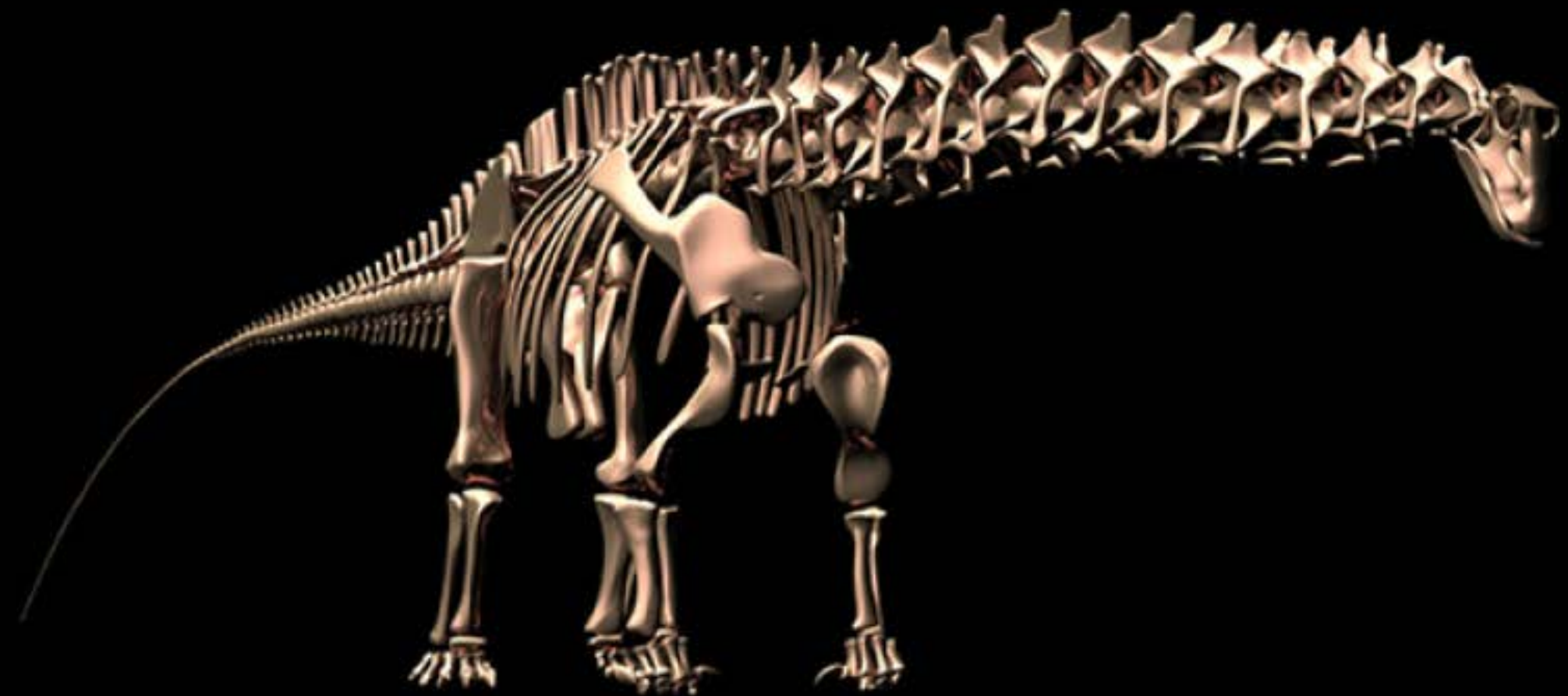


Sauropod Gigantism: A Cross-Disciplinary Approach



Sauropod Gigantism: A Cross-Disciplinary Approach

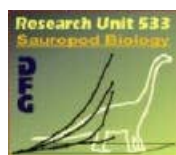
Sauropod dinosaurs were the largest terrestrial animals to roam the Earth, exceeding all other land-dwelling vertebrates in both mean and maximal body size. While convergently evolving many features seen in large terrestrial mammals, such as upright, columnar limbs and barrel-shaped trunks, sauropods evolved some unique features, such as the extremely long neck and diminutive head they are famous for.

The unique gigantism of sauropod dinosaurs has long been recognized as an important problem in the evolution of vertebrates, raising questions as to why no other land-based lineage has ever reached this size, how these dinosaurs functioned as living animals and how they were able to maintain stable populations over distinct geological time periods.

This new PLOS Collection discusses major efforts by evolutionary biologists and paleontologists to understand sauropods as living animals and to explain their evolutionary success and uniquely gigantic body size. The articles address these questions from the widest selection of disciplinary viewpoints, including those of ecology, engineering, functional morphology, animal nutrition and palaeontology.

This Collection was funded by DFG Research Unit 533. The Coordinating Author was Dr. Martin Sander, Professor of Palaeontology, Universität Bonn.

Many thanks to Andrew A. Farke, Peter Dodson, David Carrier and David C. Evans, who acted as Academic Editors for the Collection.





PLOS

COLLECTIONS

www.ploscollections.org

Overview

An Evolutionary Cascade Model for Sauropod Dinosaur Gigantism - Overview, Update and Tests

Sander MP

Page 5

Nutrition

Herbivory and Body Size: Allometries of Diet Quality and Gastrointestinal Physiology, and Implications for Herbivore Ecology and Dinosaur Gigantism

Clauss M, Steuer P, Müller DWH, Codron D, Hummel J

Page 28

Head & Neck

Biomechanical Reconstructions and Selective Advantages of Neck Poses and Feeding Strategies of Sauropods with the Example of Mamenchisaurus youngi

Christian A, Peng G, Sekiya T, Ye Y, Wulf MG, et al.

Page 44

The Articulation of Sauropod Necks: Methodology and Mythology

Stevens KA

Page 52

The Effect of Intervertebral Cartilage on Neutral Posture and Range of Motion in the Necks of Sauropod Dinosaurs

Taylor MP, Wedel, MJ

Page 80

Torsion and Bending in the Neck and Tail of Sauropod Dinosaurs and the Function of Cervical Ribs: Insights from Functional Morphology and Biomechanics

Klein N, Preuschoft H

Page 97

Locomotion

March of the Titans: The Locomotor Capabilities of Sauropod Dinosaurs
Sellers WI, Margetts L, Coria RA, Manning PL

Page 113

Quantitative Interpretation of Tracks for Determination of Body Mass
Schanz T, Lins Y, Viefhaus H, Barciaga T, Laübe S, et al.

Page 134

Growth

Preliminary Analysis of Osteocyte Lacunar Density in Long Bones of Tetrapods: All Measures Are Bigger in Sauropod Dinosaurs
Stein KWH, Werner J

Page 146

Thermo-physiology

Sauropod Necks: Are They Really for Heat Loss?
Henderson DM

Page 155

Body Temperatures in Dinosaurs: What Can Growth Curves Tell Us?
Griebeler EM

Page 163

Caudal pneumaticity and pneumatic hiatuses in Apatosaurus and Giraffatitan
Wedel MJ, Taylor MP

Page 175

Evolutionary Ecology

Ecological Interactions in Dinosaur Communities: Influences of Small Offspring and Complex Ontogenetic Life Histories
Codron D, Carbone C, Clauss M

Page 189

New Insights into Non-Avian Dinosaur Reproduction and Their Evolutionary and Ecological Implications: Linking Fossil Evidence to Allometries of Extant Close Relatives
Werner J, Griebeler EM

Page 201



An Evolutionary Cascade Model for Sauropod Dinosaur Gigantism - Overview, Update and Tests

P. Martin Sander*

Steinmann Institute of Geology, Mineralogy and Paleontology, University of Bonn, Bonn, Germany

Abstract

Sauropod dinosaurs are a group of herbivorous dinosaurs which exceeded all other terrestrial vertebrates in mean and maximal body size. Sauropod dinosaurs were also the most successful and long-lived herbivorous tetrapod clade, but no abiological factors such as global environmental parameters conducive to their gigantism can be identified. These facts justify major efforts by evolutionary biologists and paleontologists to understand sauropods as living animals and to explain their evolutionary success and uniquely gigantic body size. Contributions to this research program have come from many fields and can be synthesized into a biological evolutionary cascade model of sauropod dinosaur gigantism (sauropod gigantism ECM). This review focuses on the sauropod gigantism ECM, providing an updated version based on the contributions to the PLoS ONE sauropod gigantism collection and on other very recent published evidence. The model consist of five separate evolutionary cascades ("Reproduction", "Feeding", "Head and neck", "Avian-style lung", and "Metabolism"). Each cascade starts with observed or inferred basal traits that either may be plesiomorphic or derived at the level of Sauropoda. Each trait confers hypothetical selective advantages which permit the evolution of the next trait. Feedback loops in the ECM consist of selective advantages originating from traits higher in the cascades but affecting lower traits. All cascades end in the trait "Very high body mass". Each cascade is linked to at least one other cascade. Important plesiomorphic traits of sauropod dinosaurs that entered the model were ovipary as well as no mastication of food. Important evolutionary innovations (derived traits) were an avian-style respiratory system and an elevated basal metabolic rate. Comparison with other tetrapod lineages identifies factors limiting body size.

Citation: Sander PM (2013) An Evolutionary Cascade Model for Sauropod Dinosaur Gigantism - Overview, Update and Tests. PLoS ONE 8(10): e78573. doi:10.1371/journal.pone.0078573

Editor: Andrew A. Farke, Raymond M. Alf Museum of Paleontology, United States of America

Received: June 6, 2013; **Accepted:** September 20, 2013; **Published:** October 30, 2013

Copyright: © 2013 P. Martin Sander. This is an open-access article distributed under the terms of the Creative Commons Attribution License, which permits unrestricted use, distribution, and reproduction in any medium, provided the original author and source are credited.

Funding: This study was funded by the DFG (Deutsche Forschungsgemeinschaft/FOR 533: Biology of the Sauropod Dinosaurs: The Evolution of Gigantism). The funder's URL is www.dfg.de. The funders had no role in study design, data collection and analysis, decision to publish, or preparation of the manuscript.

Competing Interests: The author has declared that no competing interests exist.

* E-mail: martin.sander@uni-bonn.de

Introduction

Dinosaurs of the clade Sauropoda were the largest terrestrial animals that ever lived [1,2,3]. They also were the herbivorous vertebrates that were predominant in terrestrial ecosystems for the longest time of any major clade, around 120 million years, from the Middle Jurassic to the end of the Cretaceous [4,5]. Obviously, understanding their evolution and biology is a research program appropriate in size and importance to these extinct animals. The new millennium has witnessed an enormous growth in studies on sauropods, reflected by three edited volumes [3,6,7]. Since the interrelationships of major sauropod clades have largely been clarified (e.g., [8]), the focus has shifted to understanding sauropods as living animals and, through this, their remarkable evolutionary success and their evolution of their unique body size [1,2,3].

Scientists from many fields of biology and other backgrounds, sometimes far removed from traditional paleontology, have become interested in sauropods, recognizing them as models for understanding vertebrate evolution. Research has become increasingly quantitative and model-oriented. Starting with the simple quantification of sauropod body size in comparison with other clades of vertebrates [9,10,11], amazing progress has been made in quantifying dinosaur ecology [9,11,12,13,14,15]. Modeling is worthwhile in sauropod research because, for one, sauropods

went extinct 65 million years ago, making direct observation not an option, and also because of the great progress in computer applications and in the quantification and comparison of the biology of living animals and their ecosystems. The sauropod gigantism collection is meant to bring together current research on sauropods going beyond new finds in the field, beyond new phylogenies, and beyond new quantitative analyses of their fossil record. These areas of research, however, will remain as the foundation of research into sauropod gigantism.

An evolutionary cascade model for sauropod dinosaur gigantism

Recently a new evolutionary perspective has been brought to understanding the uniquely gigantic body size of sauropod dinosaurs [2], an evolutionary cascade model (ECM) of sauropod dinosaur gigantism. This ECM posits that the evolution of sauropod gigantism was the result of the unique historical interplay of plesiomorphic (primitive) and derived traits, covering many aspects of sauropod biology, and selection pressure for ever larger body size [2]. There are two important premises to the sauropod gigantism ECM: for one, that sauropod gigantism as an evolutionary phenomenon was made possible by intrinsic, biological factors alone, without the need to hypothesize an

[17] to sexual selection in birds [16], it is not yet widely used in organismal evolutionary biology.

The concept of evolutionary cascade is related to that of evolutionary constraint [18,19] in two ways. An evolutionary cascade may result from the effects of several constraints arranged in a specific sequence, but an evolutionary cascade may also result from breaking one or more constraints by key innovations. The concept of evolutionary cascade thus seeks to go beyond the simpler concept of evolutionary constraint. Similarly, the concept of evolutionary cascade reaches beyond the concept of key innovation because it identifies multiple primitive traits, key innovations, and causations that shaped the evolutionary history of a group. All of these concepts have a historical perspective in common, explaining a pattern that is observed, usually over geological time scales. This perspective should not be confused with the experimental and process perspective commonly employed in the evolutionary biology of extant organisms.

Several cascades and their interplay have affected the evolutionary history of a clade. These cascades and their interplay may be described and visualized in an evolutionary cascade model such as the one for sauropod gigantism. An evolutionary cascade model is a tool that reveals the complex interplay of evolutionary constraints and historical contingencies that have allowed a lifestyle or trait to evolve. An ECM is thus a framework that explains the success and peculiarities of an animal lineage, independent of whether it is fossil or living. The nature of evolutionary cascade models, like that of all models, is heuristic, bringing interactions and constraints in an evolving lineage into sharper focus. In addition to traits and selection pressures acting on them, evolutionary cascade models can include feedback loops, making such links self-amplifying (Fig. 1). Note that an ECM essentially is a flow diagram, not a network diagram. This is unlike the correlated progression concept of Kemp [20], in which links between different traits are hypothesized but neither sequentiality nor causation of traits are addressed.

Testing ECMs

Testing an evolutionary cascade model consists of testing its components, i.e., observed and inferred traits, evolutionary causations (i.e., selective advantages), and feedback loops. Inferred traits can be falsified by research specifically directed at this trait or by published evidence (Fig. 2). The same approach applies to hypothesized causal relationships, i.e., selective advantages and feedback loops. If the majority or all of the traits, selective advantages, and feedback loops are unfalsified, the ECM has passed the initial test and greater confidence can be placed in it. However, the predictions of the ECM must continually be tested, and the model modified, and ideally simplified, accordingly.

Update on Sauropod Evolution and Paleobiology

New taxa, finds, and phylogenies since 2009

New taxa. New sauropod taxa continue to be found or recognized through taxonomic work at a fast rate, underscoring the importance of sauropods in terrestrial ecosystems of the Jurassic and Cretaceous. While Mannion et al. [4] gave an early 2010 census of 175 valid genera, this number is up to 204 in early 2013, according to the Paleobiology Database (www.paleodb.org). There are no specific trends regarding where this new material comes from, but South America probably is the leader in diversity increase, the majority of new taxa pertaining to titanosaurs. Disparity does not seem to have increased markedly through these discoveries. Here I do not offer a comprehensive review but

highlight only a few important finds, particularly those extending geographic and temporal ranges.

Tapuiasaurus macedoi from the Early Cretaceous (Aptian) of Brazil [21] preserves the oldest typical titanosaur skull, indicating that advanced titanosaurs had evolved 30 million years earlier than previously believed. *Atacamatitan chilensis* from the Late Cretaceous of the Atacama Desert, Chile, is the first named sauropod from the western side of the Andes [22]. Likewise, the basal somphospondyliian *Angolatitan adamastor* is the first sauropod from Angola and one of the few known from the Late Cretaceous of Africa [23]. Its Turonian age combined with its basal position in the cladogram suggest that *Angolatitan* may have been a relic form [23].

Already diverse sauropod faunas have become even more diverse, with a new diplodocine from the Late Jurassic Morrison Formation of northern Wyoming described as *Katedocus siberi* [24] and new titanosaurs from the Later Cretaceous of Patagonia, Argentina, such as *Elatitan lilloi* [25] and *Narambuenatitan palomoi* [26]. Bone histology indicates that the Morrison Formation species *Suuwassea emilieae* is a valid taxon because is not a juvenile of another Morrison Formation taxon [27] and phylogenetic analysis indicates it to be a dicraeosaurid [27], the first from North America. Particularly, the Morrison Formation taxa raise the question again about true sauropod diversity in this, the most species-rich of all sauropod-bearing formations.

New finds. Not only new taxa, but new discoveries and reanalyses of known taxa may be relevant for our understanding of sauropod biology and gigantism. A case in point is the putative early theropod dinosaur *Eoraptor* from the Carnian (Late Triassic) Ischigualasto Formation of Argentina. This small biped turns out to be one of the most basal sauropodomorph dinosaurs instead, consistent with the sistergroup relationship of theropods and sauropodomorphs [28]. No later than the early Late Jurassic, sauropods had reached gigantic proportions as indicated by the remains of a mamenchisaurid from the Shishugou Formation of western China that include an ulna that is over 1 m long [29], indicating a humerus of around 1.5 m [27] and suggesting a femur of around 2.2 m in length. The large long bone shafts from the classical Late Triassic English locality of Aust Cliff remain enigmatic and cannot be assigned to Sauropoda [30]. At the other end of the stratigraphic column and the cladogram are the remains of gigantic individuals of the Maastrichtian titanosaur *Alamosaurus* from New Mexico [31,32], comparable in size to the Argentinian giant titanosaurs *Argentinosaurus*, *Futalongkosaurus*, and *Puertasaurus*. These new finds [29,31,32] underscore the early evolution of giant sauropods no later than the Middle Jurassic and their later ubiquity, already apparent from the giant sauropods *Turiasaurus* (Late Jurassic, Spain), *Paralititan* (Early Cretaceous, Egypt), and *Sauroposeidon* (Early Cretaceous, USA), in addition to the giant Argentinian taxa mentioned above (see review in [2]). At the other end of the size spectrum, the island dwarf *Europasaurus* from the Late Jurassic of Germany continues to surprise in that the material from the type locality, and only geological horizon represents growth series of two morphs [33]. The morphs differ in final size, and previous body mass estimates of 800 kg apply to the large one [33]. Note that body mass estimate of “<5 t” by given Wilson & Curry Rogers [34] is misleading. It is uncertain whether the two morphs of *Europasaurus* represent different populations or species separated in time or possibly sexual morphs. Sauropod dinosaurs are now known from all continents, with a first record from Antarctica, a titanosaur tail vertebra having been described in 2012 [35].

New phylogenies and the emergence of the sauropod body plan. The part of the sauropodomorph tree (Fig. 3) crucial for understanding sauropod gigantism is in the transition from derived

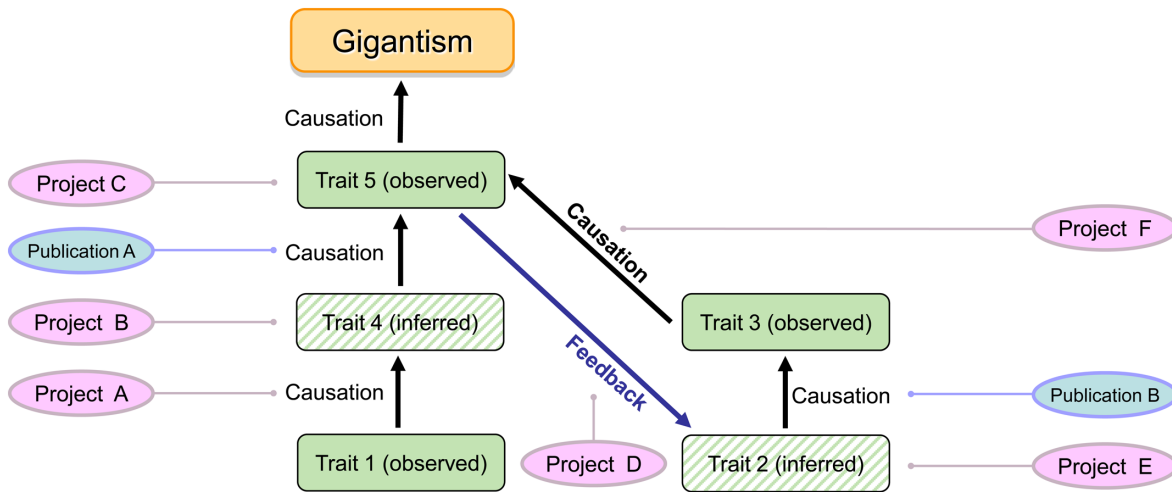


Figure 2. Testing an ECM by testing inferred traits and hypotheses of causation through transdisciplinary paleobiological research. Note that tests may consist of research projects designed for the specific purpose of falsification, come from published studies, and also may employ phylogenetic approaches.

doi:10.1371/journal.pone.0078573.g002

non-sauropod sauropodomorphs to Sauropoda. Among sauropodomorphs, Yates et al. [36] recognize an obligatorily quadrupedal clade consisting of Melanorosauridae and Sauropoda, with *Antetonitrus* being the most basal sauropod. Sauropoda are defined as “the most inclusive clade containing *Saltasaurus loricatus* but not *Melanorosaurus readi*” [37]. Closer to the traditional concept of Sauropoda, before the intermediate forms such as *Antetonitrus* were known, is the taxon Gravisauria, which is defined as “the least inclusive clade containing *Vulcanodon karibaensis* and *Saltasaurus loricatus*” [37]. In Gravisauria, the typical sauropod body plan and all characters and traits relevant to the discussion of sauropod gigantism had evolved. Body size appears to increase to typical sauropod size in Gravisauria, but the rate of this increase is difficult to quantify because of the fragmentary nature of large basal and/or early sauropods. This prevents us from optimizing body size on the sauropod phylogeny at a higher resolution than was done before [2], because only smaller taxa are represented in the phylogeny.

While the phylogenetic relationships of the major sauropod clades to each other have been pretty well understood for the last 15 years [8], the ingroup relationships of Macronaria and particularly titanosaurs *sensu lato* have been difficult to resolve (Fig. 3). This situation is improving with recent analyses [21,33,38,39,40]. While these analyses differ in important details, they generally recover a monophyletic Brachiosauridae, different clades of basal titanosaurs, and well constrained Titanosauria.

Also, with the description of new taxa, hypotheses of their relationships are needed, which in turn improves our understanding of specific branches of the sauropod tree as well as its overall topology. A case in point is the study by Carballido et al. [41] on *Comahuesaurus*, which also resolves the interrelationships of Rebbachisauridae. A very similar topology but with fewer taxa was found by Mannion et al. [40]. The relationships of Diplodocoidea were recently reanalysed by Whitlock [42], including the largest number of taxa considered so far.

Evolution and extinction

Our current understanding remains that gravisaurian sauropods first appear in the Late Triassic (Norian) but only become the dominant terrestrial herbivores in the Middle Jurassic after the

extinction of non-sauropod sauropodomorphs [4]. The major clades of neosauropods (Diplodocoidea and Macronaria) originated in the Middle Jurassic, and already outside of these clades, gigantic forms evolved among Turiasauridae and Mamenchisauridae [29,43]. The Late Jurassic saw the greatest diversification of the Diplodocoidea while the Early Cretaceous record is dominated by basal macronarians. The discovery [21] of an advanced titanosaur from the late Early Cretaceous (125–112 mya) explains the previously puzzling global distribution of the group in the Late Cretaceous, and suggests vicariance as the explanation of this pattern. Titanosaurs seem to have undergone an opportunistic radiation in the middle of the Cretaceous instead of competitively replacing diplodocoids and basal macronarians, gradually substituting them as the landmasses drifted apart [21,39]. This scenario is consistent with the lack of evidence for a mid-Cretaceous terrestrial tetrapod extinction event [5].

All sauropod dinosaurs went extinct at the end of the Cretaceous. An analysis of Late Cretaceous sauropod diversity in southwestern Europe indicates no decline towards the K/Pg boundary [44], which is in agreement with catastrophic extinction not driven by biotic interaction but by an extrinsic cause. Ecological modeling of dinosaur, including sauropod, size-specific competition based on the scaling and disparity between parent and offspring size now suggests a possible explanation of why the generally large, oviparous dinosaurs would have been more vulnerable to extrinsic causes of extinction [12] than the contemporary viviparous small mammals. The model shows that after an extrinsically caused population collapse, large dinosaurs failed to re-establish populations as opposed to mammals. Based on a case study from the Dinosaur Park Formation of Alberta, Canada [45,46], the assumption of the model of a strong left skew of body mass [12] was questioned and explained as a bias in the fossil record against small dinosaurs instead. The global nature of such a bias appears unlikely because the Dinosaur Park Formation is not representative of other Late Cretaceous dinosaur-bearing formations. Before the K/Pg extinction event, only the northern part of North America lacked sauropods [47], the extreme size of which are central to the model. The bias hypothesis was also refuted by a new compilation of vertebrate body size distribution through time [9] that had not been published at the time of the

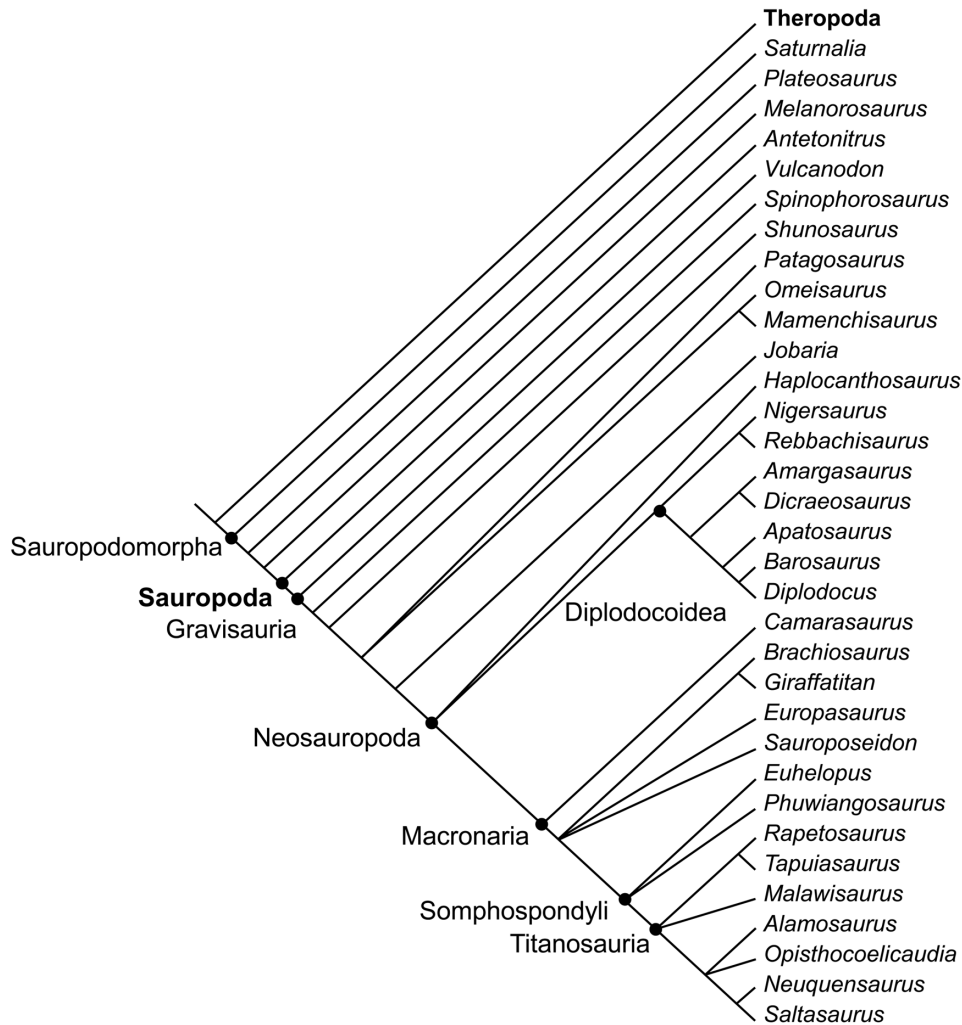


Figure 3. Simplified consensus phylogeny of Sauropoda at the genus level, containing only the best known and complete genera. Based on information in [21,33,36,38,39,40,188]. Dots indicate higher taxa. Note that no distinction is made between node-based and stem-based taxa.

doi:10.1371/journal.pone.0078573.g003

discussion about the extinction modeling [12,46,47]. The modeling approach [12] thus lends credence to an extrinsic cause for dinosaur extinction such as the meteorite impact creating the Chicxulub structure in Mexico [48].

Seemingly, this hypothesis about dinosaur extinction [12] is contrary to the hypothesis of Janis & Carrano [14,49] that ovipary made dinosaur populations less at risk of extinction than populations of mammals of the same body size. However, the two hypotheses do not necessarily contradict each other since one [12] is comparing coexisting mammals and dinosaurs, while the other [49] addresses the question of what limits body size in the two groups.

Diversity and biogeography

The emerging picture of sauropod diversity and biogeography also continues to solidify with a number of recent studies directed at refining our view of the patterns. The following section, on ecosystems, will explore some of the causations of these patterns. The diversity of dinosaurs, including sauropods, is commonly expressed by the total number of genera, with a 2010 census noting 175 sauropod genera, 325 theropod genera, and 223

ornithischian genera [50]. While there have been estimates of the total number dinosaur genera that ever lived (3500[11,51]), these may well be overestimates because of the limited comparability of mammalian and dinosaurian ecosystem structure: dinosaurian ecosystems were characterized by a great size disparity between neonate and parent, resulting in a lack of parental care and ontogenetic niche shifting. This was particularly true for sauropods [52,53,54], and one dinosaur species may have occupied several niches as the individuals grew through several orders of magnitude in body size [12,52]. In a similar mammalian ecosystem, these niches would be occupied by different species, thus leading to a greater species diversity in the mammals compared to the dinosaurs [12].

Progress has been made in reconstructing sauropod diversity through time [4], with reliable estimates for most time bins (geological stages) but not all, for example, the Late Cretaceous. The discovery of *Tapuiasaurus* serves as a reminder of the nature of the sauropod fossil record in that the major patterns of diversification are well understood but that the specifics of time and place are just now emerging. In the broader analysis of dinosaur diversity through time, a new study [5] suggests that dinosaur faunas on the northern continents were never dominated

by ornithischian dinosaurs, contrary to long-held beliefs. The only exception that appears to be remaining is the Campanian–Maastrichtian faunas of North America. Thus, the statement that “many terrestrial ecosystems were dominated by sauropods” [2] probably has to be modified to “most terrestrial ecosystems”, underscoring the importance of understanding sauropod gigantism.

The limitations of extrapolating from present patterns to the Mesozoic may be shown by an analysis of latitudinal distribution of diversity in dinosaur faunas [55]. Unlike in the modern world, where the tropics are the centers of diversity, dinosaurs appear to have been most diverse at mid- to high latitudes in temperate climates. This signal is well expressed in sauropodomorphs, particularly in the southern hemisphere. This diversity pattern also correlates with land area and may be partially explained by the weaker climate gradient in the Mesozoic [55].

Ecosystems

Improvements in our understanding of ecosystems inhabited by sauropod dinosaurs have come from two different sources: the direct evidence provided by paleontology (including paleobotany), geology, and geochemistry, and the comparison with modern, mammal-dominated ecosystems. Whereas the former is based on generalizing from case studies, i.e., specific sauropod-bearing rock formations, the latter takes the opposite approach, using general relationships in ecosystems that are consistent with the fossil and rock record.

Arguably the most important source of information about sauropod dinosaurs and their environment has been the Upper Jurassic Morrison Formation of the western United States [56]. Although often portrayed as a semiarid habitat with low “fern prairies”, this is difficult to imagine considering the energy needs of the sauropod population. Growing evidence for conifer-dominated forest vegetation in the Morrison Formation suggests a much more mesic habitat [57] that would have been able to support the sauropods so amply documented by their fossils. An alternative solution to the problem of “feeding your sauropod” in the semiarid Morrison basin is offered by cyclicity in Sr isotope geochemistry in sauropod teeth, suggesting annual migrations of sauropods to the highlands bordering the basin in the west, possibly to cope with seasonal food shortages [58].

These observations partially support (migration) and partially contradict (aridity) the assumptions made by the most refined effort to quantitatively describe a sauropod ecosystem [59], again that of the Morrison Formation. This study by Farlow et al. incorporates the greatest range of information on extant animals as well observations from deep time, thus incorporating both approaches; its goal being to estimate the population density of dinosaurian megaherbivores, primarily sauropods. Farlow et al. estimate that endothermic dinosaurian megaherbivores would have had densities of “a few tens” of individuals of all ages but only a few subadults and adults per square kilometer [59]. Counts for dinosaurs with an intermediate metabolism would have been up to an order of magnitude greater. Farlow et al. [59] make no explicit distinction between sexually reproductive animals and juveniles, but only distinguish between “large subadults and adults” and “others”. Making this distinction would be the first step in using the result of Farlow et al. [59] to estimate the density of sauropod breeding populations in models of population growth rates, e.g., [12,14,49].

Recent studies using the general ecological approach would suggest that limitations in food availability would have affected sauropod populations less than mammalian megaherbivore populations because of the much lower minimum population

densities of the former [11,12,14,49,52,59]. Low viable population densities could have been afforded by sauropods for two reasons: their ovipary [14,49,52] and the strong left skew of sauropod body mass distribution [9] combined with the scaling of basal metabolic rate (BMR) [11]. Estimates of density of sauropods in the environment [12,52,59] thus are an order of magnitude lower than observed in modern mammalian ecosystems. This low density, however, was combined with a herbivore biomass that, at least at the global level, may have been one or more orders of magnitude higher in dinosaur (mostly sauropod) ecosystems than in modern ecosystems [11]. This study, however, did not take the different ontogenetic stages of large-bodied species into account, although it discusses their effects [11].

From all of this work, it is becoming increasingly clear that the key to understanding dinosaur ecosystems is the great size disparity between neonates and adults, epitomized by sauropods (see also section Cascade “Reproduction”). Only when researchers fully embrace this difference between dinosaurs and mammals in their analyses, will a profound understanding of dinosaurian ecosystems emerge.

Test of the Sauropod Gigantism ECM by New Evidence

The evolutionary cascade model for sauropod gigantism

As originally proposed [2], the evolutionary cascade model for sauropod gigantism consists of three basal traits that are plesiomorphic at the level of Sauropoda and two basal traits that are derived (Fig. 1). The plesiomorphic traits are “Many small offspring”, “No gastric mill”, and “No mastication”. The derived traits are “Avian-style lung” and “High BMR”. These traits are at the base of five cascades, only one of which (cascade “Reproduction”) is completely independent of the others. The other four (“Feeding”, “Head and neck”, “Respiration”, “Metabolism”) are interconnected to varying degrees, with one basal trait “No mastication” feeding into two cascades (“Feeding” and “Head and neck”). The original ECM does not visualize the distinction between observed and inferred traits.

The new evidence bearing on the sauropod gigantism ECM is organized topically within the individual cascade, going up each of the cascades from the basal trait to the final one, very high body mass (Figs. 4, 5, 6, 7, 8). Cascades consist of traits, hypothesized selective advantage,s and feedback loops. Unlike in the original model, an explicit distinction is made between observed and inferred traits. However, before each cascade is discussed, new developments regarding the premises underlying research on sauropod gigantism in general and the ECM in particular need to be addressed.

Testing the premises

One of the basic assumptions of the ECM was that the evolution of sauropod gigantism is primarily under intrinsic control, meaning that it was driven by biological factors [2]. Extrinsic controls, such as changing global environmental parameters, were largely excluded from consideration in the ECM because those environmental parameters that are known or can be reasonably well inferred show no correlation with sauropod body size evolution [2]. This hypothesis of no correlation was tested by Sookias et al. [13] using maximum-likelihood analyses of Late Paleozoic to Jurassic terrestrial vertebrate evolution, and they showed that biological factors alone are sufficient to explain patterns of size evolution in dinosaurs [13]. The Cretaceous was not covered by this analysis [13], which should not be a problem in the current context because sauropod gigantism already had

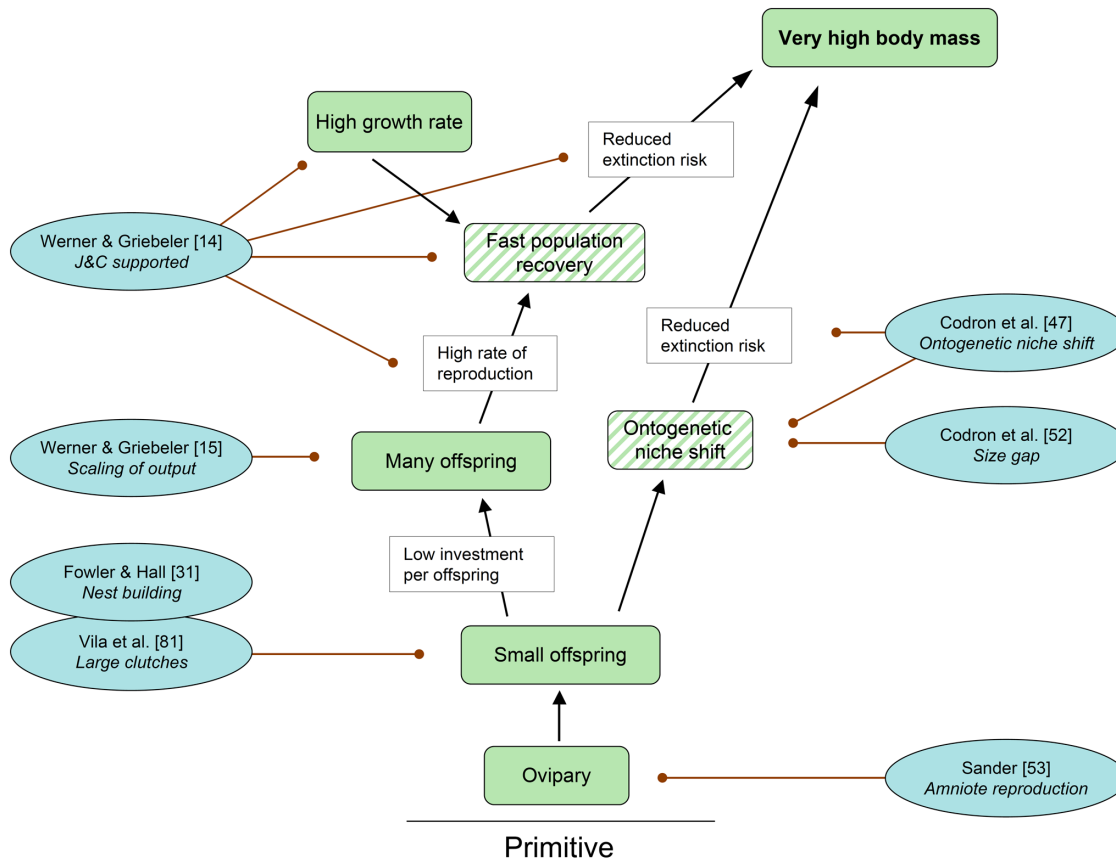


Figure 4. Cascade “Reproduction” with pertinent references published since 2010. Each reference includes a keyword indicating the aspect relevant to the cascade. In this cascade are the same as in Fig. 1, except that a distinction is made between observed traits (solid color) and inferred traits (oblique stripes). The trait “High growth rate” is part of the cascade “Metabolism”. “J&C supported” stand for the Janis & Carrano hypothesis of dinosaur body size distribution [49]. See text for further explanations.
doi:10.1371/journal.pone.0078573.g004

evolved in the Late Triassic and Jurassic. However, recently a specific hypothesis of extrinsic control by Midgley et al. [60], invoking raised levels of carbon dioxide during the Mesozoic to account for dinosaur gigantism, was resurrected [61] and awaits further scrutiny.

Among the several drivers of evolutionary body size increase in dinosaurs [9,62,63], also known as “Cope’s Rule” [64,65,66,67], predation pressure has received renewed attention. Ecological models suggest that in dinosaur ecosystems, there was a size threshold above which theropods could not subsist on prey much smaller than themselves but had to hunt prey of their own body mass [52]. This threshold, which is 21.5 kg body mass in modern terrestrial ecosystems [68], may have been 25 to 30 kg for dinosaur ecosystems [52]. This means that theropod predation pressure on sauropods must have been strong before the individuals exceeded the largest theropods in their habitat in body mass, as is the case in modern mammal ecosystems with the largest herbivores [69,70]. At least in modern large-mammal ecosystems, the largest predators generally do not take prey that is significantly larger than themselves, not even by pack-hunting [68,69,70,71].

Predation pressure by large theropods on sauropods also hinges on the question if such giants as *Tyrannosaurus* indeed were actively hunting their prey or if they only were scavengers. Models of carrion encounter vs. prey encounter support active hunting because large theropods would have been the last ones to have

found any carrion which would have been consumed by smaller theropods and juveniles first [72]. Other lines of evidence that large theropods were active hunters were reviewed by Brusatte et al. [73]. The most recent addition to the discussion is direct evidence of predation [74]. However, abundance of *Tyrannosaurus* in the Late Cretaceous Hell Creek Formation of Montana (USA) suggests that at least adult tyrannosaurs may also have subsisted on carrion [75]. While scavenging may have been a way of life in some large theropods, such as *Tyrannosaurus*, the sum of the evidence argues for large theropods generally having been active predators.

Predation pressure on herbivorous dinosaurs, i.e., ornithischians and sauropods, thus probably explains the strong left skew seen in body size histograms of these dinosaur groups [9,12].

Traits of sauropod reproductive biology, i.e., the lack of parental care and the large number of small offspring, also must have resulted in increased predation pressure which in turn would have led to strong selection for larger body size. In particular, because unlike in modern meager herbivores no trophic energy was lost due to parental care [76], juveniles of even the largest herbivorous dinosaur species were available to predators. This provided the predators with a greater resource base compared to modern ecosystems, which would have facilitated larger predator body size [52,76], raising the body size ante for sauropods even further. This effect was not limited to sauropods, of course, but would have influenced ornithischian-dominated ecosystems as well.

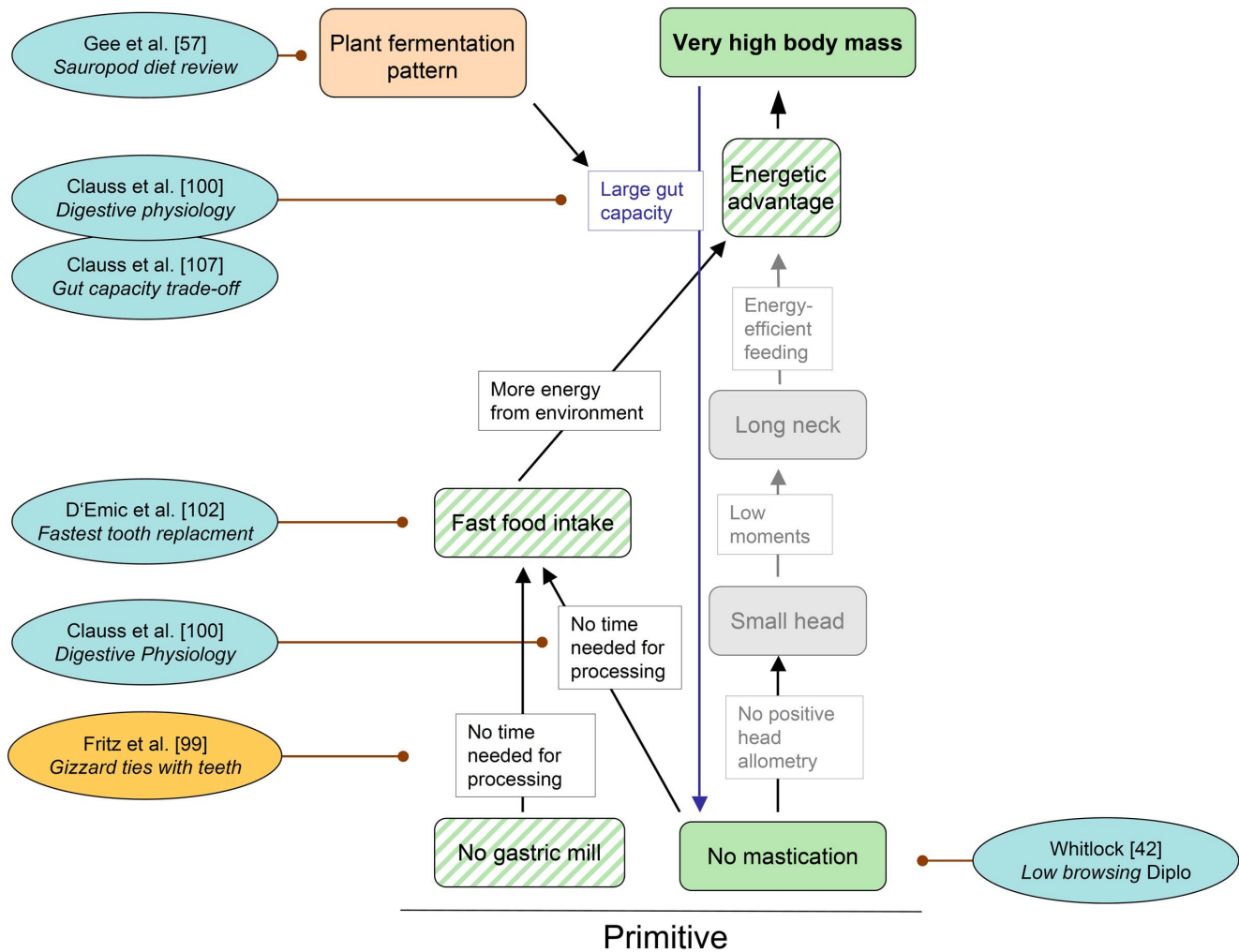


Figure 5. Cascade “Feeding” with pertinent references published since 2009. Each reference includes a keyword indicating the aspect relevant to the cascade. Conventions used in this cascade are the same as in Fig. 1, except that a distinction is made between observed traits and premises (solid color) and inferred traits or premises (oblique stripes). The orange references call the respective selective advantage into question. Grey indicates parts of another cascade that share traits with this one. See text for further explanations.
doi:10.1371/journal.pone.0078573.g005

Trait. Very high body mass

This trait will be discussed first because all cascades culminate in it. The discussion of this trait only covers the most recent developments and literature because an in-depth review is found in Sander et al. [2].

Finds of exceptionally large sauropod individuals continue to be made (see above), making the trait “Very high body mass” immediately obvious. Compilations from the literature also drive home the point [3,12]. Dinosaurs show little overlap with mammals in body mass to species richness plots and show a strongly left-skewed distribution compared to the strongly right-skewed distribution of extant and fossil mammals, with sauropods occupying the far right of the body mass spectrum [9,12].

Much of the work underlying the ECM requires accurate estimates of body masses of sauropods at the level of the individual. Classically, two approaches have been taken for estimating body mass in extinct tetrapods: mass estimates based on body volume estimates and mass estimates based on scaling of long bone dimensions in extant tetrapods. The most general dataset compiled so far offers a universal scaling relationship of long bone circumference and body mass in tetrapods [10]. Values for

sauropods calculated from this relationship are similar to estimates obtained by earlier workers, e.g., 35,780 kg for the Berlin skeleton of *Giraffatitan* [10]. Volume-based estimates also have become more refined such as the “minimum convex hull method” [77] which was calibrated using extant animals of known mass. This method resulted in a seemingly “low” estimate of 23,200 kg for the Berlin *Giraffatitan* [77].

A novel approach to “weighing” sauropods is using soil mechanics to estimate the mass of a trackmaker from the substrate deformation it caused [78]. Dinosaur tracks in a trackway always include a kinetic component in the forces that generated them in addition to the static component. However, in large slow-moving animals with columnar legs such as elephants and sauropods, the static component greatly exceeds the kinetic component. Thus, soil mechanical finite element models were calibrated for estimating sauropod masses by experiments with an elephant [78].

Cascade “Reproduction” (Fig. 4)

Trait (observed and inferred). Many small offspring

Sauropod dinosaurs, like all extinct and living dinosaurs and all archosaurs, reproduced via ovipary, presumably being constrained

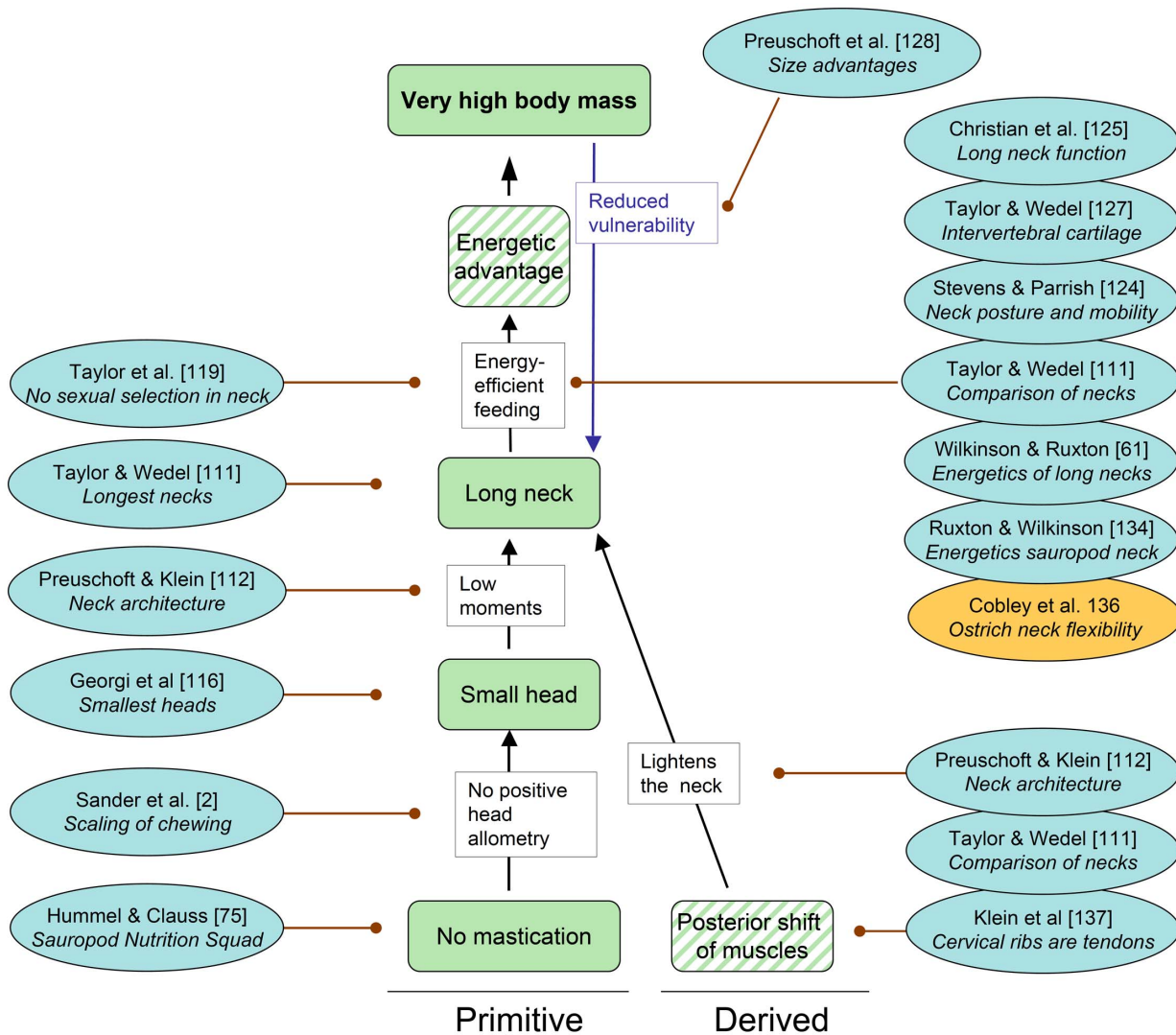


Figure 6. Cascade “Head and neck” with pertinent references published since 2011. Each reference includes a keyword indicating the aspect relevant to the cascade. Conventions used in this cascade are the same as in Fig. 1, except that a distinction is made between observed traits (solid color) and inferred traits (oblique stripes). See text for further explanations. doi:10.1371/journal.pone.0078573.g006

to this mode of reproduction by their calcified eggshells [79]. This seemingly straightforward statement takes on a new meaning when one considers that the biomechanical upper limits to egg mass [52,53,71,80], derived from work on bird eggs [71,80], means that sauropod hatchlings must have been very small compared to the adult [12,14,52]. This is in accordance with the fossil record that shows that all known sauropod eggs had a volume not exceeding 5 liters [80,81,82] and that most were buried in the substrate [81,83,84].

The small size of the offspring relative to the adult led to the hypothesis [53] that large sauropods must have laid hundreds of eggs per year in several clutches to have a biologically realistic reproductive output. This hypothesis recently found support in a detailed analysis of scaling of egg mass, clutch mass, and annual clutch mass in the extant phylogenetic bracket of sauropods [15]. This study concluded that medium to large sauropods may have laid as many as 200 to 400 eggs per year, and smaller ones <200 eggs per year.

Particularly, the laying of several clutches and the size difference between hatchling and adult make any form of parental care

unlikely. Lack of parental care is also suggested by the burial of the egg clutches by scratch-digging of the female sauropod [81,83] as practiced by extant turtles [83]. Distribution of the annual reproductive effort, i.e., annual clutch mass [15], of large sauropods over several clutches per year is suggested by phylogenetic inference combined with scaling arguments [15] and by physiological arguments [85], both based on modern amniotes. Several clutches per year is consistent with the generally small clutch size [<15 eggs], a report of up 28 eggs per clutch [81] notwithstanding. This report [81] failed to test the hypothesis, using shell thickness, that such large egg clusters represent several superimposed or closely associated clutches. Different clutches of a single species of sauropod differ in shell thickness while eggs in a single clutch do not [53]. This kind of work on eggshell thickness variation should be extended to the extant phylogenetic bracket of dinosaurs.

The possible exception to the lack of parental care may be the unburied eggs from the Argentinian locality of Auca Mahuevo [53,86], although other studies suggest burial of these eggs as well [87,88] and thus lack of parental care.

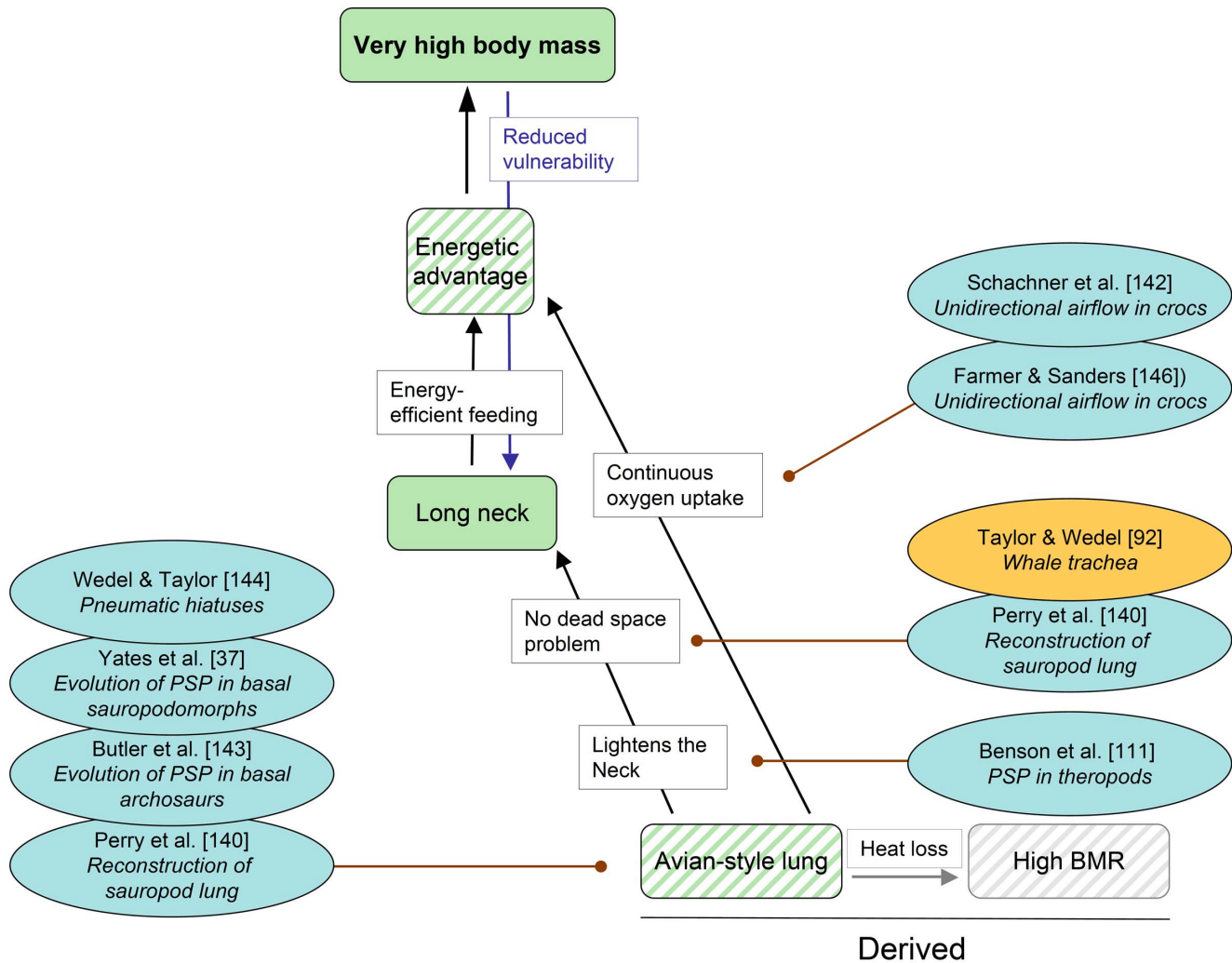


Figure 7. Cascade “Avian-style lung” with pertinent references published since 2011. Each reference includes a keyword indicating the aspect relevant to the cascade. Conventions used in this cascade are the same as in Fig. 1, except that a distinction is made between observed traits (solid color) and inferred traits (oblique stripes). See text for further explanations. doi:10.1371/journal.pone.0078573.g007

Selective advantage. High rate of reproduction

Based on data for extant birds and mammals, an early, seminal study Janis & Carrano [54] had suggested that scaling of reproductive output with body mass differs fundamentally between extant birds and mammals, and that this is linked to the oviparous mode of reproduction in birds vs. the vivipary of mammals. The latter showed negative allometry of number of offspring with body mass with increasing body mass [49], whereas birds show no decrease in reproductive output (but no increase either, i.e., no correlation) with body mass [49]. Recent analysis of a comprehensive dataset for extant birds and mammals by Werner & Griebeler [14] supports these observations, with birds showing a positive correlation between annual offspring number and body mass while mammals show a negative correlation. Werner & Griebeler [14] also noted that sauropod reproductive output was at the upper limit of that expected for a sauropod-sized bird and much higher than predicted for a sauropod-sized mammal, attributing this to the ovipary of sauropods.

Trait (inferred). Fast population recovery

Janis & Carrano [49] hypothesized that a high reproduction rate would allow fast recovery of a population after a population

crash, and this benefit also would have applied to dinosaurs [49]. The inferred trait of fast population recovery recently found support in a simple mathematical model comparing population recovery rates in a large dinosaur and a large mammal, with the dinosaur population recovering much faster [14]. However, fast population recovery also depends on a high growth rate of the offspring [14], which is lacking in extant non-avian reptiles [89,90]. Note that the trait “Fast population recovery” depends on a trait from a different cascade, the trait “High growth rate”.

Selective advantage. Reduced extinction risk

In the context of sauropod gigantism, a low reproductive output has been shown to increase the risk of extinction [14], as originally hypothesized by Janis & Carrano [49]. This will come as no surprise to a conservation biologist. Janis & Carrano [49] went on to hypothesize that reproductive output will introduce an upper limit to body size depending on reproductive output. Larger-bodied species will have lower population densities than smaller-bodied species, leading to a higher risk of population extinction through stochastic perturbations. Since the extinction risk decreases with increasing reproductive output, species with a higher reproductive output can have a larger body size than

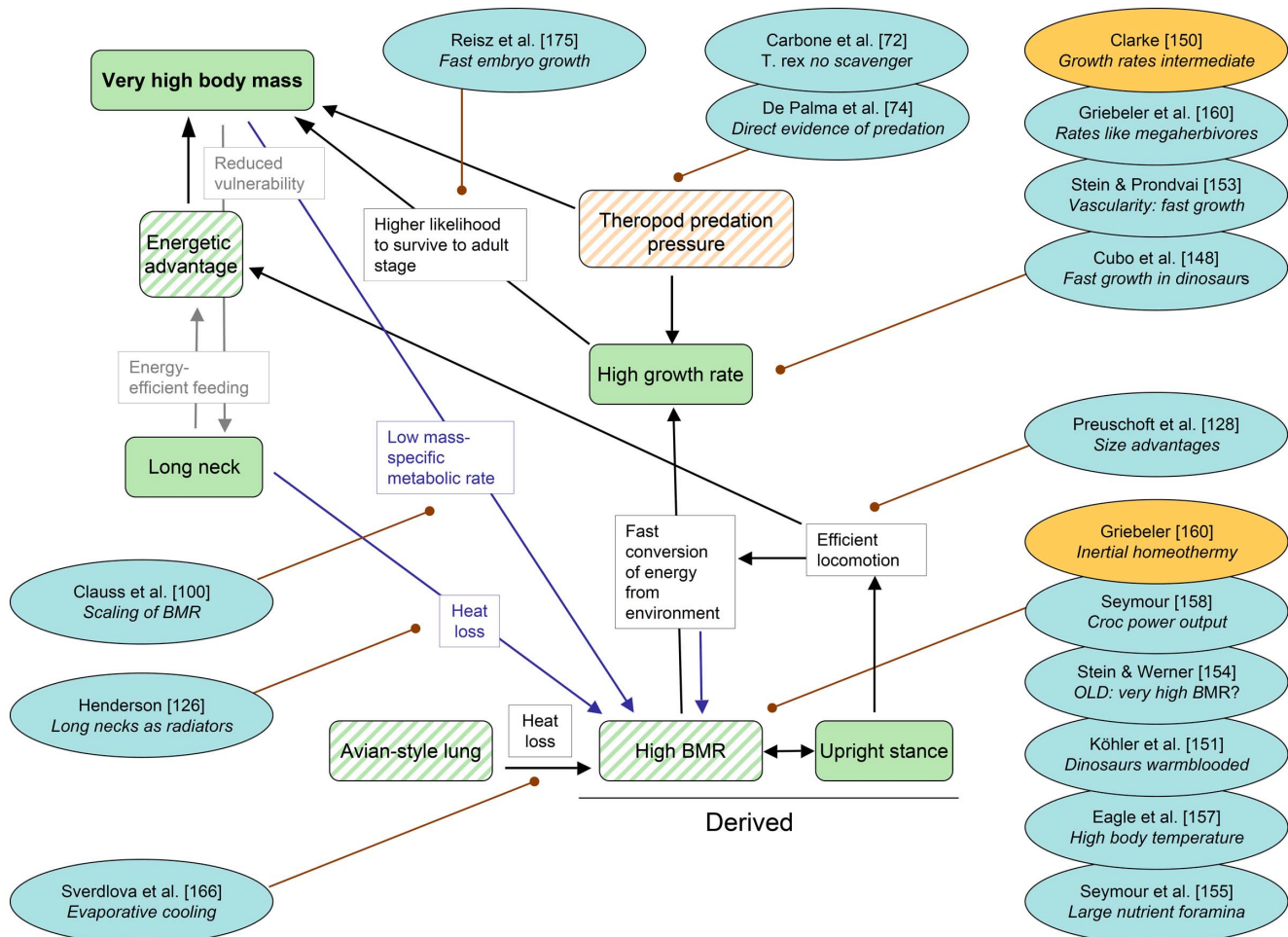


Figure 8. Cascade “Metabolism” with pertinent references published since 2011. Each reference includes a keyword indicating the aspect relevant to the cascade. Conventions used in this cascade are the same as in Fig. 1, except that a distinction is made between observed traits and premises (solid color) and inferred traits or premises (oblique stripes). Orange references call the respective trait into question. Grey indicates parts of another cascade that share traits with this one. Theropod predation pressure is an inferred premise. See text for further explanations. doi:10.1371/journal.pone.0078573.g008

species with a lower reproductive output [14,49]. This work should be extended by a comparative study of population recovery in real populations of mammals, birds, and non-avian reptiles, although likely there is much information on this subject already available in the conservation biology literature.

In sauropods, the selective advantage of a reduced extinction risk may also have resulted directly from the trait “Many small offspring”. The great size difference between hatchling and fully grown sauropods as a consequence of ovipary probably meant extensive ontogenetic niche shifting, with different life stages being adapted to different environmental conditions [12,52]. This diversity of niches in a single biological species at different times in its ontogeny is hypothesized by Codron et al. [52] to mean that in times of environmental perturbations some life stages may have been less affected or even may have preferentially survived, making the species as a whole more resilient to such perturbations. This hypothesis should be tested by studies on extant reptiles with a great size difference between offspring and parent, such as large-bodied crocodile species and marine turtles.

Cascade “Feeding” (Fig. 5)

Trait. No mastication

It is generally accepted that sauropod dinosaurs did not chew their food [91,92,93], and no evidence to the contrary has been published in recent decades. To a certain extent, lack of mastication may be a derived trait. Basal sauropodomorphs apparently possessed fleshy cheeks, a prerequisite for chewing, but fleshy cheeks were reduced in sauropods as an adaptation to bulk feeding [36]. The focus of investigations on the sauropod food gathering apparatus is now on the details of the functions of the dentition in different taxa, based on detailed descriptions of morphology and wear patterns of the dentition, macroscopic and microscopic tooth wear patterns, and muzzle shape [42], and finally biomechanical modeling using finite element analysis [92,94]. Such work lends strong support to the notion that diplodocoid sauropods were low to mid-height browsers [42]. Both generalists and specialist were found among diplodocoid sauropods, with the low browsers possibly preferring a diet of horsetails [95]. However, our understanding of the functioning of the non-masticating feeding apparatus will remain incomplete without an explanation of the common finds of isolated tooth rows in many sauropod taxa, e.g., *Giraffatitan* [96]. Possibly, the tooth row was strengthened by a keratinous sheath that covered the exposed part of the roots as suggested for dinosaurs in general [97]. Such a

sheath may or may not be homologous to the small lower bill that may have been present in some basal sauropodomorphs [28]. An improved understanding of the implications of the trait “No mastication” may come from experimental work on extant herbivorous reptiles. Herbivorous birds are not informative in this regard because they use a gastric mill to comminute plant matter instead of a dentition (see following section).

Trait. No gastric mill

In the absence of a chewing dentition, sauropod dinosaurs classically were believed to have processed their plant fodder in a gastric mill similar to granivorous birds [98]. The comparative analysis of ostrich feces and mammalian herbivore feces indicates that a gastric mill is as effective in particle size reduction as a chewing dentition [99]. However, multiple lines of evidence based on observations on extant birds make it unlikely that sauropods possessed a gastric mill [98], including the rarity of potential gastroliths found with seemingly complete sauropod skeletons compared to their consistent presence and significant mass in herbivorous birds (approx. 1% of body mass [98]).

Selective advantage. No time needed for processing

The selective advantage of not reducing fodder particle size is that no time is needed to do so. Time needed for chewing scales positively with body mass in extant mammals [69,100], limiting mammalian herbivore body size to a mass of about 18 t, at which the animal would have to spend 24 hours a day feeding [69,100]. Even if this scaling relationship for extant mammals may not have applied to chewing dinosaurs such as hadrosaurs and ceratopsians, it is likely that chewing would have limited their body size as well.

While similar data about scaling of duration of gastric mill use are lacking for birds, we cannot be sure that particle size reduction in a gastric mill limits body size. However, all birds and non-avian dinosaurs that have a gastric mill are small (dinosaurs, >25 kg) or medium-sized (birds, >250 kg) [99], suggesting other limitations to their body size. Contrary to the suggestion by Sander & Clauss [1] and Sander et al. [2], the lack of a gastric mill thus may not have been a prerequisite for sauropod gigantism.

Trait (inferred). Fast food intake

Food intake rate can only be observed in extant animals, but a high food intake rate has been inferred for sauropod dinosaurs for two reasons [1,91,101]: lack of mastication and high energy demand. The hypothesis of fast food intake can be tested by quantifying tooth wear which should increase with intake rate. Indeed, the common Morrison Formation sauropod *Diplodocus* has recently been shown to have the second-highest tooth replacement rate known among archosaurs [102]. Based on the analysis of overlapping daily growth increments in successive replacement teeth, replacement rates on the order of 35 days are reconstructed for *Diplodocus* [102]. Approximately 62 days were estimated for *Camarasaurus* [102], which is bracketed by the rates for hadrosaurs. The highest rates (“less than 30 days” [103], now refined to “15–30” days [102]) had previously been reported for *Nigersaurus* but it was not known whether this was representative for sauropods in general because of the extremely modified dentition of this taxon [103]. The new study [102] suggests that all neosauropods at least had such high tooth replacement rates, indicating fast tooth wear. Because of the small size of sauropod teeth compared to the bulk of their bearer, such high replacement rates may not be entirely surprising but clearly indicate extreme abrasion of teeth. Unlike grasses and with the exception of horsetails, Mesozoic sauropod food plants were not particularly abrasive [95], suggesting high intake rates as the explanation. Although grass phytoliths were discovered in putative sauropod coprolites from the Late Cretaceous of India [104], the sauropod affinity of these coprolites cannot be established [105,106]. A comparison of sauropod tooth

abrasion rates with those of functionally analogous non-chewing teeth (i.e., incisors) of herbivorous mammals should be done to further test the hypothesis of fast food intake.

Selective advantage. More energy from the environment

Provided that plant resources are not limited in the environment, an animal with a greater capacity for food intake rate will be able to take up more energy from the environment than an animal with a lower capacity [100]. This is supported by empirical data on extant mammals, reviewed in [100]. This increased energy taken up from the environment translates directly into an energetic advantage.

Trait (inferred). Energetic advantage

Four evolutionary cascades end in this trait, indicating that at least four traits contributed to the energetic advantage permitting sauropod gigantism, but the trait per se has not received further comparative study in extant or extinct animals since the sauropod gigantism ECM was formulated.

Feedback loop. Large gut capacity

In the original version of the ECM, a feedback loop leads from the trait “Very high body mass” to the trait “No mastication” [1,2]. This feedback loop, called “Large gut capacity” posited that very high body mass is favored by the positive scaling of the retention time of the ingested food in the gut, based on data from extant animals [107,108]. This would have allowed sauropods to compensate for the lack of mechanical breakdown of their fodder by increasing food retention time [107,108], leading to greater digestive efficiency in large-bodied dinosaurs, following the Jarman-Bell Principle in extant animals [69]. This idea was supported by the isometric scaling of gut volume compared to the negative allometry of energy requirement. However, recent work [100,109,110] called the hypothesis of positive scaling of ingesta retention time in extant animals into question because of the lack of empirical data, which instead tend to show that food retention time is independent of body mass. Accordingly, other factors than scaling of digestive physiology may have facilitated sauropod gigantism [100].

Nonetheless, isometric scaling of gut capacity would have generated the feedback loop “Large gut capacity” because of the negative allometry of BMR, but the feedback loop is probably weaker than originally envisaged. With an isometric increase in gut volume, larger animals can digest more food at the same time and thus subsist on lower-quality forage. Sauropods would have needed excessively large guts to compensate for the lack of particle reduction. In fact, the sauropod body cavity appears to have provided sufficient space for such large guts [100].

Cascade “Head and neck” (Fig. 6)

Trait. No mastication

The observed trait of no mastication has been discussed above. In addition to the selective advantage of “No time needed for food processing”, this trait provides a crucial selective advantage associated with the sauropod neck [111,112].

Selective advantage. No positive head allometry

Because of the scaling effects surrounding mastication, extant masticators show positive head allometry [2], and this may have applied to masticating dinosaurs as well, as suggested by the scaling of skull size in ceratopsian dinosaurs [113]. This is because chewing performance scales with the second power, while body mass scales with the third power. The reason for chewing performance scales with the second power is that chewing performance is determined by two surface areas: that of the combined tooth grinding surface and that of the chewing muscle cross section (the power of a muscle being determined by its cross section, not its volume). The positive head allometry of chewing

herbivores resulting from these scaling effects is weakened by the negative allometry (exponent of 0.66 to 0.75) of energy demand, i.e., BMR, to body mass, well known from extant animals (for a discussion of this scaling relationship, see [100]). Nevertheless positive head allometry appears to be the inescapable effect faced by any chewer, as seen, e.g., in the ontogeny of the hadrosaur *Prosaurolophus* [114]) and in horse evolution [115].

Trait. Small head

Sauropod dinosaurs had the relatively smallest heads in length and mass of any non-avian dinosaur [113,116] and likely of any terrestrial tetrapod, although comparative data across extinct and extant Tetrapoda have not been compiled. The small head of sauropods had to serve three major functions, the space required for all of which apparently shows a negative allometry with body mass. These functions are: food intake, housing of the sense organs, and housing of the brain and inner ear. The relatively very small brain of sauropods [117,118] stands in stark contrast with many other aspects of sauropod biology, such as their high BMR, and remains enigmatic.

Selective advantage. Low moments

The obvious selective advantages of a small head are the low moments of force that it bestows on the neck [112], permitting a longer neck than would be possible with a larger head [111,112]. The importance of moments of force in the biomechanics of long-necked mammals and birds has received much attention and most recently has been reviewed by Taylor & Wedel ([111], but see also [119,120,121,122,123,124]).

Trait. Long neck

The defining feature of sauropod dinosaurs, their uniquely long neck, received a thorough review by Taylor & Wedel ([111], see also [119,120,121,122,123,124]). This review includes a list of traits making the evolution of the long neck possible, most of which are derived from comparison with extant animals [111]. This list contains the ones discussed in depth here, as well as some more general and obvious traits such as large body size, quadrupedal stance, a phylogenetically flexible number of cervical vertebrae (unlike in mammals that are constrained to seven cervicals), and elongation of the cervical vertebrae [111].

Considering the importance of the neck, this collection contains no fewer than four contributions on the subject [112,125,126,127], including detailed studies on the osteology and posture of the neck [112,125,127]. Based on various lines of evidence, the majority of studies suggest a diversity of neck postures in sauropods, from steeply inclined to horizontal, depending on taxon. Articulation of fossil necks in the osteologically neutral pose, on the other hand, suggests a subhorizontal neck posture for all sauropods [123,124]. The topics of neck posture and flexibility will be revisited below from the perspective of the major selective advantage provided by the long neck, i.e., the selective advantage “Energy-efficient feeding”.

Although neck length would have been constrained by mechanical factors [111,112,128], the question has recently been raised whether there were neuroanatomical constraints as well, i.e., the travel times of nerve signals from the tip of the tail to the brain [129]. Signal travel times must have been up to half a second in a large sauropod based on the comparison with extant animals. Since the connection between brain and tip of tail is established by a single nerve cell, cell size might have posed an upper limit to sauropod body size [129].

Selective advantage. Energy-efficient feeding

The central hypothesis of the ECM possibly is that the long neck of sauropods facilitated highly energy-efficient feeding, both by giving access to tall vegetation and by extending the reach of the head without moving the heavy body. While it is clear that a

longer neck confers advantages to an animal of any size [2,61,128], as shown by studies on extant animals [61], the important point with regard to sauropods is that this advantage favorably scales with body mass. The scaling effect lies in the scaling of acceleration and deceleration of the body because larger animals are less “athletic” than smaller ones because muscle power only increases with the square of linear size whereas mass increases with the third power (see reviews in [130,131]).

A premise of the hypothesis of energy-efficient feeding is that the main function of the long neck indeed was feeding and not some other function in physiology, reproduction or behavior. In particular, the hypothesis that sauropod neck elongation was a result of runaway sexual selection [132], as had been hypothesized for giraffes [119], can now be rejected [119].

Several kinds of new model calculations, on the other hand, do support the hypothesized selective advantage ([61,128,133,134], see also [135]). Model calculations addressing high browsing based on *Euhelopus* and *Giraffatitan* [133] indicate that the energetic advantage of this design outweighs its metabolic costs (i.e. raising the neck and supplying it and the head with blood). Model calculations specifically addressing low browsing in sauropods [61,128] also confirm the hypothesis that the long neck greatly reduced the need for the animal to change its location during feeding. This would have resulted in energy savings of 80% in a *Brachiosaurus* bearing a nine-meter neck compared to a minimally-necked one [61]. Both studies [61,128] independently concluded that the energetic advantage of neck length levels off eventually with increasing neck length. The energetic advantage is particularly apparent if target vegetation has a patchy distribution as shown by a case study on the relatively longest-necked sauropod, *Mamenchisaurus* [125]. Therefore, there is strong support for the hypothesis that the long neck of sauropods provided a major energetic and thus selective advantage in feeding efficiency.

While both an erect and a horizontal neck convey major energetic advantages, the crucial question of neck flexibility is still surrounded by controversy [111,123,124], exemplified by papers in this collection [125,127] and another recent one [136]. The flexibility of the neck, which particularly in the low-browsing posture determines whether the animal can browse on a volume or only a large surface area, with the obvious implications for feeding efficiency. Neck flexibility was constrained by the long cervical ribs in most sauropods except diplodocoids. Diplodocoid sauropods had evolutionarily reduced the long posterior process of the cervical ribs so that they do not extend across intervertebral joints, which would have increased neck flexibility [111,112,125,137,138].

Virtual articulation of neck vertebrae and simplified models suggests that sauropod necks were held largely horizontally and may not have been flexible enough to cover a volume but only a surface [123,124]. Similarly, physical articulation of a *Mamenchisaurus* neck and optimization of intervertebral articular surface pressure indicate a horizontal posture and partitioning of flexibility along the vertebral column, with a relatively stiff middle neck region [123,124,125]. However, the same methodological approach concludes that basal marconarians held their necks at a steep angle [123,124,125].

A full understanding of sauropod neck posture and flexibility is hampered by the need to reconstruct the thickness of the cartilage covering the intervertebral joints and the zygapophyses [127,136]. With mammals and crocodiles generally having thicker cartilage than birds, the choice of either of these extant taxa for comparison results in either a more flexible or less flexible neck. Evidence from successive sauropod neck vertebrae fossilized in articulation suggests relatively thick cartilage covers and thus flexible necks

[127]. The discrepancy in the results of these studies [112, 123,124,125,127] make sensitivity analyses of neck posture advisable, quantifying the effect of different hypothetical cartilage covers on flexibility and resulting feeding volume. Also, more necks preserved *in situ* should be studied to address the issue of joint cartilage thickness. In addition, a new study on ostrich neck flexibility [136] reveals the influence of soft tissue, particularly musculature. In the ostrich, this places greater limits on flexibility than the cervical vertebrae and cartilage alone, suggesting that sauropod necks were less flexible than previously hypothesized and that the animals accordingly had to change their feeding station more often, diminishing the energetic advantage of the long neck.

Feedback loop. Reduced vulnerability

Long necks, particularly when their flexibility was limited by cervical ribs [112,125,137], would seem to be vulnerable to predator attack and thus be selected against. However, evolutionary increase in body size in adult sauropods beyond the prey spectrum of even the largest theropods would represent an active feedback loop in which the long neck allows larger body sizes, which in turn decreases neck vulnerability [128].

Trait (new, inferred). Posterior shift of neck muscles

The importance of the long neck for sauropod gigantism is emphasized by a new trait (inferred), the posterior shift of neck muscles, also observed in extant birds [139]. Already basal sauropodomorphs such as *Plateosaurus* have greatly elongated cervical ribs, extending backwards from the vertebra over two intervertebral joints. Such posteriorly elongated cervical ribs are present in most sauropods, reaching lengths of up to 340 cm [111], with only diplodocoids having short neck ribs (see above). The long ossified cervical ribs of most sauropods suggest a great posterior shift of the hypaxial muscles that attached to them [111,137].

These muscles either belong to the *m. longus colli* group based on the homology with birds [111,137,139], or alternatively, the muscles belong to the *m. scaleni* group based on the homology with crocodiles [112]. Torsion would have been important in the sauropod neck as soon as it was moved laterally, and contralateral activation of these muscles would have efficiently counteracted torsional forces, as it does in modern crocodiles during their “death roll” behavior [112]. Torsional forces would have been particularly pronounced during the lateral movement of a horizontally held neck, consistent with the extreme development of cervical ribs in *Mamenchisaurus* [125]. The torsion hypothesis could be tested by studying long-necked-birds that hold their necks horizontally during flight.

Selective Advantage. Lightens the neck

Among several beneficial effects of having long ossified cervical ribs [111,112], the lightening of the neck by moving heavy muscle mass backwards [111,137] appears particularly relevant in the context of gigantism. This selective advantage acted in concert with the lightening of the neck through diverticula of the respiratory system (see below). Lightening of the neck probably was one of the contributing factors that facilitated the uniquely elongated neck of sauropod dinosaurs.

Cascade “Respiration” (Fig. 7)

Trait (inferred). Avian-style lung

In recent years, an avian-style respiratory system (ARS, “avian-style lung” in the figures) has become the consensus inference in the respiratory biology of saurischian dinosaurs, including sauropodomorphs [2,140,141]. The components of such a system (unidirectional airflow, postcranial pneumaticity, air sacs, and countercurrent gas exchange) do not necessarily depend on each other and could have evolved separately and at different times

[142]. Observable evidence, as osteological correlate observed in extant birds, for an ARS is postcranial skeletal pneumaticity (PSP), which now has been traced to the base of Saurischia [37,142] or even to the base of Archosauria [143], obviating the need for hypothesizing its independent evolution in Sauropodomorpha and Theropoda. Among Sauropoda, specific patterns of PSP, namely the pneumatic hiatus in some neosauropods, is an osteological correlate for thoracic air sacs [144]. In addition, cryptic diverticula (in the sense that they do not leave a trace on the skeleton) probably were widespread in sauropods if not in dinosaurs and ornithomirans in general [144]. Extrem PSP, affecting the distal tail and both limb girdles, was recently described in advanced titanosaurs [144,145]. Evidence for dorsally attached parts of the lung is also seen in the dorsal vertebral column [140]. Unidirectional airflow, long believed to be unique to birds, has now been documented for living crocodiles as well [142,146]. Extant phylogenetic bracketing thus would indicate its presence in dinosaurs, including sauropods.

The notion [142] that unidirectional airflow may not be an adaptation to a high BMR because crocodiles have a low BMR is flawed, because the low BMR of crocodylians is likely secondarily derived. The evidence is found in crocodile heart anatomy [147] and in the bone histology of fossil archosaurs that documents a decrease in growth rate from basal crocodile-line archosaurs to crown group crocodiles [148]. In addition, the crocodylian lung “appears overdesigned” [140] for an ectothermic animal. Thus, the combination of high BMR and unidirectional airflow may have been plesiomorphic for archosaurs, with further elaboration of the ARS along the line to birds [140,143,147,149]. This elaboration may well have included a refined counter-current gas exchange system that would have suited the needs of sauropod dinosaurs well [140]. In conclusion, although the sauropod respiratory apparatus may not have been fully homologous to that of birds, its function and advantages must have been very similar.

Selective advantage. Lightens the neck

Among the four major selective advantages of an ARS for sauropods, the least obvious but possibly the most important is the effect of the ARS on neck mass. While a light-weight neck would be advantageous at any size, the long, predominantly horizontal neck of large sauropods could only evolve because of PSP, a corollary of an ARS. This statement presumably applies to long-necked extant birds, long-necked non-avian theropods, and long-necked pterosaurs as well, although this has not been explored in the literature before. The crucial aspect is the development of diverticula of the respiratory tract that invade the medullary region of individual vertebrae. In non-pneumatized bones, this region is filled with bone marrow, but in pneumatized bones it is filled with air.

Pneumatization does not result in a decrease in the mass of the bone tissue *per se*, only in the replacement of bone marrow by air. A pneumatized vertebra thus is lighter than a non-pneumatized one, despite both having the same amount of bone tissue. Statements found even in the most recent literature that “cervical airsacs and extensive cervical diverticula ... would also have served to lighten long necks” [111] are not quite to the point in this regard, because it is only the cervical diverticula that lighten the neck, not the cervical airsacs. The diverticula lighten the neck by bringing air into the interior of the neck vertebrae and thus replacing heavy water-rich tissue, i.e., bone marrow, with air. Cervical airsacs exterior to the vertebrae would not have lightened the sauropod neck, they only would have increased its volume without increasing its mass. Current estimates of the specific

density of sauropod necks are commonly less than 0.5 [111], based on observed densities of bird necks [111].

In non-avian theropod dinosaurs, the hypothesis that PSP evolved to lighten the skeleton was tested recently [149], and increasing PSP was found to be linked to increasing body mass, corroborating the hypothesis. In sauropods, quantitative tests have not been performed yet, but support is found in the ontogenetic increase in PSP [144]. In light of its importance in the evolution of bird-line archosaurs, PSP deserves further study in extant birds, particularly in regard to its influence on body mass and density.

Selective advantage. No dead space problem

The respiratory dead space problem is familiar to human divers and refers to the interdependency of lung volume and tracheal length. If tracheal length is artificially increased (e.g., by a snorkel), tracheal volume may reach a limit where it takes up such a large part of the tidal volume that an insufficient volume of fresh air reaches the lung. The dead space problem affects long-necked animals as well. To avoid the dead space problem, a long neck appears only possible if the non-tracheal ventilated parts of the respiratory system (lungs, air sacs) have a volume that is an order of magnitude larger than that of the trachea. Since the amniote trachea is at least as long as the neck and requires a certain minimum diameter, the long necks of sauropods meant that the non-tracheal ventilated parts of their respiratory system must have been very voluminous [111,140]. Taylor & Wedel [111] note that sperm whales may have a trachea that is over half of their body length, questioning the importance of the dead space problem for the evolution of a long neck. However, whales as intermittent aquatic breathers may not offer a useful comparative perspective on sauropods, and work on the dead space problem in terrestrial long-necked amniotes is needed.

Selective advantage. Continuous oxygen uptake

An unquestionable selective advantage of an ARS is continuous oxygen uptake, as in birds but unlike in mammals, in which oxygen is only extracted during the inhalation part of the breathing cycle. Since the discovery of unidirectional airflow in crocodiles [112,116], continuous oxygen uptake is present in the extant phylogenetic bracket of sauropods and thus very likely was present in sauropods as well. However, the energetic advantage provided by continuous oxygen uptake compared to inhalation-only uptake still needs to be estimated for sauropods in order to assess the importance of this selective advantage. In extant amniotes, respiration takes up the largest part of the energy budget at rest [150], suggesting that continuous oxygen uptake may confer an important selective advantage, although this needs to be explored further in comparative studies of mammals and birds.

Cascade “Metabolism” (Fig. 8)

Trait (inferred). High BMR

The inferred trait of a high basal metabolic rate (BMR) in sauropods has found additional support by studies published since 2009, but some evidence to the contrary has also emerged.

Comprehensive sampling of ungulate long bone histology, both in terms of taxonomic diversity and of habitat and climate zone [151], revealed the ubiquity of lines of arrested growth in this mammal group, invalidating earlier arguments [152] that the lack of LAGs in mammals *versus* their presence in non-avian dinosaurs indicates different thermophysiology in the two groups. Improved understanding of the primary bone formation in extant tetrapods led to a refined view of the evidence for high growth rates of sauropod dinosaurs provided by bone histology [153]. Taken at face value, the unusually high density of osteocyte lacunae in sauropodomorphs [154] would suggest a BMR

significantly higher than in any other tetrapod group, but this is inconsistent with all other evidence discussed in this section for sauropod BMR having been at the mammalian level or lower. The high osteocyte lacunae density does, however, underscore the uniqueness of this evolutionary lineage. At the microanatomical level, femora of dinosaurs offer additional evidence for a high BMR (“activity metabolism” [155]) in the large nutrient foramina that enter the bone at midshaft: nutrient foramina of extant endotherms (mammals) were significantly larger than those of ectotherms (non-varanid reptiles) because of the lower blood flow to the tissues inside the bone. Non-avian dinosaurs all have large nutrient foramina and the highest estimated blood flow rates to their bone interior among the groups studied [155].

A high BMR requires integumentary insulation structures (hair, feather), at least in small animals. A well preserved small theropod fossil from the Jurassic of Germany [156] now indicates that such integumentary structures were already present in rather basal theropods, narrowing the gap in the fossil record between the integumentary insulating structures occasionally preserved in ornithischian dinosaurs on one hand and feathers on the other [156], making it likely that all dinosaurs, including sauropods, bore such structures, at least as juveniles.

Finally, while research on stable isotopes has long contributed to the endothermy/ectothermy debate, the limitation of this approach remains its proxy nature [157], only indicating temperature of hard tissue formation, not BMR. The new clumped isotope thermometry [157] is a case in point, indicating body temperatures at the endothermic level for sauropods, but these could have resulted from thermal inertia (“gigantothermy, mass homeothermy”) as well. Thermal inertia, however, would not have supported the active lifestyle of sauropods and other dinosaurs that is indicated by their upright stance (see below), because a new study on large crocodiles indicates that their power output is an order of magnitude less than that of similar-sized mammals [158].

Body temperatures can also be calculated from maximum growth rates [159,160]. These studies suggest that in dinosaurs, unlike in crocodiles, body temperature did not increase with body mass, inconsistent with thermal inertia or mass homeothermy. In fact, these studies [159,160] infer a body temperature decrease with increasing body mass for sauropods, suggesting that they had an efficient cooling system to prevent overheating [160]. Absolute body temperatures in sauropods calculated from maximum growth rates are lower than expected for a similar-sized mammal, possibly indicating a lower BMR [160], but still relatively high.

While there is thus strong evidence that sauropod dinosaurs had a BMR at least in the lower range of large mammals but possibly higher, a new study on growth rates [150], discussed below, questions this conclusion.

Feedback loop. Low mass-specific metabolic rate

The negative allometry of BMR with body mass (see [100,161,162] for a discussion of this scaling relationship) means that larger animals need to take up less energy per unit body mass to enjoy the benefits of a high BMR. This effect represents a feedback loop from the trait “Very large body mass” to the trait “High BMR”.

Feedback loop. Heat loss through long neck

A classical argument against a high BMR in sauropods has been the overheating problem faced by very large endothermic animals because of their poor surface to volume ratio. This would have limited the surface area through which the excess heat generated by the animal could have been dumped via radiative and convective heat loss [163,164]. Mechanisms such as the active control of blood flow from the body core to the body surface, as

observed in crocodiles [165], auxiliary integumentary features such as the African elephant's large ears, and nocturnal loss of heat stored during the day [164] are difficult to reconstruct for sauropods. However, the unique sauropod body plan with the long neck and long tail had a more favorable surface to volume ratio than a sauropod-sized elephant or rhino. In particular, positive allometric scaling of neck surface area with basal metabolic rate is consistent with a heat loss function of the neck [126].

A long neck also plays a role in heat loss through an avian-style respiratory system, as discussed below [166]. The long neck was thus part of a positive feedback loop, in which it supported the high BMR of sauropods through its role in thermoregulation (Fig. 8).

Selective advantage. Heat loss through ARS

In the ECM, heat loss is also hypothesized to have been a selective advantage of an ARS beyond its other roles in facilitating the long neck of sauropods. Thus, an ARS and a long neck would have acted in concert in the dumping excess heat (Fig. 8).

The respiratory system of extant birds is well known to function in body temperature control, raising the question whether this function was served by the ARS hypothesized for sauropods [140,141]. A novel modeling approach, computational fluid dynamics (CFD), can be used to assess the function of the ARS in heat loss [166]. A two-dimensional CFD model of heat exchange in the trachea and air sacs of domestic chicken was used to validate the method [166]. A three-dimensional CFD simulation of the respiratory tract of a sauropod would serve to test the hypothesis.

Selective advantage. Fast conversion of energy from environment

No new studies relevant to sauropod gigantism have been published that address the selective advantage of a high BMR, i.e., the fast conversion of energy from the environment, which in turn appears necessary for high growth rates. However, this fast conversion of energy from the environment is implicit in the most widely accepted hypothesis of the origin of endothermy, the aerobic scope hypothesis [167].

Trait. High growth rate

Unlike a high BMR, which must be inferred, growth rates can be calculated in non-avian dinosaurs based on growth marks in their long bones. While growth rates have been well constrained in theropods and ornithischian dinosaurs [168,169,170], sauropod growth rates have been difficult to estimate [171], and seemingly inflated growth rates of >5000 kg per year continue to be perpetuated even in the most recent literature [34,150,171]. A global view of dinosaur growth rates, using local tissue apposition rates as proxy, suggests that growth rates an order of magnitude higher than in living reptiles evolved in early dinosaurs and remained high throughout the group [148]. The important question regarding the trait “High growth rate” is comparative, i.e., how do sauropod growth rates compare to those of living reptiles, mammals, and birds.

A first set of comparative data for growth rates in non-titanosaurian sauropods based on long bone histology is now available [89], and a single but well constrained data point was derived from growth marks in ribs [172]. These studies indicate that non-titanosaurian sauropod growth rates were in the realm of scaled-up modern ratite birds and mammalian megaherbivores, but were lower than the average mammal [89]. Titanosaur growth rates still have defied quantification, but qualitative evidence from long bone histology (i.e., modified laminar bone) suggests a phylogenetic reduction in growth rates in many smaller titanosaurs [173,174], albeit not accompanied by a reduction in BMR [173,174].

In general, growth rate data for sauropods remain more poorly constrained than for any other dinosaur group that has been sampled histologically to any extent because of the rarity and poor development of growth marks in sauropod long bones [173,174]. Growth rate estimates based on the growth mark record thus probably represent minimum growth rates [171].

The link between maximum growth rate (MGR) and BMR in vertebrates was first explored by Case [90], who calculated regression lines for major extant vertebrate groups and noted that terrestrial endotherms (mammals and birds) have an order of magnitude higher MGRs than ectothermic amniotes. Surprisingly, this link between MGR and BMR has received little attention since, not even from the perspective of the metabolic theory of ecology. In a new study, Clarke [150] compared dinosaurian MGR with those of extant mammals and reptiles, using the dataset of Case [141]. The regression for dinosaur growth rates, including those of sauropods, was intermediate between those for mammals and reptiles. Clarke [150] then entered the comparative data on growth rates into a model of the energy budget of various dinosaurs and concluded that most of the observed growth rates could have been achieved with a reptilian energy budget and BMR, concluding that this evidence made a high BMR in non-avian dinosaurs unlikely.

There are several points in the approach of Clarke [150] that require modification and further work, if it is to serve as a test of the trait “High growth rate”. For one, the Case dataset [90] is not up to date and could be replaced by a current one, which is available in the literature. Also, there are no large fast-growing non-avian reptiles, placing the data points for all sauropodomorphs outside the point cloud for non-avian reptiles, and a separate comparison of sauropodomorphs and mammals should be done. Finally, as already noted, current estimates of sauropod growth rates probably underestimate true rates considerably. Nevertheless, a certain contradiction remains between the evidence for high growth rates from bone histology [148,171] and lower growth rates from modeling of growth [160] and energy budget [150]. The influence of parental energy transfer on MGR remains poorly understood as well and should be studied in extant animals. Any kind of parental care, even simple guarding behavior, represents an energy transfer from parent to offspring, increasing offspring growth rate. With sauropods presumably lacking any form of parental care (see above), their offspring was fully autonomous, possibly limiting its growth rate as well as our ability to predict BMR from MGR.

In conclusion, the trait “High growth rate” in the evolutionary cascade has not been falsified because all studies agree that sauropod MGR experienced a manifold evolutionary increase compared to their closest living and non-dinosaurian extinct relatives.

Selective advantage. High likelihood to survive to adult stage

Independent of the necessity of a high BMR to achieve fast growth, the selective advantage of a high growth rate appears clear. Especially in animals that, like no other amniote, had an extreme size difference between embryo and adult [12,14,52], fast growth to survive to adulthood would have been of great selective advantage, considering the formidable predation pressure faced by juvenile sauropods. Such fast growth has recently been detected in embryos of the basal sauropodomorph *Lufengosaurus* [175] and has been suggested to indicate extremely fast growth in the hatchlings as well [175]. This selective advantage would be easy to test in extant animals, and tests may well be already contained in the zoological literature.

Trait. Upright stance

All large extant terrestrial tetrapods with a high BMR have an upright stance [132]. This limb posture is required for the energy-efficient mode of parasagittal locomotion in which the limbs function according to the principle of the inverted pendulum [104]. An upright stance is a derived character at the level of Dinosauria, and the upright stance was a prerequisite for sauropod gigantism not only because it preceded the graviportal stance of sauropods [176,177,178,179] but because of its link with a high BMR. Parasagittal locomotion is necessary for large animals with a high BMR to acquire enough energy from their environment to support this high BMR which, in turn, allows continuous locomotion. Thus, the causation and its direction in these two traits is not sufficiently understood (Fig. 8).

Selective advantage. Energy-efficient locomotion

Energy-efficient locomotion as a selective advantage resulting from the upright stance was discussed above, but the question could be asked whether sauropods were more efficient locomotors than extant graviportal mammals and other graviportal dinosaurs. Locomotion in sauropods can be understood from two independent and complementary lines of evidence: their skeletons and their rich track record. More efficient locomotion has not figured in previous hypotheses about sauropod gigantism, but further considerations are in order. Specifically, can we formulate hypotheses that posit that any aspect of the locomotory apparatus and locomotion facilitated the unique gigantism of sauropod dinosaurs? In particular, are there any scaling factors in locomotion that would favor larger body size over smaller body size? Negative allometry of the cost of transportation might be one such factor but it could not be detected in the study by Preuschoft et al. [128].

Future research concerning the hypothesis of “energy-efficient locomotion” could be based on quantitative biomechanical models, but it will require an improved understanding of sauropod gaits. These have not been reliably reconstructed, neither from models nor from theoretical considerations [128]. The latter study [128] excluded all gaits with a suspended phase and all asymmetrical gaits. Current quantitative research on sauropod footprints using different approaches may improve this situation [78,180,181]. Such research also needs to include studies on extant animals with an upright stance with the aim of reconstructing gaits from trackways (e.g., [182]). Good starting points would be horses and elephants.

Discussion

Revised ECM for Sauropod Gigantism

The remarkable amount of evidence that has accumulated over the last few years, and that is the focus of this collection, considerably refines the evolutionary cascade model of sauropod gigantism proposed by Sander et al. in 2010 [2] by testing many of its components. The ECM has become more complex with the splitting of cascades, the addition of traits, and the addition of links between cascades, i.e., selective advantages and feedback loops (Fig. 9). Many of the inferred traits and hypothesized selective advantages have found support. A minority were falsified or at least called into question, without affecting the overall picture, however.

Compared to the 2010 ECM, the cascade “Reproduction” has been refined by splitting the basal trait “Many small offspring” into three different traits and by adding a subcascade that takes into account the ecological effects of the body size difference between hatchlings and adults (Fig. 4). The cascade now appears to be better supported than ever since its origin in the work of Janis & Carrano [49].

The original cascade “Feeding, Head, Neck” has also been split into two cascades, “Feeding” (Fig. 5) and “Head and neck” (Fig. 6) that are linked to each other in the trait “No mastication”. New evidence supports all traits in the cascade, including the lack of a gastric mill. However, while the hypothesis that mastication limits food intake rate has received further support, the same limitation may not apply to a gastric mill, contrary to the original ECM. One aspect of the feedback loop “Large gut capacity”, i.e., the positive scaling of food retention time with body mass (“Jarman-Bell Principle”) may not hold up [100]. This research offers an example of how work on sauropod dinosaurs can question long held views on the biology of extant animals.

The cascade “Head and neck” (Fig. 6) probably has received the most attention because researchers have come to fully appreciate the central importance of the neck in sauropod biology and evolution. New modeling approaches and a refined understanding of neck anatomy (e.g., the function of cervical ribs) have strengthened and refined this cascade, leading to the addition of the inferred trait “Posterior shift of muscle bulges” and the selective advantage of “Lightening the neck” (Fig. 6). Similarly, the cascade “Avian-style lung” has been strengthened by further evidence but without experiencing modifications (Fig. 7).

The cascade “High BMR” was amended by adding “Upright stance” as an observed trait and “Efficient locomotion” as the selective advantage (Fig. 8). Much new evidence in support of this cascade has accumulated and hypothetical selective advantages have been tested, but there is also contradictory evidence. Specifically, the trait “High growth rate” has been called into question by growth rates calculated from bone histology, while at the same time other evidence from bone histology strengthens the case for fast growth in sauropods at the mammalian level (Fig. 8). In addition, the trait “High growth rate” is important for the trait “Fast population recovery”, which had been recognized before [2] but not visualized in the original sauropod gigantism ECM.

Status of the ECM and future improvements

The ECM for sauropod gigantism is of heuristic value for explaining the unique body size of sauropod dinosaurs and the limits to body size in terrestrial amniotes in general. However, the ECM currently does not provide information about the relative contribution of the component cascades and their basal traits to gigantism (see also [2]) and if any of the traits were a necessity for sauropod gigantism. Thus, we do not know whether ovipary was more important than a high BMR or than the lack of mastication (see also the ternary diagram in Sander et al. [2]). One way to improve this situation would be to take the energetic approach to sauropod gigantism [2] to its logical conclusion by modeling the energy budget of a living sauropod dinosaur, following the approach of Clarke [150]. This is suggested by the observation that four of the cascades indicate an energetic advantage as an explanation for gigantism. The other way of testing the ECM will be to bring a phylogenetic approach to it, including character optimization, character correlation analyses, and phylogenetic comparative methods. By comparing the presence or absence of these traits in other terrestrial amniotes with their maximum body size, we can estimate the relative importance of traits, but without quantification [2]. The revised ECM allows a refined understanding of body size limits in other terrestrial amniotes beyond the discussion in Sander et al. [2].

Limits to terrestrial amniote body size

This discussion of the limits to body size is restricted to terrestrial amniotes here because so many parameters are different in the marine realm (trophic structures, cost of transport, heat

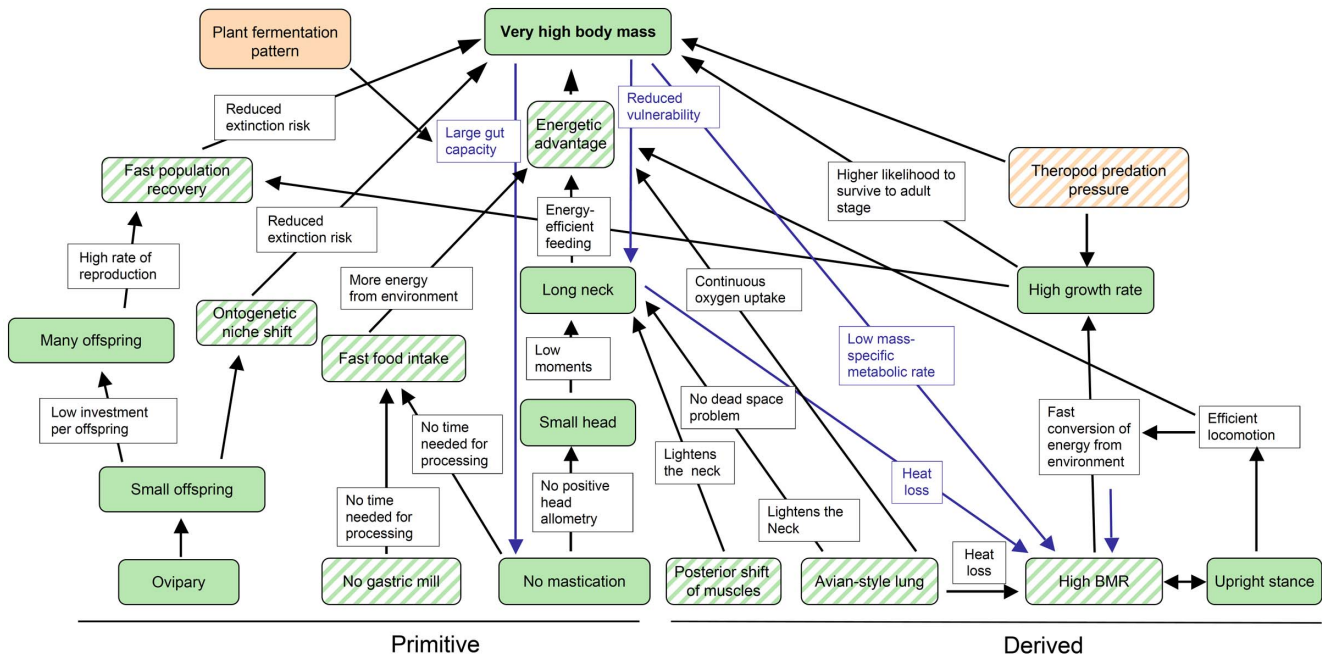


Figure 9. Revised ECM for sauropod gigantism. Conventions used are the same as in Fig. 1, except that a distinction is made between observed traits and premises (solid color) and inferred traits or premises (oblique stripes). Compared to the original ECM (Fig. 1), complexity has increased considerably as has integration, with each cascade being connected with at least one other cascade. Note the central position of the cascade “Head and neck” and the many arrows pointing at the traits “Long neck” and “Energetic advantage”. See text for further explanations. doi:10.1371/journal.pone.0078573.g009

conduction of medium, etc.) that meaningful comparisons are not obvious. Terrestrial amniotes show the following maximum body size distribution: the largest non-avian reptiles (three clades) and birds are smaller than the largest mammals; these are smaller than the largest theropod and ornithischian dinosaurs, which in turn are smaller than the largest sauropod dinosaurs. Except for non-avian reptiles, the largest (or all) species in these clades are herbivores and are an order of magnitude larger than the largest carnivorous members of their respective clades. In addition, studies of how body size is distributed across the size range of the clade [9,12] shows that sauropods differ from the other clades in that most sauropods are large. Ornithischians show a less pronounced left skew in body size distribution while mammals and birds show a strong right skew [9]. However, these studies [9,12] may suffer from the difficulty of comparability of the clades involved.

A number of factors can be identified limiting body size based on recent research and the ECM (Table 1), but a few invite further comments. The limit to body size in sauropods may well have been set by the design of the tetrapod skeleton in combination with the scaling of muscle power to body mass.

Mastication-induced positive head allometry, as predicted by scaling principles, is documented for ornithischian dinosaurs by a recent study of ontogenetic changes in the skull of a hadrosaur species [114]. The strongly positive snout allometry in this dinosaur is consistent with hadrosaurs being highly efficient chewers as shown by the complexity of their dental tissues [183].

The question of why no multi-tonne ground birds evolved in the early Tertiary after the demise of the non-avian dinosaurs remains prominent [184], considering that birds seem to show all of the traits in the revised sauropod gigantism ECM in which a gastric mill, obligatory in herbivorous birds, is not necessarily seen as limiting food intake rate (see above). Explanations are sought in features of the locomotor system and reproduction of birds that have evolved beyond the state in non-avian dinosaurs [184]. The

most obvious difference is sauropod graviportal quadrupedality vs. bird bipedality. In addition, bird hind leg posture and musculature differ from non-avian dinosaurs in that the femur is held subhorizontally, and the retraction of the leg is mainly achieved in the knee joint [178,185]. Reproduction of avian dinosaurs includes brooding and parental care, features that evolved in the most derived non-avian dinosaurs [186]. These led to a different scaling of egg size with body mass in birds [71] than

Table 1. Factors limiting body size in terrestrial herbivorous amniotes.

Sauropoda:
- Scaling of locomotory muscle power with body mass [189]
Ornithischia:
- Mastication, limiting food intake rate and neck length [100]
- Possible lack of internal respiratory cooling capabilities [166]
Mammalia:
- Mastication, limiting food intake rate and neck length [100]
- Lack of internal respiratory cooling capabilities [166]
- Reproductive output [14]
Reptilia (non-dinosaurian):
- Low BMR and low growth rate [2,14]
Aves:
- Parental care combined with ovipary [71]
- Possibly hindleg design [186]

Taxa are arranged in order of decreasing maximum size and increasing right skew of body size distribution. References are to the most recent papers only. doi:10.1371/journal.pone.0078573.t001

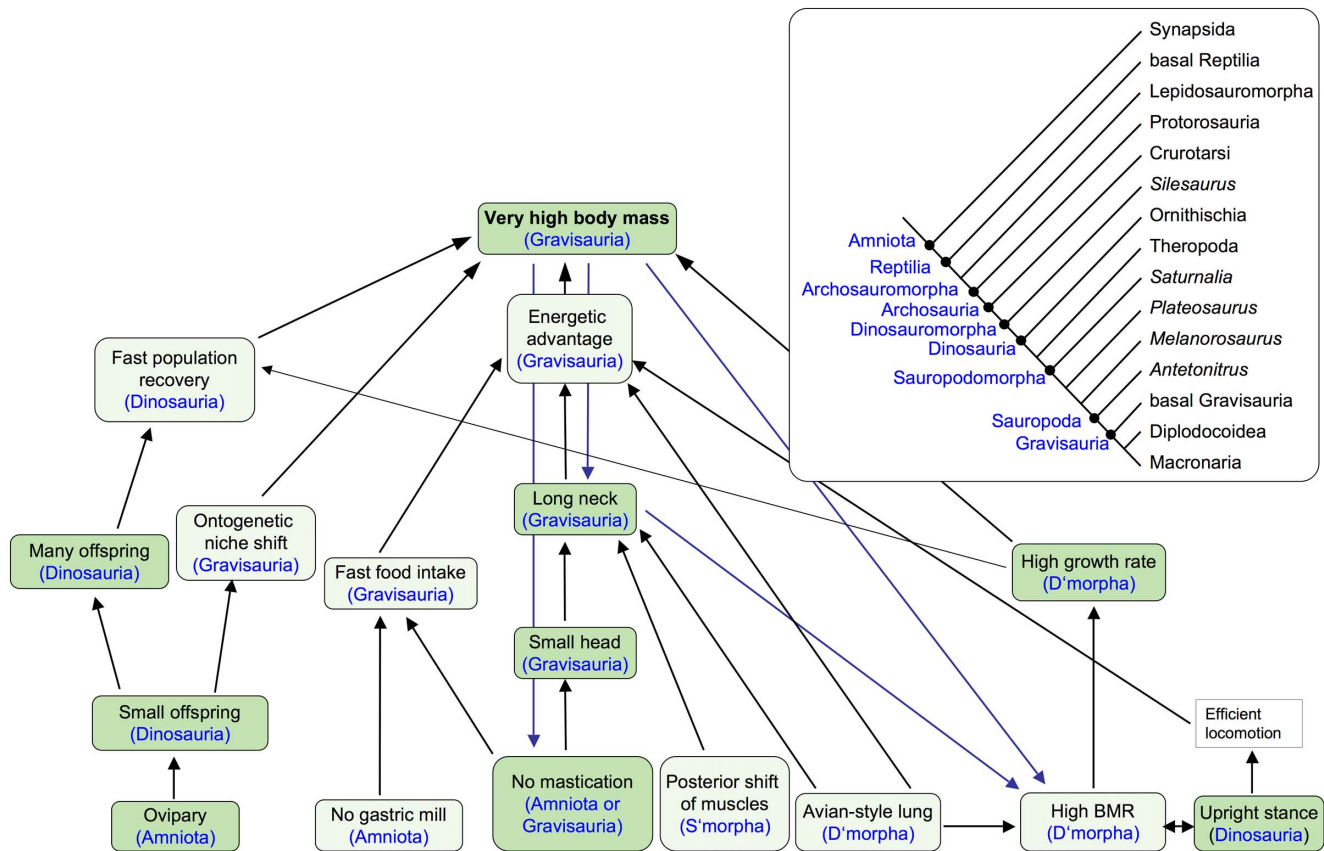


Figure 10. Phylogenetic distribution of traits in the sauropod gigantism ECM. For each trait in the model, the likely inclusive taxon in which the trait evolved is indicated. Note that Gravisauria is the taxon in which most of the classical sauropod traits appear. Darker green traits are observed, lighter green traits are inferred. Black arrows indicate evolutionary causation and blue arrows indicate feedback loops.
doi:10.1371/journal.pone.0078573.g010

in less derived dinosaurs, meaning that the upper limit of egg size apparently was reached in birds at a body mass of less than 1000 kg [71]. Body size of other extant oviparous amniotes such as turtles, lepidosaurs, and crocodiles apparently was not limited by their mode of reproduction but by a low metabolic rate [2,14].

As shown by this example of birds and extant non-avian reptiles, but also by the many other taxa and traits in Table 1, the evolution of maximal body size is often constrained by historical contingency. Traits that were highly adaptive for a lineage at small body size constrained maximum body size of the lineage later in its evolution. Only by taking the comparative approach to as many extinct and extant lineages as possible, these constraints can be understood. The study of dinosaur gigantism thus becomes a research program of general relevance in vertebrate evolutionary biology. Note that the sauropod gigantism ECM thus makes predictions about the future evolution of lineages, such as that mammals are unlikely to ever evolve the body size of sauropod dinosaurs.

Beyond the notion that some in the ECM are plesiomorphic and some are derived, the question can now be addressed of when the basal traits of each cascade arose in the phylogeny and how this coincides with body size increase. As noted earlier, it will be difficult to bring these two datasets into perfect congruency because of the difficulty of plotting the largest sauropodomorph remains from any time bin onto the phylogeny. While the traits “Ovipary”, “No gastric mill”, and “No mastication” are plesiomorphic for amniotes (Fig. 10), the avian-style lung probably evolved at the base of Dinosauria [37]. The trait “High BMR”

also evolved at the base of Dinosauria [148]. The trait “Posterior shift of muscles” in the neck was present in basal sauropodomorphs such as *Plateosaurus*, as evidenced by greatly elongated cervical ribs and their histology [112]. Greatly elongated neck ribs together with neck elongation by elongation of individual vertebrae is already seen in basal archosauromorphs such as the Late Permian *Protorosaurus* [187], but the evolution of neck ribs in archosauromorphs has not been documented in sufficient detail to exclude convergent evolution. The other traits in the ECM (Fig. 10) can also be mapped on the sauropodomorph cladogram, although this aspect of the ECM requires additional research.

Optimizing traits from the ECM onto a phylogeny that includes all the terminal taxa which exhibit the trait will be a fruitful avenue to explore. The ultimate test of the importance of the presumed factors in the evolution of amniote body size would be to test their contribution to body size across amniotes, using phylogenetic comparative methods.

Conclusions

This review of the biology of the sauropod dinosaurs and the evolution of their gigantism, condensed into the sauropod gigantism ECM, serves to compile and synthesize the rapidly expanding literature on the subject, including this collection in PLoS ONE. It also serves as an update to an earlier review [2] in which the evidence available in late 2009 was synthesized into a unified biological scenario of sauropod gigantism, using the approach of an evolutionary cascade model. Testing the premise

that it is mainly intrinsic factors rooted in the biology of the clade Sauropodomorpha that explains the historical pattern of its evolution to gigantic body size, was not the aim of this review. However, the evidence reviewed here shows at least that there is no need to invoke extrinsic, abiological factors to explain sauropod gigantism. Testing the influence of environmental change over geological time scales on the historic pattern of evolution is a valid research program, but it is not the one we pursue.

The rich new evidence accumulated in these last four years was then used to test the ECM by asking how this evidence impacted the component cascades and the entire ECM. Most of the inferred traits, selective advantages, and feedback loops in the ECM found support, sometimes strongly so, while in a few others (e.g. “High growth rate”) support weakened or relationships had to be rejected (the physiological underpinning of the feedback loop “Large gut capacity”). The ECM was also refined by splitting up traits and adding new ones. The general conclusion of Sander & Clauss [1] and Sander et al. [2] that sauropod gigantism was able to evolve because of the complex interplay of a historically contingent combination of plesiomorphic (primitive) and derived traits and characters, has emerged stronger than before. While the principle of parsimony calls for preference of simple solutions over complex ones, it is simplistic to assume that a single factor will explain

sauropod gigantism. Finally, the sauropod gigantism ECM is hoped to evolve into a comprehensive framework informing us about evolutionary body size limits in herbivorous tetrapods in particular and other terrestrial tetrapods in general.

Acknowledgments

First and foremost, I would like to thank the members of DFG Research Unit 533 for ten years of extremely fruitful intellectual interchange about sauropod gigantism. I also owe gratitude to the participants of the Second International Workshop on Sauropod Gigantism for interesting discussions and the open exchange of ideas and for accepting my invitation to submit a manuscript to the PLoS Sauropod Gigantism collection. The interaction with and questions by many science journalists and exhibition designers made me look at the big picture. Kayleigh Wiersma (Bonn) helped with editing this manuscript, and Sashima Läbe (Bonn) improved Fig. 3. Funding by the German Science Foundation (DFG) is gratefully acknowledged. This is contribution number 146 of DFG Research Unit 533 “Biology of the Sauropod Dinosaurs: The Evolution of Gigantism”.

Author Contributions

Conceived and designed the experiments: PMS. Performed the experiments: PMS. Analyzed the data: PMS. Contributed reagents/materials/analysis tools: PMS. Wrote the paper: PMS.

References

- Sander PM, Clauss M (2008) Sauropod gigantism. *Science* 322: 200–201.
- Sander PM, Christian A, Clauss M, Fechner R, Gee CT, et al. (2011) Biology of the sauropod dinosaurs: the evolution of gigantism. *Biological Reviews* 86: 117–155.
- Klein N, Remes K, Gee CT, Sander PM (2011) *Biology of the Sauropod Dinosaurs: Understanding the Life of Giants*. Bloomington: Indiana University Press.
- Mannion PD, Upchurch P, Carrano MT, Barrett PM (2011) Testing the effect of the rock record on diversity: a multidisciplinary approach to elucidating the generic richness of sauropodomorph dinosaurs through time. *Biological Reviews* 86: 157–181.
- Benson RBJ, Mannion PD, Butler RJ, Upchurch P, Goswami A, et al. (2013) Cretaceous tetrapod fossil record sampling and faunal turnover: implications for biogeography and the rise of modern clades. *Palaeogeography, Palaeoclimatology, Palaeoecology* 372: 88–107.
- Curry Rogers K, Wilson JA (2005) *The Sauropods. Evolution and Paleobiology*. Berkeley: University of California Press. 358.
- Tidwell V, Carpenter K (2005) *Thunder-Lizards. The Sauropodomorph Dinosaurs*. Bloomington and Indianapolis: Indiana University Press. 495.
- Wilson JA (2002) Sauropod dinosaur phylogeny: critique and cladistic analysis. *Zoological Journal of the Linnean Society, London* 136: 217–276.
- O’Gorman EJ, Hone DWE (2012) Body size distribution of the dinosaurs. *PLoS ONE* 7: e51925.
- Campione NE, Evans DC (2012) A universal scaling relationship between body mass and proximal limb bone dimensions in quadrupedal terrestrial tetrapods. *BMC Biology* 10: 1–22.
- Trammer J (2011) Differences in global biomass and energy use between dinosaurs and mammals. *Acta Geologica Polonica* 61: 125–132.
- Codron D, Carbone C, Müller DWH, Clauss M (2012) Ontogenetic niche shifts in dinosaurs influenced size, diversity and extinction in terrestrial vertebrates. *Biology Letters* 8: 620–623.
- Sookias RB, Benson RBJ, Butler RJ (2012) Biology, not environment, drives major patterns in maximum tetrapod body size through time. *Biology Letters* 1–4.
- Werner J, Griebeler EM (2011) Reproductive biology and its impact on body size: comparative analyses of mammalian, avian and dinosaurian reproduction. *PLoS ONE* 6: e28442.
- Werner J, Griebeler EM (2013) Reproduction in non-avian dinosaurs: linking information from the fossil record and from the allometries of extant close relatives. *PLoS ONE*.
- Westneat DF (2000) Retrospective and prospective look at the role of genetics in mating systems: toward a balanced view of the sexes. In: Apollonio M, Festa-Bianchet M, Mainardi D, *Vertebrate Mating Systems Proceedings of the 14th Course of the International School of Ethology*. Singapore: World Scientific. 253–306.
- Sachs JL, Hollowell AC (2012) The origins of cooperative bacterial communities. *mBio* 3: doi:10.1128/mBio.00099-00012.
- Schwenk K (1995) A utilitarian approach to evolutionary constraint. *Zoology* 89: 251–262.
- Futuyma DJ (2010) Evolutionary constraint and ecological consequences. *Evolution* 64: 1865–1884.
- Kemp TS (2007) The concept of correlated progression as the basis of a model for the evolutionary origin of major new taxa. *Proceedings of the Royal Society B* 274: 1667–1673.
- Zaher H, Pol D, Carvalho AB, Nascimento PM, Riccomini C, et al. (2011) A complete skull of an Early Cretaceous sauropod and the evolution of advanced titanosaurs. *PLoS ONE* 6: e16663.
- Kellner AWA, Rubilar-Rogers D, Vargas A, Suárez M (2011) A new titanosaur sauropod from the Atacama Desert, Chile. *Anais da Academia Brasileira de Ciências* 83: 211–219.
- Mateus O, Jacobs LL, Schulp AS, Polcyn MJ, Tavares TS, et al. (2011) *Angolatitan adamastor*, a new sauropod dinosaur and the first record from Angola. *Anais da Academia Brasileira de Ciências* 83: 221–233.
- Tschopp E, Mateus O (2013) Clavicles, interclavicles, gastralia, and sternal ribs in sauropod dinosaurs: new reports from Diplodocidae and their morphological, functional and evolutionary implications. *Journal of Anatomy* 222: 321–340.
- Mannion PD, Otero A (2012) A reappraisal of the Late Cretaceous Argentinian sauropod dinosaur *Argyrosaurus superbus*, with a description of a new titanosaur genus. *Journal of Vertebrate Paleontology* 32: 614–638.
- Filippi LS, Garcia RA, Garrido AC (2011) A new titanosaur sauropod dinosaur from the Upper Cretaceous of North Patagonia, Argentina. *Acta Palaeontologica Polonica* 56: 505–520.
- Hedrick BP, Tumarkin-Deratzian AR, Dodson P (2013) Bone microstructure and relative age of the holotype specimen of the diplodocoid sauropod dinosaur *Suuwassea emilieae*. *Acta Palaeontologica Polonica*.
- Martinez RN, Sereno PC, Alcober OA, Colombi CE, Renne PR, et al. (2011) A basal dinosaur from the dawn of the dinosaur era in southwestern Pangea. *Science* 331: 207–210.
- Wings O, Schwarz-Wings D, Fowler DW (2011) New sauropod material from the Late Jurassic part of the Shishugou Formation (Junggar Basin, Xinjiang, NW China). *Neues Jahrbuch für Geologie und Paläontologie Abhandlungen* 262: 129–150.
- Redelstorff R, Sander PM, Galtom PM (2013) Unique bone histology in partial large bone shafts from Aust Cliff (England, Upper Triassic): an early independent experiment in gigantism. *Acta Palaeontologica Polonica*.
- Fowler DW, Sullivan RM (2011) The first giant titanosaurian sauropod from the Upper Cretaceous of North America. *Acta Palaeontologica Polonica* 56: 685–690.
- D’Emic MD, Wilson JA, Williamson TE (2012) A sauropod dinosaur pes from the latest Cretaceous of North America and the validity of *Alamosaurus sanjuanensis* (Sauropoda, Titanosauria). *Journal of Vertebrate Paleontology* 31: 1072–1079.
- Carballido JL, Sander PM (2013) Postcranial axial skeleton of *Europasaurus holgeri* (Dinosauria, Sauropoda) from the Upper Jurassic of Germany: implications for sauropod ontogeny and phylogenetic relationships of basal Macronaria. *Journal of Systematic Paleontology*: 1–53.

34. Wilson JA, Curry Rogers K (2012) Sauropoda. In: Holtz TR, Brett-Surman MK, Farlow JO, The Complete Dinosaur. Second Edition. Bloomington: Indiana University Press. 444–481.
35. Cerda IA, Paulina Carabajal A, Salgado L, Coria RA, Reguero MA, et al. (2012) The first record of a sauropod dinosaur from Antarctica. *Naturwissenschaften* 99: 83–87.
36. Yates AM, Bonnan MF, Neveling J, Chinsamy A, Blackbeard MG (2010) A new transitional sauropodomorph dinosaur from the Early Jurassic of South Africa and the evolution of sauropod feeding and quadrupedalism. *Proceedings of the Royal Society B* 277: 787–794.
37. Yates AM, Wedel MJ, Bonnan MF (2012) The early evolution of postcranial skeletal pneumaticity in sauropodomorph dinosaurs. *Acta Palaeontologica Polonica* 57: 85–100.
38. Carballido JL, Rauhut OWM, Pol D, Salgado L (2011) Osteology and phylogenetic relationships of *Tehuelhesaurus benitezii* (Dinosauria, Sauropoda) from the Upper Jurassic of Patagonia. *Zoological Journal of the Linnean Society*, London 163: 605–662.
39. D’Emic MD (2012) The early evolution of titanosauriform sauropod dinosaurs. *Zoological Journal of the Linnean Society*, London 166: 624–671.
40. Mannion P, Upchurch P, Barnes R, Mateus O (2013) Osteology of the Late Jurassic Portuguese sauropod dinosaur *Lusotitan atalaiensis* (Macronaria) and the evolutionary history of basal titanosauriforms. *Zoological Journal of the Linnean Society*, London.
41. Carballido JL, Salgado L, Pol D, Canudo JL, Garrido A (2012) A new basal rebbachisaurid (Sauropoda, Diplodocoidea) from the Early Cretaceous of the Neuquén Group; evolution and biogeography of the group. *Historical Biology* 24: 631–654.
42. Whitlock JA (2011) Inferences of diplodocoid (Sauropoda: Dinosauria) feeding behavior from snout shape and microwear analyses. *PLoS ONE* 6: e18304.
43. Royo-Torres R, Cobos A, Alcalá L (2006) A giant European dinosaur and a new sauropod clade. *Science* 314: 1925–1927.
44. Vila B, Galobart A, Canudo JL, Le Louff J, Dinarès-Turell J, et al. (2012) The diversity of sauropod dinosaurs and their first taxonomic succession from the latest Cretaceous of southwestern Europe: clues to demise and extinction. *Palaeogeography, Palaeoclimatology, Palaeoecology*
45. Brown C, Evans D, Campione N, O’Brien L, Eberth D (2013) Evidence for taphonomic size bias in the Dinosaur Park Formation (Campanian, Alberta), a model Mesozoic terrestrial alluvial-paralic system. *Palaeogeography, Palaeoclimatology, Palaeoecology* 372: 108–122.
46. Brown C, Campione N, Giacomini H, O’Brien L, Vavrek M, et al. (2012) Ecological modelling, size distributions, and taphonomic size bias in dinosaur faunas: a comment on Codron et al. *Biology Letters* 9: 20120582.
47. Codron D, Carbone C, Müller DWH, Clauss M (2012) Ecological modelling, size distributions and taphonomic size bias in dinosaur faunas: reply to Brown et al. *Biology Letters* 9: 20120922.
48. Schulte P, Alegret L, Arenillas I, Arz JA, Barton PJ, et al. (2010) The Chicxulub asteroid impact and mass extinction at the Cretaceous-Paleogene boundary. *Science* 327: 1214–1218.
49. Janis CM, Carrano M (1992) Scaling of reproductive turnover in archosaurs and mammals: why are large terrestrial mammals so rare? *Acta Zoologica Fennica* 28: 201–216.
50. Mannion PD, Upchurch P (2010a) A quantitative analysis of environmental associations in sauropod dinosaurs. *Paleobiology* 36: 253–282.
51. Russell DA (1995) China and the lost worlds of the dinosaurian era. *Historical Biology* 10: 3–12.
52. Codron D, Carbone C, Clauss M (2013) Ecological interactions in dinosaur communities: influences of small offspring and complex ontogenetic life histories. *PLoS ONE* 8.
53. Sander PM, Peitz C, Jackson FD, Chiappe LM (2008) Upper Cretaceous titanosaur nesting sites and their implications for sauropod dinosaur reproductive biology. *Palaeontographica A* 284: 69–107.
54. Griebeler EM, Werner J (2011) The life cycle of sauropod dinosaurs. In: Klein N, Remes K, Gee CT, Sander PM, *Biology of the Sauropod Dinosaurs: Understanding the Life of Giants*. Bloomington and Indianapolis: Indiana University Press. 263–275.
55. Mannion PD, Benson RBJ, Upchurch P, Butler RJ, Carrano MT, et al. (2012) A temperate palaeodiversity peak in Mesozoic dinosaurs and evidence for Late Cretaceous geographical partitioning. *Global Ecology and Biogeography* 21: 898–908.
56. Foster JR (2007) *Jurassic West. The Dinosaurs of the Morrison Formation and their World*. Bloomington: Indiana University Press. 389.
57. Gee CT, Dayvault RD, Tidwell WD, Stockey RA (in press) A remarkable increase in conifer seed and pollen cone biodiversity in the Late Jurassic Morrison Formation, USA. *Palaeobiodiversity and Palaeoenvironments*.
58. Fricke HC, Henceroth J, Hoerner ME (2011) Lowland–upland migration of sauropod dinosaurs during the Late Jurassic epoch. *Nature* 480: 513–515.
59. Farlow JO, Coroian D, Foster JR (2010) Giants on the landscape: modeling the abundance of megaherbivorous dinosaurs of the Morrison Formation (Late Jurassic, western USA). *Historical Biology* 22: 403–429.
60. Midgley JJ, Midgley G, Bond WJ (2002) Why were dinosaurs so large? A food quality hypothesis. *Evolutionary Ecology Research* 4: 1093–1095.
61. Wilkinson DM, Ruxton GD (2011) Understanding selection for long necks in different taxa. *Biological Reviews* 87: 616–630.
62. Carrano MT (2006) Body-size evolution in the Dinosauria. In: Carrano MT, Blob RW, Gaudin T, Wible, J., *Amniote Paleobiology: Perspectives on the Evolution of Mammals, Birds, and Reptiles*. Chicago: University of Chicago Press.
63. Hone DWE, Keesey TM, Pisani D, Purvis A (2005) Macroevolutionary trends in the Dinosauria: Cope’s rule. *Journal of Evolutionary Biology* 18: 587–595.
64. Gould GC, MacFadden BJ (2004) Gigantism, dwarfism, and Cope’s rule: “nothing in evolution makes sense without a phylogeny”. *Bulletin of the American Museum of Natural History* 285: 219–237.
65. Hone DWE, Benton MJ (2005) The evolution of large size: how does Cope’s Rule work? *Trends in Ecology and Evolution* 20: 4–6.
66. Polly PD (1998) Cope’s rule. *Science* 282: 47.
67. Bonner JT (2006) *Why Size Matters: from Bacteria to Blue Whales*. Princeton University Press.
68. Carbone C, Mace G, Roberts S, Macdonald D (1999) Energetic constraints on the diet of terrestrial carnivores. *Nature* 402: 286–288.
69. Owen-Smith RN (1988) Megaherbivores. The Influence of Very Large Body Size on Ecology. Cambridge: Cambridge University Press. 369.
70. Owen-Smith RN, Mills MGL (2008) Predator–prey size relationships in an African large-mammal food web. *Journal of Animal Ecology* 77: 173–183.
71. Birchard G, Deeming D (2009) Avian eggshell thickness: scaling and maximum body mass in birds. *Journal of Zoology* 279: 95–101.
72. Carbone C, Turvey ST, Bielby J (2011) Intra-guild competition and its implications for one of the biggest terrestrial predators, *Tyrannosaurus rex*. *Proceeding of the Royal Society B* 278: 2682–2690.
73. Brusatte SL, Norell MA, Carr TD, Erickson GM, Hutchinson JR, et al. (2010) *Tyrannosaurus* paleobiology: new research on ancient exemplar organisms. *Science* 329: 1481–1485.
74. DePalma RA, Burnham DA, Martin LD, Rothschild BM, Larson PL (2013) Physical evidence of predatory behavior in *Tyrannosaurus rex*. *Proceedings of the National Academy of Sciences, USA*.
75. Horner J, Goodwin M, Myhrvold N (2011) Dinosaur census reveals abundant *Tyrannosaurus* and rare ontogenetic stages in the Upper Cretaceous Hell Creek Formation (Maastrichtian), Montana, USA. *PLoS ONE* 6: e1657.
76. Hummel J, Clauss M (2008) Megaherbivores as pacemakers of carnivore diversity and biomass: distributing or sinking trophic energy. *Evolutionary Ecology Research*.
77. Sellers WI, Bates KT, Brassey CA, Egerton VM, Falkingham PL, et al. (2012) Minimum convex hull mass estimations of complete mounted skeletons. *Biology Letters* 8: 842–845.
78. Schanz T, Lins Y, Viehhaus H, Barciaga T, Läbe S, et al. (2013) Quantitative interpretation of tracks for determination of body mass. *PLoS ONE* 8.
79. Sander PM (2012) Reproduction in early amniotes. *Science* 337: 806–808.
80. Ar A, Rahn H, Paganelli CV (1979) The avian egg: mass and strength. *Condor* 81: 331–337.
81. Vila B, Jackson FD, Fortuny J, Sellés AG, Galobart A (2010) 3-D modelling of megaloolithid clutches: insights about nest construction and dinosaur behaviour. *PLoS ONE* 5: e10362.
82. Wilson JA, Mohabey DM, Peters SE, Head JJ (2010) Predation upon hatchling dinosaurs by a new snake from the Late Cretaceous of India. *PLoS Biology* 8: e1000322.
83. Fowler DW, Hall LE (2011) Scratch-digging sauropods, revisited. *Historical Biology* 23: 27–40.
84. Deeming DC (2006) Ultrastructural and functional morphology of eggshells supports the idea that dinosaur eggs were incubated buried in a substrate. *Palaeontology* 49: 171–185.
85. Seymour RS (1979) Dinosaur eggs: gas conductance through the shell, water loss during incubation and clutch size. *Paleobiology* 5: 1–11.
86. Jackson FD, Varricchio DJ, Jackson RA, Vila B, Chiappe LM (2008) Comparison of water vapor conductance in a titanosaur egg from the Upper Cretaceous of Argentina and a *Megaloolithus siruguei* egg from Spain. *Paleobiology* 34: 229–246.
87. Grellet-Tinner G, Chiappe L, Coria R (2004) Eggs of titanosaurid sauropods from the Upper Cretaceous of Aca Mahuevo (Argentina). *Canadian Journal of Earth Sciences* 41: 949–960.
88. Grellet-Tinner G, Fiorelli LE, Salvador RB (2012) Water vapor conductance of the Lower Cretaceous dinosaurian eggs from Sanagasta, La Rioja, Argentina: paleobiological and paleoecological implications for South American favoolithid and megaloolithid eggs. *Palaios* 27: 35–47.
89. Griebeler EM, Klein N, Sander PM (2013) Aging, maturation and growth of sauropodomorph dinosaurs as deduced from growth curves using long bone histological data *PLoS ONE* 8: e67012.
90. Case TJ (1978) On the evolution and adaptive significance of postnatal growth rates in the terrestrial vertebrates. *The Quarterly Review of Biology* 53: 243–282.
91. Hummel J, Clauss M (2011) Sauropod feeding and digestive physiology. In: Klein N, Remes K, Gee CT, Sander PM, *Biology of the Sauropod Dinosaurs: Understanding the Life of Giants*. Bloomington and Indianapolis: Indiana University Press. 11–33.
92. Young MT, Rayfield EJ, Holliday CM, Witmer LM, Button DJ, et al. (2012) Cranial biomechanics of *Diplodocus* (Dinosauria, Sauropoda): testing hypotheses of feeding behaviour in an extinct megaherbivore. *Naturwissenschaften* 99: 637–643.

93. Chure D, Britt BB, Whitlock JA, Wilson JA (2010) First complete sauropod dinosaur skull from the Cretaceous of the Americas and the evolution of sauropod dentition. *Naturwissenschaften* 97: 379–391.
94. Witzel U, Mannhardt J, Goessling R, de Micheli P, Preuschoft H (2011) Finite element analyses and virtual syntheses of biological structures and their application to sauropod skulls. In: Klein N, Remes K, Gee CT, Sander PM, *Biology of the Sauropod Dinosaurs: Understanding the Life of Giants*. Bloomington and Indianapolis: Indiana University Press. 171–181.
95. Gee CT (2011) Dietary options for the sauropod dinosaurs from an integrated botanical and paleobotanical perspective. In: Klein N, Remes K, Gee CT, Sander PM, *Biology of the Sauropod Dinosaurs: Understanding the Life of Giants Life of the Past*. Bloomington and Indianapolis: Indiana University Press. 34–56.
96. Janensch W (1935–1936) Die Schädel der Sauropoden *Brachiosaurus*, *Barosaurus* und *Dicraeosaurus* aus den Tendaguruschichten Deutsch-Ostafrikas. *Palaeontographica* (Supplement 7) 2: 147–298.
97. Morhardt AC, Bonnan MF, Keillor T (2009) Dinosaur smiles: correlating premaxilla, maxilla, and dentary foramina counts with extra-oral structures in amniotes and its implications for dinosaurs. *Journal of Vertebrate Paleontology* 29: 152A.
98. Wings O, Sander PM (2007) No gastric mill in sauropod dinosaurs: new evidence from analysis of gastrolith mass and function in ostriches. *Proceedings of the Royal Society B* 274: 635–640.
99. Fritz J, Hummel J, Kienzle E, Wings O, Streich WJ, et al. (2011) Gizzard vs. teeth, it's a tie: food-processing efficiency in herbivorous birds and mammals and implications for dinosaur feeding strategies. *Paleobiology* 37: 577–586.
100. Clauss M, Steuer P, Müller DWH, Codron D, Hummel J (2013) Herbivory and body size: allometries of diet quality and gastrointestinal physiology, and implications for herbivore ecology and dinosaur gigantism. *PLoS ONE* 8.
101. Clauss M (2011) Sauropod biology and the evolution of gigantism: what do we know? In: Klein N, Remes K, Gee CT, Sander PM, *Biology of the Sauropod Dinosaurs: Understanding the Life of Giants Life of the Past*. Bloomington and Indianapolis: Indiana University Press. 3–7.
102. D'Emic M, Whitlock J, Smith K, Fisher D, Wilson JA (2013) Evolution of high tooth replacement rates in sauropod dinosaurs. *PLoS ONE* 8: e69235.
103. Sereno PC, Wilson JA, Witmer LM, Whitlock JA, Maga A, et al. (2007) Structural extremes in a Cretaceous dinosaur. *PLoS One* 2: e1230.
104. Prasad V, Strömberg CAE, Alimohammadian H, Sahni A (2005) Dinosaur coprolites and the early evolution of grasses and grazers. *Science* 310: 1177–1180.
105. Mohabey DM (2005) Late Cretaceous (Maastrichtian) nests, eggs, and dung mass (coprolites) of Sauropods (Titanosaurs) from India In: Tidwell V, Carpenter K, editors. *Thunder-Lizards. The Sauropodomorph Dinosaurs*. Bloomington: Indiana University Press. 466–489.
106. Sander PM, Gee CT, Hummel J, Clauss M (2010) Mesozoic plants and dinosaur herbivory. In: Gee CT, *Plants in Mesozoic Time: Morphological Innovations, Phylogeny, Ecosystems*. Bloomington: Indiana University Press. 331–359.
107. Clauss M, Nunn C, Fritz J, Hummel J (2009) Evidence for a tradeoff between retention time and chewing efficiency in large mammalian herbivores. *Comparative Biochemistry and Physiology, Part A: Molecular and Integrative Physiology* 154: 376–382.
108. Franz R, Hummel J, Kienzle E, Kölle P, Gunga H-C, et al. (2009) Allometry of visceral organs in living amniotes and its implications for sauropod dinosaurs. *Proceedings of the Royal Society B* 276: 1731–1736.
109. Steuer P, Südekum K-H, Müller DWH, Kaandorp J, Clauss M, et al. (2013) Fibre digestibility in large herbivores as related to digestion type and body mass - an in vitro approach. *Comparative Biochemistry and Physiology Part A: Molecular & Integrative Physiology* 164: 319–326.
110. Müller DWH, Codron D, Meloro C, Munn A, Schwarm A, et al. (2013) Assessing the Jarman-Bell Principle: scaling of intake, digestibility, retention time and gut fill with body mass in mammalian herbivores. *Comparative Biochemistry and Physiology Part A: Molecular & Integrative Physiology* 164: 129–140.
111. Taylor MP, Wedel MJ (2013) Why sauropods had long necks; and why giraffes have short necks *Peer J* 2013: 1–41.
112. Preuschoft H, Klein N (2013) Sauropod necks can resist twisting, tails resist bending. Including a theoretical approach to the function of cervical ribs. *PLoS ONE* 8.
113. Sereno PC, Zhao XJ, Brown L, Tan L (2007) New psittacosaurid highlights skull enlargement in horned dinosaurs. *Acta Palaeontologica Polonica* 52: 275–284.
114. McGarrity CT, Campione NE, Evans DC (2013) Cranial anatomy and variation in *Prosauroplophus maximus* (Dinosauria: Hadrosauridae). *Zoological Journal of the Linnean Society*, London 167: 531–568.
115. MacFadden BJ (1994) Fossil Horses. Systematics, Paleobiology, and Evolution of the Family Equidae. Cambridge: Cambridge University Press.
116. Georgi JA, Sipla JS, Forster CA (2013) Turning semicircular canal function on its head: dinosaurs and a novel vestibular analysis. *PLoS ONE* 8: e58517.
117. Knoll F, Witmer LM, Ortega F, Ridgely RC, Schwarz-Wings D (2012) The braincase of the basal sauropod dinosaur *Spinophorosaurus* and 3D reconstructions of the cranial endocast and inner ear. *PLoS ONE* 7: e30060.
118. Knoll F, Ridgely RC, Ortega F, Sanz JL, Witmer LM (2013) Neurocranial osteology and neuroanatomy of a Late Cretaceous titanosaurian sauropod from Spain (*Ampelosaurus* sp.). *PLoS ONE* 8: e54991.
119. Taylor MP, Hone DWE, Wedel MJ, Naish D (2011) The long necks of sauropods did not evolve primarily through sexual selection. *Journal of Zoology* 285: 150–161.
120. Christian A (2002) Neck posture and body design in sauropods. *Mitteilungen aus dem Museum für Naturkunde in Berlin, Geowissenschaftliche Reihe* 5: 271–281.
121. Christian A, Dzemski G (2011) Neck posture in sauropods. In: Klein N, Remes K, Gee CT, Sander PM, *Biology of the Sauropod Dinosaurs: Understanding the Life of Giants*. Bloomington and Indianapolis: Indiana University Press. 251–260.
122. Dzemski G, Christian A (2007) Flexibility along the neck of the ostrich (*Struthio camelus*) and consequences for the reconstruction of dinosaurs with extreme neck length. *Journal of Morphology* 268: 707–714.
123. Stevens KA, Parrish JM (2005a) Neck posture, dentition, and feeding strategies in Jurassic sauropod dinosaurs. In: Tidwell V, Carpenter K, *Thunder-Lizards. The Sauropodomorph Dinosaurs*. Bloomington: Indiana University Press. 212–232.
124. Stevens KA, Parrish JM (2005b) Digital reconstructions of sauropod dinosaurs and implications for feeding. In: Curry Rogers KA, Wilson JA, *The Sauropods. Evolution and Paleobiology*. Berkeley and Los Angeles: University of California Press. 178–200.
125. Christian A, Peng G, Sekiya T, Ye Y, Wulf M, et al. (2013) Biomechanical reconstructions and selective advantages of neck poses and feeding strategies of sauropods with the example of *Mamenchisaurus youngi*. *PLoS ONE* 8.
126. Henderson D (2013) Sauropod necks: are they really for heat loss? *PLoS ONE* 8.
127. Taylor MP, Wedel MJ (2013) The effect of intervertebral cartilage on neutral posture and range of motion in the necks of sauropod dinosaurs. *PLoS ONE* 8.
128. Preuschoft H, Hohn B, Stoinski S, Witzel U (2011) Why so huge? Biomechanical reasons for the acquisition of large size in sauropod and theropod dinosaurs. In: Klein N, Remes K, Gee CT, Sander PM, *Biology of the Sauropod Dinosaurs: Understanding the Life of Giants*. Bloomington and Indianapolis: Indiana University Press. 197–218.
129. Wedel MJ (2012) A monument of inefficiency: the presumed course of the recurrent laryngeal nerve in sauropod dinosaurs. *Acta Palaeontologica Polonica* 57: 85–100.
130. Alexander RM (1989) *Dynamics of Dinosaurs and Other Extinct Giants*. New York: Columbia University Press.
131. Hildebrand M, Goslow GE (2001) *Analysis of Vertebrate Structure*. Fifth Edition. New York: J. Wiley & Sons. 635.
132. Senter P (2007) Necks for sex: sexual selection as an explanation for sauropod dinosaur neck elongation. *Journal of Zoology* 271: 45–53.
133. Christian A (2010) Some sauropods raised their necks – evidence for high browsing in *Euhelopus zdanskyi*. *Biology Letters* 6: 823–825.
134. Ruxton GD, Wilkinson DM (2011) The energetics of low browsing in sauropods. *Biology Letters* 7: 779–781.
135. Seymour RS (2009) Raising the sauropod neck: it costs more to get less. *Biology Letters* 5: 317–319.
136. Copley M, Rayfield E, Barrett PM (2013) Inter-vertebral flexibility of the ostrich neck: implications for estimating sauropod neck flexibility. *PLoS ONE* 8: e72187.
137. Klein N, Christian A, Sander PM (2012) Histology shows that elongated neck ribs in sauropod dinosaurs are ossified tendons. *Biology Letters* 8: 1032–1035.
138. Christian A, Dzemski G (2011) Neck posture in sauropods. In: Klein N, Remes K, Gee CT, Sander PM, *Biology of the Sauropod Dinosaurs: Understanding the Life of Giants*. Bloomington and Indianapolis: Indiana University Press. 251–260.
139. Wedel MJ, Sanders RK (2002) Osteological correlates of cervical musculature in Aves and Sauropoda (Dinosauria: Saurischia), with comments on the cervical ribs of *Apatosaurus*. *PaleoBios* 22: 1–6.
140. Perry SF, Breuer T, Pajor N (2011) Structure and function of the sauropod respiratory system. In: Klein N, Remes K, Gee CT, Sander PM, *Biology of the Sauropod Dinosaurs: Understanding the Life of Giants Life of the Past* (series ed Farlow, J) Bloomington: Indiana University Press.
141. Wedel MJ (2003) Vertebral pneumaticity, air sacs, and the physiology of sauropod dinosaurs. *Paleobiology* 29: 243–255.
142. Schachner ER, Hutchinson JR, Farmer CG (2013) Pulmonary anatomy in the Nile crocodile and the evolution of unidirectional airflow in Archosauria *Peer J* 2013: 1–10.
143. Butler RJ, Barrett PM, Gower DJ (2012) Reassessment of the evidence for postcranial skeletal pneumaticity in Triassic archosaurs, and the early evolution of the avian respiratory system. *PLoS ONE* 7: e34094.
144. Wedel MJ, Taylor MP (2013) Caudal pneumaticity and pneumatic hantuses in the sauropod dinosaurs *Giraffatitan* and *Apatosaurus*. *PLoS ONE* 8.
145. Cerda IA, Salgado L, Powell JE (2012) Extreme postcranial pneumaticity in sauropod dinosaurs from South America. *Paläontologische Zeitschrift* 86: 441–449.
146. Farmer CG, Sanders K (2010) Unidirectional airflow in the lungs of alligators. *Science*: 327 338–340.

147. Seymour RS, Bennett-Stamper CL, Johnston SD, Carrier DR, Grigg GC (2004) Evidence for endothermic ancestors of crocodiles at the stem of archosaur evolution. *Physiological and Biochemical Zoology* 77: 1051–1067.
148. Cubo J, Le Roy N, Martínez-Maza C, Montes LP (2012) Paleohistological estimation of bone growth rate in extinct archosaurs. *Paleobiology* 38: 335–349.
149. Benson RBJ, Butler RJ, Carrano MT, O'Connor PM (2012) Air-filled postcranial bones in theropod dinosaurs: physiological implications and the 'reptile'–bird transition. *Biological Reviews* 87: 168–193.
150. Clarke A (2013) Dinosaur energetics: setting the bounds on feasible physiologies and ecologies. *The American Naturalist* 182: 283–297.
151. Köhler M, Marín-Moratalla N, Jordana X, Aanes R (2012) Seasonal bone growth and physiology in endotherms shed light on dinosaur physiology. *Nature* 487: 358–361.
152. Chinsamy A, Hillenius WJ (2004) Physiology of non-avian dinosaurs. In: Weishampel DB, Dodson P, Osmólska H, *The Dinosauria*. Second Edition. Berkeley: University of California Press. 643–659.
153. Stein K, Prondvai E (2013) Rethinking the nature of fibrolamellar bone: an integrative biological revision of sauropod plexiform bone formation. *Biological Reviews of the Cambridge Philosophical Society*.
154. Stein K, Werner J (2013) Preliminary analysis of osteocyte lacunar density in long bones of tetrapods: all measures are bigger in sauropod dinosaurs. *PLoS ONE* 8.
155. Seymour RS, Smith SL, White CR, Henderson DM, Schwarz-Wings D (2011) Blood flow to long bones indicates activity metabolism in mammals, reptiles and dinosaurs. *Proceeding of the Royal Society B* 279: 451–456.
156. Rauhut OWM, Foth C, Tischlinger H, Norell MA (2012) Exceptionally preserved juvenile megalosauroid theropod dinosaur with filamentous integument from the Late Jurassic of Germany. *Proceedings of the National Academy of Sciences, USA* 109: 11746–11751.
157. Eagle RA, Tütken T, Martin TS, Tripathi AK, Fricke HC, et al. (2011) Dinosaur body temperatures determined from isotopic (^{13}C - ^{18}O) ordering in fossil biominerals. *Science* 333: 443–445.
158. Seymour RS (2013) Maximal aerobic and anaerobic power generation in large crocodiles versus mammals: implications for dinosaur gigantothermy. *PLoS ONE* 8: e69361.
159. Gillooly JF, Allen AP, Charnov EL (2006) Dinosaur fossils predict body temperatures. *PLoS Biology* 4: 1467–1469.
160. Griebeler EM (2013) Body temperatures in Sauropodomorpha: the hypothesis of inertial homeothermy revisited. *PLoS ONE* 8.
161. Hudson L, Isaac N, Reuman D (2013) The relationship between body mass and field metabolic rate among individual birds and mammals. *Journal of Animal Ecology*.
162. McNab BK (2008) An analysis of the factors that influence the level and scaling of mammalian BMR. *Comparative Biochemistry and Physiology, Part A* 151: 5–28.
163. Paladino FV, Spotila JR, Dodson P (1997) A blueprint for giants: modeling the physiology of large dinosaurs. In: Farlow JO, Brett-Surman MK, *The Complete Dinosaur*. Bloomington: Indiana University Press. 491–504.
164. Rowe MF, Bakken GS, Ratliff JJ, Langman VA (2013) Heat storage in Asian elephants during submaximal exercise: behavioral regulation of thermoregulatory constraints on activity in endothermic gigantotherms. *The Journal of Experimental Biology* 216: 1774–1785.
165. Farlow JO, Hayashi S, Tattersall G (2010) Internal vascularity of the dermal plates of *Stegosaurus* (Ornithischia: Thyreophora). *Swiss Journal of Geosciences* 103: 173–186.
166. Sverdllova NS, Lambert M, Witzel U, Perry SF (2012) Boundary conditions for heat transfer and evaporative cooling in the trachea and air sac system of the domestic fowl: A two-dimensional CFD analysis. *PLoS ONE* 7: e45315.
167. Clarke A, Pörtner H-O (2010) Temperature, metabolic power and the evolution of endothermy. *Biological Reviews* 85: 703–727.
168. Erickson GM, Curry Rogers K, Yerby SA (2001) Dinosaurian growth patterns and rapid avian growth rates. *Nature* 412: 429–433.
169. Bybee PJ, Lee AH, Lamm E-T (2006) Sizing the Jurassic theropod dinosaur *Allosaurus*: assessing growth strategy and evolution of ontogenetic scaling of limbs. *Journal of Morphology* 267: 347–359.
170. Lee AH, Werning S (2008) Sexual maturity in growing dinosaurs does not fit reptilian growth models. *Proceedings of the National Academy of Sciences, USA* 105: 582–587.
171. Sander PM, Klein N, Stein K, Wings O (2011) Sauropod bone histology and its implications for sauropod biology. In: Klein N, Remes K, Gee CT, Sander PM, *Biology of the Sauropod Dinosaurs*. Bloomington and Indianapolis: Indiana University Press.
172. Waskow K, Sander PM (in press) Growth record and histological variation in the dorsal ribs of *Camarasaurus* sp. (Sauropoda). *Journal of Vertebrate Paleontology*.
173. Stein K, Csiki Z, Rogers KC, Weishampel DB, Redelstorff R, et al. (2010) Small body size and extreme cortical bone remodeling indicate phyletic dwarfism in *Magyarosaurus dacus* (Sauropoda: Titanosauria). *Proceedings of the National Academy of Sciences, USA* 107 9258–9263.
174. Klein N, Sander PM, Stein K, Le Loeuff J, Carballido JL, et al. (2012) Modified laminar bone in *Ampelosaurus atacis* and other titanosaurs (Sauropoda): implications for life history and physiology. *PLoS ONE* 7: e36907.
175. Reisz RR, Huang TD, Roberts EM, Peng S, Sullivan C, et al. (2013) Embryology of Early Jurassic dinosaur from China with evidence of preserved organic remains. *Nature* 469: 210–214.
176. Benton MJ (1990) Origin and interrelationships of dinosaurs. In: Weishampel DB, Dodson P, Osmólska H, *The Dinosauria*. Berkeley: University of California Press. 11–29.
177. Charig AJ (1972) The evolution of the archosaur pelvis and hindlimb: an explanation in functional terms. In: Joysey KA, Kemp TS, *Studies in Vertebrate Evolution*. Oliver and Boyd: Edinburgh. 121–155.
178. Hutchinson JR (2006) The evolution of locomotion in archosaurs CR *Palevol* 519–530.
179. Parrish JM (1986) Locomotor adaptations in the hindlimb and pelvis of the Thecodontia. *Hunteria* 1: 1–35.
180. Falkingham PL, Bates KT, Margetts L, Manning PL (2010) Simulating sauropod manus-only trackway formation using finite-element analysis. *Biology Letters*.
181. Vila B, Oms O, Galobart À, Bates KT, Egerton VM, et al. (2013) Dynamic similarity in titanosaur sauropods: ichnological evidence from the Fumanya dinosaur tracksite (southern Pyrenees). *PLoS ONE* 8: e57408.
182. Thompson ME, White RS, Morgan GS (2007) Pace versus trot: can medium speed gaits be determined from fossil trackways? In: Spielmann L, Lockley MG, *Cenozoic Vertebrate Tracks and Traces*. New Mexico Museum of Natural History and Science, Bulletin, 42. 309–314.
183. Erickson GJ, Krick BA, Hamilton M, Bourne GR, Norell MA, et al. (2012) Complex dental structure and wear biomechanics in hadrosaurid dinosaurs. *Science* 338: 98–101.
184. Deeming C, Birchard G (2009) Why were extinct gigantic birds so small? *Avian Biology Research* 1: 187–194.
185. Gatesy SM (2002) Locomotor evolution on the line to modern birds. In: Chiappe L, Witmer LM, *Mesozoic Birds: Above the Heads of Dinosaurs*. Berkeley: University of California Press. 432–447.
186. Varrichio DJ, Moore JR, Erickson GM, Norell MA, Jackson FD, et al. (2008) Avian paternal care had dinosaur origin. *Science* 322: 1826–1828.
187. Gottmann-Quesada A, Sander PM (2009) A redescription of the early archosauromorph *Protosaurus speneri* MEYER, 1832, and its phylogenetic relationships. *Palaeontographica A* 287: 123–220.
188. Mannion PD, Upchurch P, Mateus O, Barnes RN, Jones MEH (2012) New information on the anatomy and systematic position of *Dinheirosaurus lourinhanensis* (Sauropoda: Diplodocoidea) from the Late Jurassic of Portugal, with a review of European diplodocoids. *Journal of Systematic Palaeontology* 10: 521–551.
189. Hokkanen JEI (1986) The size of the biggest land animal. *Journal of Theoretical Biology* 118: 491–499.

Review

Herbivory and Body Size: Allometries of Diet Quality and Gastrointestinal Physiology, and Implications for Herbivore Ecology and Dinosaur Gigantism

Marcus Clauss^{1*}, Patrick Steuer², Dennis W. H. Müller³, Daryl Codron^{1,4}, Jürgen Hummel^{2,5}

1 Clinic for Zoo Animals, Exotic Pets and Wildlife, Vetsuisse Faculty, University of Zurich, Zurich, Switzerland, **2** Institute of Animal Science, University of Bonn, Bonn, Germany, **3** National Park 'Bavarian Forest', Grafenau, Germany, **4** Florisbad Quaternary Research, National Museum, Bloemfontein, South Africa, **5** Ruminant Nutrition, Department of Animal Sciences, University of Göttingen, Göttingen, Germany

Abstract: Digestive physiology has played a prominent role in explanations for terrestrial herbivore body size evolution and size-driven diversification and niche differentiation. This is based on the association of increasing body mass (BM) with diets of lower quality, and with putative mechanisms by which a higher BM could translate into a higher digestive efficiency. Such concepts, however, often do not match empirical data. Here, we review concepts and data on terrestrial herbivore BM, diet quality, digestive physiology and metabolism, and in doing so give examples for problems in using allometric analyses and extrapolations. A digestive advantage of larger BM is not corroborated by conceptual or empirical approaches. We suggest that explanatory models should shift from physiological to ecological scenarios based on the association of forage quality and biomass availability, and the association between BM and feeding selectivity. These associations mostly (but not exclusively) allow large herbivores to use low quality forage only, whereas they allow small herbivores the use of any forage they can physically manage. Examples of small herbivores able to subsist on lower quality diets are rare but exist. We speculate that this could be explained by evolutionary adaptations to the ecological opportunity of selective feeding in smaller animals, rather than by a physiologic or metabolic necessity linked to BM. For gigantic herbivores such as sauropod dinosaurs, other factors than digestive physiology appear more promising candidates to explain evolutionary drives towards extreme BM.

Introduction

1.1 Reconstructing dinosaur feeding behaviour and trophic niches

Dinosaur gigantism, in particular in its spectacular form of the sauropod dinosaurs, has fascinated scientists for centuries [1]. Sauropods dominated terrestrial ecosystems for more than a hundred million years [1]. Coupled with this evidence of ecophysiological success, their existence raises the question what factors selected for their very large body size? Among the various possible answers, advantages in digestive physiology bestowed by large body size have been suggested [1]. This review will examine the role of digestive physiology as a driver for increasing body mass in herbivores by reviewing evidence accumulated from studies of contemporary herbivores.

There are generally two ways to reconstruct dinosaur feeding behaviour, trophic niches and digestive physiology: using morphological characteristics of the cranium, the neck or even the whole body, and using (quantitative and qualitative) extrapolations

based on body mass (BM). Differences in skull anatomy, dentition, neck height and position, tooth microwear and stable isotope composition between different sauropod clades have been presented and used to evoke niche separation and differential resource use in different and also in sympatric sauropod species [2–11], and are not reviewed here. The second option – reconstructions by extrapolating from extant animals, based on relationships between BM and diet quality, diet selection, and digestive physiology – has also been used extensively in reconstructing dinosaur physiology [12–14] and is the topic of this review.

1.2 The use of allometries

Dealing with extrapolations based on BM, one usually refers to allometric relations that are described by the equation $y = a \cdot BM^b$. Usually, b is different from 1, i.e. the relationship is not linear (i.e., does not follow the 'same measure' in 'iso-metry') but follows 'another measure' (hence the term 'allo-metry'). If b is smaller than 1, the measure, expressed in % of BM, will decrease with increasing BM. This relation is sometimes also referred to as a 'lower mass-specific measure with increasing BM'. In the scientific literature on allometries, the (exact) magnitude of the exponent is often an important part of a concept, such as in the metabolic theory of ecology [15]. In this review, we mostly refrain from citing or analysing the magnitude of the exponent unless it is necessary for the argument. We do this to avoid confusion, because the different published allometric exponents were derived with considerable discrepancy between publications, both in terms of the species set used (which may, for example, include mammals, or only mammalian herbivores, African mammalian herbivores, ruminants, grazing ruminants etc.), and in terms of the methods

Citation: Clauss M, Steuer P, Müller DWH, Codron D, Hummel J (2013) Herbivory and Body Size: Allometries of Diet Quality and Gastrointestinal Physiology, and Implications for Herbivore Ecology and Dinosaur Gigantism. PLoS ONE 8(9): e68714. doi:10.1371/journal.pone.0068714

Editor: Peter Dodson, University of Pennsylvania, United States of America

Published: September 26, 2013

Copyright: © 2013 Clauss et al. This is an open-access article distributed under the terms of the Creative Commons Attribution License, which permits unrestricted use, distribution, and reproduction in any medium, provided the original author and source are credited.

Funding: This work was funded by the German Science Foundation (DFG, CL 182/3-1,3-2,5-1,6-1; HU 1308/2-1). It is publication no. xx of the DFG Research Unit FOR 533 "The Biology of the Sauropod Dinosaurs: The Evolution of Gigantism". The funders had no role in study design, data collection and analysis, decision to publish, or preparation of the manuscript.

Competing Interests: The authors have declared that no competing interests exist.

* E-mail: mclauss@vetclinics.uzh.ch

employed (which may or may not include the use of one mean value per species or log-transformation prior to model fitting, or account for the phylogenetic structure of the dataset etc.). For example, scaling exponents can vary significantly depending on whether the phylogenetic structure of the data is accounted for or not [16,17]. Another important problem in comparing allometries is that the compatibility of the different measures that all scale to BM must be given [18]. If we use, for example, faecal nitrogen as a proxy for diet quality, and assume that a 10 kg animal has values of 4% nitrogen in the organic matter of the faeces (OM), and a 3000 kg animal 0.8%OM (which is roughly the range covered in [18]), the resulting allometric scaling exponent for diet quality would be $BM^{-0.28}$. If we use these faecal nitrogen values, however, to calculate organic matter digestibility of the diets (using the curvilinear regression equation of Lukas et al. [19]), the resulting values are 77.6% and 29.5% for the small and the large animal, respectively, yielding a scaling of $BM^{-0.17}$. The question which of the two scaling exponents should be used in further calculations is difficult to answer, but mixing them or using them to frame a range of options is akin to lumping length measurements taken in centimetres and inches. Ideally, all measures used in such allometry-based concepts should be linked in a logical, physical (and hence mathematical) way, as for example food intake, retention time of digesta in the gastrointestinal tract, digestibility and gut fill that are linked via a physical principle [16,20]. All these difficulties make comparisons of different allometric exponents from different publications unreliable, unless they are controlled for in a single analysis. We will mention several methodological aspects of using allometries in the text below (see also [21]).

One of the most important misunderstandings when dealing with allometries [22] shall, however, be mentioned here already; it is for example evident when citing the following passage from Geist [23] explaining the Jarman-Bell-principle: *‘The daily energy and protein requirements of mammals are a function of their body weight raised to the power of 0.75. For this reason, small-bodied species require more energy and protein per day per unit of body weight than do large-bodied forms (assuming identical work regime and exposure to temperature and wind). The high metabolism of small-bodied species can be sustained only on highly digestible forage. Since digestibility, and hence daily intake of forage, is a function of the fiber and protein content of the forage, small-bodied ungulates require a forage of relatively low fiber content and high protein content; large-bodied ungulates can feed on forage with higher fiber and lower protein content since their requirement for energy and nutrients per unit of body weight are lower.’* Presented like this, this argument has no power as the scaling of a single measure (here, energy requirement) in itself explains nothing. Only when compared against a scaling of another measure (such as intake or intake capacity) do further deductions become feasible. The expression of the allometric relationship as ‘smaller species requiring more per unit body weight’, while mathematically correct, would only explain anything if it was shown that some other factor relates directly to ‘unit body weight’. The statement that smaller animals ‘have higher mass-specific metabolic requirements than large animals’ expresses the same fact as the statement that smaller animals ‘have the same metabolic requirements as large animals on a metabolic body weight basis’ (note that the allometric relationship also allows to correctly state that ‘smaller animals have lower absolute metabolic requirements than large animals’). In the scenario outlined in the citation, one can only conclude that

a) Requirements scale to $BM^{0.75}$, so the intake of a specific diet should scale to $a BM^{0.75}$.

- b) Animals faced with a lower-quality diet will have to eat more of this diet (this is valid for animals *of all size classes*). Intake of this diet will therefore scale to $c BM^{0.75}$, where $c > a$.
- c) Animal faced with a higher-quality diet will have to eat less of this diet (again, this is valid for animals *of all size classes*). One could assume that intake of this diet should therefore scale to $d BM^{0.75}$, where $d < a$.

Other conclusions are not valid based on the citation alone. In particular, the single scaling can give no compelling reason why a certain size class requires a different diet quality than another. Evidently, if intake capacity could be shown to be constrained in smaller animals, so that reaction b) was not possible, or if encounter rate was constrained in larger animals so that reaction c) was not possible, this would have great explanatory power. But the words ‘higher mass-specific requirements’ do not represent such evidence.

Concepts of Herbivore Body Size and Diet Quality

2.1 Body size and food abundance

We think that in general, there is consensus that herbivores of higher BM ingest diets of lower quality. This is due to the fact that larger animals require larger quantities of food, yet in terrestrial ecosystems, the more abundant plants and plant parts (such as stems or twigs) are generally of lower nutritional quality than less abundant, higher-quality parts (such as leaves or fruit) [24]; note that this applies to both browse and grass forage. This observation is part of a general concept that links the diets of animals to the abundance of their food (Fig. 1), and both large carnivores and large herbivores have to focus on those food items of which they can find sufficient amounts of accessible packages to satisfy their requirements – in herbivores, this is abundant low-quality forage, in carnivores, large (and high-quality) vertebrate prey [25,26]. Because of basic geometry, and also in order to meet their high absolute food requirements, the feeding apparatus of larger species is often of a dimension that in itself prevents selective foraging in terms of both, selecting of small, high-quality plant species, and selecting high-quality plant parts [27,28]. Thus, on land, large herbivore BM will most likely imply a low quality diet because of biomass availability and the ability to feed selectively, but it does not physiologically oblige animals to consume such diets if higher quality food is available in reasonable amounts. In the marine environment, where high-quality food exists in spatially and temporally aggregated lumps of krill or fish that can be easily harvested, gigantism occurs in conjunction with this high-quality food ([29]; note that the lower-quality primary production - algae - is of a dimension that makes it unfeasible for harvest by larger organisms).

Nevertheless, actual proofs of the relationship between herbivore BM and diet quality are rare in the scientific literature (see below). Most comparative datasets on this topic represent studies on African savannah systems (Fig. 2 and 3), but the clarity of the result often depends on the assemblage of species, feeding types (grazing/browsing) and digestion types (ruminant/hindgut fermenter) used. In combinations of small browsing ruminants, grazing ruminants of all sizes, and hindgut fermenters in the ruminant size range (warthog, zebra), trends of decreasing diet quality with increasing BM are mostly evident. If, however, additional species are included in the dataset, such as large browsing ruminants, rhinoceroses, hippopotamus, and elephant, these latter species often oppose the clear trend observed in the other species (see below), which evidently has important implications for any concept that links body size and diet quality. One of

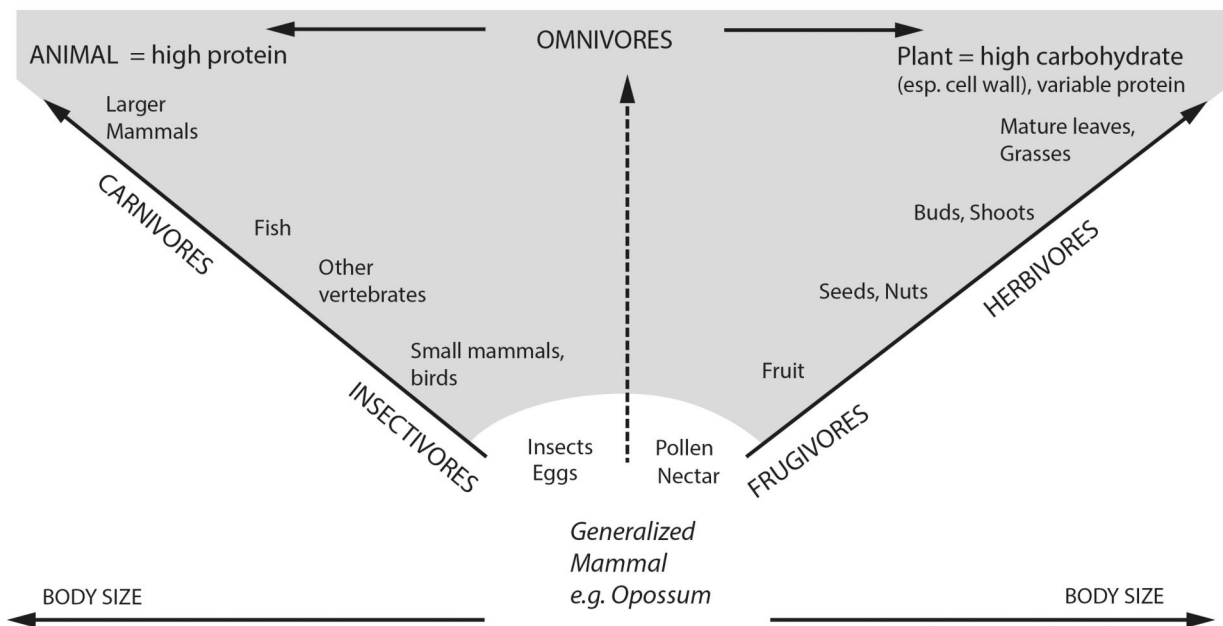


Figure 1. The link between body size and availability of prey in sufficient amounts/packages in terrestrial vertebrates. Modified from Hiiemae [131]. Note that large body size is linked to prey (package) abundance and accessibility, not necessarily to low diet quality per se. doi:10.1371/journal.pone.0068714.g001

these implications is that differences in organismal design can blur patterns related to BM only [16] – which might make simple relationships with BM questionable in the first place.

2.2 Setting the question: Can low food quality drive body size evolution?

The observation of the association of large BM and low diet quality allows the following (non-exhaustive) combinations of hypotheses

1. Low diet quality is an unavoidable consequence of large herbivore BM and
 - a) large BM provides advantages that specifically enhance the use of low quality diets or
 - b) large herbivores have to (and evidently can) cope with low quality diets without being endowed with specific advantages linked to their large BM.

The important difference between hypothesis 2a and 2b is that if 2a is true, then we could postulate selective pressure for larger BM and even gigantism by paleoenvironments in which diets were of inherently low quality [14,30]; if 2b is true, then other factors must have driven evolution towards gigantism. In the literature on species diversification and niche differentiation of extant large herbivores, it is widely assumed that *'size itself is an important adaptation, because the effect of lower selectivity in large animals would appear to be easily outweighed by their greater digestive efficiency and fasting endurance'* (p. 85 in [31]), supporting hypothesis 2a.

Characterising Diet Quality and Herbivore Adaptations

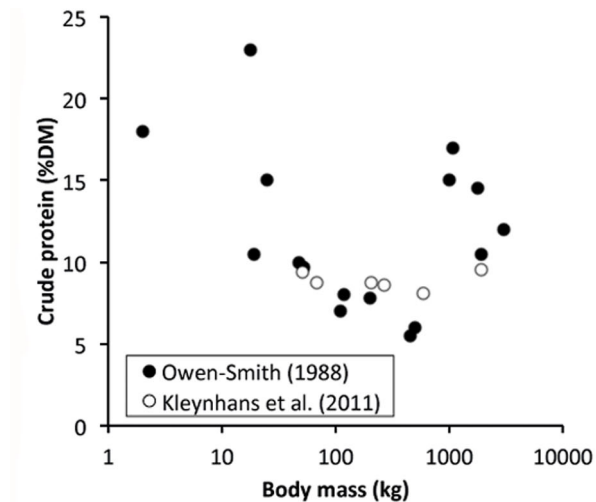
In order to investigate these hypotheses, we need to use different definitions of how 'low diet quality' can be quantified. With respect to the most often cited criteria for low diet quality, we differentiate between

- a high content of plant secondary plant metabolites such as tannins (e.g. [30]),
- a low content of protein (measured as nitrogen, and also expressed as the carbon:nitrogen [C:N] ratio) [14,30],
- a high content of slowly digestible and/or indigestible fibre components such as (hemi)cellulose or lignin [24]
- and finally a generally low 'digestibility' – a measure all three previous measures, but especially cellulose and lignin, are linked to.

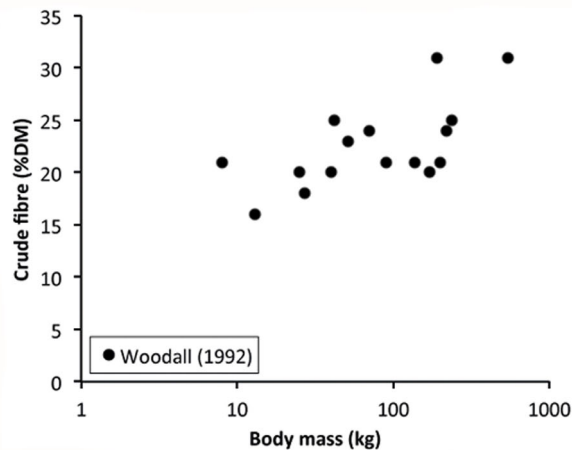
When investigating the effects of these properties, we require both logical concepts (why they are a consequence of large herbivore BM and why large BM might represent an adaptation to them), and empirical data supporting these concepts.

3.1 Diet quality: Plant secondary metabolites

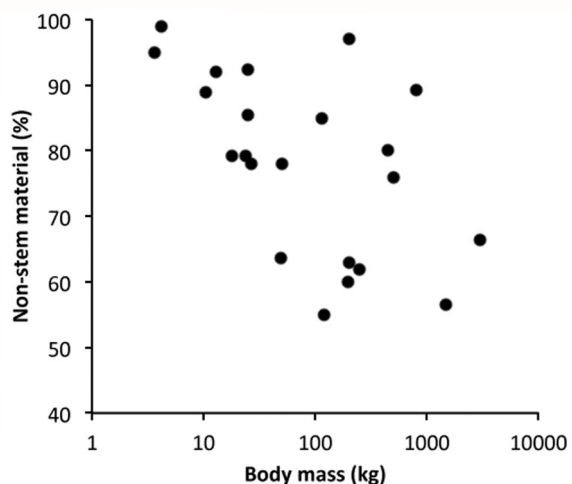
To our knowledge, no empirical evidence exists that larger herbivores ingest diets that have higher contents of plant secondary metabolites (PSM). However, it has been postulated that larger herbivores need to reduce the level of any specific PSM, assuming that their lower mass-specific metabolic rate is also linked to a generally lower detoxification metabolism [32]. In an analysis of the feeding records of 74 animal species, Freeland [32] demonstrated that the number of plant species included in a natural diet increases with BM, thus limiting the proportion of a single species within the total diet. A wider range of different forage species is commonly associated with a wider range of different PSM, and dietary variety is therefore commonly interpreted as a strategy to avoid the accumulation of any one particular PSM to toxic levels (e.g. [33,34]). Therefore, Freeland [32] hypothesized that the body size-diet variety relationship exists because small animals can detoxify larger amounts of a particular plant toxin and thus do not need to show the same degree of dietary variety as larger animals. According to this logic (which we do not accept, see below), higher levels of PSM would prevent the evolution, or drive the extinction, of larger BM. In line with this



a



b



c

Figure 2. Relationship between herbivore body mass (BM) and characteristics of the natural diet that are indicators of diet quality from comparative studies in African mammals. a) BM and nitrogen concentration in (fore)stomach contents [42] or the measured diet [43]; note that large herbivores (giraffe, rhinos, hippo, elephant) oppose the trend in the smaller species; b) BM (estimated from other sources) and the crude fibre concentration in rumen contents (data on ruminants only) [52]; c) BM and the proportion of non-stem material in the rumen [42,53,91,133–140]; note that browsing ruminants of very small (dikdik), small (duiker, steenbok), intermediate (bongo) and large size (giraffe) show less systematic variation with BM, but their selective inclusion/exclusion will influence the data set; note also that the African buffalo (and also the hippo) do not follow the clear negative trend seen in smaller grazers. doi:10.1371/journal.pone.0068714.g002

concept, Guthrie [35] hypothesized that a reduction in available plant variety causes the decline of very large species, a case he exemplifies with the well-recorded decline in variety of diet that preceded the extinction of the Shasta ground sloth (*Nothotheriops shastense*). To our knowledge, no association between plant variety and dinosaur gigantism was made to date in corresponding analyses for dinosaurs (e.g. [36]).

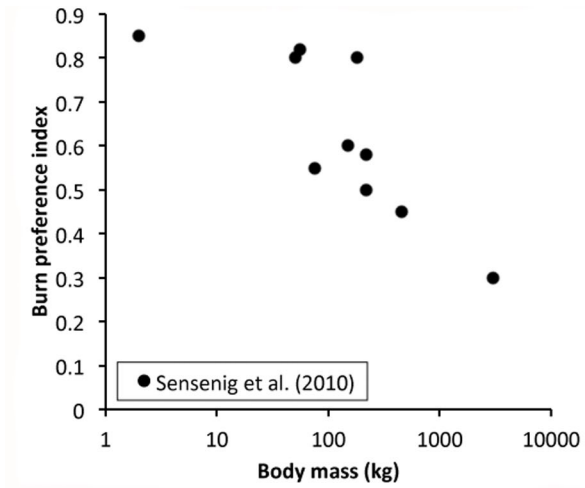
The logic of the detoxification-rate argument requires closer scrutiny. The statement that larger animals have ‘lower mass-specific metabolic rates’ (i.e., lower metabolism per unit BM) is true, yet explains nothing – the scaling of one single parameter in itself has no explanatory power unless it is related to the scaling of another parameter (cf. section 1.2). Even if detoxification metabolism were linked to overall metabolic rate – a fact that would require empirical support (see below) –, this would only represent a constraint *if PSM intake scaled differently than metabolism*. Note that larger animals also have ‘lower mass-specific food intake rates’ [16]. Basal metabolism of large mammals roughly scales to $BM^{0.72}$ [37]; in larger herbivores, evidence suggests a higher scaling of dry matter intake of about $BM^{0.84}$ [16]. Thus, in theory, if detoxification metabolism for specific toxins scaled in the same way as overall basal metabolism, larger animals might indeed require a more varied diet.

These reflections are contradicted by the finding that folivorous mammals, i.e. mammals which we expect to ingest diets that contain comparatively high amounts of PSM, generally have lower mass-specific metabolic rates than mammal herbivores that consume grass, i.e. lower levels of PSM [38,39]. This actually suggests not similarity between metabolic and detoxification rates, but a trade-off between the two [40]. PSM elimination has also been associated with mechanisms not directly linked to metabolism, such as the prevention of absorption in the gut [41]. So far, a strict link between overall metabolic rate and mechanisms of toxin avoidance or detoxification has not been presented conclusively. Consequently, the intake of a varied diet will be beneficial for herbivores of any BM, and the relationship between BM and variety mentioned earlier might not reflect a systematic difference of detoxification capacities with BM, but simply the fact that larger animals encounter a higher diversity of plants in their larger home ranges and have to rely on a larger part of the potentially available biomass.

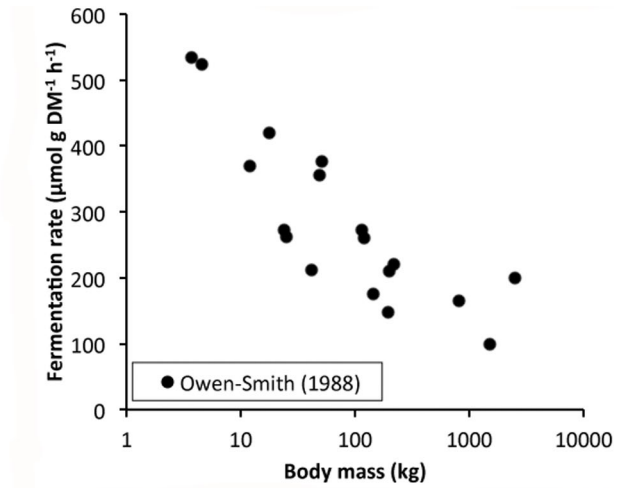
In summary, there is currently no concept that explains why a lower diet quality as defined by higher contents of secondary plant compounds could be a selective pressure for larger herbivore size. The only existing concept even points in the opposite direction, but is not backed by sufficient empirical data.

3.2 Diet quality: Protein (nitrogen)

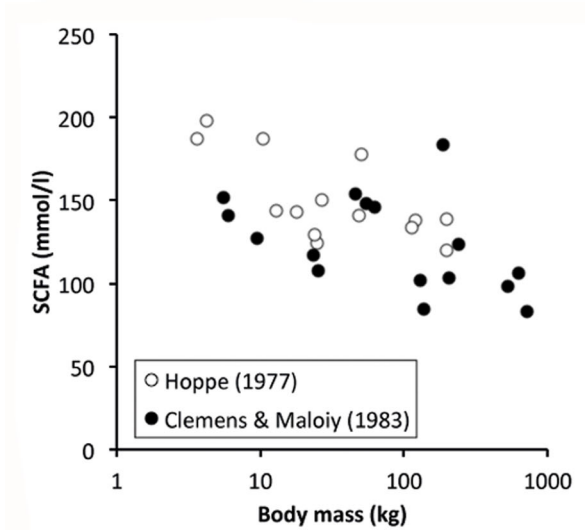
Protein is commonly measured as nitrogen, and we will use the term nitrogen (N) from here onwards. Owen-Smith [42] presented



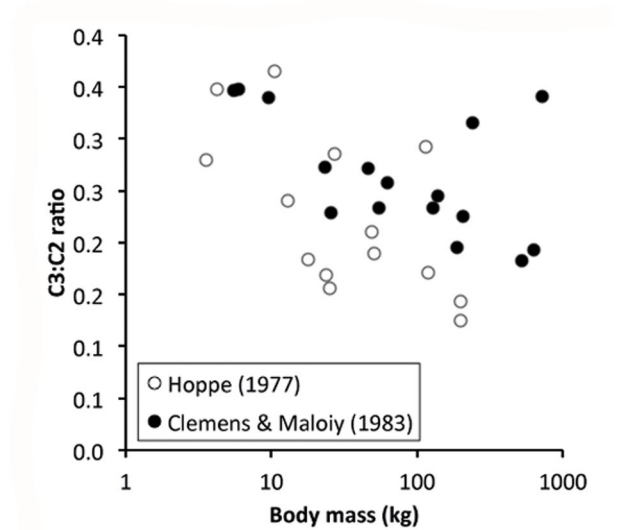
a



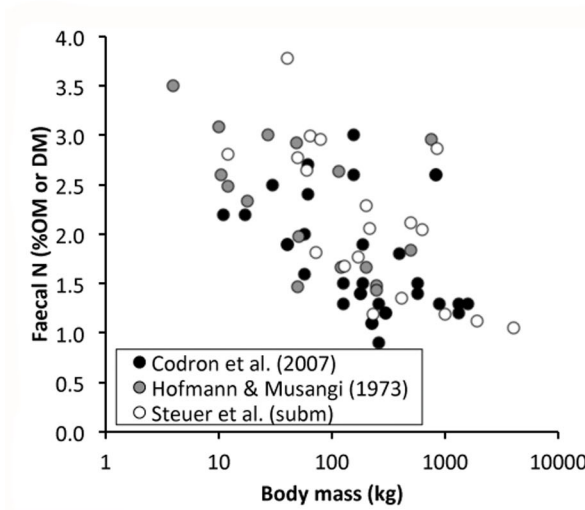
b



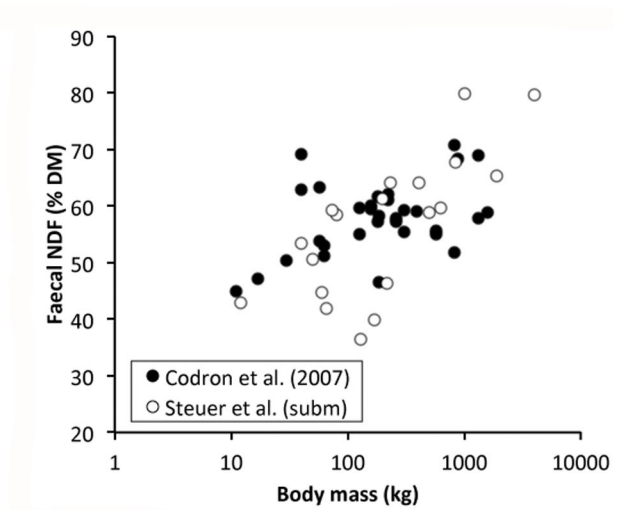
c



d



e



f

Figure 3. Relationship between herbivore body mass (BM) and characteristics of the natural diet that are indicators of diet quality/degradability from comparative studies in African mammals. a) BM and the preference for newly burned savanna patches from Sensenig et al. [55] (note that the study did not include rhinos or hippos); b) BM and in vitro fermentation rates (a proxy of microbial digestion) in rumen, forestomach (hippo) or caecum (elephant) contents [42]; c) BM and the concentration of short-chain fatty acids (SCFA, which represent products of microbial digestion) [135,141]; d) BM and the ratio of the SCFA propionate (C3) to acetate (C2) (a proxy of the proportion of easily fermentable carbohydrates in the diet) [135,141]; e) BM and nitrogen content of faeces (a proxy for diet digestibility; [18] – organic matter OM basis, [142] – OM basis, [143] – dry matter DM basis); f) BM and the neutral detergent fibre (NDF) content of faeces [18,143].
doi:10.1371/journal.pone.0068714.g003

a data collection on the relationship of diet N content (measured in stomach or forestomach contents) and herbivore BM (Fig. 2a). In that data set, there was a negative relationship between ruminant BM and dietary N, supporting the concept of decreasing diet quality with increasing herbivore size in that clade; however, dietary N levels measured for giraffe (*Giraffa camelopardalis*) and large nonruminant herbivores such as rhinoceroses (*Diceros bicornis*, *Ceratotherium simum*), hippopotamus (*Hippopotamus amphibius*) or elephant (*Loxodonta africana*) do not fit the common pattern – a fact that should not be overlooked. This result was repeated in a smaller species set, without elephants but including the white rhinoceros, by Kleynhans et al. [43], where dietary N decreased with increasing BM in the range below 1000 kg, but again with the white rhino as a notable exception (Fig. 2a). As an aside, note that while N levels in stomach contents can be regarded a direct proxy for dietary N, this is not true for faecal N levels (see section 3.4).

Among vertebrates, N requirements of individual species are closely linked to the nitrogen content of their respective diets; thus, carnivores generally have higher N requirements than herbivores, for example [44]. Midgley [45] states that “*herbivore nutritional requirements will evolve in concert with food quality.*” In species with particularly low-N diets, such as nectarivores or gummivores, extremely low N requirements have been demonstrated (e.g. [46]). If faced with a diet of low N content, animals of *any* body size would have to ingest larger quantities of that food to meet their N requirements (see section 1.2), unless they evolved specific physiological traits to reduce N requirements. An adaptive value of large BM in this respect could only be postulated if larger BM facilitated such an ingestion of larger quantities more easily.

Nevertheless, it has been suggested that large body size might represent an adaptation to food of low N content, and hence of a high C:N ratio [14,30]. While Midgley et al. [30] do not offer a mechanism by which this might occur but simply refer to the association of large body size and low diet quality, Wilkinson and Ruxton [14] do not only refer to this association, but suggest that this an effect of the discrepancy in the scaling of N requirements and energy requirements with BM. Using published equations on the scaling of N requirements and field metabolic rate for reptiles and mammals from Klaassen and Nolet [47], they calculate a scaling of the ratio of N:energy requirements of $BM^{-0.47}$ in reptiles (i.e., larger reptiles would require less N per unit energy) and $BM^{0.09}$ in mammals (i.e., larger mammals would require more N per unit energy). Linked with their assumption that large dinosaurs are best represented by extant reptiles, these scaling relationships suggest that low plant N should favour gigantism in herbivorous reptiles (and small body sizes in herbivorous mammals).

This use of allometric reasoning is instructive because of four different deficits. The first three are conceptual. First and most evidently, the discrepancy that for the association of large BM and low diet quality, the study on mammals by Owen-Smith [42] is cited (p. 131 in [14]), yet the results on the scaling of N:energy requirements in mammals would suggest that larger mammals require particularly high-quality diets (increasing N per unit energy at increasing body size), is not discussed. This discrepancy alone should caution against the use of the N:energy requirement scaling proposed by the authors.

Secondly, the argument focuses on N as the main indicator of forage quality – in contrast to most other studies in large herbivore ecology (see sections 3.3 and 3.4). Thirdly, the assumption that N requirements could scale differently than energy requirements/metabolism in vertebrates, and in particular in opposite directions in reptiles and mammals, requires a physiological concept, which is not presented. Actually, animal physiologists appear to assume, on the contrary, a scaling of N requirements that is similar to metabolic scaling ($BM^{0.75}$), which would translate into a scaling of N:energy requirements at $BM^{0.75}:BM^{0.75} \sim BM^0$ (in other words, no scaling). For example, as cited above, Geist [23] stated that “*energy and protein requirements of mammals are a function of their body weight raised to the power of 0.75.*” In his monograph on ‘Wildlife feeding and nutrition’, Robbins [48] expresses N requirements by default per unit metabolic body weight, or $BM^{0.75}$. When publishing their famous mouse-to-elephant curve that supported the concept of metabolism scaling to $BM^{0.73}$, Brody et al. [49] also reported a mouse-to-cattle curve on endogenous urinary N losses scaling to $BM^{0.72}$, indicating a similarity in scaling of N and energy requirements and, consequently, no scaling (BM^0) of the ratio of N:energy requirements. Actually, it is the most parsimonious explanation that all processes responsible for maintenance protein requirements, such as replacement of degraded body protein or enzyme production, are proportional to energy metabolism. Note that the numerical difference between the scaling factors (e.g. 0.73 for metabolism and 0.72 for endogenous urinary N losses in Brody et al. [49]) in itself does not mean much as long as it is not demonstrated that their 95% confidence intervals do not overlap [21].

The fourth concern with this approach relates to the use of empirical data. A closer look at the data from Klaassen and Nolet [47] that resulted in the scaling relationships reported by Wilkinson and Ruxton [14] show that neither author team checked whether the 95% confidence intervals (CI) for the scaling exponents they used overlapped. Using the data supplement from Klaassen and Nolet [47] to calculate these confidence intervals, one notices that the scaling of N requirements in reptiles (at $BM^{0.473}$ (95%CI: -2.179;3.126), based on a dataset of $n = 3$ species) is not significant as the 95%CI of the exponent includes zero, and also includes the scaling of field metabolic rate in reptiles (at $BM^{0.889}$ (95%CI 0.830;0.948), $n = 55$ species). For mammals, the 95% CI for N requirement scaling (at $BM^{0.863}$ (95%CI 0.769;0.956), $n = 11$ species) and field metabolic rate scaling (at $BM^{0.772}$ (95%CI 0.730;0.815), $n = 79$ species) also overlap, again not excluding a similar scaling. Thus, in both cases, a scaling of N:energy requirements at BM^0 cannot be excluded, in accord with current physiological theory.

In summary, evidence for decreasing dietary N content with increasing herbivore BM in the range of ungulate herbivores is equivocal so far, but is expected based on the considerations in section 2.1. There is currently no concept that explains why a lower diet quality as defined by lower contents of N could be a selective pressure for larger herbivore BM; current knowledge and data rather support the notion that dietary N content is unrelated to the evolution of BM.

3.3 Diet quality: Fibre content

Dietary fibre can be measured in many different ways. In herbivore research, the most commonly used is the system that analyzes acid detergent lignin (ADL; usually considered completely indigestible), acid detergent fibre (ADF; representing ADL plus cellulose), and neutral detergent fibre (NDF, representing ADF plus hemicellulose) by Van Soest [50]. Typically, increasing fibre content decreases overall digestibility, and increasing ADL content in particular reduces fibre digestibility [50]. There is one important difference between these fibre fractions: whereas hemicellulose and cellulose mainly decrease fermentation rate (measured as % per hour) but not necessarily the overall potential digestibility (measured as total %), because they are slowly-fermenting substrates, lignin does not necessarily reduce fermentation rate but does reduce overall potential digestibility, because it is basically indigestible for gut microbes [51].

To our knowledge, only one data collection exists that provides comparative data on the fibre content of (fore)stomach contents, in African ruminants [52]; higher fibre levels in larger ruminants are evident (Fig. 2b). The only other study that gives a proxy for fibre content is again by Owen-Smith [42], who showed that the ratio of foliage:stem material (i.e., the proportion of non-stem material) in the stomach decreases with increasing herbivore BM, which can be interpreted as an increase in fibre (and a decrease in nitrogen). Re-analysing that dataset for ruminants only, however, and including an additional source for another browsing ruminant of the intermediate body size range (the bongo *Tragelaphus eurycerus* [53]), also allows the interpretation that this ratio mainly separates browsers from grazers. This is also confirmed by the position of the elephant as an intermediate feeder. Hence, any relationship with BM will depend on the selection of browsing species included in the dataset (Fig. 2c); additionally, the hippopotamus does not fit the pattern found in grazing ruminants. In a more recent study, the enormous flexibility of elephants was demonstrated, with the proportion of stems, bark and roots increasing from approximately 30% in the wet season up to 94% in the hot dry season [54]; this wide range indicates that large body size may be linked with the variety of plant parts that can be used, in particular the harder tissues that may be difficult to crop for smaller species. Sensenig et al. [55] showed in a sample of ten African grazing herbivores that the preference for recently burned areas (which contain young regrowth, i.e., plant material of lower fibre and higher nitrogen content than non-burnt patches, but lower standing biomass) decreased with BM (Fig. 3a); notably, neither rhinos nor the hippo were part of that experiment. Results of similar studies with smaller numbers of species suggest that the white rhino would probably be, again, an outlier to this pattern [56,57]. Using a similar reasoning by deducting forage quality and abundance from climate, geology and landscape indicators, it was demonstrated that herbivore BM distribution followed the distribution patterns expected if larger species require more abundant food (of inherently lower quality) [58–60]. Another, similar study showed that larger species were more evenly distributed across habitats than smaller species, corresponding to smaller species relying on spatially less homogeneously distributed higher-quality forage [61]; again, the white rhino appeared as an outlier to that pattern. Similarly, the habitat use of three browsing ruminants showed an increasing habitat diversity with body size [62]. White rhinos often (though not always) feed on ‘grazing lawns’, where forage quality is comparatively high due to the regular cropping [63]. By comparison, one would assume that if the hippopotamus, another very large herbivore, would be included in such studies, it would similarly represent an outlier due to a similar feeding behaviour [64].

These studies all draw on the concept of the ‘fibre curve’, in which it is demonstrated that forage abundance is related to its fibre content, with more fibrous feeds more abundant [24,65–67]. Historically, it has been suggested that large body size confers a digestive advantage in terms of a longer digesta retention time and hence a higher digestive efficiency (reviewed in [16] - see that text for detailed references, and [68,69]). This concept was repeatedly explained as deriving from a difference in scaling between two digestive parameters: while gut capacity is assumed to scale to $M^{1.0}$, energy requirements and food intake was assumed to scale to $M^{0.75}$. Thus, one would assume larger animals to have a higher gut capacity per unit ingested food, and should therefore have a longer digesta retention time. This should scale at about $M^{1.0-0.75} = 0.25$ (Fig. 4a). This explanation is explicitly or implicitly used in a very large number of ecological studies, including examples cited above.

This use of allometric reasoning is again instructive because of four different deficits. The first three are again conceptual, of which the first relates to the nature of how forage quality can decline [18]. If lower forage quality is assumed to be mainly characterised by slower microbial fermentation rates, as one would expect by an increasing proportion of (hemi)cellulose, then an increase in retention times could compensate for this phenomenon (by giving gut microbes more time for fermentation). If, however, forage quality is mainly characterised by a lower overall potential digestibility, as one would expect by an increasing proportion of lignin, then increasing retention times would not be of any help, but would actually represent a disadvantage (because indigestible material would just be carried in the gut for a longer period of time) [51]. Thus, the scenario of increasing retention times and digestibility with increasing BM could, if at all, only apply for certain conditions of forage quality decline.

The second conceptual deficit relates to the logic of the scaling derivation: retention time is not only a function of gut capacity and intake, but also of digestibility itself [20,21]. If digestibility is higher, more food will be absorbed from the digestive tract, will hence not push on along the digestive tract, and hence retention time will be longer (Fig. 4b). When deriving the scaling of retention time from the scaling of gut capacity and food intake, one therefore inadvertently makes an implicit assumption about the scaling of digestibility itself; hence using the resulting scaling to make predictions on digestive efficiency again amounts to circular reasoning [16,70]. That is unless one also assumes that the increasing digestive efficiency of larger animals exactly out-compensates the decreasing diet quality, and hence leads to no change in the actually achieved digestibility.

The third conceptual problem is that there are several other animal factors than retention time that have an influence on digestive efficiency [71]. For example, digestion rate is slower for larger particles, and digesta particle size increases with BM in herbivorous mammals [72], reptiles [73] and birds [74] (Fig. 5a). Energetic losses due to methane production appear to increase disproportionately with increasing BM in herbivorous mammals [75,76] and reptiles [77] (Fig. 5b). These putative digestive disadvantages of large BM would have to be factored into any calculations of the scaling of digestive efficiency with BM.

Finally, empirical data do not match the predicted pattern of longer digesta retention or higher digestive efficiency in larger herbivores above a threshold of about 1–10 kg: digesta retention time does not scale as predicted (dataset from the large comparative study of [66], re-analysed by [16,42]; analyses of large compiled mammal datasets by [16,78,79]; new large comparative mammal study by [80]; compiled datasets herbivorous birds in [81] and on herbivorous reptiles in [82]) but shows a

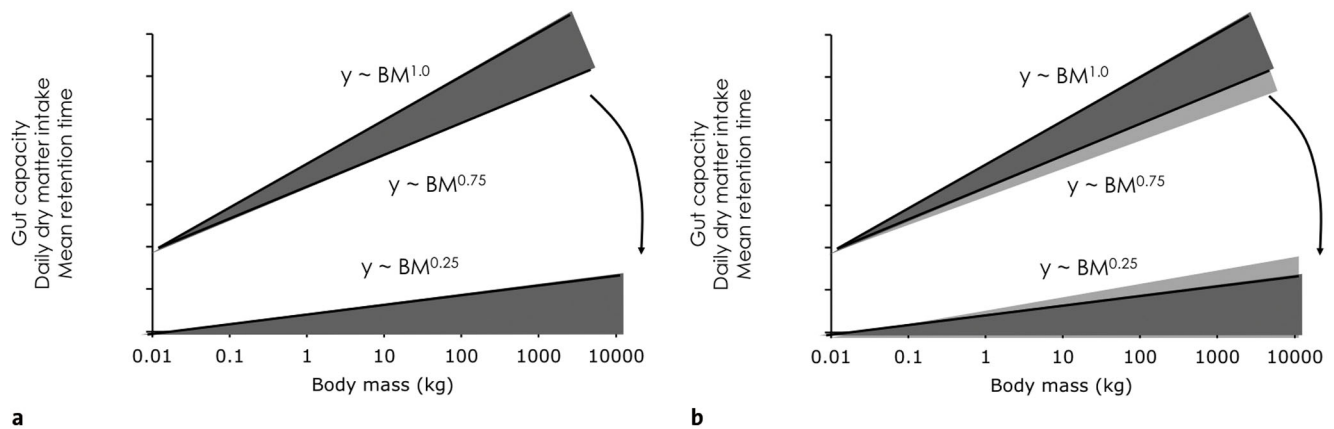


Figure 4. Schematic explanation of circular reasoning in the traditional approach of explaining a positive effect of body mass on digestibility. a) The difference in the scaling of gut capacity (measured as wet or dry gut contents; $BM^{1.0}$) and daily dry matter intake ($BM^{0.75}$), or actual dry matter gut fill rate, results in more gut available per unit digesta at higher BM, and should hence lead to increased mean retention times at higher BM ($BM^{0.25}$). If these increased retention times are used to postulate a higher digestibility at higher BM, the situation in b) occurs: The increasing digestibility reduces the actual gut fill rate, hence increases the difference in the scaling of gut capacity and gut fill rate even more, which should translate into even longer retention times.
doi:10.1371/journal.pone.0068714.g004

less clear-cut or no relationship with BM (Fig. 5c and d). Correspondingly, there is little indication for a systematic effect of body size on digestibility – neither in compiled datasets [71,83,84] (Fig. 5e), in compiled datasets when diet quality was statistically controlled for [82,85], nor in studies in which the same diets were fed to a variety of species (dataset from the large comparative study of [66], re-analysed by [16,86–88]; new large comparative mammal study by [86]) (Fig. 5f and g). Instead, digestive efficiency appears to be rather independent from BM in these studies.

In summary, although not documented in detail, the association of low diet quality and large terrestrial herbivore size is usually not questioned, but the outlying position of some megaherbivores such as white rhinos or hippos challenge the overall concept. In contrast to a long-standing view of a digestive advantage conferred by large BM in terms of digestive efficiency, neither conceptual nor empirical approaches can support this interpretation.

3.4 Diet quality: digestibility/degradability

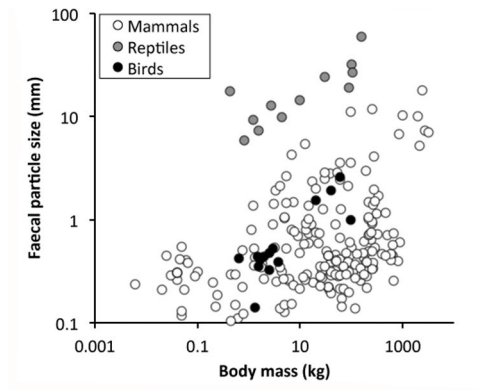
As already evident in the section above, the term ‘digestibility’ is ambiguous because it usually refers to a measurement (intake minus excretion, divided by intake) in a specific animal (with its species-specific digestive efficiency) on a specific diet (with its diet-specific degradability) in a defined time period (conventionally, 5–7 successive days) [48]. The measure will thus integrate both animal and diet factors. Therefore, other terms like ‘in vitro digestibility’, ‘potential digestibility’ or (here) ‘degradability’ are used to describe the diet-specific component of an actually occurring digestibility [18]. Degradability of a diet represents an integrative measure that is influenced by its fibre, N and PSM content, amongst other factors [51,89].

Because herbivores rely on symbiotic gut microbes for digestion [90], various proxies of microbial digestion are used to quantify diet degradability. While the degradability can be assessed by in vitro assays, the sampling of the diet itself, as consumed by the animal, is often logistically challenging. For comparative studies, therefore, samples for analysis are commonly taken after the animals performed their diet selection, either by sampling (fore)stomach contents or faeces. Analyses on forestomach contents in herbivores could be assumed to yield similar results as the

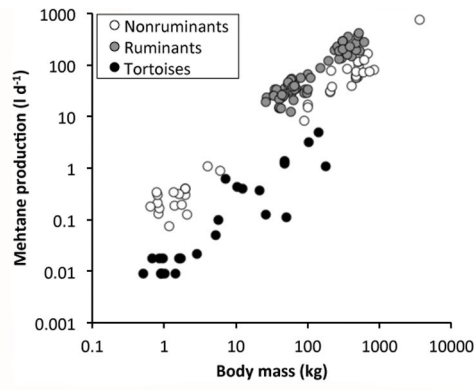
originally selected forage in in vitro assays, i.e. without a major influence of the digestive efficiency of the animal. However, this assumption might be misleading due to differences in feeding bout intervals and hence the likelihood that sampling was performed on stomach contents consisting of freshly ingested forage or forage that was already subjected to longer microbial digestion. In this respect, the extremely frequent feeding intervals for example in the small dikdik (*Madoqua* spp.) [91] could mean that forestomach contents of hunted animals will always be comparatively homogenous with respect to their digestion state, whereas for example the one nocturnal feeding bout in hippos [92] leads to the risk that forestomach contents of hunted animals may be quite pre-digested before sampling for comparative analyses. In this respect, comparative studies of (fore)stomach contents will provide results that integrate both diet quality and feeding bout frequency.

Microbial digestion is characterised by a fermentation rate: This is commonly measured as gas production in vitro, and was shown to decrease with increasing BM in African herbivores [42] (Fig. 3b). It should be noted that values from the caecum of hindgut fermenters, such as the elephant in this dataset (which already appears as an outlier due to its comparatively high values), are not strictly comparable, because the digesta entering the caecum will necessarily be of a lower quality, due to the preceding digestion in the small intestine, than digesta from the (fore)stomach. Alternatively, one can transform gas production rate into short-chained fatty acid (SCFA) production rate, which yields a similar result ([93]; note that this transformation assumes that the conversion of gas production into SCFAs does not scale with BM). Gut microbes produce SCFAs, and their concentration in rumen contents of African ruminants has been shown to decrease with increasing BM in two independent datasets (Fig. 3c). The ratio of the two major SCFAs, propionate:acetate, which decreases with a decreasing proportion of easily digestible carbohydrates and increasing proportion of fibre, decreased with increasing BM in the same two datasets, with large browsers as outliers (Fig. 3d). For the same reasons mentioned above, these comparisons are necessarily limited to foregut fermenters, i.e. mostly ruminants.

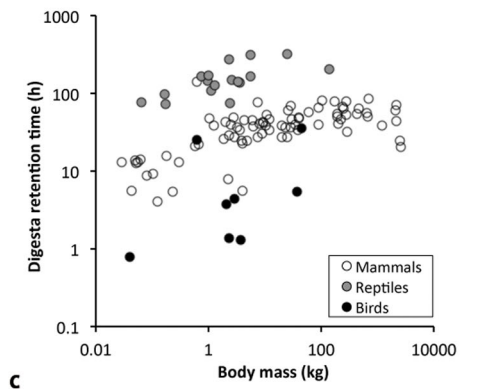
Faecal material will necessarily integrate both diet and animal effects. Estimating diet quality from faecal measures, therefore, requires a priori knowledge of factors that determine digestive



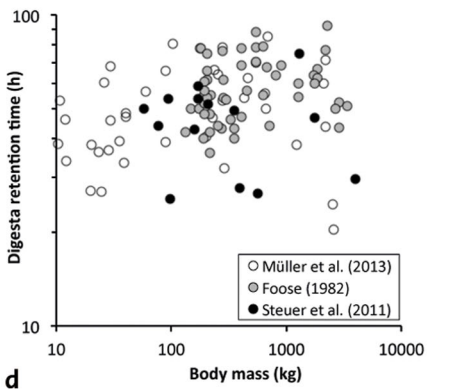
a



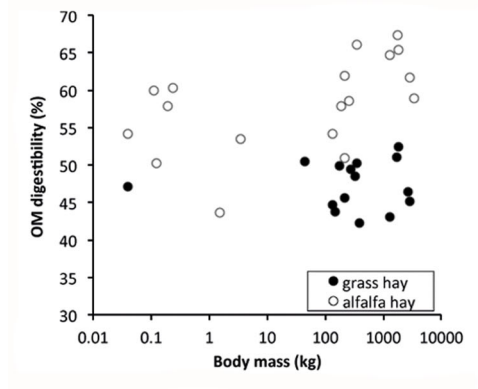
b



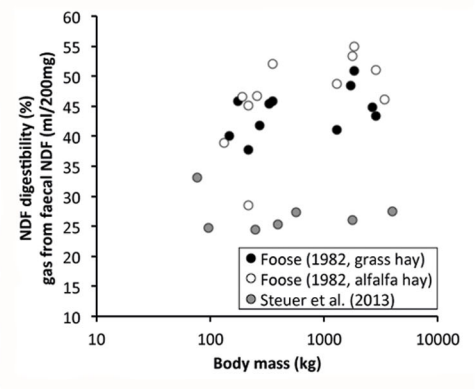
c



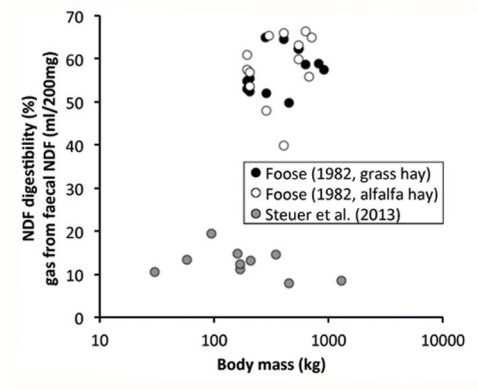
d



e



f



g

Figure 5. Relationships of body mass (BM) and aspects of the digestive physiology of herbivorous vertebrates. a) BM and faecal particle size in mammal, reptile and avian herbivores [72–74]; b) BM and methane production in ruminant and nonruminant mammal herbivores and tortoises (herbivorous reptiles) [75–77]; c) BM and particle mean retention time in herbivorous mammals, reptiles and birds [16,81,112] (note little increase above BM of 1 kg); d) BM and particle mean retention time in three independent datasets on large herbivorous mammals [16,66,80] (note the absence of relevant scaling); e) BM and organic matter digestibility in mammalian hindgut fermenters [71] (note that there is no clear scaling pattern); f) BM and NDF digestibility on two different forages [66] and in vitro faecal NDF gas production (an inverse proxy for fibre digestibility) [86] in mammal hindgut fermenters and g) ruminants (note that there are no clear scaling patterns). doi:10.1371/journal.pone.0068714.g005

efficiency: Given the finding mentioned in section 3.3 that, on a consistent diet, digestibility (which will, on that diet, only vary according to the animal factor digestive efficiency) does not scale with BM (Fig. 5e–g), any scaling of a digestibility proxy as derived from faeces in free-ranging animals will therefore necessarily indicate a scaling of diet degradability, i.e. diet quality [18]. Because herbivores rely on symbiotic gut microbes for digestion, and microbes contain high proportions of nitrogen (N), total faecal nitrogen (TFN) and metabolic faecal nitrogen (MFN, the faecal N not derived from undigested plant N) are proxies for the proportion of microbial matter in faeces; this proportion will be higher on more digestible diets [94,95]. The principle of using TFN as a proxy for digestibility was experimentally validated in domestic cattle and sheep [19,96], horses [97] as well as in more limited studies in wild sheep [98], deer [99], antelopes and equids [100,101] and rodents [102]. In animals that ingest high amounts of plant secondary metabolites such as tannins, higher TFN values will reflect not only digestibility but also the fact that tannins bind protein, render it indigestible, and lead to higher faecal N excretions on lower-quality (i.e., high-tannin) diets [103]; TFN is therefore limited to animals not consuming significant amounts of tannin-containing forage. TFN has been shown to decrease with increasing BM in free-ranging African herbivores, with an outlier position of the giraffe in three datasets (Fig. 3e), corresponding to this species' high tannin intake in the wild via acacia browse [104]. At the same time, fibre contents increased in the same faecal samples (Fig. 3f). Although faecal fibre has not been validated as an indicator of diet quality, we can assume that a higher faecal fibre content represents a higher proportion of undigested plant residue and hence also a proxy for diet degradability. Recently, Steuer et al. [18] presented data on MFN that indicate that when using this proxy of diet degradability, giraffe appear as no outlier to the overall decreasing trend with increasing BM – suggesting that MFN might be more suitable than TFN to compare a wide range of herbivore species.

In summary, digestibility proxies give the strongest direct support so far for a decreasing diet quality with increasing BM in free-ranging herbivores. While many proxies in gut contents are limited in their use to ruminants, faecal indicators of diet degradability have a high potential to demonstrate variation in herbivores in general. So far, these indicators do not allow conclusions on physiological mechanisms that could bestow larger herbivores with a digestive advantage.

Food Intake

4.1 Herbivores and diet quality: compensating by food intake

If we accept a decrease of diet quality with increasing BM, there are basically two options how herbivores could cope with this predicament [16].

1. If intake and metabolic requirements have the same scaling with BM, then larger animals need a higher digestive efficiency.
2. If larger animals do not achieve higher digestive efficiencies, then the scaling of intake and metabolic requirements must differ; there are three options:
 - a. Metabolic requirements are lower in large herbivores than in other mammals; i.e. while intake scaling is similar across mammals, metabolic scaling is lower in large herbivores.
 - b. Food intake is higher in large herbivores than in other mammals; i.e. while metabolic scaling is similar across mammals, intake scaling is higher in large herbivores.
 - c. A combination of a. and b. could apply.

Although option 1 has been traditionally used to explain large herbivore niche differentiation and diversification, little evidence exists to support it, as described in the chapters above. For option 2a, there is currently no evidence. The most comprehensive comparison of energy intake in herbivores and carnivores (though limited due to a series of assumptions) is probably that of Farlow [105], which shows overlap in the 95% CI for the scaling between the groups. The possibility that herbivores have lower levels of metabolism than vertebrate-eating carnivores has been discussed [38], but this refers to the *level* of metabolism, not its *scaling*. In the study of Capellini et al. [106] where basal metabolic rate was analysed phylogenetically, the scaling in Carnivora was not different from that of other mammalian groups. Nevertheless, the possibility that some megaherbivores have reduced metabolism, as suggested in feeding trials in hippos [107] or potentially in the particularly long gestation period of giraffes and perissodactyls [17], might deserve attention in the future.

In contrast, there is evidence for option 2b, because two independent studies (using different datasets) found that dry matter intake in large herbivores scales to a higher exponent ($BM^{0.84-0.90}$) [16,108] than that of mammalian metabolism ($BM^{0.72}$) [37,106], with confidence intervals not overlapping. Correspondingly, Bourlière [109] found that dry matter intake scaled to $BM^{0.72}$ in 12 carnivorous and to $BM^{0.84}$ in 12 herbivorous species. In a word, larger herbivores do not digest better, they simply eat more.

4.2 Does intake capacity increase with body size?

Could it be that large body size represents an advantage with respect to simply 'eating more'? If this could be demonstrated, then the evolution of large BM might still be driven by lower diet quality. The original concept of the Jarman-Bell-principle (reviewed in [16]) stated a difference in the scaling of gut capacity as measured by wet gut contents, which scales approximately linearly (reviewed in [79]), i.e. to $BM^{1.0}$ (Fig. 6a), and metabolic requirements ($BM^{0.75}$). This difference was interpreted as indicating that in larger animals, more gut capacity is available per unit energy requirement. This could, in theory, also mean more leeway for larger animals in terms of food intake. Empirical tests of this concept are difficult, however, and existing data are controversial.

So far, no easily available proxy exists for intake capacity. The scaling of wet gut contents might be complicated by the possibility that moisture content of digesta increases systematically with BM

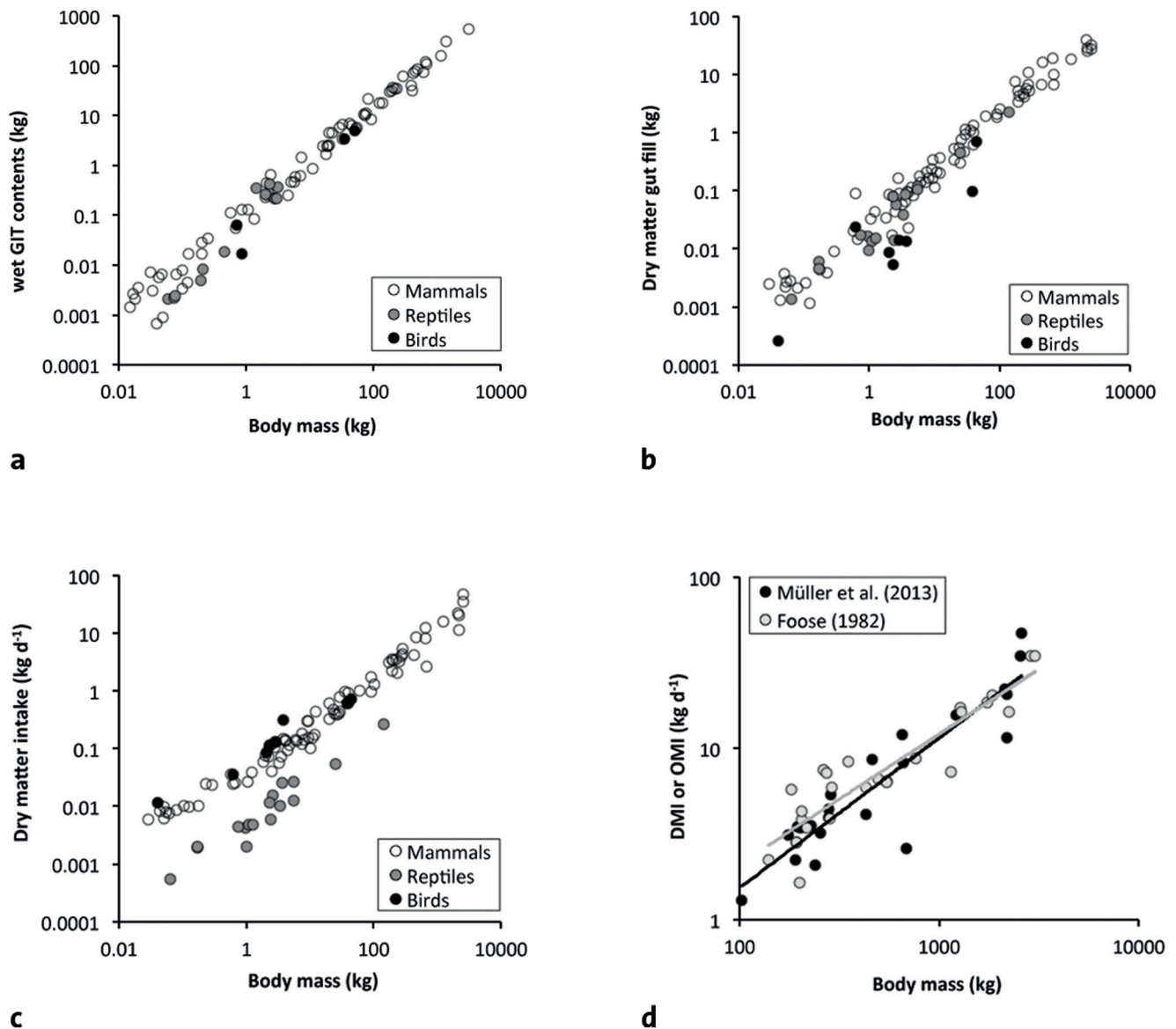


Figure 6. Relationships between body mass (BM) and aspects of the digestive physiology of herbivorous vertebrates. a) wet gut contents [79,122]; note the similarity in all three vertebrate clades, with a duck species (a flying bird) as a notable outlier; b) dry matter gut contents as calculated from simultaneous passage and digestion studies [16,81,82]; note the similarity in the scaling of both measures of gut fill in all three vertebrate clades, with herbivorous birds falling into two categories (flying birds with lower gut fills; flightless or flight-reduced birds such as hoatzin and ostrich with gut fill as in mammals); c) dry matter intake in feeding studies in captivity [16,81,82]; note the generally lower intake in reptiles as compared to mammals and birds; a curvature in mammals is evident with a lower scaling in smaller and a steeper scaling in larger species; d) dry matter intake (DMI, on a variety of diets) [16] or organic matter intake (OMI, on a consistent diet) [66] in mammal herbivores >100 kg (no smaller species included in the Foose dataset); note a tendency for a lower scaling in the Foose dataset (see text) that is not significant, raising the question whether the steeper intake scaling in larger herbivores in the Müller et al. dataset is a reaction to a putative decreasing diet quality with increasing BM.
doi:10.1371/journal.pone.0068714.g006

[16,83], for example to compensate for the increasing diffusion distances in the more voluminous guts of larger herbivores [71]. This would mean that the part of gut capacity that is relevant in terms of nutrient intake, i.e. dry matter gut contents (Fig. 6b), has a slightly lower scaling than one would expect based on wet gut content data. Experimental data from various herbivores in captivity indicate that no statistical difference in the scaling of intake (Fig. 6c) and dry matter gut capacity can be demonstrated [16], but nevertheless they both scale higher than metabolism in large herbivores. Yet, the fact that larger animals increase intake

or gut contents more than metabolism in empirical datasets, where the diet is not controlled, such as in wet gut contents from animals taken from the wild (Fig. 6a), or in data compilations from a variety of feeding studies in captivity (Fig. 6bc) where diet quality might for example systematically differ with BM as in the wild (as suggested by faecal N data for zoo animals in [94]), might simply represent an actual condition where larger animals need to compensate for lower diet quality more distinctively, *and not that smaller animals cannot do so*. They simply might not have to do so under the conditions where the data

were generated – not in the wild, because they can select higher-quality diets, nor in captivity, where they might be fed such diets. Comparing the scaling of intake from a compiled dataset and from a dataset where a consistent diet was fed to large herbivores (Fig. 6d) could suggest this possibility: on the consistent diet, the scaling of intake is numerically lower (i.e., smaller animals eat more) than in the compiled dataset (note that the data scatter is too high and the sample size too low for statistical significance).

Additionally, selected examples could indicate that differences in intake capacity can occur between species of the same body size range, which would make this attribute rather independent from BM but a characteristic of a specific *bauplan*. Apparently, hippos are much more constrained in their capacity for high food intake, in contrast to elephants [110]. On the other end of the BM range, rabbits (*Oryctolagus cuniculus*) are known to have difficulties to maintain condition on low-quality roughage (e.g. [111]), whereas this is not evident in guinea pigs (*Cavia porcellus*), which in comparison feed less selectively and have higher gut fills [112]. Selectively including one or the other species in a comparative dataset could thus yield different conclusions as to effects of BM on intake capacity. To date, current data cannot be reliably used to prove or exclude the possibility that larger body size is linked to a disproportionately higher intake capacity.

4.3 Instantaneous or anticipatory compensation of low diet quality and fasting endurance

Appealing as the concept that larger animals compensate for lower diet quality by a generally increased intake may be, intraspecific data do not unanimously indicate such a strategy. In contrast, larger herbivores typically show a strategy that could be called ‘anticipatory’, with a higher food intake on higher quality diets, and a reduction in food intake on lower quality diets [113]. In particular, reasons for a reduction of intake on lower quality diets remain to be investigated. Traditionally, the reason for this has been sought in a dichotomy between ruminants, which are supposed to be physically limited in their intake capacity by low-quality forage because of rumen physiology, and hindgut fermenters, which should not be thus constrained (reviewed in [113]). Empirical data, however, do not support this dichotomy, and hindgut fermenters also appear to reduce food intake on low quality forages. Reasons for the reduction of food intake on lower quality diets therefore might rather be related either to gut fill limitations on lower quality forages that apply to all herbivores, or to higher endogenous and metabolic losses on such diets. Only in some smaller herbivores (who also practice coprophagy, which reduces endogenous/metabolic losses) was an ‘instantaneous’ compensation - increasing food intake with lower diet quality – observed [113]. This difference matches the higher capacity for resource accretion as body (adipose) tissue and the corresponding higher fasting endurance in larger animals [114–116]. In addition to a strategy of accreting body reserves, larger animals are also more likely to adopt a strategy of migration to ensure high forage quality [117]. In contrast, smaller animals are mostly unable to evade their habitat in times of lower food quality, and need to resort either to energy saving via a reduction in metabolism, such as hibernation, or to food caching, or have to live on the lower quality food. Fasting endurance is an important benefit bestowed by large body size [31], but is notably not a direct effect of alterations in digestive physiology.

Relevance for Dinosaur Gigantism

What conclusions do these physiological reflections allow for giant dinosaur herbivores? From comparisons with extant representatives of putative dinosaur food plants [118], there do not appear to be major differences in the fermentation characteristics between dinosaur forage and important extant mammal herbivore forage like browse [51,89]. Possible differences in nitrogen content [14,89] and plant secondary compounds cannot be considered as drivers of directed body size evolution, as explained in sections 3.1 and 3.2.

Sauropod dinosaurs are peculiar due to the absence of a particle size reduction mechanism (chewing teeth or gastric mill) [119]. Given indications for a high level of metabolism in sauropods due to their fast growth [1], we would thus expect a food intake level comparable to mammals (Fig. 6c) combined with digesta particle sizes comparable to reptiles (Fig. 5a). The faster digesta passage, i.e. the shorter retention times in mammals as compared to reptiles are usually interpreted as possible due to the higher degree of particle size reduction, because smaller particles can be fermented faster by microorganisms [82,120], and a compensation between retention time and chewing efficiency is also evident in mammals [87,121]. Therefore, we would expect retention times in sauropod dinosaurs to be more similar to those of reptiles (Fig. 5c), to efficiently digest the non-comminuted digesta. Because of a link between food intake and retention time (times are shorter at higher intake levels) (Fig. 7a) [81,112], a plausible mechanism to maintain a reptile retention time at a mammalian food intake would be to have higher gut capacities than reported for both reptiles and mammals (Fig. 6ab). Actually, a comparison of the reconstructed volume of the coelomic cavity of a sauropod with the volume of the organs within that cavity suggest sufficient spare capacity of that coelomic cavity to accommodate disproportionately large guts [122]. Based on this logic, we would expect non-chewing herbivorous dinosaurs with a high metabolism, such as sauropods, to have comparatively larger coelomic cavities than chewing herbivorous dinosaurs, such as ornithopods. This hypothesis awaits testing. Another hypothesis, namely ontogenetically reduced metabolic rates in adult sauropods [123], provides a convenient *ad hoc* explanation yet is more difficult to test.

Allometries related to chewing and particle size reduction can potentially indicate that the absence of chewing in sauropods is a condition that does not necessarily drive but facilitate gigantism [1,123]. An important part of mammalian foraging time is dedicated to the act of (ingestive) mastication [21]. According to the scaling of foraging time [42] (Fig. 7b), mammal nonruminant herbivores above a BM threshold of 18 tons would require more than 24 h of foraging time per day. Evidently, the database for this allometry consists of few species, and the magnitude of scaling would change distinctively if only a few values were added or existing ones modified. Nevertheless, it is intriguing that none of the largest chewing herbivores, neither the largest mammal, the *Indricotherium* [124], nor the large ornithischians with their impressive chewing dentition [125] – such as *Shantungosaurus* [126], surpass this mass threshold [127]. The interpretation appears attractive that herbivores, once they evolved the very efficient adaptation of mastication, were generally prevented from evolving giant body size because this would have necessitated a secondary loss of mastication. Thus, it seems that a primitive feature of sauropods – the absence of mastication – allowed them to enter the niche of giants. It remains to be seen whether findings of ornithischians beyond the BM threshold do or do not show characteristics of a chewing dentition.

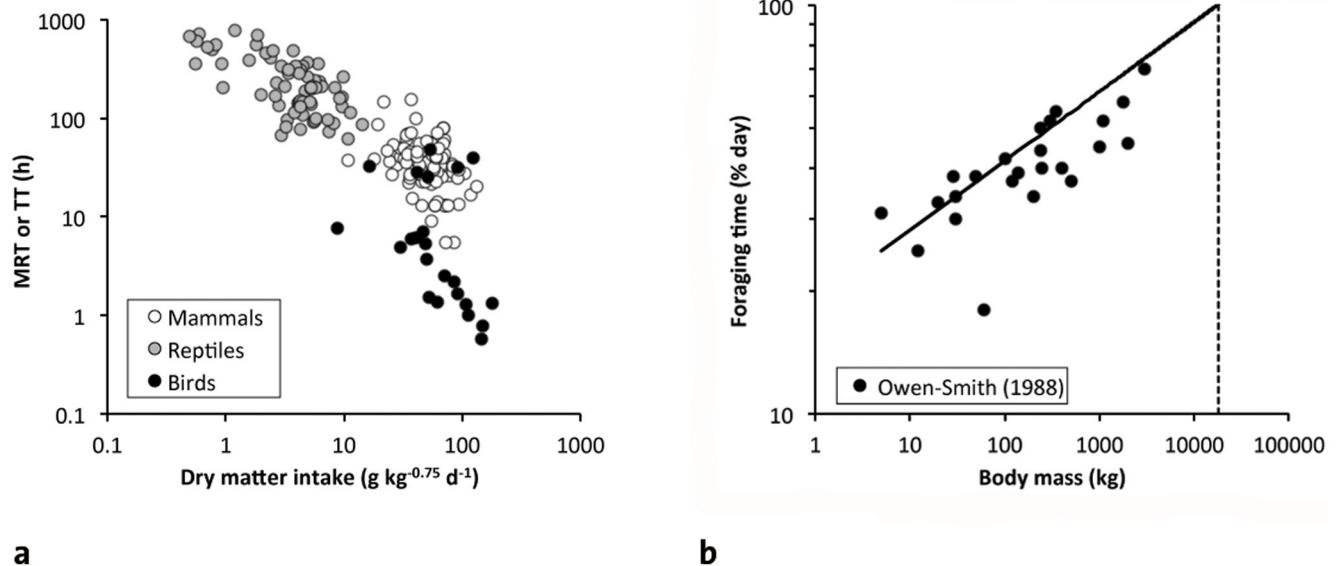


Figure 7. Relationships between aspects of the digestive physiology of herbivorous vertebrates. a) the relative food intake (per unit metabolic body weight) and the passage of digesta through the gastrointestinal tract (measured as mean retention time MRT or, in the case of some reptiles, as transit time TT) [81,112]; note that species/individuals with a higher food intake have shorter retention times; note that flying birds show a similar relationship on a lower level, potentially due to their smaller gut capacity (cf. Fig. 6b); b) body mass and foraging time for hindgut fermenters and ruminants [42] (regression given for hindgut fermenters; extrapolation to 100% of the day yields an upper BM limit of app. 18 tons). doi:10.1371/journal.pone.0068714.g007

Finally, with respect to another digestive side-effect, as long as the few existing indications that herbivorous birds, which are closer related to dinosaurs, have a dramatically lower methane production than mammals (reviewed in [81]) are not refuted, extrapolations on the production of methane by dinosaur faunas based on mammal data (e.g. [128]) should be viewed with scepticism.

To conclude, we think that existing data suggest that other putative advantages of large body size [1] are more promising candidates for the explanation of the evolution of gigantism than digestive physiology.

Outlook on Outliers: Which Rule Do Exceptions Prove?

In mammals, birds and reptiles, small-bodied herbivore species have been described that appear to ‘break’ or ‘bend’ the ‘ecophysiological rule’ that small BM must be linked to high-quality diets [83,129,130]. What do these outliers tell us? The traditional approach to such species is to identify physiological mechanisms that allow them to use these unexpected resources. We want to propose a different scenario, based on the logic outlined in section 1.2 that a ‘higher mass-specific metabolic requirement’ in itself has no explanatory power. Rather than using a physiological argument, we suggest an ecological one.

If we accept the theoretical possibility that animals of any size can use diets of any quality, given that these diets are available in sufficient quantity and accessible packages, we will, in terrestrial systems, still end up with a dichotomy of choices: because of forage abundance and the impracticability of selective feeding, larger herbivores are (mostly) confined to low quality diets. Small herbivores, however, theoretically have both options – because of their smaller absolute requirements, and their smaller feeding apparatus, they can use both, high and low quality diets. Smaller animals might be excluded from a

certain range of plants or plant parts because of physical limitations, especially in the cropping of larger-diameter lignified tissues (stems and twigs); yet, adaptations to such diets exist, as in the gnawing feeding style of rodents [131]. Note that this is a physical argument related to the mechanics of feeding, not to digestive physiology.

Rather than suggesting that small herbivores *cannot* use the lower diet quality, we could ask – why *should* they? Given their opportunity to use the higher-quality resource, it appears plausible that they would focus on the latter, and potentially even lose, over evolutionary time, adaptations to cope with the former – *not because of a body size-driven physiological necessity, but because of ecological opportunity*. Exploring this scenario, and testing it against patterns actually observed, could represent a promising approach to understand ecological and evolutionary patterns in herbivores. It might also allow to integrate the under-emphasized outlier position of extant megaherbivores in many datasets presented in this review, and link herbivore nutritional ecology by unifying concepts of biomass availability and food accessibility to that of omnivores and carnivores. Shifting the focus from a putative link with digestive physiology that might, in many cases, rest on a rhetoric misunderstanding, to an ecological approach, might finally yield better theories about the relationship of diet and body size that match actually observed patterns both in extant herbivores and in the fossil record (e.g. [132]).

Acknowledgments

We thank Peter Dodson, Norman Owen-Smith and an anonymous reviewer for their comments on the manuscript.

Author Contributions

Conceived and designed the experiments: MC JH. Performed the experiments: MC PS JH. Analyzed the data: MC PS DM DC JH. Wrote the paper: MC PS DM DC JH.

References

- Sander PM, Christian A, Clauss M, Fechner R, Gee CT, et al. (2011) Biology of the sauropod dinosaurs: the evolution of gigantism. *Biological Reviews* 86: 117–155.
- Calvo JO (1994) Jaw mechanics in sauropod dinosaurs. *GAIA* 10: 183–193.
- Christiansen P (2000) Feeding mechanisms of the sauropod dinosaurs *Brachiosaurus*, *Camarasaurus*, *Diplodocus*, and *Dicraeosaurus*. *Historical Biology* 14: 137–152.
- Upchurch P, Barrett PM (2000) The evolution of sauropod feeding mechanisms. In: Sues HD, editor. *Evolution of herbivory in terrestrial vertebrates Perspectives from the fossil record*. Cambridge: Cambridge University Press. pp. 79–122.
- Fiorillo AR (1998) Dental microwear of sauropod dinosaurs *Camarasaurus* and *Diplodocus*: evidence for resource partitioning in the Late Jurassic of North America. *Historical Biology* 13: 1–16.
- Galton PM (1986) Herbivorous adaptations of Late Triassic and Early Jurassic dinosaurs. In: Padian K, editor. *The beginning of the age of the dinosaurs*. Cambridge: Cambridge University Press. pp. 203–221.
- Bakker R (1986) *The dinosaur heresies*. Harlow, UK: Longman Scientific & Technical.
- Barrett PM, Upchurch P (2005) Sauropod diversity through time: possible macroevolutionary and palaeoecological implications. In: Curry-Rogers KA, Wilson J, editors. *The sauropods: evolution and paleobiology*. Berkeley: University of California Press. pp. 125–156.
- Tütken T (2011) The diet of sauropod dinosaurs: implications of carbon isotope analysis on teeth, bones, and plants. In: Klein N, Remes K, Gee CT, Sander PM, editors. *Understanding the life of giants The biology of the sauropod dinosaurs*. Bloomington: Indiana University Press. pp. 57–79.
- Stevens KA, Parrish JM (2005) Neck posture, dentition, and feeding strategies in Jurassic sauropod dinosaurs. In: Tidwell V, Carpenter K, editors. *Therapsids: The sauropodomorph dinosaurs*. Bloomington: Indiana University Press. pp. 212–232.
- Christian A, Dzemski G (2011) Neck posture in sauropods. In: Klein N, Remes K, Gee CT, Sander PM, editors. *Understanding the life of giants The biology of the sauropod dinosaurs*. Bloomington: Indiana University Press. pp. 251–260.
- Farlow JO, Coroian ID, Foster JR (2010) Giants on the landscape: modelling the abundance of megaherbivorous dinosaurs of the Morrison Formation (Late Jurassic, western USA). *Historical Biology* 22: 403–429.
- Farlow JO (1987) Speculations about the diet and digestive physiology of herbivorous dinosaurs. *Paleobiology* 13: 60–72.
- Wilkinson DM, Ruxton GD (2013) High C/N ratio (not low-energy content) of vegetation may have driven gigantism in sauropod dinosaurs and perhaps omnivory and/or endothermy in their juveniles. *Functional Ecology* 27: 131–135.
- Sibly RM, Brown JH, Kodric-Brown A, editors (2012) *Metabolic ecology. A scaling approach*. Chichester, UK: Wiley-Blackwell.
- Müller DWH, Codron D, Meloro C, Munn AJ, Schwarm A, et al. (2013) Assessing the Jarman-Bell Principle: scaling of intake, digestibility, retention time and gut fill with body mass in mammalian herbivores. *Comparative Biochemistry and Physiology A* 164: 129–140.
- Clauss M, Dittmann MT, Müller DHW, Zerbe P, Codron D (2013) Low scaling of a life history variable: analysing eutherian gestation periods with and without phylogeny-informed statistics. *Mammalian Biology* (in press) doi 10.1016/j.mambio.2013.01.002.
- Steuer P, Südekum K-H, Tütken T, Müller DHW, Bucher M, et al. (subm.) Large herbivore body mass does not convey a digestive advantage.
- Lukas M, Südekum K-H, Rave G, Friedel K, Susenbeth A (2005) Relationship between fecal crude protein concentration and diet organic matter digestibility in cattle. *Journal of Animal Science* 83: 1332–1344.
- Holleman DF, White RG (1989) Determination of digesta fill and passage rate from non absorbed particulate phase markers using the single dosing method. *Canadian Journal of Zoology* 67: 488–494.
- Hummel J, Clauss M (2011) Feeding and digestive physiology. In: Klein N, Remes K, Gee CT, Sander PM, editors. *Understanding the life of giants The biology of the sauropod dinosaurs*. Bloomington: Indiana University Press. pp. 11–33.
- McNab BK (1999) On the comparative ecological and evolutionary significance of total and mass-specific rates of metabolism. *Physiological and Biochemical Zoology* 72: 642–644.
- Geist V (1974) On the relationship of social evolution and ecology in ungulates. *American Zoologist* 14: 205–220.
- Demment MW, Van Soest PJ (1985) A nutritional explanation for body size patterns of ruminant and nonruminant herbivores. *American Naturalist* 125: 641–672.
- Carbone C, Mace GM, Roberts SC, Macdonald DW (1999) Energetic constraints on the diet of terrestrial carnivores. *Nature* 402: 286–288.
- Carbone C, Teacher A, Rowcliffe JM (2007) The costs of carnivory. *PLoS Biology* 5: e22.
- Christiansen P (1999) On the head size of sauropodomorph dinosaurs: implications for ecology and physiology. *Historical Biology* 13: 269–297.
- Gordon JJ, Illius AW (1988) Incisor arcade structure and diet selection in ruminants. *Functional Ecology* 2: 15–22.
- Potvin J, Goldbogen JA, Shadwick RE (2012) Metabolic expenditures of lunge feeding rorquals across scale: implications for the evolution of filter feeding and the limits to maximum body size. *PLoS ONE* 7: e44854.
- Midgley JJ, Midgley G, Bond WJ (2002) Why were dinosaurs so large? A food quality hypothesis. *Evolutionary Ecology Research* 4: 1093–1095.
- Illius AW, Gordon JJ (1999) The physiological ecology of mammalian herbivory. In: Jung HJG, Fahey GC, editors. *Nutritional ecology of herbivores*. Savoy, IL: The American Society of Animal Science. pp. 71–96.
- Freeland WJ (1991) Plant secondary metabolites: biochemical coevolution with herbivores. In: Palo RT, Robbins CT, editors. *Plant defenses against mammalian herbivory*. Boca Raton: CRC Press Inc. pp. 61–81.
- Westoby M (1974) An analysis of diet selection by large generalist herbivores. *American Naturalist* 108: 290–304.
- Marsh KJ, Wallis IR, McLean S, Sorensen JS, Foley WJ (2006) Conflicting demands on detoxification pathways influence how common brushtail possums choose their diets. *Ecology* 87: 2103–2112.
- Guthrie RD (1984) Mosaics, allelochemicals and nutrients: an ecological theory of late Pleistocene gigantism. In: Martin PS, Klein RG, editors. *Quaternary extinctions. A prehistoric evolution*. Tucson: University of Arizona Press. pp. 259–298.
- Butler RJ, Barrett PM, Kenrick P, Penn MG (2009) Diversity patterns amongst herbivorous dinosaurs and plants during the Cretaceous: implications for hypotheses of dinosaur/angiosperm co-evolution. *Journal of Evolutionary Biology* 22: 446–459.
- Müller DWH, Codron D, Werner J, Fritz J, Hummel J, et al. (2012) Dichotomy of eutherian reproduction and metabolism. *Oikos* 121: 102–115.
- McNab BK (2008) An analysis of the factors that influence the level and scaling of mammalian BMR. *Comparative Biochemistry and Physiology A* 151: 5–28.
- Cork SJ, Foley WJ (1991) Digestive and metabolic strategies of arboreal mammalian folivores in relation to chemical defenses in temperate and tropical forests. In: Palo RT, Robbins CT, editors. *Plant defenses against mammalian herbivores*. Boca Raton: CRC Press. pp. 133–166.
- Sorensen JS, Dearing MD (2004) Physiological limitations of dietary specialization in herbivorous woodrats (*Neotoma* spp.). *International Congress Series* 1275: 313–320.
- Sorensen JS, Dearing MD (2003) Elimination of plant toxins by herbivorous woodrats: revisiting an explanation for dietary specialization in mammalian herbivores. *Oecologia* 134: 88–94.
- Owen-Smith N (1988) Megaherbivores - the influence of very large body size on ecology. Cambridge: Cambridge University Press.
- Kleynhans EJ, Jolles AE, Bos MRE, Olff H (2011) Resource partitioning along multiple niche dimensions in differently sized African savanna grazers. *Oikos* 120: 591–600.
- Morris JG, Rogers QR (1986) Comparative nitrogen nutrition of carnivorous, herbivorous and omnivorous mammals. *Archives of Animal Nutrition* 36: 234–245.
- Midgley JJ (2005) Why don't leaf-eating animals prevent the formation of vegetation? Relative vs. absolute dietary requirements. *New Phytologist* 168: 271–273.
- Smith AP, Green SW (1987) Nitrogen requirements of the sugar glider (*Petaurus graciceps*) an omnivorous marsupial, on a honey-pollen diet. *Physiological Zoology* 60: 82–92.
- Klaassen M, Nolet BA (2008) Stoichiometry of endothermy: shifting the quest from nitrogen to carbon. *Ecology Letters* 11: 785–792.
- Robbins CT (1993) *Wildlife feeding and nutrition*. San Diego: Academic Press.
- Brody S, Procter RC, Ashworth US (1934) Basal metabolism, endogenous nitrogen, creatinine and neutral sulphur excretions as functions of body weight. *University of Missouri Agricultural Experimental Station Residential Bulletin* 220: 1–40.
- Van Soest PJ (1994) *Nutritional ecology of the ruminant*. Ithaca: Cornell University Press. 476 p.
- Hummel J, Südekum K-H, Streich WJ, Clauss M (2006) Forage fermentation patterns and their implications for herbivore ingesta retention times. *Functional Ecology* 20: 989–1002.
- Woodall PF (1992) An evaluation of a rapid method for estimating digestibility. *African Journal of Ecology* 30: 181–185.
- Hillman JC, Gwynne MD (1987) Feeding of the Bongo antelope (*Tragelaphus eurycerus*) in south west Sudan. *Mammalia* 51: 53–64.
- Owen-Smith N, Chafota J (2012) Selective feeding by a megaherbivore, the African elephant (*Loxodonta africana*). *Journal of Mammalogy* 93: 698–705.
- Sensign R, Demment MW, Laca EA (2010) Allometric scaling predicts preferences for burned patches in a guild of East African grazers. *Ecology* 91: 2898–2907.
- Cromsigt JPM, Olff H (2006) Resource partitioning among savanna grazers mediated by local heterogeneity: an experimental approach. *Ecology* 87: 1532–1541.
- Arsenault R, Owen-Smith N (2008) Resource partitioning by grass height among grazing ungulates does not follow body size relation. *Oikos* 117: 1711–1717.

58. Olff H, Riechert ME, Prins HHT (2002) Global environmental controls of diversity in large herbivores. *Nature* 415: 901–904.
59. Bholá N, Ogotu JO, Piepho H-P, Said MY, Reid RS, et al. (2012) Comparative changes in density and demography of large herbivores in the Masai Mara Reserve and its surrounding human-dominated pastoral ranches in Kenya. *Biodiversity and Conservation* 21: 1509–1530.
60. Hopcraft JGC, Anderson TM, Pérez-Vila S, Mayemba E, Olff H (2012) Body size and the division of niche space: food and predation differentially shape the distribution of Serengeti grazers. *Journal of Animal Ecology* 81: 201–213.
61. Crooms J, Prins HHT, Olff H (2009) Habitat heterogeneity as a driver of ungulate diversity and distribution patterns: interaction of body mass and digestive strategy. *Diversity and Distributions* 15: 513–522.
62. du Toit JT, Owen-Smith N (1989) Body size, population metabolism, and habitat specialization among large African herbivores. *American Naturalist* 133: 736–740.
63. Shrader A, Owen-Smith N, Ogotu JO (2006) How a mega-grazer copes with the dry season: food and nutrient intake rates by white rhinoceros in the wild. *Functional Ecology* 20: 376–384.
64. Olivier RCD, Laurie WA (1974) Habitat utilization by hippopotamus in the Mara River. *African Journal of Ecology* 12: 249–271.
65. Demment MW (1983) Feeding ecology and the evolution of body size of baboons. *African Journal of Ecology* 21: 219–233.
66. Foote TJ (1982) Trophic strategies of ruminant versus nonruminant ungulates. Chicago: University of Chicago.
67. Owen-Smith N, Novellie P (1982) What should a clever ungulate eat? *American Naturalist* 119: 151–178.
68. Van Soest PJ (1996) Allometry and ecology of feeding behavior and digestive capacity in herbivores: a review. *Zoo Biology* 15: 455–479.
69. Karasov WH (2012) Terrestrial vertebrates. In: Sibly RM, Brown JH, Kodric-Brown A, editors. *Metabolic ecology. A scaling approach*. Chichester, UK: Wiley-Blackwell. pp. 212–224.
70. Taylor SCS, Murray JI (1987) Genetic aspects of mammalian survival and growth in relation to body size. In: Hacker JB, Ternouth JH, editors. *The nutrition of herbivores*. Sydney: Academic Press. pp. 487–533.
71. Clauss M, Hummel J (2005) The digestive performance of mammalian herbivores: why big may not be *that* much better. *Mammal Review* 35: 174–187.
72. Fritz J, Hummel J, Kienzle E, Arnold C, Nunn C, et al. (2009) Comparative chewing efficiency in mammalian herbivores. *Oikos* 118: 1623–1632.
73. Fritz J, Hummel J, Kienzle E, Streich WJ, Clauss M (2010) To chew or not to chew: faecal particle size in herbivorous reptiles and mammals. *Journal of Experimental Zoology A* 313: 579–586.
74. Fritz J, Hummel J, Kienzle E, Wings O, Streich WJ, et al. (2011) Gizzard vs. teeth, it's a tie: food-processing efficiency in herbivorous birds and mammals and implications for dinosaur feeding strategies. *Paleobiology* 37: 577–586.
75. Franz R, Soliva CR, Kreuzer M, Hummel J, Clauss M (2011) Methane in rabbits (*Oryctolagus cuniculus*) and guinea pigs (*Cavia porcellus*) on a hay-only diet: implications for the scaling of methane production with body mass in nonruminant mammalian herbivores. *Comparative Biochemistry and Physiology A* 158: 177–181.
76. Franz R, Soliva CR, Kreuzer M, Steuer P, Hummel J, et al. (2010) Methane production and body mass in ruminants and equids. *Evolutionary Ecology Research* 12: 727–738.
77. Franz R, Soliva CR, Kreuzer M, Hatt J-M, Furrer S, et al. (2011) Methane output of tortoises: its contribution to energy loss related to herbivore body mass. *PLoS One* 6: e17628.
78. Müller DWH, Caton J, Codron D, Schwarm A, Lentle R, et al. (2011) Phylogenetic constraints on digesta separation: variation in fluid throughput in the digestive tract in mammalian herbivores. *Comparative Biochemistry and Physiology A* 160: 207–220.
79. Clauss M, Schwarm A, Ortmann S, Streich WJ, Hummel J (2007) A case of non-scaling in mammalian physiology? Body size, digestive capacity, food intake, and ingesta passage in mammalian herbivores. *Comparative Biochemistry and Physiology A* 148: 249–265.
80. Steuer P, Südekum K-H, Müller DWH, Franz R, Kaandorp J, et al. (2011) Is there an influence of body mass on digesta mean retention time in herbivores? A comparative study on ungulates. *Comparative Biochemistry and Physiology A* 160: 355–364.
81. Fritz J, Hammer S, Hebel C, Arif A, Michalke B, et al. (2012) Retention of solutes and different-sized particles in the digestive tract of the ostrich (*Struthio camelus massaicus*), and a comparison with mammals and reptiles. *Comparative Biochemistry and Physiology A* 163: 56–65.
82. Franz R, Hummel J, Müller DWH, Bauert M, Hatt J-M, et al. (2011) Herbivorous reptiles and body mass: effects on food intake, digesta retention, digestibility and gut capacity, and a comparison with mammals. *Comparative Biochemistry and Physiology A* 158: 94–101.
83. Justice KE, Smith FA (1992) A model of dietary fiber utilization by small mammalian herbivores, with empirical results for *Neotoma*. *American Naturalist* 139: 398–416.
84. Wenninger PS, Shipley LA (2000) Harvesting, rumination, digestion, and passage of fruit and leaf diets by a small ruminant, the blue duiker. *Oecologia* 123: 466–474.
85. Pérez-Barbería FJ, Elston DA, Gordon IJ, Illius AW (2004) The evolution of phylogenetic differences in the efficiency of digestion in ruminants. *Proceedings of the Royal Society B* 271: 1081–1090.
86. Steuer P, Südekum K-H, Müller DWH, Kaandorp J, Clauss M, et al. (2013) Fibre digestibility in large herbivores as related to digestion type and body mass - an in vitro approach. *Comparative Biochemistry and Physiology A* 164: 319–326.
87. Clauss M, Nunn C, Fritz J, Hummel J (2009) Evidence for a tradeoff between retention time and chewing efficiency in large mammalian herbivores. *Comparative Biochemistry and Physiology A* 154: 376–382.
88. Duncan P, Foote TJ, Gordon IJ, Gakahu CG, Lloyd M (1990) Comparative nutrient extraction from forages by grazing bovinds and equids: a test of the nutritional model of equid/bovid competition and coexistence. *Oecologia* 84: 411–418.
89. Hummel J, Gee CT, Südekum K-H, Sander PM, Nogge G, et al. (2008) In vitro digestibility of fern and gymnosperm foliage - implications for sauropod feeding ecology and diet selection. *Proceedings of the Royal Society B* 275: 1015–1021.
90. Stevens CE, Hume ID (1998) Contributions of microbes in vertebrate gastrointestinal tract to production and conservation of nutrients. *Physiological Reviews* 78: 393–427.
91. Hoppe PP, Van Hoven W, von Engelhardt W, Prins RA, Lankhorst A, et al. (1983) Pregastric and caecal fermentation in dikdik (*Madoqua kirki*) and suni (*Nesotragus moschatus*). *Comparative Biochemistry and Physiology A* 75: 517–524.
92. Field CR (1970) A study of the feeding habits of the hippopotamus in the Queen Elizabeth National Park, Uganda, with some management implications. *Zoologica Africana* 5: 71–86.
93. Gordon IJ, Illius AW (1994) The functional significance of the browser-grazer dichotomy in African ruminants. *Oecologia* 98: 167–175.
94. Schwarm A, Schweigert M, Ortmann S, Hummel J, Jarssens G, et al. (2009) No easy solution for the fractionation of faecal nitrogen in captive wild herbivores: results of a pilot study. *Journal of Animal Physiology and Animal Nutrition* 93: 596–605.
95. Wehausen JD (1995) Fecal measures of diet quality in wild and domestic ruminants. *Journal of Wildlife Management* 59: 816–823.
96. Wang CJ, Tas BM, Glindemann T, Rave G, Schmidt L, et al. (2009) Fecal crude protein content as an estimate for the digestibility of forage in grazing sheep. *Animal Feed Science and Technology* 149: 199–208.
97. Mésochina P, Martin-Rosset W, Peyraud J, Duncan P, Micol D, et al. (1998) Prediction of the digestibility of the diet of horses: evaluation of faecal indices. *Grass and Forage Science* 53: 189–196.
98. Irwin LL, Cook JG, McWhirter DE, Smith SG, Arnett EB (1993) Assessing winter dietary quality in bighorn sheep via fecal nitrogen. *Journal of Wildlife Management* 57: 413–421.
99. Osborn RG, Ginnett TF (2001) Fecal nitrogen and 2,6-diaminopimelic acid as indices to dietary nitrogen in white-tailed deer. *Wildlife Society Bulletin* 29: 1131–1139.
100. Jhala YV (1997) Seasonal effects on the nutritional ecology of blackbuck (*Antelope cervicapra*). *Journal of Applied Ecology* 34: 1348–1358.
101. Wrench JM, Meissner HH, Grant CC (1997) Assessing diet quality of African ungulates from faecal analyses: the effect of forage quality, intake and herbivore species. *Koedoe* 40: 125–136.
102. Loeb SC, Schwab RG (1989) An evaluation of three methods for determining diet quality of free-ranging small herbivorous mammals. *Canadian Journal of Zoology* 67: 96–102.
103. Robbins CT, Hanley TA, Hagermann AE, Hjeljord O, Baker DL, et al. (1987) Role of tannins in defending plants against ruminants: reduction in protein availability. *Ecology* 68: 98–107.
104. Furstenburg D, van Hoven W (1994) Condensed tannin as anti-defoliate agent against browsing by giraffe (*Giraffa camelopardalis*) in the Kruger National Park. *Comparative Biochemistry and Physiology A* 107: 425–431.
105. Farlow JO (1976) A consideration of the trophic dynamics of a late cretaceous large-dinosaur community (Oldman Formation). *Ecology* 57: 841–857.
106. Capellini I, Venditti C, Barton RA (2010) Phylogeny and metabolic scaling in mammals. *Ecology* 91: 2783–2793.
107. Schwarm A, Ortmann S, Hofer H, Streich WJ, Flach EJ, et al. (2006) Digestion studies in captive *hippopotamidae*: a group of large ungulates with an unusually low metabolic rate. *Journal of Animal Physiology and Animal Nutrition* 90: 300–308.
108. Hackmann TJ, Spain JN (2010) Ruminant ecology and evolution: perspectives useful to ruminant livestock research and production. *Journal of Dairy Science* 93: 1320–1334.
109. Bourlière F (1975) Mammals, small and large: the ecological implications of size. In: Golley FB, Petruszewicz K, Ryszkowski L, editors. *Small mammals: their productivity and population dynamics*. Cambridge: Cambridge University Press. pp. 1–8.
110. Clauss M, Streich WJ, Schwarm A, Ortmann S, Hummel J (2007) The relationship of food intake and ingesta passage predicts feeding ecology in two different megaherbivore groups. *Oikos* 116: 209–216.
111. Udén P, Van Soest PJ (1982) Comparative digestion of timothy fiber by ruminants, equines and rabbits. *British Journal of Nutrition* 47: 267–272.
112. Franz R, Kreuzer M, Hummel J, Hatt J-M, Clauss M (2011) Intake, selection, digesta retention, digestion and gut fill of two coprophagous species, rabbits

- (*Oryctolagus cuniculus*) and guinea pigs (*Cavia porcellus*), on a hay-only diet. *Journal of Animal Physiology and Animal Nutrition* 95: 564–570.
113. Meyer K, Hummel J, Clauss M (2010) The relationship between forage cell wall content and voluntary food intake in mammalian herbivores. *Mammal Review* 40: 221–245.
 114. Barboza PS, Hume ID (2006) Physiology of intermittent feeding: integrating responses of vertebrates to nutritional deficit and excess. *Physiological and Biochemical Zoology* 79: 250–264.
 115. Lindstedt SL, Boyce MS (1985) Seasonality, fasting endurance, and body size in mammals. *American Naturalist* 125: 873–878.
 116. Millar JS, Hickling GJ (1990) Fasting endurance and the evolution of mammalian body size. *Functional Ecology* 4: 5–12.
 117. Fryxell JM, Sinclair AJ (1988) Causes and consequences of migration by large herbivores. *Trends in Ecology and Evolution* 3: 324–341.
 118. Gee CT (2011) Dietary options for the sauropod dinosaurs from an integrated botanical and paleobotanical perspective. In: Klein N, Remes K, Gee CT, Sander PM, editors. *Understanding the life of giants The biology of the sauropod dinosaurs*. Bloomington: Indiana University Press. pp. 34–56.
 119. Wings O, Sander PM (2007) No gastric mill in sauropod dinosaurs: new evidence from analysis of gastrolith mass and function in ostriches. *Proceedings of the Royal Society B* 274: 635–640.
 120. Karasov WH, Petrossian E, Rosenberg L, Diamond JM (1986) How do food passage rate and assimilation differ between herbivorous lizards and nonruminant mammals? *Journal of Comparative Physiology B* 156: 599–609.
 121. Schwarm A, Ortmann S, Wolf C, Streich WJ, Clauss M (2009) More efficient mastication allows increasing intake without compromising digestibility or necessitating a larger gut: comparative feeding trials in banteng (*Bos javanicus*) and pygmy hippopotamus (*Hexaprotodon liberiensis*). *Comparative Biochemistry and Physiology A* 152: 504–512.
 122. Franz R, Hummel J, Kienzle E, Kölle P, Gunga HC, et al. (2009) Allometry of visceral organs in living amniotes and its implications for sauropod dinosaurs. *Proceedings of the Royal Society B* 276: 1731–1736.
 123. Sander PM, Clauss M (2008) Sauropod gigantism. *Science* 322: 200–201.
 124. Fortelius M, Kappelman J (1993) The largest land mammal ever imagined. *Zoological Journal of the Linnean Society* 107: 85–101.
 125. Erickson GM, Krick DA, Hamilton M, Bourne GR, Norell MA, et al. (2012) Complex dental structure and wear biomechanics in hadrosaurid dinosaurs. *Science* 338: 98–101.
 126. Horner JR, Weishampel DB, Forster CA (2004) Hadrosauridae. In: Weishampel DB, Dodson P, Osmólska H, editors. *The dinosauria*. Berkeley: University of California Press. pp. 438–463.
 127. Clauss M (2011) Sauropod biology and the evolution of gigantism: what do we know? In: Klein N, Remes K, Gee CT, Sander PM, editors. *Understanding the life of giants The biology of the sauropod dinosaurs*. Bloomington: Indiana University Press. pp. 3–7.
 128. Wilkinson DM, Nisbet EG, Ruxton GD (2012) Could methane produced by sauropod dinosaurs have helped drive Mesozoic climate warmth? *Current Biology* 22: R292–R293.
 129. Espinoza RE, Wiens JJ, Tracy CR (2004) Recurrent evolution of herbivory in small, cold-climate lizards: breaking the ecophysiological rules of reptilian herbivory. *Proceedings of the National Academy of Science* 101: 16819–16824.
 130. Foley WJ, Cork SJ (1992) Use of fibrous diets by small herbivores: how far can the rules be 'bent'? *Trends in Ecology and Evolution* 7: 159–162.
 131. Hiimeae KM (2000) Feeding in mammals. In: Schwenk K, editor. *Feeding Form, function, and evolution in tetrapod vertebrates*. San Diego CA: Academic Press. pp. 411–448.
 132. Zanno LE, Makovicky PJ (2013) No evidence for directional evolution of body mass in herbivorous theropod dinosaurs. *Proceedings of the Royal Society B* 280: 20122526.
 133. Hoppe PP, Qvortrup SA, Woodford MH (1977) Rumen fermentation and food selection in East African sheep, goats, Thomson's gazelle, Grant's gazelle and impala. *Journal of Agricultural Science (Cambridge)* 89: 129–135.
 134. Hoppe PP, Qvortrup SA, Woodford MH (1977) Rumen fermentation and food selection in East African Zebu cattle, wildebeest, Coke's hartebeest and topi. *Journal of Zoology* 181: 1–9.
 135. Hoppe PP (1977) Rumen fermentation and body weight in African ruminants. In: Peterle TJ, editor. *13th Congress of Game Biology*. Washington DC: The Wildlife Society. pp. 141–150.
 136. Hall-Martin AJ (1974) Food selection by Transvaal lowveld giraffe as determined by analysis of stomach contents. *Journal of the South African Wildlife Management Association* 4: 191–202.
 137. Scotcher JSB, Stewart DRM, Breen CM (1978) The diet of the hippopotamus in Ndumu game reserve, Natal, as determined by faecal analysis. *South African Journal of Wildlife Research* 8: 1–11.
 138. Jarman PJ, Sinclair ARE (1979) Feeding strategy and the pattern of resource partitioning in ungulates. In: Sinclair ARE, Norton-Griffiths M, editors. *Serengeti: dynamics of an ecosystem*. Chicago: University of Chicago Press. pp. 130–163.
 139. Barnes RFW (1982) Elephant feeding behaviour in Ruaha National Park, Tanzania. *African Journal of Ecology* 20: 123–136.
 140. Irby LR (1977) Food habits of Chanler's mountain reedbeek in a Rift valley ranch. *East African Wildlife Journal* 15: 289–294.
 141. Clemens ET, Maloiy GMO (1983) Digestive physiology of East African wild ruminants. *Comparative Biochemistry and Physiology A* 76: 319–333.
 142. Hofmann RR, Musangi RS (1973) Comparative digestibility coefficients of domestic and game animals from marginal land in East Africa. *Bulletin of Epizootic Diseases in Africa* 21: 385–388.
 143. Codron D, Lee-Thorp JA, Sponheimer M, Codron J, de Ruiter D, et al. (2007) Significance of diet type and diet quality for ecological diversity of African ungulates. *Journal of Animal Ecology* 76: 526–537.

Biomechanical Reconstructions and Selective Advantages of Neck Poses and Feeding Strategies of Sauropods with the Example of *Mamenchisaurus youngi*

Andreas Christian^{1*}, Guangzhao Peng², Toru Sekiya², Yong Ye², Marco G. Wulf¹, Thorsten Steuer¹

¹ Abteilung für Biologie und ihre Didaktik, Universität Flensburg, Flensburg, Germany, ² Zigong Dinosaur Museum, Dashanpu, Zigong City, Sichuan Province, China

Abstract: A very long neck is a characteristic feature of most sauropod dinosaurs. In the genus *Mamenchisaurus*, neck length is extreme, greater than 40 percent of total body length. However, the posture, utilization, and selective advantage of very long necks in sauropods are still controversial. An excellently preserved skeleton of *Mamenchisaurus youngi*, including a complete neck, provides an opportunity for a comprehensive biomechanical analysis of neck posture and mobility. The biomechanical evidence indicates that *Mamenchisaurus youngi* had a nearly straight, near horizontal neck posture and browsed at low or medium heights. The results differ from the findings for some other sauropod species, like *Euhelopus*, *Diplodocus*, and *Giraffatitan* (*Brachiosaurus*) that had been analyzed in previous studies with similar methods. The selective advantage of extreme neck length in sauropods is likely advantageous for different feeding strategies.

Introduction

The very long neck is a characteristic feature of most sauropods [1,2] and possibly a key innovation for sauropod gigantism [1], though shorter necks occur in some species [3]. The implications of having a long neck have been intensively discussed, not only for sauropods but other extinct and living vertebrates as well [4]. According to recent findings, sauropods grew fast and consequently had a high metabolic rate (e.g., [1,5]). Therefore, the rate of food intake must have been very high, and access to substantial food resources would have been essential.

Long necks appear to be obviously beneficial for high browsing because sauropods would have had access to food resources other herbivores could not reach (e.g., [6,7]). However, the question whether some sauropods like *Giraffatitan* (formerly *Brachiosaurus brancai* [8–10] actually browsed at great heights with a steeply inclined neck remains controversial [11,12]. For other genera like *Diplodocus*, *Apatosaurus* [13], and *Nigersaurus* [14] most researchers agree on a low browsing strategy, though high browsing in a bipedal or tripod stance appears possible for some sauropods that are usually regarded as low-browsers like *Diplodocus* [15]. Similar to high browsing, low browsing with a long neck might have been useful for reaching otherwise difficult or impossible to exploit resources, e.g., at shorelines or in swampy environments [12,13].

The major selective advantage of a long neck might have been a reduction in energy costs because less energy was needed to move the long but lightly built neck than the very large, massive body (e.g., [1,16,17]). Depending on the distribution of food, this argument holds true for browsing at great heights [18] as well as for browsing at medium or low heights [19], even if high browsing evoked a very high blood pressure (see e.g., [18] versus [20]). In

this study browsing height is classified relative to the dimensions of the sauropod instead of using absolute values. The term low browsing is used for feeding with the head below the height of the shoulders, or more precisely, with the head below the height of the vertebral centra at the neck-trunk transition, so that the neck is in a declining position. There is no clear separation between medium and great heights. However, with medium heights we classify here browsing with the head kept between shoulder level and a half neck length above the shoulders which means a neck inclination of about 30 degrees. Browsing with a neck that is inclined by more than 30 degrees is classified as high browsing.

Another advantage of a very long neck could have been a reduction in the time intervals between feedings, thus a higher percentage of active time of a sauropod could have been used for feeding (see discussion). Explanations for the extreme neck length of sauropods different from feeding advantages, e.g. sexual selection or thermoregulation, appear unlikely [4,21].

Among terrestrial vertebrates, very long necks are not common. Because of the success of sauropods and the rare exceptions of shorter necks among this group of dinosaurs, it appears reasonable to assume that the selective advantage of a very long neck was enhanced by other characteristic sauropod features such as the bird-like respiratory system with air sacs in the neck, which reduced neck weight without reducing lever arms of neck muscles, tendons and ligaments; the absence of mastication, which meant the skull could remain small; and the high metabolic rate for which a high rate of food intake was necessary [1]. Very long necks were not restricted to sauropods of very large size, but are also common among much smaller species, like *Europasaurus* [22], as well. Therefore, the selective advantage of a long neck was not firmly correlated with very large body size [4].

Citation: Christian A, Peng G, Sekiya T, Ye Y, Wulf MG, et al. (2013) Biomechanical Reconstructions and Selective Advantages of Neck Poses and Feeding Strategies of Sauropods with the Example of *Mamenchisaurus youngi*. PLoS ONE 8(10): e71172. doi:10.1371/journal.pone.0071172

Editor: Andrew A. Farke, Raymond M. Alf Museum of Paleontology, United States of America

Received: April 8, 2013; **Accepted:** June 25, 2013; **Published:** October 30, 2013

Copyright: © 2013 Christian et al. This is an open-access article distributed under the terms of the Creative Commons Attribution License, which permits unrestricted use, distribution, and reproduction in any medium, provided the original author and source are credited.

Funding: The study has been funded by DFG (Deutsche Forschungsgemeinschaft) FOR 533 "Biology of the Sauropod Dinosaurs: The Evolution of Gigantism". The funders had no role in study design, data collection and analysis, decision to publish, or preparation of the manuscript.

Competing Interests: The authors have declared that no competing interests exist.

* E-mail: christian@uni-flensburg.de

Extreme neck length, even in comparison to other sauropods, is a characteristic feature of mamenchisaurids [23–25]. This study focuses on *Mamenchisaurus youngi* with a neck length of about 41% of the total body length [23,24]. The skeleton of specimen ZDM0083 is excellently preserved, including a complete neck and head [23,24], making *Mamenchisaurus youngi* an ideal example for studying the neck mechanics and the feeding strategy of a sauropod with an extremely long neck. The neck skeleton was analyzed in order to reconstruct its posture and mobility. Based on the results of the biomechanical analysis, possible feeding strategies are discussed for *Mamenchisaurus youngi*.

Materials and Methods

Materials

Measurements were taken from the skeletal remains of *Mamenchisaurus youngi*, specimen ZDM0083 of the Zigong Dinosaur Museum, Zigong, Sichuan, China [23]. Additional data were taken from the description and the illustrations by Ouyang and Ye [24]. Data lacking due to damaged vertebrae were interpolated.

Osteologically Neutral Pose (ONP) and neck mobility

The ONP of the neck is the zygapophyseal alignment posture. The ONP was determined by bringing the post- and prezygapophyses of adjacent vertebrae into contact, so that the joint between the centra was articulated and the joint facets of the pre- and postzygapophyses were centered above each other.

For this analysis, depending on their shapes, cotyles were placed into the adjacent condyles so that a close and smooth fit between both surfaces was obtained. The layer of cartilage between cotyles and condyles of adjacent vertebrae was assumed to be thin, between one or two centimeters on average for most parts of the neck and even less in the foremost region of the neck. Depending on the shape of cotyles and condyles the cartilage might have been thicker at some midpoints of the intervertebral joints; this, however, would not have affected the analysis. The assumption of rather thin layers of cartilage between the vertebral centra was derived from the usually close fit of cotyles and condyles. The neck of *Mamenchisaurus youngi* was preserved in articulation [23]. Although some vertebrae were separated after death, others were still found in close contact. A large fraction of the cotyle of the fifteenth cervical is still sitting deeply in the condyle of the sixteenth cervical, leaving not much space for cartilage. Several articulated neck vertebrae of related species can be found in situ in the bone beds of Zigong. The close and tight fit of these vertebrae corroborates the assumption of a rather thin layer of cartilage between cotyles and condyles. Therefore, the possible error in the estimated angulations of adjacent vertebrae due to uncertainties in the estimates of the thickness of joint cartilage is not more than two or three degrees.

Maximum dorsal mobility was estimated by tilting articulated vertebrae dorsally until the bone stopped further movement. Ventral and lateral flexibility are more difficult to estimate [26]. For ventral flexibility, it was assumed that the articulating zygapophyseal surfaces did not completely lose contact [26]. Lateral flexibility was only roughly estimated by the size of the zygapophyseal joint surfaces. The dorsoventral mobility of adjacent vertebrae was tested directly by bringing articulated vertebrae into the extreme positions described above, or, if this was not possible, e.g., due to deformations of the vertebrae, maximum excursions at the intervertebral joints were tested with the help of photographs taken of the vertebrae in side-view.

The surface area of the joint facets of the zygapophyses was estimated by assuming an elliptical shape. For the calculation of a

surface area, its length and width were used as major axes of the ellipse. Of the two zygapophyseal joints between adjacent vertebrae, the best preserved joint facet was used for the estimates. The data are presented in Table S1.

Stress in the intervertebral cartilage

Based on the dimensions of the neck skeleton, the volume of each neck segment was estimated, assuming that the dorsoventral outlines of the neck closely fit the reconstruction of the neck skeleton given in Plate II in [24]. An elliptical shape was assumed for most parts of the neck, with the transversal diameter being three quarters of the dorsoventral diameter. From the first to the fourth cervical vertebrae, additional mass was added for extra muscles that were needed for neck movements (e.g., [18,26–28]). From the 15th to the 18th cervical vertebrae, a transition towards a round cross-section was assumed because of the considerable increase in the transversal diameter of the cervicals starting around the 15th neck vertebra (for the basic data see Table S2). Mass distribution along the neck was reconstructed under the assumption of a very low neck density (0.5 g cm^{-3}) due to large air volumes, generally suggested for sauropods by recent research (e.g., [29–31]). The mass of the head was approximated by assuming an ellipsoid fit closely around the head skeleton and a density of 0.9 g cm^{-3} . A sensitivity analysis was conducted by using a horizontal neck posture and varying neck density between 0.4 g cm^{-3} and 0.7 g cm^{-3} . Additionally, for a horizontal position of the neck with a density of 0.5 g cm^{-3} , the mass of the head and the foremost section of the neck were varied. Also, a calculation was conducted with a very light base of the neck in order to demonstrate that the method is very robust against errors in mass estimates for the caudal section of the neck.

For different hypothetical neck postures, the stress in the intervertebral cartilage was calculated along the neck (Preuschoft-method; for a detailed description see [18,27,28,32,33]). The Preuschoft-method is based on the assumption of equal stress in the intervertebral cartilage along the neck in habitual neck postures [33]. This assumption is a consequence of Wolff's law [34] applied to cartilage. According to Wolff's law, bone adapts to loads. Bone is added where stress is high and removed where stress is low, so that under typical loading conditions stress is more or less constant throughout the bone, as has been corroborated in several recent studies (e.g., [35]). This concept was applied to intervertebral cartilage by Preuschoft [36] in order to reconstruct the spatial orientation of a vertebral column. The assumption of mean average stress in the intervertebral cartilage along the vertebral column was successfully tested for several terrestrial vertebrates [32,33]. For camels and giraffes it was shown that the Preuschoft-method is a robust and reliable instrument for the reconstruction of the habitual neck posture of long-necked terrestrial vertebrates [33].

For sauropods, stress in the intervertebral cartilage is mainly due to bending moments along the neck. These bending moments are counteracted at the intervertebral junctions by tensile forces in epaxial muscles, tendons, or ligaments [32,33,36]. The tensile force of the epaxial muscles, tendons and ligaments produces a compressive force of the same magnitude that acts on the cartilage in the intervertebral joint in addition to gravity [32,33,36]. Thus, knowing the cross-sectional area of an intervertebral joint, the stress acting in the cartilage can be calculated [32,33,36,37].

The lever arms of the epaxial forces were estimated by the vertical distances between the centers of the intervertebral joints and the tips of the neural spines [32,33]. The cross-sectional area of the intervertebral joints is calculated by assuming an elliptical shape of the joints, with the transversal and dorsoventral diameters

of the cranial surface of the adjacent vertebral centrum used as the major axes [32,33]. Forces different from static or quasistatic forces are neglected, assuming that forces due to accelerations or other activities are negligible, except in the foremost region of the neck, where forces for positioning and accelerating the head cannot be excluded [27,32,33]. A hypothetical posture of the neck is rejected if the stress is not approximately constant along the neck. The basic data for the calculations of stress values are presented in Tables S2, S3, S4.

In order to compare the variation of stress values along the neck, mean stress (MS) and standard deviation (SD) of stress values divided by mean stress in the intervertebral cartilage (SD/MS) are calculated for the intervertebral joints along the neck for all hypothetical neck postures, starting at the intervertebral joint between the fifth and sixth vertebrae (c5–c6) and ending at the joint behind the fourteenth vertebra. The foremost section of the neck is not included in the calculations because the stress values in the foremost section of the neck are biased by additional forces for moving and positioning the head. The caudal section of the neck was not included because of a probable bias due to muscles and ligaments that might have been located well above the neural spines [32,33]. The higher SD/MS the lower is the probability of the neck reconstruction.

If a sauropod frequently used different neck postures, the Preuschoft-method reveals the posture that evokes the highest stress along the neck. In the case that the stress curves of different frequently used neck postures intersect, the situation becomes complicated because the dimensions of the intervertebral discs in different sections of the neck might be determined by different neck poses.

Results

ONP and neck flexibility

The optimal fit of the pre- and postzygapophyseal joint surfaces yields a nearly straight neck posture with a slight upward bend at the base of the neck and a slight downward bend close to the head. Assuming the vertebral column of the trunk was slightly declining towards the shoulders because of the greater length of the hindlimbs compared to the forelimbs [24], the neck was kept close to the horizontal with an upward inclination of about 20 degrees.

Estimates of maximum dorsoventral flexion at the intervertebral joints of the neck and the foremost section of the trunk are presented in Figure 1 and Table S5. According to results on living vertebrates with long necks, the estimated limits for dorsal flexion by bone-bone contact of adjacent vertebrae appear to be close to the excursion that can occur during daily activities. However, such extreme excursions do not occur frequently. For *Mamenchisaurus*, excursions close to bone contact are only likely at the neck-trunk transition, where the vertebral bone appears to form broad contact areas that prevented peak forces during extreme dorsal flexion. Therefore, the values presented in Figure 1 are extremes that were possibly reached rarely if at all. Ventral flexion might have not usually exceeded about two thirds of the values given in Figure 1, so that an overlap of one third of the joint surfaces in the zygapophyses was maintained. For ventral flexibility, extreme values probably were restricted to short sections of the neck. In the case that a long ligament extended above the tips of the neural spines, as it was observed in extant vertebrates with long necks [26], maximum flexion was restricted if long sections of the neck were involved. The dorsoventral flexibility is much lower if a minimum overlap of the zygapophyseal joint facets of 50% is assumed [13]. This assumption, however, appears not justified in the light of the results on extant vertebrates with long necks [26].

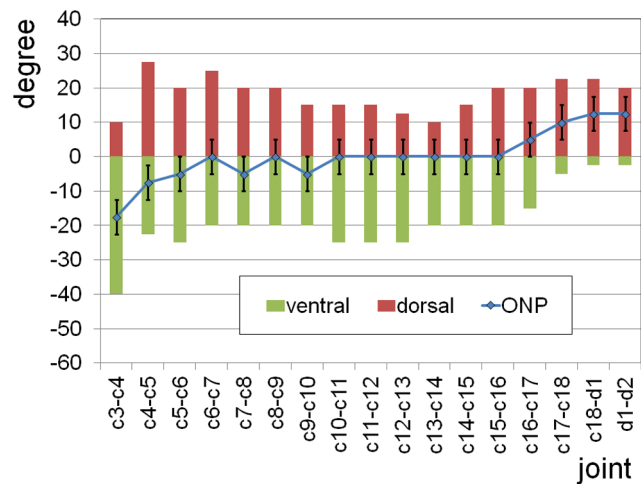


Figure 1. Osteologically Neutral Pose (ONP) and maximum dorsoventral excursions at the intervertebral joints along the neck and at the neck-trunk transition of *Mamenchisaurus youngi*. The angles are relative to a straight line of the middle axes of the vertebral centra. Positive angles mean dorsiflexion. For most joints in the midsection of the neck the ONP is straight. c1–c18, cervical vertebrae, d1,d2, first two dorsal vertebrae. An error of up to 5 degrees has to be taken into account for all angles due to deformations of the vertebrae and uncertainties in the estimate of the thickness of the intervertebral cartilage.

doi:10.1371/journal.pone.0071172.g001

Despite the problems in defining the actual limits in dorsoventral excursions at the intervertebral joints, the results allow for some basic conclusions to be made on neck mobility in *Mamenchisaurus youngi*. Dorsoventral flexibility of the vertebral column of the neck decreases from head to trunk, similar to the ostrich [26], but less pronounced. Data are missing for the joint between the second and the third cervical vertebrae because the zygapophyses were not sufficiently preserved. The high ventral and low dorsal flexibility between the third and the fourth cervical indicate a predominance of downward movements in the foremost section of the neck. Dorsal flexibility reaches a maximum but decreases towards the midsection of the neck, where ventral flexibility is high. Further posterior, dorsal flexibility increases and ventral flexibility decreases. At the neck-trunk transition dorsal flexibility is comparatively high whereas ventral flexibility is very low.

Lateral flexibility of the neck is more difficult to derive from the skeleton alone [26]. However, the size and the shape of the zygapophyses provide some hints about the general pattern [13,26,38]. Between the second and third cervical vertebrae, the zygapophyseal joint facet is broad and compared to the length of the vertebrae rather large. Behind the fourth vertebra, the zygapophyseal joints are more or less of elliptical shape with the long axis approximately parallel to the neck and comparatively small. The joint facets are medially inclined by roughly 45 degrees. Starting at around the 15th cervical, the vertebrae become much wider thereby increasing the lateral distance between the zygapophyses on both sides of the vertebrae. Simultaneously, the joint facets of the zygapophyses become much larger (Figure 2, Table S1), especially in width, so that starting around the 14th cervical, the orientation of the long axis of the zygapophyseal joint facets is more lateral than longitudinal, and towards the neck-trunk transition, the inclination of the zygapophyseal joint facets is reduced. These findings indicate that lateral mobility is low in

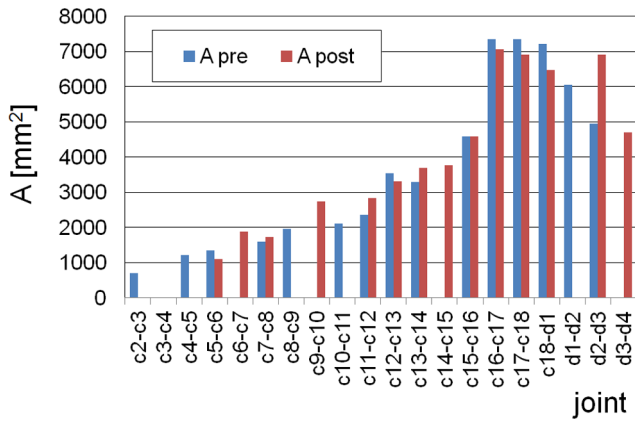


Figure 2. The size of the zygapophyseal joint facets. The surface area A of the joint facets is estimated for the prezygapophyses (A pre) and for the postzygapophyses (A post) by assuming an elliptical shape. Of both zygapophyseal joints between adjacent vertebrae, the best preserved joint facet is used for the estimates. In case of slight deformations or other damages, the joint surface was reconstructed, and in case of severe damage, no data are given. The estimated error due to deformation and deviation from elliptical shape of the joint facets is about ten percent.
doi:10.1371/journal.pone.0071172.g002

most parts of the neck, except the foremost section, but considerably increases towards the neck-trunk transition.

Neck mass and stress in the intervertebral joint cartilage

The estimated combined mass of neck and head of *Mamenchisaurus youngi* is approximately 391 kg. With a straight neck, the distance between the snout and the base of the neck is estimated at 6.47 m. The data on neck segment length and mass used for the mechanical calculations are given in Table S2 and Table S3. The data on lever arms and cross-sectional areas of the intervertebral joints are presented in Table S4. Neck and head mass estimates for different neck shapes and densities are presented in Table 1 and Table S3.

For some hypothetical neck postures, the calculated stresses in the intervertebral joints along the neck are presented in Figure 3 and Table S6; average values and standard deviations divided by mean values are given in Table 1. The magnitude of the stress values is similar to estimates for other sauropods [18,27] as well as our own estimates for some living vertebrates, and is also in accordance to the results of in vivo measurements of the pressure in an intervertebral disc of a human, which were 0.5 MPa for relaxed standing and 1.1 MPa for standing flexed forward [39]. Therefore, the overall mass estimate for the neck appears reasonable. A variation of neck density between 0.4 gcm^{-3} and 0.6 gcm^{-3} , which is equivalent to a variation of neck mass by 20%, yields reasonable results for stress (Figure 4, Table 1). With a neck density of 0.7 gcm^{-3} , which is equivalent to a 40% higher estimate of neck mass, stress values in the cartilage along the neck are about 1 MPa in a horizontal position and appear rather high for a relaxed pose of the neck. This indicates that even higher mass estimates for the neck of *Mamenchisaurus youngi* do not appear reasonable.

Nearly constant stress values in the intervertebral cartilage along the neck were obtained in straight neck poses for a slightly declined neck up to an inclination of the neck of about 45 degrees (Figure 3, Table 1). Because of uncertainties in the estimates of head and neck segment masses, habitual neck postures inside this range of inclinations are possible. Considerably bended neck postures (e.g.,

Table 1. Stress values along the neck of *Mamenchisaurus youngi* for different neck reconstructions.

Reconstruction	d [gcm^{-3}]	m [kg]	MS	SD/MS
horizontal	0.5	391.25	0.793	0.040
inclined sigmoid	0.5	391.25	0.640	0.134
declined (-15°)	0.5	391.25	0.645	0.040
inclined 45°	0.5	391.25	0.741	0.051
inclined 60°	0.5	391.25	0.506	0.069
horizontal d 0.4	0.4	318.00	0.708	0.061
horizontal d 0.6	0.6	464.50	0.877	0.041
horizontal d 0.7	0.7	537.75	0.962	0.055
heavy head (horizontal)	0.5	398.20	0.890	0.060
light head (horizontal)	0.5	384.30	0.696	0.049
light neck base (horizontal)	0.5	357.99	0.793	0.040

Mean stress (MS) and standard deviation (SD) divided by mean stress in the intervertebral cartilage along the neck for the different neck reconstructions in Figures 3–5, starting at the intervertebral joint between the fifth and sixth vertebrae (c5–c6) and ending at the joint behind the fourteenth vertebra. The higher SD/MS is the lower is the probability of the neck reconstruction. For further explanation see the text. Estimated head mass is 25 kg, except for the “heavy head” and the “light head” reconstructions. In the “heavy head” reconstruction head mass is 30 kg and the mass of the foremost neck section between the first and the third cervical vertebrae is also increased by 20% (approximately 2 kg). In the “light head” reconstruction head mass is 20 kg and the mass of the foremost neck section between the first and the third cervical vertebrae is reduced by 20% (approximately 2 kg). In the “light neck base” reconstruction, the shape of the neck is maintained elliptical at its base instead of becoming circular towards the end. Segment mass estimates are presented in Table S3, stress values are given in Table S6. d, assumed density of the neck; m, combined mass of neck and head.
doi:10.1371/journal.pone.0071172.t001

[24], Plate II) do not fit the expectation of constant stress in the intervertebral cartilage along the neck. These results indicate that the neck was generally kept in a more or less straight pose, with possible exceptions at both ends, close behind the head and in the region of the neck-trunk transition.

Very low stress close behind the head and high stress at the neck-trunk transition are observed in all poses tested for

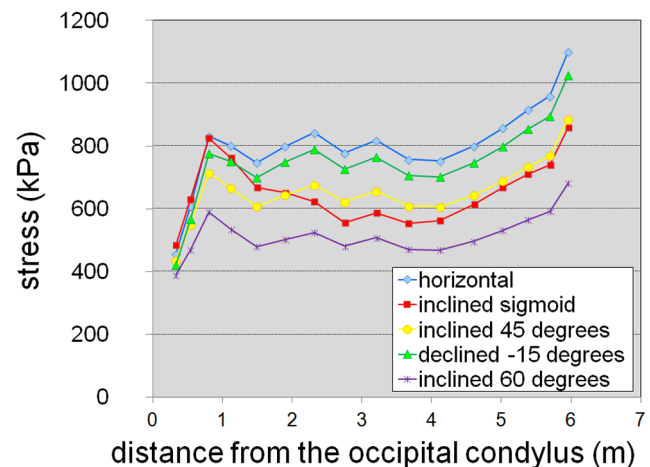


Figure 3. Stress in the intervertebral cartilage along the neck for different hypothetical neck postures (four straight postures and a sigmoid posture [24, Plate II]).
doi:10.1371/journal.pone.0071172.g003

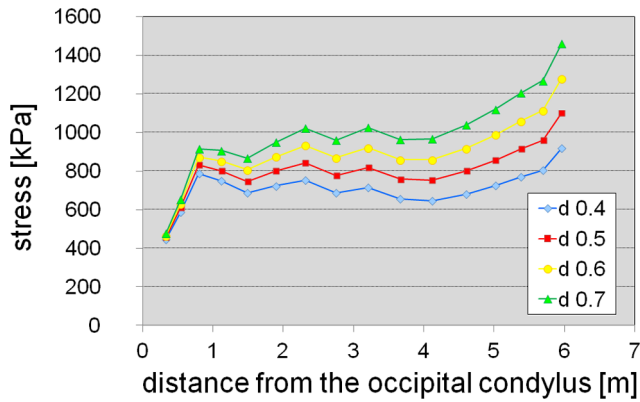


Figure 4. Stress in the intervertebral cartilage along the neck for different neck densities. The neck was assumed to be in a horizontal position. d 0.4–d 0.7, neck reconstructions assuming a density between 0.4 gcm^{-3} and 0.7 gcm^{-3} . doi:10.1371/journal.pone.0071172.g004

Mamenchisaurus youngi. These stress levels are seen in other sauropods as well (e.g., [18,27,33]). The low values observed close behind the head indicate additional forces due to head movements [18,27]. The high values at the posterior end of the neck indicate that the lever arms of epaxial forces are underestimated. Presumably neck muscles, tendons or ligaments that connected the trunk with the neck were located well above the neural spines at the base of the neck as suggested for other sauropods [18,27,28,33].

The sensitivity analysis with varied neck density (Figure 4, Table 1) and mass distribution along the neck (Figure 5, Table 1) reveals that moderate errors in the estimated mass distribution along the neck do not affect the general result of approximately constant stress values in a horizontal position of the neck, although mass variations of the head and the foremost section of the neck considerably influence the stress along the neck due to the long lever arms of the weight forces at the distal end of the neck.

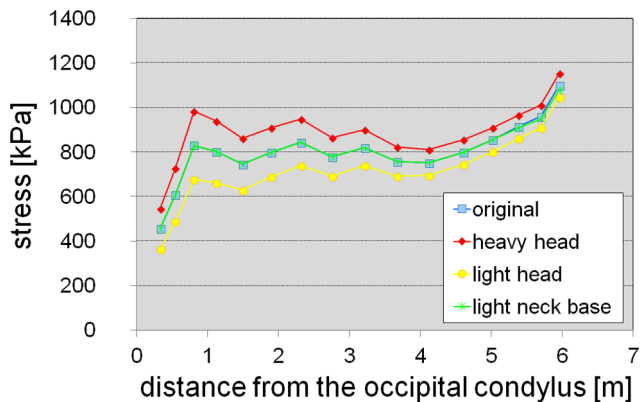


Figure 5. Stress in the intervertebral cartilage along the neck for different mass distributions along head and neck. The neck was assumed to be in a horizontal position. Neck density was assumed as 0.5 gcm^{-3} . Original, mass distribution as used for the calculations in Figure 3; heavy head, 20% mass were added to the head and to the foremost section of the neck from c1 to c3; light head, 20% mass was subtracted from the head and from the foremost section of the neck from c1 to c3; light neck base, the base of the neck was assumed to remain elliptical with a width of three quarters of the height instead of becoming circular towards the base of the neck. doi:10.1371/journal.pone.0071172.g005

Discussion

Neck posture and feeding strategy

Both the results on vertebral articulation and the results on stress in the intervertebral joint cartilage along the neck support the reconstruction of a nearly straight neck for *Mamenchisaurus youngi*. The orientation of the neck in a habitual posture could have been between slightly declined or inclined up to about 45 degrees. Assuming that the section of the vertebral column behind the second vertebra of the trunk was declining in cranial direction by 10 or 20 degrees (see e.g., Plate II in [24]), the neck in ONP was inclined by about 20 degrees. This result is not very different from the approximately horizontal neck postures that were reconstructed for several sauropods based on the ONP [13,38].

Recently, it has been questioned whether zygapophyseal alignment yields habitual positions of sauropod necks [27,40]. Studies on the neck postures of living vertebrates with long necks [26,27] indicate that the ONP usually is closer to the neck posture during locomotion than to the position of the neck at rest, which is usually by 10 or 20 degrees higher. The comparatively low neck posture during locomotion may be used for increasing forces in epaxial elastic elements along the neck during activity or for shifting forward the center of gravity of the body [26,27]. Especially in sauropods, a low position of the head during locomotion might be related to a higher metabolic rate compared to standing at rest. With the head well above the heart, an increased blood pressure evokes an additional energy consumption that is proportional to the metabolic rate [20].

In summary, for *Mamenchisaurus youngi*, the results indicate a more or less horizontal, declined, or slightly inclined position of the neck during feeding, a habitual neck posture during locomotion with a slight inclination of about 20 degrees and a habitual neck position during standing at rest with an inclination of approximately 30 or 40 degrees. The pattern of the stress as well as the magnitude of stress values in the intervertebral cartilage along the neck is in accordance with both a horizontal and an inclined position of the neck at rest. Because sauropods would have had a better view over the surrounding area and reduced their vulnerability, it appears reasonable to assume that the neck was kept in an inclined position during standing at rest. The dorsal flexibility at the neck-trunk transition fits this assumption.

A steep inclined or nearly vertical position of the neck is very unlikely even for short time intervals because this would have forced several joints into an extreme position. *Mamenchisaurus youngi*, therefore, probably did not browse at great heights by raising the neck. On the other hand, compared to other neck sections, high ventral flexibility in the midsection of the neck indicates frequent browsing at low heights. In *Diplodocus carnegii* [13,26], the head could be lowered to ground level by flexion at the base of the neck but also in the midsection of the neck, so that the height of the more massive posterior end of the neck did not change much. Compared to *Diplodocus carnegii*, the overall pattern of dorsoventral flexibility was similar in *Mamenchisaurus youngi*. In contrast to *Diplodocus carnegii*, however, in *Mamenchisaurus youngi* the base of the neck appears to have been rather inclined as opposed to declined, and the neck appears to have been straighter. These features resemble the similarly-sized *Euhelopus zdanskyi* [18,41,42]. However, in *Euhelopus zdanskyi*, the vertebral column apparently was flexed more dorsally at the neck-trunk transition than in *Mamenchisaurus youngi* [18], so that the neck possibly was kept in a more inclined position and browsing at great heights cannot be excluded. These findings indicate that *Mamenchisaurus youngi* browsed at lower heights than *Euhelopus zdanskyi*, although the neck mechanics were probably very similar. The comparatively

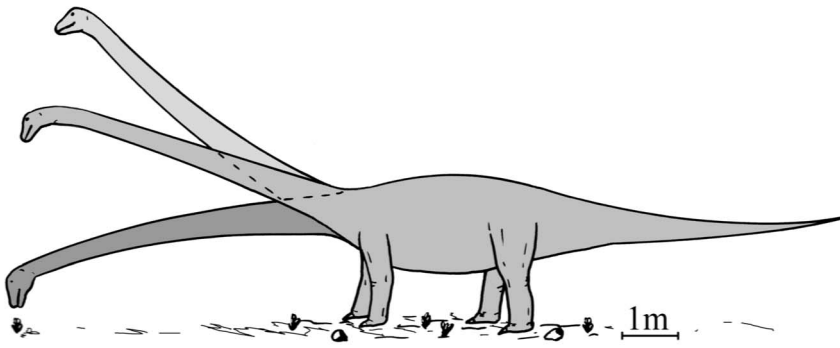


Figure 6. Suggested neck poses for *Mamenchisaurus youngi*. The neck is shown during low browsing, in ONP (middle pose), and in an alert position.

doi:10.1371/journal.pone.0071172.g006

long forelimbs and studies on the intervertebral stress indicate that *Giraffatitan brancai* resembled *Euhelopus* instead of *Mamenchisaurus* in feeding behavior [27]. The posture and utilization of the neck differed more between *Mamenchisaurus youngi* and *Diplodocus carnegii*, though both sauropods may have browsed at low heights. *Mamenchisaurus youngi* may have browsed at medium heights as well.

Like *Euhelopus* and *Giraffatitan* but different from diplodocids, the cervical ribs were very long and overlapping in *Mamenchisaurus*. The evidence recently put forward by Klein et al. [43] supports the hypothesis that cervical ribs were used for transmitting tensile forces along the neck. Yet, the mechanical function of high ventral forces along the neck is not fully clear. Strong tensile structures on the ventral side of the neck might be needed even in a more or less horizontal position of the neck for reducing swinging of the head during locomotion.

The long cervical ribs of *Mamenchisaurus* also support the idea that many sauropod necks had little flexibility. The size, location and orientation of the zygapophyses also indicate little lateral flexibility along the neck. Lateral movements of the neck were more or less restricted to the base of the neck as is frequently found in vertebrates [44]. The wide vertebrae with large, rather flat zygapophyses, starting around the 15th cervical, are well suited for maintaining contact between the pre- and postzygapophyseal joint facets during lateral excursions and for resisting torsion due to sideward movements of the more cranial parts of the neck. In contrast to dorsoventral movements, lateral movements do not imply vertical shifts of the center of mass of the neck. Therefore, it appears reasonable that frequent dorsoventral movements, e.g., during feeding, took place in the more cranial section of the neck (as observed in camels and ostriches (see, e.g., [26]).

Advantages of a very long neck

The selective advantages of a very long neck, as discussed in the introduction, include increasing access to food, especially for high browsers or reducing energy expenditures, especially in low browsers (e.g., [1,4,12,18,19]). Simple estimates of energy expenditures have been used to demonstrate advantages of a long neck for different feeding strategies depending on the distribution of food sources [17–19].

In addition to increased access to resources and more efficient browsing, a long neck might also have been useful in saving time during feeding intervals. Especially with a patchy distribution of food, with distances between food sources below neck length, the long neck could have served for moving the head quickly from one source to the next. This behavior would not only save energy due to a reduction in body movements and accelerations [17] but

would also shorten time intervals between feeding, so that absolute food intake could be increased during a day or during competitive exploration of an area with other herbivores present.

For *Mamenchisaurus youngi*, different selective advantages for a very long neck appear possible. Because of the rather low position and the little flexibility of the neck, it was not useful for exploiting resources at great heights, and it is unlikely that *Mamenchisaurus youngi* walked through dense vegetation. Therefore, it appears reasonable to assume a patchy distribution of food sources. Under this condition, the selective advantage of the long neck might have been to save energy and time by reducing distances that had to be traveled, especially in difficult terrains, or reducing the need to turn or accelerate the whole body. The results may be applied to other mamenchisaurids with similarly constructed necks (e.g., [23–25,45]).

Conclusions

The evidence put forward here indicates that the neck of *Mamenchisaurus youngi* was kept in a more or less straight, not steeply inclined, pose with little mobility in most parts of the neck, as suggested for most sauropods with long necks (e.g., [38,46]). The functional specialization of the neck sections supports the idea of browsing at low or medium heights: The foremost neck section was comparatively mobile, allowing quick movements over short distances of the head during feeding. Low stress under static conditions in the foremost intervertebral joints indicates muscle activity due to head movements during feeding. The midsection of the neck could be flexed ventrally for low browsing or kept straight or flexed slightly dorsally for browsing at medium heights. The posterior neck section was used for lateral movements of the whole neck, and at the neck-trunk transition, dorsal flexion was performed for raising the neck, e.g. into a resting position. The rather stiff construction of the neck may be related to a low density of vegetation, so that sideward movements of the neck or turning with the whole body were not much restricted by environmental obstacles (see also [15]). During locomotion the neck was slightly inclined. During standing at rest or in an alert position the inclination of the neck could be increased to 30 or 40 degrees (Figure 6).

The results presented here on the neck mechanics and feeding behavior of *Mamenchisaurus youngi*, when compared with the results on other sauropods like *Diplodocus*, *Giraffatitan*, or *Euhelopus*, indicate different ways of using a very long neck among sauropods. Also, there is a considerable variation in body size, dentition and environmental conditions of sauropods (e.g., [47–51]) with very long necks, so that niche partitioning among sauropods appears

reasonable [47]. Therefore, it has to be concluded that the selective advantage of a long neck was not restricted to the distribution of food, feeding habits, or a very large body size. It appears that multiple advantages made a very long neck stable during the long-term evolution of sauropods [1]. For a greater insight into the selective factors that favored the evolution of very long necks in sauropods, it would be worthwhile to investigate those sauropods that show a reduction in neck length.

Supporting Information

Table S1 Dimensions of the zygapophyseal facets at the cervical joints of *Mamenchisaurus youngi*. Estimated surface areas of the prezygapophyses (A_{pre}) and the postzygapophyses (A_{po}) along the neck of *Mamenchisaurus youngi*. The surface areas are calculated from the length and width of the zygapophyseal joint facets as explained in the text. l_{pre} , length of the prezygapophyses; w_{pre} , width of the prezygapophyses; l_{po} , length of the postzygapophyses; w_{po} , width of the postzygapophyses. Values are rounded because of deformations of the vertebrae. (DOC)

Table S2 Estimated dimensions of neck segments in *Mamenchisaurus youngi*. Segment lengths are taken from Table 4 in [24]. Segment heights, segment widths and volumes are estimated as described in the text. For segment volumes, a systematic error up to some ten percent cannot be excluded due to wrong estimates of neck dimensions. This systematic error would be similar for all neck sections. However, a higher error at both, the cranial and caudal ends of the neck are possible because of possible deviations in neck shape in these sections of the neck (see text). Additionally, a statistical error up to 5 percent due to deformations in the vertebrae is possible. Values for volumes are rounded. (DOC)

Table S3 Estimated mass distributions along the neck of *Mamenchisaurus youngi*. Different estimates of the mass distribution along the head and neck of *Mamenchisaurus youngi* that were used for the calculations of intervertebral stress (Figures 3–5). d 0.5, basic neck reconstruction with a density of 0.5 g cm^{-3} based on the estimated segment volumes given in Table S2; d 0.4, neck with a density of 0.4 g cm^{-3} ; d 0.6, neck with a density of 0.6 g cm^{-3} ; d 0.7, neck with a density of 0.7 g cm^{-3} ; hh, heavy head, neck with a density of 0.5 g cm^{-3} and an increased mass of the head and the foremost section of the neck; lh, light head, neck with a density of 0.5 g cm^{-3} and a reduced mass of the head and the foremost section of the neck; lnb, light neck base, neck with a density of 0.5 g cm^{-3} and a reduced mass of the basal section of the neck. For further explanation see the text. (DOC)

Table S4 Mechanically relevant dimensions at the cervical joints of *Mamenchisaurus youngi*. The lever arms

(h) of epaxial tensile forces and the cross-sectional area (A) of the compressed intervertebral cartilage at the neck joints are estimated as described in the text. a, width of the cotyle; b, height of the cotyle. For a and b rounded values were used at most joints because of slight deformations of the vertebrae. For further explanation see the text.

(DOC)

Table S5 Dorsoventral flexibility along the neck of *Mamenchisaurus youngi*. Osteologically Neutral Pose (ONP) and maximum possible dorsoventral excursion angles at the intervertebral joints along the neck of *Mamenchisaurus youngi*. Dorsal excursions are positive. The estimated error is 5 degrees for all values. For further explanation see the text. (DOC)

Table S6 Stress in intervertebral cartilage along the neck of *Mamenchisaurus youngi*. Calculated stress in the intervertebral cartilage along the neck of *Mamenchisaurus youngi* for different hypothetical neck postures and mass distributions along head and neck; b, basic mass reconstruction (with a density of 0.5 g cm^{-3}) with a horizontal neck posture; is, basic mass reconstruction with an inclined sigmoidal neck posture; i 45, basic mass reconstruction with a neck inclination of 45 degrees; i 60, basic mass reconstruction with a neck inclination of 60 degrees; de, basic mass reconstruction with a declining neck (-15 degrees); d 0.4, horizontal neck with a density of 0.4 g cm^{-3} ; d 0.6, horizontal neck with a density of 0.6 g cm^{-3} ; d 0.7, horizontal neck with a density of 0.7 g cm^{-3} ; hh (heavy head), horizontal neck with a density of 0.5 g cm^{-3} and an increased mass (20%) of the head and the foremost section of the neck; lh (light head), horizontal neck with a density of 0.5 g cm^{-3} and a reduced mass (20%) of the head and the foremost section of the neck; lnb, light neck base, horizontal neck with a density of 0.5 g cm^{-3} and reduced mass of the basal section of the neck (elliptical shape instead of a transition to a round shape). For further explanation see the text. (DOC)

Acknowledgments

We thank the staff of the Zigong Dinosaur Museum, Zigong, Sichuan, China, for the friendly support in collecting data. We thank Martin Sander for all his valuable support, Nicole Klein for helping taking photographs of vertebrae, Kent A. Stevens for critical and inspiring comments on the manuscript, and Jessica Mitchell for a linguistic survey of the manuscript. We thank the Academic Editor, Andrew A. Farke, Mike P. Taylor, and an anonymous reviewer for critical and constructive comments on the manuscript. This is contribution No 148 of the DFG Research Unit ‘Biology of the Sauropod Dinosaurs: The Evolution of Gigantism’.

Author Contributions

Conceived and designed the experiments: AC. Performed the experiments: AC MGW TS. Analyzed the data: AC GP TS YY MGW TS. Contributed reagents/materials/analysis tools: AC GP TS YY. Wrote the paper: AC. Took part in designing the experiments: GP TS YY MGW TS.

References

- Sander MP, Christian A, Clauss M, Fechner R, Gee CT, et al. (2011) Biology of sauropod dinosaurs: the evolution of gigantism. *Biol Rev* 86: 117–155.
- Upchurch P, Barrett PM, Dodson P (2004) Sauropoda. In: Weishampel DB, Dodson, Osmólska H, editors. *The Dinosauria*, 2nd edition. Berkeley, CA: University of California Press. pp. 259–322.
- Rauhut OWM, Remes K, Fecher R, Cladera G, Puerta P (2005) Discovery of a short-necked sauropod dinosaur from the Late Jurassic period of Patagonia. *Nature* 435: 670–672.
- Wilkinson DM, Ruxton GD (2012) Understanding selection for long necks in different taxa. *Biol Rev Camb Philos Soc* 87(3): 616–630.
- Sander PM, Clauss M (2008) Sauropod Gigantism. *Science* 322: 200–201.
- Bakker RT (1986) *The dinosaur heresies*. New York: Citadel Press. 481p.
- Paul GS (1988) The brachiosaur giants of the Morrison and Tendaguru with a description of a new subgenus, *Giraffatitan*, and a comparison of the world's largest dinosaurs. *Hunteria* 2(3): 1–14.
- Taylor MP (2009) A re-evaluation of *Brachiosaurus altithorax* Riggs 1903 (Dinosauria, Sauropoda) and its generic separation from *Giraffatitan brancai* (Janensch 1914). *J Vertebr Paleontol* 29(3): 787–806.
- D’Emic MD (2012) The early evolution of titanosauriform sauropod dinosaurs. *Zool J Linn Soc-Lond* 166: 624–671.
- Mannion PD, Upchurch P, Barnes RN, Mateos O (2013) Osteology of the Late Jurassic Portuguese sauropod dinosaur *Lusotitan atalaiensis* (Macronaria) and the

- evolutionary history of basal titanosauriforms. *Zool J Linn Soc-Lond* 168: 98–206.
11. Seymour RS (2009) Sauropods kept their heads down. *Science* 323: 1671.
 12. Sander PM, Christian A, Gee CT (2009) Response to sauropods kept their heads down. *Science* 323: 1671–1672.
 13. Stevens KA, Parrish MJ (1999) Neck posture and feeding habits of two Jurassic sauropod dinosaurs. *Science* 284: 798–800.
 14. Sereno PC, Wilson JA, Witmer LM, Whitlock JA, Maga A, et al. (2007) Structural extremes in a Cretaceous dinosaur. *PLoS ONE* 2(11): 1–9.
 15. Mallison H (2011) Rearing giants: Kinetic-dynamic modelling of sauropod bipedal and tripodal poses. In: Klein N, Remes K, Gee CT, Sander PM, editors. *Biology of the sauropod dinosaurs: understanding the life of giants*. Bloomington, IN: Indiana University Press. pp. 237–250.
 16. Martin J (1987) Mobility and feeding of *Cetiosaurus* (Saurischia: Sauropoda) - why the long neck? In: Curry PJ, Koster EH, editors. *Fourth Symposium on Mesozoic Terrestrial Ecosystems*. Drumheller, Alberta: Tyrell Museum of Paleontology. pp. 154–159.
 17. Preuschoft H, Hohn B, Stoinski S, Witzel U (2011) Why so huge? Biomechanical reasons for the acquisition of large size in sauropod and theropod dinosaurs. In: Klein N, Remes K, Gee CT, Sander PM, editors. *Biology of the sauropod dinosaurs: understanding the life of giants*. Bloomington, IN: Indiana University Press. pp. 197–218.
 18. Christian A (2010) Some sauropods raised their necks: evidence for high browsing in *Euhelopus zdanskyi*. *Biol Lett* 6: 823–825. (doi:10.1098/rsbl.2010.0359)
 19. Ruxton GD, Wilkinson DM (2011) The energetics of low-browsing in sauropods. *Biol Lett* 7: 779–781.
 20. Seymour RS (2009) Raising the sauropod neck: it costs more to get less. *Biol Lett* 5: 317–319.
 21. Taylor MP, Hone DWE, Wedel MJ, Naish D (2011). The long necks of sauropods did not evolve primarily through sexual selection. *J Zool* 285: 150–161.
 22. Sander PM, Mateus O, Laven T, Knötschke N (2006) Bone histology indicates insular dwarfism in a new Late Jurassic sauropod dinosaur. *Nature* 441: 739–741.
 23. Pi L, Ou Y, Ye Y (1996) A new species of sauropod from Zigong, Sichuan, *Mamenchisaurus youngi*. 30th International Geological Congress, Papers on Geosciences. Beijing, China. pp.87–91.
 24. Ouyang H, Ye Y (2002) The first Mamenchisaurian skeleton with complete skull: *Mamenchisaurus youngi*. Chengdu: Sichuan Science and Technology Press. 111 p.
 25. Sekiya T (2011) Re-examination of *Chuanjiesaurus anaensis* (Dinosauria: Sauropoda) from the Middle Jurassic Chuanjie Formation, Lufeng County, Yunnan Province, Southwest China. *Memoir of the Fukui Prefectural Dinosaur Museum* 10: 1–54.
 26. Dzemski G, Christian A (2007) Flexibility along the neck of the ostrich (*Struthio camelus*) and consequences for the reconstruction of dinosaurs with extreme neck length. *J Morph* 268: 701–714.
 27. Christian A, Dzemski G (2007) Reconstruction of the cervical skeleton posture of *Brachiosaurus brancai* Janensch, 1914 by an analysis of the intervertebral stress along the neck and a comparison with the results of different approaches. *Fossil Record* 10: 37–48.
 28. Christian A, Dzemski G (2011) Neck posture in sauropods. In: Klein N, Remes K, Gee CT, Sander PM, editors. *Biology of the sauropod dinosaurs: understanding the life of giants*. Bloomington, IN: Indiana University Press. pp. 251–260.
 29. Wedel MJ (2005) Postcranial skeletal pneumaticity in sauropods and its implications for mass estimates. In: Wilson JA, Curry-Roger K, editors. *The sauropods: Evolution and paleobiology*. Berkeley: University of California Press. pp. 201–228.
 30. Henderson DM (2004) Tippy punters: sauropod dinosaur pneumaticity, buoyancy and aquatic habits. *Proc Royal Soc London B (Supplement)* 271: 180–183.
 31. Taylor MP, Wedel MJ (2013) Why sauropods had long necks; and why giraffes have short necks. *PeerJ* 1:e36 <http://dx.doi.org/10.7717/peerj.36>
 32. Christian A, Preuschoft H (1996) Deducing the body posture of extinct large vertebrates from the shape of the vertebral column. *Palaeontology* 39(4): 801–812.
 33. Christian A (2002) Neck posture and overall body design in sauropods. *Mitt Mus Natkd Berl, Geowiss Reihe* 5: 269–279.
 34. Wolff J (1892) *Das Gesetz der Transformation der Knochen*. Berlin/Germany: Verlag August Hirschwald. 152 p.
 35. Sverdllova NS, Witzel U (2010) Principles of determination and verification of muscle forces in the human musculoskeletal system: Muscle forces to minimise bending stress. *J Biomech* 43(3): 387–396.
 36. Preuschoft H (1976) Funktionelle Anpassung evolvierender Systeme. *Aufsätze und Reden der Senckenbergischen Naturforschenden Gesellschaft* 28: 98–117.
 37. Alexander R McN (1985) Mechanics of posture and gait of some large dinosaurs. *Zool J Linn Soc* 83(1): 1–25.
 38. Stevens KA, Parrish MJ (2005) Digital reconstructions of sauropod dinosaurs and implications for feeding. In: Wilson JA, Curry-Roger K, editors. *The sauropods: Evolution and paleobiology*. Berkeley: University of California Press. pp. 178–200.
 39. Wilke HJ, Neef P, Caimi M, Hoogland T, Claes L (1999) New in vivo measurements of pressures in the intervertebral disc in daily life. *Spine* 24,8: 755–762.
 40. Taylor MP, Wedel MJ, Naish D (2009) Head and neck posture in sauropod dinosaurs inferred from extant animals. *Acta Palaeontol Pol* 54: 213–220.
 41. Wiman C (1929) *Die Kreide-Dinosaurier aus Shantung*. *Palaeontol sinica Ser C*, 6: 1–67.
 42. Wilson JA, Upchurch P (2009) Redescription and reassessment of the phylogenetic affinities of *Euhelopus zdanskyi* (Dinosauria: Sauropoda) from the Early Cretaceous of China. *J Syst Palaeontol* 7(2): 199–239.
 43. Klein N, Christian A, Sander PM (2012) Histology shows elongated neck ribs in sauropod dinosaurs are ossified tendons. *Biol Lett* 8(6): 1032–1035.
 44. Vidal PP, Graf W, Berthoz A (1986) The orientation of the cervical vertebral column in unrestrained awake animals. *Exp Brain Res* 61(3): 549–559.
 45. Young CC, Zhao X (1972) *Mamenchisaurus*. *Szechuan Academica Sinica, Inst Vert Paleont Ser A*, 1(8): 1–30.
 46. Berman DS, Rothschild BM (2005) Neck posture of sauropods determined using radiological imaging to reveal three-dimensional structure of cervical vertebrae. In: Tidwell V, Carpenter K, editors. *Thunder Lizards: The Sauropodomorph Dinosaurs*. Bloomington: Indiana University Press. pp. 233–247.
 47. Dodson P (1990) Sauropod paleoecology. In: Weishampel DB, Dodson P, Osmólska H, editors. *The dinosauria*. Berkeley, CA: University of California Press. pp. 402–407.
 48. Upchurch P, Barrett PM (2000) The evolution of sauropod feeding mechanisms. In: Sues HD, editor. *Evolution of herbivory in terrestrial vertebrates: perspectives from the fossil record*. Cambridge, UK: Cambridge University Press. pp. 79–122.
 49. Sereno PC, Wilson JA (2005) Structure and evolution of a sauropod tooth battery. In: Wilson JA, Curry-Roger K, editors. *The sauropods: Evolution and paleobiology*. Berkeley: University of California Press. pp. 157–177.
 50. Gee CT (2011) Dietary options for the sauropod dinosaurs from an integrated botanical and paleobotanical perspective. In: Klein N, Remes K, Gee CT, Sander PM, editors. *Biology of the sauropod dinosaurs: understanding the life of giants*. Bloomington, IN: Indiana University Press. pp. 34–56.
 51. Parrish JM (2006) The origins of high browsing and the effects of phylogeny and scaling on neck length in Sauropodomorpha. In: Carrano MT, Gaudin TJ, Blob RW, Wible JR, editors. *Amniote Paleobiology: Phylogenetic and Functional Perspectives on the Evolution of Mammals, Birds and Reptiles*. Chicago: University of Chicago Press. pp. 201–224.

The Articulation of Sauropod Necks: Methodology and Mythology

Kent A. Stevens*

Department of Computer and Information Science, University of Oregon, Eugene, Oregon, United States of America

Abstract

Sauropods are often imagined to have held their heads high atop necks that ascended in a sweeping curve that was formed either intrinsically because of the shape of their vertebrae, or behaviorally by lifting the head, or both. Their necks are also popularly depicted in life with poses suggesting avian flexibility. The grounds for such interpretations are examined in terms of vertebral osteology, inferences about missing soft tissues, intervertebral flexibility, and behavior. Osteologically, the pronounced opisthocoely and conformational central and zygapophyseal articular surfaces strongly constrain the reconstruction of the cervical vertebral column. The sauropod cervico-dorsal vertebral column is essentially straight, in contrast to the curvature exhibited in those extant vertebrates that naturally hold their heads above rising necks. Regarding flexibility, extant vertebrates with homologous articular geometries preserve a degree of zygapophyseal overlap at the limits of deflection, a constraint that is further restricted by soft tissues. Sauropod necks, if similarly constrained, were capable of sweeping out large feeding surfaces, yet much less capable of retracting the head to explore the enclosed volume in an avian manner. Behaviorally, modern vertebrates generally assume characteristic neck postures which are close to the intrinsic curvature of the undeflected neck. With the exception of some vertebrates that can retract their heads to balance above their shoulders at rest (e.g., felids, lagomorphs, and some ratites), the undeflected neck generally predicts the default head height at rest and during locomotion.

Citation: Stevens KA (2013) The Articulation of Sauropod Necks: Methodology and Mythology. PLoS ONE 8(10): e78572. doi:10.1371/journal.pone.0078572

Editor: Andrew A. Farke, Raymond M. Alf Museum of Paleontology, United States of America

Received: April 12, 2013; **Accepted:** September 20, 2013; **Published:** October 30, 2013

Copyright: © 2013 Kent A. Stevens. This is an open-access article distributed under the terms of the Creative Commons Attribution License, which permits unrestricted use, distribution, and reproduction in any medium, provided the original author and source are credited.

Funding: The author has no support or funding to report.

Competing Interests: The author has declared that no competing interests exist.

* E-mail: kent@cs.uoregon.edu

Introduction

Sauropod necks were but one remarkable aspect of an altogether remarkable vertebrate. The necks of many sauropod taxa comprised a larger proportion of the presacral axial skeleton than found in any extant non-avian, with individual vertebrae representing extremes of pneumaticity, elongation, and size. The combination of relatively tiny head, elongate neck, and enormous body has posed fascinating questions regarding sauropods, including how they fed, moved, and simply how they appeared in life.

Since only their fossilized bones remain, and usually incomplete and imperfectly preserved at that, even their skeletal reconstructions have been subject to differences in interpretation and sometimes artistic liberties. The overall bauplan of these great giants remains controversial (see below), let alone how they might have held their heads and used their necks in life. Settling the essential questions of sauropod feeding habits and the role of their remarkable necks in feeding will be challenging, since the origin and role of the long neck of the giraffe remains controversial despite their being available for direct observation, as living and behaving animals. Even if alive today, some contention could be expected regarding how the sauropod got its long, long neck. But given only their fossils, much must be inferred and little can be observed directly. This review attempts to summarize what can be concluded about sauropod neck articulation based on correlations between function and (osteological) form. The methodology is necessarily inferential and incremental, accumulating a coherent

explanation that, while highly incomplete and speculative, is at least consonant with what can be derived from other sources.

What if Giraffes Were Extinct?

By analogy, imagine that giraffes were extinct, and known only by their desiccated bones, with some cervical columns remaining in apparently close articulation but in opisthotonic pose [1], while others are found associated but disarticulated. The skeletal structure could still be reconstructed with reasonable accuracy to reveal the overall conformation of the axial skeleton, however, revealing the abrupt rise of the neck at the shoulders, the straight mid-neck, the downward-tilted skull, and the resultant head height – all surmised by reassembling the bones with the joints in their neural, undeflected state (Figure 1). The neck's range of motion could then be explored by re-articulating the cervical vertebrae (spaced appropriately to account for the missing cartilage), revealing differences in lateral versus dorsoventral flexibility, and variation in flexibility along the length of the neck (the consequences of which are observable in life). Suspicion would likely arise that the neck's limited ventral flexibility posed a problem for reaching down to water, requiring splayed forelimbs or bent elbows. As will be reviewed, preventing disarticulation ultimately limits joint range of motion, and soft tissues further constrains flexibility. Ligamentous synovial capsules surrounding the zygapophyses arrest deflection prior to their disarticulation, plus layers of deep and superficial musculature and fascia would further restrict the effective range of motion (see below). While joint geometry may allow some estimation of joint flexibility and

provide some insight into posture and feeding envelope, it would not go far towards revealing behavioral specializations in feeding or other roles of the neck. This is the situation faced by paleontologists when seeking answers to just those questions for sauropods. While estimating sauropod neck curvature and flexibility from fossilized bones based on extant models is necessarily speculative, support is unfortunately even more tenuous regarding speculations related to behavior.

The Necessity of Speculation

Unlike other sciences where the subjects under study are extant and their behaviors (e.g., physical, chemical, psychological, societal) can be observed directly, in paleontology, when the subjects are extinct their behaviors can only be inferred. The process of scientific inference regarding extinct behavior is therefore indirect and conjectural, and many of the presumptions about how these animals lived out their lives rely on tacit intuition and the selection of modern examples that appear to support a given conjecture.

Since their first discovery, sauropods have long been the subject of speculation, e.g., that they had a sprawling stance [2,3], used their long necks as snorkels while walking along the bottoms of lakes [4], walked bipedally [5,6], used their tails as supersonic bullwhips [7], used their hindlimbs to kick predators [8], sat down to eat [9], held their heads so high as to require multiple hearts to create sufficient blood pressure [10,11], and long necked or short, habitually dorsiflexed the base of their long necks to achieve maximum head elevation [12].

Note that the above speculations are suggestions not only about potential function (snorkeling, standing on hind legs, whipping, kicking, sitting, and holding the head high) but about behavior, and unless outright refuted as physically impossible, are subsequently adopted – or not – based on their appeal and support by analogical reasoning (see below). There is also a tendency to propose conjectures that are not scientifically testable (i.e., not

refutable) yet seem compelling, popular, and make for a satisfactory story [13]. For example, Paul [14] argues that “... a low neck increases the risk of not spotting attackers ... and so appears illogical”. Long necks that reach high allow the owner to see approaching predators, to see where they are going, to eat what others with shorter necks could not reach, and to keep their necks out of reach of predators’ jaws [15]. For sauropods to have not used their long necks to elevate the head, and to keep it elevated habitually when not drinking or browsing low vegetation, would have been to miss the best part of having a long neck. Even sauropods such as *Diplodocus* with shorter forelimbs (and seemingly ill-adapted to a life of high browsing) are expected to have raised their heads skyward habitually (by bending the neck sharply upward at the base and tucking the chin down to level out at the head) [12]. While sauropods with soaring necks is congruous with childhood expectations, these often-repeated and seldom-challenged speculations amount to little more than scientific mythology.

Recently, however, there has been increasing use of a method to challenge the mythology using observations of modern vertebrates and certain bridging assumptions to ‘ground-truth’ proposals about sauropod pose, flexibility, and behavior. The application of this methodology to examine the mythology is the subject of this review.

Conjectures about sauropod neck function, physiology, and feeding behavior are invariably based on skeletal reconstructions by illustrations or mounts and while such reconstructions are very familiar and seemingly authoritative, they often amount to hypotheses or conjectures incorporating significant artistic interpretation (see below). Some effort will be devoted to this issue, since sauropod reconstructions, whether physical or pictorial, are often used uncritically, as will be discussed. The relationships between osteological form and biological function in general, and of vertebral articular geometry and joint articulation in particular are becoming increasingly understood, and recent studies are confirming that vertebral osteology can tell us something about pose and flexibility. The vertebrate neck is not merely a chain of bones and joints, but a system, and observable correlates between structure and function in the necks of extant vertebrates are becoming better understood, thus permitting more principled application towards interpreting sauropod neck function.

The Appeal of Simple Explanations

“... the truth will out. Nature’s phenomena will agree or they’ll disagree with your theory. Although you may gain some temporary fame and excitement, you will not gain a good reputation as a scientist if you haven’t tried to be very careful...” [16].

There seems a universal tendency to confer greater trust upon simple parsimonious explanations of natural phenomena, those that capture some essence in few words and to hold broadly without exception. It has been suggested that, based on how extant amniotes hold their heads in alert rest, that sauropods assumed a posture with the neck is maximally extended (dorsiflexed) at the base and the head maximally ventrified [12,17], giving weight to the popular expectation that sauropods indeed held their heads up. Disregarding for the moment whether amniotes actually raise their heads maximally when in alert rest, it represents an attempt to ground speculations by more than just an appeal to common sense. Whether sauropods held their heads in such a state is not expected to be directly testable i.e., refutable. Instead, an indirect



Figure 1. Intrinsic neck curvature starts with the bones. In (A), cervical vertebrae C4 and C5 of *Giraffatitan brancai* specimen SI are shown articulated and undeflected, i.e., in osteologically neutral pose (ONP). Their vertebral axes, shown in red, naturally create a slight downward bend in ONP, contributing to the subtle ventral osteologically induced curvature (OIC) likely shared with other sauropod necks cranially (Figure 5). In (B) the giraffe *Giraffa camelopardalis*, cervical vertebrae C6 and C7 are shown also in ONP, revealing the naturally-ascending slope characteristic of giraffe necks at the base. Note the similarity in their opisthocoelous central articulations compared to the sauropod above. Vertebrae to scale; scale bar equals 10 cm. Giraffatitan photographs courtesy Christopher McGowan; giraffe photographs courtesy Brian Curtice.

doi:10.1371/journal.pone.0078572.g001

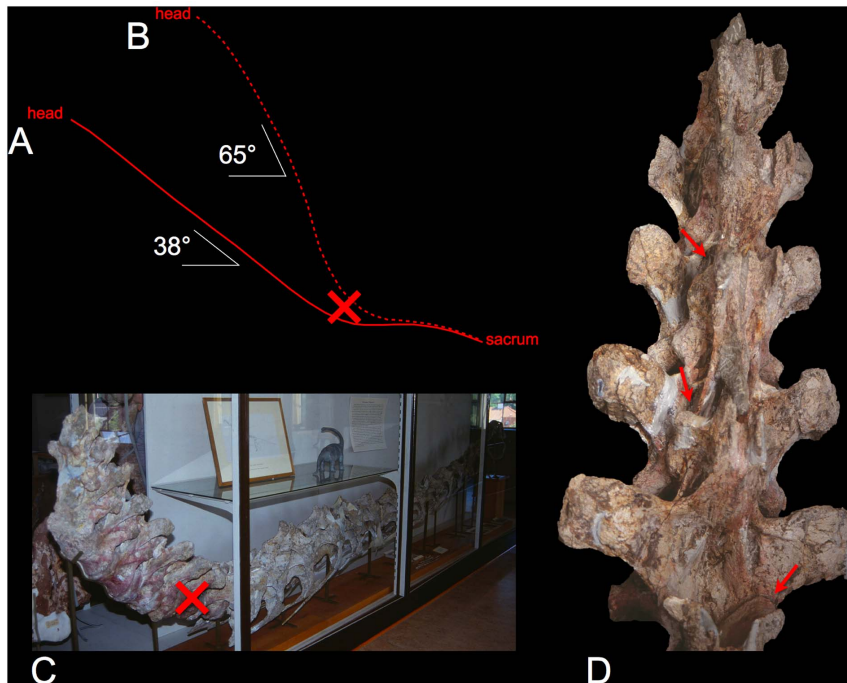


Figure 2. The life and death of *Euhelopus zdanskyi*. In 1929, Wiman illustrated this sauropod in life with a decidedly giraffe-like pose, rising at a slope of 38° (vertebral axes indicated by the solid red line in A, derived from [4:fig. 3 and pl. 3], see also [32:fig. 9]). In the life reconstruction the base of the neck was given the same curvature as the opisthotonic pose in which the original specimen was found (C). It has subsequently been depicted with a steeper slope (dashed red line in B, from [14]) that even exceeds the death pose in which bone already contacts bone (indicated by the red arrows in D). While the neck has also been regarded as more moderately curved [33], *Euhelopus* may in fact have had a straight neck in the cervicodorsal region in ONP [31–32]. Photographs courtesy Valérie Marin-Rolland of the *E. zdanskyi* specimen PMU 24705, Paleontological Museum of Uppsala University.

doi:10.1371/journal.pone.0078572.g002

argument is provided based on an observable (and refutable) relationship in extant organisms to support the untestable speculation. In brief, the method, the ‘Extent Phylogenetic Bracket’, or EPB (discussed in more detail below). In brief, if a given unpreserved property such as a behavior is exhibited by a specifically-defined extant cohort of related organisms, there is reason to speculate that the extinct organism also shared this property. But as cautioned by the proponents of this approach [18,19], even speculations that are successfully supported by the method remain guesses, only more ‘educated’ or ‘informed’ guesses. Following Witmer [19] “... the term speculation is not used here in its more common, pejorative sense, and implies no de facto absence of testability ... we need greater methodological rigor in order to determine the limits of our objective inferences – that is, to constrain, not completely eliminate, speculation.” The EPB method provides at least some grounds for speculations that, by their very nature, cannot be empirically verified.

Polarized Conjectures

The necessarily speculative nature of theorizing in paleontology is unfortunately susceptible to the social phenomenon of ‘group polarization’, as speculations are adopted and repeated by secondary sources [21,22,23]: “... as individuals learn that most of the other group members lean in one direction on some issue, they may adopt a more extreme attitude in the same direction” [24]. Group polarization may create a false dichotomy when outgroup opinions are stereotyped and misrepresented in stating the strengths of one idea or the weaknesses of another, and a general failure to acknowledge implicit bridging assumptions, exceptions, and potential pitfalls in subsequent citations.

Regarding sauropod necks, for instance, while historically they have long been depicted with a wide range of combinations neck curvature (from straight to sharply reflex-curved) and slope at mid-neck (from horizontal, or even downward-sloping to vertical or even past vertical) [25,26,4,14,27,28,29,30–33], there is a tendency for subsequent retrospectives and reviews to categorize, to simplify, and to polarize: “Sauropods can be broadly grouped into forms with ... a presumably upright neck ... and forms ... with a presumably more horizontal neck” [34]. The expectation for increasingly high head elevation is exemplified by *Euhelopus zdanskyi* (Figure 2) which was originally depicted in 1929 with a slope of 38° [4] but that was later revised to 68° [14]. *Mamenchisaurus hochuanensis* was originally depicted with a descending neck [35], yet mamenchisaurids have subsequently been illustrated [14,29] and mounted [Zigong Dinosaur Museum] with subvertical necks. Even *Opisthocoelicaudia sharzynskii*, found without a neck and originally reconstructed with a horizontal neck [36] was later given a swan-like neck [14,29]. *Giraffatitan brancai*, perhaps the iconic swan-necked sauropod, was given one when first described and mounted has been depicted with increasingly steep neck in both mounts (Figure 3) and illustrations (Figure 4) [27,14,29]. *Camarasaurus* was originally depicted without a swan neck [37], but soon acquired one [38], and to this day, camarasaurids are generally reconstructed as having a vertical or even past-vertical neck [14,29]. The dichotomy of ‘upright’ versus ‘horizontal’ is not absolute. Even *Giraffatitan* has been given comparatively low-neck interpretations [39,31,32,40]. But while some other sauropod taxa are reconstructed with descending necks at shoulders (e.g., *Dicraeosaurus hansemanni* [41,42,31–32,43] and *Nigersaurus taqueti* [44]), it has



Figure 3. Impressive sculpture. The *Giraffatitan brancai* mount at the Humboldt Museum of Natural History has been restored with an extraordinarily steep neck at the base, with an ascending neck that appears to be in ONP. While the neural arches in the cervico-dorsal region were not preserved, the centra were, and the sculpture in the mounted skeleton deviates significantly from the actual fossil material (see Figure 4). Photographs by the author.

doi:10.1371/journal.pone.0078572.g003

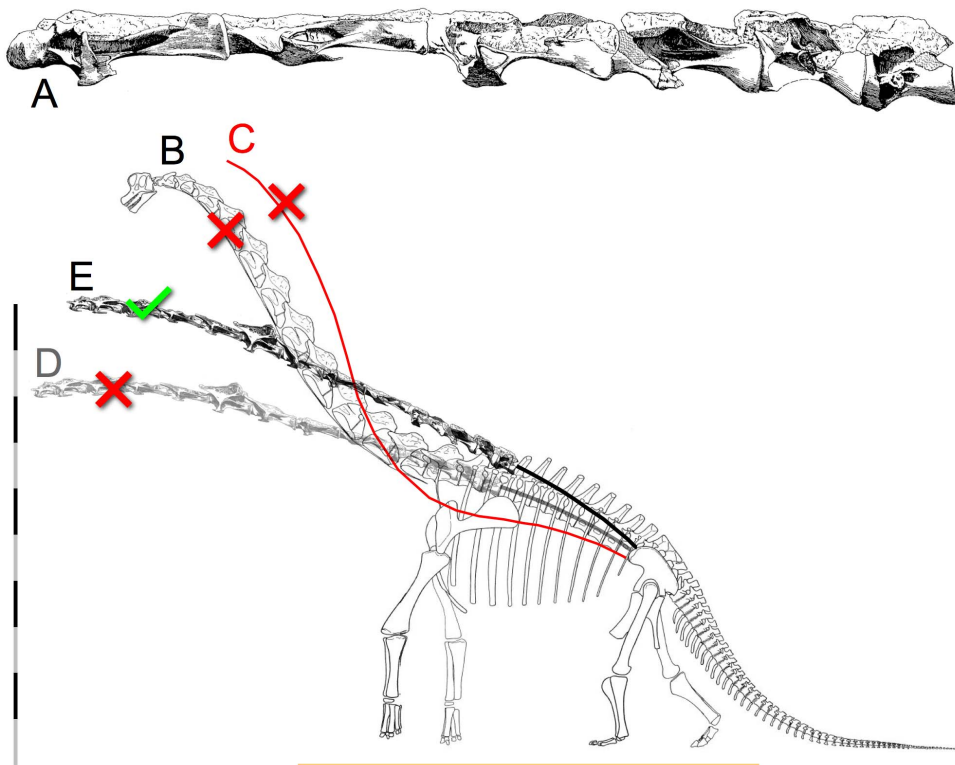


Figure 4. The iconic swan neck of *Giraffatitan brancai*. Janensch [104] (A) illustrated the original fossil material in the cervico-dorsal vertebrae (C10 to D2) as they were found, in articulation, and despite their missing the neural spines, the centra are collinear and appear close to ONP based on their central articulations. Janensch's skeletal reconstruction [27] (B), however, does not reflect this osteology; instead a gracefully-curved swan neck was illustrated, complete with restoring the vertebrae at the base of the neck as if wedge-shaped to formed that elegant rising curve in ONP. The slope of the neck increased further in some later illustrations, e.g., the red curve (C) is drawn from Paul's reconstruction [14; 32:fig. 6]. The centra at the base of the neck are straight, elongated cylinders with parallel anterior and posterior central margins (A) and not wedge-shaped with convergent margins (as inevitably, mis-represented) like those of a giraffe, there is no osteologically-induced bend at the base of the neck. Substituting an ONP reconstruction of the complete vertebral series from C3 to D2 based entirely on Janensch's individual vertebral illustrations (see text) two alternatives are presented (D and E). In D the slope of the anterior column matches that of the original skeletal reconstruction by Janensch [27], which has relatively high placement of the pectoral girdles upon the ribcage (but lower placement than Paul [14] illustrated, which caused his reconstruction to have a lower vertebral column at the base of the neck). If the scapulocoracoids are reconstructed as closely separated medially and more ventrally placed upon the ribcage, the resultant slope of the anterior dorsals rises necessarily. This raises the head height to 10 m, while the Berlin mount goes to 11, or more. Scale bar is 10 m. The horizontal line represents the ground plane according to revised appendicular reconstructions.

doi:10.1371/journal.pone.0078572.g004

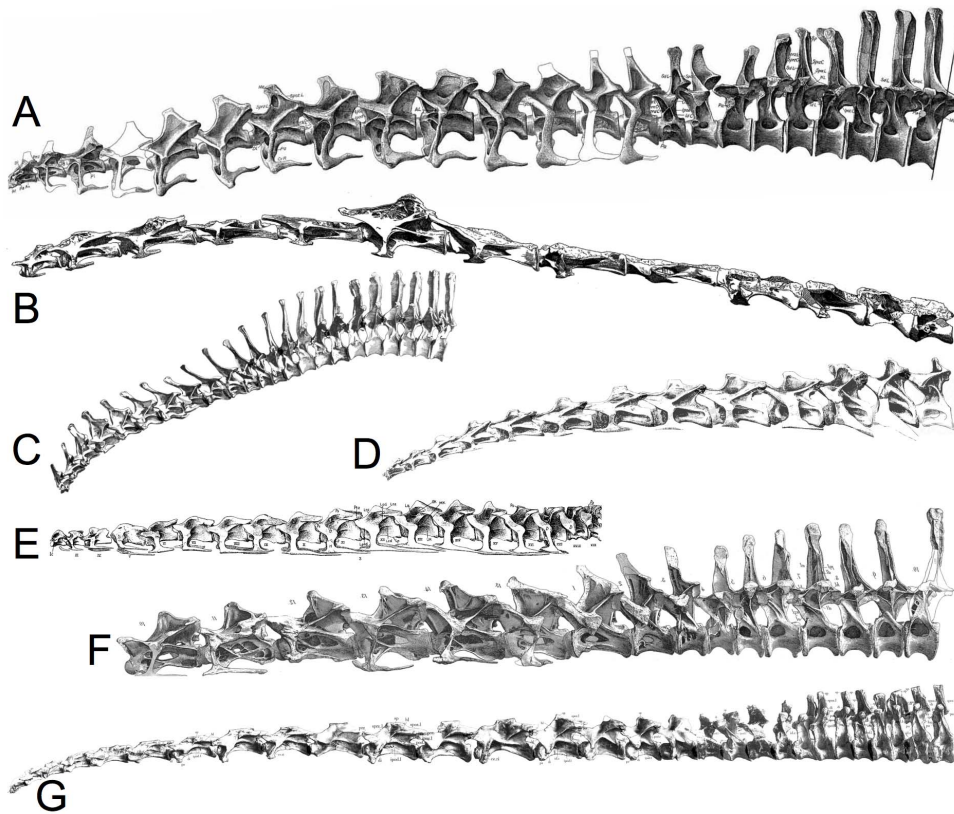


Figure 5. Estimation of sauropod ONP from illustrations. Composite figures are assembled into approximate ONP for partial or complete presacral columns for various sauropods: A: *Apatosaurus louisae* [45], B: *Giraffatitan brancai* [27], C: *Dicraeosaurus hansemanni* [86], D: *Cetiosaurus oxoniensis*, E: *Euhelopus zdanskyi* [4], F: *Diplodocus carnegii* [26], and G: *Mamenchisaurus youngi* [35]. Note that some exhibit a slight dorsal OIC cranially, and all are straight caudally. *Cetiosaurus* illustrations courtesy John Martin. The reconstructions are not to scale, however, the individual vertebrae within a column were adjusted as necessary to the same scale within each vertebral column [31,32]. doi:10.1371/journal.pone.0078572.g005

recently been argued that all sauropods held their heads high [12], as will be reviewed below. The presumption that many – perhaps most – sauropods held their heads high above ground level has become deeply entrenched and incorporated in derivative research regarding their physiology and behavior. Sauropod reconstructions are necessarily speculative, however, and likely have been subject to polarization, especially in the frequent absence of quantitative measurements (of slope and curvature) associated with the reconstructions.

Analysis of neck curvature in modern vertebrates provides a means to estimate neck curvature in sauropods. The starting point is to distinguish intrinsic curvature as that which remains in a vertebral column when all intervertebral joints are in an undeflected state. Osteological mounts of extant vertebrates are valuable resources illustrating intrinsic curvature and how it arises from their particular osteology. When the vertebral columns of extant birds, reptiles and mammals are assembled with the successive vertebrae spaced according to their separations in life, and with each joint undeflected, the columns assume a familiar and characteristic intrinsic curve associated with that taxon in an osteologically neutral pose (ONP). The process of estimating intrinsic curvature is of course neither absolute nor exact, nor is it immune to artistic bias and measurement error, in particular as regards speculation about the thickness of the intervertebral separation for extinct vertebrates.

Despite their common depiction with rising curvature at the base of the neck, reconstructions of the undeflected neck in

sauropods in the cervico-dorsal vertebral columns suggest they were straight where the neck transitions into the anterior dorsals [30–32] (Figure 5). This basic finding is at odds with many depictions of sauropods, particularly brachiosaurids and camarasaurids, as will be discussed, but subsequent polarization of this work have summarily equated ‘straight’ (i.e., a lack of curvature) with ‘horizontal’ as: “When sauropod necks are reconstructed in ONP, their necks are horizontal” [17]. Straight, yes, but not necessarily horizontal. The goal of the 1999 study [30] was comparative neck flexibility, however, wherein *Diplodocus* sp. was found to be less flexible than *Apatosaurus* sp. when both were subject to the same criteria to limit intervertebral flexibility based on a modern avian model (see below), and both were less much flexible than the avian model. Head height of course varies trigonometrically with the slope and height of the base of the neck [31–32], and if the anterior dorsal column in diplodocids had sloped downward as originally depicted [25,26,45] that would have sent the neck on a downward slope as well (Figure 6a). But the modern interpretation of the pectoral girdles [cf. 32, 46] elevates the anterior dorsal column to approximately horizontal (Figure 6c, d), and this is naturally reflected in higher head heights. The ‘straight’ sauropod neck was subsequently reconstructed clearly horizontal or upward sloping, and when the less-than-avian 1999 estimates of diplodocid neck flexibility are applied to the revised bauplan, the 2005 studies [31–32] clearly showed that even the diplodocids could reach high enough that their feeding envelopes overlapped vertically with some other sympatric

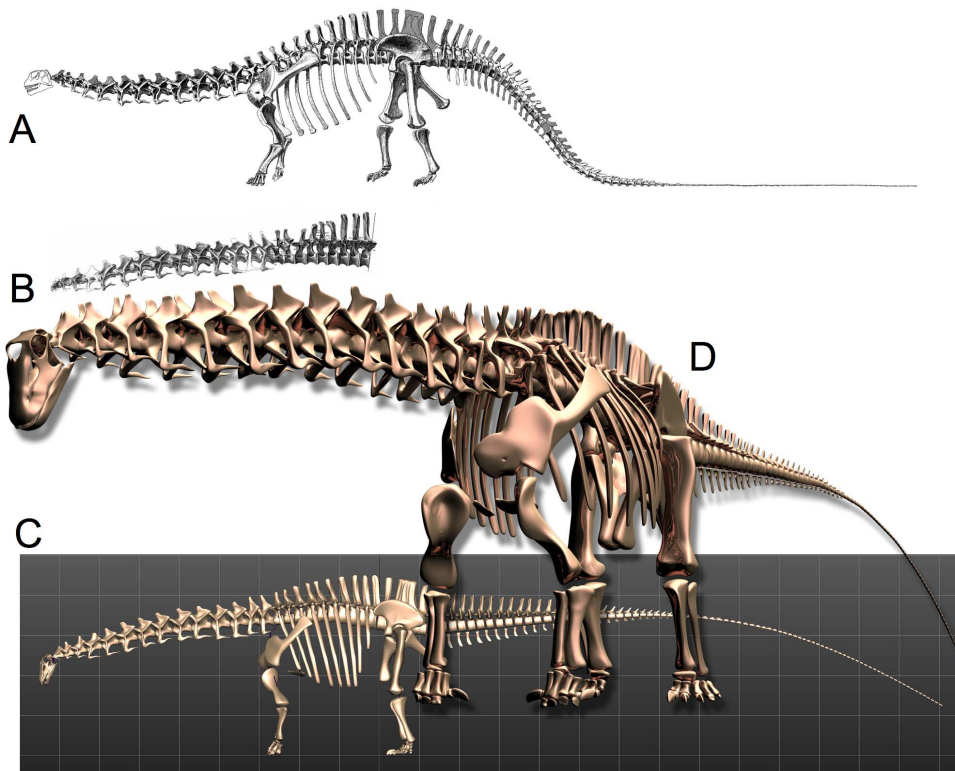


Figure 6. Revised Skeletal Reconstruction of *Apatosaurus louisae*. In the original 1936 reconstruction (A) of *Apatosaurus louisae* (CM 3018) [45] the pectoral girdles were positioned quite dorsally upon the ribcage, which created a downward slope to the anterior dorsal column at the shoulders, and hence a downward slope at the base of the neck. Reconstruction of the vertebral column from individual illustrations [B] corresponds closely to the skeletal illustration and was used as one check of the dimensional accuracy of a fully-articulated digital model of the specimen CM 3018 (C). All elements modeled individually to scale, based on archival sources [45] plus photographs and personal observation of the original material during its reassembly and remounting at Phil Fraley Studio, and scale orthographic drawings courtesy Philip Platt [pers. comm.]. In articulating and posing the digital model, the orientation and placement of the pectoral girdles and the angulation of the ribs incorporate many current contributions of studies of the articular skeleton, in particular the placement of the pectoral girdles [31–32, Phil Platt, pers. comm.]. doi:10.1371/journal.pone.0078572.g006

sauropod taxa regarded as ‘high browsers’. And yet these studies are persistently characterized as only suggesting these sauropods “... held their necks at or below horizontal, and could not raise their necks far above the horizontal” [12,17,47] and to have resulted in “low flexibility estimates” [48], promoting or perpetuating a false dichotomy, a polarization, between unnaturally-stiff-and-horizontal versus naturally-flexible-and-high-reaching.

Depolarization

To depolarize the dichotomy between sauropod necks as straight-and-stiff-and-horizontal versus curved-and-flexible-and-upright requires replication and independent confirmation, and convergence of contributions from multiple directions. This will allow for more substantive pursuits, such as seeking deeper explanations for their extreme specializations. But proposals about sauropod neck curvature, pose, head height and so forth have been confounded and conflicted in the literature, and progress will likely require that they be understood in basically the following order:

1. intrinsic curvature of the vertebral column in the undeflected state.
2. intervertebral flexibility.
3. habitual pose for a variety of activities, including feeding, locomotion, and alert rest.
4. characteristic motions involved in browsing, drinking, display, surveillance.

5. vertical and lateral reach, feeding envelopes versus reachability volumes.

Just as the sauropod neck is becoming better understood in terms of topics (1–3), the post-cervical skeleton is as well, permitting refined estimations of the motions and characteristics of the vertebrate as whole. Importantly, studies of sauropod forelimbs and pectoral girdles [32,49,50] is resulting in the reconstruction of diplodocids and camarasaurids as much taller at the shoulder [31–32,46] than when first described [26,37,45] (Figure 6). With their anterior dorsal columns no longer depicted as steeply descending, but instead horizontal or slightly rising through the shoulders, their heads would rise accordingly, and consequently even ‘low browsers’ such as *Diplodocus* could have engaged in an ecospace that many would consider as ‘high browsing’ [32] – see Figure 7. Camarasaurids and brachiosaurids were even taller at the shoulder absolutely, and had relatively longer forelimbs (compared to hindlimbs), resulting in even greater slope at the anterior dorsal column at the shoulder, and ultimately the slope of the base of the neck. Especially in the case of *Giraffatitan brancai*, one need not affix a swan-like neck for the head to rise far above that of the contemporaneous diplodocids [32]. Moreover, if much of the head elevation in the taller sauropods were achieved by leg elongation rather than neck curvature, they were still easily able to ‘high browse’ even if reaching down to feed, as modern giraffes often do today [51,52], while reducing hemostatic pressures since the head

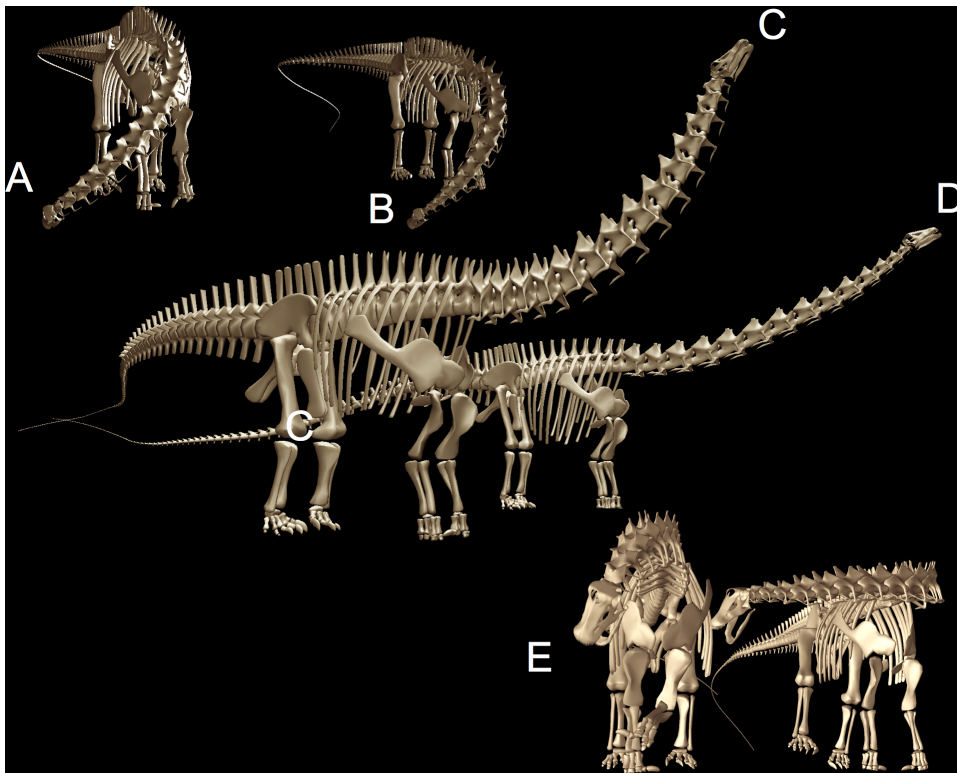


Figure 7. Diplodocids swept out a huge feeding surface, despite their relative inflexibility. *Apatosaurus* (A) and *Diplodocus* (B) are shown in extreme lateroventral flexion, reaching down and laterally to ground level, and in C and D in extremes of dorsal flexion (including dorsiflexion at the cranio-cervical joint) as if to reach as high as possible (see also overall feeding envelope visualization in Figure 20). Despite the enormous sweep of these necks, the vertebral joints, especially at the base of the neck of *Diplodocus* (C13 and C14) permit limited flexion prior to disarticulation (see Figure 9). While both necks sweep out a huge surface area, *Apatosaurus*, with its larger posterior cervical zygapophyses, could reach higher despite having a somewhat shorter neck than *Diplodocus*.
doi:10.1371/journal.pone.0078572.g007

would have usually been within a few meters of the height of the heart in ONP [H-C. Gunga, pers. comm., 53–55]. Differences in neck length and the slope at the base would differential head height and feeding specializations [56] would facilitate resource partitioning, without having to postulate that some had swan-shaped necks.

Estimates of head elevation as based on osteology alone is generally lower than that suggested by an analysis of forces and moments [57–60], and that is generally lower than the most extreme poses suggested on behavioral grounds [12]. Understanding of habitual neck postures will be refined and depolarized as better descriptions of the behavior of modern models are forwarded. At the time of this review, views on sauropod necks remain contentious primarily regarding topics (1–3), i.e., the intrinsic curvature of sauropod necks, their flexibility along their length, and especially, their pose at rest. In fact, much of the contention and polarization seems to reduce to whether these terrestrial giants held their heads swan-like or not when resting, which has little bearing on the important questions of sauropod biology, namely, how did they eat, rather than how they stood there when not eating.

Methods

Inferences about sauropod necks (their curvature, flexibility, habitual poses, characteristic motions, and the relationship between the neck and the rest of the sauropod) rapidly lead from the hard evidence, the fossil material, to speculation. Even the

reassembly of the undeflected vertebral column requires understanding how they were connected by soft tissues, and yet their intervertebral joints are not known and can only be inferred. Inferences about habitual neck posture and movement are even more derivative – and necessarily more speculative – as they build upon assumptions about intervertebral flexibility, which must build upon assumptions about the intervertebral joints, and so forth.

Supporting Conjectures about Unpreserved Properties

The Extant Phylogenetic Bracket (EPB) [18,19] is a method to support speculative inferences about properties that are not preserved in the fossil record such as a feature of soft tissue anatomy [19,20,61] or some aspect of behavior such as reproductive rate [62]). Consider some property P that is present in some taxa. Use P(t) to indicate that P is indeed present in taxon t. The EPB provides a means to support the inference P(t₀) for some extinct taxon t₀. Since P(t₀) cannot be observed directly, an indirect argument is offered that involves an ‘osteological correlate’ O that reliably co-occurs with P in extant taxa and which is reliably preserved in the fossil record. O and P should be “causally associated” [18,19], i.e.,

$$O(t) \leftrightarrow P(t) \text{ for taxon } t.$$

The co-occurrence of O and P is examined for the so-called extant phylogenetic bracket (EPB), namely the set of taxa that comprise the closest-related outgroup to the extinct taxon t_0 [18]:

$$\forall t \in \text{EPB } O(t) \leftrightarrow P(t).$$

Given the physical correlate holds for extant taxa, the presence of the physical evidence O in a fossil of an extinct taxon t_0 might be offered as evidence that this taxon also exhibited property P:

$$O(t_0) \rightarrow P(t_0).$$

If the osteological correlate O is exhibited by all taxa in the EPB, then a so-called ‘Type I’ inference is supported for the extinct taxon, i.e.,

$$(\forall t \in \text{EPB } O(t) \leftrightarrow P(t)) \rightarrow (O(t_0) \rightarrow P(t_0)).$$

While some inference about the extinct taxon is well supported by observations on extant counterparts, the inference necessarily remains a speculation – just a “more constrained speculation” [19]. The strength of inference is weakened when the osteological correlation does not hold for all taxa in the extant outgroups, i.e., where some extant taxa that exhibit P but not C (or vice versa). Such counterexamples permit at best (“Type II” and “Type III”) inferences, with gradations [19,20]. However, even in the absence of support by extant outgroups, a case may be based on a “sufficiently strong causal relationship” between C and P in extant taxa, i.e., “an argument of compelling morphological evidence [19], or ‘extrapolatory analysis’ [18]. A weaker, abbreviated form of this method, would rely on P occurring in the EPB, without support from an osteological correlate. This amounts to jumping to the conclusion without physical evidence:

$$(\forall i \in \text{EPB } P(i)) \rightarrow P(t_0).$$

An invocation of EPB is particularly weak if, in addition to neglecting osteological correlates, draws conclusions based on only a limited sampling of extant taxa that exhibit the given property:

$$(\exists i \in \text{EPB } P(i)) \rightarrow P(t_0).$$

Terminology

Osteologically Neutral Pose (ONP). The undeflected state of an intervertebral joint, geometrically defined by centering the associated pre- and postzygapophyses.

Vertebral Axis. A vector constructed from cotyle center to condyle center, used to quantify curvature along a vertebral column (Figure 1).

Intervertebral Curvature. The angular difference between successive vertebral axes. Intervertebral curvature is zero when the axes are geometrically collinear (Figure 1).

Osteologically Induced Curvature (OIC). The curvature of a vertebral column in ONP, as distinguished from curvature induced by joint deflection (Figure 1).

Range of Motion (ROM). The set of all achievable combinations of mediolateral and dorsoventral flexion. As applied to a vertebral column: the set of poses (some subset of the product space of all individual joint ROM), also termed a ‘reachability envelope’.

Osteological Stops. Contact between vertebrae that limits angular deflection at a vertebral joint and provides load-bearing bracing against disarticulation. Osteological stops may be present independently for dorsiflexion and for mediolateral flexion, or not at all.

Zygapophyseal Safety Factor (ZSF). During intervertebral joint flexion, displacement between pre- and postzygapophyses is limited by the surrounding ligamentous synovial capsule, which draws taut prior to their disarticulation, preserving a ‘safety factor’, a minimal overlap (typically 0.2–0.5 by lineal measurement). The ZSF provides a not-to-exceed limit on joint deflection, which is further restricted by soft tissues and behaviorally (see below).

Extant Phylogenetic Bracket (EPB). To support speculation that some extinct taxon had some unpreserved property (e.g., a soft tissue structure or behavior) based on 1) observation of that property in closely-related living forms, the EPB, and 2) an ‘osteological correlate’. Presence of that correlated physical evidence in the extinct taxon supports inference that the unpreserved property was also present (see below).

Estimating Intrinsic Curvature and Intervertebral Flexibility

The first two of the above five tasks concern estimation of intrinsic curvature and the extremes of what the joint geometry might allow – basic geometric (kinematic) aspects of sauropod neck shape and flexibility, and do not concern estimating their habitual poses, postural preferences, or behavioral tendencies. The success with which neck curvature and flexibility is replicated through the manipulation of the dry bones of extant vertebrates might be used to gauge the feasibility of estimating sauropod neck curvature and flexibility [12]. Clearly there would be little hope of learning about sauropod necks if extant vertebrates cannot be used as controls.

The Osteologically Neutral Pose

Quantification of intrinsic curvature and joint flexibility requires first establishing the undeflected state of the intervertebral joints. The osteologically neutral pose or ONP [30–32] (Figure 1) defines the state of an deflected vertebral column, relative to which extremes of joint dorsiflexion, ventriflexion, and mediolateral flexion are subsequently measured [15,63–65,48]. Additional refinement to the operational definition of ONP is warranted, especially when the joint geometry suggests differing degrees of dorsal versus ventral flexibility, but a satisfactory convention is to define ONP as when the pre- and post- zygapophyses are centered and maximally overlapping, which often coincides at the centrum to parallel margins of synovial capsule surrounding the condyle-cotyle. ONP is not “merely the midpoint in the range of motion” as concluded by Taylor et al. [12] – vertebral joints are not equally flexible dorsally as ventrally. That is, flexibility is measured relative to ONP, not vice versa.

A vertebral column in ONP reveals the characteristic curve of the undeflected neck, which provides an important guide to how that neck is utilized [66], as discussed below. The characteristic curve of a vertebral column that remains when all joints are undeflected is termed here osteologically induced curvature (OIC), which medically correspond to regions of kyphotic versus lordotic curvature [67], and the anatomically-defined regions of the avian neck based on curvature and maximum dorsal and ventral flexibility [68–70,64]. Determining the ONP of a sauropod’s

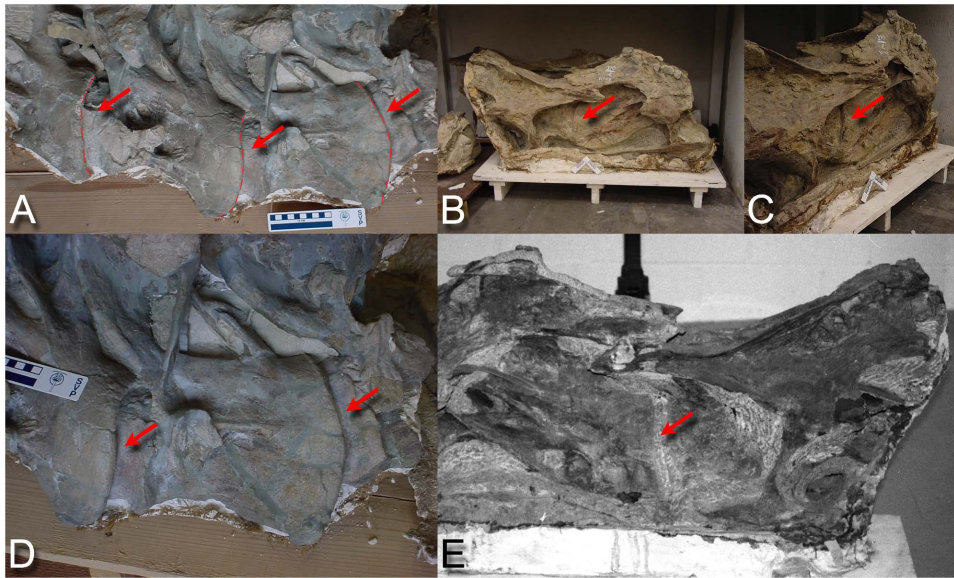


Figure 8. Sauropod intervertebral separations. Examples of articulated sauropod cervical columns with condyles deeply inserted into their associated cotyles, leaving intervertebral gaps of only a few centimeters (see arrows). *Camarasaurus lentus* (DNM 28, A and D) and *Barosaurus* (CM 11984, B, C, and E). Photographs by the author and J. Michael Parrish. doi:10.1371/journal.pone.0078572.g008

cervical vertebral column given only its bones requires is necessarily speculative since the cartilage, and thus the intervertebral spacing, is unknown.

Accounting for Unpreserved Arthrology

Intervertebral joint flexion, in general, involves one vertebra rotating about an instantaneous or ‘momentary’ center of rotation relative to the other [71]. For vertebrates with amphiarthrotic amphiplatyan central articulations (such as lagomorphs, felids and humans), the instantaneous rotation center is not fixed, but rather, shifts depending upon the mechanical properties of the soft tissues and the instantaneous loading [72,73]. Especially in those mammals such as lagomorphs whose cervical vertebrae are separated by a compressible nucleus pulposus, the resultant curvature of the column in life represents a reaction to all compressive, tensile and shearing forces imposed along the column, and a ‘dry bones’ articulation [12] would be expected to fail to predict either the column’s curvature or flexibility in life. But static reconstruction has been used successfully to estimated pose and flexibility in vertebrates with diarthrotic central articulations, such as the closely-spaced heterocoelous vertebrae of birds [74]. Diarthrotic articulation involves the sliding translation of one surface upon a conformal, apposed surface, thus the instantaneous center of rotation is strongly constrained by their conformal geometries.

Wedge-shaped intervertebral disks contribute to the intrinsic lordotic or kyphotic spinal curvature of amphiplatyan vertebral columns, such as mammalian vertebrae and particularly apparent in the human lumbar spine [75]. Thick intervertebral disks are sometimes suggested to have formed some of the upward curvature in sauropod necks, where “... the thicker the disks were, the more upwardly flexed the neck was” [14], however the intervertebral disks in birds and reptiles do not have a nucleus pulposus and birds in particular are characterized by closely-spaced, conformal, diarthrotic articular facets [76].

Numerous articulated sauropod cervical vertebral columns have been found with their central condyles deeply inserted within

cotyles (e.g., see Figure 8, and Figures 16, 17, below). The preserved small intervertebral separations leave no room for the thick wedge-shaped cartilaginous pads that have been suggested might have curved the neck [14], nor should there they be expected. Moreover, the annulus fibrosus would unlikely shrink significantly due to its high density [77]. Instead of thick pads, intervertebral separations of a few centimeters between condyle and cotyle are suggested by their difference in radii of curvature (pers. obs.), which is consistent with the tightly-fitting central articulations found by Dzemski and Christian [15] in Ostrich (<1 mm) and Giraffe (7–9 mm), given that articular cartilage is negatively allometric with body mass [78].

Estimating Intervertebral Flexibility

During joint flexion, the pronounced opisthocoely of sauropod cervical vertebrae greatly reduces uncertainty about the center of rotation, or the pivot point, about which they articulated. A cervical vertebrae can be regarded a rigid body comprised of three contact surfaces, the cotyle and plus paired postzygapophyses, moving as a unit in gliding contact over the surfaces of the condyle and paired prezygapophyses of the subsequent vertebra. As cotyle rotates over condyle, the postzygapophyses make gliding contact as they travel across their associated prezygapophyses (allowing for thin avascular layers of hyaline cartilage). Since both the central articulation and the zygapophyses are diarthrodial, with free sliding motion within their capsules, angular deflection at the centrum results in predominantly a translation or gliding motion of parallel articular surfaces, which is especially apparent as the postzygapophyses sliding across prezygapophyses. That translation must be arrested at some point otherwise disarticulation will occur. It is expected that sauropods, like modern vertebrates, arrested motion prior to disarticulation, preserving a residual overlap or zygapophyseal safety factor (ZSF).

Intervertebral joints flex dorsoventrally, mediolaterally, and in combination (dorsolaterally, etc.) to define a range of motion (ROM). Manipulation of dissections of turkey cervical columns [30] reveal that flexibility at each intervertebral joint is ultimately

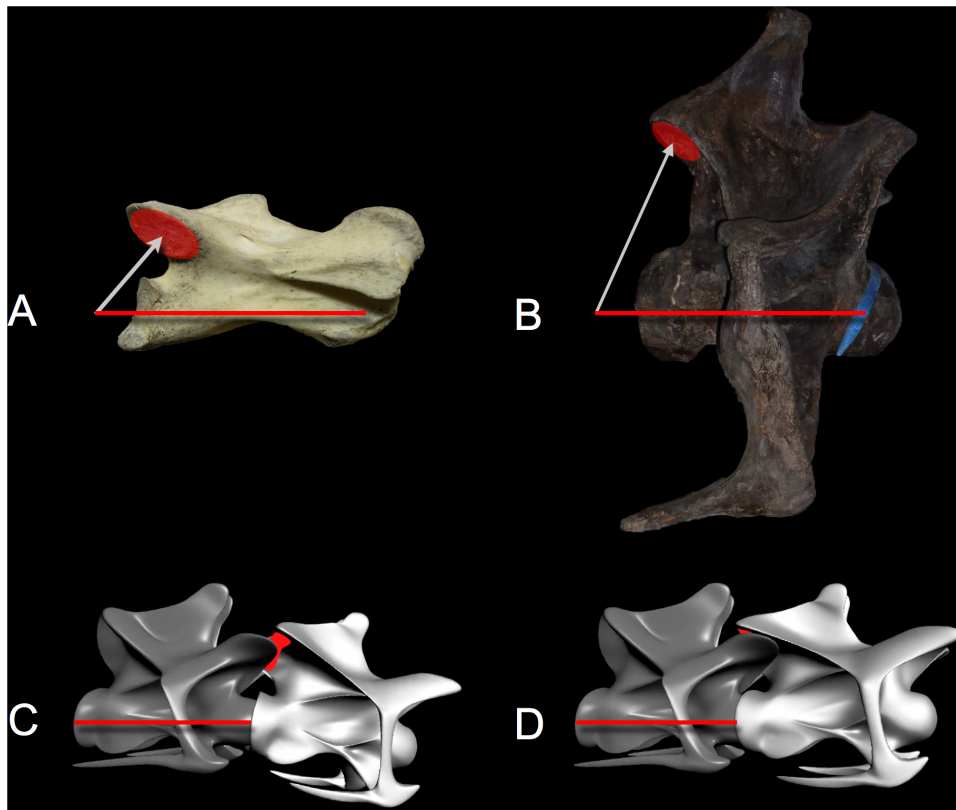


Figure 9. Sauropod necks did not have avian flexibility. Cervical vertebra C13 of the ostrich *Struthio camelus* (A) and C13 of *Apatosaurus louisae* (B) are scaled to equal vertebral axis length. The heterocoelous central articulation (A) and the opisthocoelous articulation (B), both have geometrically-defined centers of rotation defined by their centers of curvature in the sagittal plane. The ostrich postzygapophyses (red) are both relatively larger and closer to the center of rotation (white arrows) than those of the sauropod. The geometric consequence is that for any value of ZSF applied equally to the ostrich and to the sauropod, the former will have a greater range of motion. C and D show two articulated cervical vertebrae, C13 and C14, near the base of the neck of *Diplodocus carnegii* (CM 84) in maximum lateroventral flexion to the left (C) and maximum laterodorsal flexion (D), i.e., diagonal extremes of the range of motion. Note that the postzygapophyses (red regions) in C and D barely overlap their associated prezygapophyses (the ZSF is about 0.5). *Struthio* image courtesy John Martin; *Apatosaurus* image courtesy Virginia Tidwell. Supplemental material: Movie S1.
doi:10.1371/journal.pone.0078572.g009

limited by the zygapophyseal capsules which prevent disarticulation by preserving a minimum overlap or zygapophyseal safety factor (ZSF). Manual exploration of the range of motion suggested that roughly 25–50% overlap (by lineal measurement) remained when the capsules were taut [30]. This was confirmed independently by a radiographic study of neck flexibility in ostrich which found that “bone would break before the zygapophyses would disarticulate” [M. Wedel, pers. comm, 79, 32]. Limiting neck flexion by preservation of zygapophyseal overlap was met with skepticism [80] due to the remarkable dorsal flexibility exhibited by camels [81], which actually does not require disarticulation [32]. Further confirmation of this safety factor is summarized by Dzemski and Christian [15]: “Extensive observations of living giraffes [63] and observations of living camels are in accordance with the data that were determined from the skeletons”. Moreover, the expectation that “... in vivo, muscles, ligaments, and fascia may have further limited movement” [30] has recently been supported [48] for the ostrich, however flexion in living birds approaches the limits of disarticulation [15]. While the ZSF predicts ‘best case’ estimations in extant vertebrates [30] (see also Figure 12), its application may overestimate neck flexibility in sauropods with elongate tendonous cervical ribs [82].

A conservative ZSF of 0.5 was used to estimate the relative neck flexibility in two diplodocids [30]. The relatively larger zygapo-

physeal surfaces in the posterior cervicals of *Apatosaurus louisae* permitting greater dorsal and ventral flexibility compared to the more slender counterparts in *Diplodocus carnegii* (Figure 7), but compare to the ostrich (Figure 9), the relatively small zygapophyses of *Apatosaurus* suggested far less than avian flexibility. The D. carnegii reaching laterally to harass *A. louisae* (Figure 7e) illustrates how at mid-neck any further lateral flexion would disarticulate its zygapophyses. Similar constraints apply to dorsiflexion, and will be discussed in the context of bracing the neck at the limits of head elevation.

Osteological Bracing

In some vertebrates, in addition to limiting deflection by the ligamentous synovial capsule surrounding the zygapophyses, intervertebral joint flexion may be limited by physical contact between vertebrae, e.g., between the postzygapophyses of one vertebra against the neural spine of the more caudal vertebra [32,15,48]. As dorsiflexion increases, for example, the postzygapophyses of one cervical vertebra may slide posteriorly until they fit neatly into depressions located just posterior to the associated prezygapophyses (pers. obs.; see Figure 10). Osteological stops for dorsiflexion are apparent in many birds, especially those with long necks, and in the base of the neck of large mammals such as giraffids, equids, and camelids. The prevalence of osteological

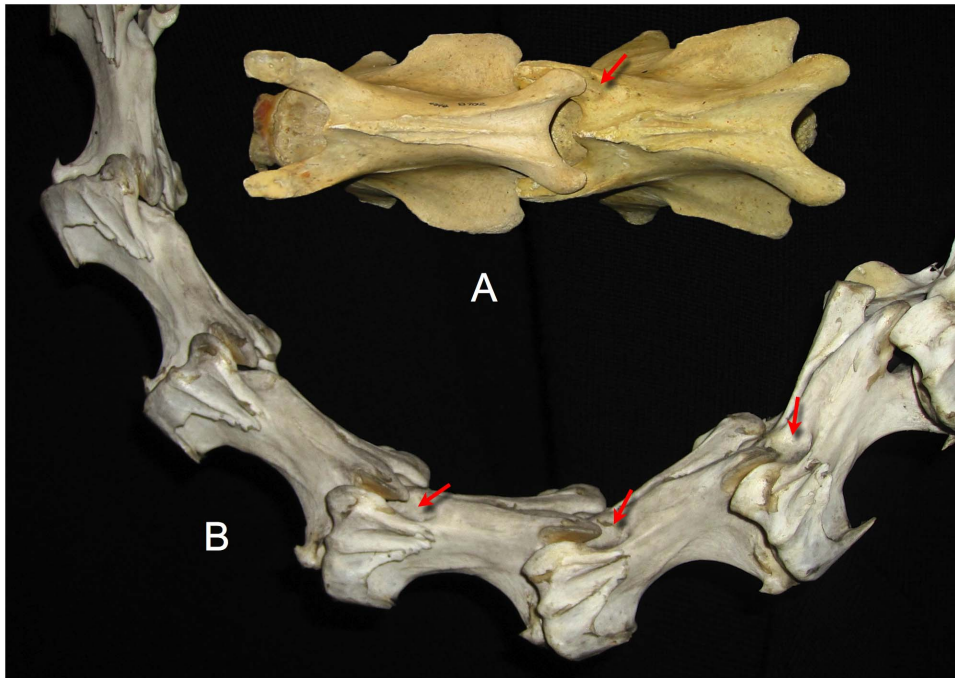


Figure 10. Osteological stops. The posterior cervicals of camel *Camelus dromedarius* (A) show pronounced depressions (see arrow) where the postzygapophyses make contact just posterior to the associated prezygapophyses with which they articulate. At the limit of travel in dorsiflexion the zygapophyses remain in overlap (contra [80]) and compression forces can be transmitted through the zygapophyses as the neck becomes effectively rigid and stable at the extremes of dorsiflexion. Pronounced osteological stops are also exhibited in many birds, such as the Greater Rhea *Rhea americana* (B, see arrows). Photographs by the author; rhea specimen at the Zoology Museum, University of Cambridge, access courtesy Matthew Lowe, and the camel vertebrae are at the Condon Museum, University of Oregon.
doi:10.1371/journal.pone.0078572.g010

stops in vertebrates is not well known, but it is noteworthy that they are clearly present in some vertebrates, and clearly absent in others (pers. obs.). Where they are present, experimental manipulation of vertebral pairs demonstrates that physical contact firmly braces the two vertebrae against further dorsiflexion (e.g., Figure 11) [15]. The neck ‘locks up’ and those vertebrae effectively becomes a rigid body protecting the intervertebral joint. Zygapophyseal bracing is also noted to be assist in stabilizing the

neck against torsion and lateral tilting [83]. Osteological bracing may also prevent excessive mediolaterally flexion in some extant vertebrates (e.g., in the base of the neck in giraffes, Figures 11b, 12, and rhinos, pers. obs.).

It has been suggested that dorsiflexion in sauropods was also limited by osteological stops, given their presence in *Camelus bactrianus*, *Giraffa Camelopardalis* and *Struthio camelus* [15]. In an earlier study [30], the sauropod *Diplodocus carnegii* was

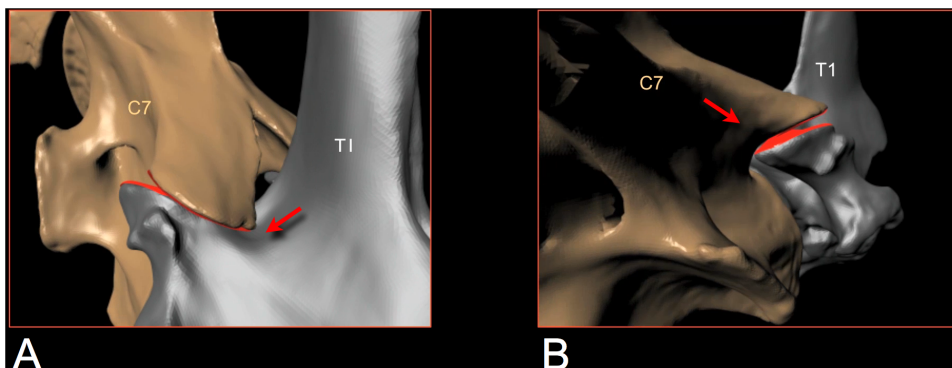


Figure 11. Bracing at the base of the giraffe's neck. The base of the giraffe's neck is braced to protect the intervertebral joints from excessive strain on their synovial capsules and to rigidify the neck as it reaches the limits of range of motion. As the neck is raised at the base (A), the postzygapophyses of C7 travel posteriorly until they wedge into depressions in the neural spines of T1 just behind the prezygapophyses (see arrow). Another bracing scheme applies when the neck is deflected laterally (B). In deflecting the neck to the left, for example, C7 bears against the left postzygapophysis of T1, see arrow. In either dorsal or lateral flexion the two vertebrae progressively lock up firmly and stably. At these extremes the zygapophyses maintain substantial overlap (roughly a ZSF of roughly 0.5). CT data provided courtesy American Museum of Natural History and Timothy Rowe, University of Texas. Supplemental material: Movie S2, Movie S3.
doi:10.1371/journal.pone.0078572.g011

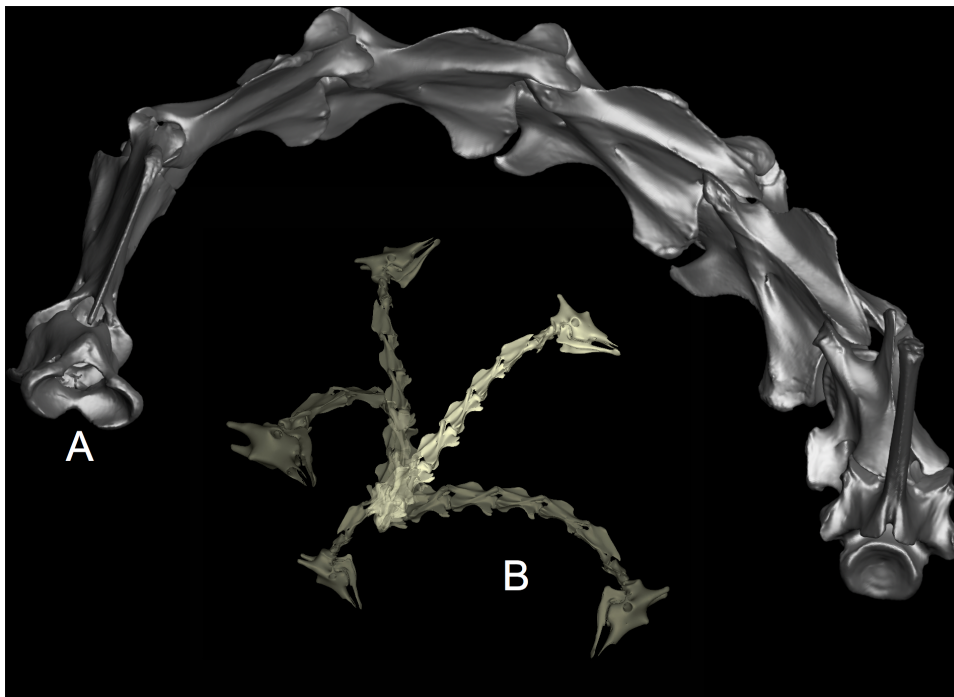


Figure 12. Giraffe flexibility is predicted by their joint geometry. The ability of a giraffe to reach vertically and to flex laterally to just reach its flanks is closely replicated by a digital model based on CT scan data of a recent giraffe (see also closeup in Figure 11). The zygapophyses remain in articulation with substantial overlap when they reach osteological stops at the base). CT data provided courtesy American Museum of Natural History and Timothy Rowe, University of Texas. Supplemental material: Movie S4. doi:10.1371/journal.pone.0078572.g012

estimated to have surprisingly little dorsal due to the relatively small zygapophyses at the base of the neck. Dzemski and Christian [15] rotated copies of Hatcher's [26] vertebra illustrations of the same specimen (*D. carnegii*, CM 84) from until the neural spines appeared to make contact in lateral view, as they do in ostriches. Their two-dimensional (2D) manipulation of illustrations, however, could not reveal that in three dimensions (3D) the zygapophyses would have been completely disarticulated far before the vertebrae would have contacted one another (Figure 9c, d). Dorsiflexion in *Diplodocus* (and likely in sauropods generally) was limited by the ZSF [30] without the additional bracing of bone against bone.

While some extant cervical vertebrae are braced ontologically as they reach the limits of dorsal or lateral deflection, many extant vertebrates do not exhibit apparent morphological adaptations (pers. obs.). Nor does osteological bracing against excessive dorsiflexion appear present in sauropods (although osteological contact may have braced the neck in extremes of lateral flexion in some sauropods [84]). In sauropod cervical vertebrae, three geometric factors argue against dorsal bracing by osteological stops: elevation of the prezygapophyses above the spinoprezygadiapophyseal laminae (sprl) [85], the ridge-like shape of the sprl, and the trajectory that the postzygapophyses would travel in dorsiflexion about the center of rotation at the centrum that would clear, rather than contact, these laminae. The sprl, which originates behind the prezygapophysis, ascends to the anterior aspect of the neural spine, and is ridge-like and devoid of a smooth depression or hollow to accept the loading by the postzygapophyses of the more anterior cervical vertebra during extreme dorsiflexion [30,86,4,37,38,45]. Moreover, the prezygapophyses project anterodorsally relative to his lamina such that the postzygapophyses, pivoting about the central condyle, would not

make contact with the sprl during its excursion posteriorly. Hence one cannot assume that sauropod vertebrae pivoted in a vertical plane until bone touched bone. Instead, dorsiflexion was likely limited by soft tissue constraints from the zygapophyseal capsule ligaments plus muscles and fascia.

Due to their nearly spherical central condyles, sauropod intervertebral articulations can be regarded as universal joints of well-defined center of rotation and angular range of motion as imposed by limiting zygapophyseal displacement to preserve a safety factor (ZSF). Each successive pair of vertebral axes (Figure 1) defines a segment of a kinematic chain from base of the neck to the cranium. With each joint in an undeflected state (ONP), the chain forms a piecewise linear curve of characteristic form, such as the familiar sigmoidal shape in avian necks. The kinematic simplification of the neck to a chain of universal joints is adopted to many studies of neck flexibility [66,15,63,87]. Since the centers of rotation are determined by the ball-and-socket geometry of the opisthocoelous central articulations, a 'bare bones' giraffe neck can be flexed to replicate observed limits flexibility by a combination of ZSF limit and osteological bracing (Figure 12).

Osteologically-Induced Curvature

The normal division of human spine into regions of intrinsically lordotic or kyphotic spinal curvature arises partly by wedge-shaped intervertebral disks as mentioned, and partly by the vertebral osteology (as well as the posture assumed by an individual, of course). The osteological contribution can be subtle but accumulative, as in the slight wedge shape of the vertebrae in the lumbar spine [88]. It can also be dramatic: much of the sharp elevation in the Giraffe neck is produced by the wedge-shaped osteology of the cervical vertebra at the base of the neck [89]; see Figure 1b, see also Figure 15b). In general, centra that are shorter dorsally than

ventrally, when articulated and aligned in ONP form a natural upward bend, such as common at the base of the neck in many extant birds and reptiles. This curvature is not due to flexion; is ‘in the bones’ but may be further accentuated by dorsiflexion, of course. Vertebral centra that are shorter dorsally than ventrally will produce dorsal OIC, typically at the base of the neck, which serves to elevate the head. Combinations of these morphologies along the cervical column produces a variety of intrinsic curves in ONP.

Many birds also have ventral OIC cranially, which together with the rise at the base of the neck, creates a sigmoid curve with an inflection in curvature mid-neck (Figure 13). Reptile necks generally form simpler curves, from varying from nearly straight in most lacertilians (Figures 14a, c) [90,91], to more elevated with a more or less pronounced built-in arc in crocodylians (Figures 14b, d) [94; pers. obs]; and turtle necks in ONP position the head in a characteristic pose, that is steeply descending caudally then rising cranially, sometimes with a sigmoidal curve in ONP (Figures 14e, f). Mammal cervical vertebral also form a simple arc-like curve (Figure 15), from nearly straight in anteaters and hares (Figures 15a, c) to more substantially curved in giraffes, horses, and camels (Figures 15b, d, f). In mammals the built-in dorsal curvature is greatest at the base and diminishes cranially. The sigmoidal shape characteristic of horse necks, incidentally, is little reflected in the osteology, but superficially by the epaxial musculature. The catenary shape of the camel neck derives from the descending slope of the anterior thoracic vertebrae combined with the dorsally curved cervical column. The underlying osteology of the mammalian cervical column is not ‘S’ shaped nor ‘U’ shaped but ‘J’ shaped, and to the extent there is an inflection point in curvature, it is not within the neck, but at the

atlantoccipital joint. Like the letter ‘J’, the column begins with high curvature which diminishes as the curve ascends.

Behaviorally-Induced Curvature

Caution is needed to distinguish between behaviorally-induced curvature and that which is intrinsic to the osteology, particularly when attempting to draw broad generalizations about default behavioral postures [12]. Neck posture varies with activity [15,63–64], from alert rest to locomotion and feeding, and vertebrates do not all assume a similar strategy for holding their head in alert rest (discussed below). The ONP provides a baseline relative to which characteristic poses for resting, locomotion and feeding can be described. The ONP corresponds to the alert rest pose in at least some birds and reptiles [95–97], and while yet to be systematically studied across mammals, ONP predicts the default alert head height for large herbivorous mammals at alert rest and in locomotion [98, pers. obs.]; Camel and Giraffe [15,63–64] often hold their heads slightly higher than predicted by ONP. Some mammals (e.g., felids and lagomorphs [95]) can assume a ‘sphinx-like’ pose by retracting their heads sufficiently to balance over their shoulders when resting (discussed further below). Others cannot, but have alternative means of minimizing energy expenditure. Also, while ONP may predict a default alert pose for birds in general, there are exceptions. Ratites such as the Ostrich (but not the Cassowary or Kiwi, pers. obs. and Figure 13d) hold their heads far above the height predicted by ONP [15,63–64].

Speculation regarding the relationship between ONP and characteristic poses of the neck during rest and locomotion for sauropods seems of less importance to understanding their biology than how they used their necks for feeding. The relationship between ONP and the characteristic pose for feeding in modern

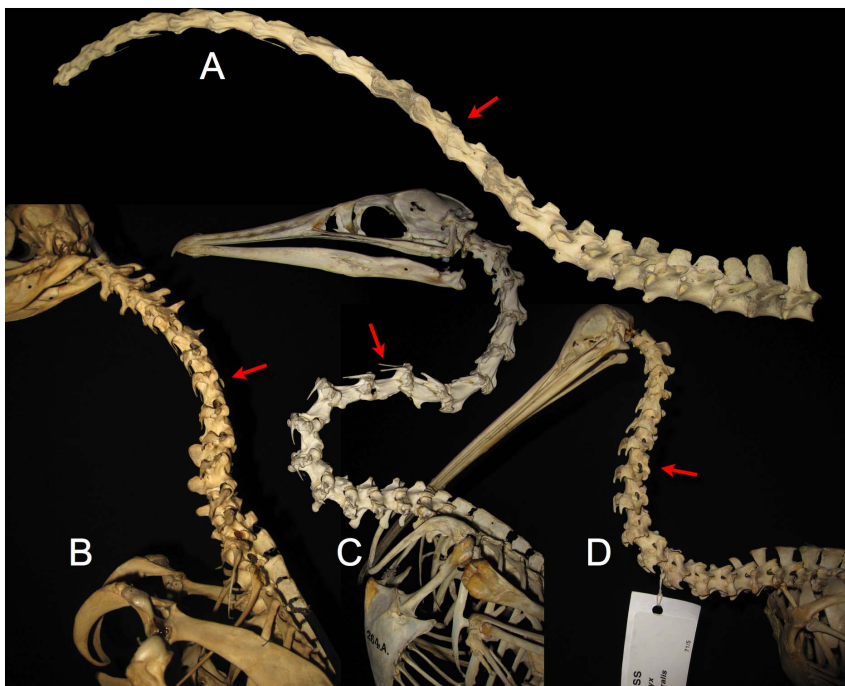


Figure 13. ONP for various birds. The avian neck has a sigmoidal curve that is formed intrinsically by its osteology when the vertebrae are articulated in ONP. The alert resting head height for the ostrich *Struthio camelus* (top) is higher than predicted by ONP [15] (and the ostrich often further retracts the head during locomotion [98]). Many other birds, however, do assume a pose close to ONP as their characteristic alert resting posture: Cape Penguin *Spheniscus demersus* (bottom left), Flightless Cormorant *Phalacrocorax harrisi* (middle), and Kiwi *Apteryx australis* (bottom right). Note inflection points (arrows). Photographs by the author and John Martin; specimens at the Zoology Museum, University of Cambridge, access courtesy Matthew Lowe.

doi:10.1371/journal.pone.0078572.g013



Figure 14. ONP for various reptiles. The Nile Monitor *Varanus niloticus* (A) and Komodo Dragon *Varanus komodoensis* (C) have very straight necks in ONP. Head elevation, if any, is primarily through the slope of the anterior dorsals. In contrast, the crocodylians Alligator mississippiensis (B) and *Crocodylus acutus* (D) have gently rising necks in ONP. The Seychelles tortoise *Testudo elephantina* (E) has an inflection in curvature; note that its characteristic head elevation arises in ONP. The cryptodiran snapping turtle *Chelydra serpentina* (F) curves monotonically from a vertical descent caudally to nearly straight cranially. Photographs by the author and John Martin of specimens at the Zoology Museum, University of Cambridge, access courtesy Matthew Lowe.
doi:10.1371/journal.pone.0078572.g014

herbivores is straightforward only for grazers, while many low browsers will take advantage of vegetation that requires raising the head above ONP, and high browsers will very frequently feed by ventriflexion far below ONP [99–103].

Skeletal Reconstructions: Illustrations, Mounts, and Models

Given the rarity and inaccessibility of physical mounts of dinosaur skeletons, skeletal drawings and composites have traditionally used to reconstruct and subsequently analyze sauropod vertebral columns. More recently, 3D digital models are being used in preference to relying on 2D artwork [31–32,104,87]. Regardless the medium, all such reference material is subject to issues of restoring missing or damaged vertebrae. Unfortunately, the illustrations and physical mounts which are frequently relied upon as primary sources of information about sauropod osteology are subject to subtle yet significant alterations. Digital 3D modeling and articulation of scan data brings with it new as well as old problems of subjectivity.

Illustrations

Skeletal illustrations have been relied upon to both summarize the bauplan of a given taxon of sauropod, and as source material on which to base estimates of head height and speculations regarding feeding, and so forth. Significant artistic liberties are sometimes noted [31,32] but usually dismissed as either within the realm of possibility, or as artwork. Nonetheless illustrations are often trusted as authoritative.

The macronarian *Camarasaurus*, for example, is usually depicted to have had a sharply rising neck at the base, largely

due to illustrations based on the juvenile *C. lentus* CM 11338. The original specimen was preserved in a severe opisthotonic posture, with the cervicals wrenched back and the zygapophyses displaced out of articulation (Figure 16a). The skeletal illustration (Figure 16b) [38: plate XVII] however, shows the neck with the same curvature but with the zygapophyses drawn as if aligned, in ONP, suggesting that the steep neck curve was intrinsic [38,14,29], likely contributed to the widespread current presumption that this sauropod had a natural swan-neck. The same depiction of death-as-life pose arises in Wiman's 1929 [4] illustration of *Euhelopus zdanskyi* in life (Figure 2) with an ascending neck drawn with precisely the same curve as when it was found, in an opisthotonic state. And as mentioned, Janensch's [27] illustration of the skeleton of *Giraffatitan brancai* (Figure 4b) depicts a steeply-ascending neck, seemingly in ONP, which, bears little resemblance to the actual fossil material in the cervico-dorsal region [105] (Figure 4a); while the neural spines were not preserved at the base of the neck, the centra were found in articulation, with central articulations approximately in ONP. In the skeletal reconstruction, however, the cervico-dorsal centra acquired a wedge shape and the neural spines are figured with aligned zygapophyses, suggesting this neck ascended in ONP. The slope subsequently been exaggerated to vertically (or past vertically) [29: fig. 20.7], however some skeletal reconstructions show the cervico-dorsal region [39,32] as close to the straight.

While skeletal reconstructions may incorporate artistic liberties, some degree of independent verification is afforded by the detailed steel engravings or photographs of the individual vertebrae illustrations were published in the original descriptions by C. Gilmore, J.B. Hatcher, W. Janensch, W. Wiman and others. These illustrations can be scanned, composited, and placed into

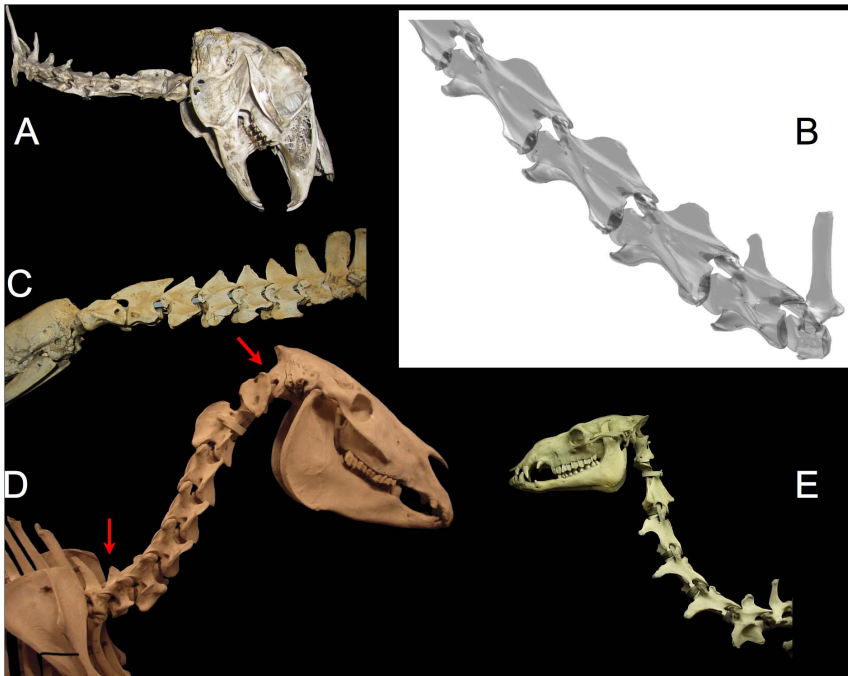


Figure 15. ONP for various mammals. Mammals have more or less dorsally-curved necks that tend to raise the head intrinsically. ONP is characteristic of mammals in alert rest and locomotion (an exception is exemplified by the Brown Hare *Lepus europaeus* (A) which assumes ONP for locomotion and exploratory behavior [97: fig. 17-3] but not in alert rest [95,96]). The giraffe *Giraffa camelopardalis* naturally rises in ONP (B, note the deep insertion of condyles within cotyles consistent with dissections [15]), and assumes approximately this pose in locomotion and alert rest [63,89,92,93]. The nearly straight necks of the Giant Anteater *Myrmecophaga tridactyla* (C), also mounted in ONP, is characteristic of habitual alert resting pose of alert rest, locomotion pose and feeding. The horse *Equus caballus* (D) and camel *Camelus dromedarius* (E) also hold their heads close to ONP in alert rest and locomotion. Note that the cranio-cervical joint is undeflected (arrow) as well as the entire cervical column. Photographs by the author (camel photograph by J. Michael Parrish); hare, anteater and horse specimens at the Zoology Museum, University of Cambridge, access courtesy Matthew Lowe. The giraffe is at the Field Museum of Natural History. The camel is at the Field Museum of Natural History. The giraffe is a 3D digital model placed in ONP based on CT data courtesy American Museum of Natural History.
doi:10.1371/journal.pone.0078572.g015

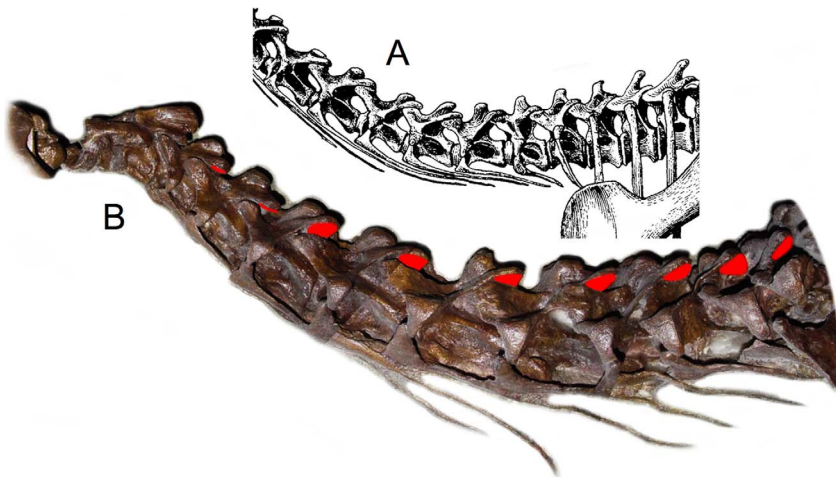


Figure 16. *Camarasaurus* had a swan neck taphonomically, but not in life. The 1925 skeletal reconstruction of the juvenile *Camarasaurus* [38] (A) accurately replicates the curvature of the neck as found (B), but the zygapophyses are illustrated misleadingly as if they were aligned, in ONP, suggesting that the upward curve is intrinsic and 'built in'. The original specimen, however, is obviously contorted into a dramatic opisthotonic pose, with the zygapophyses disarticulated throughout much of the neck. Red indicates the exposed postzygapophyses (compare with nearly identical opisthotonic pose in the larger specimen USNM 13786-310D, Figure 17). Disregard for this extreme opisthotonic distortion in subsequent skeletal depictions, some portraying the neck comfortably achieving a near vertical pose [14,29] has resulted in a nearly universal expectation that *Camarasaurus* had a natural swan-like curve to the neck. Photograph of *Camarasaurus lentus* CM 11338, by the author.
doi:10.1371/journal.pone.0078572.g016

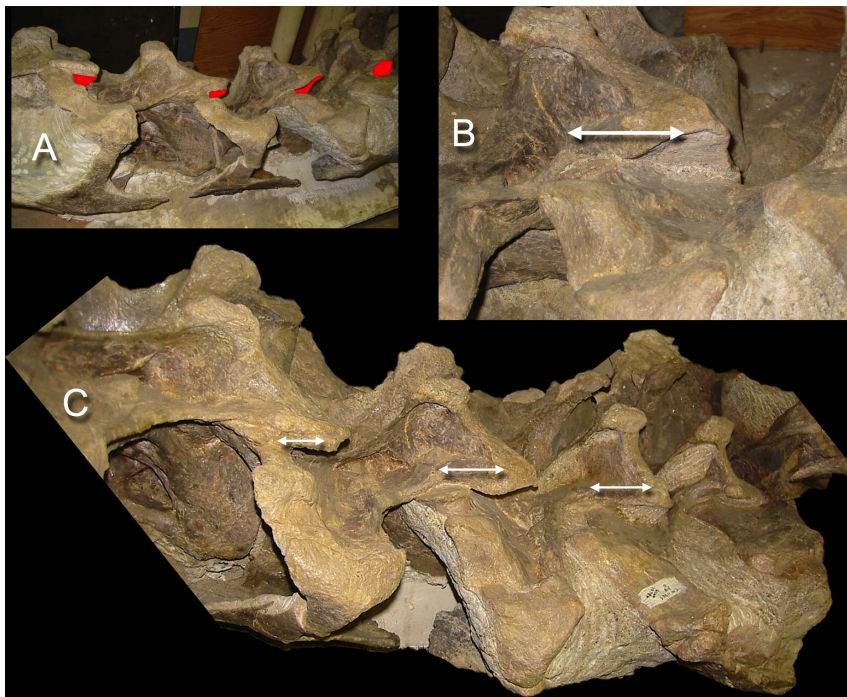


Figure 17. Another *Camarasaurus lentus* in opisthotonic pose. A partly-prepared block, USNM 13786-310D, reveals a ‘death pose’ with curvature very close to that of the more familiar juvenile specimen CM 11338 (Figure 16). In both specimens the postmortem dorsiflexion disarticulated the zygapophyses such that it was preserved in a pose that was unlikely attainable in life. Red indicates exposed postzygapophyses, and the white line segments indicate the extreme displacement of the zygapophyseal pairs from ONP. Photographs by the author. doi:10.1371/journal.pone.0078572.g017

articulation to roughly reconstruct their ONP (Figure 5) [31–32]. But 2D illustrations are of limited use, as they collapse or obscure aspects of the 3D structure that are essential in understanding their articulation, as evidenced with problems that arise in estimating flexibility, even in the case of pure dorsoventral movement from lateral views [15].

Sculpted Inaccuracies in Skeletal Mounts

The neck of the iconic *Giraffatitan brancai* mount (Figure 3) is reconstructed with its neck in ONP. The cervico-dorsal vertebrae are extensively restored, since the neural arches of the original specimens were missing. The restored vertebrae were sculpted in such a manner as to make them appear to bend naturally, with all zygapophyses aligned, centra wedge-shaped, and even the anterior and posterior margins of the condyles and cotyles made to appear undeflected in that steep curve. Not only are the missing vertebral arches fabricated to form a steeply-ascending neck, the centra are curved to follow that bend, in marked contrast to with Janensch’s illustrations [105] of the original material (c.f. Figures 3, 4e). Although only the centra were preserved in the block from C10 through D2, those vertebrae were found in articulation as a very straight column based on their collinear ventral margins, and the ridges of condyle and cotyles were parallel indicating that they were roughly in ONP. The historic and familiar swan neck of the mounted skeleton, while impressive, is a fabrication.

While extreme in the case of the Berlin mount, it is not uncommon for neural spines to be restored in sauropod skeletal mounts as if they were in ONP. The *Apatosaurus ajax* at the Yale Peabody Museum (YPM VP 001980), for instance, has a gently-curved sigmoidal-shaped neck. Close inspection shows that the zygapophyses are centered, as if the vertebrae were in ONP. Still closer inspection, requiring a ladder to reach up and tap on the

darkly-varnished plaster, reveals an artistic amalgam of real material and plaster (pers. obs.). The gracefully-ascending curve to the neck appears to have been conceived first, then the details of the restoration made to neatly fit that vision.

The neck of *Camarasaurus lentus* USNM 13786-310D (Figure 17) was preserved in articulation in a pronounced opisthotonic pose (‘death pose’). The vertebrae were dorsiflexed to the extent that the zygapophyses were disarticulated, as was the case in the juvenile *C. lentus* CM 1133 (c.f. Figures 16 and 17). This extreme state of dorsiflexion is again likely beyond what could have been achieved in life, given that degree of disarticulation. USNM 13786-319D (originally CM 11373) was used as reference for a sculpted replica for public display (M.K. Brett-Surman, pers. comm.), the opisthotonic neck curvature was accurately replicated, however the zygapophyses were sculpted as centered, as if the neck curvature were intrinsic, not due to extreme dorsiflexion. The displayed sculpture further reinforces the incorrect expectation that *Camarasaurus* had a steeply elevated neck at the base.

The Denver Museum of Nature and Science *Diplodocus longus* DMNS 1494 is also mounted with an upward bend in the neck at its base (Figure 18). Again, the vertebrae appear undeflected with zygapophyses in neutral alignment indicating that the bend is intrinsic to the neck. While the vertebra from C1–C10 are based on a cast of *Diplodocus carnegii* CM 84 (Kenneth Carpenter, pers. comm.), those posterior to C10 have restored neural spines, and the sculpting required to integrate the zygapophyses had set them into position as if the vertebra were undeflected, thereby suggesting a sharp intrinsic bend around C13–C14. The neural spine restorations are built up around the placement of the zygapophyses. The induced kink in the neck is inconsistent with other *Diplodocus* material, including the original CM 84 posterior

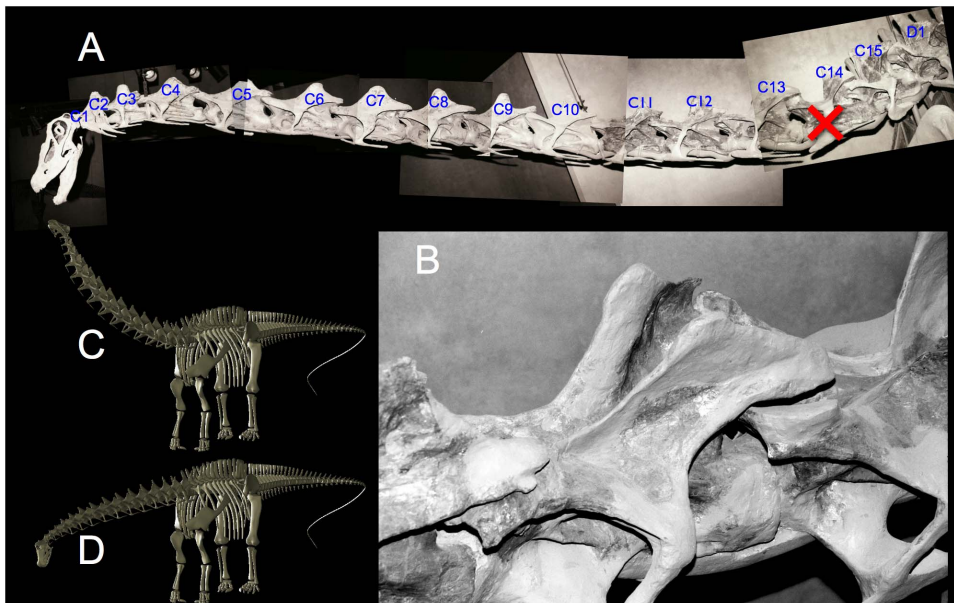


Figure 18. This *Diplodocus* has a false kink in the neck. The Denver Museum of Nature and Science mount of *Diplodocus longus* DNMS 1494 has a sharp upward bend that appears intrinsic since the vertebrae in the vicinity of C13–C15 appear undeflected. The curvature, however, is an artifact of the restoration of the fragmentary neural spines, and not exhibited by any other diplodocid specimen including the Carnegie Museum of Natural History *Diplodocus carnegii* CM 84, a cast of the first 10 cervicals of which were used for the Denver mount. Those cervicals caudal to C10 are heavily restored and induced the misleading suggestion of an upturned neck. Taylor, Wedel and Naish [12] claim that "... computerized studies are not as objective as they may appear, since seemingly Stevens and Parrish could not replicate the flexibility of actual specimens" presuming that the entire neck of DMNS 1494. In fact, the flexibility estimates from [30] would have permitted the head to have reached such heights (see [32] and C). The specimen they refer to (A) has a sculpted bend that is not representative of other, more complete specimens of *Diplodocus* that emerged straight from the shoulders (D). Photographs by the author, access courtesy Kenneth Carpenter. Supplemental material: Figure S1, Figure S2. doi:10.1371/journal.pone.0078572.g018

cervical vertebrae. Unfortunately, a subsequent study trusted the Denver mount as osteologically accurate [12].

Models

2D skeletal illustrations provide only limited insight into vertebral articulation, but have been resorted to given limited access to, and manipulation of, original specimens, especially those that are mounted. Yet entire articulated vertebral columns can be manipulated in a virtual 3D space provided their morphology is converted to digital form. Fossil vertebrae can be digitized to capture their surface morphology and subsequent digital retrodeformation [106] can remove at least some of the postdepositional distortion that would otherwise preclude their re-articulation. The problem of reconstructing missing (not merely distorted) elements remains, however. Filling in for a missing vertebra by duplicating then scaling an adjacent vertebra is not unheard of, but clearly of greater aesthetic than scientific utility.

An alternative to digitization of original material is to begin with a set of deformable 3D models can be subsequently formed to closely resemble the morphology of the original specimens. Deformable 3D surfaces can be created using subdivision surface model techniques [107], and using blend shape animation techniques [108,109], adjusted to match dimensional data from multiple sources (effectively lofting 3D surfaces to match 2D profiles derived from archival images and illustrations, or when available, 3D data from surface scans, etc.). The models can be interpolated by creating a model that is an interpolate of two such 3D shapes, creating a more accurate restorations in cases where the original reference fossil material is missing, inaccurately restored, or intractably distorted (Figure 19) – see below.

Through a laborious process of building then adjusting generic models of axial and appendicular elements to fit specimens, eventually entire articulated digital skeletons can be constructed (Figures 6, 7, 20, 22, 23) that approximate the shape and dimensions of the available reference material, faithfully replicating that morphology which is judged undistorted while attempting to correct for distortions, defects, and missing elements in the source material. Doubtless, subtle artistic license can be introduced in the digital sculpting process, just as it has been known to happen with plaster or pencil. Just as the term ‘sculpting’ may connote an artistic and often subjective process, so too is digitally-sculpted modeling. But then a digitized specimen is a model as well, and reflects subjectivity and artistic bias as a result of the many steps including decimation, filtering, and smoothing to fit a satisfactorily smooth surface that approximates the original surface prior to digitization, followed by artful manual correction of voids, registration errors, and under-sampled regions. Retrodeformation necessarily introduces subjectivity as well, e.g., in further adjusting a model to remove scaling artifacts induced by an automated retrodeformation process [106].

Results

The following general inferences regarding sauropod vertebral joints appear supported by the EPB, with avia and reptilia as outgroups:

1. Intervertebral central articulations were diarthrotic, with close intervertebral separations.
2. Anterior cervical vertebrae were essentially straight (negligible OIC in ONP).

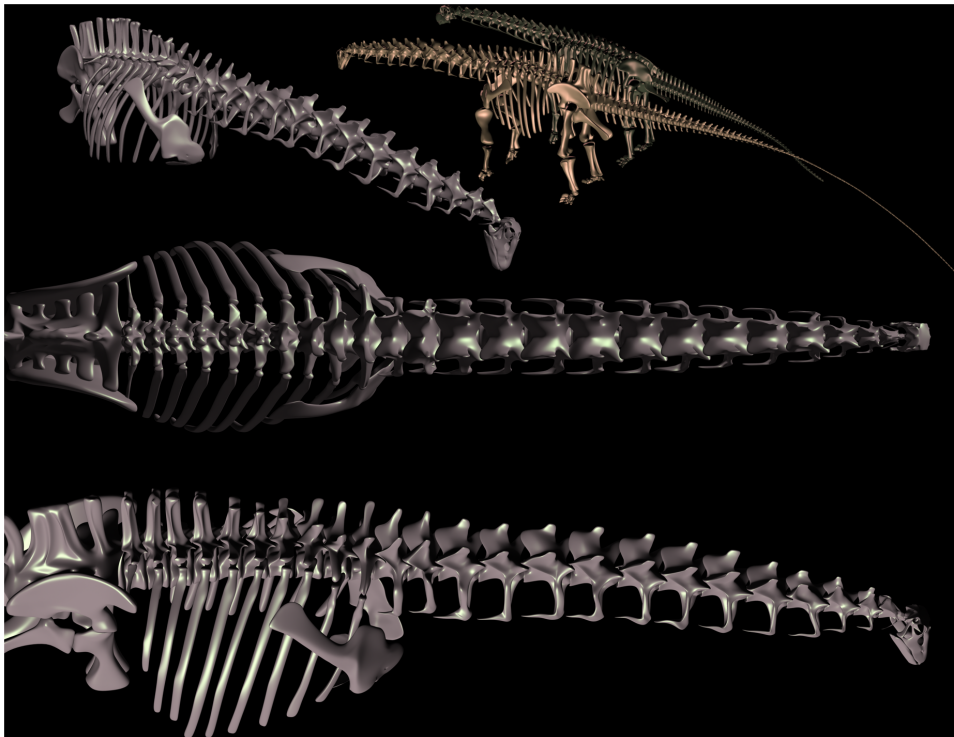


Figure 19. Details of the digital modeling of *Apatosaurus lousiae*. Archosaur vertebral morphology varies smoothly along the axial skeleton, and the gradual changes from one vertebra to the next is amenable digital modeling by ‘blend shapes’ (see text regarding digital modeling). Through a multi-step process, first deformable generic forms are created for all elements then used to create specific variations on that shep. For example, a generic dorsal rib is constructed, then several specific ribs are modeled to match the corresponding original fossil material, with the remaining intervening elements created by interpolation, and finally each element is painstakingly sculpted and adjusted to capture individualities of the original specimen such as the irregularities in the cervical ribs, compared to the original specimen (Figure 5). The process of creating a digital scale model, like sculpting in a more conventional physical medium, shares the same goals of faithfully replicating the morphology and dimensions of the original. Like physical sculptures, it is a matter of judgment as to when the resemblance is sufficient, and as to what is to be regarded as artifactual, such as an apparent distortion due to preservation. Unlike physical sculptures, these models are readily edited and successively refined, and most importantly, readily articulated without need for a physical armatures. As a visualization tool, digital models greatly facilitate the appreciation of design as the bauplan emerges from the aggregation of the component pieces (note that *A. lousiae* is accompanied by a *Camarasaurus lentus*, to scale).

doi:10.1371/journal.pone.0078572.g019

3. Posterior cervical vertebra had slight ventral OIC in ONP.
4. Intervertebral joint flexibility was limited by synovial capsules surrounding the zygapophyses which draw taut prior to permitting disarticulation, preserving a ZSF.
5. Cervical vertebrae were limited in dorsiflexion by the ZSF, not by osteological stops.

Specific conclusions regarding sauropod necks would include the need to revise the reconstructions of brachiosaurids and camarasaurids based on 1–3, above. Regarding 4 and 5, above, the relatively ‘stiff’ necks of sauropods (by avian, but not reptilian, standards) and their kinematics suggest a coherent role for the sauropods neck with regard to feeding. While not yet explored in detail, the following provides a review that draws on the deep understanding of neck function in extant vertebrates towards better understanding the corresponding function of sauropod necks. As discussed below, some of the insight derives not by analogy with birds, but by how the analogy with birds fails, and yet resembles that of another, very distant group: browsing mammalian herbivores.

Necks for Sweeping Out a Surface Versus Necks for Exploring a Volume

While the relatively inflexibility of sauropod necks compared to birds is sometimes viewed with skepticism [80,12], the kinematic implication of relatively small zygapophyseal facets (compared to their distance from the center of rotation) is clear: less angular deflection is permitted prior to their disarticulation (c.f. Figures 9). The greater intervertebral flexibility in avian intervertebral joints permits birds a greater behavioral repertoire than that of those vertebrates with stiffer, straighter necks. Kinematically, the redundancy in the avian head-neck system permits control of both the placement and orientation of the head within a volume [65], by adjusting all cervical joints to form a smooth spline-like curve that “... behaves effectively as a (pre-shaped) flexible rod that, given the orientation and position of the two endpoints, takes the shape that minimizes the bending energy” [66]. The avian neck divides into regions that can work individually or together to explore a large volume in three dimensions, e.g., for preening and selective feeding [110,111,65] (Figure 20a). In contrast to the avian sigmoidal curve, the monotonically-curved necks of lacertilians, crocodylians and mammals is simpler kinematically, with the head neck system operating primarily to direct the head in two

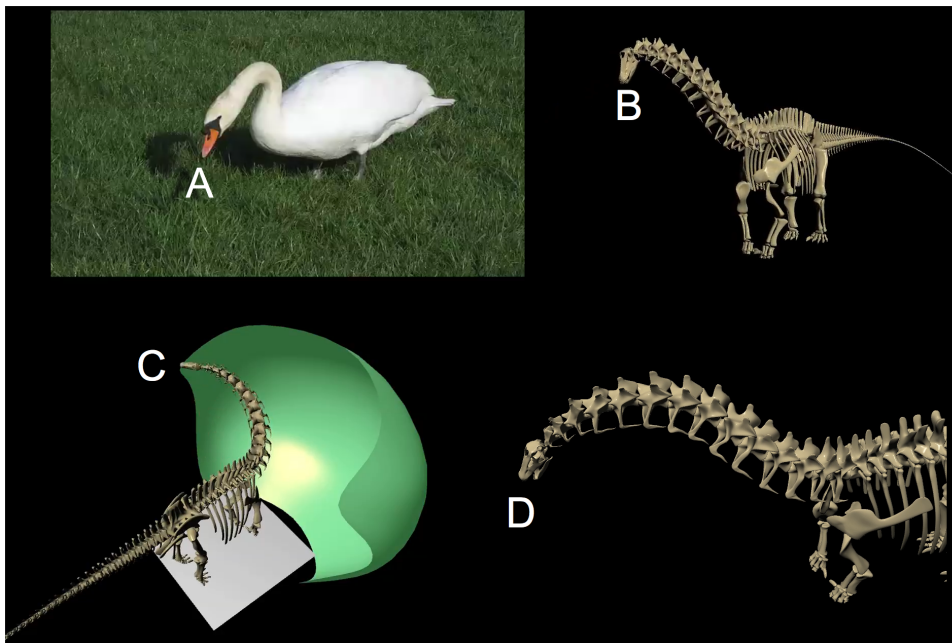


Figure 20. Long necks, but not swan necks. In addition to sweeping out a broad ‘feeding envelope’ (a curved surface of maximum reach [28]), sauropod necks are sometimes expected to be able to pull the head back to reach closer to the animal to explore the volume within this surface, (e.g., [113: fig. 12.1]), somewhat in the manner of a swan (A). While *Apatosaurus* could place its head at any point across an enormous feeding surface (C), the neck was not able to retract the head back towards the body (B, D). Supplemental material: Movie S5, Movie S6, Movie S7, Movie S8. doi:10.1371/journal.pone.0078572.g020

dimensions by flexion at the two extremes of the column [112,95–97].

The cervical column may be regarded kinematically as a spline-like chain of fixed-length links between joints of limited angular mediolateral and dorsoventral flexibility [66]. Consider first a neck that is initially completely straight. Flexion near the base of the neck reorients the distal vertebral column and results in the head sweeping across a curved surface or envelope centered upon the base of the neck. This constitutes the ‘reachability envelope’ of the neck (Figure 20c). Flexion cranially reorients the head on a smaller radius of curvature. Uniform flexion along the entire column produces an arc-like curve which indeed reduces the radial distance (the chord) from base to head but the tangent at the head is also affected. To maintain the head pointing in a given direction while retracting it back towards the base of the neck requires different segments of the column working in opposition, effectively creating a sigmoidal spline curve. The built-in sigmoidal curve in the avian cervical column permits its joint flexibility to be distributed relative to that curve, which facilitates independently controlling both the pointing direction of the head and the position of the head [66,110,111]. In contrast, a simple monotonically-curved neck in ONP must create an inflection point by dorsiflexing caudally and ventriflexing cranially (Figure 20b, d). Consequently, while mammals can achieve wide reachability envelopes (turning to point directly behind themselves [114]), and reptiles generally less so, they must strain to retract their head even moderately, often choosing instead to take a step back.

Consider the consequences of varying vertebral length, count, and flexibility, either singly or in combination. First, increasing vertebral length alone increases reach linearly and the surface area of the reachability envelope quadratically. Increasing intervertebral flexibility, particularly caudally, also increases surface area roughly linearly (and both vertebral elongation and specialized flexibility is apparent in giraffes). Next, while holding overall neck

length constant, increasing vertebral count while trading off intervertebral flexibility and vertebral length off can produce a tradeoff, resulting in the same reachability envelope. But increasing vertebral count without proportionately reducing intervertebral flexibility greatly dramatically increases the kinematic redundancy of the neck [66], and hence its repertoire of postures. Further increasing intervertebral flexibility compounds this increase in the space of possible neck configurations. Long-necked birds such as the swan and ostrich have done just that, with considerable intervertebral flexibility at each of 20 or more joints. In contrast, sauropod specialization has tended towards generally increases in vertebral length and count but not flexibility, suggesting that their necks were specialized for other tasks than those to which birds use their necks: for sweeping across a surface, not for exploring a volume.

Speculation About the Habitual Resting Pose in Sauropods

Taylor, Wedel, and Naish [12,17] argue that sauropods habitually held their heads high. With annotations Ci added in the following quotation for subsequent reference, they claim [17]: “A substantial literature on extant amniotes (mammals, turtles, squamates, crocodylians and birds) shows that:

- C0: “living animals do not habitually maintain their necks in ONP. Instead ...
 C1: “the neck is maximally extended at the cervico-dorsal junction
 C2: “and maximally flexed at the cranial-cervical junction
 C3: “so that the mid-cervical region is near vertical.
 C4: “This is true even in apparently short-necked animals. ...
 C5: “The fact that elevated, extended necks are widespread across Amniota means that

C6: “elevated necks should be assumed for sauropods in the absence of evidence to the contrary.

C7: “Elevated neck postures for sauropods are indicated by the extant phylogenetic brackets at the levels of *Saurischia*, *Archiosauria*, *Diapsida*, *Reptilia*, and *Amniota*.

Recall that the EPB method supports a Type I inference about an unpreserved property P in some extinct taxon t_0 if a physical property O is identified, that is correlated with P in all members of the extant outgroups comprising the EPB, and O is present in traces of the extinct taxon:

$$(\forall t \in \text{EPB } O(t) \leftrightarrow P(t)) \rightarrow (O(t_0) \rightarrow P(t_0))$$

and if no physical evidence O is offered then the method would degenerate to simply asserting that if the property is apparent now, it was then:

$$(\forall i \in \text{EPB } P(i)) \rightarrow P(t_0).$$

Regarding the conjectured C0–C4 [12,17], the property P is a behavior combining maximal dorsiflexion at the base of the neck and maximal ventriflexion at the head. This behavior would contort the neck far from ONP, but being ephemeral, would not be expected to have left a trace in the fossil record. Claiming that all extant amniotes assume this pose in alert rest (the validity of which is addressed momentarily), they argue that this behavior should also be assumed of sauropods (C6). While specifying extant phylogenetic brackets (C7), they offer no osteological correlates for the behavior they attribute to sauropods, nor a ‘compelling morphological evidence’ [19]. They propose a behavior of sauropods simply on the basis of the (purported) ubiquity of that behavior across Amniota. For EPB support, they cite a radiographic study of the resting posture of various laboratory animals (monkey, cat, rabbit, guinea pig, rat, chicken, lizard, and frog) [95], plus two follow-on studies [96–97]. Indeed the mammals (rat, guinea pig, rabbit, cat, and monkey) do habitually rest in an alert state, however that same study showed that the non-mammalian subjects did not assume such an extreme posture: “... in lizard and frog, the cervical column was held near earth horizontal, when animals were in a resting position” [95], refuting Taylor et al.’s [12,17] broad claim. In both the chicken and lizard *Varanus exanthematicus* radiographs revealed elevation at the base of the neck [95] but that rise is intrinsic to the neck, and evidenced in ONP (Figure 14c). Incidentally, while indeed the chicken neck also rises at the base and is vertical at mid-length, that is achieved without flexion, and some birds even have a horizontal mid-neck in ONP (in fact one that is inverted in the middle, such as the Flightless Cormorant (*Phalacrocorax harrisi*; Figure 13c).

Sauropod Necks were Cantilevered

The behavioral claims C0–C4 [12,17] are not supported by Aves and Crocodylia, let alone Amniota, leaving no EPB support for the conjecture C6. Few vertebrates rest in an alert state with their necks maximally dorsiflexed at the base and heads tucked down maximally, nor are all amniote cervical vertebral columns vertical when they rest (and moreover, many could never achieve such elevation). Lagomorphs and felids are among the relatively few mammals capable of resting with the head “... balanced and supported on top of a straight line which is collinear with the gravity vector” [95]. This ‘sphinx-like’ pose is achieved by

dorsiflexing at the cervico-dorsal junction to retract the head, while ventriflexing at the cranio-cervical junction to re-establish a horizontal head (Figure 21a, b). In those vertebrates that can successfully balance the head upon a spring-like vertical column, little further muscular effort is needed to support its weight [95]. Some long necked birds, such as the swan and ostrich, regularly rest with their heads balanced above the base of the neck, which requires significant retraction of the head in the case of the ostrich [15], while others may achieve this in closer to ONP (Figure 13). While some long-necked mammals have sufficiently flexible necks to bend back past vertical, such as giraffes and camels [81,63–64], they do not habitually rest in that pose, since that inverts the head. Maintaining a level head is a behavioral priority [95–97] across the Amniota.

While some mammals can and do rest in an alert state by retracting the head to balance it atop a subvertical column, the far more widely-adopted posture in quadrupeds is to cantilever the head and neck before the shoulders, in approximate ONP. The weight of the head and neck is then supported passively by means of suspension through some combination of dorsal musculature and ligaments in tension [114–116]. The cervical vertebral column is in low state of flexion (as observed in radiographs of reptiles and birds [95–97]). Active dorsiflexion at the base of the neck may further raise the head, of course, depending upon the state of vigilance and alarm (pers. obs.). Again, it is not sufficient to simply cite examples of this behavior in extant vertebrates to support the speculation that sauropods did as well. Osteological correlates, fortunately, have been identified in avian and crocodylian cervical and dorsal morphology [94,117,15,46,118,119,120] which allow an EPB-based inference that at least some sauropods suspended their necks in front of the body. It does not necessarily follow, however, that the neck were held in ONP. Some estimates of head elevation [58,59] predict higher elevations, and sauropods might have, for purely behavioral reasons, elevated their heads above ONP in the manner in which they are most often illustrated. Head

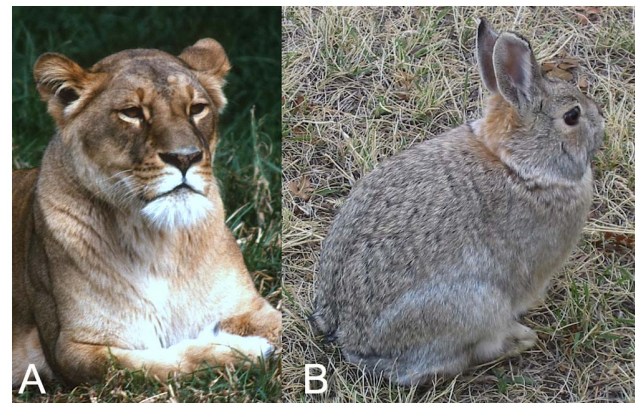


Figure 21. Some mammals relax in an alert posture by retracting their heads over their shoulders, but most do not. The sphinx-like alert resting posture in *Panthera leo* (A) and *Sylvilagus nuttallii* (B) is achieved by maximum dorsiflexion at the base of the neck (C7-T1) and maximum ventriflexion at the head to keep the head level, as shown by radiographic studies (95–97). But few mammals can achieve this feat. Most quadrupeds hold their heads cantilevered before the shoulders with the intervertebral joints in a relaxed ONP posture and the weight of the head and neck carried by dorsal ligaments and muscles. The horse, for instance, holds its head high in alert rest (as in Figure 15d), with all joints of the cervical column, including the cranio-cervical joint and the C7-T1 junction undeflected, in ONP. Photos by the author.

doi:10.1371/journal.pone.0078572.g021

elevation remains 'intuitively' logical, recall, as was discussed in the introduction. While it might be tempting to argue based solely on examples of extant behavior that support one or the other interpretation, the EPB method builds upon osteological correlates with behavior.

Evidence regarding the Gravitational Orientation of Sauropod Heads

The osseous labyrinth containing the semicircular canals constitutes a potential osteological correlate for supporting inferences about the preferred or stereotypic head posture in extinct vertebrates [121,44]. In extant vertebrates the semicircular canals sense angular accelerations in three planes [122,123]. In the alert state, vertebrates tend to hold the head such that the lateral (or 'horizontal') semicircular canal (LSC) is approximately level. If α denotes the angle between the plane of the LSC and the gravitational horizontal, α is usually inclined by roughly 5–10° for many birds and laboratory animals (e.g., domestic cats and rabbits) [124–126,111,127–130,95–97]. The study by de Beer [126] showed a remarkable alignment of the LSC with the horizontal in the alert dog and horse. Larger values of inclination α and more variability in α have been reported for some mammals (rabbit, guinea pig, rat, human) [126,95–97,124,131] and some birds such as the spoonbill *Platalea* and stork *Ciconia* [111] have negative values of α , i.e., the LSC descends).

The habitual orientation of the head relative to gravity is a behavior property, one that is fortunately correlated with the gravitational orientation of the LSC, and hence of potential use as an osteological correlate [121,44]. The utility of the LSC for inferring head orientation depends on the quality of the correlation, and by citing the greatest reported range in α (from 30° to –19° [111]), LSC would appear only to give "... only a general idea of the life posture of extinct animals' heads" [12], just as it would make a poor proxy for head orientation in cranial morphometrics [132]. The variation in α across bird taxa reported in Duijm's [111] study (Figure 22a, b) in fact provides a rather more specific idea regarding the orientation of sauropod head orientation.

An EPB-supported inference of the gravitational orientation of the cranium in the extinct vertebrate could be inferred from 1) the observed orientation of the LSC within the cranium of an extinct vertebrate [121,44], and 2) the inclination angle α in the EPB. The LSC was imaged by μ CT for the prosauropod *Massospondylus* plus the sauropods *Diplodocus longus*, *Camarasaurus lentus* and *Nigersaurus taqueti* [44]. For an assumed $\alpha = 5^\circ$, the four crania could be compared relative to a common frame of reference, namely the LSC (see also [132]). The osteology of the sauropod occiput cranium and atlas-axis is well understood [38,26,37,117], permitting confident estimation of the orientation of the atlas-axis relative to the foramen magnum and the basioccipital condyle. Thus, if the gravitational orientation of the cranium were established, that in turn would indicate the gravitational orientation of the anterior neck. For the prosauropod and the three sauropods studied, the atlas-axis was found to be close to gravitationally horizontal [44] (see Figure 22c, g).

Combining Independent Lines of Evidence

Proceeding caudally through the occiput (with the basioccipital in articulation with the atlas and the foramen magnum collinear with the neural canal of the atlas-axis), the gravitational slope of the neck at the atlas-axis is constrained as well. Three independent lines of evidence can thus be combined. The LSC data supports a postulated slope for the atlas-axis relative to horizontal, and post-cervical skeletal reconstructions suggest the gravitational slope of

the anteriormost dorsal vertebrae (i.e., how the neck emerges from the shoulders), and in the middle, ONP studies of re-articulated cervical columns in the undeflected state, suggest the relative slopes at their two ends. The three lines of evidence combine satisfactorily with the following caveats (all of which are open to eventual EPB-supported verification):

1. Sauropod heads were held in alert rest with a relatively small inclination α of the LSC.
2. Sauropod cranio-cervico joints are held undeflected in alert rest.
3. Sauropod necks are suspended, with intervertebral joints in approximate ONP (i.e., relaxed).
4. Sauropod cervico-dorsal vertebrae are held in approximately ONP in alert rest.

So progressing from the cranium through the cervical column caudally and into the cervico-dorsal transition, a consistent (but still conjectural) global picture is emerging. But speculations about how sauropods held their head in alert rest, when not otherwise occupied, has perhaps less relevance to sauropod biology compared to how the animal used its neck for feeding, and secondarily, while engaged in locomotion.

Conclusions

Starting with the bare bones, plus caveats about their intervertebral separations based on modern vertebrates with similar articulations, the cervical vertebral columns of sauropods, relieved of their opisthotonic pose (Figure 23), are revealed to be remarkably straight caudally, devoid of any intrinsic sigmoidal-shaped curvature, but some droop cranially (perhaps to re-orient the head ventrally). Osteologically, the base of the neck of all sauropods was a straight collinear extension of the anterior dorsal column. Behaviorally, modern vertebrates, with few exceptions (such as lagomorphs and felids) cantilever the neck and head by dorsal suspension, wherein the intervertebral joints are relaxed and in close to ONP, and the head elevation is that achieved by the 'pre-formed' inherent curvature of the cervical column and the slope of the anterior dorsal column at the shoulders.

Sauropod skeletal reconstructions indicate a range of slopes for the anterior dorsal columns. Variation in the resting height and gravitational orientation of the head can be attributed primarily to variations in body plan without postulating any mechanism (either osteological or behavioral) for creating an upward bend in the base of the neck. Thus despite having no intrinsic upward bend at the base of the neck ONP, the sauropod head could have been placed at a substantial elevation above the shoulders, or at or even below the shoulders, simply due to the slope of the anterior dorsal column. Even modest dorsiflexion at the base could then produce several meters of additional head elevation in those sauropods with especially long necks, and those with long necks and high resting height could also ventriflex to bring the head down to browse low (as well as drink water). The once-held distinction between low versus high browsers is not sharply defined.

Upper bounds on neck mobility are predicted geometrically for extant vertebrates, and those criteria, applied to sauropod necks, predict less-than-avian flexibility, presuming sauropod necks did not disarticulate (more than once per lifetime). Extant vertebrates that do not have a sigmoid curve to the neck, sauropod necks were well-suited for directing the head to different locations on a 'feeding envelope' surface rather than to any point within the volume within that surface (think cow not swan). While intervertebral flexibility was comparable to most that of reptiles,

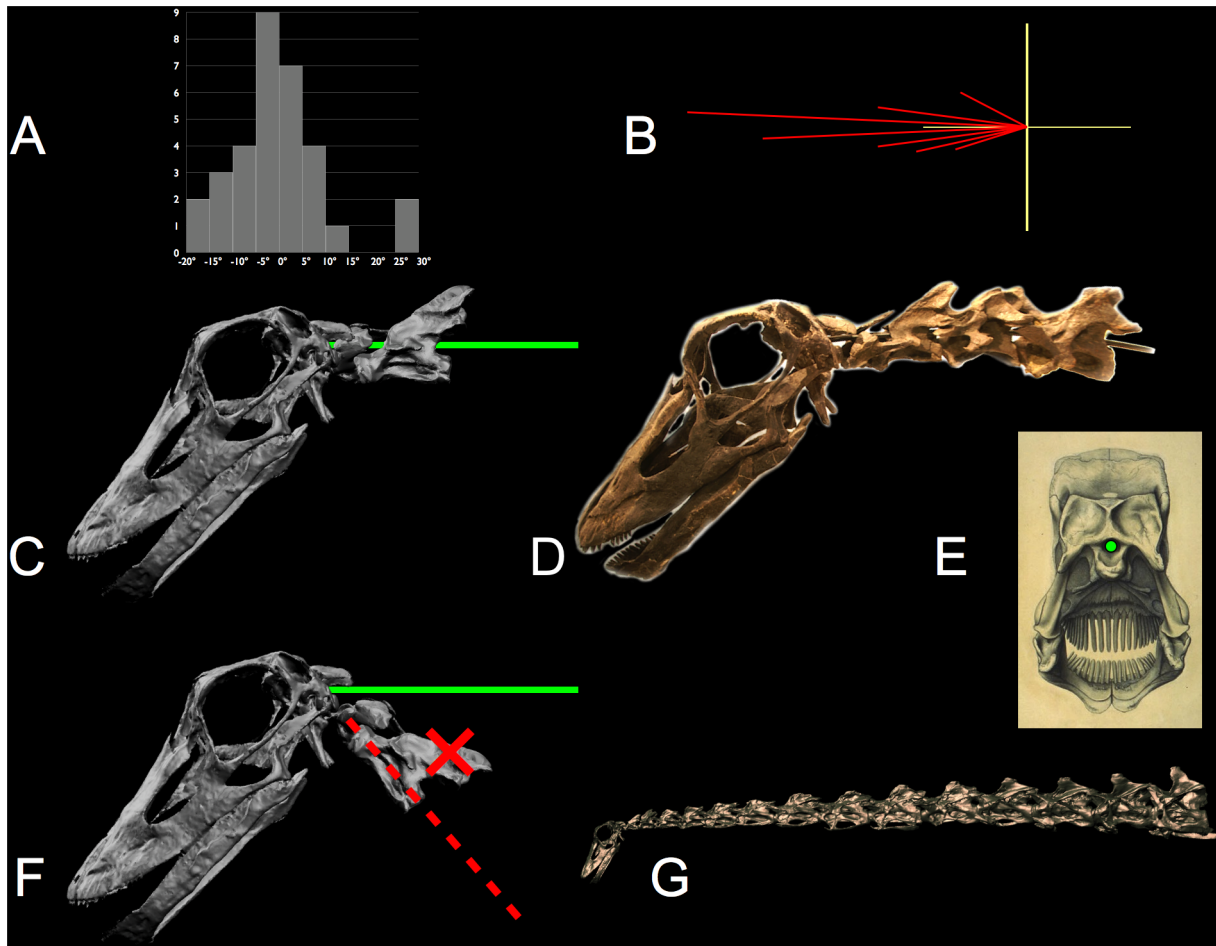


Figure 22. Inner ear orientation is consistent with subhorizontal sauropod necks. The lateral semicircular canal (LSC) is approximately horizontal in alert birds. The orientation α (see text) is plotted for 32 species of birds [111: fig 7a] as a conventional histogram (A) and polar histogram (B) with 5° intervals (c.f. expanded-scale plot in [132: fig. 2]). When a sauropod cranium is similarly oriented ($\alpha = +5^\circ$), the rostrum slopes downward (by -15° in *Camarasaurus lentus* and by -37° in *Diplodocus longus*) [44,135]. The LSC also constrains the slope of the neck cranially. The neural canal passing through the atlas-axis is *collinear* with the foramen magnum, as illustrated by the solid green line in C and the physical armature in the original specimen (D) of *Kaatedocus siberi*, SMA 0004 [133] – see also the location of the foramen magnum (indicated in green) in the posterior view (E) of *Diplodocus* [134]. Consequently, with the cranium oriented relative to gravity as indicated by the LSC, and with the cranio-cervical joint undeflected, the anterior neck is roughly *horizontal* [44]. Taylor et al. [12], however, misinterpreting the anatomy, suggest “... the foramen magnum and occipital condyle are [both] at a right angle relative to the long axis of the skull ...” so that the atlas-axis inserts posteroventrally to the cranium, and consequently they falsely conclude the anterior neck ascends steeply as indicated by the red dashed line in F, from [12: fig. 4]; they figured an even steeper neck for *Camarasaurus*. But properly interpreted, the anatomy of the occiput, the atlas-axis, and the LSC, together with observations of habitual head orientating in the EPB, supports the interpretation that the necks were habitually subhorizontal cranially in diplodocids (E) and camarasaurids (as depicted in Figure 23) [44]. The digital reconstruction (C, F, and G) is based on data courtesy Andreas Christian and Gordon Dzemeski. Photo (D) by the author. Supplemental material: Movie S9. A turntable movie depicting the spinal cord (red) entering the foramen magnum of *Kaatedocus siberi*.

doi:10.1371/journal.pone.0078572.g022

and less than most birds, they more than made up for ‘stiff’ necks by their absolute length. While some sauropods literally went to extraordinary lengths to sweep out a ‘feeding surface’ swath in front of them by flexing their necks at full extension dorsoventrally and mediolaterally, their necks were neither pre-curved avian-style nor sufficiently flexible to fully explore the volume of space contained within that surface. Despite some uvam acerbam arguments that sauropods held their heads high (based on the alert rest pose for lagomorphs, felids and some ratites) sauropod necks were incapable of the prerequisite ability to retract the head sufficiently to balance its weight above the shoulders, adopted passive suspension of the head, like extant vertebrates that share this inability. But how sauropods held their head when inactive

seems of lesser importance to understanding their feeding behavior (a point underscored by lagomorphs, felids, and some ratites).

Several of the conclusions in this review seem negative, about what sauropod necks did not look like, and what they did not do, and which popularizations are not scientifically supported and should be abandoned. For instance, none were shaped like swan necks, and there is no support for the persistent suggestion they held their heads high habitually. Perhaps the most useful such negative is that sauropods were not unique – at least, there is no evidence to suggest that what is known about the articulation, suspension, and function of extant archosaur vertebral columns does not apply as well to the sauropods, despite their extremes.

All is certainly not negative: there are many EPB-supported (or supportable) hypotheses to propose and to test, given the

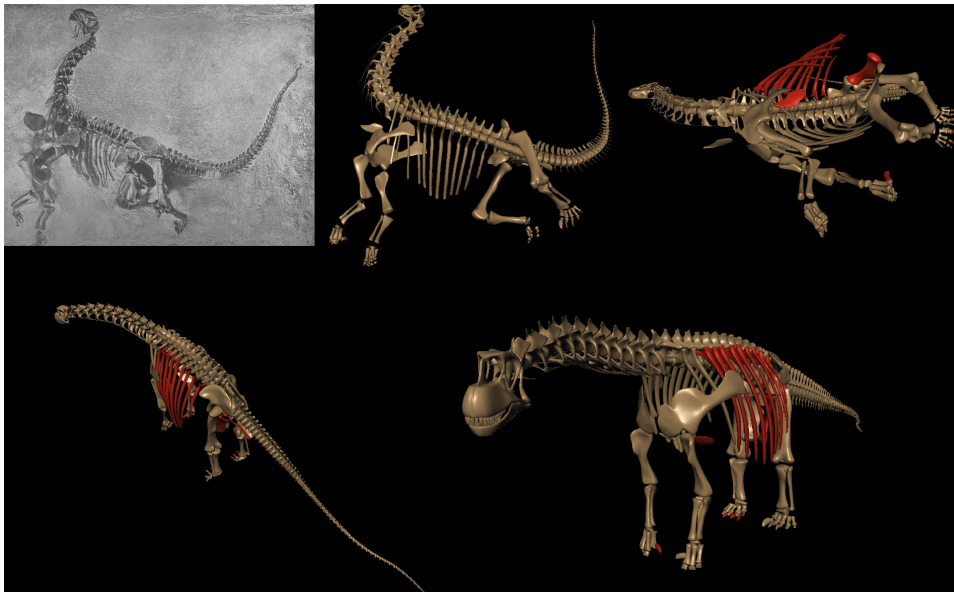


Figure 23. Resurrection of a juvenile *Camarasaurus lentus*. The iconic swan-like ascending neck of *Camarasaurus* sp. [38] likely derives from the opisthotonic pose of the remarkably complete specimen CM 11338 (upper left). However, when all elements are modeled individually and placed into ONP, the opisthotonic pose in the neck and the axial twist through the dorsal column is removed revealing that this sauropod had a rather short neck that extends straight from the anterior dorsals, which raised the neck with a slight incline (see also [136]). Red indicates elements that were missing in the original specimen. This model was created for the Carnegie Museum of Natural History, with cranial modeling contributed by Scott Ernst, forelimb modeled with reference to digitization data of AMNH 664 and scapula coracoid of CM 11338, both courtesy Ray Wilhite (see below regarding digital modeling). Supplemental material: Movie S10. Animation of *Camarasaurus* from its death pose into a life pose near ONP. doi:10.1371/journal.pone.0078572.g023

commonality between extinct and extant archosaurs – inferences which investigators have barely begun to explore. The lateral semicircular canal evidence is compelling (and likely to become more so), as is the upper-bounds on flexibility implied by vertebrates sensibly preserving a safety factor of overlap at the zygapophyses. Osteological bracing (both its presence and absence) and its relationship to loads imposed upon necks at the limit of flexibility has only been noted in a few cases. The kinematic importance of a sigmoidal intrinsic curve to the neck has been well appreciated for birds, and that extends to extinct vertebrates that share a sigmoidal design. But the implications of a neck that is a simple monotonic arc, devoid of a built-in inflection point, has not been previously explored either in extant vertebrates or in sauropods, and yet clearly has relevance to browse-gathering efficiency and behavior. Preconceived notions and ill-supported presuppositions will be replaced increasingly by newly-conceived notions as methodology replaces mythology in the study of sauropods.

Some Notes Regarding Digital Modeling

The 3D models that appear in this review have been developed in Autodesk Maya [108] by the author using standard methods of digital modeling and animation. Each model consists of a set of polygonal objects to represent the osteology, and a ‘rig’, i.e., a set of joint nodes [108] to which these objects are parented in a hierarchical fashion, using the industry convention of defining a ‘root joint’ at the sacrum. The axial skeleton then extends cranially and caudally as distinct kinematic chains, along with the left and right hindlimbs, also forming distinct chains, and continuing, and so forth, in accordance with conventional quadrupedal character rigs [108].

Regarding the modeling of individual bones, conventional digital modeling employs two somewhat disparate choices:

importing a polygonal mesh of vertices that form a piecewise planar approximation to a surface from sampled positions across the given object which, given sufficiently many samples, creates an apparently smooth replica of an actual specimen (see the giraffe CT data in Figure 24). The alternative is to create a meshes derived from mathematical representations of smooth surfaces, such as subdivision surfaces [107]. The sauropod models shown here and in Figure 25 are all based on the latter, but individually shaped to closely conform with digitization data when available (but that represents but one resource for creating dimensionally-accurate replicas of the surface morphology of fossil specimens). As in conventional sculpting, a solid form can be approximated from orthographic views (digitally, 2D source images can be superimposed on planes in the 3D modeling space). The primary benefit of using models (rather than ‘real data’ from CT or other digital sources) is permitting the creation of skeletal reconstructions that fill missing elements, provide alternative restorations to damaged specimens, and to correct distortions that are not amenable to automatic retrodeformation techniques [106].

In modeling based on deformable 3D surfaces, a set of prototypical shapes are created, each a generic form (e.g. of a femur, tibia, dorsal vertebra, rib) that represent sufficient morphology to capture the major osteological features (fenestrae, trochanters, laminae, processes, condyles, etc.) sufficient to model a range of variation across taxa for appendicular elements, and across both taxa and position within a vertebral column for axial elements. To model a specific dorsal vertebral column, for example, a generic dorsal vertebra model is duplicated multiple times to represent the first, mid, and last vertebrae of a given specimen. Each instance is then individually sculpted to match the shape and dimensions of its original counterpart, based on archival material, photographs, and, when available, digitized surface scans, CT, or other point-sampled data of actual specimens.

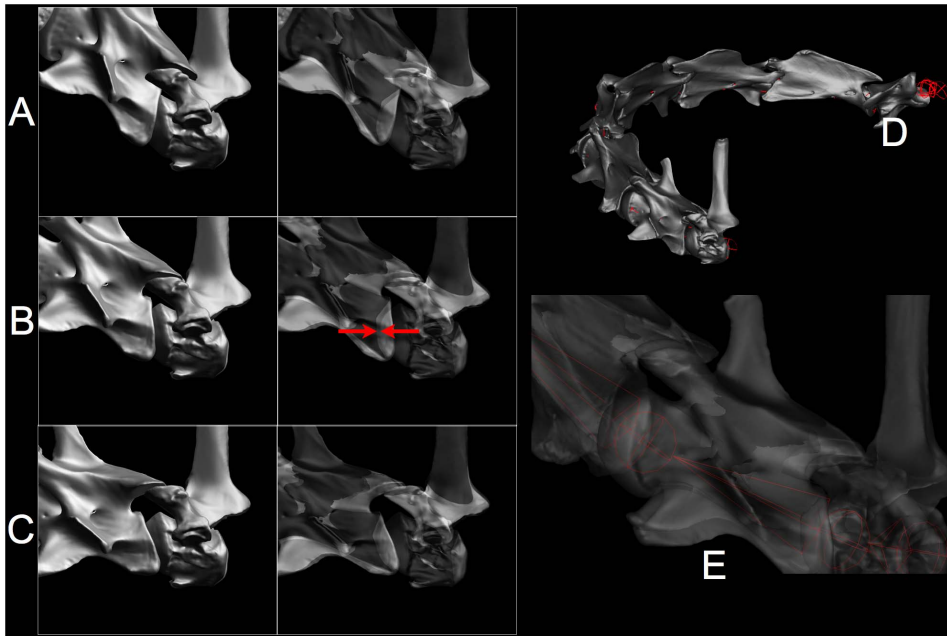


Figure 24. Digital articulation. CT data of individual vertebrae of a recent giraffe *Giraffa Camelopardalis* are articulated in Autodesk Maya [108]. Cervical vertebra C7 pivots about a center of rotation that closely corresponds to the center of curvature of the roughly hemispherical condyle of T1, confirmed by exploratory manipulation and adjustment, resulting in close intervertebral separations as reported in [15] (see red arrows). In A–C, by alternating between opaque and transparent one can observe osteological bracing dorsiflexion (A) and the ZSF at the limit of ventriflexion. With all intervertebral joints adjusted (D–E), the articulated neck approximates the range of motion observed in life (see also Figures 11, 12). This method applies equally to the similarly opisthocoelous vertebrae [30–32], see Figure 25. CT data provided courtesy American Museum of Natural History. doi:10.1371/journal.pone.0078572.g024

Vertebral osteology in archosaurs varies sufficiently smoothly that missing elements can be interpolated over small intervals. Interpolation of missing or severely damaged elements based on adjacent elements is justifiably criticized as being somewhat

speculative, as in the case of the restoration of C13–C15 in the Carnegie Museum specimen *Apatosaurus louisae* CM 3018 [137]. It is conceivable that these vertebrae were not interpolates of their neighboring vertebrae, just as C7 in Giraffe is unique and not

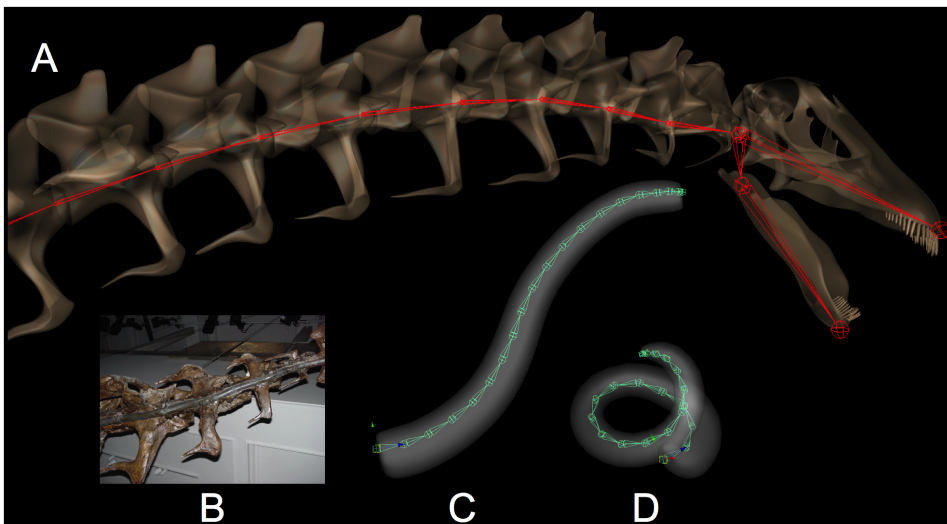


Figure 25. Creating digital, articulated skeletal models. In A, the cervical vertebrae of *A. louisae* CM 3018, modeled by subdivision surfaces (see text) are rigged to form a kinematic chain with joints at the centers of curvature of the condyles (displayed in red), with empirically-determined intervertebral separations that maximize the congruence between condyles and cotyles and associated zygapophyseal pairs at each intervertebral joint. The articulated skeleton resembles the original specimen (B), but fortunately without the rigid steel armature. In C, a digital model of an ostrich *Struthio camelus* is shown in ONP, based on published data [15] of joint-by-joint intervertebral separations and flexion limits (in both mediolateral and dorsoventral flexion), and in D, an example of its extraordinary flexibility. Supplemental material: Movie S11, Movie S12, File S1. doi:10.1371/journal.pone.0078572.g025

predicted as a straightforward interpolate of C6 and T1. But the gradual variation of morphology along sauropod axial skeletons, and the morphological similarity of corresponding cervical vertebrae across known *Apatosaurus* specimens supports the restoration of missing or damaged elements by interpolation.

Next, blend shape animation [109] permits shape interpolation to form the intermediate vertebrae as blends, to create the complete dorsal series. Due to the gradual progression of morphological variation along a vertebral column in archosaurs, linear shape interpolation between axial elements spaced by four or so vertebrae provides a good first approximation, to be followed by refinement. Finally, after establishing the general trends along the entire axial and appendicular skeletons, specific variations are added based on detailed measurements and comparison with reference material.

The skeleton is then rigged to become fully articulated (following standard rigging practices [108]), yet allowing for subsequent adjustments (e.g., of bone morphology, joints the centers of rotation for all joints including the angulation of ribs to form a ribcage, and pectoral girdle placement). Estimating range of motion in a vertebral column requires estimating the centers of rotation for intervertebral joints (see text) as well as the intervertebral separation. Fortunately, manipulation of digital models in three dimensions permits exploratory confirmation of the center of rotation and spacing between condyle and cotyle essentially simulating realtime fluoroscopy to verify the mechanics of articulation.

Once the rigged skeletal model is complete (but always open to subsequent modification and refinement), the digital joints can be exercised to explore the intervertebral range of motion along the axial skeleton, reachability envelopes, and so forth, as exemplified by the figures in this review.

Supporting Information

Figure S1
(TIF)

Figure S2
(TIF)

File S1
(ZIP)

Movie S1
(MP4)

Movie S2
(MP4)

Movie S3
(MP4)

References

- Reisdorf AG, Wuttke M (2012) Re-evaluating Moodie's Opisthotonic- Posture Hypothesis in Fossil Vertebrates Part I: Reptiles – the taphonomy of the bipedal dinosaurs *Compsognathus longipes* and *Juravenator starki* from the Solnhofen Archipelago (Jurassic, Germany). *Palaeobiodiversity and Palaeoenvironments* 92: 119–168. doi:10.1007/s12549-011-0068-y.
- Tornier G (1909) Wie war der *Diplodocus carnegii* wirklich gebaut? *Sitzungsberichte der Gesellschaft Naturforschender Freunde zu Berlin* 1909-4: 193–209.
- Hay OP (1910) On the manner of locomotion of the dinosaurs, especially *Diplodocus*, with remarks on the origin of the birds. *Proceedings of the Washington Academy of Sciences*. 12: 1–25.
- Wiman C (1929) Die Kriede-dinosaurier aus Shantung. *Palaeontologica Sinica* (Series C) 6: 1–67.
- Paul G (1998) Differing bipedal and tripodal feeding modes in sauropods. *Journal of Vertebrate Paleontology* 69: 70A.
- Mazzetta GV, Blanco RE (2001) Speeds of dinosaurs from the Albian-Cenomanian of Patagonia and sauropod stance and gait. *Acta Palaeontologica Polonica* 46: 235–246.
- Myhrvold NP, Currie PJ (1997) Supersonic sauropods? Tail dynamics in the diplodocids. *Paleobiology* 23: 393–409.
- Taylor MP, Wedel MJ, Cifelli RL (2011) A new sauropod dinosaur from the Lower Cretaceous Cedar Mountain Formation, Utah, USA. *Acta Palaeontologica Polonica* 56: 75–98.
- Siegwarth JD, Smith CN, Redman PD (2011) An alternative sauropod physiology and cardiovascular system that eliminates high blood pressures. *Lethaia* 44: 46–57.
- Bakker RT (1978) Dinosaur feeding behavior and the origin of flowering plants. *Nature* 274: 661–663.
- Choy DSJ, Altman P (1992) The cardiovascular system of *Barosaurus*: and educated guess. *Lancet* 340: 534–536.

Movie S4
(MP4)

Movie S5
(MP4)

Movie S6
(MP4)

Movie S7
(MP4)

Movie S8 A turntable movie depicting the spinal cord (red) entering the foramen magnum of *Kaatedocus siberi*.
(MP4)

Movie S9 Animation of *Camarasaurus* from its death pose into a life pose near ONP.
(MP4)

Movie S10
(MP4)

Movie S11
(MP4)

Movie S12
(MP4)

Acknowledgments

The author thanks Martin Sander, Andreas Christian, and the organizers of the DFG Research Unit 533 for the invitation to contribute to this volume. I gratefully acknowledge the contributors of many individuals over the last decade or so, including: Michael Brett-Surman, Kenneth Carpenter, Andreas Christian, Brian Curtice, Peter Dodson, Scott Ernst, Guy Leahy, Matthew Lowe, John Martin, Christopher McGowan, Mark Norell, J. Michael Parrish, Philip Platt, Timothy Rowe, Hans-Jacob (Köbi) Siber, Neil Whitely-Bolton, Eric D. Wills, Ray Wilhite, D. Cary Woodruff, Carl Zimmer, and the kind assistance of the American Museum of Natural History, Brigham Young University Museum of Paleontology, the Carnegie Museum of Natural History, the Denver Museum of Nature and Science, the Sauriermuseum Aathal, the University Museum of Zoology, University of Cambridge, the U.S. National Museum of Natural History, and the University of Texas, for access to materials. J. Michal Parrish's contributions regarding feeding by ventriflexion and its relationship to ONP in extant browsers are specially acknowledged. D. Cary Woodruff, Andrew A. Farke and an anonymous reviewer were very valuable in improving the manuscript.

Author Contributions

Conceived and designed the experiments: KAS. Performed the experiments: KAS. Analyzed the data: KAS. Contributed reagents/materials/analysis tools: KAS. Wrote the paper: KAS.

12. Taylor MP, Wedel MJ, Naish D (2009) Head and neck posture in sauropod dinosaurs inferred from extant animals. *Acta Palaeontologica Polonica* 54: 213–220. DOI: 10.4202/app.2009.0007.
13. Gould SJ (1991) *Bully for brontosaurus: reflections in natural history*. New York: W.W. Norton. 540.
14. Paul G (2000) Restoring the life appearance of dinosaurs. In: Paul GS, editor. *The Scientific American Book of Dinosaurs*. New York: Bryon Press and Scientific American. pp.78–106.
15. Dzemski G, Christian A (2007) Flexibility along the neck of the ostrich (*Struthio camelus*) and consequences for the reconstruction of dinosaurs with extreme neck length. *Journal of Morphology* 268: 701–714.
16. Feynman RP (with Leighton R, Hutchings E) (1985) “Surely you’re joking, Mr. Feynman!”: adventures of a curious character. New York: W.W. Norton. 350.
17. Naish D, Taylor MP, Wedel MJ (2009) Extant animals provide new insights on head and neck posture in sauropods. *Journal of Vertebrate Paleontology* 29: 56A.
18. Bryant HN, Russell AP (1992) The role of phylogenetic analysis in the inference of unpreserved attributes of extinct taxa. *Philosophical Transactions of the Royal Society of London B* 337: 405–418.
19. Witmer LM (1995) The extant phylogenetic bracket and the importance of reconstructing soft tissues in fossils. In: Thomason JJ, editor. *Functional Morphology in Vertebrate Paleontology*, Cambridge: Cambridge University Press. pp.19–33.
20. Carrano MT, Hutchinson JR (2002) Pelvic and hindlimb musculature of *Tyrannosaurus rex* (Dinosauria: Theropoda). *Journal of Morphology* 253: 207–228.
21. Moscovici S, Zavalloni M (1969) The group as a polarizer of attitudes. *Journal of Personality and Social Psychology* 12(2): 125–35.
22. Chandrashekanan M, Walker BA, Ward JC, Reingen PH (1996) Modeling individual preference evolution and choice in a dynamic group setting. *Journal of Marketing Research* 33: 211–223.
23. Myers DG, Lamm H (1976) The group polarization phenomenon. *Psychological Bulletin* 83: 602–627.
24. Kassin S, Fein S, Markus HR (2010) *Social Psychology*. 8th edition. Belmont, CA: Wadsworth Publishing. 613.
25. Marsh OC (1883) Principal characters of American Jurassic dinosaurs. Pt. VI. Restoration of *Brontosaurus*. *American Journal of Science (series 3)* 27: 329–340.
26. Hatcher JB (1901) *Diplodocus* (Marsh): its osteology, taxonomy and probable habits, with a restoration of the skeleton. *Memoirs of the Carnegie Museum* 1: 1–63.
27. Janensch W (1950) Die Skelettrekonstruktion von *Brachiosaurus brancai*. *Palaeontographica (Suppl. 7)* 3: 95–103.
28. Martin J (1987) Mobility and feeding of *Cetiosaurus* (Saurischia, Sauropoda) why the long neck? In: Currie PJ, Koster EH, editor. *Fourth Symposium on Mesozoic Terrestrial Ecosystems, Short Papers*. Drumheller: Boxtree Books. pp. 154–159.
29. McIntosh J, Brett-Surman MK, Farlow JO (1997) Sauropods. In: Farlow JO, Brett-Surman MK, editor. *The complete dinosaur*. Bloomington: Indiana University Press. pp. 264–290.
30. Stevens KA, Parrish JM (1999) Neck posture and feeding habits of two Jurassic sauropod dinosaurs. *Science* 284, April 30: 798–800.
31. Stevens KA, Parrish JM (2005) Neck posture, dentition and feeding strategies in Jurassic sauropod dinosaurs. In: Tidwell V, Carpenter K, editor. *Thunder-lizards: the sauropodomorph dinosaurs*. Bloomington: Indiana University Press. pp. 212–232.
32. Stevens KA, Parrish JM (2005) Digital reconstructions of sauropod dinosaurs and implications for feeding. In: Curry Rogers K, Wilson J, editor. *The Sauropods: Evolution and paleobiology*. Berkeley: University of California Press. pp. 178–200.
33. Christian A (2010) Some sauropods raised their necks: evidence for high browsing in *Euhelopus zdanskyi*. *Biol Lett* 6: 823–825. (doi:10.1098/rsbl.2010.0359).
34. Clauss M (2011) Sauropod biology and the evolution of gigantism: what do we know? In: Klein N, Remes K, Gee CT, Sander PM, editor. *Biology of the Sauropods: understanding the life of giants*. Bloomington: Indiana University Press. pp. 1–7.
35. Young CC, Zhao X-J (1972) *Mamenchisaurus hochuanensis* sp. nov. *Institute of Vertebrate Paleontology and Paleoanthropology Monographs A* 8: 1–30.
36. Borsuk-Bialynicka M (1977) A new camarasaurid sauropod, *Opisthocoelecaudia skarzynskii*, n. sp. n., from the Upper Cretaceous of Mongolia. *Acta Palaeontologica Polonica* 37: 5–64.
37. Osborn HF, Mook CC (1921) *Camarasaurus*, *Amphicoelias*, and other sauropods of Cope. *Memoirs of the American Museum of Natural History* 3: 247–287.
38. Gilmore CW (1925) A nearly complete articulated skeleton of *Camarasaurus*, a saurischian dinosaur from the Dinosaur National Monument. *Memoirs of the Carnegie Museum* 10: 347–384.
39. Czerkas SA, Czerkas SJ (1991) *Dinosaurs: a global view*. New York: Mallard Press. 247.
40. Christian A, Dzemski G (2007) Reconstruction of the cervical skeleton posture of *Brachiosaurus brancai* Janensch, 1914 by an analysis of the intervertebral stress along the neck and a comparison with the results of different approaches. *Fossil Record* 10: 37–48.
41. Janensch W (1936) Ein aufgestelltes Skelett von *Dicraeosaurus hansemanni*. *Palaeontographica (suppl. 7)*: 299–308.
42. Wilson JA (2002) Sauropod dinosaur phylogeny: critique and cladistic analysis. *Zoological Journal of the Linnean Society* 136: 217–276.
43. Rauhut OWM, Remes K, Fechner R, Cladera G, Puerta P (2005) Discovery of a short-necked sauropod dinosaur from the Late Jurassic period of Patagonia. *Nature* 435: 670–672.
44. Sereno PC, Wilson JA, Witmer LM, Whitlock JA, Maga A, et al. (2007) Structural extremes in a Cretaceous dinosaur. *PLoS ONE* 2: e1230. (DOI: 10.1371/journal.pone.0001230).
45. Gilmore CW (1936) The osteology of *Apatosaurus* with special reference to specimens in the Carnegie Museum. *Memoirs of the Carnegie Museum* 11: 175–300.
46. Schwarz D, Frey E, Meyer CA (2007) Novel reconstruction of the orientation of the pectoral girdle in sauropods. *The Anatomical Record* 290: 32–47.
47. Taylor MP (2010) *Sauropod dinosaur research*. Geological Society, London, Special Publications. 343–361–386. doi:10.1144/SP343.22.
48. Cobley MJ, Rayfield EJ, Barrett PM (2013) Inter-vertebral flexibility of the ostrich neck: implications for estimating sauropod neck flexibility. *PLoS ONE* 8: e72187. doi:10.1371/journal.pone.0072187.
49. Bonnan MF (2003) The evolution of manus shape in sauropod dinosaurs: implications for functional morphology, forelimb orientation, and sauropod phylogeny. *Journal of Vertebrate Paleontology* 23: 595–613.
50. Wilhite R (2005) Morphological variation in the appendicular skeleton of North American Upper Jurassic sauropods. In: Tidwell V, Carpenter K, editor. *Thunder-lizards: the sauropodomorph dinosaurs*. Bloomington: Indiana University Press. pp. 268–301.
51. Woolnough AP, du Toit JT (2001) Vertical zonation of browse quality in tree canopies exposed to a size-structured guild of Africa browsing ungulates. *Oecologia (Berlin)* 129: 585–590.
52. Cameron EZ, du Toit JT (2007) Winning by a neck: tall giraffes avoid competing with shorter browsers. *The American Naturalist* 169: 130–135.
53. Seymour RS (2009) Raising the sauropod neck: it costs more to get less. *Biology Letters* 5: 317–319.
54. Seymour RS (2009) Sauropods kept their heads down. *Science* 323: 1671.
55. Ganse B, Stahn A, Stoinski S, Suthau T, Gunga H-C (2011) Body mass estimation, thermoregulation, and cardiovascular physiology of large sauropods. In: Klein N, Remes K, Gee CT, Sander PM, editor. *Biology of the sauropod dinosaurs: understanding the life of giants*. Bloomington: Indiana University Press. pp. 105–115.
56. Whitlock JA (2011) Inferences of *diplodocoid* (Sauropoda: Dinosauria) feeding behavior from snout shape and microwear analyses. *PLoS ONE* 6: e18304. doi:10.1371/journal.pone.0018304.
57. Preuschoft H (1976) Funktionelle anpassung evolvierender systeme. *Aufsätze und Reden der Senckenbergischen Naturforschender Gesellschaft* 28: 98–117.
58. Christian A, Preuschoft H (1996) Deducing the body posture of extinct large vertebrates from the shape of the vertebral column. *Palaeontology* 39: 801–812.
59. Christian A (2002) Neck posture and overall body design in sauropods. *Mitteilungen des Museums für Naturkunde Berlin, Geowissenschaftliche Reihe* 5: 269–279.
60. Berman DS, Rothschild BM (2005) Neck posture of sauropods determined using radiological imaging to reveal three-dimensional structure of cervical vertebrae. In: Tidwell V, Carpenter K, editor. *Thunder-lizards: the sauropodomorph dinosaurs*. Bloomington: Indiana University Press. pp. 233–247.
61. O’Connor PM (2006) Postcranial pneumaticity: an evaluation of soft-tissue influences on the postcranial skeleton and the reconstruction of pulmonary anatomy in archosaurs. *Journal of Morphology*. 267: 1199–1226.
62. Werner J, Griebeler EM (2013) New insights into non-avian dinosaur reproduction and their evolutionary and ecological implications: linking fossil evidence to allometries of extant close relatives. *PLoS ONE* 8(8): e72862. doi:10.1371/journal.pone.0072862.
63. Dzemski G (2005) Funktionsmorphologische Betrachtung der Halsstellung bei Zoogiraffen. *Zool Garten* 3: 189–201.
64. Dzemski G (2006) Funktionsmorphologische Analysen langer Hälse bei rezenten terrestrischen Wirbeltieren zur Rekonstruktion der Stellung und Beweglichkeit langer Hälse prähistorischer Tiere. Ph.D. dissertation. Universität Flensburg Juli.
65. Van Der Leeuw AHJ, Bout RG, Zweers GA (2001) Evolutionary morphology of the neck system in raites, fowl, and waterfowl. *Netherlands Journal of Zoology* 51: 243–262.
66. Bout RG (1997) Postures of the avian craniocervical column. *Journal of Morphology* 231: 287–295.
67. Bernhardt M, Bridle KH (1989) Segmental analysis of the sagittal plane alignment of the normal thoracic and lumbar spines and thoracolumbar junction. *Spine* 14:717–721. doi: 10.1097/00007632-198907000-00012.
68. Sivers W (1934) Ein Beitrag zur Kenntnis des Vogelhalses. *Morphologischer Jahrbuecher* 74: 697–728.
69. Boas JEV (1929) Biologisch-anatomische Studien über den Hals der Vogel. *Det Kongelige Danske Videnskabernes Selskabs Skrifter* 9: 101–222.
70. Heidweiller J (1989) Postnatal development of the neck system in the chicken (*Gallus domesticus*). *American Journal of Anatomy* 186: 258–270.

71. Davies DV, Barnett CH, MacConaill MA (1961) Synovial joints. Their structure and mechanics. Springfield, Illinois: Charles C. Thomas. 304.
72. Kuznetsov AN, Tereschenko VS (2010) A method for estimation of lateral and vertical mobility of platycoelous vertebrae of tetrapods. *Paleontological Journal* 44: 209–225.
73. Schmidt H, Heuer F, Claes L, Wilke H-J (2008) The relation between the instantaneous center of rotation and facet joint forces – a finite element analysis. *Clinical Biomechanics* 23: 270–278.
74. Zweers GA, Vanden Berge JC, Koppendraier R (1987) Avian craniocervical systems. I. Anatomy of the cervical-column in the chicken (*Gallus gallus* L.). *Acta Morphologica Neerlandica-Scandinavica* 25: 131–155.
75. Pooni JS, Hukins DW, Harris PF, Hilton RC, Davies KE (1986) Comparison of the structure of human intervertebral disks in the cervical, thoracic and lumbar regions of the spine. *Surgical and Radiologic Anatomy* 8: 175–182.
76. Bruggeman BJ, Maier JA, Mohiuddin YS, Powers R, Lo Y, Guimarães-Camboa N, Evans SM, Harfe BD (2012) Avian intervertebral disc arises from rostral sclerotome and lacks a nucleus pulposus: implications for evolution of the vertebrate disc. *Developmental Dynamics* 241: 675–683.
77. Hall BK (1983) *Cartilage*, Volume 1. Academic Press. 400.
78. Malda J, de Grauw JC, Benders KEM, Kik MJ, van der Lest CHA, et al. (2013) Of mice, men and elephants: the relation between articular cartilage thickness and body mass. *PLoS ONE* 8(2): e57683.
79. Wedel MJ, Sanders RK (1999) Comparative morphology and functional morphology of the cervical series in Aves and Sauropoda. *Journal of Vertebrate Paleontology* 19: 83A.
80. Sereno PC, Beck AL, Moussa B, Dutheil D, Larsson HCE, et al. (1999) Cretaceous sauropods from the Sahara and the uneven rate of skeletal evolution among dinosaurs. *Science* 286: 1342–1347.
81. Gauthier-Pilters H, Daag AI (1981) The camel, its ecology, behavior and relationship to man. Chicago: University of Chicago Press. 208.
82. Klein N, Christian A, Sander PM (2012) Histology shows that elongated neck ribs in sauropod dinosaurs are ossified tendons. *Biology Letters*, 8: 1032–1035.
83. Schwarz-Wings D, Meyer CA, Frey E, Manz-Steiner HR, Schumacher R (2010) Mechanical implications of pneumatic neck vertebrae in sauropod dinosaurs. *Proceedings of the Royal Society of London B* 277: 11–17. doi: 10.1098/rspb.2009.1275.
84. Stevens KA, Wills ED (2001) Gracile versus robust cervical vertebral designs in sauropods. Annual Meeting of the Society of Vertebrate Paleontology, Bozeman, MT. October, 2001. *Journal of Vertebrate Paleontology* 21: 104A.
85. Wilson JA (1999) Vertebral laminae in sauropods and other saurischian dinosaurs. *Journal of Vertebrate Paleontology* 18: 639–653.
86. Janensch W (1929) Die Wirbelsäule der Gattung *Dicraeosaurus* hausemanni. *Palaontographica* 3 (Suppl. 7): 39–133.
87. Snively E, Cotton JR, Ridgely R, Witmer LM (2013) Multibody dynamics model of head and neck function in *Allosaurus* (Dinosauria, Theropoda). *Palaontologia Electronica* 16, Issue 2; 11A 29; paleo-electronica.org/content/2013/389-allosaurus-feeding.
88. Zhou SH, McCarthy ID, McGrew AH, Coombs RR, Hughes SP (2000) Geometrical dimensions of the lower lumbar vertebrae – analysis of data from digitized CT images. *European Spine Journal* 9: 242–8.
89. Solounias N (1999) The remarkable anatomy of the giraffe's neck. *Journal of Zoology* 247: 257–268.
90. Romer AS (1956) *Osteology of the Reptiles*. Chicago: University of Chicago 772.
91. Conrad JL (2006) Postcranial skeleton of *Shinisaurus crocodilurus* (Squamata: Anguimorpha). *Journal of Morphology* 267: 759–775.
92. van Sittert SJ, Skinner JD, Mitchell G (2010) From fetus to adult—an allometric analysis of the giraffe vertebral column. *Journal of Experimental Zoology (Molecular and Developmental Evolution)* 314B: 469–479.
93. Badlangana NL, Adams JW, Manger PR (2009) The giraffe (*Giraffa camelopardalis*) cervical vertebral column: a heuristic example in understanding evolutionary processes? *Zoological Journal of the Linnean Society* 155: 736–757.
94. Frey E (1988) Anatomie des Körperstammes von Alligator mississippiensis Daudin. Staatliches Museum für Naturkunde Serie A, 105.
95. Vidal PP, Graf W, Berthoz A (1986) The orientation of the cervical vertebral column in unrestrained awake animals. *Experimental Brain Research* 61: 549–559.
96. Graf W, de Waele C, Vidal PP (1992) Skeletal geometry in vertebrates and its relation to the vestibular end organs. In: Berthoz A, Graf W, Vidal PP, editor. *The Head-neck sensory motor system*. Oxford: Oxford University Press. pp. 129–134.
97. Graf W, de Waele C, Vidal PP (1995) Functional anatomy of the head-neck movement system of quadrupedal and bipedal mammals. *Journal of Anatomy* 186: 55–74.
98. Muybridge E (1957) *Animals in motion*. Mineola, NY: Courier Dover Publications. 416.
99. Leuthold W (1977) *African ungulates: a comparative review of their ethology and behavioral ecology*. Springer Verlag, Berlin, 307.
100. Leuthold B, Leuthold W (1972) Food habits of giraffe in Tsavo National Park, Kenya. *East African Wildlife Journal* 10: 129–141.
101. Owen-Smith RN (1988) Megaherbivores: the influence of very large body size on ecology. Cambridge University Press, Cambridge. 369.
102. Pellew R (1984) The feeding ecology of a selective browser, the giraffe (*Giraffa camelopardalis tippelskirchi*). *Journal of Zoology* 202: 57–81.
103. Young T, Isbell L (1991) Sex differences in giraffe feeding ecology: energetic and social constraints. *Ethology* 87: 79–89.
104. Stevens KA (2002) *DinoMorph: Parametric Modeling of Skeletal Structures*. Senckenbergiana Lethaea 82(1): 23–34.
105. Janensch W (1950) Die Wirbelsäule von *Brachiosaurus brancai*. *Palaontographica* (Suppl. 7) 3: 27–93.
106. Tschopp E, Russo J, Dzemski G. (2013) Retrodeformation as a test for the validity of phylogenetic characters: an example from diplodocid sauropod vertebrae. *Palaontologia Electronica*, 1998: 16.
107. Catmull E, Clark J (1978) Recursively generated B-Spline surfaces on arbitrary topological meshes. *Computer Aided Design*, 10: 350–355.
108. Autodesk (2013) *Maya - 3D Animation, Visual Effects & Compositing Software* [online] <http://usa.autodesk.com/maya/> [Accessed 28 August 2013].
109. Deng Z, Noh J (2008) Computer facial animation: A survey. In: Deng Z, Neumann U, editor. *Data-Driven 3D facial animation*. London: Springer-Verlag. pp.1–28.
110. Zweers GA, Bout RG, Heidweiller J (1994) Motor organization of the avian head-neck system. In: Davies MNO, Green PR, editor. *Perception and Motor Control in Birds*. Heidelberg: Springer-Verlag. pp.201–221.
111. Duijm M (1951) On the head posture in birds and its relation to some anatomical features. II. Proceedings of the Koninklijke Nederlandse Akademie van Wetenschappen, Series C 54: 202–211, 260–271.
112. Pellionisz AJ, Le Goff B, Jaczkó L (1992) Multidimensional geometry intrinsic to head movements around distributed centers of rotation: A neurocomputer paradigm. In: Berthoz A, Graf W, Vidal PP, editor. *The Head-Neck Sensory Motor System*. New York: Oxford University Press. pp. 158–167.
113. Preuschhof H, Hohn B, Stoinski S, Witzel U (2011) Why so huge? Biomechanical reasons for the acquisition of large size in sauropod and theropod dinosaurs. In: Klein N, Remes K, Gee CT, Sander PM. *Biology of the sauropods: understanding the life of gaits*. Bloomington: Indiana University Press. pp. 197–218.
114. Jouffroy FK (1992) Evolution of the dorsal muscles of the spine in light of their adaptation to gravity effects. In: Berthoz A, Graf W, Vidal PP, editor. *The Head-neck sensory motor system*. Oxford: Oxford University Press. pp. 22–35.
115. Slijper EJ (1946) Comparative biologic-anatomical investigations on the vertebral column and spinal musculature of mammals. *Verhandelingen der Koninklijke Akademie van Wetenschappen II* 42: 1–128.
116. Alexander RMcN (1985) Mechanics of posture and gait of some large dinosaurs. *Zoological Journal of the Linnean Society*, 83: 1–25. doi: 10.1111/j.1096-3642.1985.tb00871.x
117. Wedel MJ, Cifelli RL, Sanders RK (2000) Osteology, paleobiology, and relationships of the sauropod dinosaur *Sauroposeidon*. *Acta Palaontologica Polonica* 45: 343–388.
118. Tsubihiji T (2004) The ligament system in the neck of *Rhea americana* and its implication for the bifurcated neural spines of sauropod dinosaurs. *Journal of Vertebrate Paleontology*. 24: 165–172.
119. Schwarz D, Frey E, Meyer CA (2007) Pneumaticity and soft-tissue reconstructions in the neck of diplodocid and dicraeosaurid sauropods. *Acta Palaontologica Polonica* 52: 167–188.
120. O'Connor PM (2007) The postcranial axial skeleton of *Majungasaurus crenatissimus* (Theropoda: Abelisauridae) from the Late Cretaceous of Madagascar. *Journal of Vertebrate Paleontology* 27: 127–163.
121. Witmer LM, Chatterjee S, Franzosa J, Rowe T (2003) Neuroanatomy of flying reptiles and implications for flight, posture and behaviour. *Nature* 425: 950–953.
122. Rabbitt RD, Damiano ER, Grant JW (2004) Biomechanics of the semicircular canals and otolith organs. In: Highstein SM, Fay RR, Popper AN, editor. *The vestibular system*. New York: Springer Verlag. pp. 153–202.
123. Cohen B, Raphan T (2004) The physiology of the vestibulo-ocular reflex (VOR). In: Highstein SM, Fay RR, Popper AN, editor. *The vestibular system*. New York: Springer Verlag. pp.235–285.
124. Girard L (1923) Le plan des canaux semi-circulaires horizontaux considéré comme plan horizontal de la tête. *Bulletin et Mémoires de la Société d'Anthropologie de Paris*. Series 7(IV): 14–33.
125. Lebedkin S (1924) Über die Lage des Canalis semicircularis lateralis bei Säugern. *Anatomischer Anzeiger* 58: 447–460.
126. de Beer GR (1947) How animals hold their heads. *Proceedings of the Linnean Society of London* 159: 125–139.
127. Mazza D, Winterson B (1984) Semicircular canal orientation in the adult resting rabbit. *Acta Oto-Laryngologica* (Stockholm) 98: 472–480.
128. Erichsen JT, Hodos W, Evinger C, Besette BB, Phillips SJ (1989) Head orientation in pigeons: postural, locomotor and visual determinants. *Brain, Behavior and Evolution* 33: 268–278.
129. Blanks RHI, Curthoys IS, Markham CH (1972) Planar relationships of semicircular canals in the cat. *American Journal of Physiology* 223: 55–62.
130. Spoor F, Zonneveld F (1998) Comparative review of the human bony labyrinth. *Yearbook of Physical Anthropology* 41: 211–251.
131. Wilson VJ, Melville Jones G (1979) *Mammalian vestibular physiology*. Plenum Press, New York London.
132. Marugán-Lobón J, Chiappe LM, Farke AA (2013) The variability of inner ear orientation in saurischian dinosaurs: testing the use of semicircular canals as a

- reference system for comparative anatomy. *PeerJ* 1: e124; DOI: 10.7717/peerj.124.
133. Tschopp E, Mateus O (2012) The skull and neck of a new flagellicaudatan sauropod from the Morrison Formation and its implication for the evolution and ontogeny of diplodocid dinosaurs. *Journal of Systematic Palaeontology*. doi:10.1080/14772019.2012.746589.
 134. Ostrom JH, McIntosh JS (2000) *Marsh's dinosaurs. The collections of Como Bluff*. New Haven: Yale University Press. 416.
 135. Madsen, Jr. JH, McIntosh JS, Berman DS (1995) Skull and atlas-axis complex of the upper Jurassic sauropod *Camarasaurus* Cope (Reptilia: Saurischia). *Bulletin of Carnegie Museum of Natural History* 31: 115.
 136. McIntosh JS, Miles CA, Cloward KC, Parker JR (1996) A new nearly complete skeleton of *Camarasaurus*. *Bulletin of Gunma Museum of Natural History* 1: 1–87.
 137. Upchurch P (2000) Neck posture of sauropod dinosaurs. *Science* 287: 547b.

The Effect of Intervertebral Cartilage on Neutral Posture and Range of Motion in the Necks of Sauropod Dinosaurs

Michael P. Taylor^{1*}, Mathew J. Wedel²

1 Department of Earth Sciences, University of Bristol, Bristol, United Kingdom, **2** College of Osteopathic Medicine of the Pacific and College of Podiatric Medicine, Western University of Health Sciences, Pomona, California, United States of America

Abstract

The necks of sauropod dinosaurs were a key factor in their evolution. The habitual posture and range of motion of these necks has been controversial, and computer-aided studies have argued for an obligatory sub-horizontal pose. However, such studies are compromised by their failure to take into account the important role of intervertebral cartilage. This cartilage takes very different forms in different animals. Mammals and crocodylians have intervertebral discs, while birds have synovial joints in their necks. The form and thickness of cartilage varies significantly even among closely related taxa. We cannot yet tell whether the neck joints of sauropods more closely resembled those of birds or mammals. Inspection of CT scans showed cartilage:bone ratios of 4.5% for *Sauroposeidon* and about 20% and 15% for two juvenile *Apatosaurus* individuals. In extant animals, this ratio varied from 2.59% for the rhea to 24% for a juvenile giraffe. It is not yet possible to disentangle ontogenetic and taxonomic signals, but mammal cartilage is generally three times as thick as that of birds. Our most detailed work, on a turkey, yielded a cartilage:bone ratio of 4.56%. Articular cartilage also added 11% to the length of the turkey's zygapophyseal facets. Simple image manipulation suggests that incorporating 4.56% of neck cartilage into an intervertebral joint of a turkey raises neutral posture by 15°. If this were also true of sauropods, the true neutral pose of the neck would be much higher than has been depicted. An additional 11% of zygapophyseal facet length translates to 11% more range of motion at each joint. More precise quantitative results must await detailed modelling. In summary, including cartilage in our models of sauropod necks shows that they were longer, more elevated and more flexible than previously recognised.

Citation: Taylor MP, Wedel MJ (2013) The Effect of Intervertebral Cartilage on Neutral Posture and Range of Motion in the Necks of Sauropod Dinosaurs. PLoS ONE 8(10): e78214. doi:10.1371/journal.pone.0078214

Editor: Peter Dodson, University of Pennsylvania, United States of America

Received: April 8, 2013; **Accepted:** September 18, 2013; **Published:** October 30, 2013

Copyright: © 2013 Taylor, Wedel. This is an open-access article distributed under the terms of the Creative Commons Attribution License, which permits unrestricted use, distribution, and reproduction in any medium, provided the original author and source are credited.

Funding: No current external funding sources for this study.

Competing Interests: The authors have declared that no competing interests exist.

* E-mail: dino@miketaylor.org.uk

Introduction

Historical background

Sauropod dinosaurs are notable both for their very long necks [1] and their very large body sizes [2] (Figure 1). They were, by an order of magnitude, the heaviest terrestrial animals that have ever existed [3]. An extensive review of sauropod palaeobiology [4] found that the long necks of sauropods were the key factor in the evolution of their large size.

Ever since the sauropod body shape has been understood, the posture and flexibility of their necks has been of interest. Initially, the long neck was assumed to be “swanlike” and flexible [5–7], and habitually held high above the level of the torso. Elevated posture was depicted in most (though not all) life restorations of sauropods, including the classic works of Knight [8], Zallinger [9] and Burian [10], and continued to dominate the popular perception of sauropods through books such as *The Dinosaur Heresies* [11] and films such as *Jurassic Park* [12].

This changed in 1999, with the work of Stevens and Parrish [13]. In a short paper, Martin had proposed, based on his work on mounting the skeleton of the Middle Jurassic sauropod *Cetiosaurus*, that it was constrained to a relatively low, horizontal neck posture, and limited in flexibility [14]. Stevens and Parrish extended this idea to the better known Late Jurassic sauropods *Apatosaurus* and

Diplodocus, and modelled the intervertebral articulations using a computer program of their own devising named DinoMorph. They concluded that *Apatosaurus* and *Diplodocus*, and by extension other sauropods, were adapted to “ground feeding or low browsing” and stated that “*Diplodocus* was barely able to elevate its head above the height of its back”. The horizontal neck postures advocated in this widely publicised paper were quickly adopted as a new orthodoxy, and were reflected in the BBC television documentary *Walking With Dinosaurs* [15] and a special exhibition at the American Museum of Natural History. Stevens [16] subsequently published a high-level description of the DinoMorph software, and Stevens and Parrish [17,18] elaborated their earlier work with more detailed models.

Although several subsequent publications have provided evidence for a habitually raised neck posture [19–21], the only direct response to the work of Stevens and Parrish was that of Upchurch [22], a half-page technical comment. As a result, certain other flaws in this influential study have so far remained unaddressed. This is unfortunate, as the digital modelling approach pioneered by the DinoMorph project is potentially very useful: as a result of the lack of serious critique, this approach has not yet matured into the powerful and informative tool that it should have become.

The year after the DinoMorph work was published, Gregory Paul ([23]: 92–93) pointed out the importance of cartilage in understanding posture:

A problem with estimating neck posture is that it is highly sensitive to the thickness of the cartilage separating the vertebrae, especially the discs. The computer-generated studies [of Stevens and Parrish] have assumed that the discs separating the vertebrae were thin; but so closely spacing the neck vertebrae jams the aft rim of one vertebra's centrum into the base of the rib of the following vertebra in some sauropods. It is therefore probable that at least some sauropods had thick intervertebral discs. The thicker the discs were, the more upwardly flexed the neck was.

But this was rejected by Stevens and Parrish ([18]: 214), as follows:

Paul (2000, 92) suggests that some sauropod necks had thick intervertebral discs, effectively wedged between successive centra, which induced an upward curve at their base. Sauropod necks, however, were strongly opisthocoelous,



Figure 1. The world's biggest mounted skeleton: the sauropod *Giraffatitan brancai*. Mounted skeleton of *Giraffatitan brancai* paratype MB.R.2181 at the Museum für Naturkunde Berlin, Berlin, Germany. Lead author for scale, by the skeleton's elbow. This is the largest mounted skeleton in the world based primarily on real remains rather than sculptures. It is 13.27 m tall, and represents an animal that probably weighed about 20–30 tonnes[61]. Much larger sauropods existed, but they are known only from fragmentary remains. doi:10.1371/journal.pone.0078214.g001

with central articulations that closely resemble the mammalian opisthocoelous biomechanical design, consisting of condyles that insert deeply in cotyles of matching curvature, leaving little room for cartilage. In modern quadrupeds with opisthocoelous cervicals, such as the horse, giraffe, and rhino, the central condyle and cotyle are separated by only a few millimeters. In avians, heterocoely is similarly associated with very precisely matching articular facets and tight intervertebral separations. Across a large range of extant vertebrates, while substantial intervertebral separations are associated with platycoelous vertebrae, vertebrae with nonplanar central articular geometry generally have little intervening cartilage (pers. obs.), and thus little room for conjecture regarding their undeflected state.

A more general survey of difficulties with the DinoMorph work will be published elsewhere (Taylor and Wedel in prep.) In this contribution, we ignore problems such as the imperfect preservation of the sauropod vertebrae, and investigate in detail the consequences of just one oversimplification: the neglect of articular cartilage in the models used for this work. We show that this significantly affects both the neutral posture recovered and the range of motion found possible.

We examine preserved intervertebral gaps in sauropod necks where CT scans are available, and compare with data obtained from extant animals.

Basic vertebral architecture

The vertebrae of all tetrapods are broadly similar in construction, and those of sauropods and birds particularly resemble each other as a consequence of their close evolutionary relationship (Figure 2). The body of a vertebra is called the centrum, and is usually a fairly simple shape resembling a cylinder. The anterior and posterior facets (i.e., the front and back) of each centrum

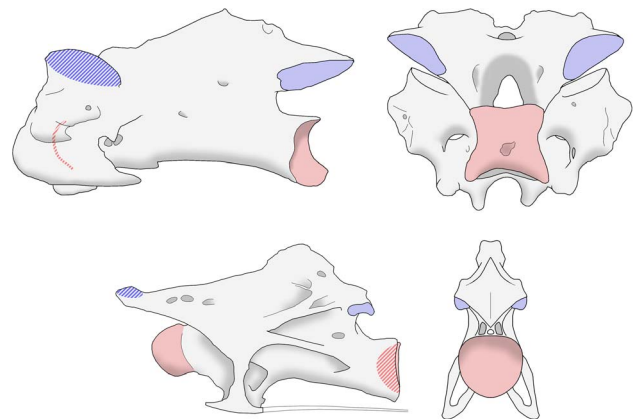


Figure 2. Cervical vertebrae of a turkey and a sauropod. Representative mid-cervical vertebrae from a turkey (top) and the sauropod *Giraffatitan brancai* (bottom), not to scale. Each vertebra is shown in left lateral view (on the left) and posterior view (on the right). Articular surfaces, where each vertebra meets its neighbour, are highlighted in red (for the centra) and blue (for the zygapophyses). Articular surfaces that are concealed from view are cross-hatched: prezygapophyses face upwards and inwards, so that the facets are inclined towards the midline. In sauropods, the centra have ball-and-socket joints. In birds, the joints are saddle-shaped, and the anterior articular surface is hidden in lateral view. Despite numerous differences in detail, the bird and sauropods vertebrae strongly resemble each other in fundamentals. doi:10.1371/journal.pone.0078214.g002

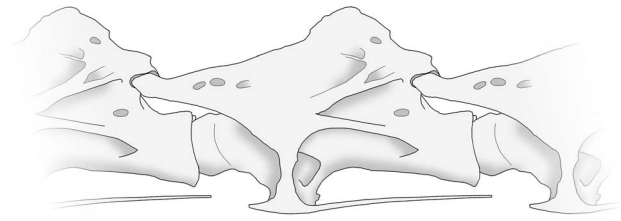


Figure 3. Articulated sauropod vertebrae. Representative mid-cervical vertebra of *Giraffatitan brancai*, articulating with its neighbours. The condyle (ball) on the front of each vertebra's centrum fits into the cotyle (socket) at the back of the preceding one, and the prezygapophyses articulate with the preceding vertebra's postzygapophyses. These vertebrae are in Osteological Neutral Pose, because the pre- and postzygapophyseal facets overlap fully.
doi:10.1371/journal.pone.0078214.g003

articulate with the centra of the previous and subsequent vertebrae in the column. Above the centrum is a more elaborate construction called the neural arch. (The neural canal runs from front to back down the middle of the vertebra, between the centrum and arch, and houses the spinal cord.) As well as the centra, adjacent vertebrae also touch at another pair of points above the centra, the zygapophyses. Each vertebra has two pairs of these: prezygapophyses in front and postzygapophyses at the back. Each vertebra's prezygapophyses articulate with the postzygapophyses of the preceding vertebra (Figure 3).

For the purposes of this work, other vertebral features (neural spines, cervical ribs, epiphyses, etc.) are ignored.

The role and form of intervertebral cartilage

The bone of one vertebra never directly touches the next: instead, the articular surfaces are covered with a thin layer of cartilage, which is softer, smoother and more resilient than bone. Except in rare cases (e.g., [24,25]), cartilage is not preserved in fossils, and we are unaware of any preserved articular cartilage in

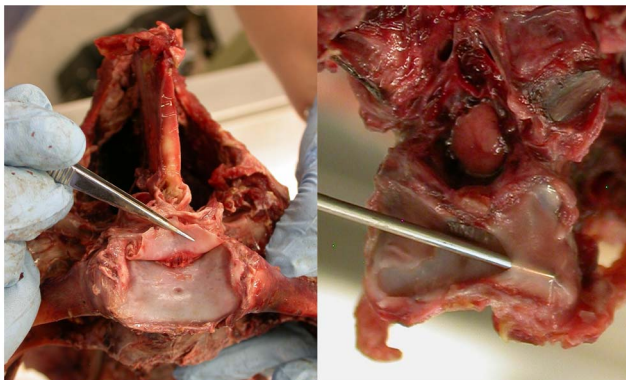


Figure 4. Intervertebral articular discs of an ostrich. Intervertebral articular discs of an ostrich (not to scale). Left: first sacral vertebra in anterior view, showing articular disc of joint with the last thoracic vertebra. Right: posterior view view of a cervical vertebra, with probe inserted behind posterior articular disc. The cervical vertebra is most relevant to the present study, but the the sacral vertebra is also included as it shows the morphology more clearly. These fibrocartilaginous articular discs divide the synovial cavity, like the articular discs in the human temporomandibular and sternoclavicular joints, and should not be confused with the true intervertebral discs of mammals and other animals, which consist of a nucleus pulposus and an annulus fibrosus.
doi:10.1371/journal.pone.0078214.g004

sauropod vertebrae. When we speak of fossil vertebrae in this paper, we are referring only to fossilised bone.

The layers of cartilage covering the articular surfaces of vertebrae do not always closely follow the shape of the underlying bone, but can vary significantly in thickness. For example, the thickness of cartilage between adjacent vertebrae of a king penguin (*Aptenodytes patagonica*) ([26]: figure 4) is more than twice as thick at mid-height as it is at the dorsal and ventral margins. The shape of articular bony surfaces cannot therefore be assumed to indicate the functional shape of those surfaces in life. This is probably true of tetrapods in general but it is particularly important for large non-avian dinosaurs, in which extensive cartilage was present at many joints and did not always reflect the morphology of the underlying bones ([25,27,28] but see also [29]).

The morphology of cartilage in intervertebral joints varies significantly among taxa. In most animals, there is a distinct fibrocartilaginous element, known as a disc, between the centra of consecutive vertebrae. These discs consist of an *annulus fibrosus* (fibrous ring), made of several layers of fibrocartilage, surrounding a *nucleus pulposus* (pulpy centre) with the consistency of jelly [30,31]. But in birds, uniquely among extant animals, there is no separate cartilaginous element. Instead, the articular surfaces of the bones are covered with layers of hyaline cartilage which articulate directly with one another, and are free to slide across each other. The adjacent articular surfaces are enclosed in synovial capsules similar to those that enclose the zygapophyseal joints [32].

The difference between these two constructions is very apparent in dissection: in birds, adjacent vertebrae come apart easily once the surrounding soft tissue is removed; but in mammals, it is very difficult to separate consecutive vertebrae, as they are firmly attached to the intervening intervertebral disc.

Crucially, the extant phylogenetic bracket (EPB) [33] does not help us to establish the nature of the intervertebral articulations in sauropods, as the two extant groups most closely related to them have different articulations. As noted, birds have synovial joints; but crocodylians, like mammals, have fibrocartilaginous intervertebral discs.

To complicate matters further, thin articular discs occur in the necks of some birds – for example, the ostrich (*Struthio camelus*) (Figure 4), the swan (*Cygnus atratus*) ([34]: figure 3), and the king penguin ([26]: figure 4). But these discs do not occur in all birds – for example, they are absent in the turkey (*Meleagris gallopavo*) and the rhea (*Rhea americana*). When they are present, these articular discs divide the synovial cavity and prevent the (cartilage-covered) bones on either side from ever articulating directly with each other, just like the articular discs in the human temporomandibular and sternoclavicular joints. These discs are thinner than the true intervertebral discs of mammals and crocodylians; and they are different in composition, lacking the annulus/nucleus structure and consisting of a simple sheet of fibrocartilage.

The thickness of cartilage between consecutive cervical vertebrae is considerable in at least some taxa. For example, in the dromedary camel (*Camelus dromedarius*), mounted skeletons that omit spacers where the cartilage would have been in life instead have large gaps between the centra, even when the neck is posed well below habitual posture (Figure 5).

In this paper, we express thickness of cartilage as a cartilage/bone percentage. This is not to be confused with the percentage of total segment length that is accounted for by cartilage: when a 10 cm bone has 1 cm of cartilage on the end, the cartilage/bone ratio is 10%, but cartilage accounts for only 9.09% – one eleventh – of the total segment length.



Figure 5. Intervertebral gaps in camel necks. Head and neck of dromedary camels. Top: UMZC H.14191, in right lateral view, posed well below habitual posture, with apparently disarticulated C3/C4 and C4/C5 joints. Photograph taken of a public exhibit at University Museum of Zoology, Cambridge, UK. Bottom: OUMNH 17427, in left lateral view, reversed for consistency with Cambridge specimen. Photograph taken of a public exhibit at Oxford University Museum of Natural History, UK. Inset: detail of C4 of the Oxford specimen, showing articulations with C3 and C5. The centra are separated by thick pads of artificial “cartilage” to preserve spacing as in life. doi:10.1371/journal.pone.0078214.g005

Osteological neutral pose (ONP) and range of motion (ROM)

Stevens and Parrish [13] introduced the notion of Osteological Neutral Pose (ONP), which is attained when the centra abut without gaps and the zygapophyseal facets of consecutive vertebrae are maximally overlapped. The vertebrae in Figure 3 are in ONP.

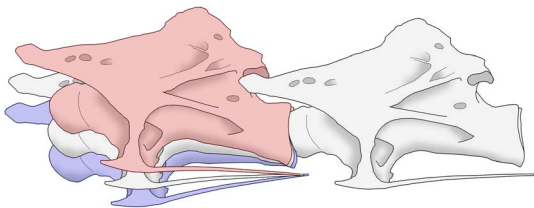


Figure 6. Range of motion in a vertebral joint. Range of Motion (ROM) illustrated schematically for a single intervertebral joint of *Giraffatitan brancai*. The grey-scale vertebrae are shown in Osteological Neutral Pose. The red vertebra has been rotated upwards (“extended”) until its postzygapophyseal facet overlaps 50% with the prezygapophyseal facet of the succeeding vertebra, in accordance with the assumption of Stevens and Parrish. Similarly, the blue vertebra has been rotated downwards (“flexed”) until 50% zygapophyseal overlap is achieved. Because the zygapophyseal articulations in the neck of *Giraffatitan* are some way anterior to the those of the centra, the relative movement of the articulating zygapophyseal facets is anteroventral–posterodorsal; in taxa such as the turkey in which the zygapophyseal articulation are directly above those of the centra, relative movement is anterior–posterior. doi:10.1371/journal.pone.0078214.g006

When the neck extends or flexes (bends upwards or downwards respectively) the centra remain in articulation, rotating against each other, and the zygapophyses glide past each other. The point around which a pair of consecutive centra rotate with respect to one another is called their centre of rotation. Various factors limit how far a given intervertebral joint can rotate: in the extreme case, bone collides with bone, creating an osteological stop. More often, rotation is inhibited before this point is reached by limits to zygapophyseal travel. The joint between one vertebra’s postzygapophysis and the prezygapophysis of the next is enclosed in a delicate synovial capsule which cannot be stretched indefinitely. Stevens and Parrish stated that “pre- and postzygapophyses could only be displaced to the point where the margin of one facet reaches roughly the midpoint of the other facet” [13], citing unpublished data. Range Of Motion (ROM) in their sense is the degree of movement that can be attained while retaining at least 50% overlap between zygapophyseal facets (Figure 6). Although this figure remains to be demonstrated, and is in fact contradicted by Stevens and Parrish themselves ([17]: 191), who observed that when giraffes bend their necks laterally there is almost no zygapophyseal overlap, we provisionally accept the 50% overlap criterion here.

For the purposes of this discussion, ROM is considerably simplified from the reality. The shapes of zygapophyseal facets can be complex, and limit or facilitate motion. The inclination of facets introduces further complexity. As shown in Figure 6, anterior positioning of the zygapophyses in some sauropods (unlike the situation in birds) means that zygapophyseal displacement is primarily dorsoventral rather than anteroposterior. In some cases, zygapophyseal facets can pull apart rather than remaining in articulation. As a final simplification, in this paper we consider only vertical movement of the neck, not lateral movement or twisting. Despite these simplifications, ROM remains a useful abstraction, and its relation to zygapophyseal facet size is apparent: ROM varies more or less linearly with facet size and inversely with distance from zygapophyses to the centre of rotation. Equal ranges of motion can be achieved by small zygapophyseal facets close to the centre of rotation, or larger facets further from it.

Materials and Methods

Extinct animal specimens

OMNH 53062 is the holotype of the long-necked basal titanosauriform *Sauroposeidon*. The specimen consists of four articulated mid-cervical vertebrae. Portions of the three more anterior vertebrae were CT scanned in January 1998 to image their pneumatic internal structures [35–37]. This is the first time that these scans have been used to investigate the shapes of the articular surfaces of the vertebrae or to estimate the thickness of the intervertebral cartilage.

CM 3390 and CM 11339 are two partial skeletons of juvenile individuals of *Apatosaurus*. They were collected from the Carnegie Museum Quarry at Dinosaur National Monument, which also yielded CM 3018, the holotype of *Apatosaurus louisae*. To date, no single quarry has produced members of more than one valid species of *Apatosaurus*, and according to McIntosh ([38]: 26) these specimens “show no characters to distinguish them from the above [holotype] specimens of *Apatosaurus louisae*.” For the purposes of this discussion, we accept this tentative referral.

Extant animal specimens

It is impossible to fully determine the effect of articular cartilage on ONP and ROM of sauropod necks directly due to the paucity

of specimens with preserved cartilage. As a proxy, we took measurements from the neck of a domestic turkey, sourced from a local butcher. We interpreted these as proportions of whole-neck length, vertebra length and zygapophysis length.

Turkeys are a reasonable model organism for these purposes, as birds are the closest living relatives of sauropods and their cervical architecture is similar [1,39], but see the discussion below of other animals' necks that are used as well.

The complete neck of the turkey is made up of 14 vertebrae [40], of which the last few are functionally part of the torso. However, the neck obtained for this work is incomplete, consisting of only eight vertebrae. Based on the absence of carotid processes in the most posterior vertebra, this is probably C13, meaning that the available neck segments represent C6–C13. This is consistent with the profiles of the vertebrae illustrated by Harvey et al. ([40]: plate 65). Although the absence of the first five vertebrae is regrettable, it is not critical as the base of the neck is the region where flexion and extension have the greatest effect on posture.

We also obtained less detailed cartilage measurements for a selection of other extant animals as detailed below. The ostrich, rhea, alligator (*Alligator mississippiensis*) and horse (*Equus caballus*) are all salvage specimens, and they were obtained, dissected, and photographed with the approval of the Institutional Animal Care and Use Committee at Western University of Health Sciences. The camel is a mounted museum specimen, the dog is a veterinary subject, and the giraffe was obtained from an anonymous zoo via the Royal Veterinary College, UK.

We are all too aware that the wildly different provenances and ages of these specimens, and the different measurement techniques used, make direct comparisons problematic. As noted in the Future Work section below, we hope subsequent studies will be able to take advantage of a wider and more controlled range of specimens.

Fossil CT scanning protocol

Sauropod vertebrae were CT scanned at the University of Oklahoma Medical Center in Oklahoma City in January 1998 (*Sauroposeidon*) and January 2000 (both specimens of *Apatosaurus*). CT scans were performed using a General Electric 9800 Highlight Advantage 4th generation scanner. Scout images were obtained in lateral projection with a technique setting of 120 kVp (kilovolt peak) and 40 mA (milliamperes). Axial images were produced at 120 kVp and 120 mA. Data were reconstructed in bone algorithm using a Star Tech, Inc., One Sun CPU computed tomography array imaging processor and the GE Advantage version 1.0 imaging software package.

Vertebra measurement protocol

In order to determine the thickness of intervertebral cartilage and possible other soft-tissue, it is necessary to accurately measure the length of both intact neck segments and their constituent vertebrae.

Measuring the lengths of intact necks is awkward, even when the heads and torsos have been removed. Contraction of dorsal tension members causes them to curl up, which impedes attempts to find the straight-line length. It is necessary to hold a neck straight, and simultaneously to gently compress it end-to-end in order to prevent artificial elongation due to post-mortem separation of adjacent vertebrae. This is hard to achieve without buckling the neck out of the straight line. With the neck straightened and longitudinally compressed, a measurement must be taken along the neck, between perpendiculars, from the front of the anteriormost vertebra to the back of the posteriormost.

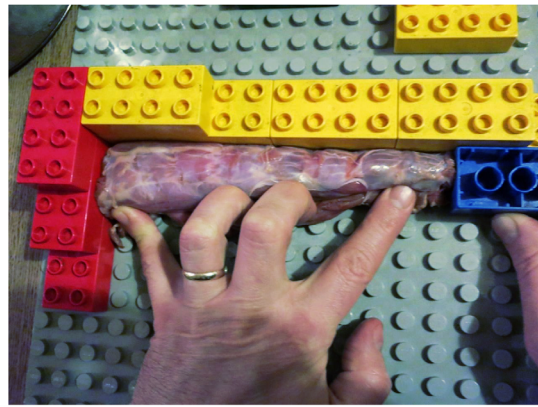


Figure 7. Measurement rig for necks. Measurement rig for intact turkey necks, constructed from Duplo bricks and baseboard. The neck is pushed into the angle between the back wall (yellow) and the left wall (red), and held straight along the back wall. The marker brick (blue) abuts the end of the neck: the distance between the left wall and the marker brick is the length of the neck between perpendiculars. doi:10.1371/journal.pone.0078214.g007

To solve this problem, a simple measurement rig was constructed from Duplo bricks and a baseboard. The bricks were used to construct an 'L'-shaped bracket (Figure 7). The neck is then laid in this bracket with its dorsal side facing away and into the back wall. It is unrolled and straightened against that wall. Once the neck is in place, with its posterior end hard against the left wall, a marker brick is used to locate the position of the anteriormost part of the neck, sliding along the back wall until the neck prevents further travel. If this is done correctly, there is very little movement: the entire series of vertebrae is lined up and solidly abutted, with bone pushing against the left wall and the marker brick. The distance between left wall and this brick is then the length of the neck. It is easy to remove the neck (without moving the marker brick) and measure this distance.

Measuring the length of individual cervical vertebrae is also problematic, due to the complex saddle shape ("heterocoely") of



Figure 8. Cervical vertebra 7 from a turkey. Cervical vertebra 7 from a turkey: anterior view on the left; dorsal, left lateral and ventral views in the middle row; and posterior on the right. doi:10.1371/journal.pone.0078214.g008

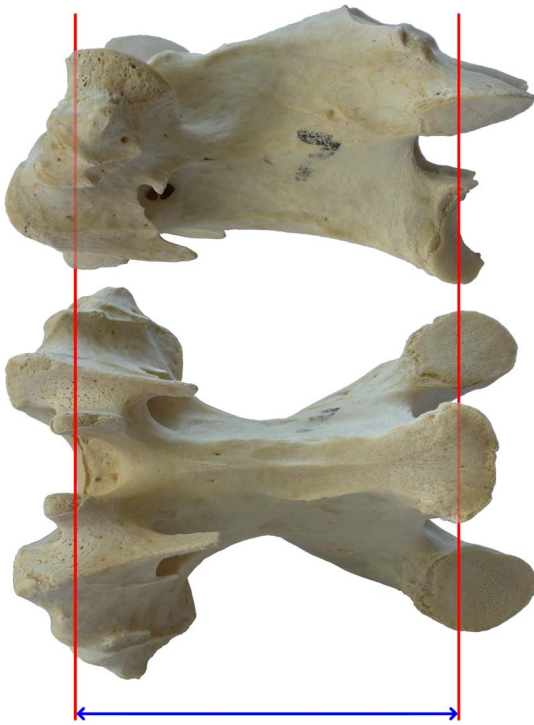


Figure 9. Functional length of a cervical vertebra. Functional centrum length of a cervical vertebra of a turkey. The measurement is taken between the inflection points of the saddle-shaped articulations at each end of the centrum, shown here by the blue arrow connecting the red lines that mark the position of the saddle points. doi:10.1371/journal.pone.0078214.g009

the articular faces of the centrum (Figure 8). The anterior articular surface is convex dorsoventrally but concave transversely, and is not the most anterior part of the vertebra; and the posterior face is concave dorsoventrally and convex transversely. For our purposes, the most interesting metric is not total length (which would include the anteriorly projecting cervical-rib loops and in some cases overhanging postzygapophyses) but functional length.

We define *functional length* as the straight-line distance between the most anterior point on the midline of the anterior face, and the most anterior point on the midline of the posterior face – for birds, that is between the saddle points of the anterior and posterior articular surfaces of the centrum (Figure 9). Functional length can also be thought of as the distance between the same point on two consecutive vertebrae when they are articulated. This definition works for vertebrae of any shape – for example, those of sauropods, which have ball-and-socket joints rather than saddle-shaped joints, also have a functional length equal to the distance between the most anterior points on the midlines of the anterior and posterior faces. Functional length may be measured either including or excluding articular cartilage. We use it exclusive of cartilage except where otherwise noted.

We use functional, rather than total, length because it has the important property that the sum of the functional lengths of a sequence of vertebrae is equal to the functional length of the sequence as a whole.

To measure the functional length of the turkey vertebrae, we glued a tooth onto one jaw of the calipers, facing the other jaw, and recalibrated them so that they read zero when the tooth was in contact with the opposing jaw. Then we placed the vertebra between the jaws of these modified calipers, with the tooth



Figure 10. Modified calipers for measuring functional vertebral length. Modified calipers used to measure functional length of a turkey vertebra. The tooth glued to the left jaw protrudes into the transverse concavity of the anterior articular surface and the dorsoventral concavity of the posterior articular surface straddles the right jaw. doi:10.1371/journal.pone.0078214.g010

protruding into the transverse concavity of the anterior articular surface of the centrum, and with the dorsoventral concavity of the posterior articular surface straddling the unmodified jaw (Figure 10).

We also measured the anteroposterior length of all four zygapophyseal facets of each vertebra with unmodified calipers.

Each measurement (functional centrum length and four zygapophyseal facet lengths) was made three times: once on the freshly dissected-out vertebrae; once after they had been simmered and cleaned, and cartilage had been removed from the articular surfaces; and once more after being degreased in dilute hydrogen peroxide and thoroughly dried. The bones of living animals most closely resemble the first of these measurements, while fossil bones most closely resemble the last. The differences between these sets of measurements show how calculations based on fossils mislead as to the behaviour of bones in living animals.

Results

Data from sauropod CT scans

Sauroposeidon OMNH 53062. The four vertebrae that make up the holotype of *Sauroposeidon* are inferred to represent C5–C8 [35,36], and we refer to them as such here. The specimen therefore includes three intervertebral joints: between C5 and C6, between C6 and C7, and between C7 and C8. C7 and C8 are simply too large to pass through a medical CT scanner, but the other two joints have been imaged. At the C5/C6 joint, the condyle of C6 is centered in the cotyle of C5, and the zygapophyses on the right are in articulation (Figures 11 and 12). (The left sides of the vertebrae were facing up in the field and were badly damaged by erosion prior to excavation.) As in *Apatosaurus* CM 3390, the cotyle is more rounded than the condyle, so the radial spacing between the vertebrae varies from the rim of the cotyle to the centre. The spacing from the front of the condyle of C6 to the deepest point in the cotyle of C5 is 52 mm, but the minimum radial spacing between the condyle and the cotyle rim is only 31 mm.

C6 is slightly flexed relative to C7, and the condyle of C7 is displaced toward the top of the cotyle of C6, rather than being maximally engaged like the C5/C6 joint. The condyle of C7 has a very odd shape. Although the condyle has a maximum dorsoventral diameter of just over 170 mm, it is only about 30 mm long (Figure 13). The unusually flattened shape cannot be an artefact of

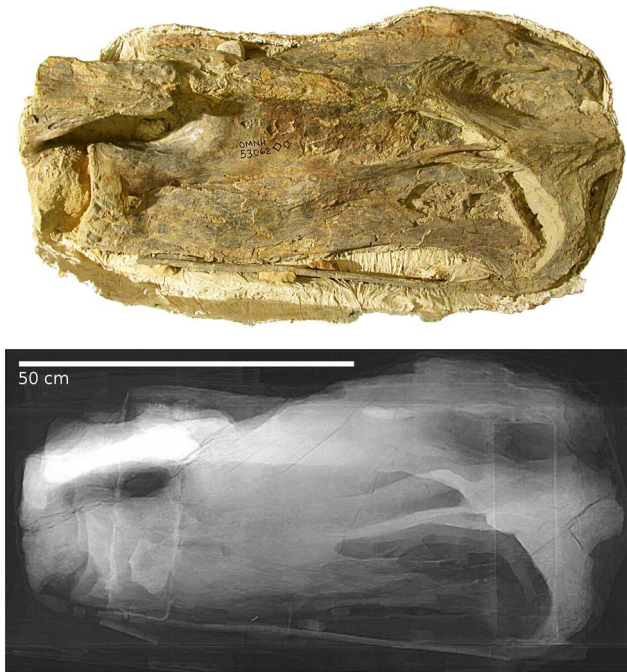


Figure 11. Fifth and partial sixth cervical vertebrae of *Sauroposeidon*. Photograph and x-ray scout image of C5 and the anterior portion of C6 of *Sauroposeidon* OMNH 53062 in right lateral view. The anterior third of C5 eroded away before the vertebra was collected. C6 was deliberately cut through in the field to break the multi-meter specimen into manageable pieces for jacketing (see [37] for details). Note that the silhouettes of the cotyle of C5 and the condyle of C6 are visible in the x-ray.
doi:10.1371/journal.pone.0078214.g011

preparation or damage because the anterior end of the condyle is covered by matrix and surrounded by the cotyle. It is difficult to imagine a form of taphonomic distortion that would act only on the vertebral condyle, and the rest of the vertebrae are anything but anteroposteriorly compressed. Although it looks odd, the condyle of C7 is consistent with the condyle of C6 and with that of D2 in CM 3390 in having a broader, flatter curvature than the cotyle with which it articulated. Assuming a minimum 30 mm radial spacing around the rim of the cotyle, as at the C5/C6 joint, gives a maximum anteroposterior spacing at the centre of about 60 mm.

Conceptually, we might expect cartilage in a ball-and-socket joint to approach one of two simple conditions: a constant radial thickness, or a constant anteroposterior thickness (Figure 14: parts A and B). Note that in these simple models the condyle is assumed to have the same basic shape as the cotyle. At the two intervertebral joints in *Sauroposeidon* that have been imaged, this expectation is not met – in both cases, the cotyle is deeper and more strongly curved than the condyle. However, at the C5/C6 joint the anteroposterior separation between the condyle and cotyle is almost constant, at least in the sagittal plane (Figure 14: part C). But this even separation is achieved by having a condyle that is much smaller in diameter than the cotyle, and of a different shape. The condyle of C6 is not as flattened as the condyle of C7, but it is still much flatter than the condyles in cervicals of *Giraffatitan* ([41]: figures 17–46) and North American cervicals referred to *Brachiosaurus* ([42]: figure 7.2). It is tempting to speculate that the flattened condyles and nearly constant thickness of the intervertebral cartilage are adaptations to bearing weight,

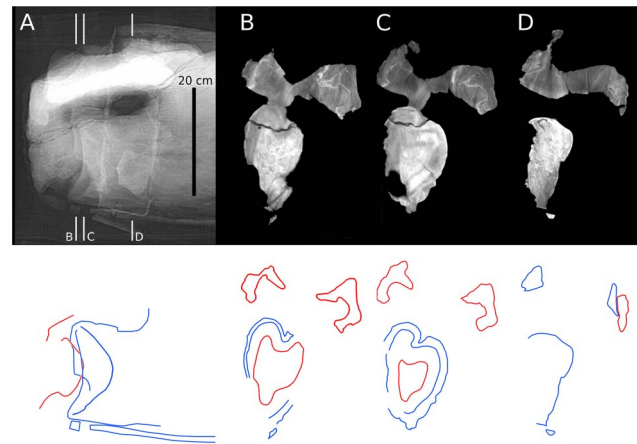


Figure 12. CT slices from fifth cervical vertebrae of *Sauroposeidon*. X-ray scout image and three posterior-view CT slices through the C5/C6 intervertebral joint in *Sauroposeidon* OMNH 53062. In the bottom half of figure, structures from C6 are traced in blue and those from C5 are traced in red. Note that the condyle of C6 is centered in the cotyle of C5 and that the right zygapophyses are in articulation.
doi:10.1371/journal.pone.0078214.g012

which must have been an important consideration in a cervical series more than 11 meters long, no matter how lightly built.

The cotyles of C5 and C6 are both 65–70 mm deep. So the distance from the foremost point of the C6 condyle to the deepest point of its cotyle includes the centrum length (1220 mm) minus the depth of the C6 cotyle (67 mm), for a total of about 1153 mm from cotyle to cotyle. The maximum cartilage thickness of 52 mm therefore accounts for 4.5% of the bone length, which is proportionally thinner than in most of the other animals we have sampled.

Centrum shape is conventionally quantified by Elongation Index (EI), which is defined as the total centrum length divided by the dorsoventral height of the posterior articular surface. *Sauroposeidon* has proportionally very long vertebrae: the EI of C6 is 6.1. If instead it were 3, as in the mid-cervicals of *Apatosaurus*, the centrum length would be 600 mm. That 600 mm minus 67 mm for the cotyle would give a functional length of 533 mm, not 1153, and 52 mm of cartilage would account for 9.8% of the length of that segment. And, of course, not all of the cervicals in *Sauroposeidon* were so long. Assuming a cervical count of thirteen, multiplying by an average of 52 mm of cartilage per segment comes to 67 cm of cartilage in the neck. Assuming a summed vertebral length of 11.5 meters (based on comparisons with *Brachiosaurus* and *Giraffatitan* [36]), the neck in life would have been just over 12 meters long, for a cartilage/bone ratio of 5–6%.

Apatosaurus louisae CM 3390

CM 3390 includes a pair of articulated anterior dorsal vertebrae (Figure 15). The vertebrae lack hyposphenes, as expected for anterior dorsals of *Apatosaurus* ([43]: 201), and based on the centrum proportions and the low positions of the parapophyses on the centra (Figure 15 part A), the vertebrae probably represent the first two dorsals – rather than posterior cervicals, as posited by Wedel ([44]: 349 and figure 7). D2 has a centrum length of 90 mm, a cotyle height of 58 mm, and so an EI of about 1.5. The equivalent vertebra in the mounted holotype of *A. louisae*, CM 3018, has a cotyle height of 225 mm, about 3.9 times the linear size of CM 3390.

The slice thickness in the CT scan is 3 mm, with 1 mm of overlap on either side, yielding a distance of 2 mm from the centre

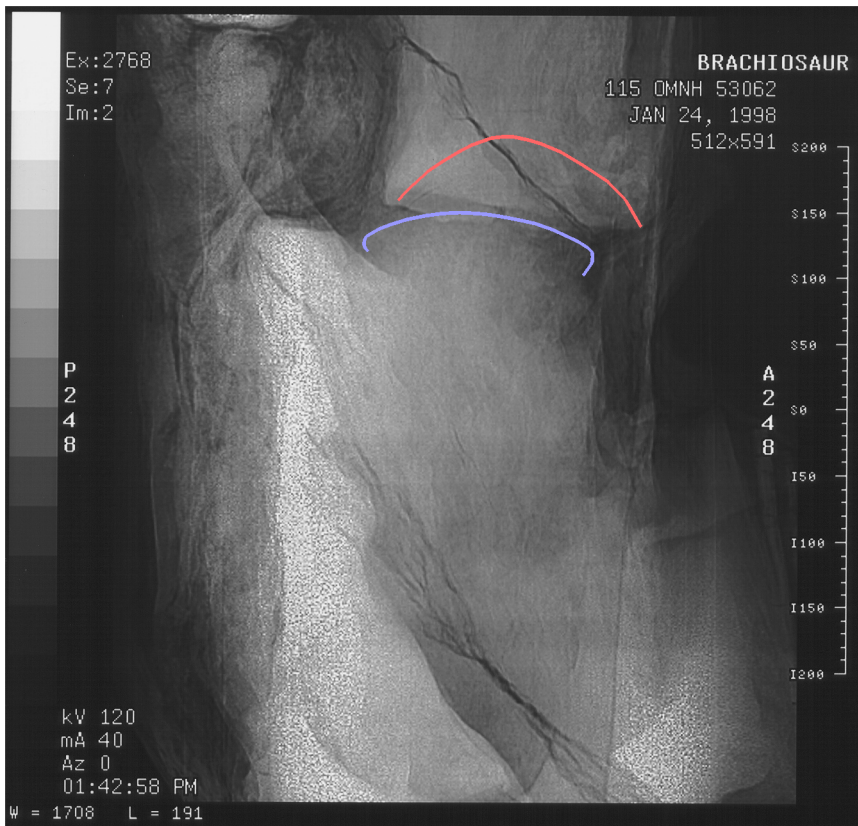


Figure 13. Joint between sixth and seventh cervicals vertebrae of *Sauroposeidon*. X-ray scout image of the C6/C7 intervertebral joint in *Sauroposeidon* OMNH 53062, in right lateral view. The silhouette of the condyle is traced in blue and the cotyle in red. The scale on the right is marked off in centimeters, although the numbers next to each mark are in millimeters.
doi:10.1371/journal.pone.0078214.g013

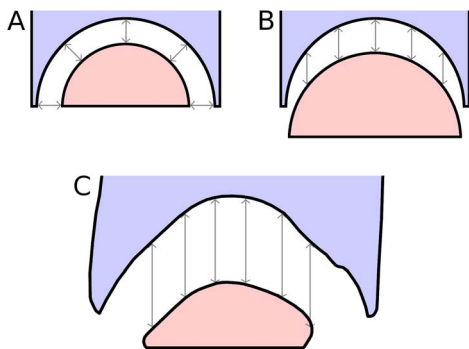


Figure 14. Geometry of opisthocoelous intervertebral joints. Hypothetical models of the geometry of an opisthocoelous intervertebral joint compared with the actual morphology of the C5/C6 joint in *Sauroposeidon* OMNH 53062. A. Model in which the condyle and cotyle are concentric and the radial thickness of the intervertebral cartilage is constant. B. Model in which the condyle and cotyle have the same geometry, but the condyle is displaced posteriorly so the anteroposterior thickness of the intervertebral cartilage is constant. C. the C5/C6 joint in *Sauroposeidon* in right lateral view, traced from the x-ray scout image (see Figure 12); dorsal is to the left. Except for one area in the ventral half of the cotyle, the anteroposterior separation between the C5 cotyle and C6 condyle is remarkably uniform. All of the arrows in part C are 52 mm long.
doi:10.1371/journal.pone.0078214.g014

of one slice to the next. Resolution within each slice is 0.571 mm/pixel (44.5 dpi). In this and all other scans, the slices are numbered from anterior to posterior.

The deepest part of the cotyle of D1 is first visible in slice 25 (Figure 15 part B). The condyle of D2 is first apparent in slice 31 (Figure 15 part C). However, we cannot tell where in the 2 mm thickness represented by slice 25 the cotyle actually begins, and the same uncertainty applies to the most anterior point of the condyle within slice 31. The spacing between the vertebrae is therefore at least five slices (26–30) and no more than 7 (25–31, inclusive), or 10–14 mm. The first clear slice through the cotyle of D2 is in slice 61 (Figure 15 part G). So the functional length of D2, measured from the foremost part of the condyle to the deepest part of the cotyle is 29–31 slices or 58–62 mm. The gap for cartilage accounts for $12 \pm 2 / 60 \pm 2$, a cartilage/bone ratio of $20 \pm 4\%$.

Juvenile sauropods have proportionally short cervicals ([36]: 368–369, figure 14, and table 4). The scanned vertebrae are anterior dorsals with an EI of about 1.5. Mid-cervical vertebrae of this specimen would have EIs about 2, so the same thickness of cartilage would yield a cartilage/bone ratio of $12 \pm 2 / 80 \pm 2$ or $15 \pm 3\%$. Over ontogeny the mid-cervicals telescoped to achieve EIs of 2.3–3.3. The same thickness of cartilage would then yield a cartilage/bone ratio of 9–13%, which is consistent with the thickness we calculated for an adult *Apatosaurus* based on *Sauroposeidon*, above. Intervertebral cartilage would still be 10–15% of bone length in the proportionally shorter cervicodorsals. Averaged over the whole neck, in the adult cartilage probably contributed about 10–12% to the length of the neck.

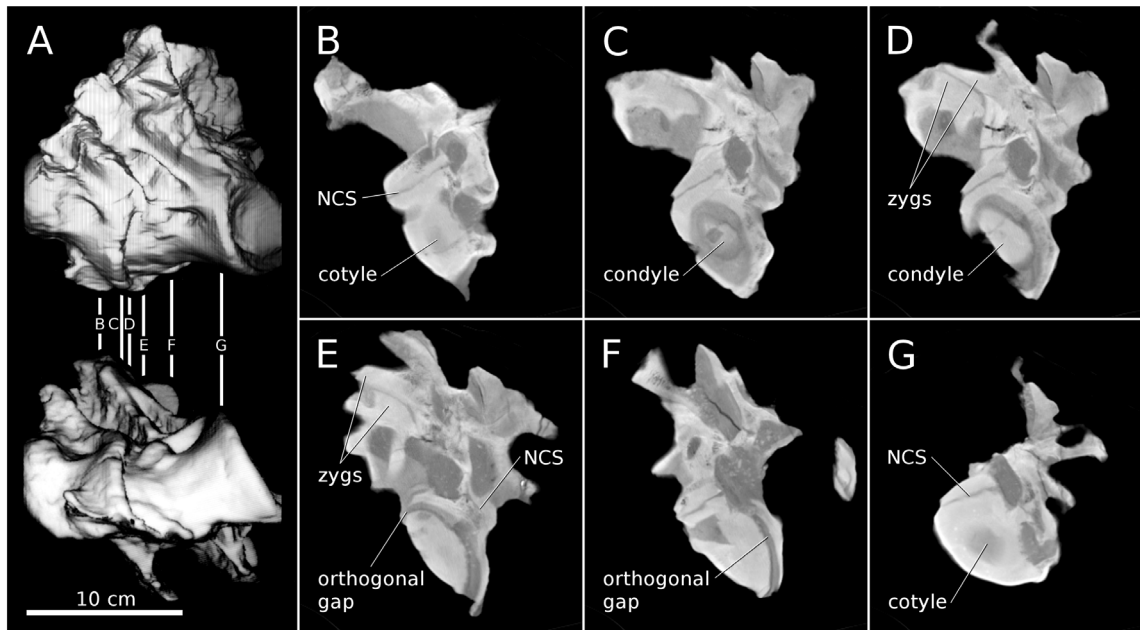


Figure 15. First and second dorsal vertebrae of *Apatosaurus* CM 3390. Articulated first and second dorsal vertebrae of *Apatosaurus* CM 3390. A. Digital model showing the two vertebrae in articulation, in left lateral (top) and ventral (bottom) views. B-G. Representative slices illustrating the cross-sectional anatomy of the specimen, all in posterior view. B. Slice 25. C. Slice 31. D. Slice 33. E. Slice 37. F. Slice 46. G. Slice 61. Orthogonal gaps are highlighted where the margins of the condyle and cotyle are parallel to each other and at right angles to the plane of the CT slice. 'Zygs' is short for 'zygapophyses', and NCS denotes the neurocentral synchondroses. doi:10.1371/journal.pone.0078214.g015

Unfortunately, none of the slices provide us with as clear an image of the condyle-cotyle separation as at the C5/C6 joint in *Sauroposeidon*. But we can investigate which of the hypothetical models (Figure 14) the real vertebrae more closely approach by measuring the thickness of the cartilage gap not only at the deepest part of the cotyle but also at its margins. By analysing the full sequence of slices we can see that in slice 46 (Figure 15 part F), the lateral walls of condyle and cotyle are orthogonal to the plane of the section (so the cartilage gap is not artificially inflated by measuring its width on a slice that cuts it at an angle). In that slice, the separation between condyle and cotyle is about 3.5 mm. In slice 37 (Figure 15 part E), the uppermost margins of condyle and cotyle are orthogonal to the plane of slice, and the separation is about 4 mm. These results are consistent with each other, showing that the condyle was not displaced toward the margin of the cotyle. However, this radial thickness of cartilage at the rim of the condyle and cotyle is only about one third of the maximum anteroposterior thickness of the cartilage from the front of the condyle to the deepest part of the cotyle. This indicates that the condyle is not concentric with the cotyle – in fact, it is considerably less rounded, just as in *Sauroposeidon*. As more articulated sauropod vertebrae are scanned, it will be interesting to see if this geometry of the intervertebral joint is a convergent feature of *Apatosaurus* and *Sauroposeidon* or something common to most or all sauropods.

Slice 33 is of particular interest because it shows the condyle centred in the cotyle and the left zygapophyses in articulation (Figure 15 part D). Adjacent slices confirm that the left zygapophyses are in tight articulation over their entire length. Cartilage thickness between the zygapophyses is 1–2 mm. Unfortunately, the zygapophyses on the right are not preserved. The tight articulation of the left zygapophyses combined with the centring of the condyle of D2 in the cotyle of D1 indicates that this posture was achievable in life.

Using various landmarks we estimate that D1 is extended 31–36° relative to D2. This degree of extension is noteworthy; it is considerably more than the ~6° of extension that Stevens & Parrish [13,17] estimated between the cervical vertebrae of adult specimens of *Apatosaurus* and *Diplodocus*. The anterior dorsals have very large zygapophyseal facets that are not as far from the centre of rotation as they are in most of the cervical series, and these large, advantageously-positioned zygapophyses may have facilitated a greater range of motion than is found in the middle of the neck. This is consistent with the finding that most extant tetrapods raise and lower their heads by extending and flexing at the cervicodorsal junction, rather than bending in the middle of the neck [45,46]. It also reinforces the argument that flexibility of the anterior dorsal vertebrae should be considered when trying to estimate the range of motion of the head and neck [22].

***Apatosaurus louisae* CM 11339.** CM 11339 includes a pair of articulated middle or posterior dorsal vertebrae, with hyposphene/hypanttrum articulations (Figure 16). The more posterior of the two vertebrae has a cotyle height of 94 mm. Middle and posterior dorsal vertebrae of CM 3018 have cotyle heights of 315–365 mm, or 3.4–3.9 times the linear size of CM 11339. The individuals represented by CM 3399 and CM 11339 are therefore about the same size, roughly one quarter of the size of the large and presumably adult CM 3018. (They cannot however both represent the same individual as they contain overlapping elements – specifically, most of the dorsal column.)

The slice thickness in the CT scan is 5 mm, with 1.5 mm of overlap on either side, yielding a distance of 3.5 mm from the centre of one slice to the next. The cotyle of the anterior vertebra is first revealed in slice 39 (Figure 16 part B). The condyle of the second vertebra first appears in slice 43 (Figure 16 part C). The spacing between the vertebrae is therefore four slices (plus or minus one slice, as discussed above for CM 3390) or 14 ± 3.5 mm. The first clear slice through the cotyle of the second vertebra is in

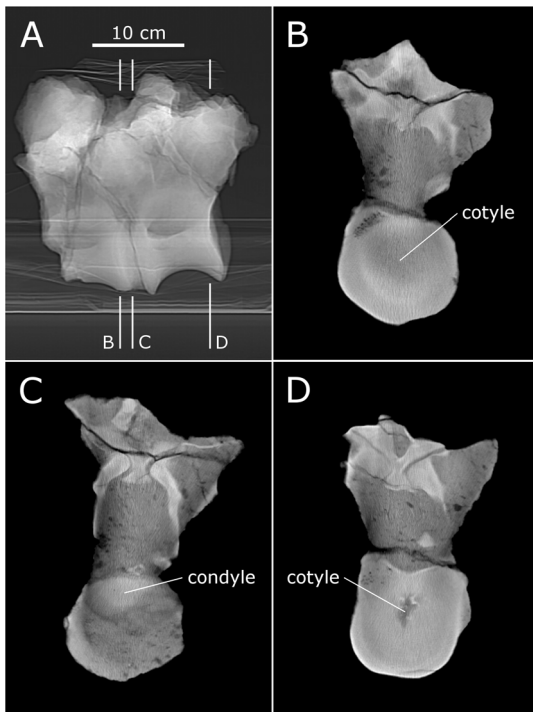


Figure 16. Dorsal vertebrae of *Apatosaurus* CM 11339. Articulated middle or posterior dorsal vertebrae of *Apatosaurus* CM 11339. A. X-ray scout image showing the two vertebrae in articulation, in left lateral view. B–D. Slices 39, 43 and 70 in posterior view, showing the most anterior appearance of the condyles and cotyles. doi:10.1371/journal.pone.0078214.g016

slice 70 (Figure 16 part D). So the functional length of the second vertebra is 27 ± 1 slices or 94.5 ± 3.5 mm. The cartilage/bone ratio is therefore $14 \pm 3.5/94.5 \pm 3.5$ or $15 \pm 4\%$.

Data from turkey neck

Tables 1 and 2 contain all measurements made of the dissected turkey neck. The banner figures are as follows:

The intact neck segment measured 189.5 mm from the most anterior to most posterior bone. Once the neck had been dissected apart into individual vertebrae, the length of the column of these vertebrae was 186.0 mm. After removing all cartilage and other soft tissue and drying the vertebrae, the articulated sequence shrank to 179.0 mm. And after degreasing in dilute hydrogen peroxide and fully drying, the same articulated column measured 178.0 mm. The intact neck, then, was 6.46% longer than the length derived from fully cleaned vertebrae whose condition would most closely approach that of fossilised vertebrae.

Therefore, in order to reconstruct the in-vivo length of any vertebra, it is necessary to add 6.46% to the length of the dry bone. The effect of this is shown in Figure 17. (For simplicity, we added the whole 6.46% to one of the articulating surfaces rather than adding 3.23% to each.) Although this illustration is only schematic, it gives a reasonable indication of the magnitude of the effect: measuring from the composite image, we find that the inclusion of articular cartilage increases intervertebral elevation by about 15° per joint. If this were replicated along a neck of 14 vertebrae, the resulting additional deflection of the anteriormost vertebra would be an enormous 210° .

An additional extension of 210° in neutral pose is plainly impractical as it would result in the head being carried upside-down

and directed backwards. What this really shows is simply that necks are not habitually held in neutral posture [20].

The changes in measured zygapophyseal length were less consistent than those in centrum length, due to the difficulty of measuring the facets accurately: the limits of the facets are difficult to make out, especially when soft tissue is present. Although the general trend was for the measurements of any given facet to decrease as soft-tissue was removed, in a few cases the lengths measured for cleaned, degreased and dried zygapophyseal facets were longer than those taken from the vertebrae when freshly dissected. It seems unlikely that these measurements are correct: probably the earlier measurements underestimated the facet lengths. However, we have used the figures as measured rather than “fudging”, in the hope that any over- and under-measurements cancel out across the whole data set.

With these caveats, the key zygapophyseal measurements are that the average lengths of pre- and postzygapophyseal facets when freshly dissected (i.e., including cartilage) were 8.30 and 8.51 mm respectively; and that the corresponding lengths from cleaned, degreased and dried facets were 7.41 and 7.73 mm. This means that the additional length contributed by cartilage is 12% for prezygapophyses and 11% for postzygapophyses, an average of about 11%. Measurement error means that the true figure may be rather more than this (or conceivably slightly less), but we will use the figure 11%.

Data from other animals

Turkeys are not the only animals whose intervertebral cartilage can shed light on that of sauropods. Some data are available for certain other animals, though not yet in as much detail as above. Note, however, that these data are only indicative, and cannot in general be compared directly with those above as they were obtained by a variety of different methods.

The cartilage of other birds is also informative, since all modern birds are equally closely related to sauropods. Of particular interest is the ostrich, as it is the largest extant bird. In a sequence of 14 cervical vertebrae (C3–C16) the total length of the centra when wet and with cartilage intact was 865.5 mm, but after drying and removal of cartilage only 814 mm [47]. Thus intervertebral cartilage accounted for an increase of 51.5 mm, or 6.3% over the length of bone alone.

The rhea is closely related to the ostrich, but has very different intervertebral cartilage. Measuring the cartilage thickness on both sides of the vertebrae of a sagittally bisected rhea neck (Figure 18), we found that on average cartilage added 2.59% to the length of the vertebrae (Table 3).

Among extant animals, crocodylians are the next closest relatives to sauropods. Therefore, birds and crocodylians together form an extant phylogenetic bracket. We examined a sagittally bisected frozen American alligator. This animal was wild-caught and so its exact age is not known, but the snout-vent length of 51 cm suggests an age of about one year. We measured the thickness of intervertebral cartilage from photographs (Figure 19) using GIMP [48], a free image-editing program similar to PhotoShop. We found that of a total neck length of 779 pixels, 101 pixels were cartilage, constituting 14.9% of the length of the bone (678 pixels).

The horse is of interest as a good-sized animal with a reasonably long neck and strongly opisthocoelous cervical vertebrae – that is, having vertebrae with pronounced condyles and cotyles rather than flat articular surfaces. From photographs of a sagittally bisected horse head and neck (Figure 20), we measured the thickness of intervertebral cartilage for three vertebrae (C2, C3 and C4). C5 was broken and more posterior vertebrae were absent. Of a total C2–C4 neck length of 940 pixels, 61 pixels were

Table 1. Measurements of individual vertebrae of a turkey neck: anteroposterior lengths of centra and zygapophyseal facets, measured “wet” (freshly dissected), “dry” (after removal of all flesh and one day’s drying) and “degreased” (after one day in dilute hydrogen peroxide and one week’s thorough drying).

WET											
Vertebra	Centrum	Prezyg		Postzyg							
	Length	L	R	L	R						
A	22.5	6.78	7.3	7.86	8.48						
B	24.5	7.53	7.43	8.28	7.53						
C	25.05	7.43	6.76	7.63	8.87						
D	24.5	7.47	8.11	8.88	8.83						
E	24.5	8.45	8.86	8.96	9.27						
F	24	8.58	8.76	8.12	9.53						
G	22.8	9.28	9.51	8.46	9.67						
H	19.6	9.57	10.93	7.2	8.61						
Total/Avg	187.45	8.14	8.46	8.17	8.85						
		8.3		8.51							
DRY											
Vertebra	Centrum	Prezyg		Postzyg		RATIO wet:dry					
	Length	L	R	L	R	Vertebra	Centrum	Prezyg	Postzyg		
							Length	L	R	L	R
A	23.28	5.95	6.44	6.72	6.63	A	0.966	1.139	1.134	1.170	1.279
B	23.88	6.59	6.56	7.22	7.21	B	1.026	1.143	1.133	1.147	1.044
C	23.96	6.54	6.5	7.8	7.82	C	1.045	1.136	1.040	0.978	1.134
D	23.6	7.23	7.17	7.84	7.81	D	1.038	1.033	1.131	1.133	1.131
E	23.54	7.74	7.61	8.54	8.46	E	1.041	1.092	1.164	1.049	1.096
F	23.01	7.61	7.96	8.24	8.34	F	1.043	1.127	1.101	0.985	1.143
G	22.05	8.1	8.34	8.46	7.97	G	1.034	1.146	1.140	1.000	1.213
H	18.56	9.39	9.56	6.59	7.07	H	1.056	1.019	1.143	1.093	1.218
Total/Avg	181.88	7.39	7.52	7.68	7.66	Average	1.031	1.104	1.123	1.069	1.157
		7.46		7.67				1.114		1.113	
DEGREASED											
Vertebra	Centrum	Prezyg		Postzyg		RATIO wet:degreased					
	Length	L	R	L	R	Vertebra	Centrum	Prezyg	Postzyg		
							Length	L	R	L	R
A	23.15	5.89	6.5	6.42	7.84	A	0.972	1.151	1.123	1.224	1.082
B	23.72	6.6	6.52	7.17	7.43	B	1.033	1.141	1.140	1.155	1.013
C	23.8	6.39	6.37	7.67	7.54	C	1.053	1.163	1.061	0.995	1.176
D	23.56	6.93	7.06	8.25	7.69	D	1.040	1.078	1.149	1.076	1.148
E	23.52	7.83	7.55	8.55	8.39	E	1.042	1.079	1.174	1.048	1.105
F	22.96	7.48	7.95	8.18	7.98	F	1.045	1.147	1.102	0.993	1.194
G	22	8.08	7.56	7.78	7.58	G	1.036	1.149	1.258	1.087	1.276
H	18.52	10.1	9.7	8.01	7.17	H	1.058	0.948	1.127	0.899	1.201
Total/Avg	181.23	7.41	7.4	7.75	7.7	Average	1.035	1.107	1.142	1.060	1.149
		7.41		7.73				1.124		1.11	

All lengths in mm. This table is also available as file S1.
doi:10.1371/journal.pone.0078214.t001

cartilage, constituting 6.9% of bone length (879 pixels). This thickness of neck cartilage is consistent with those illustrated in veterinary radiographs [49–52].

Camels also have long necks and opisthocoelous cervical vertebrae. We might expect their necks to be similar to those of horses, but X-rays show that they are very different (Figure 21). While the condyles of horses’ cervicals are deeply inserted into their corresponding cotyles, those of the camel do not even reach the posterior lip of their cotyles, so that a clear gap is visible

between centra in lateral view. (The same is true in alpacas [53,54].) It is difficult to measure the thickness of cartilage when much of it is hidden inside the cotyle; however, we were able to obtain a rough measurement of 13% the length of the bones, by measuring cartilage space from condyle rim to cotyle margin. The example of the camel contradicts Stevens and Parrish’s claim, quoted in the introduction, that “the mammalian opisthocoelous biomechanical design [consists] of condyles that insert deeply in cotyles of matching curvature, leaving little room for cartilage [...]

Table 2. Length measurements of a turkey neck.

Condition of neck	Length	Intact as
	(mm)	proportion
Intact before dissection	189.5	0.00%
Articulated sequence of wet vertebrae immediately after dissection	186	1.88%
Sum of lengths of individual wet centra	187.45	1.09%
Articulated sequence of vertebrae after removal of all flesh and drying	179	5.87%
Sum of lengths of individual dry centra	181.88	4.19%
Articulated sequence of vertebrae after degreasing in H2O2 and drying	178	6.46%
Sum of lengths of individual degreased centra	181.23	4.56%

For each measurement, the length of the intact neck is given as a proportion, indicating by what factor the various measurements would need to be increased to yield the true length in life.

doi:10.1371/journal.pone.0078214.t002

vertebrae with nonplanar central articular geometry generally have little intervening cartilage (pers. obs.), and thus little room for conjecture regarding their undeflected state”. Instead, the situation

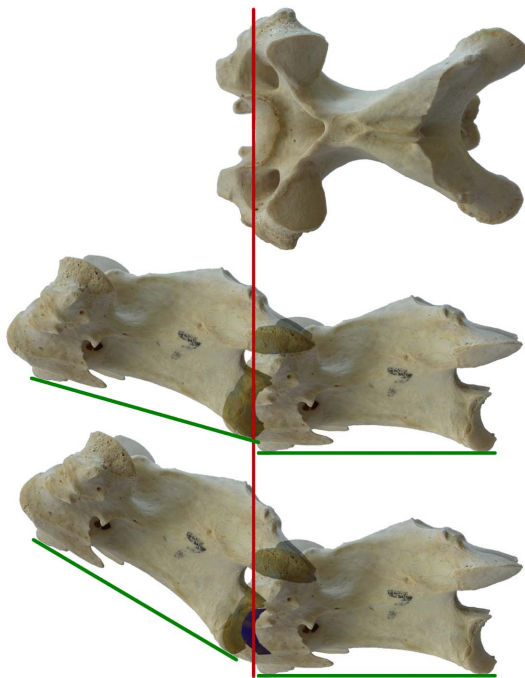


Figure 17. Effect on neutral pose of including cartilage on ONP. Effect on neutral pose of including cartilage. Top: dorsal view of a turkey cervical vertebra: vertical red line indicates the position of the most anterior part of the midline of the anterior articular surface, which is obscured in later view. Second row: two such vertebrae arranged in osteological neutral pose, with the articular surfaces of the centra abutting and the zygapophyseal facets maximally overlapped. The anterior vertebra is inclined by about 16° relative to the posterior. Third row: two such vertebrae, with the centrum of the more posterior one elongated by 6.46% to allow for intervertebral cartilage (shown in blue), and the more anterior positioned with its centrum articulating with the cartilage and the zygapophyses maximally overlapped. The anterior vertebra is inclined by about 31°. The inclusion of cartilage has raised neutral posture by 15°. Green lines represent a horizontal baseline, joining the most ventral parts of the anterior and posterior ends of the vertebrae.

doi:10.1371/journal.pone.0078214.g017

is more complex: different animals have very different arrangements and the bones alone may not convey sufficient information.

From a veterinary X-ray of a dog (*Canis familiaris*) we measured a total length from the posterior margin of C2 to that of C6 of 881 pixels (Figure 22). The intervertebral gaps behind the four vertebrae C2–C5 were 28, 34, 37 and 39 pixels, for a total of 138. This constitutes 18.6% of bone length (743 pixels). However, the true thickness of cartilage was probably greater, since the intervertebral gaps visible in lateral view are from the posterior margin of the cotyle to the anterior margin of the condyle. Allowing for the additional thickness of cartilage within the cotyles would add perhaps 1/4 to these measurements, bringing the cartilage proportion up to 23%. This neck X-ray is consistent with those of other dogs illustrated in the veterinary literature [55–57].

The best extant sauropod analogue would be the giraffe (*Giraffa camelopardalis*), due to its larger size and much longer neck. Unfortunately, giraffe necks are difficult to come by, and the only data we have been able to gather was from the neck of a young juvenile, two weeks old at the time of death. When intact, the neck was 51 cm in length; but when the vertebrae were prepared out and cleaned of cartilage, they articulated to form a misleading cervical skeleton that is only 41 cm long (Figure 23). In this neck, intervertebral cartilage contributes 24% of the length that the bones themselves contribute. No doubt this very high ratio is



Figure 18. Cartilage in the neck of a rhea. Joint between cervicals 11 (left) and 10 (right) of a rhea, sagittally bisected. Left half of neck in medial view. The thin layers of cartilage lining the C11 condyle and C10 cotyle are clearly visible.

doi:10.1371/journal.pone.0078214.g018

Table 3. Measurements of centrum lengths and intervertebral cartilage in the sagittally bisected neck of a rhea.

	Segment length			Condyle cartilage			Cotyle cartilage			Bone Length	Cartilage%	
	Left	Right	Avg.	Left	Right	Avg.	Left	Right	Avg.		Of bone	Of total
C4	32.3	31.9	32.1			0.43	0.51		0.51	31.2	3.00	2.91
C5	36.1	36.8	36.5	0.41		0.41	0.93		0.93	35.1	3.82	3.68
C6	39.3	39.2	39.3		0.57	0.57	0.58		0.58	38.1	3.02	2.93
C7	39.9	40.3	40.1			0.43	0.74	0.47	0.61	39.1	2.64	2.57
C8	41.5	41.1	41.3			0.43	0.44	0.39	0.42	40.5	2.08	2.03
C9	41.8	42.4	42.1	0.36		0.36	0.57	0.43	0.50	41.2	2.09	2.04
C10	40.6	41.0	40.8		0.42	0.42	0.53	0.43	0.48	39.9	2.26	2.21
C11	38.3	38.6	38.5	0.31	0.47	0.39	0.32	0.38	0.35	37.7	1.96	1.92
C12	37.4	37.0	37.2	0.39	0.43	0.41	0.40	0.35	0.38	36.4	2.16	2.11
C13	34.2	33.8	34.0	0.48	0.39	0.44	0.58	0.47	0.53	33.0	2.91	2.82
Avg.	38.14	38.21	38.2	0.39	0.46	0.42	0.56	0.42	0.53	37.2	2.59	2.52

All measurements are in mm. "Segment" here means a centrum including its anterior and posterior articular cartilage. Empty cells represent surfaces so torn up by the bandsaw used in bisection that accurate measurements were impossible. There are more of these empty cells on the right than on the left because of how the saw trended; the cut was not perfectly on the midline. For C4, C7 and C8, condyle cartilage thickness could not be accurately measured on either side, so an estimate of the average was used. This table is also available as file S2.

doi:10.1371/journal.pone.0078214.t003

largely due to the incomplete ossification of the bones of a young juvenile: it would be interesting to carry out the same exercise with the neck of an adult giraffe, to see whether giraffes more closely resemble camels or horses in the thickness of their intervertebral cartilage.

Finally, Evans [58] measured the thickness of intervertebral cartilage preserved in the complete, articulated fossilised necks of two plesiosaurs. He found that it came to 14% of centrum length in *Muraenosaurus* and 20% in *Cryptoclidus*.

These results are summarised in Table 4. Across all 13 surveyed animals, and using midpoints of ranges for *Apatosaurus*, the mean cartilage/bone ratio is 12.5%, and the median is 14.0%. But there is a great deal of variation (standard deviation = 6.9%). For this reason, and because some juvenile individuals were included, and because the measurements were obtained by a variety of different methods, simple averages are not reliable. With that caveat, averages by clade are as follows: sauropods 13.2%, birds 4.5%, crocodylians 14.9%, mammals 15.2% and plesiosaurus 17%.

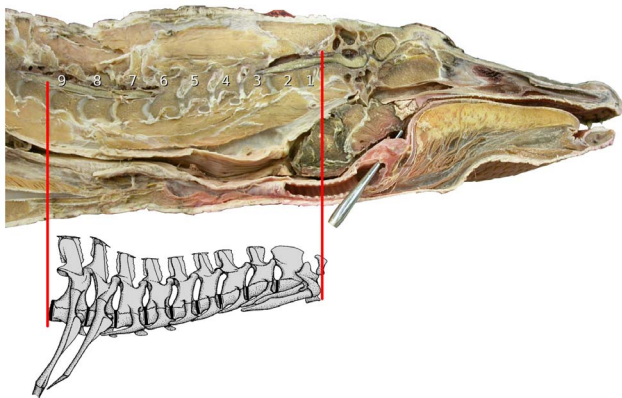


Figure 19. Alligator head and neck. Sagittally bisected head and neck of American alligator, with the nine cervical vertebrae indicated. Inset: schematic drawing of these nine vertebrae, from ([62]: figure 1), reversed.

doi:10.1371/journal.pone.0078214.g019

Discussion

Implications for sauropod necks

The morphology of intervertebral cartilage in the sauropods is not known, and cannot presently be determined from osteological correlates, as none have yet been identified for bird- and mammal-style intervertebral joints. It is notable that in the examined extant animals with true intervertebral discs (crocodylians and mammals) the cartilage:bone ratios are three times higher than in birds. The relatively low cartilage ratio for *Sauroposeidon* and the high ratio for *Apatosaurus*, taken in isolation, perhaps suggests some variation in morphology within Sauropoda, with *Sauroposeidon* having bird-style synovial intervertebral joints and *Apatosaurus* having true discs. Such variation would not be unprecedented: the presence of simple articular discs in the ostrich and their absence in the rhea shows that variation exists even at low taxonomic levels. However, the difference in proportional cartilage thickness between these two sauropods is more parsimoniously explained as due to the



Figure 20. Horse head and neck. Sagittally bisected head and anterior neck of a horse. The first four cervical vertebrae are complete, but the posterior part of the fifth is absent. Note that the condyles are deeply embedded in their cotyles.

doi:10.1371/journal.pone.0078214.g020

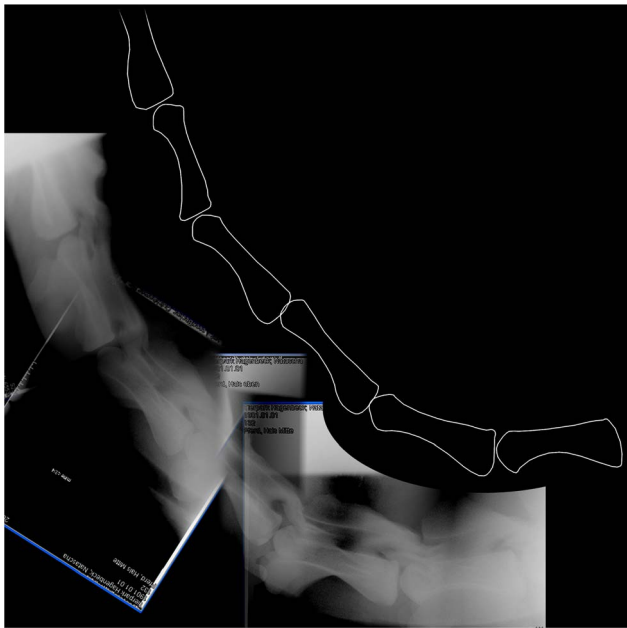


Figure 21. Camel neck in X-ray. X-ray image of a camel, with tracing to highlight the centra of cervical vertebrae 2–7. (C1 and the anterior part of C2 are obscured by the skull.) Note that most of the condyles do not even reach the posterior margins of their corresponding cotyles, let alone embed deeply within them.
doi:10.1371/journal.pone.0078214.g021

elongation of the *Sauroposeidon* vertebrae and the juvenile nature of the *Apatosaurus* specimens.

As shown by the contrasting morphology of horse and camel necks, similarly shaped vertebrae of different animals may be augmented by a dramatically different shape and amount of cartilage. It may be that, in the same way, different sauropods had significantly different cartilaginous contributions to their necks. Given information regarding one sauropod group, we must be cautious not to assume that it generalises to all others.

With these caveats in mind, and based on the limited information currently available, it is reasonable to guess that most adult sauropods had cartilage/bone ratios of about 5–10% – that the lower figure for *Sauroposeidon* is a result of its extreme vertebral elongation and the higher figure for *Apatosaurus* is due to its proportionally shorter vertebrae. We obtained similar estimates for the cartilage thickness in an adult *Apatosaurus* neck by scaling up from the juvenile material and scaling down, proportionally, from

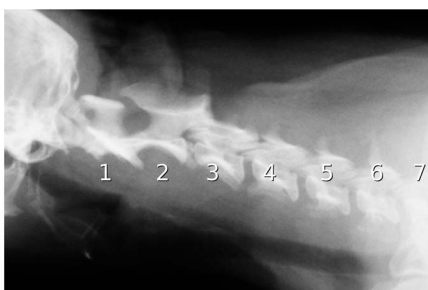


Figure 22. Dog neck in X-ray. Neck of a dog (dachshund), in X-ray, with the seven cervical vertebrae indicated. This photo has been used with permission from the Cuyahoga Falls Veterinary Clinic.
doi:10.1371/journal.pone.0078214.g022

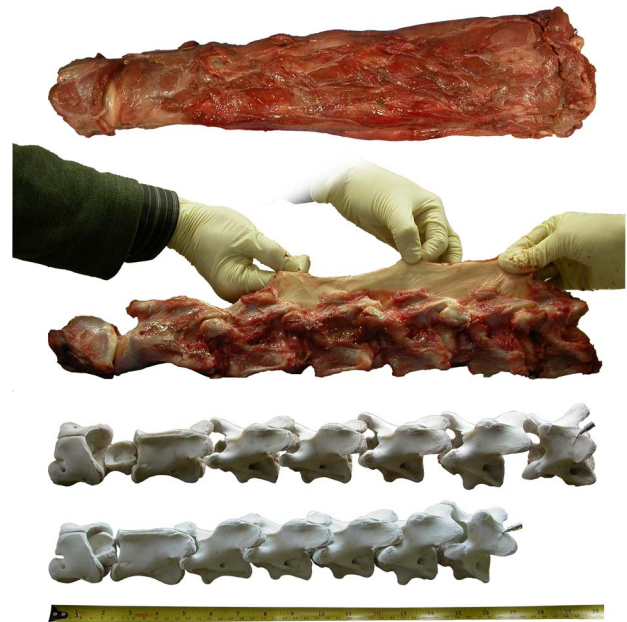


Figure 23. Neck of a young juvenile giraffe. Neck of a young juvenile giraffe, in various states of dissection, to scale. Top, the neck as received, skinned and stripped of skin, oesophagus and trachea. Second, the neck with most muscle removed and the nuchal ligament stretched out. Third, the vertebrae cleaned of soft tissue and cartilage, laid out with equal intervertebral spacing to attain the same total length as when intact (51 cm). Fourth, the vertebrae in the same condition but articulated as closely as possible, forming a misleading cervical skeleton measuring only 41 cm. Top image in left lateral view; second in right lateral view, reversed; third and fourth in left dorsolateral.
doi:10.1371/journal.pone.0078214.g023

Sauroposeidon, which suggests that unlike mammals, juvenile sauropods may not have had proportionally thicker intervertebral cartilage than adults.

In the neck of a turkey, adding 4.56% to bony centrum length to restore the absent cartilage resulted in neutral pose being raised by 15° at each joint. This increase in extension is roughly proportional to the proportion of cartilage restored and inversely proportional to the height of the zygapophyses above the centre of rotation – very high zygapophyses would mean that the increased length of the centrum with cartilage restored would subtend only a small angle at the zygapophyses, while low zygapophyses would result in a wider angle. Zygapophysis height varies among different sauropods, and along the neck of each; but as a proportion of centrum length it is generally reasonably close to that of turkey cervicals. It therefore seems reasonable to conclude that restoring the missing cartilage to sauropod vertebrae would raise neutral posture commensurately, although it is not possible to give meaningful quantitative results without detailed modelling.

If the neutral posture of each joint in a sauropod's neck was raised, perhaps by as much as 15°, it may seem that this would result in an absurd neutral posture in which the neck curls back over the torso. In practice, as has often been noted [20,45,46], animals do not hold their necks in neutral posture, but habitually extend the base of the neck and flex the more anterior portion. This pattern of behaviour combined with more extended neutral postures than previously envisaged indicates that swan-like postures may have been very common, and that in some sauropods it may have been common to hold the middle region of the neck at or even beyond vertical.

Table 4. Cervical intervertebral cartilage thickness in a variety of taxa, expressed as a percentage of bony centrum length.

Taxon	Thickness	Reference	Notes
<i>Sauroposeidon</i>	4.50%	This study	Measurements from CT scan of articulated material. Vertebrae are proportionally long mid-cervicals; averaged over the whole neck the thickness is estimated to have been 5.8%.
<i>Apatosaurus</i> CM 3390	16–24%	This study	Measurements from CT scan of articulated material. Vertebrae are most anterior dorsals.
<i>Apatosaurus</i> CM 11339	14.80%	This study	Measurements from CT scan of articulated material. Vertebrae are middle or posterior dorsals.
Turkey	4.56%	This study	Difference in measurements of intact neck and articulated sequence of cleaned, degreased and dried vertebrae.
Ostrich	6.30%	[47]	Difference in measurements of individual vertebrae with and without cartilage.
Rhea	2.59%	This study	Measurement of <i>in situ</i> cartilage in bisected neck.
Alligator	14.90%	This study	Measurement of <i>in situ</i> cartilage from photograph of cross section.
Horse	6.90%	This study	Measurement of <i>in situ</i> cartilage from photograph of cross section.
Camel	13.00%	This study	Crude measurement from condyle margin to cotyle lip of lateral-view X-ray. This is an interim measurement, which we hope to improve on when we obtain better images.
Dog	17.00%	This study	Measurement of intervertebral gaps in lateral-view X-ray, uncorrected for likely concavity of cotyles.
Giraffe	24.00%	This study	Difference in measurement of intact neck and closely articulated sequence of cleaned vertebrae. Young juvenile specimen.
<i>Muraenosaurus</i>	14.00%	[58]	Measurement of <i>in situ</i> cartilage in fossils.
<i>Cryptoclidus</i>	20.00%	[58]	Measurement of <i>in situ</i> cartilage in fossils.

doi:10.1371/journal.pone.0078214.t004

We found that the anteroposterior length of the zygapophyseal facets of turkey cervicals were, on average, 11% longer when cartilage was intact than after it was removed. It is reasonable to assume that a similar proportion held for sauropods. The effect of longer zygapophyseal facets on ROM is very straightforward: ROM increases more or less linearly with zygapophyses length, so an 11% increase in the latter translates directly to an 11% increase in dorsoventral flexibility at each neck joint. Of course, if the neck were thought for other reasons to be very inflexible, an 11% increase in small ROM angles would not make a particularly big difference. Calculating absolute values for ROM requires detailed modelling that is beyond the scope of this study.

In apparent contradiction to this, recent work [47] shows that ostrich necks with their soft tissue in place are less flexible than bones alone indicate, and suggests that the same would have been true of sauropod necks. In interpreting this result, it is important to bear two things in mind. First, whatever it may do to range of motion, including intervertebral cartilage unquestionably raises neutral pose: it is for this reason that the habitual life posture of rabbits is more raised than can be attained by the bones of the neck even in maximum extension [20]. Second, the effect of soft tissues on neck flexibility differs among taxa. For example, in humans, where the cervical vertebrae are mildly amphicoelous, there is no ball-and-socket joint, so no obvious way for one vertebra to rotate with respect to those before and after it. But the thick intervertebral discs, with their roughly spherical nuclei, provide a centre of rotation: as the neck flexes and extends, the discs become wedge-shaped to accommodate motions that the bones alone would not permit [59]. More comparative work is needed to determine the different effects of soft tissue on flexibility in different taxa, and to enable conclusions to be drawn regarding extinct animals.

In summary, including cartilage in our models of sauropod necks shows that they were longer, more raised and probably more flexible than previously recognised.

Future work

This study represents only a beginning, not an end, to the work on the neck cartilage of sauropods (and other extinct animals). We would like to see future work extend this in the following ways.

- CT scans of more sauropod neck segments that preserve vertebrae in articulation – ideally much more complete necks than the ones described here.
- Measurements of intervertebral cartilage thickness and zygapophyseal cartilage extent for more extant animals: especially birds and crocodylians, which together form an extant phylogenetic bracket for sauropods; and an adult giraffe, which has much the longest neck of any extant animal.
- Intervertebral and zygapophyseal cartilage measurements for individuals of different growth stages within single species, to determine how the amount and shape of cartilage varies through ontogeny.
- Work to determine whether dry bones have any osteological correlates that are informative regarding the morphology of intervertebral cartilage: true intervertebral discs, or synovial joints with or without articular discs.
- Finally, we would very much like to see the results of re-running the DinoMorph software with its models updated to take into account intervertebral and zygapophyseal cartilage. At present this is the only software that has been used to model intervertebral joints; if it remains unavailable then it may be possible to use more general-purpose CAD packages to achieve the same ends.

Conclusions

A survey of intervertebral spacing and cartilage thickness in extinct and extant amniotes reveals several factors that affect any attempts to model vertebral articulations:

1. The thickness of intervertebral cartilage is highly variable among taxa, ranging from 2.6% of centrum length in a rhea to 24% of centrum length in a baby giraffe. Even if we restrict the sample to presumably adult animals, the range is 2.6% to 20% – a factor of almost eight.
2. There seem to be some systematic differences among clades: mammals and other non-avian amniotes typically have thicker intervertebral cartilage than birds. Intervertebral spacing is particularly high in plesiosaurs, perhaps because of their proportionally short vertebral centra (i.e., the cartilage was not thicker absolutely than in similarly sized animals, but only in comparison to the shorter vertebrae).
3. Based on our admittedly limited sample, sauropods appear to have been intermediate between birds and other amniotes in the thickness of the intervertebral cartilage in the neck, with cartilage accounting for 5–10% of the lengths of the centra in adults.
4. Although only two of our sampled sauropod specimens have strongly opisthocoelous centra, in both of those cases the bony condyle is not shaped to fit the cotyle, and the intervertebral cartilage is thicker anteroposteriorly at the centre than radially at the cotyle rim. More sampling is required to determine if this is a general feature of sauropods, convergent in *Apatosaurus* and *Sauroposeidon*, or variable among individuals and along the column.
5. At present, there are no known osteological correlates of different intervertebral joint types (intervertebral disc, synovial joint, synovial joint with articular disc).
6. At present, there are no known osteological correlates of thick versus thin intervertebral cartilage. For example, horses and camels both have strongly opisthocoelous cervical vertebrae, but their intervertebral spacing is very different: in camels, the condyles do not even reach the rims of the cotyles, much less articulate with them directly.

These difficulties and uncertainties do not render attempts to model intervertebral joint mechanics uninformative or worthless. However, it is clear that intervertebral cartilage is a significant fraction of the length of the bony cervical series in most amniotes, as well as highly variable among taxa. Therefore, assumptions about intervertebral cartilage in biomechanical models must be explicit in choice of reference taxa, type of intervertebral joint, and thickness of cartilage. Sensitivity analyses using DinoMorph or other CAD software to quantify the variation in ONP and ROM imposed by different starting assumptions would be extremely valuable; indeed it is difficult to see how digital ONP and ROM estimates can be useful in the absence of such analyses. Recent work on the prosauropod *Plateosaurus* [28,60] shows how this can be done for extinct dinosaurs; applying these techniques to sauropod necks would be informative.

More generally, we need to look more carefully at both fossils and extant organisms. In the extant realm, a search for possible osteological correlates of intervertebral joint type and cartilage

thickness is very badly needed. But aside from that, simply documenting the cartilage thickness in a wider range of taxa will be useful in elucidating ontogenetic, phylogenetic, and size-related variation among individuals and clades. The same survey can be extended to articulated fossil material. Although complete, undistorted cervical material is rare for sauropods, a more extensive and careful survey of articular morphology will allow future workers to better constrain their models, and may also turn up characters of potential biomechanical and phylogenetic interest, such as the unusually flattened condyles in middle cervical vertebrae of *Sauroposeidon*. All specimens that have both centra and zygapophyses in articulation should be CT scanned where this is logistically feasible.

We have attempted a first step toward understanding how intervertebral cartilage affected the postures and ranges of motion of sauropod necks. We hope that further work makes this paper obsolete very quickly.

Supporting Information

File S1 Data from Table 1 in more useful format.
(XLS)

File S2 Detailed data on rhea neck cartilage.
(XLS)

Acknowledgments

We thank Matt Lamanna, David Berman, and Amy Henrici for access to Carnegie Museum *Apatosaurus* specimens, and Rich Cifelli, Nick Czaplewski, and Jennifer Larsen for access to the *Sauroposeidon* specimen. The staff of the Oklahoma University Medical Center Department of Radiological Sciences assisted with CT scans of sauropod vertebrae: we especially thank B. G. Eaton for access to CT facilities, Thea Clayborn, Kenneth Day, and Susan Gebur for performing the scans, and R. Kent Sanders for overseeing the scanning, reconstructing the data, and interpreting the results. We also thank Eileen Foate, Elizabeth Mock, and Tami Miller of Western University Veterinary Medicine for help with animal specimens and for dissecting tools and support. Thanks are also due to Kevin Vale of Vale Butchers, Drybrook, UK, for providing the turkey neck, John Hutchinson of the Royal Veterinary College, UK, for providing the juvenile giraffe neck, Ruth Elsey of Rockefeller Wildlife Refuge, Grand Chenier, Louisiana, for providing the alligator, the College of Veterinary Medicine at Western University of Health Sciences, California, for access to the hemisectioned horse head and neck, Cuyahoga Falls Veterinary Clinic in Cuyahoga Falls, Ohio (<http://fallsvetclinic.com/>) for providing the dog X-ray image, Gordon Dzemski of the University of Flensburg, Germany, for the camel X-ray, and the Museum für Naturkunde Berlin for permission to use the *Giraffatitan* photograph.

Finally, we thank our handling editor Peter Dodson and our reviewers Heinrich Mallison and Andreas Christian for their clear and helpful comments.

Author Contributions

Conceived and designed the experiments: MPT MJW. Performed the experiments: MPT MJW. Analyzed the data: MPT MJW. Wrote the paper: MPT MJW.

References

1. Taylor MP, Wedel MJ (2013) Why sauropods had long necks; and why giraffes have short necks. *PeerJ* 1: e36. doi:10.7717/peerj.36.
2. Paul GS (1988) The brachiosaur giants of the Morrison and Tendaguru with a description of a new subgenus, *Giraffatitan*, and a comparison of the world's largest dinosaurs. *Hunteria* 2(3): 1–14.
3. Carpenter K (2006) Biggest of the big: a critical re-evaluation of the mega-sauropod *Amphicoelias fragillimus* Cope, 1878. *New Mexico Museum of Natural History and Science Bulletin* 36: 131–137.
4. Sander PM, Christian A, Clauss M, Fehner R, Gee CT, et al. (2011) Biology of the sauropod dinosaurs: the evolution of gigantism. *Biological Reviews* 86: 117–155. doi:10.1111/j.1469-185X.2010.00137.x.
5. Marsh OC (1883) Principal characters of American Jurassic dinosaurs. Pt. VI. Restoration of *Brontosaurus*. *American Journal of Science, Series 3* 26: 81–85.
6. Hatcher JB (1901) *Diplodocus* (Marsh): its osteology, taxonomy and probable habits, with a restoration of the skeleton. *Memoirs of the Carnegie Museum* 1: 1–63.
7. Matthew WD (1905) The mounted skeleton of *Brontosaurus*. *The American Museum Journal* 5: 62–70.

8. Knight CR (1897) Restoration of *Brontosaurus*. Hall of Saurischian Dinosaurs, American Museum of Natural History. Guache on artist board.
9. Zallinger RF (1947) The Age of Reptiles. Mural in the Dinosaur Hall, Yale Peabody Museum.
10. Burian Z (1941) Snorkelling *Brachiosaurus*. Reproduced in: Augusta, Joseph (1957) *Prehistoric Animals*. London: Spring Books.
11. Bakker RT (1986) The Dinosaur Heresies. New York: Morrow. 481 p.
12. Spielberg S (1993) Jurassic Park. Amblin Entertainment.
13. Stevens KA, Parrish JM (1999) Neck posture and feeding habits of two Jurassic sauropod dinosaurs. *Science* 284: 798–800.
14. Martin J (1987) Mobility and feeding of *Cetiosaurus* (Saurischia: Sauropoda) - why the long neck? Occasional Papers of the Tyrrell Museum of Palaeontology (Fourth Symposium on Mesozoic Terrestrial Ecosystems) 3: 154–159.
15. Haines T (1999) Walking with Dinosaurs. BBC Worldwide.
16. Stevens K (2002) DinoMorph: Parametric modeling of skeletal structures. *Senckenbergiana Lethaea* 82: 23–34.
17. Stevens KA, Parrish JM (2005) Digital reconstructions of sauropod dinosaurs and implications for feeding. In: Tidwell V, Carpenter K, editors. *The Sauropods: Evolution and Paleobiology*. Berkeley: University of California Press. pp. 178–200.
18. Stevens KA, Parrish JM (2005) Neck posture, dentition, and feeding strategies in Jurassic sauropod dinosaurs. In: Curry Rogers K, Wilson J, editors. *Thunderlizards: the sauropodomorph dinosaurs*. Bloomington: Indiana University Press. pp. 212–232.
19. Dzemski G, Christian A (2007) Flexibility along the neck of the ostrich (*Struthio camelus*) and consequences for the reconstruction of dinosaurs with extreme neck length. *Journal of Morphology* 268: 701–714. doi:10.1002/jmor.10542.
20. Taylor MP, Wedel MJ, Naish D (2009) Head and neck posture in sauropod dinosaurs inferred from extant animals. *Acta Palaeontologica Polonica* 54: 213–220.
21. Christian A (2010) Some sauropods raised their necks — evidence for high browsing in *Euhelopus zdanskyi*. *Biol Lett* 6: 823–825. doi:10.1098/rsbl.2010.0359.
22. Upchurch P (2000) Neck Posture of Sauropod Dinosaurs. *Science* 287: 547b.
23. Paul GS (2000) Restoring the life appearances of dinosaurs. In: Paul GS, editor. *The Scientific American book of dinosaurs*. New York: St. Martin's Press. pp. 78–106.
24. Schwarz D, Wings O, Meyer CA (2007) Super sizing the giants: first cartilage preservation at a sauropod dinosaur limb joint. *Journal of the Geological Society* 164: 61–65. doi:10.1144/0016-76492006-019.
25. Mallison H (2010) CAD assessment of the posture and range of motion of *Kentrosaurus aethiopicus* Hennig 1915. *Swiss Journal of Geosciences* 103: 211–233.
26. Emerson CL, Eurell JAC, Brown MD, Walsh M, Odell D, et al. (1990) Ruptured intervertebral disc in a juvenile king penguin (*Aptenodytes patagonica*). *Journal of Zoo and Wildlife Medicine* 21: 345–350.
27. Holliday CM, Ridgely RC, Sedlmayr JC, Witmer LM (2010) Cartilaginous epiphyses in extant archosaurs and their implications for reconstructing limb function in dinosaurs. *PLoS ONE* 5: e13120. doi:10.1371/journal.pone.0013120.
28. Mallison H (2010) The digital *Plateosaurus* II: an assessment of the range of motion of the limbs and vertebral column and of previous reconstructions using a digital skeletal mount. *Acta Palaeontologica Polonica* 55: 433–458. doi:10.4202/app.2009.0075.
29. Bonnan MF, Sandrik JL, Nishiwaki T, Wilhite DR, Elsej RM, et al. (2010) Calcified cartilage shape in archosaur long bones reflects overlying joint shape in stress-bearing elements: Implications for nonavian dinosaur locomotion. *The Anatomical Record: Advances in Integrative Anatomy and Evolutionary Biology* 293: 2044–2055. doi:10.1002/ar.21266.
30. Wake MH, editor (1992) Hyman's comparative vertebrate anatomy, 4th ed. University of Chicago Press. Available: <http://books.google.co.uk/books?hl=en&lr=&id=VKIWjdOkMwC&oi=fnd&pg=PR9&dq=Hyman%27s+Comparative+Vertebrate+Anatomy&ots=KfhjZ2q4BS&sig=-Hqon9F-i3hNllwJ7cUWr5NItv4>. Accessed 13 August 2013.
31. Liem KF, Walker WF, Bemis WE, Grande L (2001) Functional anatomy of the vertebrates: an evolutionary perspective. Harcourt College Publishers Philadelphia. Available: <http://library.wur.nl/WebQuery/clc/1869344>. Accessed 13 August 2013.
32. Baumel JJ, King AS, Brezile JE, Evans HE, Berge JCV (1993) *Handbook of Avian Anatomy: Nomina Anatomica Avium*, Second Edition. Cambridge/Massachusetts: Nuttall Ornithological Club. 779 p.
33. Witmer LM (1995) The extant phylogenetic bracket and the importance of reconstructing soft tissues in fossils. In: Thomason JJ, editor. *Functional morphology in vertebrate paleontology*. Cambridge, UK: Cambridge University Press. pp. 19–33.
34. Hultgren BD, Wallner-Pendleton E, Watrous BJ, Blythe LL (1987) Cervical dorsal spondylosis with spinal cord compression in a black swan (*Cygnus atratus*). *J Wildl Dis* 23: 705–708.
35. Wedel MJ, Cifelli RL, Sanders RK (2000) *Sauroposeidon proteles*, a new sauropod from the Early Cretaceous of Oklahoma. *Journal of Vertebrate Paleontology* 20: 109–114.
36. Wedel MJ, Cifelli RL, Sanders RK (2000) Osteology, paleobiology, and relationships of the sauropod dinosaur *Sauroposeidon*. *Acta Palaeontologica Polonica* 45: 343–388.
37. Wedel MJ, Cifelli RL (2005) *Sauroposeidon*: Oklahoma's native giant. *Oklahoma Geology Notes* 65: 40–57.
38. McIntosh JS (1981) Annotated catalogue of the dinosaurs (Reptilia, Archosauria) in the collections of Carnegie Museum of Natural History. *Bulletin of the Carnegie Museum* 18: 1–67.
39. Wedel MJ, Sanders RK (2002) Osteological correlates of cervical musculature in Aves and Sauropoda (Dinosauria: Saurischia), with comments on the cervical ribs of *Apatosaurus*. *PaleoBios* 22: 1–6.
40. Harvey EB, Kaiser HE, Rosenberg LE (1968) An atlas of the domestic turkey (*Meleagris gallopavo*): myology and osteology. U.S. Atomic Energy Commission, Division of Biology and Medicine. 268 p.
41. Janensch W (1950) Die Wirbelsäule von *Brachiosaurus brancai*. *Palaeontographica* (Suppl 7) 3: 27–93.
42. Wedel MJ (2005) Postcranial skeletal pneumaticity in sauropods and its implications for mass estimates. *The Sauropods: Evolution and Paleobiology*. Berkeley: University of California Press. pp. 201–228.
43. Gilmore CW (1936) Osteology of *Apatosaurus*, with special reference to specimens in the Carnegie Museum. *Memoirs of the Carnegie Museum* 11: 175–298.
44. Wedel MJ (2003) The evolution of vertebral pneumaticity in sauropod dinosaurs. *Journal of Vertebrate Paleontology* 23: 344–357.
45. Vidal PP, Graf W, Berthoz A (1986) The orientation of the cervical vertebral column in unrestrained awake animals. *Exp Brain Res* 61: 549–559. doi:10.1007/BF00237580.
46. Graf W, De Waele C, Vidal PP (1995) Functional anatomy of the head-neck movement system of quadrupedal and bipedal mammals. *J Anat* 186: 55–74.
47. Cobley MJ, Rayfield EJ, Barrett PM (2013) Inter-vertebral flexibility of the ostrich neck: implications for estimating sauropod neck flexibility. *PLOS ONE* 8: e72187. doi:10.1371/journal.pone.0072187.
48. Kimball S, Mattis P (2010) GIMP - The GNU Image Manipulation Program. Available: <http://www.gimp.org/>. Accessed 10 March 2013.
49. Wagner PC, Bagby GW, Grant BD, Gallina A, Ratzlaff M, et al. (1979) Surgical Stabilization of the Equine Cervical Spine. *Veterinary Surgery* 8: 7–12. doi:10.1111/j.1532-950X.1979.tb00596.x.
50. Papageorges M, Gavin PR, Sande RD, Barbee DD, Grant BD (1987) Radiographic and Myelographic Examination of the Cervical Vertebral Column in 306 Ataxic Horses. *Veterinary Radiology* 28: 53–59. doi:10.1111/j.1740-8261.1987.tb01725.x.
51. Whitwell KE, Dyson S (1987) Interpreting radiographs 8: Equine cervical vertebrae. *Equine Veterinary Journal* 19: 8–14. doi:10.1111/j.2042-3306.1987.tb02568.x.
52. Hudson NPH, Mayhew IG (2005) Radiographic and myelographic assessment of the equine cervical vertebral column and spinal cord. *Equine Veterinary Education* 17: 34–38. doi:10.1111/j.2042-3292.2005.tb00333.x.
53. Glass K, Baird AN, Baird DK, Del Piero F (2003) Vertebral malformation in two alpacas. *The Camelid Quarterly* June 2003: 1–2.
54. McKenzie EC, Seguin B, Cebra CK, Margiocco ML, Anderson DE, et al. (2010) Esophageal dysfunction in four alpaca crias and a llama cria with vascular ring anomalies. *J Am Vet Med Assoc* 237: 311–316. doi:10.2460/javma.237.3.311.
55. McKee WM, Butterworth SJ, Scott HW (1999) Management of cervical spondylopathy-associated intervertebral, disc protrusions using metal washers in 78 dogs. *J Small Anim Pract* 40: 465–472.
56. Levitski RE, Lipsitz D, Chauvet AE (1999) Magnetic Resonance Imaging of the Cervical Spine in 27 Dogs. *Veterinary Radiology & Ultrasound* 40: 332–341. doi:10.1111/j.1740-8261.1999.tb02120.x.
57. Da Costa RC, Parent J, Dobson H, Holmberg D, Partlow G (2006) Comparison of magnetic resonance imaging and myelography in 18 Doberman pinscher dogs with cervical spondylomyelopathy. *Vet Radiol Ultrasound* 47: 523–531.
58. Evans M (1993) An investigation into the neck flexibility of two plesiosauroid plesiosaurs: *Cryptoclidus eurymerus* and *Muraenosaurus leedsii*. University College: MSc thesis. London p.
59. Kapandji IA (2008) The physiology of the joints: annotated diagrams of the mechanics of the human joints Vol. 3, Vol. 3. Edinburgh [etc.]: Churchill Livingstone/Elsevier.
60. Mallison H (2010) The digital *Plateosaurus* I: body mass, mass distribution, and posture assessed using CAD and CAE on a digitally mounted complete skeleton. *Palaeontologia Electronica* 13. Available: http://www.uv.es/~pardomv/pe/2010_2/198/abstracts.html. Accessed 24 November 2012.
61. Taylor MP (2009) A re-evaluation of *Brachiosaurus altithorax* Riggs 1903 (Dinosauria, Sauropoda) and its generic separation from *Giraffatitan brancai* (Janensch 1914). *Journal of Vertebrate Paleontology* 29: 787–806.
62. Frey E (1988) Anatomie des Körperstammes von *Alligator mississippiensis* Daudin. *Stuttgarter Beiträge zur Naturkunde* 424: 1–106.

Torsion and Bending in the Neck and Tail of Sauropod Dinosaurs and the Function of Cervical Ribs: Insights from Functional Morphology and Biomechanics

Holger Preuschoft¹, Nicole Klein^{2*}

¹ Anatomical Institute, Ruhr University Bochum, Bochum, Germany, ² Staatliches Museum für Naturkunde Stuttgart, Stuttgart, Germany

Abstract

The long necks of sauropods have been subject to many studies regarding their posture and flexibility. Length of the neck varies among groups. Here, we investigate neck posture and morphology in several clades from a mechanical viewpoint. Emphasis is put on comparing sauropod necks and tails with structures in living archosaurs and mammals. Differences in the use made of necks and tails lead to clear-cut differences in the mechanical loads occurring in the same models. Ways of sustaining loads are identified by theoretical considerations. If the observed skeletal structures are suited to resist the estimated loading in a particular posture, this concordance is taken as an argument that this posture or movement was of importance during the life of the individual. Apart from the often-discussed bending in side view, we analyze the often overlooked torsion. Because torsional stresses in a homogenous element concentrate near the periphery, a cylindrical cross section gives greatest strength, and the direction of forces is oblique. In a vertebrate neck, during e.g. shaking the head and twisting the neck, oblique muscles, like the mm. scaleni, if activated unilaterally initiate movement, counterbalance the torsional moments and keep the joints between neck vertebrae in equilibrium. If activated bilaterally, these muscles keep the neck balanced in an energy-saving upright posture. The tendons of the mm. scaleni may have ossified as cervical ribs. The long cervical ribs in brachiosaurids and mamenchisaurids seem to have limited flexibility, whereas the shorter cervical ribs in Diplodocidae allowed free movement. The tails of sauropods do not show pronounced adaptation to torsion, and seem to have been carried more or less in a horizontal, extended posture. In this respect, sauropod tails resemble the necks of herbivorous cursorial mammals. These analyses provide an improved understanding of neck use that will be extended to other sauropods in subsequent studies.

Citation: Preuschoft H, Klein N (2013) Torsion and Bending in the Neck and Tail of Sauropod Dinosaurs and the Function of Cervical Ribs: Insights from Functional Morphology and Biomechanics. PLoS ONE 8(10): e78574. doi:10.1371/journal.pone.0078574

Editor: Andrew A. Farke, Raymond M. Alf Museum of Paleontology, United States of America

Received: June 14, 2013; **Accepted:** September 20, 2013; **Published:** October 30, 2013

Copyright: © 2013 Preuschoft and Klein. This is an open-access article distributed under the terms of the Creative Commons Attribution License, which permits unrestricted use, distribution, and reproduction in any medium, provided the original author and source are credited.

Funding: NK (second and corresponding author) was funded by the DFG (DFG Projekt FOR 533/N2). The funders had no role in study design, data collection and analysis, decision to publish, or preparation of the manuscript.

Competing Interests: The authors have declared that no competing interests exist.

* E-mail: nicole.klein@smns-bw.de

Introduction

Neck Length and Neck Posture in Sauropod Dinosaurs

Sauropoda are a major clade of the Dinosauria (Saurischia) and the largest animals that ever lived on land, reaching body masses up to 70 tons or even more (summarized in [1], appendix). In spite of a high taxonomic diversity, all Sauropoda share a characteristic body plan, consisting of a small head, an elongated neck, a barrel-shaped trunk on four column-like limbs, and an elongated tail. The very long neck is one major hallmark of sauropod dinosaurs and may be a key innovation for their success and gigantism [2,3]. Although all sauropods have a long neck, they show differences in neck length, morphology, and probably also in neck posture. The “morphological disparity” among sauropods was also emphasized by Taylor and Naish [4] and Taylor and Wedel [5]. In some sauropod taxa (e.g., *Mamenchisaurus*, *Omeiosaurus*) the neck was extremely long, making up approximately half of the entire body length of the animal. This was the result of an increase in the number of cervical vertebrae (up to 19) and partially also of the elongation of the single elements [6]. The necks of most Diplodocidae are not as long as in mamenchisaurids but are still elongated, with 15 to 16 cervical vertebrae. Among Sauropoda,

one group, the brachiosaurids had longer forelimbs than hind limbs and are commonly thought to have kept their long necks in a more upright (vertical) posture. They have a lower segment number (around 14 cervical vertebrae) but the single cervicals are elongated. Camarasaurids, *Dicraeosaurus* and *Brachytrachelopan* are the exceptions among Sauropoda because they had rather short dimensioned necks (although the neck of camarasaurids is still elongated when compared e.g., to a giraffe), which possess unusually long and split neural processes. These forms are not considered here but will be the focus of a future study.

The most plausible explanation for the evolution of long necks in sauropods is that feeding becomes more energetically efficient by giving the animal long reaching distance for getting a hold of food without moving the entire body (e.g. [3,7,8,9]). Whether this long reach is actually used for harvesting vegetation close to the ground, high in the canopy, or in any other stratum, is just a matter of the preferred food--the mechanical needs are identical. The often discussed discrimination between high and low browsing confines, in fact, the general problem to just one aspect. Only if the long necks of sauropods can be flexed in all directions is the complete exploitation of the huge volume of vegetation

available for them [9]. Any restriction of neck mobility reduces the harvested volume (Fig. 1). However, strict preferences for feeding height and vegetation are common among living mammalian herbivores (e.g., giraffe [10], domestic horses, cattle, sheep, and goat [own results, data collected by Schlunk, unpublished]), although all these animals are able to make use of other strata of vegetation as well. Similar preferences for feeding heights and vegetation may also have existed in sauropods.

The true neck posture in sauropods is still unknown and controversial (e.g., papers in this collection), at least in taxa such as e.g., *Giraffatitan* and mamenchisaurids. Although some authors favored nearly vertical neck postures and specialized high-browsing [11,12], others have argued that increased horizontal feeding range has been the primary function of the neck and that the vertical range was limited [13,14]. The flexibility of the sauropod neck is also a topic of debate. Clearly, a flexible neck allows more complete exploitation of the food resources than a restricted range of movement (Fig. 1), but the use of energy-saving tensile structures like ligaments for positioning the neck instead of energy-consuming musculature may outweigh the disadvantage of such restrictions. Standard mechanical laws were used to reconstruct the neck posture of sauropods but the results are still differing. This is partly because of different interpretations of the function of mechanically relevant structures such as the cervical ribs or the assumed amount of intervertebral and zygapophyseal cartilage (e.g. [7,11-17]).

A weak point of previous approaches to neck mechanics is their bias towards bending of the neck under the influence of weight and balancing of the head and neck weight in lateral view. Several basic biomechanical facts were not given adequate attention in this context. This is particularly the occurrence of torsional loads in flexed necks that had been recognized already by Dzemski and Christian [18]. Taylor and Wedel [5] at least mention loading of the neck by lateral bending and by torsion. To improve the basic concepts of neck posture, we approach the problem here from the viewpoint of functional morphology (in a strict sense), and, literally, from different views. Essential, but also largely unknown, is the arrangement of tension-resistant structures. Since these are usually not preserved in fossils, we have to make assumptions. To narrow down the multitude of possible assumptions, we use possible homologies with crocodiles and other living vertebrates, especially birds and mammals. The biomechanical analyses will be treated as results, replacing to some extent empirical data. Our “inverse” biomechanical analysis starts off from a structure (morphology) of the skeleton, and aims to determine the (unknown) behavior. In this article, we intend to broaden the basis of analysis by including a commonly underestimated stress quality, i.e., torsion, as well as comparisons of sauropod necks with sauropod tails and non-sauropod necks. The discussion focuses on comparisons with other vertebrates, which are seen as functional analogs to sauropods.

Cervical Ribs and Ossification of Tendons

Little attention has so far been paid to the meaning of the cervical ribs, which occur in all amniotes but are often reduced; e.g., in mammals. A typical cervical rib runs nearly parallel to the neck axis and carries an anterior and a posterior process [19]. The head of a cervical rib is divided into the dorsally located tuberculum and the ventrally located capitulum. The tuberculum connects the cervical rib dorsolaterally to the diapophysis of the neural arch and the capitulum is attached ventrolaterally to the parapophysis, which can be located on the centrum or the neural arch [19]. In sauropods, the posterior processes of cervical ribs may be shorter than, as long as its corresponding vertebra, or

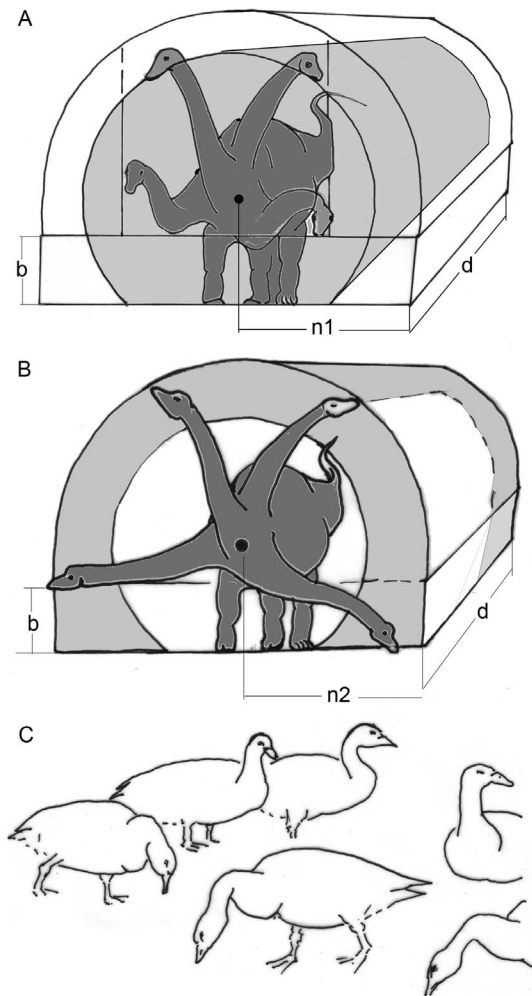


Figure 1. Influence of neck flexibility on the feeding envelope.

A) A flexible neck with limited excursion angles allows harvesting of a sector (yellow) of the theoretically possible entire feeding envelope. B) Free excursions at the basis of an otherwise stiff and inflexible neck give access to only a peripheral part of the entire potential feeding envelope. C) Long-necked Canadian geese can and do flex their necks freely. In relaxed resting as well as in watching positions, the necks are kept upright. Both neck positions keep energy requirements low. While feeding, birds usually reduce the bending moments acting along their necks by assuming a sigmoid neck posture: near the trunk the usual downward convexity, near the head a convexity directed upward. These curvatures of the neck reduce the lever lengths, specifically the distances between the neck base and the segment weights contained in the neck. Abbreviations: b = forelimb length, n = neck length, d = the distance c overed during a given time. All these values are of the same size in A and B.

doi:10.1371/journal.pone.0078574.g001

“hyperelongated” and extending back over several (two or more) cervical vertebrae. Such extremely long posterior processes of cervical ribs exist, for example, in *Giraffatitan brancai* and mamenchisaurids. In *Shunosaurus* and Diplodocoidea, the posterior processes of the cervical ribs are commonly shorter.

Frey and Martin [15] and Martin et al. [16] proposed a ventral bracing hypothesis in which the overlapping cervical ribs were bound into continuous rods by connective tissue and supported the neck ventrally. Following this hypothesis, cervical ribs transferred compressive forces and counteracted the torques of weight, which otherwise would have required a very muscular epaxial neck. The

ventral bracing hypothesis implies a rather horizontal neck posture and is only reasonable for an inflexible neck, because any deviation from a maximum ventrally flexed and extended position would have reduced the load, and thereby the bracing function, of the rod formed by the cervical ribs. Lateral flexion would have been largely restricted [20]. Contrary to the ventral bracing hypothesis, several authors [12,17,21,22] had postulated a construction which can be summarized as the “tensile member hypothesis”, in which the cervical ribs were used for transferring tensile forces over long distances, so that neck muscles could be shifted towards the trunk, thereby reducing the weight of the neck. The tensile member hypothesis is in agreement with all other tetrapod animals and allows more flexibility of the neck and is also in accordance with the dorsoventral neck mobility observed by Christian and Dzemski [20].

In two independent histological studies Cerda [23] and Klein et al. [24] found that the anterior and posterior processes of the cervical ribs of sauropods largely consist of longitudinally oriented mineralized collagen fibers, similar to what is known of the microstructure of ossified tendons [25,24]. The tuberculum and capitulum, however, consist of periosteal compression-resistant bone [24]. The anterior and posterior processes of the cervical ribs of the alligator (*Alligator mississippiensis*), of the ostrich (*Struthio camelus*), and of the sauropodomorph *Plateosaurus engelhardi*, also show longitudinal fibers instead of periosteal bone, indicating their origin as ossified tendons (Fig. 2).

In a living organism, bone is deposited in places that are not exposed to movement ([26,27], both resting on the experience of orthopedists and surgeons). If deformations (e.g., resulting from a fracture) cannot be excluded, ossification will not take place – so that a pseudarthrosis is developed instead of rigid bone. In addition, bone is modeled and remodeled under the influence of mechanical stress.

An old controversy is which sort of stress is responsible for the development of bone (older literature on mammals, summarized in [27]). Sverdlova and Witzel [28] recently have provided strong arguments that compressive stress alone leads to bone deposition, but this analysis was also confined to mammals. Among many birds (and possibly among sauropods and other dinosaurs) tendons have a marked tendency to ossify under the influence of tensile force (see also [29]) and in the absence of deformation. Forces on tendons are by definition produced by the muscles from which the tendons arise. Consequently, the only mechanical function known for all tendons is the transmission of tensile force, without regard to their being ossified or not. The strength of both ossified and fibrous tendons is largely the same. Therefore, the existence of an ossified tendon raises the question from which muscle it takes its origin and which function is performed by this muscle-tendon complex.

In a flexible neck, one insertion of an independent muscle is to be expected for each segment, although the transmission of tendon force on a bony element can also take place by passing a tendon through an annular ligament, which forces the tendon to change its direction or by crossing a protruding “hypomochlion”. The classical examples of such arrangements are the digits [30-32] and the knee joint [27,33].

The length of the ossified part of a tendon also implies that little to no deformation took place along its length, at least during development. The length of ossified tendons also tells us how far the muscle has been removed from the insertion of its tendon, although the origin of the tendon from pinnate muscle fibers may extend far into the muscle belly. A long ossified tendon thus indicates that a tensile force was exerted again and again in exactly the same direction, and that the distance between muscle belly and

insertion was long. The constant direction of pulling forces would be in agreement with the observation of a relatively stiff middle section in the necks of various animals [20]. The advantage of long tendons in slender, rapidly moved segments is convincingly explained in Klein et al. [24] by the reduction of mass along the neck and a concentration of the heavy muscle bellies in the posterior neck/anterior trunk region. The same mechanical principle has also been observed in the extremities of cursorial animals [34-36]. The great number of segments allows flexibility along the entire neck. Although necks of sauropods as well as those of birds are composed of many segments (i.e., cervical vertebrae), the range of movement of one segment against the next is limited [37]. Pronouncedly flexed neck postures seem to imply deformation of the cervical ribs, which would inhibit their ossification.

One major aim of the current paper is to understand what the longitudinal splitting of the ventrally flexing musculature (m. longus colli ventralis in birds) implies for neck posture and neck mobility in sauropod dinosaurs and how their cervical ribs can show such a marked tendency for elongation and ossification. We intend to develop a complete explanation for at least one among the varying shapes of necks in sauropods.

Methods

Premises for the Theoretical Approach

Our basic hypothesis is that all parts of the locomotor apparatus, including the neck, are optimized for fulfilling their functions that are “adapted” to sustain the loads applied during every-day life, while being as lightly built as possible with the available materials. This is in accordance with evolutionary theory and with Wolffs law [26] and Pauwels’ theory of causal morphology [27]. Both lead automatically to optimized “light-weight constructions” of the locomotor apparatus.

The most promising way to obtain better understanding of morphology is the investigation of extant vertebrates. The moments and internal forces evoked in static and kinetic conditions, as well as the skeletal and muscular structures, which resist these internal forces, can be studied directly in living forms. Because sauropods are extinct and have no living counterpart, this aim can best be approached by investigating their closest living relatives, crocodiles and birds, and functionally similar conditions in large cursorial mammals.

Crocodiles, however, do not have a very long neck, which characterizes sauropods. In addition, crocodylian tails fulfill a very special biological role, namely propelling the animal in water. Therefore, they are not fully convincing models, especially for studying the bending stresses in a long neck. The conditions of balancing the head in common terrestrial postures must be fulfilled by their morphological structures (bones, muscles and tendons) as well. Crocodiles do, however, show a behavior by which the neck is exposed to pure torsion: the often so-called “death roll” they use for hunting and feeding. As long as the animals are supported by water, no strong bending moments due to gravity obscure the torsional stressing of the neck. Special morphological traits of the crocodiles neck therefore seem to depend largely upon torsion and can be considered as “adaptations” to torsional loads. Therefore, it is reasonable to search for convergences of neck morphology between crocodiles and sauropods in spite of their obvious morphological and behavioral differences. Likewise, the tails of sauropods can be compared with those of crocodiles, although the use in each animal is different.

Obtaining data on internal forces is technically very difficult, and inflicting damage to the experimental animal is nearly inevitable. External forces can be measured with the aid of

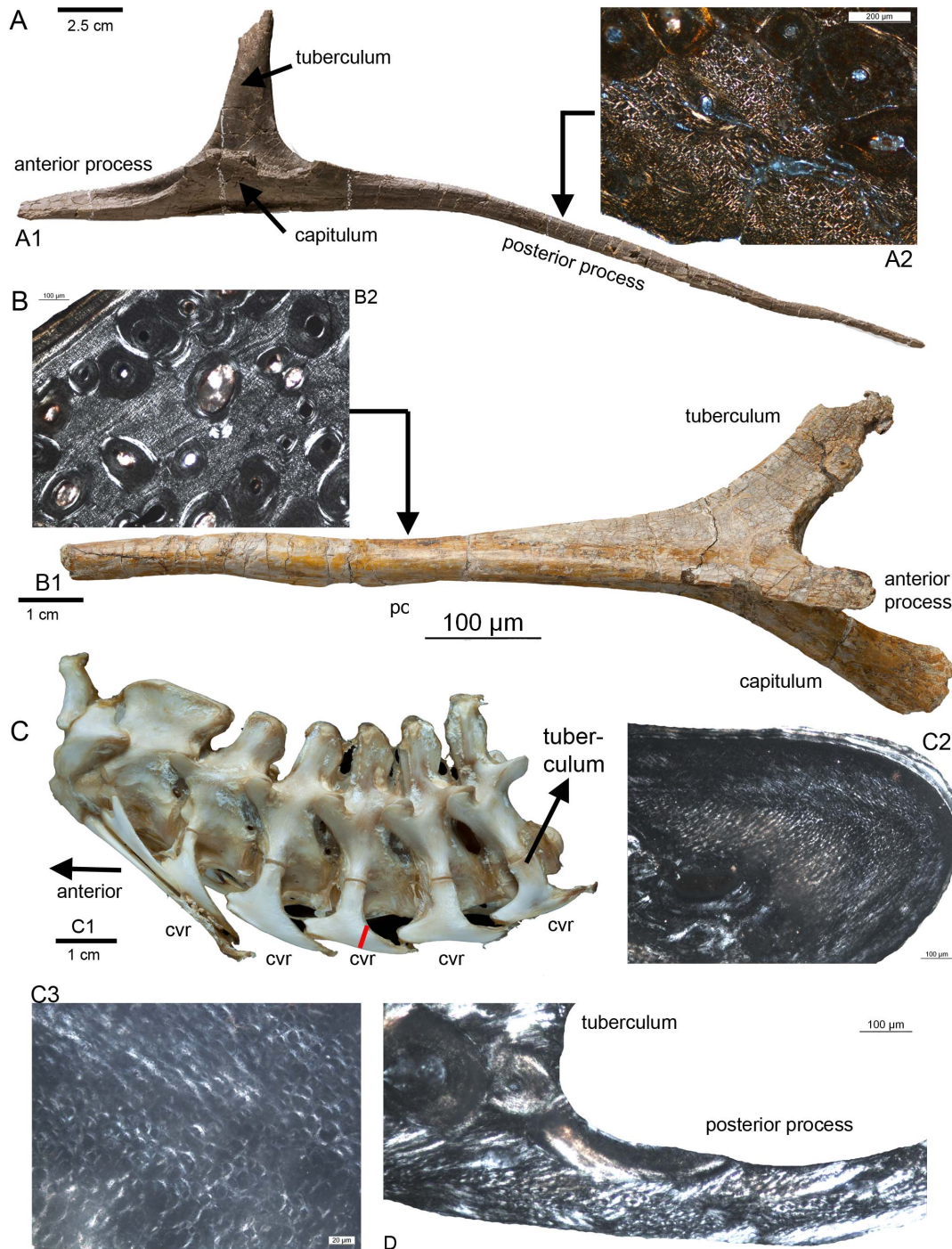


Figure 2. Longitudinal fibers in the posterior processes of cervical ribs of some archosaurs. A1) Cervical rib from the mid-neck region of a cf. *Diplodocus* sp. (Sauriermuseum Aathal, Aathal SMA HQ2) in ventromedial view. A2) Histological details of the posterior process of the cervical rib of a cf. *Diplodocus* sp. (SMA HQ2-D) in polarized light showing dense longitudinally running fibres between scattered secondary osteons. Note the diamond shape of the perpendicular cut longitudinal fibres. The fibres are surrounded by a sheath, which appears here mainly in white (see also Klein et al. 2012). B1) Cervical rib from the sauropodomorph *Plateosaurus engelhardti* (STIPB R 620) in ventrolateral view. B2) Histological details of the posterior process of the cervical rib of *Plateosaurus engelhardti* in polarized light showing dense longitudinally running fibres between scattered secondary osteons. C1) Neck from *Alligator mississippiensis* (STIPB R 599) in lateral view, exhibiting the cervical ribs still attached to the cervicals. In lateral view is only the dorsally located tuberculum visible. cvr = cervical rib. C2) Histological details of the posterior process of a mid-cervical rib of *Alligator mississippiensis* in polarized light showing dense longitudinally running fibres. C3) Enlargement of the same section, showing longitudinal running fibres. The red line on the posterior process of the mid-cervical rib marks the histological sampling location shown in C2 and C3. D) Histological sample of a posterior process of a mid-cervical rib of an ostrich (*Struthio camelus*, STIPB R 621) in lateral view and in polarized light showing longitudinally running fibres.
doi:10.1371/journal.pone.0078574.g002

extremely expensive machinery. Muscle activities are relatively easy to monitor by using the EMG technique, but the data obtained do not tell the whole story. The most relevant shortcoming is that EMG does not yield reliable data on the forces exerted by muscles. Therefore, the simplest way to develop a reliable idea about the biomechanical conditions is a theoretical approach, which is based on standard mechanical laws.

Our Theoretical Approach

The theoretical approach begins with precisely defined and plausible data and calculation of internal forces and stresses that show which structures are required and which shapes fit best. In fossils, the argument must be inverted: Only the skeletal structures are known, and we try to derive from them – under the premise of the basic working hypothesis of perfect “adaptation” of structures to function – the internal forces, the external loads, and finally body posture and the mode of locomotion. While the first step is quite reliable, the third and fourth steps are increasingly hypothetical – although still based on the laws of physics. Since these laws are generally valid, any agreement of traits in a living animal with identified mechanical rules confirms the correctness of the basic working hypothesis. The opposite, of course, is also true: If no agreement can be found, something must be wrong – in most cases, the error lies in the assumptions about stresses, which occur in particular movements.

The methods of theoretical mechanics are described in detail in several textbooks. Our preferred references are Lehmann [38] and Dubbel [39]. We use the terminology and common abbreviations developed by engineers. The most frequently used abbreviations are m for mass, F for force, r or l for length of the lever arm, or other distances. The product of the latter, the “moment” is named M . Weight is the product of mass (m) times Earth’ acceleration (g). The technical models were transformed to fit the shapes of animals. Extant animals that can be observed are the most informative, with emphasis on their neck posture and mobility as well as on their locomotive behavior. During locomotion the highest forces occur and must be sustained by the animal. If this condition is not met, the resulting failure is fatal for the animal. Lower forces, which occur in social or comfort behavior, of course can be sustained by stronger structures. Extant animals also can be dissected to identify the soft-part structures like ligaments and muscles, including their insertions at the skeleton. Information about the skeleton can be derived from both extant as well as extinct forms. Fossils only reveal information about their skeletons (bones) – the aim of our work is to obtain the missing information about their “mechanical function” in the sense of Bock and v. Wahlert [40] and understand the resulting implications for the behavior of Sauropoda.

Material

Most specimens considered in the current study are on display in public museums. All mentioned museums gave permission to study the specimens in their exhibition and/or collection. The sauropods *Brachiosaurus* (now *Giraffatitan*, Museum für Naturkunde, Berlin, Germany; MB.R.5002.1, MB.R.5002.3 - MB.R.5002.26, MB.R.5002.29, MB.R.5004, MB.R.5005.1-4 - MB.R.5007.1-19, MB.R.5000.1-25, MB.R.5000.26-50) and *Diplodocus* (e.g., *Diplodocus carnegii*, Naturmuseum Senckenberg, Frankfurt, Germany; SMF R462) were studied first hand. In addition, published illustrations of a number of other Sauropoda were considered. Our study is also based on first-hand observations and measurements of skeletons of several recent cursorial mammals in the collections of Institut dAnatomie of the Université Louis Pasteur in Strasbourg,

France, and the Naturmuseum Senckenberg, in combination with repeated observations of locomotor behavior of extant mammals. Names of the muscles follow the terminology of Fürbringer [41].

Results

Sauropod Necks in Different Views: Bending Under Weight

Seen from the side, the body of a quadrupedal animal can be compared roughly to a beam, or girder, with two cantilevers on either side, jutting out forward (head and neck) as well as rearward (tail) (Fig. 3). This construction is to be analyzed under static and under kinetic conditions. To get hold of the conditions in the three dimensions of space, the construction must be investigated from the side, top, and front. The anterior and posterior support is then, respectively, a pair of fore- and hindlimbs, and the movements – viewed from top-- of neck and tail outside the lateral plane become visible. This is not only relevant when the animal is feeding, but also during locomotion. Additional information can be supplemented by looking at the neck in the anterior or posterior views (see below). If viewed from the side, the most obvious stress quality is **bending**, evoked by the masses of the segments of the beam, or body stem, multiplied with gravity (= weight forces) and lever arms (= bending moments). The weight forces act in a vertical direction and their lever arms are greatest if the neck is kept horizontal. This leads to very high bending moments, which must be counteracted by tension-resistant structures (ligaments, muscles) on the dorsal side of the neck. The morphological “adaptations” of the sauropod neck to bending under the influence of body weight have received much attention in the literature [20,21,42,43]. While the length of the neck is documented by the fossil bones, the weight of the neck is presently under discussion. Light-weight construction, especially pneumatization of the cervical vertebrae, is responsible for the very low neck densities (< 0.5) assumed by Taylor and Wedel ([5]: p16). Even if this low value is correct, the mechanical problem of controlling enormous bending moments and mass moments of inertia persists because of the extreme length of the neck. In addition, this approach does by no means explain the function of cervical ribs, which are located ventrolaterally to the column of vertebral centra; neither does the investigation of the lateral view explain the obvious morphological differences between necks and tails of dinosaurs. If viewed from the side, both are cantilevers, consisting of a big number of long rigid segments, which must be kept in equilibrium against gravity. In spite of this similarity, their shapes deviate.

Two sometimes neglected, though very simple, conditions become clearly visible in side view: first, alone muscles can keep a neck at variable heights, while the given lengths of ligaments place it in one, invariable position. Second, the absolute maximum for all moments evoked by the neck is set by the trunk mass: Neither the static moments of the neck ($F_{mn} * l_n < F_{mt} * l_t$) nor its mass moments of inertia ($F_{mn} * l_n^2 < F_{mt} * l_t^2$) can become greater than that of trunk plus tail plus extremities. The same fact was noted by Taylor and Wedel [5].

The greatest forces are evoked by segment weights and by the inertia of their masses. The masses of head and neck – or of the tail – are distributed along the length. If cut into segments, each of the segments exerts a weight force (F_{mi}). These forces are multiplied with their distances from the pivot to yield ventrally directed bending moments ($F_{mi} * l_i$). The bending moments add up to a maximal value at the pivot that is the joint between the most proximal neck vertebra and the most cranial thoracic vertebra (Fig. 4). The envelope of all these bending moments, exerted by all segments, follows an exponential curve (Fig. 4). The moments can

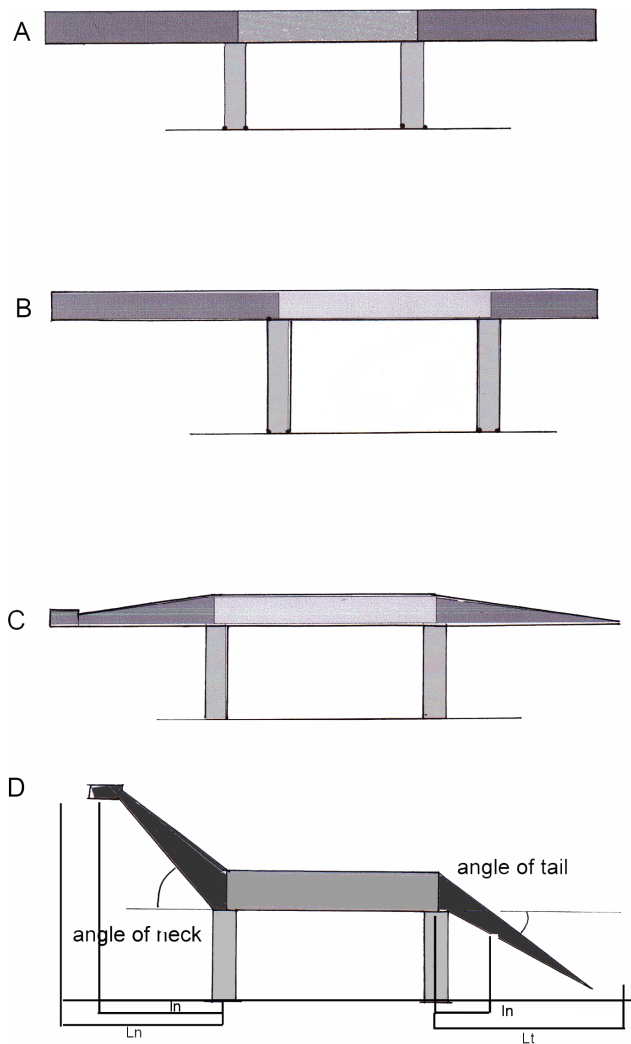


Figure 3. Simplified model of a sauropod dinosaur: A heavy beam on two pairs of support (limbs). The bending moments vary dependent from the lengths of the segments (A and B), dependent from the mass distribution (A and C), and dependent from the inclination of the cantilevers at both ends (A and D). The current study is focused on the cantilever segments (dark grey). L is full neck or tail length, l indicates the lever lengths of segment weights.
doi:10.1371/journal.pone.0078574.g003

be reduced by choosing flexed postures of the neck (Fig. 1), which reduce the lever arms. The bending moments evoked by weight in all postures must be balanced at each intervertebral joint by the moments exerted by one of the tension-resistant structures (muscles or ligaments). To allow free choice of postures, these structures must insert into each individual vertebra. If muscles (tension-resistant structures of variable lengths) are present, the positions of all segments can be chosen arbitrarily. This is not the case if ligaments (tension-resistant structures of defined lengths) counteract weight, because tough, collagenous ligaments have a length limit that cannot be exceeded and arrests further movement. If elastic ligaments are present, the force they produce depends upon the degree to which they are stretched. If such a ligament is not pre-stretched, it produces no or a very small force. If a given length is reached by stretching the elastic ligament, an equilibrium results and the elastic ligament stops further movement as long as the moving force (e.g. weight) remains unchanged.

On the other hand, if the movement leads to a relaxation of the elastic ligament, it does not exert any force on the skeletal structures, which then can be arranged in any position, without being influenced by the ligament.

The height, to which the head is lifted on the neck, influences the bending moments by reducing the lever arms (l), following the formula: $I = L * \cosine \alpha$, where L is neck length and α the angle against the horizontal (Fig. 3A).

The necks of mammals and the tails of sauropods are also characterized by tension-resistant fibrous or muscular structures that in side view space apart from the vertebral column so that they have long lever arms, which are less pronounced in transverse direction. The farther removed from the vertebral bodies, the longer the lever arms and the greater their moments around the joints between the centra. In the neck vertebrae of sauropods and of most mammals, there are no or at least no apparent dorsal extensions of the skeletal elements (= spinal processes), the whole space between the vertebrae and the contour being filled with tension-resistant soft tissues. The lever arms are long because the nuchal ligaments and the muscles have their origins at the spinal processes of the anterior dorsal vertebrae, between the transverse processes (and ribs) and their tips. The reverse is true in the tails. The spinal processes are elongated in the anterior thoracal segments, forming something like a “withers” (Fig. 5A). Although only a part of the muscle fibers is attached to the spinal processes of these trunk vertebrae, the major part of the nuchal ligament in the neck or the supraspinal ligament in the tail is attached to the tips of the long spinal processes. To better resist the high longitudinal tensile force exerted by the ligaments (Figs. 4, 5A) the spinal processes of the anterior thorax are inclined rearward. By this inclination the spinal processes have the same direction as the resultant of all major forces acting on them and bending moments do not occur while the spinal processes are under compression (Fig. 6). If, however, the muscle forces are increased, or the ligaments heavily pre-stretched, the resultants may deviate temporarily from the spinal processes, so that bending moments are evoked. In addition to their inclination, the spinal processes possess very large diameters in the direction of the tensile forces and therefore remarkable bending strength. It can be assumed, that this sort of loading is only transitory, because a new equilibrium is established rapidly by muscle reflexes.

Sauropod Necks: Twisting and Torsional Stress

Additional information can be supplemented by looking at the neck in anterior or dorsal views. Figures 7 and 8A, B show hypothetical sauropods with their necks flexed laterally and Figures 8B, C show their head turned. The neck segments proximal to the lateral flexure are exposed to torsion. The torsional moments (M_t) are defined by $M_t = F * r$, where F is the weight of the segments distal to the bend, and r the distance from the longitudinal axis of the proximal neck to the center of mass (CoM) of the laterally flexed segments. Figures 7A and 7C illustrate muscles that counteract the torsional moments and thus give the neck the characteristics of a cantilever supported solely at its base. Actual rotation about the longitudinal axis of the neck – which is impossible in extant animals [13,35] – is not necessary for evoking torsion. Along the twisted proximal part of the neck, torsional moments are constant (Fig. 7A-C). If, however, the lateral curvature of the neck is shifted proximally, the maximal torsional moments can increase with the masses of the neck segments distal to the curvature and with their lengths, which means the increase follows an exponential function (Fig. 7G).

The sort of loading which causes “torsion” (Figs. 7, 8) in the neck can best be illustrated and analyzed in crocodiles (Fig. 9).

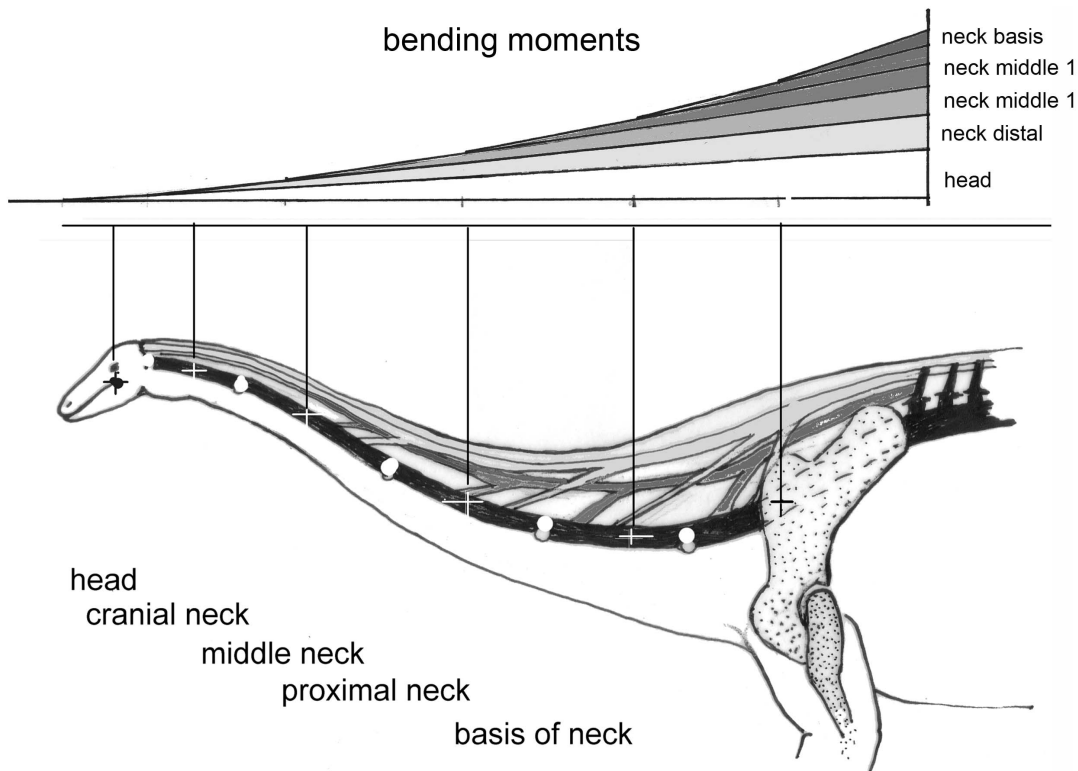


Figure 4. A) Schematic neck of a sauropod to show joints (open circles), centers of segment masses (crosses). B resulting bending moments. Skeletal structures are in black, ligaments are in dark grey and muscular structures are in light grey. The pull of these structures exerts compressive forces in the vertebral column (black). Note that muscular structures of variable lengths are needed to keep the joints in balance against segment weights, in all positions in which the ligaments are not pre-stretched. Stretching of the ligaments leads to forces which make further movement impossible, so setting limits to neck mobility.
doi:10.1371/journal.pone.0078574.g004

During the "death roll behavior", the neck is exposed to huge torsional moments when transmitting the twisting forces from the trunk to the head [44] (Fig. 9A). To keep the intervertebral joints

in balance, tensile forces running obliquely from the shoulder girdle and thorax to the head must be countered by oblique muscles, which control the position of each vertebra. These muscles are arranged in chains, and some of them act directly on the head, without contact to the neck (like the *m. collosquamosus* and *m. longissimus capitis* [45]). In a crocodile, the necessary force components are labeled F_{m1} , F_{m2} , and F_{m3} (Fig. 9B). Each component is provided by a group of muscles that block rotation of the neck around its longitudinal axis on the side where the head is forced to rotate dorsally and the trunk ventrally (own dissections, as well as [41,45,46]). The force component F_{m3} comprises the *m. trapezius* (connecting the lateral surface of the scapula with the spinal processes), *m. rhomboideus* (connecting the vertebral margin of the scapula with the spinal processes), and at the neck segments two to four, deep layers of the *m. cervicis* (= *m. multifidus*, extending from transverse processes of more caudal vertebrae to spinal processes of more cranial ones). Group F_{m2} includes the *m. levator scapulae* or *m. serratus profundus* (running from the vertebral margin of the scapula to the transverse processes of the vertebrae) and, at the posterior neck segments, the *m. multifidus*. Component F_{m1} is provided by the *m. scalenus* (or *m. costocervicalis*, see [45]), which connects the most anterior thoracic ribs to the "neck ribs", exerting force along their greatest length [44]. Thus, the tendons of the *m. scalenus* are the most probable candidates for ossification in the case of the sauropods.

Figure 5. Neck of a horse as example of a cursorial mammal. A) Horse neck plus head in side view. B) Bending moments caused by segment weights in analogy to the sauropod in Figure 4. C) Cross section through a horse neck at the level of cervical 7. This arrangement of structures is highly specialized to sustain the bending moments that occur in the mediosagittal plane and are visible in side view.
doi:10.1371/journal.pone.0078574.g005

In all tetrapods, the ventrally directed tensile forces are taken over from the transverse processes of the neck vertebrae by the fibers of the transversospinal or multifidus system. The muscle chain is continued on the contralateral side and the oblique tensile

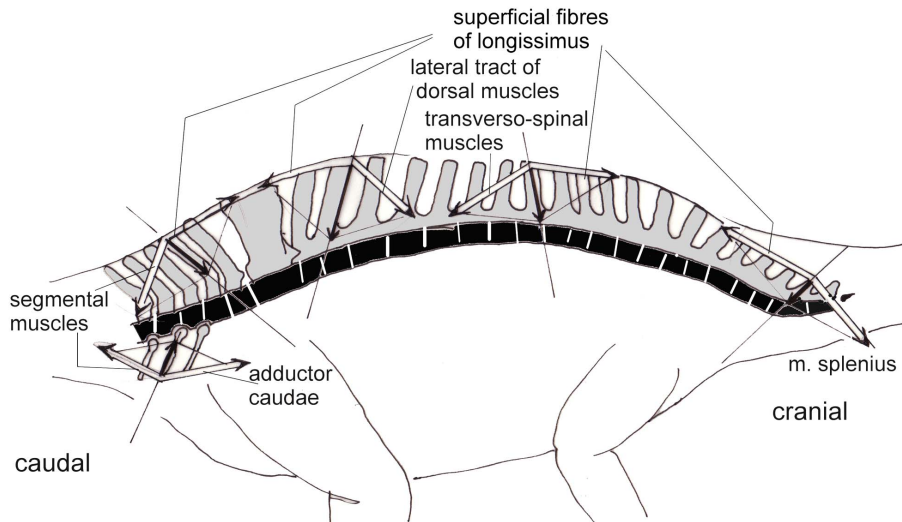


Figure 6. Direction and loading of spinal processes (neuroapophyses). The spinal processes of the tail of a sauropod are not exposed to bending if directed along the resultant of all forces acting on them. Instead of the ligamentum superspinale, a longitudinal muscle leads to the same result. If the muscle forces are increased, or the ligaments heavily prestretched, the resultants may well deviate at least temporarily from the spinal processes. In these cases, bending strength is required. doi:10.1371/journal.pone.0078574.g006

force is transmitted to the head by the *m. splenius* and *m. semispinalis capitis* (Fm3). The *m. sternomastoideus* has the same function but crosses the whole distance from sternum to head without contact to the neck vertebrae.

The parapophysis of the vertebra connect the capitulum of the cervical ribs to the axial skeleton, and the diapophysis of the vertebra connects the tuberculum of the cervical ribs to the axial skeleton, and thus both keep the twisting forces far away from the necks longitudinal axis. Their long lever arms (Figs. 8, 9) allow reduction of muscle forces but make movements slower than short lever arms would do. By being stretched passively or by active contraction, the above mentioned muscles exert compressive forces directed medially against the axial skeleton (Fig. 10C), specifically against the capitulum and tuberculum of the cervical rib as well as against the parapophysis and diapophysis of the vertebrae. Indeed, the connections between vertebrae and cervical ribs are suited to sustain compression [24]. Because the neck skeletons of crocodiles possess morphological features very similar to those that can be observed in diplodocid and brachiosaurid sauropods, the arrangement of cervical ribs and their anchoring to the neck vertebrae can be identified as “adaptations”, well suited to resisting the torsional stresses with a minimum of material.

Ossified Tendons on the Ventrolateral Side of the Neck and Their Implications for Neck Mobility

The long posterior processes of the cervical ribs of sauropods contain mostly longitudinal fibers [23,24], and therefore must be interpreted as ossified tendons. This raises two questions: first, how are tension-resistant structures or muscle-tendon complexes on the ventrolateral sides of cervical centra used, and second, to which muscle(s) could they have belonged? The answer to the first question seems to be simple: If contracted on both sides simultaneously, the muscle-tendon complexes flex the neck ventrally (like the *m. longus colli ventralis* in birds). For the development of muscle-tendon complexes it is unimportant whether intervertebral flexion takes place or not; the tensile forces are also required for keeping balance between the segments in static situations, not just for movement. The splitting of the

tendons to insert into each vertebra allows precise control of the exact position of these vertebrae.

Not so easy to answer is the question why muscles are recruited for ventral flexion in a forwardly inclined neck of a sauropod, because the weight of neck segments and the enormous distances from the segments to the base of the neck yield ventrally bending moments without any expenditure of energy – as was discussed often in the literature (e.g. [18,37,42,47]) and is illustrated in Figures 5, 6, and 7. Unilateral contraction of muscles ventral to the vertebral column (Fm3 in Fig. 9B) primarily leads to ventrolateral bending and turning the distal neck segments or the head. Even if no movement takes place, stresses occur and must be counterbalanced. If the head is kept in its position, by its weight or inertia, or by foliage resisting being cropped, the torsional stresses occurring in the neck can be taken over by the muscle of only one side.

The second question raised above, to which muscle the ossified tendons belonged, is difficult to answer because soft part anatomy is not preserved and the functional analogs are contradictory: In crocodiles as well as in sauropods, the posterior processes deviate from the vertebrae caudally, which is visible in dorsal and in lateral view. They point towards the direction of a rather lateral origin, perhaps on the anterior ribs like the *m. scalenus* (Fm3 in Fig. 9B). From a phylogenetic perspective, it is equally likely that the muscle attaching to the cervical ribs in sauropods is the *m. scalenus* as in crocodiles, rather than the *m. longissimus colli* as in birds (see below). It should be noted that the *m. longus colli* passing along the ventral surfaces of the cervical centra is present in crocodiles – similar to the arrangement in mammals [45].

Flexibility of Sauropod Necks

Sauropod necks are divided into 14 to 19 neck segments, which can be moved against each other. This is similar to the situation in birds, which has been investigated systematically by Dzemplski ([37], but see also [18,20]). The excursions in the intervertebral joints add up to the full mobility of the neck (Fig. 10). If the mobility between neighboring vertebrae as observed in ostriches is taken as an example, a total flexion of the neck by 90° is reached or exceeded by a chain of seven (proximal) segments. A greater

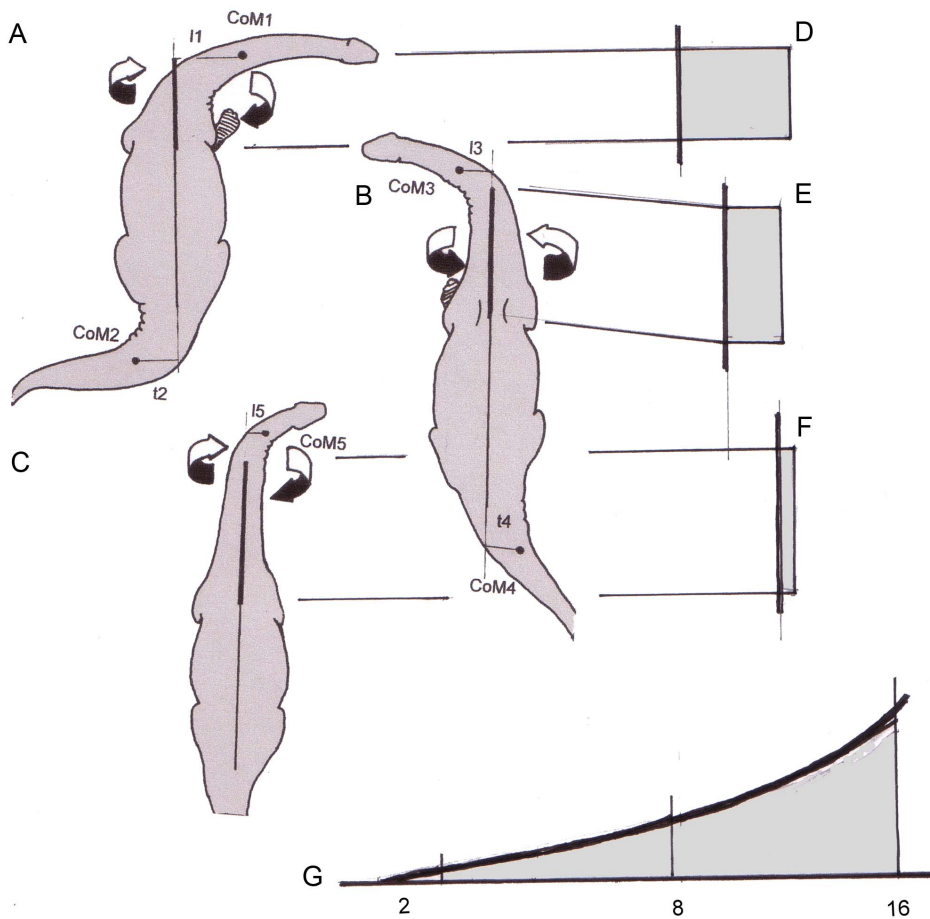


Figure 7. View from above (top) on sauropods, which flex their necks laterally. A – C) The proximal neck segments exposed to torsion are marked by a heavy long axis. The dots are the CoM (centers of mass) of the head plus neck segments distal to the flexed joints. The masses concentrated in the CoM (CoM 1, 3 or 5, respectively) become smaller with a distal shift of the flexure and their lever arms (l_1 in comparison to l_3 or l_5) become shorter. A) The moment of the heavy and long neck is so great, that the inner (right) foot must be placed laterally in order to expand the area of support and to prevent imbalance of the whole animal. B) The same is shown for flexion of the neck to the left. C) The rotating moment is so small that it does not require a lateral placement of a forefoot. D – F) Torsional moments evoked by lateral flexion remain constant along the posterior part of the neck. In all cases shown here, the tails are flexed into the direction opposite to the neck. So the imbalance caused by lateral flexion of the neck can be reduced. The degree to which the tail can be used to counterbalance the neck depends from the ratio $CoM\ 1 * l_1/CoM2 * l_2$, or $CoM3 * l_3/CoM4 * l_4$, respectively. G) Maximal torsional moments that can occur along the neck from segment 2 – segment 16. doi:10.1371/journal.pone.0078574.g007

number of segments would lead to more pronounced flexion. The degree of flexion or the “sharpness” (minimal radius) of the curvature also depends on the lengths of segments: The shorter the segments, the shorter the radius of curvature (Fig. 10C). Longer segments in turn lead to a less pronounced curvature (Fig. 10A, B). The same drawing (Fig. 10B) illustrates a side-effect of ossified tendons: if the posterior processes of the cervical ribs are shorter than or as long as the vertebrae (such as in *Diplodocus*, *Apatosaurus*, and *Alligator*), these rigid elements do not at all influence flexibility of the neck. At the level of the intervertebral junctions, the tendons consist of collagenous fibers, which can easily be deflected. If the posterior processes of the cervical ribs are longer than one segment (such as in *Giraffatitan* and mamenchisaurids), they approach the neck vertebral column on the concave side, while being removed from the vertebrae on the convex side of the flexion. If the posterior processes are ossified tendons, the lever arms of these tendons at the concave side of neck flexion (no matter in which plane it occurs, mediolateral or dorsoventral) are long at the nearest intervertebral joint, but decrease posteriorly until they make contact with the vertebral column. At the convex side of the

curvature, the lever arms of the pulling forces increase continuously in the posterior direction, making the effect of a contraction stronger and stronger. At the posterior tip of the cervical rib, the tendon must be tied to the vertebra, either by muscular fibers attached to the bony element or by tough connective tissue, which redirects the direction of pulling force. No histological evidence exists for such a tying, however [24]. In addition, the tendons cannot escape being bent – which would make ossification improbable. Thus, only one conclusion seems convincing: that active flexibility was limited where the long ossified tendons exist. Ossification can be taken as an indicator of a straight flow of forces across several joints without any change of direction.

Tails of Sauropods and Crocodylians

In the case of sauropods, no realistic idea seems to exist as to what the animals did with their tails – except keeping them horizontally and serving as the posterior insertion of the caudofemoralis muscle [48] or as a counterweight for the neck [49,50]. For comparison, we consider the tails of crocodylians that serve a clear-cut function, propulsion in water. Anyway, a major

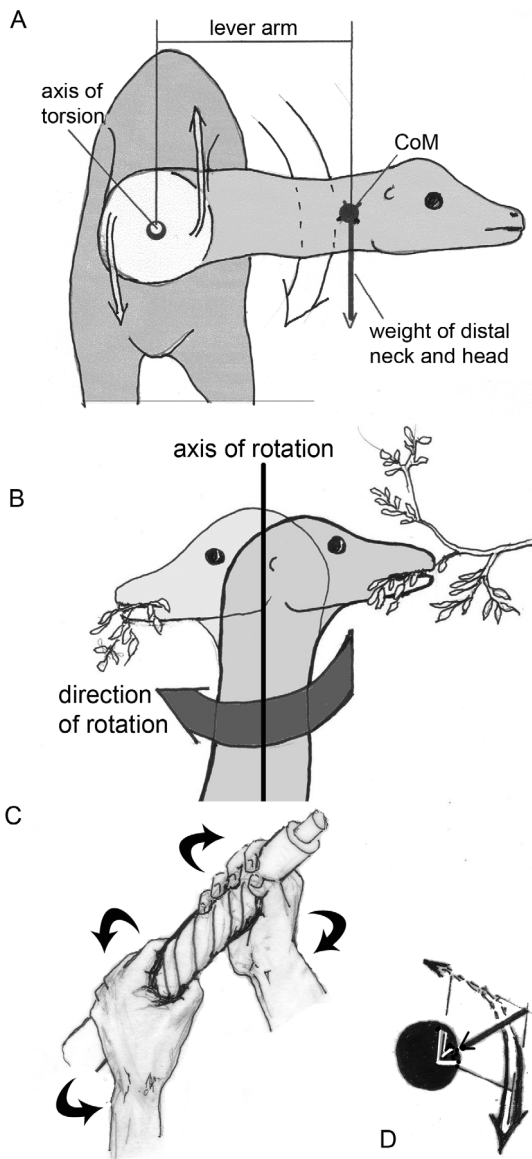


Figure 8. Torsional stresses which are evoked by twisting the neck. A) Anterior view on a sauropod flexing its neck laterally. The product of weight of neck plus head * lever arm is the torsional moment around the axis of rotation along the proximal part of the neck. F_{m1} and F_{m2} are schematic representations of the oblique neck muscles described in the text, whereby the components along the length of the neck are ignored. B) Vertical neck position and turning the head from right to left, e.g., for stripping foliage from a branch. The movement is resisted by the strength of the branch, which exerts a force directed to the right. This resistance must be overcome by active torsion of the distal neck. C) To realize torsion, imagine a wet cloth, which is wrung out by both hands. Its fibers form a spiral between the points of force application. Doing so, the length of the cloth between the hands is shortened, and at the same time the oblique fibers exert a resultant force against the center – exactly as the oblique muscles of the neck exert a re-directional force against the vertebral column (stick), which is also compressed in its longitudinal direction. doi:10.1371/journal.pone.0078574.g008

functional difference between necks and tails is the application of external forces. This difference has several reasons: In spite of the lack of a masticatory apparatus as in mammals, the heads in sauropods are usually heavier than the tips of their tails. External forces are often concentrated at the jaws, while external forces

acting against the tail are usually distributed over a considerable part or its entire length (for example water resistance in swimming, ground reaction forces compensating a part of the weight). Twisting plays a lesser role for the tails than for the necks. In addition, flexibility of the tail is less pronounced and the musculature is less differentiated than that of the neck in all land-living vertebrates [45,51,52].

Like the necks, the long tails of reptiles are exposed to bending moments because of their weight, especially if carried without ground contact more or less horizontally.

In the case of most dinosaurs no traces of drag marks of the tail have ever been found, so we may assume that this appendage was kept in a rather invariable position at the level of the pelvis, well above the ground. In view of their limited mobility, a “specialized” profile, as is characteristic for the necks of mammals (see also Fig. 5) can be expected in the tails of all sauropods. The arrangement of tension-sustaining elements with long dorsal lever arms leads to high and narrow cross sections of the tails – like in the necks of mammals (see below) and the tails of crocodiles. The arrangement of the sagittal vertebral processes, especially the presence of the neural spines on the dorsal side, limits pronounced dorsal and ventral flexion, which is in strong contrast to the situation in the neck. These processes provide firm insertions for ligaments and so reduce the need to control the tails position actively by expending muscular energy.

The tail vertebrae in sauropods as well as in crocodiles also possess ventral processes (hemapophyses) of variable length in addition to the long dorsal neural spines. In *Diplodocus*, for example, the caudal vertebrae posterior to the second caudal show hemapophyses. In all cases, the “strong”, that is broad and rearward inclined, dorsal processes are rigidly fused to the neural arches, whereas the more slender ventral processes are weaker and not rigidly fused to the centra, but attached to them in a sort of joint. Although only a part of the muscle fibers is attached to the spinal processes, the major part of the supraspinal ligament is fixed to the tips of the long spinal processes. The exact direction of the resultant of all tensile forces acting on the spinal processes is not predictable. Therefore, height resistance of the rigid dorsal processes makes sense. Their inclination keeps bending moments within the neural processes and at their bases (Fig. 6) at a low level. In addition to their inclination, the spinal processes possess a shape that provides great bending strength. Obviously, the dorsal processes are better suited to sustain the bending moments exerted by tensile structures attached to their tips than the ventral processes. The rearward inclination of the dorsal processes of the tail vertebrae corresponds to the forward directed tensile force acting on them. The anterior insertions of these tensile structures are the spinal processes of the posterior trunk, which are long and inclined somewhat forward, comparable to the withers at the base of the neck in the anterior trunk segments of cursorial mammals. The combination of rigid and long dorsal processes with ligamentous passive elements of defined lengths implies rigidity, or at least limited mobility of the tail. The bending moments occurring in the necks and tails also influence the bending of the trunk region [42,43].

If indeed the position of the tail was invariable, the tensile structures to support the tail may possess a definite length, like ligaments, rather than being able to adapt their lengths, like muscles. In fact, some dinosaurs, such as hadrosaurs, show ossified structures in their skeleton comparable to the muscle insertions in Figure 6. The advantages of ligaments and tendons are their ability to exert force (some 1700 N/cm²) without expenditure of energy and their lower weight. Muscles, by contrast, are weaker (something like 50 N/cm², the values vary tremendously), much

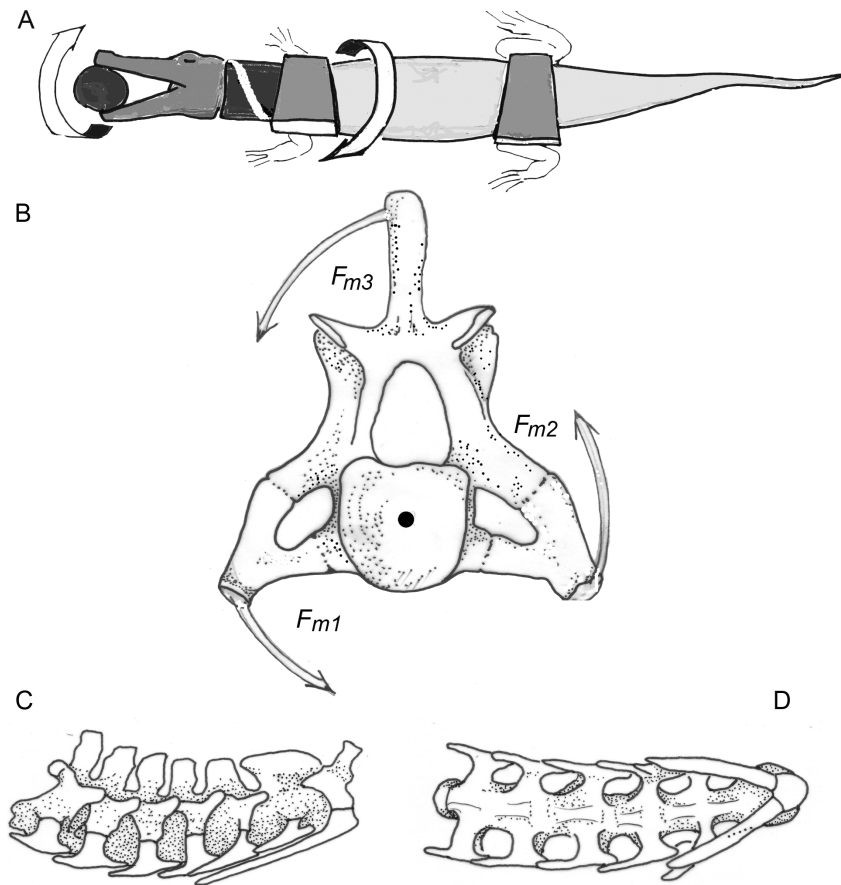


Figure 9. Death roll in a crocodile and its mechanical consequences for the neck. A) Schematic drawing of a crocodile performing the death roll. The head is anchored by the jaws, while the trunk rotates about its longitudinal axis. The neck segments are kept in equilibrium by muscles pulling in the direction of the white band. B) The seventh neck vertebra of an *Alligator mississippiensis* in posterior view. F_{m1} - F_{m3} are the muscle components in the transverse plane which counter the torsional moments exerted while performing the death roll. C) Part of the neck skeleton of the *Alligator mississippiensis* with the cervical ribs (white) in side view. D) Part of the neck skeleton of the alligator in ventral view. The head points to the right in both cases.

doi:10.1371/journal.pone.0078574.g009

heavier and require much energy if actively contracted. The musculature of sauropod tails commonly is reconstructed on the basis of homology, or as in this study, of (hypothetical!) biomechanical needs. Homology can be based on the muscles of crocodiles. Unfortunately, the information in the literature is not precise, but confined to generalized statements about the stem musculature. Often authors classify muscles just as “primitive”, meaning that muscles are segmented and arranged similar to fish tails.

As noted above, the hemapophyses of the tail vertebrae are attached to the centra by joints, which provide long lever arms for the hypaxial muscles while permitting longitudinal flexion of the skeletal elements against the body axis instead of sustaining torque. In the transverse direction, the two branches forming the hemal arch provide remarkable strength against being bent in the transverse direction. The increase of strength follows a parabolic function, corresponding to loads distributed over the whole length of the hemapophyses [53]. This makes sense in the case of crocodiles, which expose their tails to water resistance, but not in sauropods. Keeping the tail in its position requires not just strong torques in the dorsal direction by the tensile structures attached to the neural spines, but also devices for keeping balance in the opposite, ventral direction. Muscles on the ventral side may well be weaker than the epaxial muscles, and indeed many dinosaurs

possess shorter and more slender hemapophyses. As in the necks of sauropods, torsional stresses must be expected in long tails as soon as a lateral flexion takes place (Fig. 10). The arrangement of the m. caudofemoralis in fact is suited to control the torsion on the convex side of any lateral flexion.

In the absence of direct evidence for tail use and tail function in sauropods, it seems worthwhile to go into details of tail anatomy and function in their closest extant relatives. Crocodiles and also lizards usually tow their tails behind when walking on the ground, and lift it only in rare cases and for a short time off the ground. Bending and torsional moments are reduced by this behavior. In crocodiles that walk rapidly (“high walk”) or run on firm ground, the tail is partly balanced by the dorsal muscles, while during the “low walk” or slithering, the tail is propped against the ground or resting on it and gives the caudofemoralis muscle a solid, immobile caudal insertion for retroverting the hind limbs [54].

According to Gatesy [48], Fehner [55] and Mallison [50], the m. caudofemoralis was also responsible for retracting the hind limb during terrestrial locomotion of sauropods, just as in crocodiles. Because it connects the femur (fourth trochanter, see e.g., [56]) with the transverse processes of the anterior caudal vertebrae, the m. caudofemoralis exerts a ventrally flexing moment on the tail. Because no tail drag marks are known, ventral flexion of the tail during retraction of the thigh seems to be excluded in

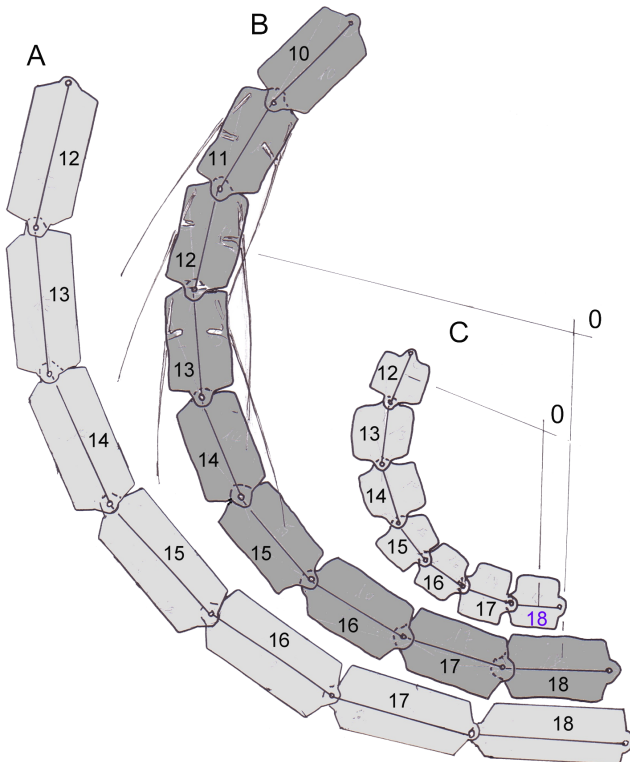


Figure 10. Proximal part of a schematic neck seen from on top illustrates flexibility. A) Elongation of the segments (cervical vertebrae) makes the radius of curvature longer. Note that the cervical ribs do not contact vertebrae because they deviate ventrally from the axes of the centra. B) The segments (cervical vertebrae) 12 – 18 are deflected by 20° each. This corresponds to the lateral deflection observed by Dzemski (2006) in the ostrich. In addition, (long) cervical ribs are shown on both sides of the vertebrae. C) Shortening of the segments leads to a sharper curvature of the neck. doi:10.1371/journal.pone.0078574.g010

terrestrial sauropods by the strong tension-producing structures, muscles or ligaments, dorsal to the axial skeleton (see above).

External Ground-Reaction Forces depending on Neck Posture

Because of its length, neck posture exerts a strong influence on the **external equilibrium** of the whole animal. The external equilibrium requires that

$$F_1 * l_1 + F_2 * l_2 + F_5 * l_5 + F_6 * l_6 + F_7 * l_7 = F_{v1} * l_f,$$

if the neck is kept horizontally, or, if the neck is elevated,

$$F_1 * l_3 + F_2 * l_4 + F_5 * l_5 + F_6 * l_6 + F_7 * l_7 = F_{v2} * l_f$$

(under the condition of equilibrium of moments: sum of all moments acting on the hind foot = 0).

From the condition of equilibrium of forces (sum of all forces = 0) follows that the sum of all segment weights (*F*) equals the sum of reaction forces (*F_v* and *F_h* in Fig. 11). Obviously, the values *F₁* * *l₁* + *F₂* * *l₂* are greater than *F₁* * *l₃* + *F₂* * *l₄*, and therefore the horizontally held neck leads to much higher ground reaction

forces in the forelimbs (*F_{v1}*), than a vertically erected neck (*F_{v2}*). In other words, the center of total body mass is shifted forward by stretching the neck horizontally, and shifted rearward by assuming a more upright position. If a mass distribution similar to Henderson [57] is taken as an example, the forelimbs carry 39% of total body weight when the neck is kept horizontally, but only 26% when the neck is elevated (Fig. 11). The difference between the reaction forces on the forelimb is 33.3%. Indeed the imprints of forelimbs in the majority of sauropod tracks cover much smaller areas than those of hind limbs (Laebe, unpublished data; [58]). This clearly indicates smaller loads on the forelimbs than on the hind limbs because the ground reaction forces are distributed over the contact area (that is the sole) of the limb. In addition, the imprints of the forefeet are shallower than those of the hind feet [58–60], which also indicates more weight on the hind limbs, although this relationship cannot yet be quantified. Especially, lateral flexion of the horizontal neck leads not only to torsional stresses at the base of the neck, but also requires lateral placements of a forefoot including abduction in the shoulder joint (Fig. 7, 10; [61]). Such a sprawling posture would be in line with the characteristic shape of the head of the humerus and the orientation of its greatest diameter transverse to the sagittal plane in sauropods.

Discussion

Sauropoda

What we can see in fossils are morphological peculiarities (characters) of the skeleton, but what is missing is the functional meaning of these characters. Nevertheless, it is quite usual to talk about “adaptations”, without considering that the use of this word implies a functional hypothesis. These hypotheses are often not justified. Only if the functional value of a character can be defined clearly (perhaps quantitatively!), we may conclude that the characters are “adapted”. According to Wolff [26] and Pauwels [27], the existing shapes are developed under the influence of mechanical stresses and therefore fit perfectly to the loads acting on them: morphology is per se “adapted” and this means that the patterns of stresses under which the shape was formed can be observed. The problem we are still facing is: What makes up the relevant functional stresses, which have shaped a particular (morphological) character? The variables we are searching for by applying inverse biomechanics are body posture and mode of locomotion. Limits (or “constraints”) of our search are given by functional analogs among mammals and recent birds.

Regardless of their preferred inclination, sauropod necks are exposed to bending. The lengths of the lever arms may vary, following the cosine of the inclination angles. Sauropod necks are also exposed to considerable torsional moments. In spite of lightweight-constructions [5,62], the enormous lengths of some sauropod necks evoke very high bending and torsional moments, especially in more or less horizontal neck postures. Counteracting against these moments requires muscle activity. The activity of muscles costs much energy, even if only slowly contracting “red” muscle fibers are involved. The fact that the lateral flexion of a more or less horizontal neck inevitably leads to torsional moments in the neck section proximal to the flexure is commonly overlooked. Our analysis shows that the structures summarized under “cervical ribs” are well suited to sustaining torsional stresses.

Cervical ribs of less than a vertebra’s length remain straight and are without influence on neck flexibility even in pronounced bending of the neck (Fig. 11). Great length of the cervical ribs requires deforming the bony elements, which inhibits the process of ossification in the tendons. A general condition for ossification is

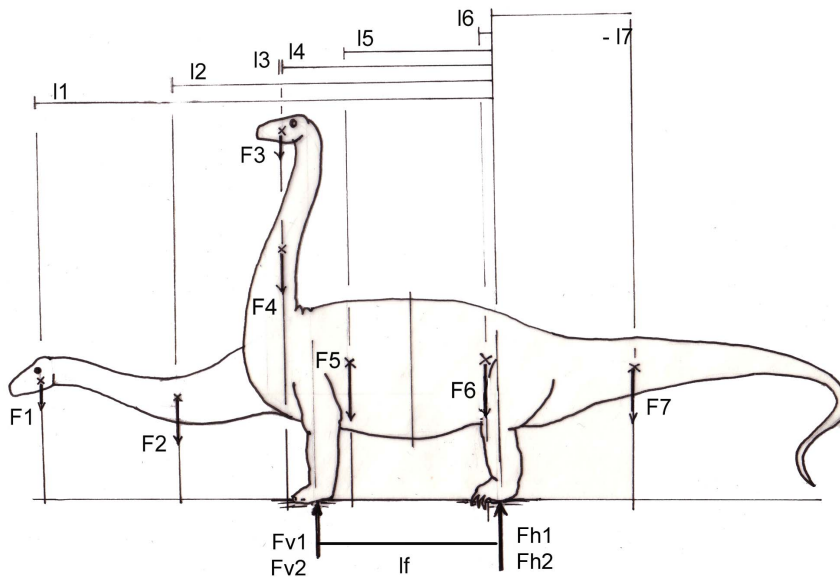


Figure 11. External equilibrium of a sauropod, depending on neck posture. External equilibrium is determined by the moments of segment weights about the hind feet, which must be equal to the ground reaction force F_{v1} or F_{v2} , respectively, exerted by the forefeet with a lever arm l_f ($F_v \cdot l_f$). Note that the tail exerts a nose up-rotating torque, because of its negative lever arm (l_7). Low neck position gives the weight forces of head and neck (F_1, F_2) long lever arms (l_1, l_2). By contrast, a high neck position entails shorter lever arms (l_3, l_4) of the same weight forces as before (F_1 and F_2). This reduces the load on the forefeet: F_{v2} in comparison to F_{v1} . The share of body weight carried by the hindlimbs (F_{h1} or F_{h2} , respectively), is total body weight $- F_v$. The elevation of the neck is equivalent to a shift of the CoM in dorsal and caudal direction.
doi:10.1371/journal.pone.0078574.g011

the absence of any deformation apart from axial strain. The conditions for ossification of tendons may well be realized within the muscular bellies, where pinnate muscle fibers are attached to the tendons as in *Meleagris* and *Grus* ([63]; Preuschoft, personal observation). Therefore, the length of an ossified tendon provides only information about the maximal distance between insertion and muscle, but not about the minimum distance, or the location of the muscle itself. This observation is in contrast to [5] as well as [24], who assume ossification alone in the free part of the tendons, outside, or distal to the muscle belly. In most galliform birds [63,64], the ossified parts of long tendons parallel the long bones especially of the hind limbs and alternate with fibrous parts near the joints (where the point of deflecting the tendon changes).

The morphology of sauropod tail skeletons is similar to that in crocodiles. These amphibious archosaurs use their tails for propulsion in water, and their tail shape is clearly adapted to the external forces that are required by this function. In the case of sauropods, tail function is unknown, and an aquatic lifestyle is not seriously considered. The above-noted opinion that tails just counterbalance neck weight does not seem satisfying, because it implies that sauropods and many other dinosaurs were carrying considerable dead weight, or ballast, which is in clear contrast to the light-weight-constructions which have evolved in other parts of the body. If the effects of body weight alone are considered, sauropod tails in fact have adapted shapes, although not all details (like the divergent shapes of hemapophyses) can be explained.

Mammals: Bending of the Neck under Weight

In mammals, necks are not really long in comparison to sauropods [5], but moderately “long” necks can be observed primarily among the large, cursorial, hooved mammals. Cattle, horses, and some cervids keep their seven-segment-necks often in a nearly horizontal posture. In most cervids, antilopes, and camelids, the posterior segments of the necks are kept horizontal, whereas the anterior segments approach the vertical. According to

Christian and Dzemski [20], these necks are kept while resting at angles of about 40° – 60° against the horizontal, and during locomotion at angles of 20° – 40° . At rest, the bending moments are reduced by lifting the necks, because the lever arms of segment weights follow the cosine of the angle of elevation. The elastic ligaments seem to be stretched to such an extent that they produce enough force, to keep the neck in balance. In locomotion, the mass moments of inertia of the body stem are increased by lowering the neck, which facilitates movements of the limbs against the trunk (Yamazaki pers. comm.; [34,35,36]).

The necks of cursorial herbivorous mammals can be classified as morphologically specialized for sustaining high bending moments in lateral view. In so far, mammalian necks and the tails of sauropods are similar. The farther removed the tension-resistant fibrous (nuchal ligaments) or muscles from the neck vertebrae, the longer are the force arms and the greater their torques. The lever arms are long because the nuchal ligaments and the muscles have their proximal insertions at the anterior thoracal vertebrae, (between the transverse processes and the ribs) and at the tips of the spinal processes. Especially the latter are elongated in the anterior thoracal segments, forming the “withers” of cursorial mammals (Fig. 6). The lack of bony outgrowth (like spinal processes or cervical ribs) on the cervical vertebrae yields freedom of mobility – but may require higher forces.

The neck construction of mammals also provides oblique muscles to sustain torsion, but these muscles usually bridge a large part or even the whole distance between thorax and the heavy head that, because of its mass, causes particularly high torsional moments (m. sternocleidomastoideus or m. brachiocephalicus; mm. splenius cervicis et capitis, m. semispinalis capitis in addition to the longus system). It should be noted that the necks of, e.g., carnivores do not have the high and narrow neck profile so typical of the large herbivores. The more circular cross sections of carnivores give their necks higher resistance against torsion. Because the necks of the hooved mammals are specialized for

sustaining high bending moments, their neck construction permits the use of horns, antlers, or simply the frontal bone in intraspecific or interspecific fights (bovids, cervids, and giraffes). In terms of mechanics, these external forces are concentrated on the head and therefore have the longest possible lever arms along the neck, which is strongly bent when transmitting the external forces to the trunk. The fighting animals take care to keep these forces more or less in the sagittal plane and thus keep torsion within narrow limits. The energetically cheapest means to control bending of the neck under the influence of ventrally flexing moments, while keeping it in various positions, are long lever arms of muscles. The latter are obviously powerful, especially in males.

The mobility of necks in the large cursorial mammals is limited; they can usually reach their hindquarters by the teeth, but often not their backs. Extreme mobility of the neck can be observed among carnivorous mammals, especially in seals and elephant seals. These necks are characterized by strong vertebrae without long bony processes, and the very strong musculature is arranged in accordance to the muscles in other mammals. It should be noted, that necks of seals are – on land, under the influence of earth gravity – rarely kept in horizontal postures without bracing their heads on the ground. By contrast, seals show a clear tendency to place their necks into a vertical position for resting, basking, or display behaviors. If submerged in water, the necks lose their weight (but not their mass!) and therefore can be kept parallel to the body axis.

The tails of most mammals are unimportant for the general equilibrium and do not play a large role, because they neither contain much mass, nor are they kept in a more or less horizontal position in which they exert influence on the system. Some exceptions from this rule can be found among marsupials.

Birds

Long-necked birds (ostriches, swans, geese, phasianids) can be seen as functional analogues of sauropods (see also [5]). During rest, slow walking and swimming, these birds regularly keep their necks upright, so that bending moments under the influence of gravity are minimized. Even in feeding, the lengths of necks are kept low by sigmoid curvatures (Fig. 2; [37]).

The usefulness of this analog, however, is doubtful, simply because the equipment with muscles theoretically can be, and in fact seems to be, quite different in both groups, in spite of the otherwise far-reaching homology of the musculature. In birds, the most obvious flexor of the neck is the *m. longus colli ventralis* [64,65]. In some species, its tendons are ossified (crane and turkey, but not in storks nor in herons (personal observations; [65])). The clearly separated tendons diverge cranio-laterally and reach separate insertions at the transverse processes of each vertebra. In the posterior direction, the muscles of both sides converge towards the crista ventralis of the thoracic vertebrae. This is not the direction of the ossified tendons in sauropod necks. The complete muscles of both sides clearly allow rapid protrusion of the head, while all cervical vertebrae are precisely controlled. This is vital for catching fast prey or in pecking, for example. In crocodiles, the *m. longus colli ventralis* is present, but not strongly developed. Functionally it is replaced by the *m. costocervicalis* (*m. scalenus* of [45]).

However, the subdivisions of the avian *m. longus colli ventralis* can hardly be considered as homologous to sauropod cervical ribs, because their common origin is along the ventral midline of the neck, instead of deviating from the midline, and because the tendons do not insert into the long and slender “processus costales” of the bird vertebrae. Instead, these structures are the insertions of the segmental *m. longus colli lateralis* [65]. In this

point we disagree with Taylor and Wedel [5], who argue for the *m. longissimus colli*.

All we know about animal behavior indicates that every possible attempt is made to reduce the expenditure of muscle force; that is, horizontal neck posture is not probable as a frequently assumed or “resting” posture. The influence of gravity on neck posture can easily be observed in many birds (Fig. 3). If a long neck is kept upright in a resting position, its center of mass may well be located behind the vertical through the neck base (Fig. 11). In this case, muscles on both sides must exert tensile force to keep the intervertebral joints in balance. Such a posture obviously requires much less energy than a horizontal posture of the long neck (Fig. 11). Active ventral flexion by muscle activity is required if the head and neck are accelerated forward. In rapid movements, ventral flexion must be induced by muscle activity to overcome mass inertia of the neck. Acceleration of the neck and head for rapid ventral flexion of the neck takes place commonly in birds during capturing prey, pecking (woodpeckers, herons for example), and all similar activities, but it does not seem probable in the case of the herbivorous, browsing sauropods. Admittedly, slower flexion of the neck is and was initiated by weight – even if the neck was kept in a more or less upright posture. Under static conditions, a slight active ventral flexion by muscle activity is only required if the neck at rest is fully erect or inclined dorsally. The only task left in sauropods for the muscle and the ossified tendons is unilateral activity in order to keep the neck in balance against torsional moments.

Superficially, snakes seem to move their most cranial parts in a way similar to that postulated here for sauropods. These anterior parts of snake bodies, however are not necks, but anterior parts of the trunk, with its common equipment: Ribs and intercostal musculature. These anatomical elements have been identified by Preuschoft et al. [66] as torsion-resisting structures, but they belong to the trunk, not to the neck.

Conclusions

Aside from the often-discussed bending in side view, necks of sauropods are exposed to torsion. This requires particular adaptations, especially because of the concentration of internal forces derived from torsion near the periphery of the twisted element. Very similar adaptations to torsional strength can be seen in crocodiles, which expose their admittedly short necks to huge torsional moments in the death roll. By contrast, the tails of sauropods do not show pronounced adaptation to torsion, and seem to have been carried more or less in a horizontal posture. In this respect, sauropod tails resemble the necks of large cursorial, herbivorous mammals. The high number of short neck segments is an indicator of neck flexibility, while long segments limit flexion, as do long dorsal and ventral apophyses.

The cervical ribs of some sauropods resemble functionally the tendons of a muscle group named in birds the *m. longus colli ventralis*, which gives rise to long tendons, inserting into each neck vertebra. The muscle bellies, however, are located more medially on the centra of the posterior vertebrae and do not insert into the processus costalis of the avian neck vertebrae. The direction of the cervical ribs in sauropods indicates a more lateral insertion, like that of the *m. scalenus* in crocodiles, which is contrary to Taylor and Wedel [5] who argue for the *m. longissimus colli ventralis*.

If acting on both sides, these muscles flex the neck ventrally – a movement that seems completely unnecessary in the heavy necks of sauropods if carried forwardly inclined. The existence of a strong ventral muscle is reasonable only if the neck is kept upright

– a posture that saves energy. According to Christian [this collection], the *m. longus colli ventralis* may have an important function to counteract passive movements of the long sauropod neck in locomotion. No doubt, the muscle of which the ossified tendons seem to be the cervical ribs is perfectly suited to keep the neck in balance against torsional moments by unilateral activity. The forces produced by these muscles are further transmitted from the transverse processes to the spinal processes by the deep fibers of the *m. longissimus* system (*multifidus cervicis*) and *m. splenius capitis*.

In conclusion, the necks of diplodocids seem to have been very flexible, permitting smooth adaptation to a variety of postures, while those of brachiosaurids were more restricted and still more so the necks of mamenchisaurids. Unilateral activation of the *m. longus colli ventralis* or the *mm. scalani* contributes in sauropods to shaking the head and twisting the neck, as well as to resisting torsional stresses in crocodiles.

Acknowledgments

We thank P. M. Sander (University of Bonn) for stimulating discussion, valuable additions and comments, and for asking questions, which

References

- Klein N, Remes K, Gee CT, Sander PM (2011) Biology of the sauropod dinosaurs: understanding the life of giants. *Life of the Past* (series ed. Farlow, J.) Bloomington: Indiana University Press. 344 pp.
- Sander PM, Christian A, Gee CT (2009) Response to sauropods kept their heads down. *Science* 323: 1671–1672.
- Sander PM, Christian A, Clauss M, Fechner R, Gee CT, et al. (2010) Biology of the sauropod dinosaurs: the evolution of gigantism. *Biol Rev* 86: 117–155.
- Taylor MP, Naish D (2007) An unusual new neosauropod dinosaur from the Lower Cretaceous Hastings Beds Group of East Sussex, England. *Palaentology* 50: 1547–1564.
- Taylor MP, Wedel MJ (2013) Why sauropods had long necks; and why giraffes have short necks. *PeerJ* 1:e36; DOI 10.7717/peerj.36.
- Upchurch P, Barrett PM, Dodson P (2004) Sauropoda. In: Weishampel DB, Dodson P, Osmolska H, eds. *The Dinosauria*. Berkeley: University of California Press, pp. 259–322.
- Christian A (2010) Some sauropods raised their necks: evidence for high browsing in *Euhelopus zdanskyi*. *Biol Lett* 6: 823–825. (doi:10.1098/rsbl.2010.0359).
- Ruxton G.D, Wilkinson DM (2011) The energetics of low-browsing in sauropods. *Biol Lett* 7: 779–781.
- Preuschoft H, Hohn B, Stoinski St, Witzel U (2011) Why so huge? Biomechanical reasons for the acquisition of large size in sauropod and theropod dinosaurs. In: Klein N, Remes K, Gee CT, Sander PM, eds. *Biology of the sauropod dinosaurs: understanding the life of giants*. Bloomington: Indiana University Press. pp. 197–218.
- Shorrocks B (2009) The behaviour of reticulated giraffe in the Laikipia district of Kenya. *Giraffa* 3(1): 22–24.
- Taylor MP, Wedel MJ, Naish D (2009) Head and neck posture in sauropod dinosaurs inferred from extant animals. *Acta Palaentol Pol* 54: 213–220.
- Christian A, Dzemski G (2011) Neck posture in sauropods. In: Klein N, Remes K, Gee CT, Sander PM, eds. *Biology of the sauropod dinosaurs: understanding the life of giants*. Bloomington: Indiana University Press. pp. 251–260.
- Stevens KA, Parrish MJ (2005) Digital reconstructions of sauropod dinosaurs and implications for feeding. In: Wilson JA, Curry Rogers K eds. *The Sauropods: evolution and paleobiology*. Berkeley, CA: University of California Press. pp. 178–200.
- Stevens KA, Parrish MJ (2005) Neck posture, dentition and feeding strategies in Jurassic sauropod dinosaurs. In: Tidwell V, Carpenter K eds. *Thunder lizards: the sauropodomorph dinosaurs*. Bloomington: Indiana University Press. pp. 212–232.
- Frey E, Martin J (1997) Long necks of sauropods. In: Currie PJ, Padian K eds. *Encyclopedia of dinosaurs*. California San Diego: Academic Press, pp. 406–409.
- Martin J, Martin-Rolland V, Frey E (1998) Not cranes or masts, but beams: the biomechanics of sauropod necks. *Oryctos* 1: 113–120.
- Christian A (2002) Neck posture and overall body design in sauropods. *Mitt Mus Natkd Berl, Geowiss Reihe* 5: 269–279.
- Dzemski G, Christian A (2007) Flexibility along the neck of the ostrich (*Struthio camelus*) and consequences for the reconstruction of dinosaurs with extreme neck length. *J Morph* 268: 701–714.
- Romer AS (1956) *Osteology of reptiles*. Chicago: University of Chicago Press.
- Christian A, Dzemski G (2007) Reconstruction of the cervical skeleton posture of *Brachiosaurus brancai* Janensch, 1914, by an analysis of the intervertebral stress

compelled us to search for reliable answers. A. Christian (University of Flensburg) provided a healthy basis for this project through his earlier analyses of sauropod necks. O. Dülfer and G. Oleschinski (both University of Bonn) are acknowledged for preparing thin sections and the excellent photographs. J. Mitchell is acknowledged for linguistic improvement and H. Mallison (MfN) for his support. NK thanks the DFG for funding. This is publication No 149 of the Research Unit “Biology of Dinosaurs, the evolution of gigantism.” We would like to thank the reviewers, A. Christian (University of Flensburg) and U. Witzel (Ruhr-University of Bochum), and the academic editor, A. Farke (Raymond M. Alf Museum of Paleontology, Claremont, California), for their very helpful comments on the manuscript.

Author Contributions

Analyzed the data: HP NK. Contributed reagents/materials/analysis tools: HP NK. Wrote the paper: HP NK. Conceived and designed the experiments (theoretical biomechanical part): HP. Conceived and designed the experiments (histology of cervical ribs): NK. Performed the experiments ((theoretical biomechanical part): HP. Performed the experiments (histology of cervical ribs): NK..

- along the neck and a comparison with the results of different approaches. *Fossil Rec* 10: 38–49.
- Christian A, Heinrich WD (1998) The neck posture of *Brachiosaurus brancai*. *Mitt Mus Natkd Berl, Geowiss Reihe* 1: 73–80.
- Wedel MJ, Cifelli RL, Sanders RK (2000) Osteology, paleobiology, and relationships of the sauropod dinosaur *Sauroposeidon*. *Acta Palaentol Pol*. 45: 343–388.
- Cerda IA (2009) Consideraciones sobre la histogénesis de las costillas cervicales en los dinosaurios saurópodos. *Ameghiniana* 46: 193–198.
- Klein N, Christian A, Sander PM (2012) Histology shows that elongated neck ribs in sauropod dinosaurs are ossified tendons. *Biol Lett*: doi: 10.1098/rsbl.2012.0778.
- Organ Ch, Adams J (2005) The histology of ossified tendons in dinosaurs. *J Vert Paleontol* 25: 602–613.
- Wolff J (1892) *Das Gesetz der Transformation der Knochen*. Berlin: Hirschwald.
- Pauwels F (1965) *Gesammelte Abhandlungen zur funktionellen Anatomie des Bewegungsapparates*. Berlin: Springer.
- Sverdllova NS, Witzel U (2010) Principles of determination and verification of muscle forces in the human musculoskeletal system: Muscle forces to minimise bending stress. *J Biomechanics* 43: 387–396.
- Knese KH, Biermann H (1958) Die Knochenbildung an Sehnen und Bandansätzen im Bereich ursprünglich chondraler Apophysen. *Zt f Zellf* 49: 142–187.
- Preuschoft H (1969) Statische Untersuchungen am Fuss der Primaten. I Phalangen und Metatarsalia. *Z Anat Entw Gesch* 129: 285–345.
- Preuschoft H (1970) Functional anatomy of the lower extremity. In: Bourne GH ed. *The chimpanzee Vol 3*. Basel: Karger-Verlag. pp. 221–294.
- Preuschoft H (1973) Functional anatomy of the upper extremity. In: Bourne G, ed. *The chimpanzee, Vol 6*. Basel: Karger-Verlag. pp.34–120.
- Kummer B (1959) *Bauprinzipien des Säugerskeletts*. Stuttgart: Georg-Thieme-Verlag.
- Witte H, Preuschoft H, Recknagel S (1991) Human body proportions explained on the basis of biomechanical principles. *Zt Morphol Anthropol* 78: 407–423.
- Preuschoft H, Witte H (1993) Die Körpergestalt des Menschen als Ergebnis biomechanischer Erfordernisse. In: Voland E ed. *Evolution und Anpassung—Warum die Vergangenheit die Gegenwart erklärt*. Stuttgart: Hirzel Verlag. pp 43–74.
- Preuschoft H, Witte H, Christian A, Recknagel S (1994) Körpergestalt und Lokomotion bei großen Säugetieren. *Verhand dt Ges Zool* 87: 147–163.
- Dzemski G (2006) Funktionsmorphologische Analysen langer Hälse bei rezenten terrestrischen Wirbeltieren zur Rekonstruktion der Stellung und Beweglichkeit langer Hälse prähistorischer Tiere. Ph.D. Dissertation. Flensburg: University of Flensburg. 155p.
- Lehmann T (1974–77) *Elemente der Mechanik, Band 1–3*. Braunschweig: Vieweg & Sohn.
- [39] Dubbel H (1981) *Taschenbuch für den Maschinenbau*. Berlin: Springer. 1495p.
- Bock WJ, v. Wahlert G (1965) Adaptation and the form-function-complex. *Evol* 19: 269–299.
- Fürbringer M (1876) *Zur vergleichenden Anatomie des Schultergürtels, 3. Teil*, *Morph Jb* 1: 636–816.

42. Preuschoft H (1976) Funktionelle Anpassung evolvierender Systeme. 5. Arbeitsgespräch zu Phylogenetik und Systematik, Lochmühle/Spessart. Aufsätze und Reden der Senckenberg. Naturforsch. Ges. Evolvierende Systeme I und II. Frankfurt: Kramer-Verlag. pp 98–117.
43. Alexander RM (1985) Mechanics of posture and gait of some large dinosaurs. *Zool J Linn Soc* 83:1–25.
44. Walmsley CW, Smits PD, Quayle MR, McCurry MR, Richards HS, et al. (2013) Why the long face? The mechanics of mandibular symphysis proportions in crocodiles. *PLoS ONE* 8(1): e53873. doi:10.1371/journal.pone.0053873.
45. Nishi S (1938) Muskeln des Rumpfes. In: Bolk L, Göppert E, Kallius E, Lubosch W, eds. *Handbuch der vergleichenden Anatomie der Wirbeltiere*. Berlin: Urban & Schwarzenberg. pp 351–446.
46. Hohn B (2011) Walking with the shoulder of giants: biomechanical conditions in the tetrapod shoulder girdle as a basis for sauropod shoulder reconstruction. In: Klein N, Remes K, Gee CT, Sander PM, eds. *Biology of the sauropod dinosaurs: understanding the life of giants*. Bloomington: Indiana University Press. pp 182–196.
47. Wedel MJ, Sanders RK (2002) Osteological correlates of cervical musculature in Aves and Sauropoda (Dinosauria: Saurischia), with comments on the cervical ribs of *Apatosaurus*. *PaleoBios* 22: 1–6.
48. Gatesy SM (1990) Caudofemoral musculature and the evolution of theropod locomotion. *Paleobiology* 16(2): 170–186.
49. Mallison H, Pfretzschner HU (2005) Walking with sauropods: modeling dinosaur locomotion in MSC visual NASTRAN 4D. *J Vert Pal* 25: 88A.
50. Mallison H (2011) Rearing giants. Kinetic-dynamic modeling of sauropod bipedal and tripodal poses. In: Klein N, Remes K, Gee CT, Sander PM, eds. *Biology of the sauropod dinosaurs: understanding the life of giants*. Bloomington: Indiana University Press. pp. 237–250.
51. Guibé J (1970) La musculature. In: Grasse PP, editor. *Traite de Zoologie*. Paris: Masson. Tome XIV, Fasc II:701–812.
52. Gasc JP (1981) Axial musculature. In: Gans C, Parsons TS (eds.). *Biology of the Reptilia*. London: Academic Press Vol. 11, pp. 355–435.
53. Preuschoft H, Reif WE, Muller WH (1974) Funktionsanpassungen in Form und Struktur an Haifischzähnen. *Zt Anat Entwlg* 143: 315–344.
54. Willey JS, Biknevicius AR, Reilly SM, Earls KD (2003) The tale of the tail: limb function and locomotor mechanics in *Alligator mississippiensis*. *J Expl Biol* 207: 553–563.
55. Fechner R (2009) Morphofunctional Evolution of the pelvic girdle and hind limb of Dinosauromorpha on the lineage to Sauropoda. Ph.D. Dissertation. München: University of München. 211p. Online available: http://edoc.ub.uni-muenchen.de/10954/1/Fechner_Regina.pdf
56. Fechner R, Stratmann M, Göbbling R, Sverdllova N (2013) The functional role of the ischiopubic membrane for the mechanical loading of the pubis in the domestic fowl (*Gallus gallus*). *J Anat* 222: 305–312.
57. Henderson DM (1999) Estimating the masses and centers of mass of extinct animals by 3-D mathematical slicing. *Paleobiology* 25: 88–106.
58. Thulborn RA (1989) The gaits of dinosaurs. In: Gillette DD, Lockley MG eds. *Dinosaur tracks and traces*. Cambridge: Cambridge University Press. pp.39–50.
59. Bird RT (1944) Did *Brontosaurus* ever walk on land? *Nat Hist* 53: 60–67.
60. Alexander RM (1989) *Dynamics of dinosaurs and other extinct giants*. New York: Columbia University Press. 167p.
61. Preuschoft H, Gudo M (2005) Die Schultergürtel von Wirbeltieren: Biomechanische Überlegungen zu den Bauprinzipien des Wirbeltierkörpers und zur Fortbewegung von Tetrapoden. *Zblt Geo Pal*, Teil II 2005: 339–361.
62. Wedel MJ (2006) Origin of postcranial skeletal pneumaticity in dinosaurs. *Integrative Zoology* 2:80.
63. Blickhan R (2007) *Biomechanik der axialen aquatischen und der pedalen terrestrischen Lokomotion*. Aachen: Shaker Verlag. p 179.
64. Nickel R, Schummer A, Seiferle E (1973) *Lehrbuch der Anatomie der Haustiere, Band 5 Anatomie der Vögel*. Stuttgart: Medizinischer Verlag.
65. Bock WJ (1974) The avian skeletomuscular system. In: Farner DS, King JR, Parkes KC (eds.). *Avian Biology Vol. 4*. New York: Academic Press, pp. 119–257.
66. Preuschoft H, Schulte D, Distler C, Witzel U, Hohn B (2007) Body shape and locomotion in monitor lizards. *Mertensiella* 16: 58–79.
67. Abel O (1909) Die Rekonstruktion des *Diplodocus*. *Abh zool-bot Ges Wien* 5:1–60.

March of the Titans: The Locomotor Capabilities of Sauropod Dinosaurs

William Irvin Sellers^{1*}, Lee Margetts², Rodolfo Aníbal Coria³, Phillip Lars Manning⁴

1 Faculty of Life Sciences, University of Manchester, Manchester, Greater Manchester, United Kingdom, **2** IT Services for Research, University of Manchester, Manchester, Greater Manchester, United Kingdom, **3** CONICET - Universidad Nacional de Río Negro - Subsecretaría de Cultura de Neuquén, Museo Carmen Funes, Plaza Huincul, Neuquén, Argentina, **4** School of Earth, Atmospheric & Environmental Sciences, University of Manchester, Manchester, Greater Manchester, United Kingdom

Abstract

Sauropod dinosaurs are the largest terrestrial vertebrate to have lived on Earth. This size must have posed special challenges for the musculoskeletal system. Scaling theory shows that body mass and hence the loads that must be overcome increases with body size more rapidly than either the ability of the muscles to generate force, or the ability of the skeleton to support these loads. Here we demonstrate how one of the very largest sauropods, *Argentinosaurus huinculensis* (40 metres long, weighing 83 tonnes), may have moved. A musculoskeletal model was generated using data captured by laser scanning a mounted skeleton and assigning muscle properties based on comparative data from living animals. Locomotion is generated using forward dynamic simulation to calculate the accelerations produced by the muscle forces, coupled with machine learning techniques to find a control pattern that minimises metabolic cost. The simulation demonstrates that at such vast body size, joint range of motion needs to be restricted to allow sufficient force generation for an achievable muscle mass. However when this is done, a perfectly plausible gait can be generated relatively easily. Whilst this model represents the best current simulation of the gait of these giant animals, it is likely that there are as yet unknown mechanical mechanisms, possibly based on passive elastic structures that should be incorporated to increase the efficiency of the animal's locomotion. It is certainly the case that these would need to be incorporated into the model to properly assess the full locomotor capabilities of the animal.

Citation: Sellers WI, Margetts L, Coria RA, Manning PL (2013) March of the Titans: The Locomotor Capabilities of Sauropod Dinosaurs. PLoS ONE 8(10): e78733. doi:10.1371/journal.pone.0078733

Editor: David Carrier, University of Utah, United States of America

Received: April 2, 2013; **Accepted:** September 22, 2013; **Published:** October 30, 2013

Copyright: © 2013 Sellers et al. This is an open-access article distributed under the terms of the Creative Commons Attribution License, which permits unrestricted use, distribution, and reproduction in any medium, provided the original author and source are credited.

Funding: Support for developing GaitSym was provided by BBSRC, NERC and the Leverhulme Trust. The funders had no role in study design, data collection and analysis, decision to publish, or preparation of the manuscript.

Competing Interests: The authors have declared that no competing interests exist.

* E-mail: William.Sellers@manchester.ac.uk

Introduction

In organismal biology, whether the focus is comparative anatomy, functional morphology or evolution, the body mass of an organism is perhaps the most important individual factor [1–4]. This is especially true in biomechanics. Here size has a pervasive influence on the performance of animals in their environments, and represents a primary determinant of how animals forage, fight, flee and interact [5]. This applies particularly to terrestrial vertebrates whose limbs must support the body mass against gravity and exert the necessary forces to locomote through an environment. Considering the limited range of biomaterials and their uniform physical properties [6] the size range of extant terrestrial vertebrates is impressive: adult pygmy shrews typically weigh about 0.002 kg while elephants are known to reach masses of 7000 kg [7,8]. However, modern day giants pale into insignificance when compared to the enormous size achieved by the largest Mesozoic dinosaurs. Predatory theropod dinosaurs like *Tyrannosaurus rex* may have reached masses in excess of 10,000 kg [9], while giant sauropods are consistently estimated to have masses in the 15,000 to 40,000 kg range [10] with some perhaps reaching masses as high as 100,000 kg [11,12].

Studies of the effects of body size on locomotor performance date back to the 1940s and the now famous Friday Evening Discourse at the Royal Institution [13]. The two fundamental

observations are (1) that muscle power is more or less proportion to muscle mass, and therefore power limited activities such as jumping should be expected to be mass independent, and (2) that muscle force is more or less proportional to muscle area which scales as mass^(2/3) so that force limited activities such as standing should be expected to become harder as mass increases. These are, of course, first approximations and most activities have a considerably more complex set of requirements. However the scaling of force with body size does mean that we would expect considerable locomotor constraints at large body mass. In terms of static forces it can be shown that both skeletal and muscular strength should scale adequately up to very large body sizes in the order of 100,000 to 1,000,000 kg [14]. However the situation for dynamic forces is considerably more complex and even among living animals we can observe locomotor kinematics changes with large body size to reduce the forces required during locomotion [15]. It is therefore clear that whilst we can get a great deal of useful information from studies of locomotion in the largest living terrestrial vertebrates (e.g. [16–19]), we should expect the locomotor kinematics of the largest sauropods to differ from those seen in modern animals since they are potentially an order of magnitude larger, and have their own unique musculoskeletal adaptations such as air sacs and bone pneumaticity [10].

Traditionally, both osteology and ichnology have been the only available tools for approaching sauropod limb kinematics [20–23].



Figure 1. *Argentinosauros huinculensis* reconstruction at Museo Municipal Carmen Funes, Plaza Huincul, Neuquén, Argentina.
doi:10.1371/journal.pone.0078733.g001

Among titanosaurs, the most common information sources lie on features of their appendicular skeleton, which include the presence of a prominent olecranon in the ulna, laterally expanded preacetabular lobe of the ilium, proximal one-third of the femoral shaft deflected medially, and extremely elliptical femoral midshaft [22,24]. These features are also useful to explain the trackway patterns of these graviportal animals. In contrast, bone scaling and biomechanical analysis shows little to distinguish sauropods from other quadrupedal dinosaurs [25]. Ichnological analysis has been used to calculate the speeds of titanosaur trackways [26,27] but this may only encompass a subset of possible gaits due to preservational bias [28], and is subject to a number of caveats in terms of accuracy [29].

Since we cannot assume, *a priori*, that sauropods used similar kinematic patterns to extant animals during locomotion, we need to generate a number of plausible locomotor patterns and test them for their efficacy in terms of biologically and mechanically meaningful measures such as skeleton and joint loading, metabolic energy cost, speed and acceleration. The general approach is to construct a computer simulation of sufficient biofidelity to capture the necessary mechanics of the system and to use this to test specific locomotor hypotheses. The earliest musculoskeletal models for use in reconstructing gait in vertebrate fossils date back to the pioneering work of Yamazaki et al. [30] who produced a highly

sophisticated neuromusculoskeletal simulation to investigate the evolution of bipedality in humans and other primates. Since then a range of other vertebrate fossils have been simulated including hominoids [31–38], terror birds [39], and dinosaurs [40–44]. These simulations can be kinematically based where a movement pattern is provided founded on extant analogues, trackway data, or theoretically derived. The model then calculates the muscle activations needed to match the input kinematics. Alternatively the simulations can use global optimisation goals to optimise some output measure such as metabolic energy cost or speed. The advantage of this latter approach is that no assumptions need to be made about the likely kinematics and this makes it very suitable for situations where there may be no reasonable modern analogue. The disadvantage is that because the input is much less constrained, the simulation needs to try many more different possibilities whilst searching for the optimal solution and this makes the process extremely computationally intensive.

Methods

Musculoskeletal systems in vertebrates are extremely complex and constructing a simulation with an appropriate level of realism to test its locomotor capabilities is a relatively time consuming process. The necessary stages are as follows.

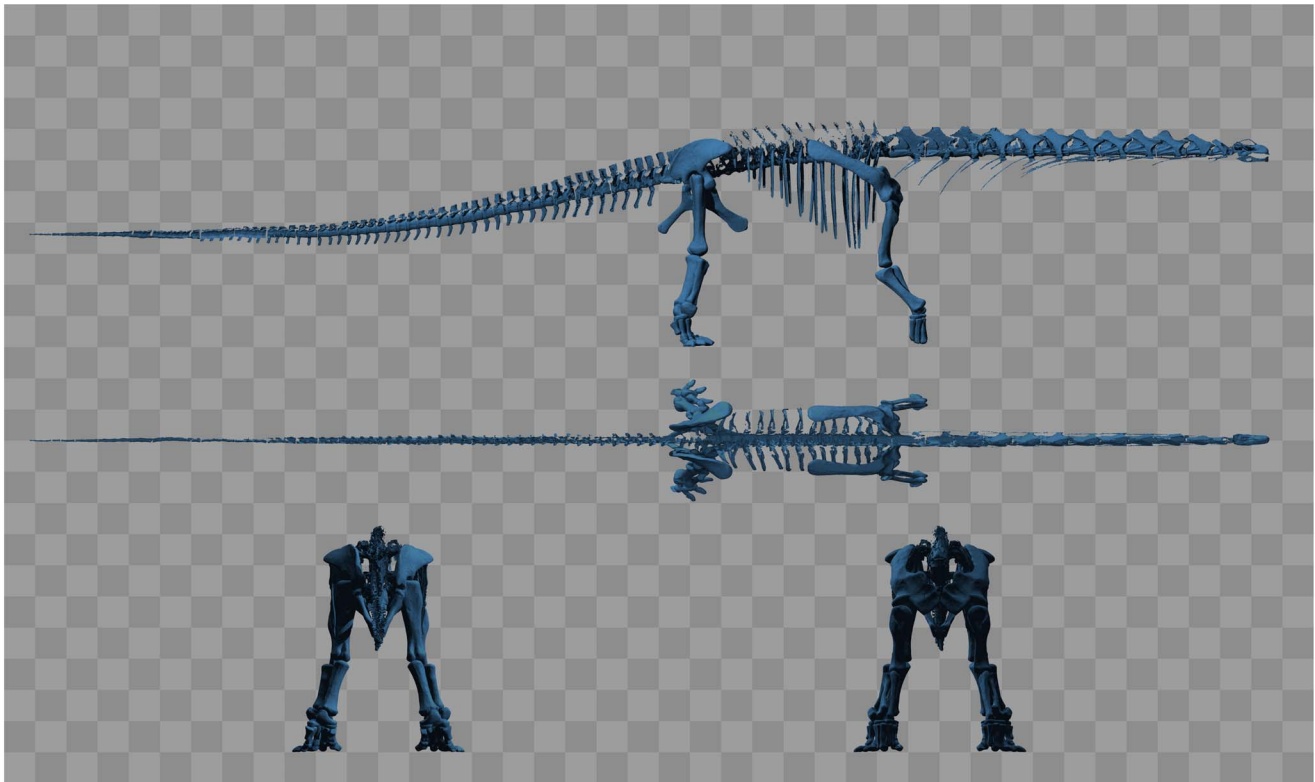


Figure 2. Multiple orthographic views of the digitised skeleton created using the POV-Ray ray-tracer (www.povray.org). The background pattern consists of 1 m squares.
doi:10.1371/journal.pone.0078733.g002

Skeletal Capture

The initial stage in building the simulation is construction an appropriate musculoskeletal model. The first step is to acquire a digital model of the skeleton of the target species. In this case, our aim is to explore the locomotor capabilities of the largest of the sauropod dinosaurs and we chose the to use *Argentinosaurus huinculensis*, as reconstructed by the Museo Municipal Carmen Funes, Plaza Huincol, Argentina, which also houses the original fossil material. Permission was granted by Museo Municipal Carmen Funes, Plaza Huincol, Argentina to scan their

reconstruction. The reconstruction was performed in-house at the museum. This reconstruction is shown in Figure 1. It is 39.7 m long and stands 7.3 m high at the shoulder. The reconstruction is based on rather fragmentary material [45] but includes well preserved fibula and vertebral elements that have allowed mass estimates to be obtained of between 60 and 88 tonnes depending on the regression equation used [46]. The reconstruction was scanned using a Z+F Imager 5006i LiDAR scanner from multiple locations in the gallery. The individual scans were aligned by Z+F Germany, using the multiple printed targets placed around the

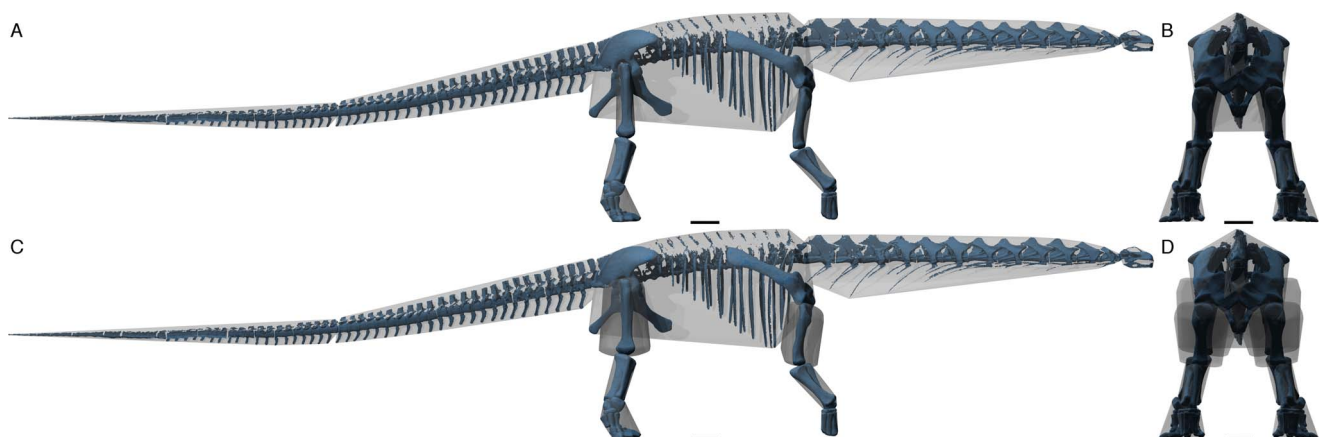


Figure 3. Orthographic views of the hulled segments created using the POV-Ray ray-tracer (www.povray.org). A, side, and B, front view of the unscaled hull model. C, side, and D, front view of the scaled model with extra mass in the thigh and forearm segments.
doi:10.1371/journal.pone.0078733.g003

Table 1. Segmental mass properties of the model as posed in the reference position.

	Position of CM (m)			Segment Mass (kg)	Moments of Inertia (kg.m ²)			Products of Inertia (kg.m ²)		
	x	y	z		I _{xx}	I _{yy}	I _{zz}	I _{xy}	I _{xz}	I _{yz}
Left Arm	3.397	1.270	3.641	2.879E+03	1.519E+03	1.281E+03	8.795E+02	1.182E+02	-6.649E+01	-2.591E+01
Left Foot	-2.977	1.913	0.589	9.761E+02	2.199E+02	1.966E+02	1.908E+02	1.485E+01	4.443E+01	-1.427E+00
Left Forearm	3.779	1.621	1.835	4.282E+02	7.766E+01	1.251E+02	6.805E+01	-9.099E+00	4.994E+01	9.129E+00
Left Hand	4.320	1.753	0.610	1.957E+02	1.774E+01	1.565E+01	9.555E+00	1.221E+00	8.048E-01	8.834E-02
Left Shank	-2.946	1.493	2.067	6.202E+02	1.636E+02	1.613E+02	6.334E+01	1.053E+00	-3.237E+01	2.818E+01
Left Thigh	-2.763	0.998	4.219	5.387E+03	4.513E+03	3.536E+03	2.659E+03	-3.189E+02	5.098E+01	3.073E+02
Right Arm	3.397	-1.270	3.641	2.879E+03	1.519E+03	1.281E+03	8.795E+02	-1.182E+02	-6.649E+01	2.591E+01
Right Foot	-2.977	-1.913	0.589	9.761E+02	2.199E+02	1.966E+02	1.908E+02	-1.485E+01	4.443E+01	1.427E+00
Right Forearm	3.779	-1.621	1.835	4.282E+02	7.766E+01	1.251E+02	6.805E+01	9.099E+00	4.994E+01	-9.129E+00
Right Hand	4.320	-1.753	0.610	1.957E+02	1.774E+01	1.565E+01	9.555E+00	-1.221E+00	8.048E-01	-8.834E-02
Right Shank	-2.946	-1.493	2.067	6.202E+02	1.636E+02	1.613E+02	6.334E+01	-1.053E+00	-3.237E+01	-2.818E+01
Right Thigh	-2.763	-0.998	4.219	5.387E+03	4.513E+03	3.536E+03	2.659E+03	3.189E+02	5.098E+01	-3.073E+02
Trunk	0.454	0.000	5.256	6.226E+04	8.831E+04	1.281E+06	1.257E+06	2.209E+03	-8.752E+04	5.735E+02

doi:10.1371/journal.pone.0078733.t001

gallery as automatically detectable shared reference points. The tail, torso, neck and head and the individual limb bones and girdles were segmented out and decimated using of Geomagic Studio (www.geomagic.com) and the resultant 3D objects posed using 3DS Max (www.autodesk.com). The quality of the scan is variable due to limitations on where the scanner could be placed. Therefore limb bones on the side that had been better scanned were mirrored to produce a completely symmetrical model and

the torso was moved slightly so that its centre of mass was exactly in the midline. This produced the reference pose illustrated in Figure 2. It was not possible to raise the scanner above floor level so the quality of the scan for dorsal elements such as neural spines is relatively poor. However the limb bones and girdles are well digitised and these are the most important in terms of subsequent modelling steps.

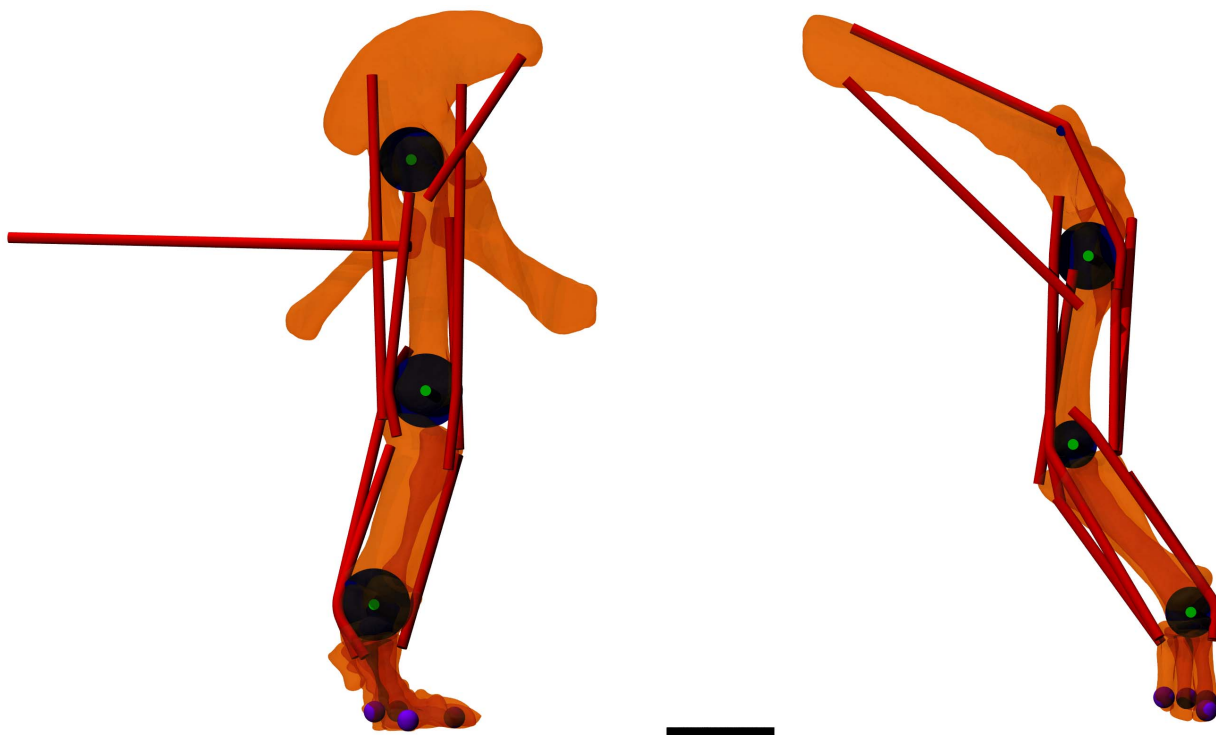


Figure 4. Orthographic views of the limb bones, muscle paths, wrapping cylinders, joint axes and contact points used in the model. The scale bar is 1 m long. Created using the POVray ray-tracer (www.povray.org). doi:10.1371/journal.pone.0078733.g004

Table 2. Reference positions of the joint centres in the model.

	X (m)	Y (m)	Z (m)
Right Hip	-2.866	-0.655	5.309
Right Knee	-2.732	-1.223	3.169
Right Ankle	-3.211	-1.708	1.186
Right Shoulder	3.409	-1.217	4.417
Right Elbow	3.268	-1.347	2.670
Right Wrist	4.359	-1.610	1.116
Left Hip	-2.866	0.655	5.309
Left Knee	-2.732	1.223	3.169
Left Ankle	-3.211	1.708	1.186
Left Shoulder	3.409	1.217	4.417
Left Elbow	3.268	1.347	2.670
Left Wrist	4.359	1.610	1.116

doi:10.1371/journal.pone.0078733.t002

Segmental Mass Properties

Once the skeleton has been captured it is necessary to define the body segments that are used in the simulation. In common with nearly all locomotor analysis, the body is treated as a series of rigid, linked segments [47]. As in all modelling exercises it is necessary to decide on the level of complexity that is going to be used. It is perfectly possible to model every single bone as a separate segment but doing so greatly increases the calculation time for the simulation and having a large mass difference between body elements tends to cause numerical instability. For the sauropod model, 3 segments were defined for each limb representing the stylopodium, zeugopodium and autopodium. The head, neck, torso and tail were considered a single combined segment. Each segment is a six degree of freedom rigid element that has a position and orientation as well as a mass and inertial tensor. In the reference pose, the position is defined as the position of the centre of mass of the segment, and the orientation is set to a rotation of zero, with the inertial tensor calculated at this orientation. In the palaeontological literature there are two approaches for generating mass properties. Firstly these can be scaled from experimentally derived data of similarly shaped modern species and this is probably the commonest approach among hominoid workers (e.g. [32,35]) with reference data from humans [48,49] or chimpanzees [50]. Secondly these can be obtained from volumetric models of the target animal [51–53]. The modern locomotor analogues for dinosaurs have very different body shapes so the scaling approach is probably less useful than the volumetric approach. However whilst these are based on external body measurements when used with living animals, for fossil animals these soft-tissue measurements cannot be measured directly. This leads to an undesirable subjective element to these reconstructions and in an attempt to improve on this we have developed an objective technique based on convex hulling [54]. In its original form, this technique produced a mathematically unique minimum wrap around the individual skeletal components to estimate body mass. However since these are simply closed 3D shapes, all the other mass properties can also be calculated. The only difficulty is that our previous analysis found that approximately 20% of the mass was lost in the minimal wrap and this needs to be recovered. Figure 3AB shows the results of convex hulling the skeletal elements. The main place where the segments are clearly far too small is the thigh

Table 3. The locations of the contact spheres attached to the autopodia of the model.

Contact Name	X (m)	Y (m)	Z (m)	Radius (m)
Left Foot 1	-3.206	2.294	0.194	0.1
Left Foot 2	-2.991	1.454	0.199	0.1
Left Foot 3	-2.895	2.734	0.112	0.1
Left Foot 4	-2.466	1.304	0.141	0.1
Left Hand 1	4.111	1.920	0.327	0.1
Left Hand 2	4.321	1.495	0.318	0.1
Left Hand 3	4.505	1.835	0.205	0.1
Left Hand 4	4.502	1.605	0.295	0.1
Right Foot 1	-3.206	-2.294	0.194	0.1
Right Foot 2	-2.991	-1.454	0.199	0.1
Right Foot 3	-2.895	-2.734	0.112	0.1
Right Foot 4	-2.466	-1.304	0.141	0.1
Right Hand 1	4.111	-1.920	0.327	0.1
Right Hand 2	4.321	-1.495	0.318	0.1
Right Hand 3	4.505	-1.835	0.205	0.1
Right Hand 4	4.502	-1.605	0.295	0.1

doi:10.1371/journal.pone.0078733.t003

and upper arm and so the missing mass was added to these segments by using an appropriate scale factors orthogonal to the long axis of the bone. Figure 3CD shows the effects of this scaling. This choice of where to put the extra mass is somewhat arbitrary but it is believed that at low speeds, the choice of mass properties in the limbs is relatively unimportant [55]. The calculated mass properties for each segment in the reference pose are shown in Table 1. The total calculated body mass for the reconstruction using convex hulling approach [54] is 83,230 kg which is within the range previously predicted for this species [46] and certainly helps us have confidence in the reconstruction. However it must be remembered that these values are necessarily estimates. We do know how much soft tissue was associated with the skeletal segments and these estimates are means based on a limited dataset of modern animals. However we also know that the choice of mass parameters has relatively little effect on experimental [55] or simulation outcomes [33,56].

Muscle and Joint Locations

From the reference skeleton it is now possible to define the joints and muscle paths, although there will always be ambiguities in specific cases. As with the choice of segments, it is necessary to simplify these to prevent undue model complexity. The joints were therefore all considered to be hinge joints operating in various parasagittal planes (i.e. with hinge axes directed laterally), with the joint centre measured from the skeleton. This is probably reasonably accurate for all the joints except the shoulder and hip joints, which should be ball-and-socket joints. However it is likely that there is very little abduction/adduction or axial rotation in normal walking so this is a reasonable approximation for a model of straight line walking and greatly simplifies the control processes. The joints chosen are listed in Table 2. It is also necessary to define contact points on the skeleton which are simply the parts of the feet that make contact with the ground. The foot contact points chosen are listed in Table 3. We also define contact points on the head and the tail but these are simply used to abort the model if the simulation falls over. Muscles are another area

Table 4. Origin and insertion positions of the muscles used in the model in the reference pose.

	Origin			Insertion			Radius 1	Radius 2
	X (m)	Y (m)	Z (m)	X (m)	Y (m)	Z (m)	(m)	(m)
Left Ankle Ext	-3.059	1.359	2.652	-3.292	1.907	0.703	0.336	
Left Ankle Ext Knee Flex	-2.883	1.037	3.556	-3.373	1.637	0.701	0.344	0.336
Left Ankle Flex	-2.431	1.327	2.573	-2.954	1.734	0.788	0.260	
Left Elbow Ext	3.273	1.383	4.289	2.948	1.381	2.302	0.219	
Left Elbow Ext Wrist Flex	3.058	1.499	3.059	4.068	2.093	0.877	0.219	0.236
Left Elbow Flex	3.669	1.077	4.174	3.644	1.510	2.604	0.223	
Left Elbow Flex Wrist Ext	3.253	1.491	2.989	4.568	1.816	0.871	0.223	0.232
Left Hip Ext	-6.594	0.055	4.586	-2.871	1.127	4.503		
Left Hip Ext Knee Flex	-3.229	0.754	6.092	-3.129	1.219	2.900	0.273	0.344
Left Hip Flex	-1.838	1.735	6.267	-2.714	1.414	4.946	0.302	
Left Hip Flex Knee Ext	-2.400	1.416	6.007	-2.523	1.654	2.438	0.302	0.288
Left Knee Ext	-2.509	1.003	4.770	-2.424	1.281	2.625	0.288	
Left Knee Flex	-2.878	1.134	5.000	-2.999	1.385	2.746	0.344	
Left Shoulder Ext	1.219	1.101	6.527	3.689	1.398	4.109	0.050	0.309
Left Shoulder Ext Elbow Flex	3.812	0.135	4.750	3.673	1.484	2.590	0.309	0.223
Left Shoulder Flex	1.161	1.588	6.046	3.337	1.587	3.943	0.315	
Left Shoulder Flex Elbow Ext	3.138	1.411	4.971	3.155	1.564	2.131	0.315	0.219
Left Wrist Ext	3.772	1.508	2.400	4.560	1.610	0.850	0.232	
Left Wrist Flex	3.115	1.720	2.174	4.085	1.904	0.831	0.236	
Right Ankle Ext	-3.059	-1.359	2.652	-3.292	-1.907	0.703	0.336	
Right Ankle Ext Knee Flex	-2.883	-1.037	3.556	-3.373	-1.637	0.701	0.344	0.336
Right Ankle Flex	-2.431	-1.327	2.573	-2.954	-1.734	0.788	0.260	
Right Elbow Ext	3.273	-1.383	4.289	2.948	-1.381	2.302	0.219	
Right Elbow Ext Wrist Flex	3.058	-1.499	3.059	4.068	-2.093	0.877	0.219	0.236
Right Elbow Flex	3.669	-1.077	4.174	3.644	-1.510	2.604	0.223	
Right Elbow Flex Wrist Ext	3.253	-1.491	2.989	4.568	-1.816	0.871	0.223	0.232
Right Hip Ext	-6.594	-0.055	4.586	-2.871	-1.127	4.503		
Right Hip Ext Knee Flex	-3.229	-0.754	6.092	-3.129	-1.219	2.900	0.273	0.344
Right Hip Flex	-1.838	-1.735	6.267	-2.714	-1.414	4.946	0.302	
Right Hip Flex Knee Ext	-2.400	-1.416	6.007	-2.523	-1.654	2.438	0.302	0.288
Right Knee Ext	-2.509	-1.003	4.770	-2.424	-1.281	2.625	0.288	
Right Knee Flex	-2.878	-1.134	5.000	-2.999	-1.385	2.746	0.344	
Right Shoulder Ext	1.219	-1.101	6.527	3.689	-1.398	4.109	0.050	0.309
Right Shoulder Ext Elbow Flex	3.812	-0.135	4.750	3.673	-1.484	2.590	0.309	0.223
Right Shoulder Flex	1.161	-1.588	6.046	3.337	-1.587	3.943	0.315	
Right Shoulder Flex Elbow Ext	3.138	-1.411	4.971	3.155	-1.564	2.131	0.315	0.219
Right Wrist Ext	3.772	-1.508	2.400	4.560	-1.610	0.850	0.232	
Right Wrist Flex	3.115	-1.720	2.174	4.085	-1.904	0.831	0.236	

Radius 1 is the proximal cylinder radius and radius 2 is the distal cylinder radius for one and two cylinder wrapping muscles.
doi:10.1371/journal.pone.0078733.t004

where simplification is necessary. It is actually very straightforward to simulate a large number of muscles and this causes very few problems, and relatively little simulation computational cost. However, each muscle needs to have its activation level controlled and therefore each additional muscle increases the dimensionality of the optimal control search space. This causes a huge additional cost in terms of search and it is therefore important to have as few functional muscles as possible. Since we also have the problem that we do not know the sizes of the individual muscles even if we can

infer their probably identity using an extant phylogenetic bracket [57] it makes sense to reduce the model's complexity by using a more idealised set of muscles that represent the functional actions that are likely to be available. These muscles can be defined with arbitrary paths and moment arms as long as they produce equivalent actions to anatomical muscles. The muscles chosen are listed in Table 4, including their origin and insertion points, and illustrated in Figure 4. Most muscles are not implemented as simple point-to-point muscles. This is because they need to wrap

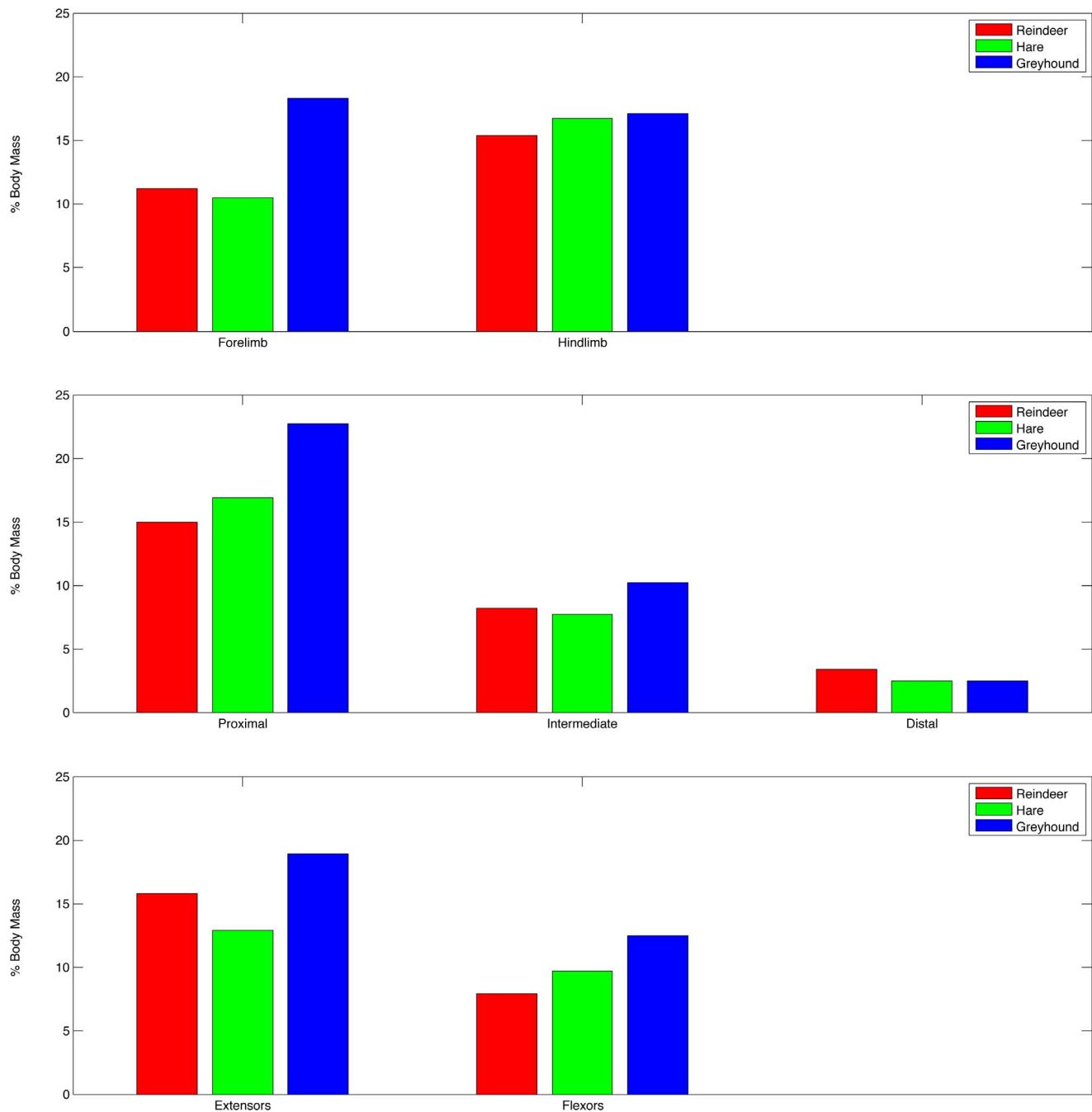


Figure 5. Charts showing the distribution of muscle mass in three species of cursorial quadruped. Data from Wareing et al. 2011. doi:10.1371/journal.pone.0078733.g005

around bones to maintain their moment arms throughout the range of movement. This effect can be achieved using multiple via points but this approach often leads to unrealistic muscle paths at the extremes of joint action. It is also possible to define the muscle as a chain of linked segments and to calculate how these would slide over the bone morphology (and even other muscles). This is very computationally expensive and can cause numerical instability issues. Instead we define cylinders or pairs of parallel cylinders that allow a wrapping path to be calculated as needed with relatively minimal cost. The radius of the cylinder is chosen to match the effective moment arm of the muscle as it wraps around the condyles of the long bones.

Muscle Properties

As has been shown on several occasions [43,56,58], the most important property to estimate correctly in locomotor simulations is muscle mass. This is because the power available is proportional to muscle mass, and the force available, which is proportional to muscle area, is therefore proportional to the (muscle mass/muscle fibre length). Limb muscle mass as a fraction of total body mass is known for a number of animals and it is usually assumed that a value of 50% is an absolute maximum [58] and with values of 25 to 35% found more typically [59]. From the limited current data an approximate partitioning can be estimated with ~60% of the muscle found around proximal joints, ~30% around the

Table 5. Fixed modelling parameters. For sources see the main text.

Model Parameter	Value
Body Mass (kg)	83,230.29
Limb Muscle Proportion	0.35
Extension to Fibre Length Ratio	0.50
Muscle Density ($\text{kg}\cdot\text{m}^{-3}$)	1056.00
Extensors Proportion	0.60
Flexors Proportion	0.40
Proximal Joints Proportion	0.60
Intermediate Joints Proportion	0.30
Distal Joints Proportion	0.10
Forelimb Proportion	0.45
Hindlimb Proportion	0.55
Muscle Force per Unit Area ($\text{N}\cdot\text{m}^{-2}$)	300,000
Activation K	0.17
VMaxFactor (s^{-1})	8.4

doi:10.1371/journal.pone.0078733.t005

intermediate, and $\sim 10\%$ around the distal joints. Similarly muscle is split approximately $\sim 60\%$ extensors to $\sim 40\%$ flexors and $\sim 45\%$ forelimb to $\sim 55\%$ hindlimb [59]. Comparative data for greyhound, hare and reindeer are shown in Figure 5 and it can be seen that there is a relatively consistent pattern even for quadrupeds of different sizes and locomotor specialisations. Knowing these patterns it is therefore possible to calculate the masses of the individual muscles in the model based on their actions. This procedure works with any number of muscles as long as we assume that the mass is distributed evenly. Multiple joint muscles are simply divided among their multiple actions. To do this we need to use the model parameters listed in Table 5. Muscle density used is 1056 kg m^{-3} [60]. Force per unit area was chosen to be $300,000 \text{ Nm}^{-2}$ [61] but there are other values in the literature: Umberger et al [62] uses $250,000 \text{ Nm}^{-2}$, Alexander [63] reports an *in vitro* maximum value of $360,000 \text{ Nm}^{-2}$ for frog and $330,000 \text{ Nm}^{-2}$ for cat for parallel fibred leg muscles. Zheng et al. [64] recommend a value of $400,000 \text{ Nm}^{-2}$ for human quadriceps, and Pierrynowski [65] suggests $350,000 \text{ Nm}^{-2}$. There is a similarly large range for maximum contraction speed. Winter [47] suggest values from 6 to 10 times the muscle's resting length per second for humans. This value is clearly highly dependent both on the fibre type composition of the muscle and on the temperature. Westneat [66] reports a range of values for fish from 3 to 10 s^{-1} for different fibre types and Umberger et al [62] recommends values of 12 s^{-1} for fast twitch and 4.8 s^{-1} for slow twitch. A value of 8.4 s^{-1} was chosen to represent a mixed fibred muscle. However it should be noted that there is data to suggest that this value reduces with body size [67] although there is very little data for large bodied animals and there is considerable scatter. The activation K value used is the recommended value for the muscle contraction and energetics model used [68].

Muscle maximum contractile force is determined by its physiological cross section area, which is calculated by dividing the muscle volume (obtained by dividing the mass by the muscle density) by the mean fibre length [47]. Unfortunately muscle fibre length is problematic to estimate. It is usually estimated by scaling from related species. This scaling can work well if there is a good modern analogue as is probably the case for early hominin

musculoskeletal models [34,35], but is considerably less reliable for morphologically more distinct species such as dinosaurs [43,61]. This is particularly problematic if muscles with a similar action are being combined together to provide a more abstract joint driver since in that case there is no single muscle that can be used as a homologous reference. However there is a possible solution to this difficulty that can be derived from what we know about how vertebrate muscle contracts. Muscle can only generate force from approximately 60% of its resting length to about 160% [69]. Since the force follows an inverted U shaped curve we would expect most muscles to operate well within these limits in normal use, and since muscle physiology appears to be well conserved among the vertebrates, that this useful fraction of muscle length to be similar for different species. The length a muscle shortens depends on the change in angle at the joint multiplied by the moment arm [70]. So if we know the likely range of motion at a joint and the moment arm then we can predict the likely change in muscle length, and hence predict the muscle fibre length.

To test this prediction that vertebrate skeletal muscles exhibit a preferred length change, a literature survey was performed to identify suitable experimental data. What was required were studies that reported muscle fibre length and where length change could be calculated from moment arm and range of motion data. Since many muscle show changes in moment arm with joint angle this restricted studies to those where moment arm was measured over a range of joint angles. It was also decided that only studies that reported a reasonably large number of muscles should be included otherwise there would be bias associated with large numbers of studies on a relatively few specific muscles. There were relatively few suitable studies found, and of these several were of closely related primate species (hominoids including humans) and it was felt that including all these would produce a taxonomic bias. In the end the following species were chosen: chimpanzees [71], greyhound [72,73], ostrich [74,75] and horse [76]. For the chimpanzee, ostrich and horse the literature gave the best-fit polynomials for the tendon travel during joint rotation so that the length change of the muscle could be calculated directly. For the greyhound, the moment arm data was integrated over the range of angles presented to calculate length change. The chimpanzee and greyhound datasets included both fore- and hindlimbs whereas the ostrich and horse were hindlimb only. Ideally for this study the joint range of motion should match that seen *in vivo* for a range of movements. This is difficult to duplicate in cadaver studies since dead bodies tend to stiffen up which can restrict movement. Conversely as muscles are dissected away the joints become more mobile and this can lead to excessive movements at joints. In the case of the ostrich the joints were only moved through the range of movement associated with running and particularly for the hip and knee this was felt to be rather restricted. The analysis was repeated using a nominal, much larger range of movement for the ostrich data but this had no effect on the results and the conclusions remained unaltered so only the data as calculated directly from the paper is reported here.

Figure 6 shows the (extension/fibre length) ratios for the 121 muscles assessed subdivided by action and location. The modal value in the pooled case is 0.4–0.6, and only in two of the subdivided cases is the mode less clearly defined (0.2–0.6 in both cases). This suggests that assuming that muscle extends 50% of its resting fibre length (or conversely, that the resting fibre length is double the extension distance) is a reasonable assumption for most muscles. Very low values are probably due to one of two of factors. Firstly these are muscles whose prime action is neither flexion nor extension and therefore do not change length appreciably during this movement at the joint. Secondly these are muscles that cross

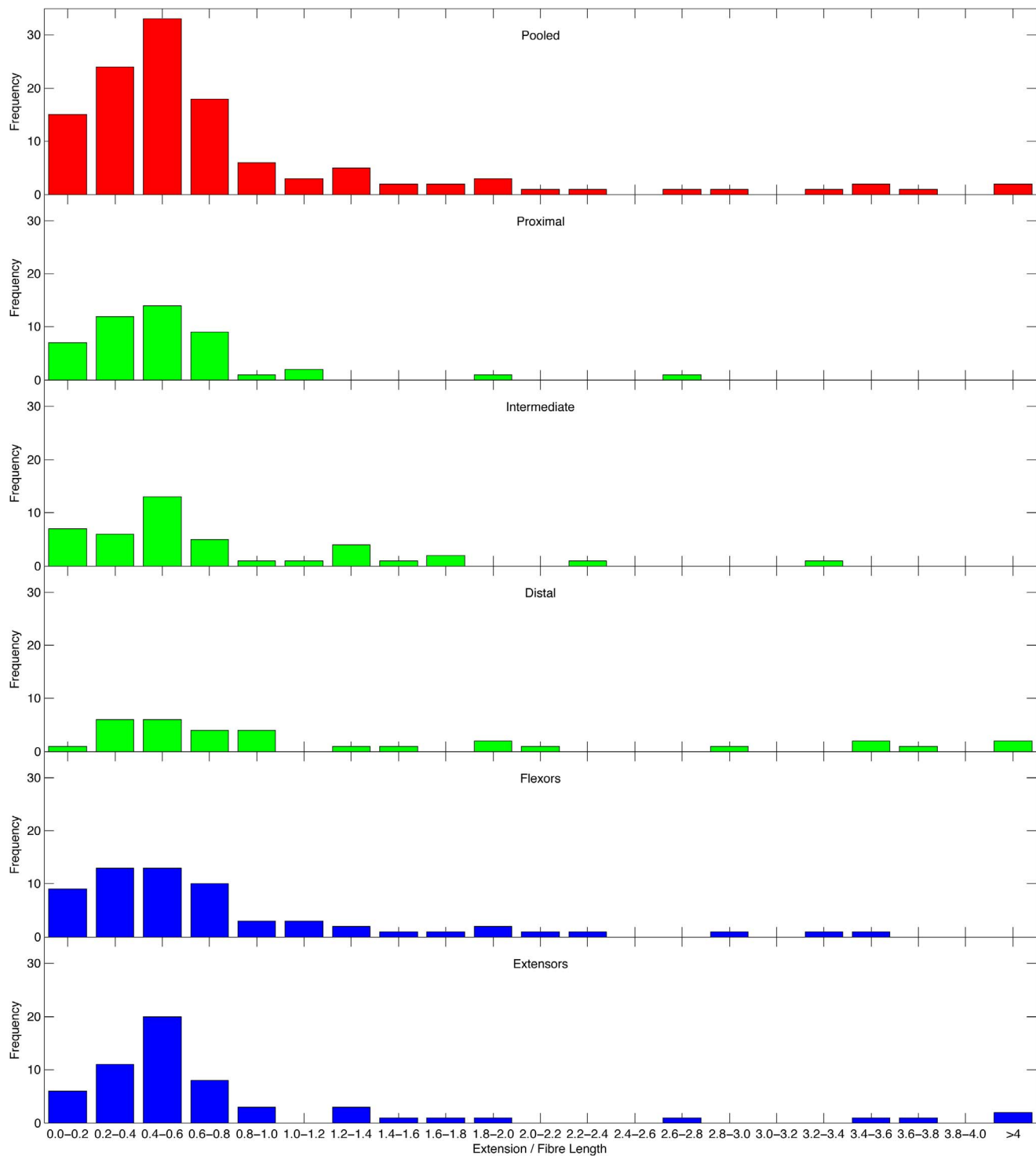


Figure 6. Charts showing the frequency distributions of the (extension/fibre length) ratio for a variety of muscles and vertebrate species.

doi:10.1371/journal.pone.0078733.g006

more than one joint but whose action is mainly over a different joint. Very high values are more interesting because muscles cannot generate active force over these large extension ratios. Again there are two possibilities. Firstly these represent muscles that do not extend over the observed *in vitro* range *in vivo*. This includes two joint muscles where the full range of movement is not

possible at both joints simultaneously. The human hamstrings are a good example of this where full hip flexion is not possible if the knee is extended. Secondly these represent muscles where part of the joint movement is accommodated by tendon stretch. The crural part of the camel *m. plantaris* is perhaps the most extreme example [77].

Table 6. Joint ranges of motion with respect to the reference pose.

		Best Estimate ROM (°)	Elephant Functional ROM (°)	Restricted Ankle ROM (°)
Hip	Min	−20	−20	−20
	Max	70	20	40
	Range	90	40	60
Knee	Min	−105	−50	−40
	Max	15	5	20
	Range	120	55	60
Ankle	Min	−10	−10	−30
	Max	55	30	0
	Range	65	40	30
Shoulder	Min	−75	−35	−40
	Max	15	10	20
	Range	90	45	60
Elbow	Min	−35	−20	−40
	Max	90	25	20
	Range	125	45	60
Wrist	Min	−50	−70	−5
	Max	65	35	25
	Range	115	105	30

Positive values allow the distal element to move anticlockwise when viewed from the right of the body.

doi:10.1371/journal.pone.0078733.t006

We can thus calculate the fibre length of the muscle by calculating the length change of the muscle which is equal to the joint range of motion multiplied by the moment arm. Moment arms are not necessarily easy to obtain for extinct species since exact points of attachment can be difficult to define. Furthermore, moment arms themselves depend on the presence of other soft tissue elements and exact instantaneous joint centres which are also unknown and need to be estimated (e.g. [42]). However if we use length change to define muscle fibre length, then the choice of moment arm does not actually matter in the simulation. If we choose a small moment arm, then we get a small length change, and hence a small fibre length. Since the volume of the muscle is defined by the mass which we have calculated *a priori*, a small fibre length leads to a large physiological cross section area which allows greater force production. Since all these relationships are directly proportional, the greater force production exactly compensates for the reduced moment arm in terms of the eventual torque around the joint. The contraction velocity is similarly exactly compensated: shorter muscle fibre, slower contraction velocity, but smaller moment arm leads to faster angular velocity around the joint. This is exactly as would be predicted from simple lever theory.

The key parameter then becomes joint range of motion. However there have been very few studies that have systematically looked at joint ranges of motion, and whilst some joint limits can be identified from skeletal features, others depend on soft tissue to limit the movement and thus can not. Ren et al. [17] compared elephant joint ranges of motion to cats, dogs, and humans and contrary to expectations did not find any body size related patterns. We thus created models with a range of different joint ranges of motion based on (1) estimation of joint range of motion from the skeleton; (2) range of motion matched to the functional range of motion for an elephant; (3) range of motion based on the previous two versions but with a restricted ankle range of motion. These ranges of motion are shown in Table 6. Using each of these

ranges of motion allows us to calculate the length change of the individual muscle groups using the attachment points and wrapping cylinders previously specified. The tendon length is simply chosen so that the muscle tendon unit is slack when the joint is halfway between its maximum and minimum excursion. The calculated values for the muscles under the different range of motion conditions are shown in Table 7. Again there is no good comparative data on slack lengths and it is difficult to obtain since there is appreciable post mortem shrinkage and stiffening so that measurements taken from cadavers are probably not useful. Measuring passive elastic moments [78], as has been done for human models [79], might allow this to be calculated but the data would have to be taken from anaesthetised animals which would make it much more difficult to collect.

One useful side effect of calculating muscle fibre length from joint range of motion is that you can calculate the minimum muscle mass needed for joint extensors to be able to support a particular load. This is easiest to see for the ankle or wrist but is applicable for all the joints in each limb. If we consider Figure 7 which represents the ankle joint supporting the body weight of the animal (or some fraction thereof for multi-legged animals), we can see that the torque around the ankle (T) must be equal or greater to the ground reaction force (F) multiplied by the moment arm (M). This torque is generated by the ankle extensors, and using the methodology for specifying muscle fibre length outlines above we can show that:

$$T = \frac{Kkm}{\Delta\theta\rho} \quad (1)$$

Where K is the peak force generated per unit cross section area ($\text{N}\cdot\text{m}^{-2}$) as specified in Table 5; k is the (extension/fibre length) ratio chosen (0.5); m is the mass of the muscle (kg); $\Delta\theta$ is the joint range of motion (radians); and ρ is the muscle density ($\text{Kg}\cdot\text{m}^{-3}$).

Table 7. Muscle properties for each of the joint range of motion conditions.

Joint Range of Motion	Muscle Group	Min (m)	Max (m)	Extension (m)	FL (m)	Mass (kg)	PCSA (m ²)	Tendon Length (m)
Best Estimate	Ankle Ext	2.115	2.485	0.371	0.741	320.44	0.4095	1.559
	Ankle Ext Knee Flex	2.340	3.462	1.122	2.245	400.55	0.1690	0.656
	Ankle Flex	1.494	1.962	0.468	0.935	320.44	0.3244	0.793
	Elbow Ext	1.802	2.360	0.558	1.116	589.89	0.5004	0.965
	Elbow Ext Wrist Flex	2.104	3.189	1.086	2.171	382.34	0.1668	0.476
	Elbow Flex	1.251	1.830	0.579	1.159	393.26	0.3213	0.382
	Elbow Flex Wrist Ext	1.865	2.919	1.054	2.107	327.72	0.1473	0.285
	Hip Ext	3.611	4.631	1.020	2.040	1922.62	0.8925	2.081
	Hip Ext Knee Flex	2.419	3.656	1.238	2.476	1201.64	0.4597	0.562
	Hip Flex	1.179	1.722	0.543	1.086	1281.75	1.1174	0.364
	Hip Flex Knee Ext	2.620	4.235	1.616	3.231	1121.53	0.3287	0.196
	Knee Ext	2.076	2.688	0.612	1.225	961.31	0.7433	1.157
	Knee Flex	1.498	2.376	0.878	1.755	480.65	0.2593	0.182
	Shoulder Ext	3.727	4.211	0.484	0.968	1573.05	1.5387	3.001
	Shoulder Ext Elbow Flex	2.128	3.109	0.982	1.963	983.16	0.4743	0.655
	Shoulder Flex	2.442	3.118	0.676	1.352	1048.70	0.7347	1.429
	Shoulder Flex Elbow Ext	2.013	3.284	1.271	2.542	819.30	0.3053	0.107
	Wrist Ext	1.522	2.004	0.482	0.963	262.18	0.2577	0.800
	Wrist Flex	1.348	2.009	0.661	1.322	174.78	0.1252	0.357
	Elephant Functional	Ankle Ext	2.115	2.343	0.228	0.455	320.44	0.6666
Ankle Ext Knee Flex		2.685	3.259	0.574	1.147	400.55	0.3307	1.825
Ankle Flex		1.692	1.962	0.269	0.538	320.44	0.5636	1.289
Elbow Ext		1.905	2.112	0.206	0.413	589.89	1.3542	1.596
Elbow Ext Wrist Flex		2.090	2.820	0.731	1.461	382.34	0.2478	0.994
Elbow Flex		1.469	1.750	0.281	0.561	393.26	0.6634	1.048
Elbow Flex Wrist Ext		2.340	2.941	0.601	1.202	327.72	0.2583	1.439
Hip Ext		3.611	4.141	0.530	1.059	1922.62	1.7190	2.817
Hip Ext Knee Flex		2.677	3.359	0.682	1.364	1201.64	0.8343	1.654
Hip Flex		1.496	1.722	0.226	0.452	1281.75	2.6825	1.157
Hip Flex Knee Ext		3.366	3.959	0.593	1.187	1121.53	0.8950	2.476
Knee Ext		2.137	2.413	0.276	0.552	961.31	1.6492	1.723
Knee Flex		1.947	2.316	0.369	0.739	480.65	0.6161	1.393
Shoulder Ext		3.754	3.996	0.242	0.484	1573.05	3.0764	3.390
Shoulder Ext Elbow Flex		2.343	2.838	0.495	0.990	983.16	0.9400	1.600
Shoulder Flex		2.753	3.090	0.337	0.674	1048.70	1.4727	2.247
Shoulder Flex Elbow Ext		2.521	3.008	0.487	0.974	819.30	0.7962	1.790
Wrist Ext		1.659	2.084	0.425	0.850	262.18	0.2922	1.022
Wrist Flex		1.273	1.879	0.606	1.213	174.78	0.1365	0.363
Restricted Ankle		Ankle Ext	2.002	2.172	0.170	0.340	320.44	0.8914
	Ankle Ext Knee Flex	2.640	3.175	0.535	1.069	400.55	0.3547	1.838
	Ankle Flex	1.904	2.055	0.151	0.301	320.44	1.0067	1.678
	Elbow Ext	1.764	2.092	0.328	0.657	589.89	0.8508	1.272
	Elbow Ext Wrist Flex	2.343	2.750	0.407	0.814	382.34	0.4445	1.732
	Elbow Flex	1.501	1.854	0.353	0.707	393.26	0.5268	0.970
	Elbow Flex Wrist Ext	2.403	2.757	0.354	0.709	327.72	0.4378	1.871
	Hip Ext	3.611	4.377	0.766	1.531	1922.62	1.1888	2.462
	Hip Ext Knee Flex	2.755	3.544	0.789	1.578	1201.64	0.7212	1.572
	Hip Flex	1.364	1.722	0.358	0.717	1281.75	1.6939	0.826
Hip Flex Knee Ext	3.009	3.909	0.901	1.801	1121.53	0.5896	1.658	

Table 7. Cont.

Joint Range of Motion	Muscle Group	Min (m)	Max (m)	Extension (m)	FL (m)	Mass (kg)	PCSA (m ²)	Tendon Length (m)
	Knee Ext	2.041	2.363	0.323	0.645	961.31	1.4103	1.557
	Knee Flex	2.027	2.406	0.379	0.759	480.65	0.6001	1.458
	Shoulder Ext	3.700	4.022	0.323	0.645	1573.05	2.3085	3.216
	Shoulder Ext Elbow Flex	2.307	2.963	0.656	1.312	983.16	0.7095	1.323
	Shoulder Flex	2.711	3.146	0.435	0.870	1048.70	1.1415	2.058
	Shoulder Flex Elbow Ext	2.343	3.044	0.701	1.401	819.30	0.5538	1.292
	Wrist Ext	1.700	1.822	0.122	0.244	262.18	1.0178	1.517
	Wrist Flex	1.632	1.825	0.193	0.386	174.78	0.4288	1.343

doi:10.1371/journal.pone.0078733.t007

Since $T = FM$ we can rearrange this equation to calculate the minimum extensor mass:

$$m = \frac{BgM\Delta\theta\rho}{Kk} \quad (2)$$

Where B is the effective body mass (kg); and g is the acceleration due to gravity ($m.s^{-2}$). Effective body mass is the body mass that would need to be supported by this leg alone. This would be equal to the body mass for a biped but would equal 1/3 of the body mass if we assume that 3 legs were on the ground at all times.

Of these values, only $\Delta\theta$ is unknown for a fossil animal and thus the muscle mass is directly proportional to the joint range of motion chosen. In fact the effect of joint range of motion may be greater than that because a larger range of motion may lead to a larger horizontal moment arm too. We performed this calculation for the *Argentinosaurus* model for all the joints using the maximum possible moment arm, as calculated by the maximum horizontal distance from the foot centre of pressure to the joint centre at either full extension or full flexion, as a way of checking that the model had adequate muscle to function.

Gait Simulation

Once all the muscle, joints, segments, and contacts have been defined it is necessary to find an appropriate activation pattern for the muscles that produces effective walking. To do this we use a feed-forward control system where a central pattern generator sends out muscle activation signals. This is a very simple approach but it is effective in a simulation environment which is entirely uniform. For these simulations we have adopted boxcar functions for the activation patterns [35]. A boxcar function is a rectangular function that has a zero value for a specified time and then a non-zero value for another specified time before falling back to zero. A boxcar function can thus be specified by 3 parameters: a delay, a width, and a height. This is a very concise way, in terms of control parameters, of specifying an activation pattern. If more precise control is required then two or more boxcar functions can be summed which rapidly allows very complex activation shapes to be generated, although single boxcar functions are the only ones that have been used in these simulations. The boxcar functions are duration normalised so that they work in a time interval from 0 to 1, and wrap around. The cycle time for all the functions is specified by a single master cycle time. The gait is assumed to be symmetrical so the left hand side drivers are identical to the right hand side drivers but are half a cycle out of phase. For these experiments the cycle phase was fixed externally. Since the model

has 19 muscle groups per side, this equates to 57 unknown parameters to control the model.

We need to do two things: (1) find a good set of values for these parameters to allow high quality locomotion; (2) find a set of starting conditions that allow the simulation to work in a cyclic steady state. We do this using our now standard procedure of starting our simulant in its reference pose with all segments set at zero velocity, and using a genetic algorithm multiparameter optimisation procedure to find a pattern that maximises the forward distance moved by the model in fixed time. Once we have found a pattern that manages a good degree of forward movement, we use the segment poses and velocities from the middle of this simulation as a new set of starting conditions, and use the solution set as a best estimate solution set for a new optimisation run. This time the optimisation criteria is the maximum distance forward for a given amount of metabolic energy as calculated by the simulation. Once a good solution has been found, we repeat the process of selecting a mid-simulation set of velocities and poses, and reusing the solution set for a new optimisation run. In this way we bootstrap our start conditions, and eventually we end up converging on a largely steady state simulation that minimises the cost of locomotion since this is commonly considered the major goal of low speed locomotion [34,35].

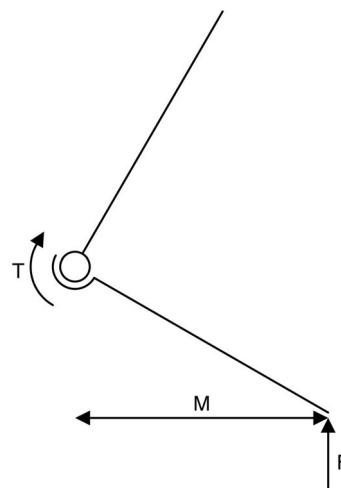


Figure 7. Diagram showing how the minimum ankle torque required to support an animal can be calculated.

doi:10.1371/journal.pone.0078733.g007

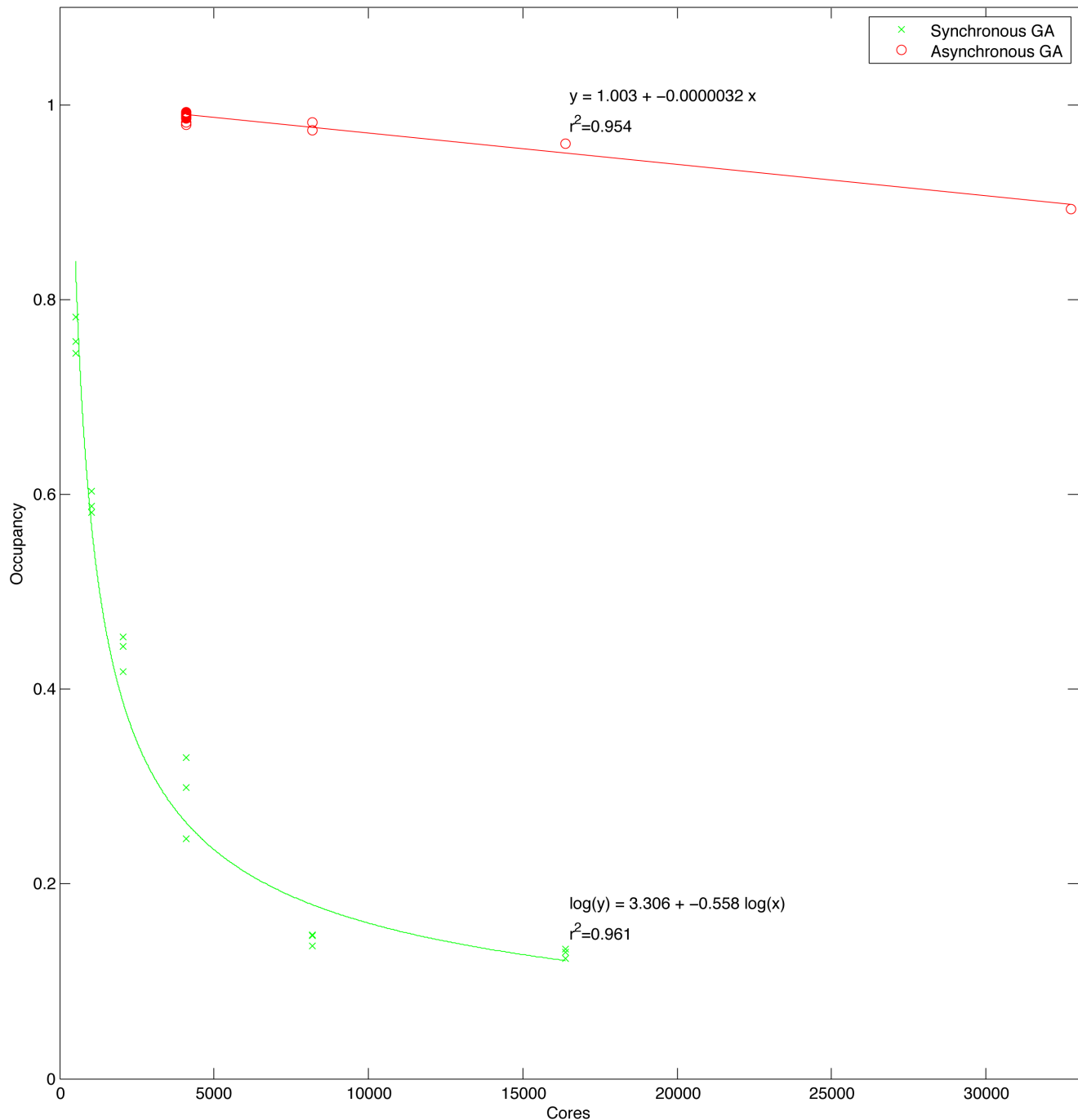


Figure 8. Chart showing the performance characteristics of asynchronous versus synchronous genetic algorithm implementations on varying numbers of CPU cores.
doi:10.1371/journal.pone.0078733.g008

The simulation was performed using our in-house open source simulator, GaitSym. The software and the model specification files can be downloaded from www.animalsimulation.org. The simulation runs at about half real time on a modern processor, so a typical simulation run takes about 30 seconds of CPU core time. A single optimisation run requires 100,000 repeats of the simulation run, and typically 30 repeats of the bootstrap process are needed to get convergence. This equates to about 25,000 CPU core hours for each run condition tested. We had access to the HECToR, the UK National Supercomputer Service (www.hector.ac.uk) and

were able to access up to 32,768 CPU cores at any one time. Our previous traditional genetic algorithm implementation [44] was very successful up to 512 cores but did not scale well for use with larger numbers of cores. Traditional genetic algorithms are highly synchronised [80], effectively because they use a seasonal breeding model. We re-implemented the algorithm using a continuous breeding and therefore asynchronous model and achieved excellent scaling up to 32,768 CPU cores (see Figure 8) which allowed us to explore considerably more options in terms of gait generation in a reasonable length of time.

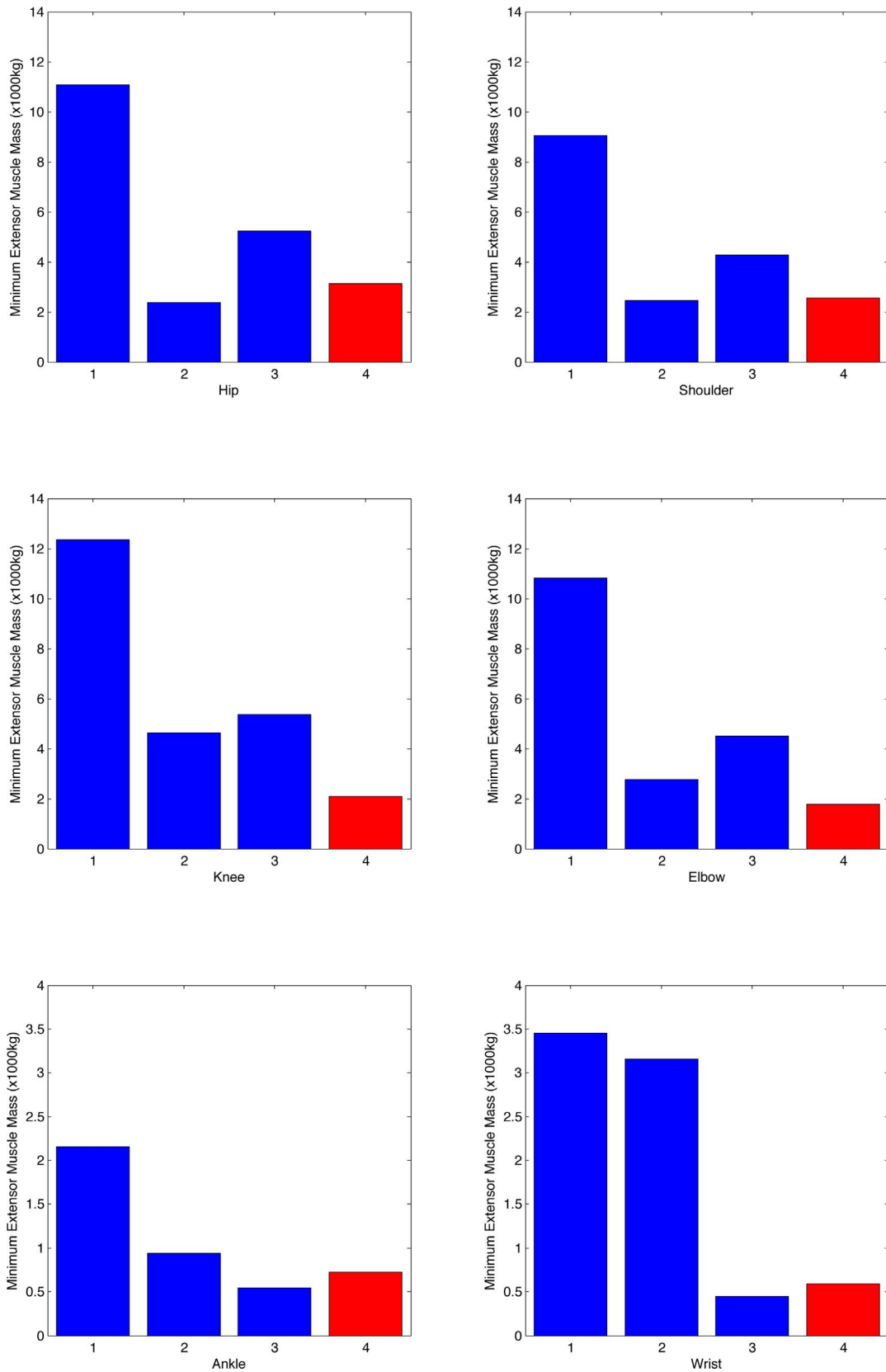


Figure 9. Charts showing the minimum extensor muscle mass required (1,2,3) and the muscle mass available (4) around individual joints for the different joint range of motion cases. 1, best estimate range of motion; 2, elephant functional range of motion; 3, restricted ankle range of motion; 4, muscle mass in model.
 doi:10.1371/journal.pone.0078733.g009

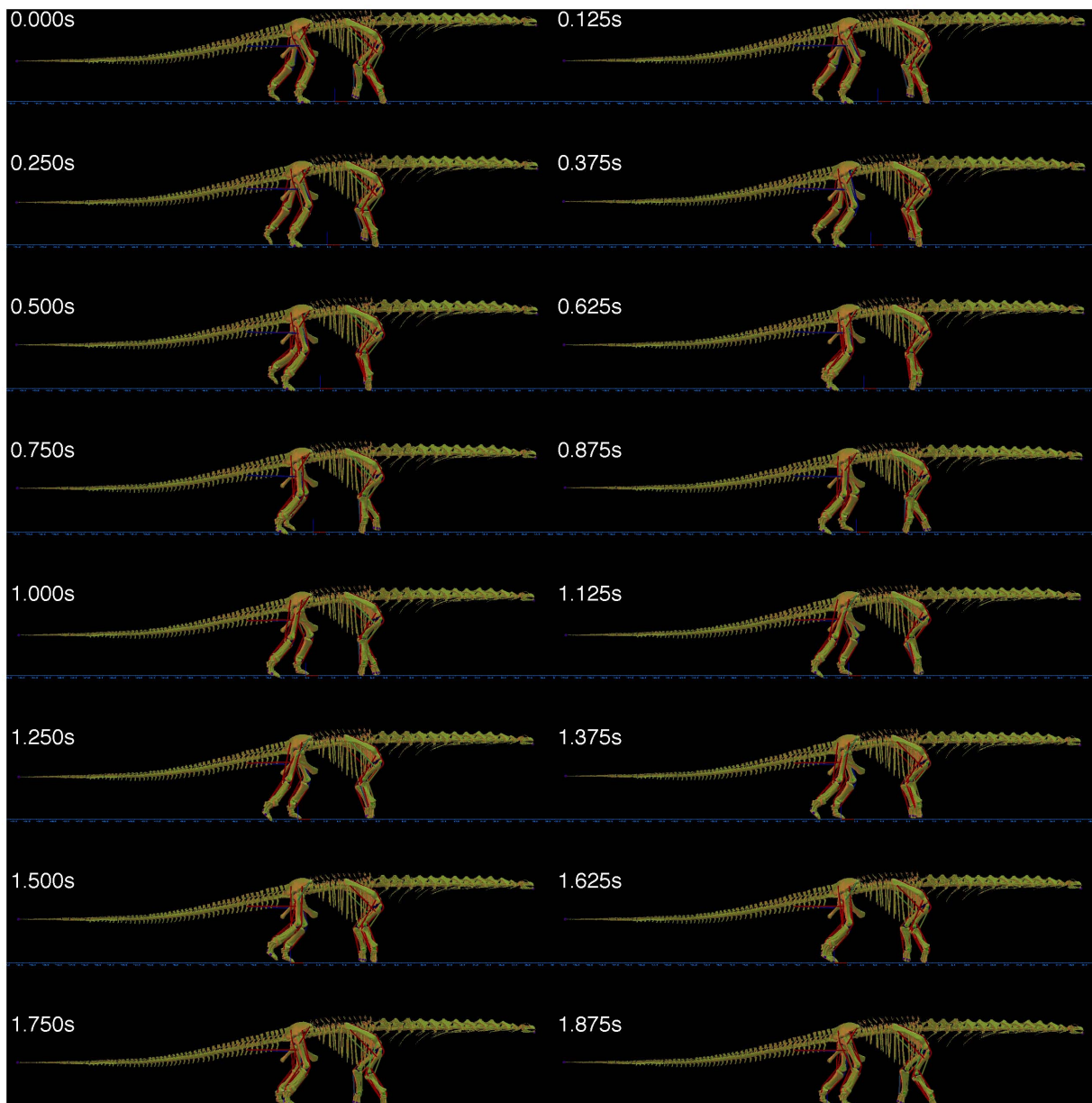


Figure 10. Animation frames generated by GaitSym (www.animalsimulation.org) for the 2 second gait cycle time.
doi:10.1371/journal.pone.0078733.g010

Results

We ran the complete bootstrap process for the three joint range of motion conditions multiple times. The initial standing start was run at least 10 times in each case but only continued to the second stage if a run was found with appreciable forward movement. However the best estimate joint range of motion model was never able to generate a cyclic walking gait. The elephant functional range of motion model was able to generate cyclic gait but it did so by allowing the wrist joint to lock at a position of maximum flexion and producing a gait somewhat reminiscent of a chimpanzee knuckle walking. The restricted ankle range of motion model was able to generate good quality gait. To explore the reasons for this we calculated the minimum muscle mass required for the joint extensors for each of the cases using equation 2 and estimating the maximum possible moment arm for the available range of motion.

These results are shown in Figure 9. From this it is clear why the best estimate joint range of motion model failed since there is clearly insufficient muscle mass around all of the joints to support the body with even moderate levels of joint excursion. The elephant functional range of motion model is very weak around the wrist which again matches the simulation findings where the wrist joint collapsed to full flexion. The restricted ankle range of motion model is slightly vulnerable, particularly around the knee and elbow extensors, but these values assume the maximum possible moment arm which is unlikely to be actually achieved at any point (and can to some extent be actively avoided by the global optimisation procedure), so this model is the only functional one.

The model was optimised to move the greatest distance forward for a fixed amount of energy and as expected this generated a slow, walking gait. This is illustrated in Figure 10 for a gait with a 2

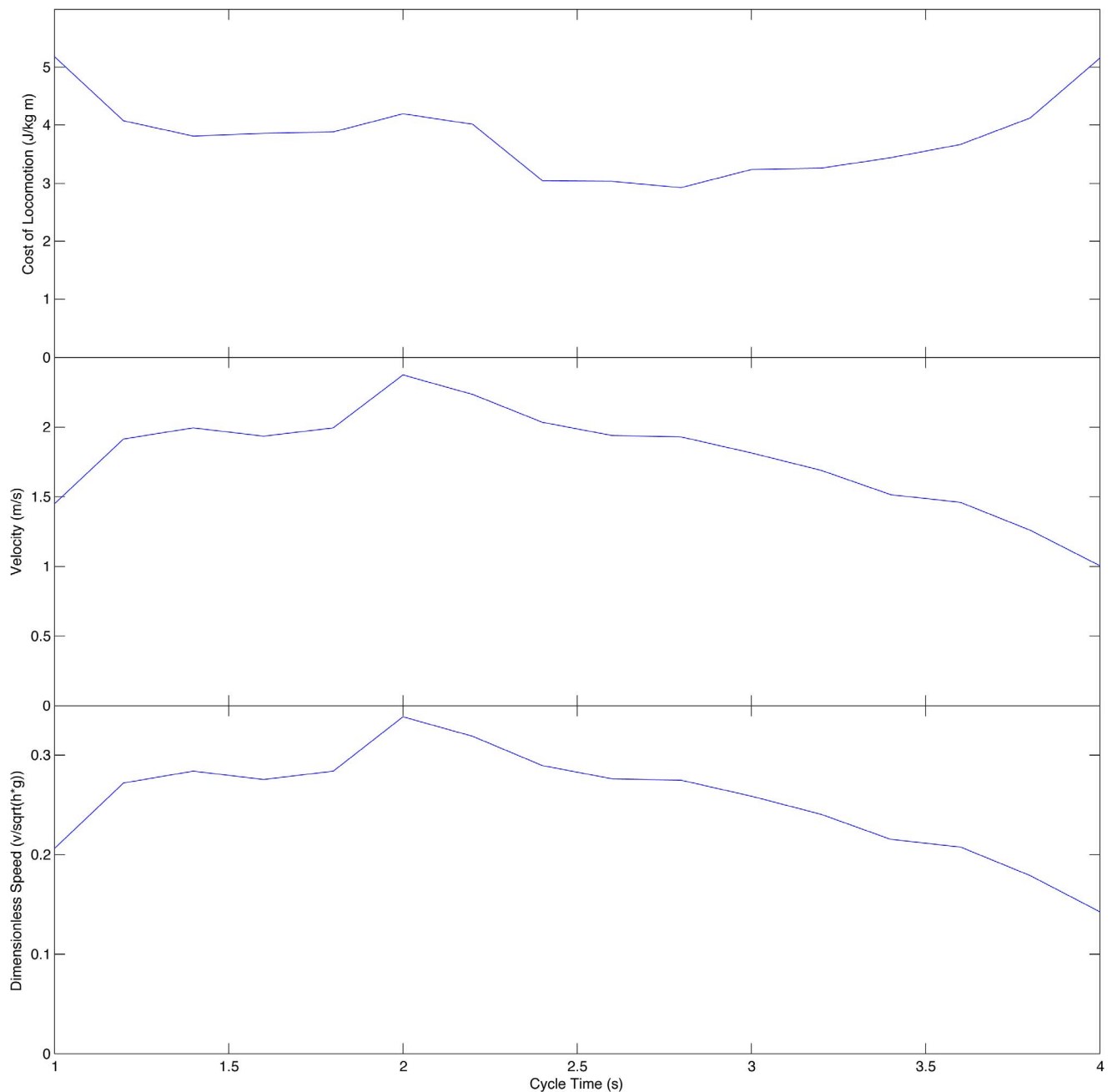


Figure 11. Charts showing the cost of locomotion and walking speeds for the best simulations generated with different gait cycle times.

doi:10.1371/journal.pone.0078733.g011

second cycle time. A range of different gait cycle times were tried from 1.0 s to 4.0 s and the animations produced are available in the supplementary data. Because of the pendular nature of walking gaits it was expected that considerable differences would be seen in the cost of locomotion for different cycle times. As can be seen in Figure 11, the most efficient gait had a cycle frequency of 2.8 s which is relatively close to the natural frequencies of the fully extended legs (3.1 s for the forelimb and 3.7 s for the hindlimb) There was a greater difference in locomotor speed with the longer cycle times producing the fastest gaits, and the longest stride lengths, although as can be seen from the dimensionless speed

(calculated as the square root of the Froude number, velocity/ $\sqrt{(\text{hip height} \times g)}$, following Alexander [20]). For comparison, the maximum speed obtained is equivalent to a human with 0.9 m leg length walking at 1 ms^{-1} [63] which, although slower than the mean, is well within the normal range of typical walking speeds seen in free ranging humans [81]. The gait produced was typically a diagonal gait with lateral couplets [82]: foot fall sequence left hindfoot, right forefoot, right hindfoot, left forefoot; and the ipsilateral forefoot and hind foot on the ground for a greater proportion of the gait cycle than the contralateral forefoot and hind foot. However the phase difference was very small and the

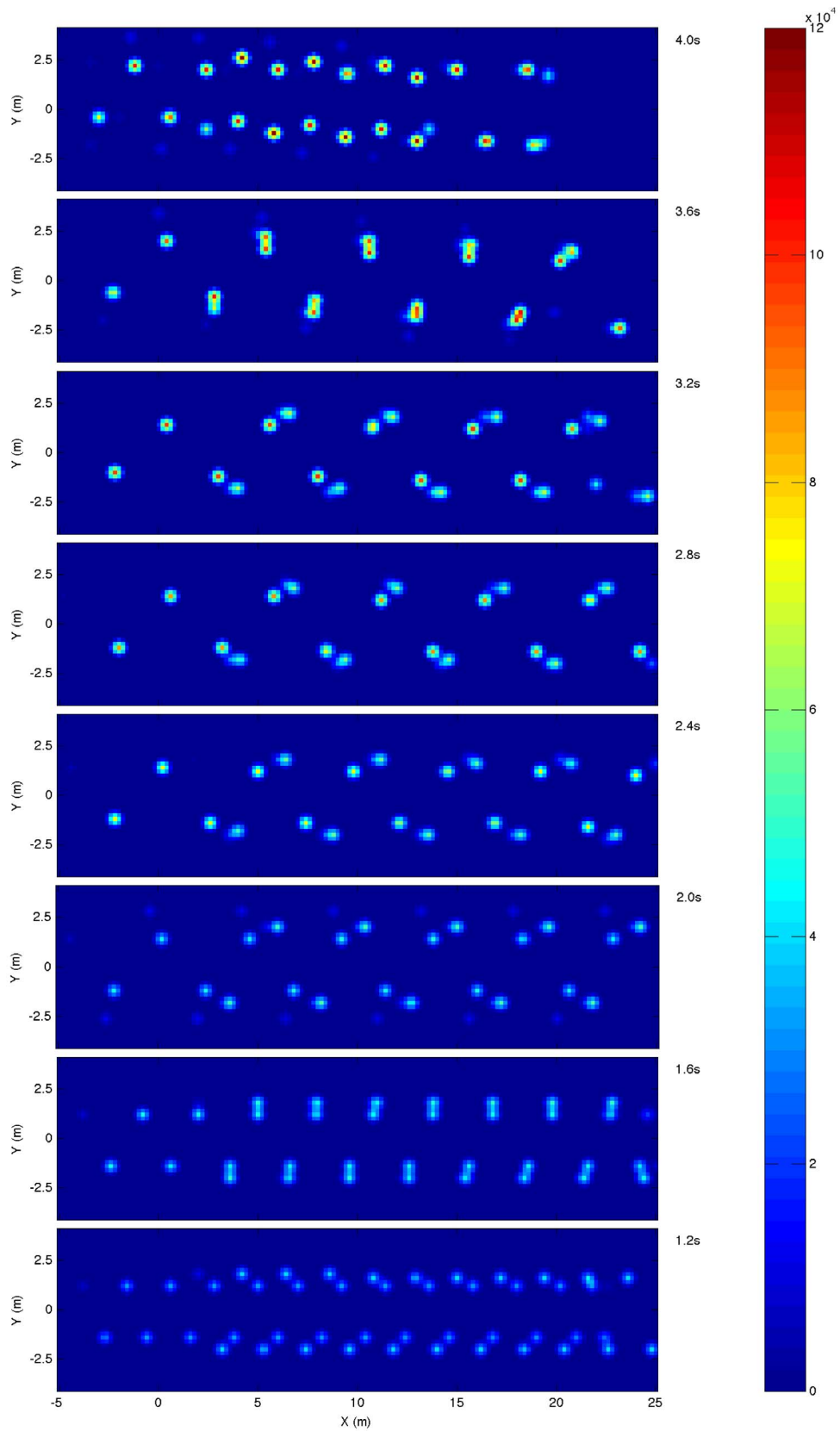


Figure 12. Simulated trackways generated by spatially summing the impulse between the foot contacts and the substrate.
 doi:10.1371/journal.pone.0078733.g012

gaits generated were very close to a pace, particularly when the cycle time was reduced. It is also useful to compare the generated gaits to trackway data. Figure 12 shows a spatial plot of the underfoot impulse which shows where individual footprints would be formed. At intermediate cycle times (2.4 to 3.2 s) these show marked similarity to standardised depictions of sauropod trackways [20].

Discussion

The process of creating a forward dynamic simulation of *Argentinosaurus* has highlighted a number of interesting aspects of its biology. The mass estimate of 83 tonnes using the convex hull technique is relatively robust provided that the reconstruction is accurate. That it agrees broadly with estimates based on single bone allometric relationships is encouraging given the fragmentary nature of the fossil material on which it is based. Reconstructing the soft tissue parameters correctly are, of course, essential for an accurate assessment of its locomotor capabilities, and the process described here illustrates how comparative approaches can be used to find appropriate values for these parameters. However it also highlights the dearth of suitable data. Many vertebrates have been carefully dissected and their internal anatomy described in exquisite detail. Unfortunately very few vertebrates have been dissected quantitatively, and the lack of soft tissue measurements means that we do not know whether the trends that have been identified concerning muscle mass distribution are widely applicable among cursorial vertebrates. The same issues are present for joint ranges of motion: both for functional range of motion during gait and for maximum ranges of motion during other activities. The findings for muscle fibre length as a function of length change are based on a large number of muscles but relatively few (if diverse) species. Ideally this would be extended to more species but because there is a strong physiological basis for the 50% (extension/fibre length) ratio, it is likely that this finding is robust. A large data set would improve the estimate of the mode and might reveal patterns between muscles that have different primary functions. However the individual variation in this ratio is very large and deciding a specific, muscle by muscle value, for fossil animals may prove difficult.

The predictions of equation 2 fall directly from the (extension/fibre length) ratio argument and have profound effects for locomotor modelling in extinct animals. It is usually impossible, based on the fossil remains, to know how muscle is partitioned. However this equation generates a functional minimum for the muscle mass around a particular joint once a range of motion has been specified. It is particularly the case in theropod dinosaurs, with their relatively long metatarsus, that lack of sufficient ankle extensor muscle has caused problems in our earlier simulation models, and has been highlighted as a speed limiting factor in static models [42,58]. There may be mechanical systems that can avoid this problem. Distal muscles can use parallel and serial connective tissue to increase the passive elasticity of muscles and this might allow much of the movement at the joint to be accommodated by elastic stretch rather than active contraction. There is considerable difference between the passive properties of different muscles (e.g. frog hindlimb muscles [83]) but little systematic biomechanical analysis. Similarly, clever use of multiple joint muscles with moment arms that change with joint angle may also minimise the force required at particular stages in the locomotor cycle. Alternatively, control heuristics can ensure that the load moment arm is always small when high loads are applied. In practice, it is likely that all these mechanisms come into play, but there are clear lower limits to the amount of muscle necessary

to allow active force generation in situations where large ranges of joint motion are required such as standing up.

The simulation outputs reveal that it is indeed possible to generate convincing gaits using a global optimisation system provided that the fundamental mechanics of the system are gait compatible. This in itself is useful since it provides a functional bracket to soft-tissue reconstructions. However it is clear that generating efficient gait is rather difficult. The metabolic cost of locomotion has been shown to scale negatively with body mass [$C = 10.79 \text{ m}^{-0.31}$ [84]]. This equation would predict a value of $0.322 \text{ J kg}^{-1} \text{ m}^{-1}$ which is far lower than the $3.81 \text{ J kg}^{-1} \text{ m}^{-1}$ found by the simulation. It may be that this relationship cannot be extrapolated to large body masses depending on how the mechanical cost of locomotion scales [85] since the mechanical cost per kilogram may be mass independent at approximately $1 \text{ J kg}^{-1} \text{ m}^{-1}$ and the metabolic cost cannot be lower than the mechanical cost. The largest animal that we have good data for the metabolic cost of locomotion is the horse with values of about $1.5 \text{ J kg}^{-1} \text{ m}^{-1}$ for a mean body mass of 515 kg. It is possible that the control pattern, based on 57 parameters, is simply not complex enough, to specify highly efficient gait. Locomotor control is certainly an area where further work is necessary, but increasing the sophistication of the control system increases the number of search parameters and this can actually lead to worse solutions being found. Systems that use incremental search are therefore potentially useful such as increasing the control complexity in subsequent repeats. Heuristics such as phase resetting may prove helpful in this context [86]. The choice of footfall pattern selected by the model is interesting because the model is free to choose footfall patterns, and there are considerable footfall pattern differences found among living species [87]. However it is clear from other work on simulation of quadrupedal gait [88] that a considerable number of repeats need to be performed before conclusions about gait selection can be made. The gaits generated are also somewhat slow but this may be a function of the relatively minimal muscle availability, or perhaps also due to the lack of elastic support structures which would stiffen the limbs and increase elastic recoil. It is clear that such passive structures, such as the stay apparatus in the horse [89], are essential for effective quadrupedal locomotion and we would predict that such would be found in sauropod dinosaurs.

There are a number of areas where the model needs to be improved. There is a great shortage of comparative neontological data and this needs to be collected to improve any soft tissue reconstruction. The model has limited biorealism at present, and future models should incorporate a full myological reconstruction. In addition spinal mobility, particularly at the neck and tail, should also be investigated. Similarly, increased complexity in the control system, particularly feedback from skeletal loading, should be incorporated. The model relies heavily on the full body skeletal reconstruction and more work needs to be done on other, more complete sauropod specimens to confirm any findings. Finally the model should be validated using a Monte Carlo sensitivity analysis [90] to investigate which parameters have the greatest effect on the model's predictions and how these individual parameters might interact.

Conclusions

Forward dynamic simulations shows that an 83 tonne sauropod is mechanically competent at slow speed locomotion. However it is clear that this is approaching a functional limit and that restricting the joint ranges of motion is necessary for a model without hypothetical passive support structures. Much larger terrestrial

vertebrates may be possible but would probably require significant remodelling of the body shape, or significant behavioural change, to prevent joint collapse due to insufficient muscle.

Supporting Information

Movie S1 Lateral view movie file generated from the best example using a 1.0 s gait cycle time. (MPG)

Movie S2 Lateral view movie file generated from the best example using a 1.2 s gait cycle time. (MPG)

Movie S3 Lateral view movie file generated from the best example using a 1.4 s gait cycle time. (MPG)

Movie S4 Lateral view movie file generated from the best example using a 1.6 s gait cycle time. (MPG)

Movie S5 Lateral view movie file generated from the best example using a 1.8 s gait cycle time. (MPG)

Movie S6 Lateral view movie file generated from the best example using a 2.0 s gait cycle time. (MPG)

Movie S7 Lateral view movie file generated from the best example using a 2.2 s gait cycle time. (MPG)

Movie S8 Lateral view movie file generated from the best example using a 2.4 s gait cycle time. (MPG)

Movie S9 Lateral view movie file generated from the best example using a 2.6 s gait cycle time. (MPG)

Movie S10 Lateral view movie file generated from the best example using a 2.8 s gait cycle time. (MPG)

Movie S11 Lateral view movie file generated from the best example using a 3.0 s gait cycle time. (MPG)

Movie S12 Lateral view movie file generated from the best example using a 3.2 s gait cycle time. (MPG)

Movie S13 Lateral view movie file generated from the best example using a 3.4 s gait cycle time. (MPG)

Movie S14 Lateral view movie file generated from the best example using a 3.6 s gait cycle time. (MPG)

Movie S15 Lateral view movie file generated from the best example using a 3.8 s gait cycle time. (MPG)

Movie S16 Lateral view movie file generated from the best example using a 4.0 s gait cycle time. (MPG)

Data File S1 GaitSym model specification file used to generate Movie S1. (XML)

Data File S2 GaitSym model specification file used to generate Movie S2. (XML)

Data File S3 GaitSym model specification file used to generate Movie S3. (XML)

Data File S4 GaitSym model specification file used to generate Movie S4. (XML)

Data File S5 GaitSym model specification file used to generate Movie S5. (XML)

Data File S6 GaitSym model specification file used to generate Movie S6. (XML)

Data File S7 GaitSym model specification file used to generate Movie S7. (XML)

Data File S8 GaitSym model specification file used to generate Movie S8. (XML)

Data File S9 GaitSym model specification file used to generate Movie S9. (XML)

Data File S10 GaitSym model specification file used to generate Movie S10. (XML)

Data File S11 GaitSym model specification file used to generate Movie S11. (XML)

Data File S12 GaitSym model specification file used to generate Movie S12. (XML)

Data File S13 GaitSym model specification file used to generate Movie S13. (XML)

Data File S14 GaitSym model specification file used to generate Movie S14. (XML)

Data File S15 GaitSym model specification file used to generate Movie S15. (XML)

Data File S16 GaitSym model specification file used to generate Movie S16. (XML)

Acknowledgments

We would like to thank Zoller + Fröhlich Germany and Manchester for their assistance with the laser scanning, and the staff at the Museo Municipal Carmen Funes, Plaza Huincul, Argentina, for their assistance accessing specimens. High performance computing on HECToR and N8 was provided by EPSRC.

Author Contributions

Conceived and designed the experiments: WIS PLM LM RC. Performed the experiments: WIS PLM RC. Analyzed the data: WIS PLM LM RC. Contributed reagents/materials/analysis tools: WIS PLM LM RC. Wrote the paper: WIS PLM LM RC.

References

- Cope ED (1896) The Primary Factors of Organic Evolution. New York: Open Court Publishing Co.
- Coombs WP (1978) Theoretical aspects of cursorial adaptations in dinosaurs. Quarterly Review of Biology 53: 393–418.
- Biewener AA (1989) Scaling body support in mammals: limb posture and muscle mechanics. Science 245: 45–48.
- Carrano MT (2006) Body-size evolution in the Dinosauria. In: Carrano MT, Blob RW, Gaudin TJ, Wible JR, editors. Amniote paleobiology: perspectives on the evolution of mammals, birds, and reptiles. Chicago: University of Chicago Press. 225–268.
- Schmidt-Nielsen K (1984) Scaling: Why is animal size so important? Cambridge: Cambridge University press.
- Currey JD (2002) Bones, structures and mechanics. Princeton: Princeton University Press.
- Wood GL (1972) Animal Facts and Feats. New York: Doubleday.
- Christiansen P (2004) Body size in proboscideans, with notes on elephant metabolism. Zoological Journal of the Linnean Society 140: 523–549.
- Hutchinson JR, Ng-Thow-Hing V, Anderson FC (2007) A 3D interactive method for estimating body segmental parameters in animals: Application to the turning and running performance of *Tyrannosaurus rex*. Journal of Theoretical Biology 246: 660–680.
- Sander PM, Christian A, Clauss M, Fechner R, Gee CT, et al. (2011) Biology of the sauropod dinosaurs: the evolution of gigantism. Biological Reviews 86: 117–155.
- Paul GS (1997) Dinosaur models: The good, the bad, and using them to estimate the mass of dinosaurs. In: Wolberg DL, Stump E, Rosenberg GD, editors. Dinofest International Society Proceedings. Philadelphia: Academy of Natural Sciences. 129–154.
- Carpenter K (2006) Biggest of the big: a critical re-evaluation of the mega-sauropod *Amphicoelias fragillimus*. In: Foster JR, Lucas SG, editors. Paleontology and geology of the Upper Jurassic Morrison Formation. New Mexico: New Mexico Museum of Natural History and Science Bulletin. 131–133.
- Hill AV (1950) The dimensions of animals and their muscular dynamics. Science Progress 38: 209–230.
- Hokkanen JEI (1986) The size of the largest land animal. Journal of Theoretical Biology 118: 491–499.
- Biewener AA (1991) Musculoskeletal design in relation to body size. Journal of Biomechanics 24: 19–29.
- Genin JJ, Willems PA, Cavagna GA, Lair R, Heglund NC (2010) Biomechanics of locomotion in Asian elephants. Journal of Experimental Biology 213: 694–706.
- Ren L, Butler M, Miller C, Paxton H, Schwerda D, et al. (2008) The movements of limb segments and joints during locomotion in African and Asian elephants. Journal of Experimental Biology 211: 2735–2751.
- Marey EJ, Pagès C (1887) Locomotion comparée: mouvement du membre pelvien chez l'homme, l'éléphant et le cheval. Comptes Rendus de l'Académie des Sciences 105: 149–156.
- Muybridge E (1899) Animals in motion. London: Chapman & Hall.
- Alexander RM (1989) Dynamics of dinosaurs and other extinct giants. Cambridge: Cambridge University Press.
- Johnson RE, Ostrom JH (1995) The forelimb of *Torosaurus* and an analysis of the posture and gait of ceratopsians. In: Thomasson J, editor. Functional morphology in vertebrate paleontology. New York: Cambridge University Press. 205–218.
- Wilson JA, Carrano M (1999) Titanosaurs and the origin of “wide-gauge” trackways: A biomechanical and systematic perspective on sauropod locomotion. Paleobiology 25: 252–267.
- Otero A, Vizcaino SF (2008) Hindlimb musculature and function of *Neuquensaurus australis* Lydekker (Sauropoda: Titanosauria). Ameghiniana 45: 333–348.
- Wilson JA (2005) Overview of sauropod phylogeny and evolution. In: Curry Rogers KA, Wilson JA, editors. The sauropods: evolution and paleobiology. Berkeley: University of California Press. 15–49.
- Carrano MT (2005) The evolution of sauropod locomotion. In: Curry Rogers KA, Wilson JA, editors. The sauropods, evolution and paleobiology. Berkeley: University of California Press. 229–251.
- González Riga BJ (2011) Speeds and stance of titanosaur sauropods: analysis of *Titanopodus* tracks from the Late Cretaceous of Mendoza, Argentina. Anais da Academia Brasileira de Ciências 83: 279–290.
- Vila B, Oms O, Galobart À, Bates KT, Egerton VM, et al. (2013) Dynamic similarity in titanosaur sauropods: ichnological evidence from the Fumanya dinosaur tracksite (Southern Pyrenees). PLoS ONE 8: e57408.
- Falkingham PL, Bates KT, Margetts L, Manning PL (2011) The ‘Goldilocks’ effect: preservation bias in vertebrate track assemblages. Journal of the Royal Society, Interface 8: 1142–1154.
- Manning PL (2004) A new approach to the analysis and interpretation of tracks: examples from the dinosauria. In: McIlroy D, editor. The application of ichnology to palaeoenvironmental and stratigraphic analysis: Geological Society, London, Special Publications. 93–123.
- Yamazaki N, Hase K, Ogihara N, Hayamizu N (1996) Biomechanical analysis of the development of human bipedal walking by a neuro-musculo-skeletal model. Folia Primatologia 66: 253–271.
- Crompton RH, Li Y, Wang W, Günther MM, Savage R (1998) The mechanical effectiveness of erect and “bent-hip, bent-knee” bipedal walking in *Australopithecus afarensis*. Journal of Human Evolution 35: 55–74.
- Kramer PA (1999) Modelling the locomotor energetics of extinct hominids. Journal of Experimental Biology 202: 2807–2818.
- Sellers WI, Dennis LA, Wang WJ, Crompton RH (2004) Evaluating alternative gait strategies using evolutionary robotics. Journal of Anatomy 204: 343–351.
- Sellers WI, Cain GM, Wang W, Crompton RH (2005) Stride lengths, speed and energy costs in walking of *Australopithecus afarensis*: using evolutionary robotics to predict locomotion of early human ancestors. Journal of the Royal Society, Interface 5: 431–441.
- Nagano A, Umberger BR, Marzke MW, Gerritsen KGM (2005) Neuromusculoskeletal computer modeling and simulation of upright, straight-legged, bipedal locomotion of *Australopithecus afarensis* (A.L. 288-1). American Journal of Physical Anthropology 126: 2–13.
- Ogihara N, Yamazaki N (2006) Computer simulation of bipedal locomotion: toward elucidating correlations among musculoskeletal morphology, energetics, and the origin of bipedalism. In: Ishida H, Tuttle R, Pickford M, Nakatsukasa M, editors. Human origins and environmental backgrounds. New York: Springer. 167–174.
- Sellers WI, Pataky TC, Caravaggi P, Crompton R H (2010) Evolutionary robotic approaches in primate gait analysis. International Journal of Primatology 31: 321–338.
- Crompton RH, Pataky TC, Savage R, D’Aouit K, Bennett MR, et al. (2012) Human-like external function of the foot, and fully upright gait, confirmed in the 3.66 million year old Laetoli hominin footprints by topographic statistics, experimental footprint-formation and computer simulation. Journal of the Royal Society, Interface 9: 707–719.
- Blanco RE, Jones WW (2005) Terror birds on the run: a mechanical model to estimate its maximum running speed. Proceedings of the Royal Society of London B 272: 1769–1773.
- Gatesy SM, Middleton KM, Jenkins FA, Jr, Shubin NH (1999) Three-dimensional preservation of foot movements in Triassic theropod dinosaurs. Nature 399: 141–144.
- Stevens KA (2002) DinoMorph: parametric modeling of skeletal structures. Senckenbergiana Lethaea 82: 23–34.
- Hutchinson JR, Anderson FC, Blemker SS, Delp SL (2005) Analysis of hindlimb muscle moment arms in *Tyrannosaurus rex* using a three-dimensional musculo-skeletal computer model: implications for stance, gait, and speed. Paleobiology 31: 676–701.
- Sellers WI, Manning PL (2007) Estimating dinosaur maximum running speeds using evolutionary robotics. Proceedings of the Royal Society of London B 274: 2711–2716.
- Sellers WI, Manning PL, Lyson T, Stevens K, Margetts L (2009) Virtual palaeontology: gait reconstruction of extinct vertebrates using high performance computing. Palaeontologia Electronica 12: 11A.
- Bonaparte J, Coria R (1993) Un nuevo y gigantesco sauropodo titanosaurio de la Formación Rio Limay (Albiano-Cenomaniano) de la Provincia del Neuquen, Argentina. Ameghiniana 30: 271–282.
- Mazzetta GV, Christiansen P, Fariña RA (2004) Giants and bizarres: body size of some southern South American Cretaceous dinosaurs. Historical Biology 65: 1–13.
- Winter DA (1990) Biomechanics and motor control of human movement. New York: John Wiley and Sons.
- Chandler RF, Clauser CE, McConville JT, Reynolds HM, Young JW (1975) Investigation of inertial properties of the human body. Ohio: Aerospace Medical Research Laboratories, Wright-Patterson Air Force Base. AMRL-TR-74-137, AD-A016-485. DOT-HS-801-430.
- Zatvorski VM, Seluyanov V (1983) The mass and inertia characteristics of the main segments of the human body. In: Matsui H, Koayashi K, editors. Biomechanics VIII-B. Champaign, Illinois: Human Kinetic Publishers. 1154–1159.
- Crompton RH, Li Y, Alexander RM, Wang W, Günther MM (1996) Segment inertial properties of primates - new techniques for laboratories and field studies of locomotion. American Journal of Physical Anthropology 99: 547–570.
- Hanavan EP (1964) A mathematical model of the human body. Ohio: Aerospace Medical Research Laboratories, Wright-Patterson Air Force Base. AMRL-TR-64-102, AD-608-463 AMRL-TR-64-102, AD-608-463.
- Yeardon MR (1990) The simulation of aerial movement-II. A mathematical inertia model of the human body. Journal of Biomechanics 23: 67–74.
- Bates KT, Manning PL, Hodgetts D, Sellers WI (2009) Estimating mass properties of dinosaurs using laser imaging and 3D computer modelling. PLoS ONE 4: e4532.
- Sellers WI, Hepworth-Bell J, Falkingham PL, Bates KT, Brassey CA, et al. (2012) Minimum convex hull mass estimations of complete mounted skeletons. Biology Letters 8: 842–845.
- Yoko T, Takahashi A, Okada H, Ohyama KB, Muraoka M (1998) Is the selection of body segment inertia parameters critical to the results of kinematic

- and kinetic analysis of human movement? *Anthropological Science* 106: 371–383.
56. Bates KT, Manning PL, Margetts L, Sellers WI (2010) Sensitivity analysis in evolutionary robotic simulations of bipedal dinosaur running. *Journal of Vertebrate Paleontology* 30: 458–466.
 57. Witmer LM (1995) The Extant Phylogenetic Bracket and the importance of reconstructing soft tissues in fossils. In: Thomason JJ, editor. *Functional morphology in vertebrate paleontology*. Cambridge: Cambridge University Press. 19–33.
 58. Hutchinson JR, Garcia M (2002) Tyrannosaurus was not a fast runner. *Nature* 415: 1018–1021.
 59. Wareing K, Tickle P, Stokkan KA, Codd JR, Sellers WI (2011) The musculoskeletal anatomy of the reindeer (*Rangifer tarandus*): fore- and hindlimb. *Polar Biology* 34: 1571–1578.
 60. Méndez J, Keys A (1960) Density and composition of mammalian muscle. *Metabolism* 9: 184–188.
 61. Hutchinson JR (2004) Biomechanical modeling and sensitivity analysis of bipedal running ability. II. Extinct taxa. *Journal of Morphology* 262: 441–461.
 62. Umberger BR, Gerritsen KGM, Martin PE (2003) A model of human muscle energy expenditure. *Computational Methods in Biomechanics and Biomedical Engineering* 6: 99–111.
 63. Alexander RM (2003) *Principles of Animal Locomotion*. Princetown, NJ: Princetown University Press.
 64. Zheng N, Fleisig GS, Escamilla RF, Barrentine SW (1998) An analytical model of the knee for estimation of internal forces during exercise. *Journal of Biomechanics* 31: 963–967.
 65. Pierrynowski MR (1995) Analytical representation of muscle line of action and geometry. In: Allard P, Stokes IAF, Blanch JP, editors. *Three-dimensional analysis of human movement*. Champaign, Illinois: Human Kinetic Publishers. 215–256.
 66. Westneat MW (2003) A biomechanical model for analysis of muscle force, power output and lower jaw motion in fishes. *Journal of Theoretical Biology* 223: 269–281.
 67. Medler S (2002) Comparative trends in shortening velocity and force production in skeletal muscles *American Journal of Physiology - Regulatory, Integrative and Comparative Physiology* 283: 368–378.
 68. Minetti AE, Alexander RM (1997) A theory of metabolic costs for bipedal gaits. *Journal of Theoretical Biology* 186: 467–476.
 69. McGinnis PM (1999) *Biomechanics of Sport and Exercise*. Champagne, Illinois: Human Kinetics.
 70. An KN, Takahashi K, Harrigan TP, Chao EY (1984) Determination of muscle orientations and moment arms. *Transactions of the American Society of Mechanical Engineers* 106: 280–283.
 71. Thorpe SKS, Crompton RH, Günther MM, Ker RF, Alexander RM (1999) Dimensions and moment arms of the hind- and forelimb muscles of common chimpanzees (*Pan troglodytes*). *American Journal of Physical Anthropology* 110: 179–199.
 72. Williams S, Wilson A, Daynes J, Peckham K, Payne R (2008) Functional anatomy and muscle moment arms of the thoracic limb of an elite sprinting athlete: the racing greyhound (*Canis familiaris*). *Journal of Anatomy* 213: 373–382.
 73. Williams S, Wilson A, Rhodes L, Andrews J, Payne R (2008) Functional anatomy and muscle moment arms of the pelvic limb of an elite sprinting athlete: the racing greyhound (*Canis familiaris*). *Journal of Anatomy* 213: 361–372.
 74. Smith NC, Wilson AM, Jespers KJ, Payne RC (2006) Muscle architecture and functional anatomy of the pelvic limb of the ostrich (*Struthio camelus*). *Journal of Anatomy* 209: 765–779.
 75. Smith NC, Payne RC, Jespers KJ, Wilson AM (2007) Muscle moment arms of pelvic limb muscles of the ostrich (*Struthio camelus*). *Journal of Anatomy* 211: 313–324.
 76. Crook TC, Cruickshank SE, McGowan CM, Stubbs N, Wilson AM, et al. (2010) A comparison of the moment arms of pelvic limb muscles in horses bred for acceleration (Quarter Horse) and endurance (Arab). *Journal of Anatomy* 217: 26–37.
 77. Alexander RM, Maloiy G, Ker RF, Jayes AS, Warui CN (1982) The role of tendon elasticity in the locomotion of the camel (*Camelus dromedarius*). *Journal of Zoology* 198: 293–313.
 78. Silder A, Whittington B, Heiderscheit B, Thelen DG (2007) Identification of passive elastic joint moment-angle relationships in the lower extremity. *Journal of Biomechanics* 40: 2628–2635.
 79. Arnold EM, Ward SR, Lieber RL, Delp SL (2010) A model of the lower limb for analysis of human movement. *Annals of Biomedical Engineering* 38: 269–279.
 80. Mühlhain H (1991) Asynchronous parallel search by the parallel genetic algorithm. *Proceedings of the Third IEEE Symposium on Parallel and Distributed Processing*, Dallas, Texas. 526–533.
 81. Bornstein MN, Bornstein HG (1976) The pace of life. *Nature* 259: 557–558.
 82. Hildebrand M (1965) Symmetrical gaits in horses. *Science* 150: 701–708.
 83. Wilkie DR (1968) *Muscle*. Institute of Biology's Studies in Biology no 11. London: Edward Arnold (Publishers) Ltd.
 84. Full RJ, Zuccarello DA, Tullis A (1990) Effect of variation in form on the cost of terrestrial locomotion. *Journal of Experimental Biology* 150: 233–246.
 85. Nudds RL, Codd JR, Sellers WI (2009) Evidence for a mass dependent step-change in the scaling of efficiency in terrestrial locomotion. *PLoS ONE* 4: e6927.
 86. Yamasaki T, Nomura T, Sato S (2003) Phase reset and dynamic stability during human gait. *Biosystems* 71: 221–232.
 87. Hildebrand M (1980) The adaptive significance of tetrapod gait selection. *American Zoologist* 20: 255–267.
 88. Sellers WI, Margetts L, Bates KT, Chamberlain AT (2013) Exploring diagonal gait using a forward dynamic 3D chimpanzee simulation. *Folia Primatologica* 84: 180–200.
 89. Skerritt GC, McLelland J (1984) *Introduction to the functional anatomy of the limbs of the domestic animals*. Bristol: Wright.
 90. Campolongo F, Saltelli A, Sørensen T, Taratola S (2000) Hitchhikers' guide to sensitivity analysis. In: Saltelli A, Chan K, Scott EM, editors. *Sensitivity analysis*. Chichester: Wiley. 15–47.

Quantitative Interpretation of Tracks for Determination of Body Mass

Tom Schanz^{1*}, Yvonne Lins¹, Hanna Viefhaus¹, Thomas Barciaga¹, Sashima Läbe², Holger Preuschoft³, Ulrich Witzel⁴, P. Martin Sander²

1 Lehrstuhl für Grundbau, Boden- und Felsmechanik, Ruhr-Universität Bochum, Bochum, Germany, **2** Steinmann-Institut für Geologie, Mineralogie und Paläontologie, Universität Bonn, Bonn, Germany, **3** Abteilung für Funktionelle Morphologie, Institut für Anatomie, Ruhr-Universität Bochum, Bochum, Germany, **4** Forschungsgruppe Biomechanik, Lehrstuhl für Maschinenelemente und Konstruktionslehre, Ruhr-Universität Bochum, Bochum, Germany

Abstract

To better understand the biology of extinct animals, experimentation with extant animals and innovative numerical approaches have grown in recent years. This research project uses principles of soil mechanics and a neoichnological field experiment with an African elephant to derive a novel concept for calculating the mass (i.e., the weight) of an animal from its footprints. We used the elephant's footprint geometry (i.e., vertical displacements, diameter) in combination with soil mechanical analyses (i.e., soil classification, soil parameter determination in the laboratory, Finite Element Analysis (FEA) and gait analysis) for the back analysis of the elephant's weight from a single footprint. In doing so we validated the first component of a methodology for calculating the weight of extinct dinosaurs. The field experiment was conducted under known boundary conditions at the Zoological Gardens Wuppertal with a female African elephant. The weight of the elephant was measured and the walking area was prepared with sediment in advance. Then the elephant was walked across the test area, leaving a trackway behind. Footprint geometry was obtained by laser scanning. To estimate the dynamic component involved in footprint formation, the velocity the foot reaches when touching the subsoil was determined by the Digital Image Correlation (DIC) technique. Soil parameters were identified by performing experiments on the soil in the laboratory. FEA was then used for the backcalculation of the elephant's weight. With this study, we demonstrate the adaptability of using footprint geometry in combination with theoretical considerations of loading of the subsoil during a walk and soil mechanical methods for prediction of trackmakers weight.

Citation: Schanz T, Lins Y, Viefhaus H, Barciaga T, Läbe S, et al. (2013) Quantitative Interpretation of Tracks for Determination of Body Mass. PLoS ONE 8(10): e77606. doi:10.1371/journal.pone.0077606

Editor: Peter Dodson, University of Pennsylvania, United States of America

Received: May 3, 2013; **Accepted:** September 6, 2013; **Published:** October 30, 2013

Copyright: © 2013 Schanz et al. This is an open-access article distributed under the terms of the Creative Commons Attribution License, which permits unrestricted use, distribution, and reproduction in any medium, provided the original author and source are credited.

Funding: No current external funding sources for this study.

Competing Interests: The authors have declared that no competing interests exist.

* E-mail: tom.schanz@rub.de

Introduction

Since the first massive bones of sauropods were discovered, many scientists have investigated how these animals evolved to their gigantic size [1–3]. Analyses and interpretation of sauropod gigantism are essential for the understanding of evolutionary constraints and how these constraints impact Earth's geological and biological history. Bones of sauropods, of course, are not their only remains in the fossil record, but the second most common evidence for their former existence are footprints and entire trackways. The track record is important because it provides anatomical details and locomotion patterns of the trackmaker. Unlike bones, which are often transported, trace fossils are autochthonous and provide unequivocal information about the actual habitat of the trackmaker. The enormous tracks of gigantic sauropod dinosaurs occur in sediments from the Late Triassic [4] to Cretaceous all over the world [5]: e.g., in tidal flat deposits of the Paluxy River tracksite in Texas, USA [6]; in fluvial deposits [7,8] and in lacustrine carbonate sediments of the Morrison Formation [9,10] or in lagoonal deposits in Münchhagen, Germany [11,12]. A comprehensive listing and review is found in [13].

In the past, mostly descriptive studies of tracks were done, but currently the focus is on understanding the paleobiology of the trackmaker. In general, it is possible to estimate anatomical details like hip heights [14] of the trackmaker from the tracks or to estimate walking velocity from measurements of pace and stride [15–17]. Modern vertebrate ichnology deals with experiments on living animals e.g., [18,19], artificial indenters in the laboratory e.g., [20,21], and computer-aided approaches e.g., [22,23]. Common methods for calculating body mass based on body volume and density were done with models [24], 3D scanning [25,26], or numerical methods [27]. Current numerical studies [28–31] have as their main objective to qualitatively better understand the kinematics of the foot indenting the subsoil and to relate subsoil properties to footprint quality and preservation.

Quantitative approaches to dinosaur footprints offer the perspective of addressing a fundamental question in dinosaur paleobiology, i.e., mass estimation. However, a reliable quantitative method for weight reconstruction from dinosaur footprints has not been developed so far, even though this is of major importance, especially for gigantic sauropods [32].

Here we introduce an approach for weight estimation based on footprint geometry using soil mechanical concepts. These can be used to back calculate the load applied to the subsoil by the

trackmaker's feet. The geometry of the footprint (i.e., vertical displacements and diameter) is strongly influenced by the applied stress and the constitutive characteristics of the subsoil. Note that we use the term "geometry" in a different way than in the literature on dinosaur ichnology where it refers to the parameters of entire trackways. However, we only study the individual footprint, not the trackway. The value of the stress applied to the subsoil depends on the weight of the dinosaur (i.e., a static component) as well as on the deceleration that the dinosaur foot experiences when coming into contact with the subsoil (i.e., a dynamic component). In addition, biomechanical aspects, such as gait and weight distribution among the four limbs of the trackmaker, have to be taken into account when dealing with this problem. An important step towards the application of the soil-mechanical approach to fossil footprints is the validation by work on extant tracks, also known as the actualistic approach in paleontology. The African elephant (*Loxodonta africana*) is the largest terrestrial animal today, just as the sauropods were in the Mesozoic. Considering elephants and sauropods show similarities in foot morphology, quadrupedality and massive, graviportal limbs, elephants have often been included as recent analogs in sauropod research e.g., [19,23]. The field part of our study was conducted at the Zoological Gardens Wuppertal, Germany. Briefly, after weighing an African elephant cow was walked across a prepared sand bed to produce footprints. Based on the footprint geometry, gait analysis and soil mechanical properties of the subsoil, the Finite Element Analysis (FEA) was adopted to back calculate the weight of the elephant. For simplicity, in this analysis we only consider layered subsoil properties that are homogenous within each layer. We are aware that the situation in track formation often is much more complex, especially for a foot penetrating soft layers in a large deformation type of kinematics before finding resistance at a competent layer below, see [30,33]. For this study we focus on sand as subsoil material because in a next step we will target sauropod footprints preserved in sandstones.

Well known sauropod track sites in sandstones are the Late Jurassic sites of Barkhausen [34,35] and Copper Ridge (Utah, USA) [7,36], and the Early Cretaceous site of MÜNCHENHAGEN [11,12], also Germany. Barkhausen shows several trackways of relatively small sauropods together with one theropod trackway in a fine-grained sand. The surface on which the animals walked is well preserved as indicated by the distinctive sediment bulges caused by the feet. The same applies to the Copper Ridge site which was made by a large sauropod that walked on a 15 cm thick bed of medium sand underlain by a mudstone. The MÜNCHENHAGEN site records numerous long trackways impressed in a 25 cm thick medium sandstone also underlain by a mudstone. Some of the tracks are partially eroded at this site, making them unsuitable for the soil mechanical approach to weight estimation. However, note that this paper only reports on a first step in methods development, showing that weight estimation from footprints is possible. Considerably more research is necessary before reliable results can be obtained for sauropods, let alone other dinosaurs. Note also that elephants and sauropods are particularly suitable for this approach because of their graviportal stance and locomotion and their simple foot morphology.

Methods and Materials

For the present research, FEA, gait analysis and Digital Image Correlation (DIC) technique were carried out, the specifics of both of which are described below. The subsoil used in the field experiment was classified and soil parameters were determined

with precision by performing several experiments in the laboratory. These parameters were needed as input parameters in the FEA simulations.

Finite element analysis (FEA) using an advanced constitutive soil model

For the numerical simulation of the observed elephant footprint geometry (i.e., vertical displacements and diameter) FEA was used. In routine soil mechanics applications we normally derive settlements from the applied load. However, in the current study, we took the opposite approach by applying a specific type of so called back analysis (inverse analysis) in order to determine the load from the settlements. Inverse analysis is a well established tool in soil mechanics (for an overview see [37]). The FEA code used in this study considers three spatial dimensions and was originally developed for the analysis of deformations in geotechnical applications. Soil behavior is simulated in a non-linear elastic-plastic manner. Several soil models, e.g., the Mohr-Coulomb model and the hardening soil model [38], that differ in accuracy, are implemented in the FEA code to model the mechanical behavior of soil. The Mohr-Coulomb model is an elastic-plastic material model, that assumes a constant stiffness of the material (i.e., the stiffness of the soil) with the depth. However, this condition is generally not met by the mechanical behavior of soils. The Mohr-Coulomb model is mostly used in initial approaches to numerical modeling of soil mechanical behavior only, but it is physically wrong for solving deformation problems as in this research.

A more realistic material model for the simulation of the behavior of different types of soil is the hardening soil model. When soil is subjected to primary loading, it shows an increase in stiffness with increasing stress and develops an irreversible plastic strain. In contrast to the Mohr-Coulomb model, the hardening soil model implements the stress dependent stiffness behavior of the soils, i.e., the hardening of the soil is taken into account. In addition to the material parameters used in the Mohr-Coulomb model, i.e., friction angle ϕ [°], cohesion c [kN/m²], dilatancy ψ [°], the hardening soil model requires further input parameters. These include the stiffness modulus E_{oed} [kN/m²] for primary compression loading (derived from one-dimensional compression tests), the unloading and reloading stiffness modulus E_{ur} [kN/m²] (derived from one-dimensional compression tests), as well as the deviatoric stiffness E_{50} [kN/m²] (derived from triaxial tests). In reality, all loading conditions and loading directions may occur simultaneously, depending on the spatial position of an observation point. Therefore a constitutive model as used in this study is required that automatically analyzes the loading conditions and applies the relevant stiffness. Considering the fact that stiffnesses may vary by a factor of 7 to 10, we have to admit that less realistic soil models than the hardening soil model cannot be used for quantitative analyses. The required input parameters were determined in standard soil mechanics laboratory experiments that we performed with the material used as subsoil in the elephant field experiment.

Method of digital image correlation (DIC)

As noted, the stress transmitted to the subsoil during animal walking has a dynamic and a static component. Subsoil deformation is a consequence of the maximum load, which either corresponds to the maximum static load $\sigma_{stat,max}$ or to the sum of dynamic load and the corresponding static load $\sigma_{dyn+stat}$. To determine the velocity of the elephant's foot at the time of contact with the subsurface, the DIC technique was used. The elephant's walk was recorded by a high speed camera (Casio Exilim EX-F1,

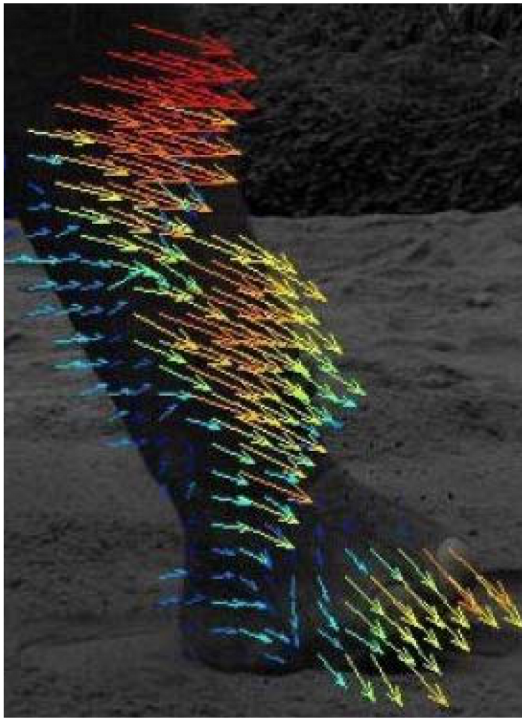


Figure 1. Vectors of displacement of elephant’s forelimb obtained by DIC technique. The vectors illustrate the amount (length and color of arrows) and direction (orientation of arrows) of displacement.
doi:10.1371/journal.pone.0077606.g001

60 frames per second) and deformation of pixel clusters was analyzed for the defined time interval (Figure 1). See reference [39], for details of the DIC technique. The velocity vectors obtained by the DIC technique permit calculation of the dynamic stress applied to the subsoil based on the following equation:

$$\sigma_{dyn} = \frac{m \cdot v_1^2}{2 \cdot s \cdot A} \quad (1)$$

where m [kg] is the mass in motion (i.e., the weight distributed over the limb considered); v_1 [m/s] is the velocity of the mass (i.e., the velocity of the limb) on impact on the subsoil; s [m] is the path of deceleration (i.e., the deformation of the subsoil); and A [m²] is the area of the foot obtained from footprint geometry. If the state of dynamic loading corresponds to the maximum load, a factor f_{dyn} [-] can be obtained that relates $\sigma_{dyn+stat}$ to σ_{stat} :

$$f_{dyn} = \frac{\sigma_{dyn+stat}}{\sigma_{stat}} \quad (2)$$

Thus, the stresses determined by FEA (i.e., $\sigma_{dyn+stat}$) can then be related to the weight of the elephant:

$$m_e = \frac{\sigma_{dyn+stat} \cdot A}{f_{dyn} \cdot g \cdot f_{wd}} \quad (3)$$

where m_e [kg] is the mass of the elephant; g [m/s²] is the acceleration of gravity; and f_{wd} [-] is the factor considering weight

distribution on the limbs, i.e., gait, by relating the mass carried by the particular limb (m_{limb} [kg]) to the total mass (m_{tot} [kg]):

$$f_{wd} = \frac{m_{limb}}{m_{tot}} \quad (4)$$

In summary, the factors f_{dyn} [-] and f_{wd} [-] differ for varying loading situations (i.e., combination of footfalls and walking velocity), but do not depend on the total mass of the elephant. Thus, application of Equation 3 to weight estimation of any other animal requires considerations of the anatomical characteristics and locomotion patterns of the trackmaker.

3D scanner

Footprint geometry was captured with a portable laser scanner designed and constructed for this purpose. The scanner (see Figure 2) covers an area of 800×800 mm. The 3D surface scan provides very precise ($\pm 75 \mu\text{m}$) information of the settlements in the subsoil produced by the weight of the elephant. This information is later needed for calculating the weight of the elephant using FEA.

Classification of the soil used and derivation of soil parameters

It is important to note that the general approach (including its accuracy) suggested in this paper does not depend on the type of subsoil. Different constitutive models are available and well validated in soil mechanics to consider, for example, cohesive soils or low permeability soils including consolidation analysis [40]. The sediment used in the neoichnological experiment was the so called Rhine sand. The grain-size distribution of Rhine sand is given in Figure 3. As can be seen from the grain-size distribution curve, grain-sizes range between 0.1 and 4.0 mm in diameter. The estimated coefficient of curvature $C_c = d_{30}^2 / (d_{60} \cdot d_{10})$ and the coefficient of uniformity $C_u = d_{60} / d_{10}$, lead to the conclusion that the sediment is a poorly graded medium sand. Based on Hazen’s formula[41], a permeability coefficient of $k = 0.0003$ m/s was calculated. The loose density was found to be $\rho_{min} = 1.51$ g/cm³, and the dense density was found to be $\rho_{max} = 1.79$ g/cm³, which correspond to a loose void ratio of $e_{max} = 0.75$ and a dense void ratio of $e_{min} = 0.48$.



Figure 2. 3D laser scanner developed and custom-built for recording animal tracks. The scanner covers an area of 800×800 mm.
doi:10.1371/journal.pone.0077606.g002

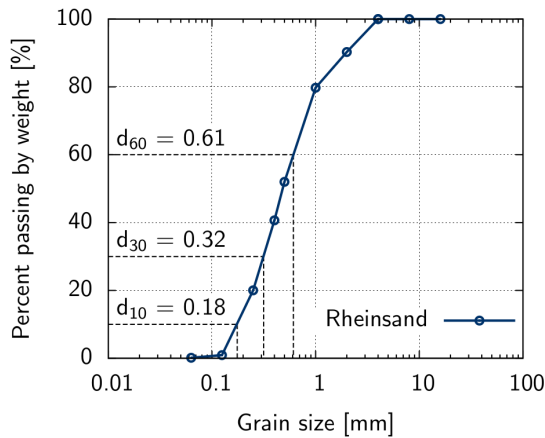


Figure 3. Grain-size distribution of Rhine sand. Grain sizes are given for characteristic values, i.e., for 10% (d_{10}), 30% (d_{30}), and 60% (d_{60}) of the sand passing the corresponding mesh size by weight. doi:10.1371/journal.pone.0077606.g003

Several tests are available in soil mechanics to measure the stress-strain behavior of a soil, e.g., the isotropic compression test, the one-dimensional compression test, the triaxial test, and the direct shear test [42].

In the present study, the stress-strain behavior of the soil was investigated using a one-dimensional compression and rebound test. This type of test is performed in conventional oedometer cells. Results derived from the one-dimensional compression and rebound test conducted on Rhine sand are shown in Figure 4 and Figure 5. This test includes the application of stress to a soil sample along the vertical axis, while the strain in the horizontal direction is restricted. To determine stress-strain behavior, the one-dimensional compression and rebound test is often used because it is simple to perform. We also used this test because the strain condition in the soil sample is approximately similar to the situation in the center of the load generated by the elephant's foot on the subsoil. Important parameters derived from one-dimensional compression test are the stiffness moduli E_{oed} [kN/m²] and E_{ur} [kN/m²] that describe the stress dependent stiffness in a soil [43]. The stress dependent stiffness moduli E_{oed} and E_{ur} can be calculated based on Equation 5, where E_{oed}^{ref} is the reference stiffness modulus for initial loading and E_{ur}^{ref} is the reference stiffness modulus for the unloading/reloading path determined for a reference stress $\sigma_{ref} = 100$ kN/m² and m is a dimensionless parameter [44,45]:

$$E_{oed} = E_{oed}^{ref} \cdot \left(\frac{\sigma}{\sigma_{ref}} \right)^m \quad E_{ur} = E_{ur}^{ref} \cdot \left(\frac{\sigma}{\sigma_{ref}} \right)^m \quad (5)$$

The parameter m and the normalized stiffness modulus E_{oed}^{ref} and E_{ur}^{ref} are derived from a regression analysis, that is presented in the diagram in Figure 5. To linearize the function of vertical net stress against strain $\varepsilon(\sigma)$, the logarithm of the strain $\ln(\varepsilon)$ and the logarithm of the normalized stress $\ln(\sigma/\sigma_{ref})$ is used:

$$\ln(\varepsilon) = \alpha \cdot \ln\left(\frac{\sigma}{\sigma_{ref}}\right) + \beta \quad E_{oed,ur}^{ref} = \frac{1}{\alpha} \cdot \frac{\sigma_{ref}}{\exp^{\beta}} \quad m = 1 - \alpha \quad (6)$$

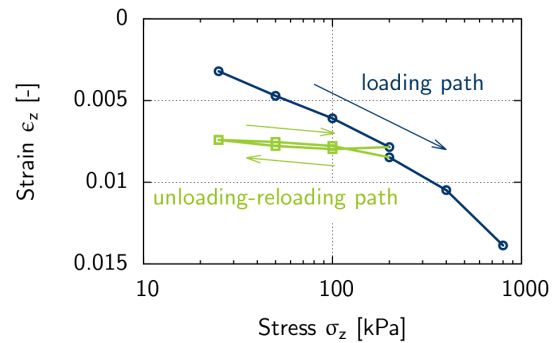


Figure 4. One dimensional compression and rebound test results for Rhine sand with an initial density of $e = 0.6$. Initial loading was conducted towards a value of 200 kPa followed by an unloading-reloading path down to 25 kPa. Initial loading was then continued towards a value of 800 kPa. doi:10.1371/journal.pone.0077606.g004

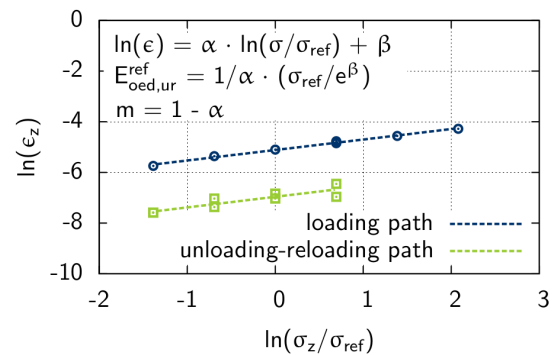


Figure 5. One dimensional compression and rebound regression analysis for Rhine sand with an initial density of $e = 0.6$. Parameters α and β of linear functions for initial loading and unloading-reloading path lead to the stiffness value E_{oed}^{ref} and E_{ur}^{ref} , respectively. doi:10.1371/journal.pone.0077606.g005

where α and β are the slope and the intersection with the y-axis, respectively.

A triaxial test was performed to predict shear parameters such as friction angle, cohesion and angle of dilatancy [46]. Triaxial tests are conducted in a cell, where a cylindrical sample is subjected to a confining pressure σ_3 (radial stress). Increasing axial stress σ_1 is applied to the sample by a vertical loading that causes shear failure in the sample. Figures 6 and 7 show results derived from triaxial tests conducted on Rhine sand at a cell pressure of $\sigma_3 = 50; 100; 150$ kN/m² (i.e., the confining pressure), where maximum shear stress is plotted against effective normal stress (Figure 6), and deviatoric stress is plotted against axial strain (Figure 7). Based on Equation 7, the initial loading of the soil was described by the stress-dependent secant stiffness E_{50} [kN/m²] (see Figure 7), that is the secant stiffness over the first 50% of the deviatoric stress:

$$E_{50} = E_{50}^{ref} \cdot \left(\frac{\sigma_3}{\sigma_{ref}} \right)^m \quad (7)$$

where E_{50}^{ref} is the stress-dependent secant stiffness at reference stress $\sigma_{ref} = 100$ kN/m². The friction angle was calculated from

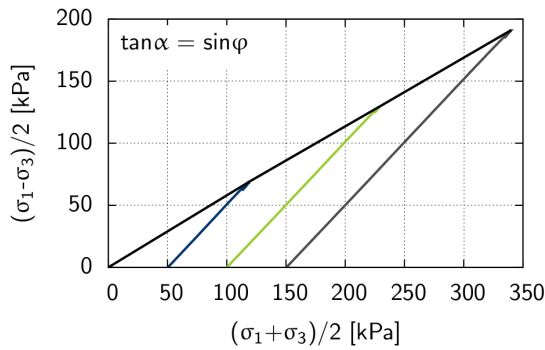


Figure 6. Triaxial test results for the determination of shear parameters of Rhine sand with an initial density of $e = 0.6$. Black line: Maximum shear stress is plotted against effective normal stress associated with cohesion c [kN/m²] and friction angle ϕ [°]. Blue, green and grey line: Stress paths for experiments conducted at 50 kN/m², 100 kN/m², and 150 kN/m² confining pressure, respectively. doi:10.1371/journal.pone.0077606.g006

the maximum shear stress-effective normal stress diagram (see Figure 6) between the x-axis and the linear function through the points of maximum shear stress. The linear function intersects with the point of origin and leads to a cohesion value $c = 0$ kN/m².

The hardening soil model parameters determined from triaxial and oedometer tests for Rhine sand with an initial density $e = 0.6$ (average density of Rhine sand in the field) are summarized in Table 1. For this type of subsoil material, i.e. sand, water content is of no significance, because additional strength and stiffness from capillary pressure is in the range of a few kN/m² only. Also, permeability of the sand is so high that undrained conditions during loading do not have to be considered.

Field experiment

The field experiment was carried out in the Zoological Gardens Wuppertal, Germany, with the tame African elephant cow Sweeny walking on a sand bed prepared in advance.

Because our goal was to back calculate the elephant's weight from a single footprint, some considerations on the gaits of elephants are in order here. Elephants differ remarkably from large hooved mammals in their locomotor repertoire by being confined to symmetrical gaits. In view of their great size (up to 5.5 tons), it is not clear whether this confinement depends on their unique size and thus is relevant for sauropods, or on some other reason. A simple theoretical consideration (detailed e.g. in [47]) may help. The speed reached in any gait is defined by the distance covered in one step cycle ('stride length') multiplied by cycle frequency. Since limb length as well as excursion angles are limited, great step lengths can only be reached by intercalating phases of suspension without ground contact into each step cycle. In combination with step frequency, this leads to a shortening of the ground contacts. Because the sum of impulses exchanged between the animal and the ground must be equal to its constantly acting body weight, the immediate consequence of a suspension phase are increased ground reaction forces. To avoid exceeding the strength limits of the limbs, suspension phases must be kept short or eliminated completely. In reference [48] the authors have calculated the ground reaction forces in dependence of the intervals available for ground contacts. According to these calculations, the mass of large sauropods alone compelled them to have used elastic damping mechanisms in order to avoid dangerous stressing of limbs even during a walk. This would have

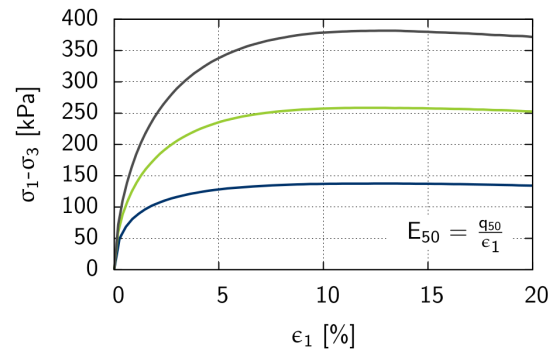


Figure 7. Triaxial test results for the determination of stiffness E_{50} [kN/m²] of Rhine sand with an initial density of $e = 0.6$. Blue, green and grey line: Deviatoric stress is plotted against axial strain for experiments conducted at 50 kN/m², 100 kN/m², and 150 kN/m² confining pressure, respectively. The stiffness E_{50} is the secant stiffness over the first 50% of the deviatoric stress. doi:10.1371/journal.pone.0077606.g007

Table 1. Hardening soil model parameters.

Parameter	Rhine sand
m [-]	0.4
E_{oed}^{ref} [MN/m ²]	42
E_{ur}^{ref} [MN/m ²]	208
ϕ [°]	35
ψ [°]	5
c [kN/m ²]	0
E_{50}^{ref} [MN/m ²]	42

doi:10.1371/journal.pone.0077606.t001

excluded the option of a further shortening of ground contact intervals which are typical for asymmetric gaits.

The gaits used by elephants for slow locomotion is a walk, the walk being a 4-beat rhythm with intervals between footfalls of 25% of cycle duration. To move faster, elephants change to a gait very similar to an 'amble' (a 4-beat rhythm with higher frequency than the walk) by elongating their steps [48,49]. This is possible by intercalating a phase without ground contact, first with the hindlimbs and then with the forelimbs. This step elongation seems to be facilitated by marked elastic up and down-movements of the heavy head [48].

Before the experiment the weight of Sweeny was carefully measured using the special scale kept in the elephant enclosure for this purpose. As can be seen in Figure 8, the weight was measured under several conditions to determine the weight borne by each limb of the elephant. The following loads were measured: a) the elephant was standing with all limbs on the scale ($m = 2530$ kg), b) the load carried by both hindlimbs ($m = 1125$ kg), c) the load carried by both forelimbs ($m = 1530$ kg), and d) the load carried by one forelimb ($m = 1390$ kg). If it is known from biomechanical considerations how the weight of the moving trackmaker is distributed on its limbs and which type of gait was used during track formation (according to f_{dyn} and f_{wd} in Equation 3), analysis of just one print will be sufficient for determining the trackmakers weight.



Figure 8. Weighing the elephant cow Sweeny. The following loads were measured: a) the elephant was standing with all limbs on the scale ($m = 2530$ kg), b) the load carried by both hindlimbs ($m = 1125$ kg), c) the load carried by both forelimbs ($m = 1530$ kg), and d) the load carried by one forelimb ($m = 1390$ kg).
doi:10.1371/journal.pone.0077606.g008

Prior to the experiment, a test field had been prepared for the elephant to cross. This consisted of an excavation in the elephant enclosure of 5.25 m in length, 2.20 m in width, and 0.90 m in depth, which was refilled with the experimental subsoil. The sand fill was prepared in three layers with each layer being compacted with a hand-pulled roller after dumping into the test field. Soil samples were obtained from the prepared test field by manual sampling with a metal tube and taken to the lab to determine density and water content. Dry density and water content of the samples are given in Figure 9. The average dry density was found to be $\rho_d = 1.6$ g/cm³. Homogeneity was an important experimental condition for the volume of soil influenced by the loading. This volume can be estimated as a cube with a side length of about twice the relevant loading dimension, which was foot diameter in our case. As noted, the subsoil was put into place in three layers, and each of these layers was verified for the target void ratio.

The elephant enclosure and the location of the test field is shown in Figure 10. Guided by one of her keepers, Sweeny walked across the test field during the experiment and left several footprints in the sand bed. A total of six footprints were scanned using the 3D laser scanner (see Figure 11). The area of the forefeet and hindfeet is about the same, whereas lengths ratio of forefeet to hindfeet is about 0.85, and the widths ratio is about 1.18. Visual analysis of the actual footprints and of the scanned prints indicates that the loading area is the same as the area imprinted on the subsoil. However, for practical reasons, we restricted the FEA to the footprints of the forelimbs. Based on the 3D scanner results, average footprint length is 0.32 m, average width is 0.30 m, and the average depths of the three scanned forefoot impressions is 0.020 m, 0.021 m, and 0.026 m, respectively.

Results

Our 3D FEA model consists of a soil volume 2 m in width, 2 m in length and 1 m in depth and a circular plate 0.32 m in diameter that simulates the elephant’s forefoot. Since the rigid plate differs from the soft sole of the elephant’s foot, the numerical results for the vertical deformation were multiplied by a factor of 1/0.75 based on the DIN 4019-1 standard to take into account the flexible loading characteristics produced by the foot [50]. The geometry of the FE model, including the mesh generated, is given in Figure 12. The boundary conditions were set to the bottom of the model volume being fully fixed. The sides of the model were vertically unconstrained but fixed in all other directions. To simulate the subsoil-foot interaction, interfaces were introduced into the model around the circular plate. The outer interface were assigned the normal parameters of the subsoil, but reduced soil parameters were assigned to the inner interface to model smooth contact between the subsoil and the elephant’s foot. The numerical simulation is a forward simulation, i.e., stress is applied through the plate to the soil, and then the settlements are derived. As described above, the hardening soil model was used for describing the mechanical behavior of the soil. The model input parameters were experimentally determined as described above.

Two approaches were used in the numerical simulations. The first approach included the numerical simulation of the vertical displacements of the subsoil by the elephant’s weight. The calculation is based on the results of the gait analysis, the application of the DIC technique, and the elephant’s weight. The numerical simulation was performed using several phases. The initial phase included the generation of initial conditions in the soil, i.e., the configuration of the initial geometry and the initial stress state (e.g., effective stresses, state parameters). In the second phase, the circular

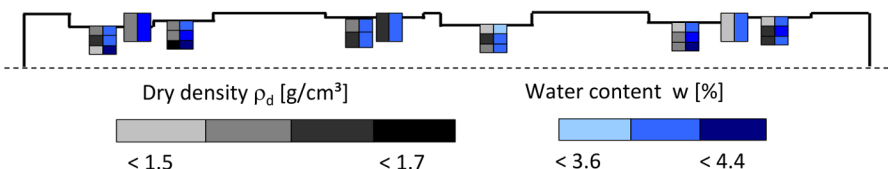


Figure 9. Results of dry density and water content profile measurements. Soil samples were obtained from the prepared test field by manual sampling with a metal tube. Samples were taken inside and outside several footprints, indicated by differing sampling depths, i.e., differing starting points of the top of the tube. Footprints are displayed schematically, for detailed information see Figure 11.
doi:10.1371/journal.pone.0077606.g009

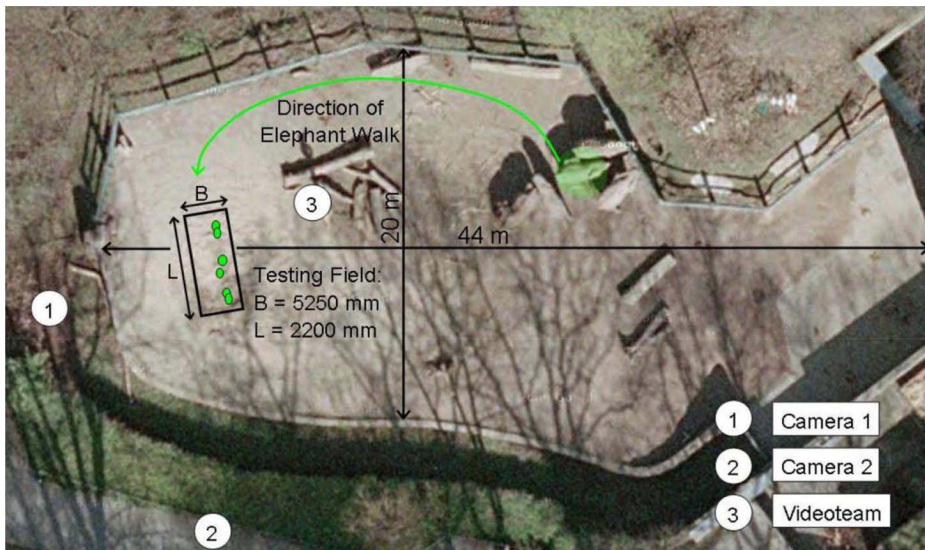


Figure 10. Satellite image of elephant enclosure (and elephants) at the Zoological Gardens Wuppertal including the testing field (www.google.de). Positions of the scanned footprints are marked in green within the prepared testing field.
doi:10.1371/journal.pone.0077606.g010

plate was activated, without applying stress to the soil. In the following phases, the stresses induced by the weight of the elephant were applied successively. From the sequence of footfalls in the elephant walk (see Figure 13), four scenarios of static loading were simulated as loads applied to the circular plate simulating the elephant's forefoot. Application of a stress of $\sigma = 93 \text{ kN/m}^2$ (loading step 1) simulated the standing elephant (i.e., the weight is distributed to all four limbs, where 60% of the weight is carried by the forelimbs and 40% is carried by the hindlimbs). Loading step 2 ($\sigma = 99 \text{ kN/m}^2$) simulated the load on one forelimb with both forelimbs touching the ground but one hindlimb not touching the ground.

Loading step 3 ($\sigma = 166 \text{ kN/m}^2$) simulated the load on one forelimb with the other not touching the ground but both hindlimbs touching the ground. Loading step 4, representing the maximum static stress $\sigma_{max} = 185 \text{ kN/m}^2$ below the forefoot, simulated only one forelimb and one hindlimb touching the ground, as when the animal was progressing in a walk. In a final step (loading step 5), we added the dynamic component of the foot to the model by introducing the relevant stress $\sigma_{dyn+stat}$ for the simulation of the settlements, i.e., the sum of the static stress of loading step 2 and the dynamic stress:

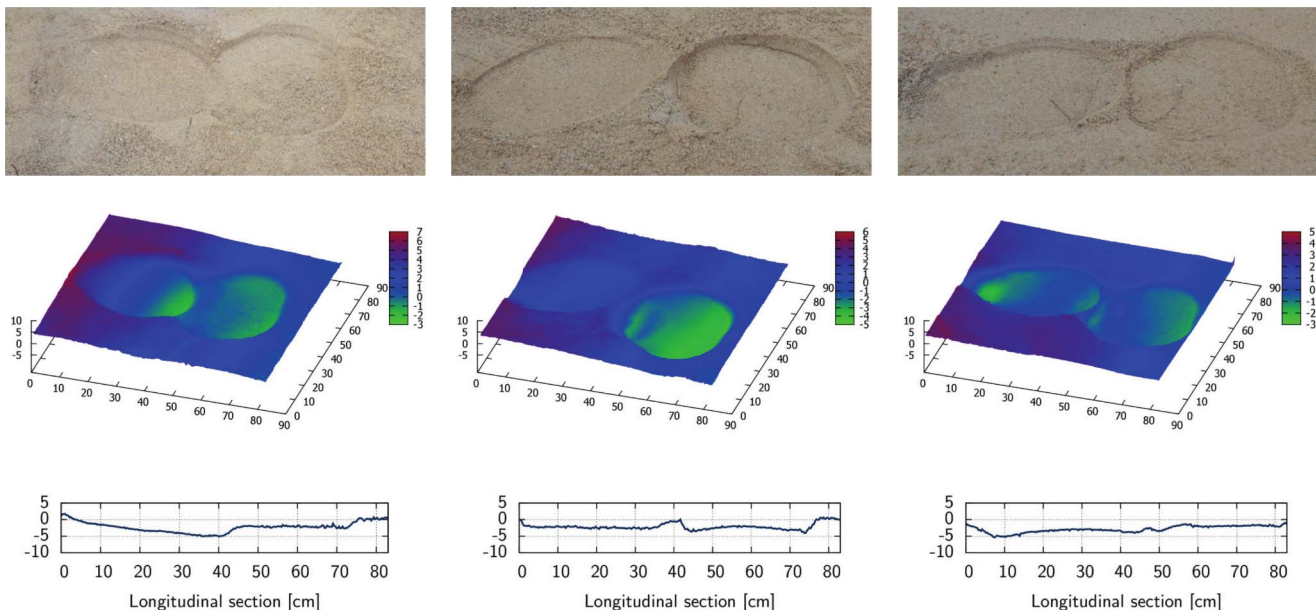


Figure 11. Capture of elephant footprints geometry using 3D laser scanner. A total of six footprints were scanned, i.e., three pairs, each of them consisting of one forefoot imprint (right) and one hindfoot imprint (left). Each pair is pictured by a photograph (top), 3D surface plot (center), and a 2D longitudinal section plot (bottom).
doi:10.1371/journal.pone.0077606.g011

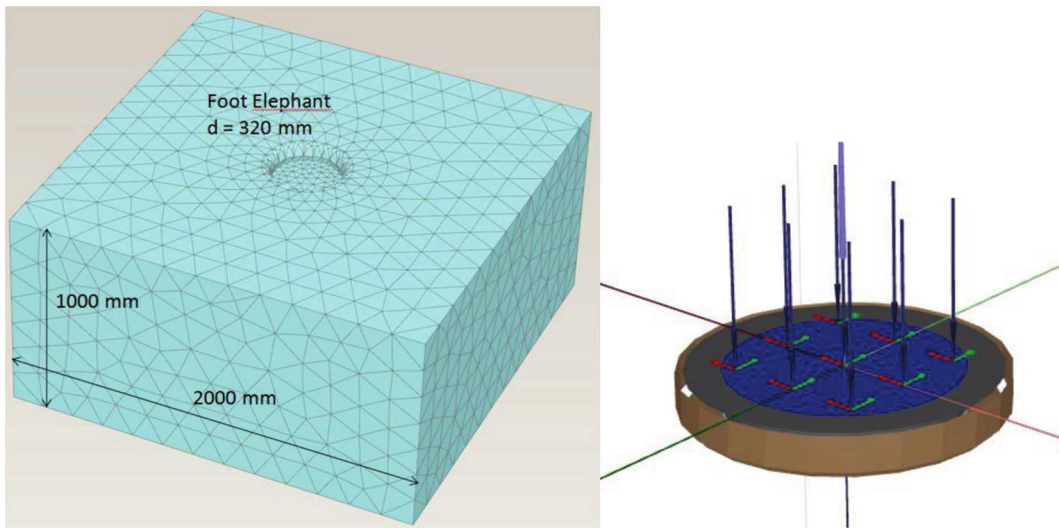


Figure 12. Geometry and generated mesh of the FEA model and interfaces. See text for a detailed description of the model. doi:10.1371/journal.pone.0077606.g012

$$\sigma_{stat} + \sigma_{dyn} = \sigma_{dyn+stat} \rightarrow 99\text{kN/m}^2 + 245\text{kN/m}^2 = 344\text{kN/m}^2 \quad (8)$$

The factors f_{wd} and f_{dyn} , which determine the stresses applied during the loading steps according to Equation 3 are summarized in Table 2.

The results of the numerical simulation are shown in Figures 14 and 15, in which the vertical deformations are presented. For loading step 1, a deformation $u = 0.003$ m was calculated, loading step 2 resulted in a deformation of $u = 0.004$ m, loading step 3 in a deformation of $u = 0.007$ m, and loading step 4 in a deformation of $u = 0.008$ m. As expected the largest deformation was found for loading step 5 with $u = 0.018$ m.

In order to determine the weight of a dinosaur based on back analysis of vertical settlements, a second approach was developed. In this approach, numerical simulations were carried out for Rhine sand subsoil with relative densities of $I_D = 0.22; 0.41; 0.59; 0.81; 1.00$ and applied stresses of $\sigma = 50; 100; 150; 200; 250; 300; 350; 400$ kN/m², respectively. The relative density is calculated as follows:

$$I_D = \left(\frac{e_{max} - e}{e_{max} - e_{min}} \right) \quad (9)$$

where e_{max} and e_{min} are the maximum and minimum void ratio of the soil and e is the void ratio of the soil. For each simulation, hardening soil model parameters were calculated from experimental results carried out on Rhine sand samples with the appropriate void ratio. In Figures 16 and 17, the results of the

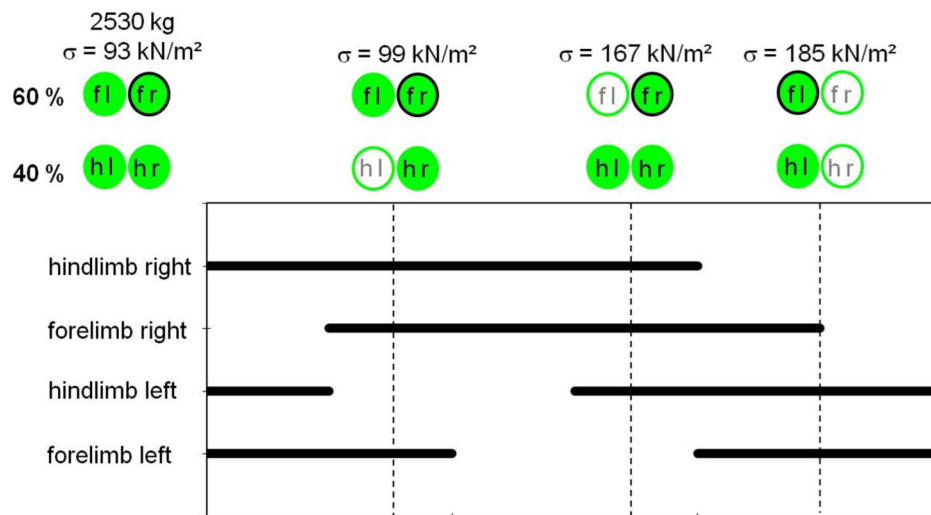


Figure 13. Sequence of footfalls in elephant walk after [5]. The static loading conditions (loading steps 1 to 4) simulated by FEA are marked and quantified within the sequence. The leftmost loading step is loading step 1, with the elephant at a standstill. Black bars indicate ground contact of the respective foot. fl = left forefoot, fr = right forefoot, hl = left hindfoot, hr = right hindfoot. See text for a detailed description of the loading steps.

Table 2. Factors f_{wd} and f_{dyn} determining total mass distribution on the limbs during the elephant's walk.

	Forelimb	Hindlimb
f_{wd}		
4 limbs	0.3	0.2
3 limbs (2 fore-, 1 hind-)	0.32	0.36
3 limbs (1 fore-, 2 hind-)	0.54	0.23
2 limbs (1 fore-, 1 hind-)	0.6	0.4
f_{dyn}	3.5	1.6

doi:10.1371/journal.pone.0077606.t002

second approach are presented that allows determination of the stress applied to a specific subsoil and thus the total mass of an animal (see Equation 3). To use the diagram, only two values have to be known: the relative density of the subsoil I_D [-] and footprint geometry (i.e., vertical displacement and diameter). In the case of

the elephant's footprints, the relative density of the subsoil was found to be between 0.30 and 0.47, and measured vertical displacements were between 0.020 m and 0.026 m. Using these results as input values in the diagram in Figure 16, applied stress with an average value of about 360 kN/m² can be obtained. Using Equation 3, an average mass of about 2635 kg can be back-calculated from the geometry of the elephant footprints and the relative density of the soil.

Discussion

The present study illustrates the successful application of soil mechanical concepts to the quantitative interpretation of the soil deformation represented by footprints. Two aspects have to be taken into account accurately: (1) the simulation of the behavior of the subsoil using corresponding soil parameters and (2) the relationship between applied stress and total mass of the animal. The constitutive soil model used in this study for FEA describes soil behavior in a most realistic manner since it takes into account stress and loading direction dependent soil stiffness. The geometry, initial conditions and boundary conditions of the model, as well as

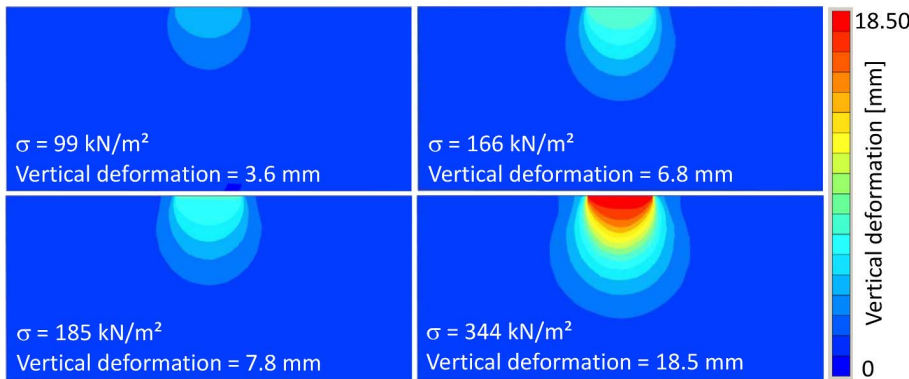


Figure 14. Vertical sections of FEA model at loading steps 2 to 5. Colors indicate amount of deformation. doi:10.1371/journal.pone.0077606.g014

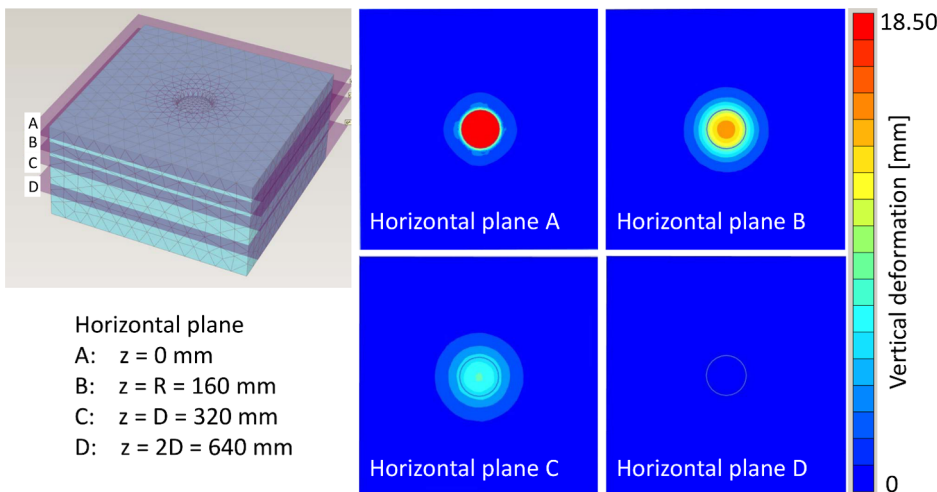


Figure 15. Four horizontal sections of FEA model of loading step 5. Horizontal plane A is at surface, horizontal plane B is at the depth of the radius R of the circular plate that was loaded to simulate the elephant's foot, horizontal plane C is at the depth of the diameter D of the circular plate, and horizontal plane D is at twice the depth of the diameter D of the circular plate. Colors indicate amount of deformation. doi:10.1371/journal.pone.0077606.g015

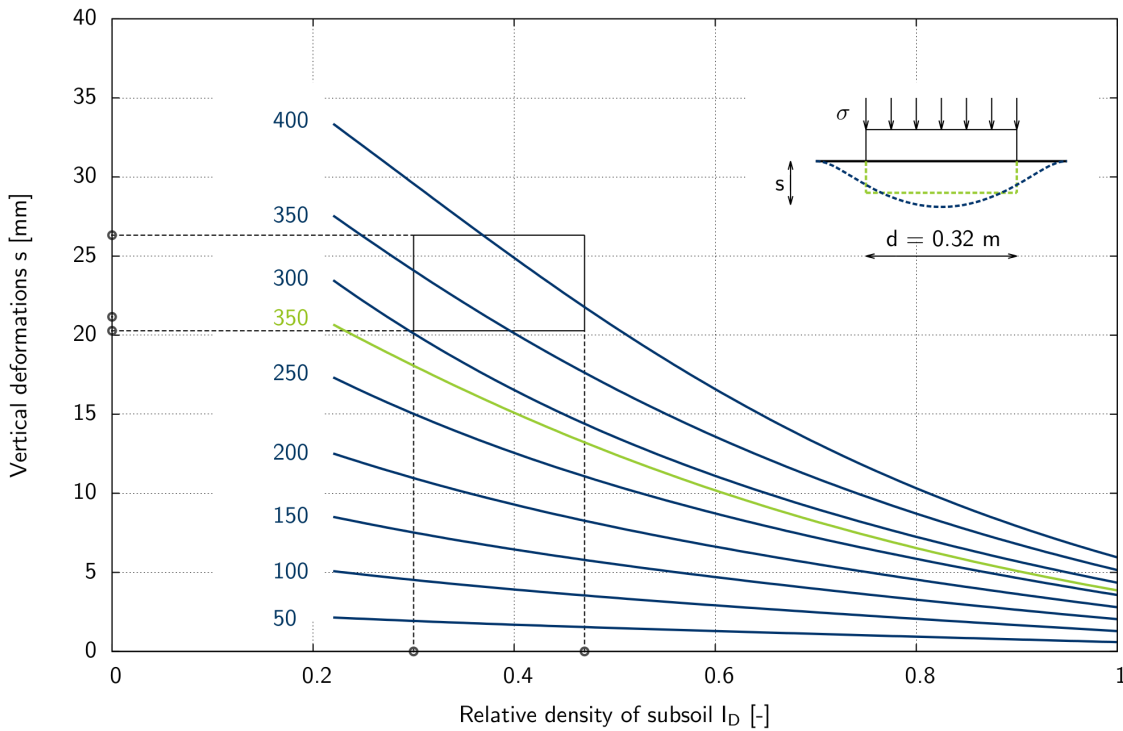


Figure 16. 2D-plot of relative density versus settlements for back analysis of applied stress σ [kN/m²] by FEA for a circular plate ($d = 0.32$ m). The diagram applies to subsoil conditions of Rhine sand. According to the deformation characteristics illustrated at the top right corner of the diagram, blue curves apply to the flexible loading characteristics of the elephant's foot, and the green curve ($\sigma = 350$ kN/m² \approx loading step 5) applies to rigid loading characteristics used in the FEA model. The relationship is detailed in the text. The range of stresses that can be back-calculated from in situ conditions of relative density of subsoil I_D (0.3 and 0.47) and measured values of s (20.28 mm, 21.16 mm, and 26.32 mm) is marked by a box.
doi:10.1371/journal.pone.0077606.g016

the input parameters characterizing soil behavior, influence the results of subsoil deformation and have to be accurately identified.

The present research study indicates that the dynamic component of the trackmaker has a significant influence on subsoil deformation. A factor of approximately 3.5 relating $\sigma_{stat+dyn}$ to σ_{stat} was identified using the DIC technique to

quantify the velocity of the elephant's foot when coming into contact with the subsoil. The outcome of our numerical simulation is that the average vertical displacement $u_{Exp} = 0.022$ m measured in the field experiment is in good agreement with the numerically calculated vertical displacement $u_{FEA} = 0.018$ m as a result of the maximum applied stress $\sigma_{stat+dyn}$.

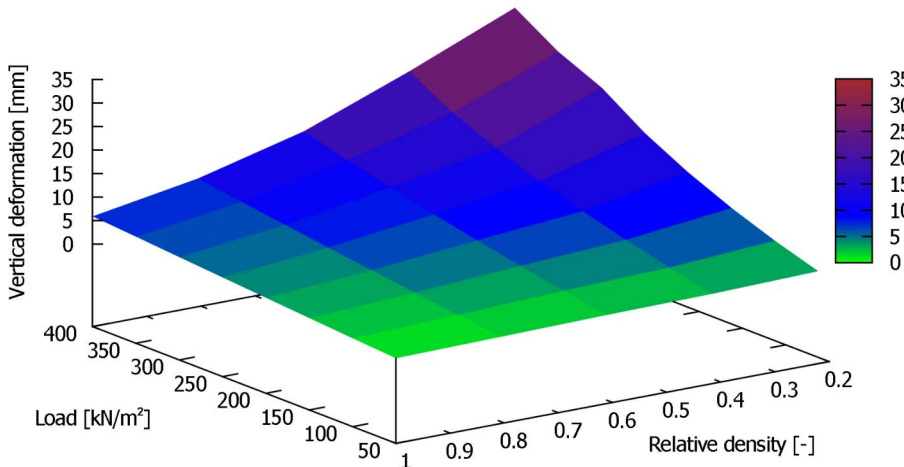


Figure 17. 3D-plot of relative density versus settlements for back analysis of applied stress σ [kN/m²] by FEA for a circular plate ($d = 0.32$ m). The diagram applies to subsoil conditions of Rhine sand. This diagram can be used to estimate the load having produced a fossil footprint if the original subsoil parameters were the same as our experimental subsoil, Rhine sand.
doi:10.1371/journal.pone.0077606.g017

Conclusions

We conclude that a reliable method for weight reconstruction from footprints has been developed, implemented and validated. Our inverse approach, as shown in Figure 16 and 17, allows the stress applied to a specific subsoil to be determined. In addition, the total weight of an animal (see Equation 3) can be determined with an error of about 15%.

Our work represents a first step in the direction of back calculating the weight of extinct animals such as sauropod dinosaurs from their footprint. However, several additional footprint and subsoil characteristics have to be considered before reliable results can be obtained for fossils. These include geological processes that alter the original subsoil deformation such as the (1) influence of overburden pressure on subsoil deformations after the footprint was created, (2) identification of the type of fossil footprint (i.e., undertrack, overtrack, true track), (3) surface weathering, and (4) the soil profile, including constitutive parameters and layering of the subsoil. Accordingly, in ongoing research using micro-CT analysis, realistic stiffness parameters of

fossil subsoils are estimated from the granulometric properties of the rock in which the footprint is preserved. It thus is clear that detailed sedimentological study must precede the soil mechanical approach in the study of sauropod footprints.

Acknowledgments

The authors thank the Zoological Gardens Wuppertal (Wuppertal, Germany) for permitting and supporting the field experiment with the elephant cow Sweeny. We thank Dr. Ulrich Schürer, Dr. Arne Lawrence and the staff of the elephant house for their kind assistance on the research project. Finally, we thank R. Hodge for correcting the English and the academic editor Peter Dodson, the reviewer Peter Falkingham and the anonymous reviewer for their helpful reviews and comments.

Author Contributions

Conceived and designed the experiments: TS YL UW PMS. Performed the experiments: TS YL HV UW SL. Analyzed the data: TS YL HV HP. Contributed reagents/materials/analysis tools: TB. Wrote the paper: TS YL HV SL HP PMS.

References

- Klein N, Remes K, Gee CT, Sander PM, editors (2011) *Biology of the Sauropod Dinosaurs -Understanding the Life of Giants*. Life of the past. Bloomington and Indiana: Indiana University Press.
- Sander PM, Clauss M (2008) Sauropod gigantism. *Science* 322: 200–201.
- Sander PM, Christian A, Clauss M, Fechner R, Gee CT, et al. (2011) Biology of the sauropod dinosaurs: the evolution of gigantism. *Biological Reviews* 86: 117–155.
- Lockley MG, Wright JL, Hunt AP, Lucas SG (2001) The Late Triassic sauropod track record comes into focus: old legacies and new paradigms. *Guidebook New Mexico Geological Society* 52.
- Wright JL (2005) Steps in understanding sauropod biology. In: Curry Rogers K, editor, *The Sauropods*, Berkeley: Univ. of California Press. pp. 252–280.
- Farlow JO, Pittman JG, Hawthorne JM (1989) *Brontopodus birdi* Lower Cretaceous sauropod footprints from the U.S. Gulf Coastal Plain. In: Gillette DD, Lockley MG, editors, *Dinosaur Tracks and Traces*, Cambridge: Cambridge Univ. Press. pp. 371–394.
- Barnes FA, Lockley MG (1994) Trackway evidence for social sauropods from the Morrison Formation, Eastern Utah (USA). *GAIA : Revista de geociências* 10: 37–41.
- Foster JR, Lockley MG (2006) The vertebrate ichnological record of the Morrison Formation (Upper Jurassic, North America) 36: 203–213.
- Lockley MG, Houk KJ, Prince NK (1986) North America's largest dinosaur trackway site: implications for Morrison Formation paleoecology. *Geological Society of America Bulletin* 97: 1163–1176.
- Prince NK, Lockley MG (1989) The sedimentology of the Purgatoire tracksite region, Morrison Formation of southeastern Colorado. In: Gillette DD, Lockley MG, editors, *Dinosaur Tracks and Traces*, Cambridge: Cambridge Univ. Press. pp. 155–163.
- Fischer R (1998) Das Naturdenkmal Saurierfahrten Munchenhagen. *Mitteilungen aus dem Institut für Geologie und Palaontologie der Universit at Hannover* 37.
- Lockley MG, Wright JL, Thies D (2004) Some observations on the dinosaur tracks at Münchenhagen (Lower Cretaceous), Germany. *Ichnos* 11: 261–274.
- Mannion PD, Upchurch P (2010) A quantitative analysis of environmental associations in sauropod dinosaurs. *Paleobiology* : 253–282.
- Henderson D (2003) Footprints, trackways, and hip heights of bipedal dinosaurs - Testing hip height predictions with computer models. *Ichnos* 10: 99–114.
- Alexander RM (1976) Estimates of speeds of dinosaurs. *Nature* 261: 129–130.
- Alexander RM (2006) Dinosaur biomechanics. *Proceedings of the Royal Society B: Biological Sciences* 273: 1849–1855.
- Thulborn T (1990) *Dinosaur Tracks*. New York: Chapman and Hall, 1 edition.
- Milán J (2006) Variations in the morphology of emu (*Dromaius novaehollandiae*) tracks reflecting differences in walking pattern and substrate consistency: ichnotaxonomic implications. *Palaentology* 49: 405–420.
- Platt BF, Hasiotis ST, Hirmas DR (2012) Empirical determination of physical controls on megafaunal footprints formation through neoichnological experiments with elephants. *Palaos* 27: 725–737.
- Jackson SJ, Whyte MA, Romano M (2010) Range of experimental dinosaur (*Hypsilophodon foxii*) footprints due to variation in sand consistency: How wet was the track? *Ichnos* 17: 197–214.
- Manning PL (2004) A new approach to the analysis and interpretation of tracks: examples from the Dinosauria. In: McIlroy D, editor, *The Application of Ichnology to Palaeoenvironmental and Stratigraphic Analysis*. Geological Society, London, Special Publications 228, London, volume 228. pp. 94–123. doi:10.1144/GSL.SP.2004.228.01.06.
- Falkingham PL, Bates KT, Margetts L, Manning PL (2011) Simulating sauropod manus-only trackway formation using finite-element analysis. *Biology Letters* 7: 142–145.
- Henderson DM (2006) Burly gaits: Centers of mass, stability, and the trackways of sauropod dinosaurs. *Journal of Vertebrate Paleontology* 26: 907–921.
- Colbert EH (1962) The weights of dinosaurs. *American Museum Novitates* : 1–16.
- Gunga HC, Suthau T, Bellmann A, Friedrich A, Schwanebeck T, et al. (2007) Body mass estimations for Plateosaurus engelhardti using laser scanning and 3D reconstruction methods. *Naturwissenschaften* 94: 623–630.
- Gunga HC, Suthau T, Bellmann A, Stoinski S, Friedrich A, et al. (2008) A new body mass estimation of Brachiosaurus brancai Janensch, 1914 mounted and exhibited at the Museum of Natural History (Berlin, Germany). *Fossil Record* 11: 33–38.
- Henderson DM (1999) Estimating the masses and centers of mass of extinct animals by 3-D mathematical slicing. *Paleobiology* 25: 88–106.
- Falkingham PL, Margetts L, Smith IM, Manning PL (2009) Reinterpretation of palmate and semi-palmate (webbed) fossil tracks; insights from finite element modelling. *Palaeogeography, Palaeoclimatology, Palaeoecology* 271: 69–76.
- Falkingham PL, Margetts L, Manning PL (2010) Fossil vertebrate tracks as paleopenetrometers: Confounding effects of foot morphology. *Palaos* 25: 356–360.
- Falkingham PL, Bates KT, Margetts L, Manning PL (2011) The 'Goldilocks' effect: preservation bias in vertebrate track assemblages. *Journal of the Royal Society: Interface* 61: 1142–1154.
- Bates KT, Savage R, Pataky TC, Morse SA, Webster E, et al. (2013) Does footprint depth correlate with foot motion and pressure? *Journal of the Royal Society: Interface* 83.
- Campione NE, Evans DC (2012) A universal scaling relationship between body mass and proximal limb bone dimensions in quadrupedal terrestrial tetrapods. *BMC Biology* 10.
- Gatesy S (2003) Direct and Indirect Track Features: What Sediment Did a Dinosaur Touch? *Ichnos* 10.
- Kaever M, de Lapparent AF (1974) Les traces de pas de Dinosaures du Jurassique de Barkhausen (Basse Saxe, Allemagne). *Bulletin de la Socié Gologique de France* 16: 516–525.
- Diedrich C (2011) Upper Jurassic tidal at megatracksites of Germany - coastal dinosaur migration highways between European islands, and a review of the dinosaur footprints. *Palaeobiodiversity and Palaeoenvironments* 91: 129–155.
- Ishigaki S, Matsumoto Y (2009) Off-tracking"-like phenomenon observed in the turning Sauropod trackway from the Upper Jurassic of Morocco. *Memoir of the Fukui Prefectural Dinosaur Museum* 8: 1–10.
- Knabe T, Datcheva M, Lahmer T, Cotecchia F, Schanz T (2013) Identification of constitutive parameters of soil using an optimization strategy and statistical analysis. *Computers and Geotechnics* 49: 143–157.
- Schanz T, Vermeer P, Bonnier P (1999) The hardening soil model: Formulation and verification. Rotterdam: Balkema.
- Röchter L (2011) Systeme paralleler Scherbänder unter Extension im ebenen Verformungszustand. Ph.D. thesis, Ruhr-Universität at Bochum.
- Knabe T, Schweiger HF, Schanz T (2012) Calibration of constitutive parameters by inverse analysis for a geotechnical boundary problem. *Canadian Geotechnical Journal* 49: 170–183.
- Hazen A (1892) Some physical properties of sands and gravels, with special reference to their use in filtration. 24th Annual Rep, Massachusetts State Board of Health : 539–556.

42. Lambe TW, Whitman RV (1969) Soil Mechanics. John Wiley & Sons.
43. Schanz T, Vermeer P (1998) On the stiffness of sands. *Géotechnique Special issue on Pre-failure Deformation Behaviour of Geomaterials* : 383–387.
44. Ohde J (1939) Zur Theorie der Druckverteilung im Baugrund. *Bauingenieur* 20: 93–99.
45. Schanz T (1998) Zur Modellierung des mechanischen Verhaltens von Reibungsmaterialien. Institut für Geotechnik, Universität Stuttgart: Mitteilung 45.
46. Schanz T, Vermeer P (1996) Angles of friction and dilatancy of sand. *Géotechnique* 46: 145–151.
47. Preuschoft H, Hohn B, Stoinski S, Witzel U (2011) Why so huge? Biomechanical Reasons for the Acquisition of Large Size in Sauropod and Theropod Dinosaurs. In: Klein N, Remes K, Gee CT, Sander PM, editors, *Biology of the Sauropod Dinosaurs - Understanding the Life of Giants*, Bloomington and Indiana: Indiana University Press, Life of the past. pp. 197–218.
48. Christian A, Müller RHG, Christian G, Preuschoft H (1999) Limb swinging in elephants and giraffes and implications for the reconstruction of limb movements and speed estimates in large dinosaurs. *Fossil Record* 2: 81–90.
49. Hutchinson JR, Famini D, Lair R, Kram R (2003) Biomechanics: Are fast-moving elephants really running? *Nature* 422: 493–494.
50. DIN 4019-1 (1979) Setzungsberechnungen bei lotrechter, mittiger Belastung.
51. Genin JJ, Willems PA, Cavagna GA, Lair R, Heglund NC (2010) Biomechanics of locomotion in Asian elephants. *Journal of Experimental Biology* 213: 694–706.

Preliminary Analysis of Osteocyte Lacunar Density in Long Bones of Tetrapods: All Measures Are Bigger in Sauropod Dinosaurs

Koen W. H. Stein^{1*}, Jan Werner²

1 Steinmann Institut für Geologie, Mineralogie und Paläontologie, University of Bonn, Bonn, Germany, **2** Institut für Zoologie, Abteilung Ökologie, Johannes Gutenberg-Universität Mainz, Mainz, Germany

Abstract

Osteocytes harbour much potential for paleobiological studies. Synchrotron radiation and spectroscopic analyses are providing fascinating data on osteocyte density, size and orientation in fossil taxa. However, such studies may be costly and time consuming. Here we describe an uncomplicated and inexpensive method to measure osteocyte lacunar densities in bone thin sections. We report on cell lacunar densities in the long bones of various extant and extinct tetrapods, with a focus on sauropodomorph dinosaurs, and how lacunar densities can help us understand bone formation rates in the iconic sauropod dinosaurs. Ordinary least square and phylogenetic generalized least square regressions suggest that sauropodomorphs have lacunar densities higher than scaled up or comparably sized mammals. We also found normal mammalian-like osteocyte densities for the extinct bovid *Myotragus*, questioning its crocodylian-like physiology. When accounting for body mass effects and phylogeny, growth rates are a main factor determining the density of the lacunocanalicular network. However, functional aspects most likely play an important role as well. Observed differences in cell strategies between mammals and dinosaurs likely illustrate the convergent nature of fast growing bone tissues in these groups.

Citation: Stein KWH, Werner J (2013) Preliminary Analysis of Osteocyte Lacunar Density in Long Bones of Tetrapods: All Measures Are Bigger in Sauropod Dinosaurs. PLoS ONE 8(10): e77109. doi:10.1371/journal.pone.0077109

Editor: David C. Evans, Royal Ontario Museum, Canada

Received: April 9, 2013; **Accepted:** September 3, 2013; **Published:** October 30, 2013

Copyright: © 2013 Stein, Werner. This is an open-access article distributed under the terms of the Creative Commons Attribution License, which permits unrestricted use, distribution, and reproduction in any medium, provided the original author and source are credited.

Funding: This work was supported by the German Research Foundation (DFG) as part of the third funding period of the Research Unit FOR 533 "Biology of the Sauropod Dinosaurs". The funders had no role in study design, data collection and analysis, decision to publish, or preparation of the manuscript.

Competing Interests: The authors have declared that no competing interests exist.

* E-mail: koen_stein@yahoo.co.uk

‡ Current address: Museum für Naturkunde, Leibniz Institute for Research on Evolution and Biodiversity Berlin, Germany

Introduction

Osteocytes

Osteocytes and osteocyte characters observed in fossil bone provide an untapped reserve of information for paleobiological studies. Osteocyte features have recently been shown to provide information on growth rates as well as muscle attachment sites of extinct taxa [1,2]. Moreover, osteocytes may have the potential to preserve proteins of extinct vertebrates [3,4]. Osteocytes are the most common cells in intramembranously formed bone tissues. They derive from bone forming osteoblasts which become incorporated into the bone matrix during bone growth (for a review see [5]). An osteocyte resides inside the bony tissue in an osteocyte lacuna, and remains in direct contact with other osteocytes through small pores called canaliculi [6]. This osteocyte canalicular network functions as a mechanosensing sensory network [7–9]. Osteocytes help maintain bone homeostasis by signalling other osteocytes, osteoblasts and osteoclasts about adjacent tissue damages or even changes in stress and strain in their local environment, inhibiting or promoting bone remodelling [8,9,10].

The factors determining the density of osteocytes in the lacunocanalicular network remain unclear. In comparison with teleost fishes, amphibians and other terrestrial vertebrates have

much better developed osteocyte-lacunocanalicular systems, however, these differences may not be directly related to aquatic habitats [11]. Cubo et al. [1] found cellular density, among a number of other histomorphometric parameters, to be significantly correlated to femoral growth rate. Bromage et al. [12] found a relationship between the osteocyte density of lamellar bone and body mass of mammals. This relationship between osteocyte lacunar density (OLD) and body mass (BM) is described by an allometric function of the form $OLD = a BM^b$ (or $\log OLD = \log a + b \log BM$, to get a linear relationship). The exponent b has a negative value, indicating a decrease in OLD with increasing body mass. The authors concluded from this that OLD reflects the rate of osteoblast proliferation, transformation, and incorporation into bone as osteocytes during growth. Lacunar densities should therefore be higher in mammals with rapid growth, small body mass, and whose osteoblast proliferation rates would lead to higher osteocyte lacunar densities.

Osteocyte lacunar density may thus have the potential to provide significant information about bone cell proliferation, physiology and life history of vertebrates [1,5,12]. So far it has been the focus of (osteoporosis) studies in humans (e.g. [13–16]), and to some extent also in other mammals [17–21,12]. Osteocytes themselves are rarely preserved in fossilized bone, but the lacunae provide a good proxy for the shape and maximum possible size as

well as density of the osteocytes. Because lacunar density is a feature that can be measured relatively easily in fossil bone, it is surprising that almost no comparative data are known for extinct vertebrates.

Sauropods and Bone Histology

Because of their unsurpassed body masses, sauropod dinosaurs have been the focus of an increasing number of paleohistological investigations [22–28]. Sauropod long bones are made of highly vascularized fast growing tissues, consisting of a thin woven bone trabecular framework compacted with highly organized primary bone (HOPB *sensu* [28]). In the diapsid lineage, these highly vascularized long bone tissues were already present in basal Archosauria [1,29–31]. Highly vascularized long bone tissues can also be found in mammals, a feature which evolved basally in therapsids, possibly even in synapsids [32–33].

Life history features, like growth rates, are of high interest for many researchers studying bone histology (e.g. [34–42]). Most of these skeletochronological studies aim to model growth dynamics and estimate growth rates of tetrapods using lines of arrested growth (LAGs) or other types of growth mark (*cf.* [41–42]). In extant animals, LAGs and other growth marks are the result of a seasonal cessation or slowdown of growth respectively [43–46]. Skeletochronology, however has its limitations. In the femur of an alligator, Klein et al. [47] found a number of growth marks different from the actual known age. Sauropod dinosaurs only exceptionally preserve such growth marks in their long bones. In the case of the dwarfed sauropod *Europasaurus* [48], a tibia (DFMMh/FV495.5) and femur (DFMMh/FV495.9) of one individual show a different number of growth marks (6 and 4 respectively, KS, Pers. Obs.). Moreover, reported variabilities in the histology of different elements of other dinosaurs calls for caution in element selection and accounting for missing growth marks [49]. These complications make life history studies of sauropod dinosaurs difficult, and their growth rates not fully understood. Here we explore how paleocytological characters of sauropods and basal sauropodomorphs, compared to other tetrapods, can help us assess growth rates.

Aim of the Study

High OLD indicates high cell proliferation rates and high local apposition and metabolic rates [1,12]. Therefore, given the presence of highly vascularized bone tissues, high growth rates comparable to mammals [24,50–52] and assumed high basal metabolic rates of sauropodomorphs (and dinosaurs in general), we hypothesized the OLD in sauropodomorphs to be similar to mammals. Furthermore, we hypothesize that OLD will decrease with body mass in Sauropodomorpha, because small taxa like *Saturnalia* should exhibit higher local apposition rates than large sauropods. Although overall increase in absolute body size in sauropods may be larger than in small sauropodomorphs, the local mitotic rates of the osteoblasts will be higher in these smaller taxa, similar to mammals. In a broader phylogenetic context, tetrapods with known low growth rates, like amphibians, crocodiles and squamate reptiles are hypothesized to have low OLD.

The aim of this preliminary investigation is thus to obtain a better understanding of the nature of the lacunocanalicular network in tetrapods, with a focus on sauropodomorphs, and following Stein and Prondvai [28] how sauropodomorph bone tissue is organized on a cellular level.

Materials and Methods

We used thin sections of histological cores (*cf.* [25,53] of long bones of 12 sauropodomorph taxa (*Saturnalia tupiniquim*, *Thecodontosaurus*, *Plateosaurus*, *Spinophorosaurus*, *Brachiosaurus*, *Europasaurus*, *Apatosaurus*, *Dicraeosaurus*, *Barosaurus*, *Janenschia*, *Phuwiangosaurus* and *Alamosaurus*, see Table 1) from the thin section collection at the Steinmann Institut in Bonn. Further sampled tetrapod taxa include a non-therapsid synapsid (*Dimetrodon natalis*, histological analysis in [54]), squamate reptiles (*Iguana iguana*, *Varanus niloticus*, *Varanus timorensis*, *Tupinambis teguixin*), basal archosauromorphs (*Trilophosaurus sp.*, *Hyperodapedon sp.*, *Rhamphorhynchus muensteri* (histological analysis in [39]), two alligators (*Alligator mississippiensis*, histological analysis in [47] and [55] respectively), large theropod dinosaurs (*Albertosaurus*, *Gorgosaurus* and *Tyrannosaurus*, histological analysis in [36,6–57]), and two birds (*Buteo buteo* and *Struthio camelus*). As non-amniote representatives, a Jurassic salamander (*Kokartus*, described in [58]), a common European frog (*Rana temporaria*) and *Diadectes sp.* were sampled. Mammal lacunar densities were taken from Bromage et al. [12] (Table 2). We measured OLDs of two additional extant mammal taxa, a guinea pig (*Cavia porcellus*) and an Indian elephant (*Elephas maximus*) to extend the range of body masses for mammals. Furthermore, we measured OLD in primary cortical bone of *Myotragus balearicus*, an extinct island-dwarf bovid, that has been reported to have a crocodile-like physiology and growth rate [59]. Thin sections of extant specimens were studied in their repository collections, or samples were taken from salvage specimens (*i.e.* animals which died of natural causes). All measured specimens with collection numbers, body mass estimates and osteocyte lacunar densities are listed in Table 1.

Bromage et al. [12] provided osteocyte densities of fully grown mammals. For a meaningful comparison, we required osteocyte densities of adult individuals. Therefore, we used only the largest individuals in our regression analyses if OLD's of more than one individual of the same species were available. Additionally, osteocyte lacunar density was measured in the outer third of the bone cortex of the midshaft of transverse sections of mostly femora, but in some cases tibiae or humeri. In the case of sauropods, only individuals of at least histological ontogenetic stage 9 (HOS, [60–61]) were chosen. Sauropods of HOS 9 or above usually have laminar or plexiform bone with well defined primary osteons and a progressed state of cortical remodelling. Animals at this stage are not growing at the incredible juvenile rate anymore, and are putting more energy in maintenance than growth. Apart from being sexually mature, skeletal maturity may also have been reached if an EFS is present [60]. For all taxa with highly vascularized tissues, osteocyte lacunar density was measured in the parallel-fibred or rather highly organized primary bone (HOPB *sensu* [28]) matrix of the composite cortical bone. It should be noted that Hernandez et al. [19] found no significant difference between OLD of lamellar cortical bone and OLD of periosteal woven bone in the rat. However, Bromage et al. [12] measured lacunar density in HOPB, allowing direct comparison with their published data. The main reason for choosing HOPB to measure OLD is that taxa without highly vascularized long bone tissues only possess HOPB. Other reasons include the proportion of HOPB matrix is much larger than that of woven bone, which makes counting a significant number of osteocyte lacunae in woven bone nearly impossible; osteocyte lacunae in HOPB do not have irregular shapes as in woven bone, and are therefore easier to recognise with polarized light microscopic methods. Furthermore, a sample site without cracks, diagenetic alteration, and if possible, vascular canals, is also easier to locate.

Table 1. Specimens with body masses and measured osteocyte densities.

Taxon	specimen nr.	et	el (mm)	BM (kg)	OLD (#/mm ³)	BM source or method
<i>Kokartus</i>	ZIN.PH 43/47	fe		0.05	8601	P. Skutchas p.c.
<i>Rana temporaria</i>	IPB no nr.	fe		0.039	13828	species average
<i>Diadectes</i>	IPB no nr.	fe	130	35	29741	[99]
<i>Dimetrodon natalis</i>	IPB SABCBB 2010–26	fe	98	23	47413	[99]
<i>Dimetrodon natalis</i>	IPB SABCBB 2010–1	fe	108	28	34364	[99]
<i>Myotragus balearicus</i>	MBCN SM-T-8829-?/?	ti	183	20	26867	[100]
<i>Elephas maximus</i>	IPB no nr. female	fe		3000	19264	species average
<i>Cavia porcellus</i>	IPB no nr.	fe		0.7	36190	species average
<i>Iguana iguana</i>	AC 1896 288	fe	74.23	5	20534	V. de Buffr�n�il p.c.
<i>Tupinambis teguixin</i>	MK 53531/VB	fe		1.5	61118	V. de Buffr�n�il p.c.
<i>Varanus niloticus</i>	FAOTD39	fe		11	42977	V. de Buffr�n�il p.c.
<i>Varanus timorensis</i>	MK 52920	fe	33.41	0.8	53806	V. De Buffr�n�il p.c.
<i>Trilophosaurus</i>	TMM 31025-786	fe		14.8	37.037	[99]
<i>Trilophosaurus</i>	TMM 31025-885 avg.	fe		14.5	38117	[99]
<i>Trilophosaurus</i>	TMM 31025-67-02 avg.	fe		14.0	27051	[99]
<i>Trilophosaurus</i>	TMM 31025-67-01	fe		13.5	36.795	[99]
<i>Trilophosaurus</i>	TMM 31025-787	fe		13.3	27.505	[99]
<i>Hyperodapedon</i>	MCP PV0247	ti		188	23054	[99]
<i>Hyperodapedon</i>	MCP PV0407	hu		41	55787	[99]
<i>Hyperodapedon</i>	MCP PV408	hu		41	53129	[99]
<i>Rhamphorhynchus</i>	BSPG 1960 I 470a	ti		0.0834	52714	[39]
<i>Rhamphorhynchus</i>	BSPG 1929 I 69	fe		2.085	36859	[39]
<i>Rhamphorhynchus</i>	BSPG 1877 ×1	fe		0.112	46786	[39]
<i>Alligator mississippiensis</i>	SMNS 10481	fe		100	9064	[47]
<i>Alligator mississippiensis</i>	IPB "Babette" posterior	fe		6.86	18455	wet specimen measure
<i>Buteo buteo</i>	IPB no nr.	fe		1.3	59350	species average
<i>Struthio camelus</i>	IPB 5y old male	tt		115	46001	species average
<i>Gorgosaurus</i>	TMP 99.33.1	fi		607	15546	[36]
<i>Gorgosaurus</i>	TMP 99332	fi		607	17846	[36]
<i>Albertosaurus</i>	TMP 2002.45	fi		50.3	16294	[36]
<i>Albertosaurus</i>	TMP 86.64.1	fi		762	18790	[36]
<i>Albertosaurus</i>	TMP 86.64.1	fe		762	16765	[36]
<i>Albertosaurus</i>	TMP 81.10.1	fi		1142	17499	[36]
<i>Tyrannosaurus</i>	TMP 81.6.1	ilb		3230	13528	[36]
<i>Tyrannosaurus</i>	TMP 81.6.1	ilb		3230	12153	[36]
<i>Tyrannosaurus</i>	TMP 81.6.1	ilb		3230	12027	[36]
<i>Saturnalia</i>	MCP PV3845	fe		20	53432	[99]
<i>Thecodontosaurus</i>	IPB no nr.	ti		24.6	47611	[26]
<i>Plateosaurus</i>	SMNS F14A	fe	655	780	23300	[52]
<i>Plateosaurus</i>	SMNS F8	fe	740	900	20776	[52]
<i>Spinophorosaurus</i>	NMB 1698-R	hu	1121	6600	27392	U. Joger, p.c.
<i>Apatosaurus</i>	SMA "Jaques"	fe	1640	10000	33202	[26]
<i>Barosaurus</i>	MfN XV15	fe	790	1500	45480	[99]
<i>Barosaurus</i>	MfN Ki2	fe	1190	11000	41878	[99]
<i>Dicraeosaurus</i>	MfN T31a	fe	980	3000	58540	[99]
<i>Dicraeosaurus</i>	MfN dd3032	fe	1140	4635	48500	[99]
<i>Europasaurus</i>	DFMMh/FV 415	fe	510	690	39386	[99]
<i>Brachiosaurus</i>	MfN dd452	fe	1350	10000	35647	[26]
<i>Brachiosaurus</i>	BYU 725-17336	fe	1750	19000	21923	[26]

Table 1. Cont.

Taxon	specimen nr.	et	el (mm)	BM (kg)	OLD (#/mm ³)	BM source or method
<i>Janenschia</i>	MfN Nr.22	fe	1270	14029	43241	[26]
<i>Janenschia</i>	MfN Nr.22	fe	1270	14029	56715	[26]
<i>Phuwingsosaurus</i>	PC.DMR K21	fe	1120	9046	31866	[99]
<i>Alamosaurus</i>	TMM 43090-1	hu	1300	16000	26246	[99]

Abbreviations: **et**, element type (fe, femur; fi, fibula; hu, humerus; ilb, indeterminate long bone; ti, tibia; tt, tibiotarsus); **el**, element length (given where known); **BM**, body mass; **OLD**, osteocyte lacunar density; **p.c.**, personal communication. Institutional abbreviations: **BSPG**, Bayerische Staatssammlung für Paläontologie und Geologie; **BYU**, Earth Sciences Museum, Brigham Young University, Provo, Utah; **DFMMh/FV**, Dinosaurier-Freilichtmuseum MÜNCHENHAGEN/Verein zur Förderung der Niedersächsischen Paläontologie (e.V.), Germany; **IPB**, Institut für Paläontologie, Bonn, Germany; **MBCN**, Museu Balear de Ciències Naturals, Mallorca, Spain; **MCP**, Museu de Ciències e Tecnologia PUCRS, Porto Alegre, Brazil; **MFN**, Museum für Naturkunde, Berlin, Germany; **MK**, Museum König, Bonn, Germany; **NMB**, Naturhistorisches Museum Braunschweig, Germany; **PC.DMR**, Paleontological Collection, Department of Mineral Resources, Khon Kaen Province, Kalasin, Thailand; **SMA**, Saurier Museum Aathal, Switzerland; **SMNS**, Staatliches Museum für Naturkunde Stuttgart, Germany; **TMM**, Texas Memorial Museum, Austin, Texas; **TMP**, Royal Tyrell Museum of Paleontology, Drumheller, Alberta, Canada. **ZIN.PH**, Zoological Institute, Russian Academy of Sciences, Paleoherpelological Collection, St. Petersburg, Russia.

doi:10.1371/journal.pone.0077109.t001

The method for measuring lacunar densities used here is similar to that of Bromage et al. [12], albeit with a less sophisticated, low-cost image processing technique (Fig. 1). Using a Leica DMLP microscope at 40× magnification, a 257-µm wide by 192 µm high XY field of view was chosen for each specimen as described above. Once an XY field was selected, a z-stack of images with a spacing of 5 µm was acquired using a Leica FireCam and processed with Leica Imageaccess software. Individual lacunae were identified in the three-dimensional image stacks and then projected on a two-dimensional plane. From these images, all identified lacunae were counted manually.

Thickness of the thin sections was determined with a standard microscopic procedure. The sample was brought in focus on the upper surface of the epoxy resin. The stage was then lowered until the lower scratched surface of the epoxy resin was in focus. The difference in stage height setting, as read off the fine focus dial, was multiplied with the refractive index of the resin. The Araldite™ two component resin used in our lab has a refractive index of 1.554 when hardened. This refractive index measure of the resin was provided by the manufacturer. The obtained thickness was controlled with the number of images in the z-stack with 5 µm distanced focal planes. The obtained thickness was multiplied with the surface area of the sample, corrected for any blood vessels, to obtain the total volume of bone. All measurements were then standardised by extrapolation of the number of lacunae per measured volume of bone to a 1 mm³ unit value.

To avoid the large potential errors involved in estimating body masses of extinct animals, femur length should be used as proxy for body size. However, longitudinal bone growth may be faster than appositional growth in some species. Moreover, here, OLD is measured in a volume (i.e. 3 dimensions), and is thus more appropriately compared with a volumetric body mass. Bromage et al. [12] provided body masses obtained from literature species averages for their mammal samples (T. Bromage, Pers. Comm.). Body masses of the extinct animals in this study were collected from previously published literature sources or estimated with different methods (listed in Table 1). It should be emphasised that usage of sauropod dinosaur (but also other extinct animal) body mass estimates should be done with caution, as many well known potential problems are involved e.g. overestimating body density because of the airsac system, unknown humerus to femur ratio (see [62–63] for an introduction). However, the obtained body masses for this study were log-transformed to reduce this potential source of error.

Lacunar densities were log-transformed and plotted against the log-transformed body masses. Phylogenetic generalized least square regressions (PGLS, [64–66]) were calculated in R (version 2.15.2, [67]) for the whole dataset and separately for different groups containing at least six species (e.g. sauropodomorphs, mammals and reptiles, Table 3) using the generalized linear square method (gls) from the nlme package and the corPagel correlation structure from the ape package. Additionally we used a weighting structure in our PGLS analyses because the phylogenetic tree used was not ultrametric (containing extinct taxa). The weighting structure was calculated from the phylogeny by extracting the vector containing the branch lengths from the root to every tip (weights (W) = diag(vcv.phylo(tree))). Thus our final PGLS model was defined in R as

$$\text{gls}(\log_{10}(\text{OLD}) \sim \log_{10}(\text{BM}),$$

$$\text{correlation} = \text{corPagel}(1, \text{tree}), \text{weights} = \text{varFixed}(\sim W))$$

where OLD = osteocyte lacuna density, BM = body mass tree = phylogenetic tree, W = weights.

To solve the problem that no complete phylogeny was available for all species, we constructed a new tree based on different published phylogenetic trees. Branch lengths were calculated from estimated divergence times of the different nodes taken from the literature, because characters and clustering methods used to construct trees might have been different and thus might have affected branch lengths. Phylogenetic trees were constructed from Vidal and Hedges [68], Mulcahy et al. [69] and Amer and Kumazawa [70] for squamates; Hackett et al. [71] for birds; Marjanovic and Laurin [72] and Clack [73] for non-amniote tetrapods; Bennett [74] and Nesbitt [75] for non-dinosaurian archosaurs; Pisani et al. [76] and Brusatte et al. [77] for tyrannosaurid dinosaurs; Yates [78–79]; Sereno [80]; Allain and Aquesbi [81]; Remes et al. [82] for Sauropodomorpha and Beck et al. [83] and Perelman et al. [84] for mammals using Mesquite v. 2.75 [80]. Additional information on node divergence times was taken from Benton et al. [85] and Müller and Reisz [86]. Specific taxon ranges were obtained from the paleobiology database on 26/06/2013, except for *Phanourios minutus* (= *Hippopotamus minutus*) and *Spinophorosaurus* for which stratigraphic data were obtained from Van der Geer et al. [87] and Remes et al. [82] respectively. A nexus file containing our calibrated tree can be found in Nexus S1.

Table 2. Mammal body masses and osteocyte lacunar densities from Bromage et al. [12].

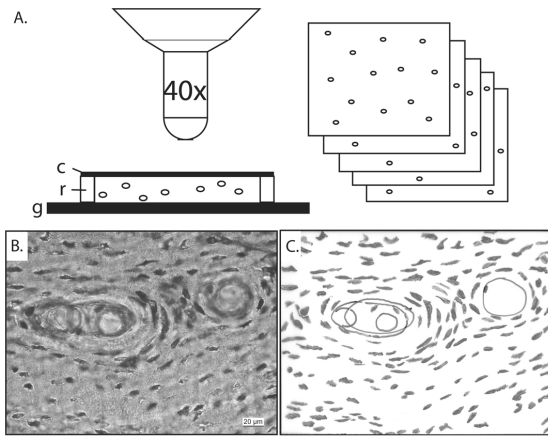
Taxon	BM (kg)	OLD (#/mm ³)
<i>Rattus norvegicus</i>	0.3	58000
<i>Phanourios minutus</i>	200	23641
<i>Hippopotamus amphibius</i>	2000	16667
<i>Otolemur crassicaudatus</i>	1.15	44353
<i>Chlorocebus aethiops</i>	3.515	32012
<i>Pan troglodytes</i>	33.7	18706
<i>Homo sapiens</i>	62	20444
<i>Galago moholi</i>	0.244	51724
<i>Cheirogales major</i>	0.4	31526
<i>Macaca mulatta</i>	3	22222

doi:10.1371/journal.pone.0077109.t002

To test for differences in slopes and in intercepts of the regressions of the different taxonomic groups we performed pairwise comparisons using t-tests. If variances of intercept or slope were statistically unequal t-test for unequal variances were used otherwise not. For further comparisons we also calculated the 95% prediction interval of the phylogenetic controlled mammal regression using standard methods.

Results

In general, OLD and BM were correlated with each other and this yielded to significant regression models except for reptiles (Table 3). With the exception of the regression model over all available data points and the reptile regression residuals were normally distributed (Shapiro-Wilk normality test; all: $W = 0.9296$, $p\text{-value} = 0.01257$; reptiles: $W = 0.7924$, $p\text{-value} = 0.03442$; mammals: $W = 0.9592$, $p\text{-value} = 0.7407$; sauropodomorphs: $W = 0.9485$, $p\text{-value} = 0.6145$) However, removing the *Alligator* from the reptile sample which might be an outlier (see Figure 2) produced a significant regression model for reptiles (Table 3) with normally distributed residuals (Shapiro-Wilk normality test; $W = 0.8141$, $p\text{-value} = 0.07835$). Comparing pairwise the taxonomic groups with each other, which contained at least six species (mammals, reptiles, reptiles without *Alligator*, sauropodomorphs), showed that all slopes were statistical not different (Table 4). Comparing the intercepts revealed that the sauropodomorph intercept was different from that of mammals and reptiles, whereas the intercepts of mammals and reptiles were statistical not different

**Figure 1.** Method for acquiring z-stacks, and counting lacunae.

A. Z-stack acquisition and thickness measurement. Thin sections were imaged at 40 \times magnification, the first image taken at the uppermost scratched surface of the specimen. The stage was then lowered with 5 μm for every subsequent image, until the lowermost scratched surface of the section was reached. Thickness of the sections was determined with a standard microscopic procedure. The sample was brought in focus on the upper surface of the epoxy resin. The stage was then lowered until the lower scratched surface of the epoxy resin was in focus. The difference in stage height setting, as read off the fine focus dial, was multiplied with the refractive index of the resin. This measurement was controlled with the number of images taken at 5 μm intervals. B,C, Lacunae identified in the z-stacks were projected on a two dimensional plane, and manually counted. The volume of bone was corrected for any vascular spaces, like in this example of *Dicraeosaurus*, any lacunae within the marked boundaries were ignored. The resulting volumetric density was then standardised to a volume of 1 mm³. **Abbreviations:** c, cover slip; g, glass slide; r, epoxy resin. doi:10.1371/journal.pone.0077109.g001

from each other (Table 4). However, the reptile regression model without the *Alligator* had a significant different intercept in comparison to the mammal regression. (Table 4).

Using the mammal regression and the 95% prediction interval of the mammal regression as a baseline for comparison revealed that amphibians and the *Alligator* had low OLD's in comparison to all other taxa (Figure 2B). The bird species *Struthio camelus*, and sauropodomorphs (with exception of *Plateosaurus* and) had higher OLD values as observed in mammals (Figure 2B). All other OLD's were within the mammalian range considering so diverse taxa like theropods, extant ectothermic reptiles, reptiliomorphs, synapsids as well as Pterosauria (Figure 2B). A pairwise comparison [88] in Mesquite [89] yielded similar results, i.e. that there is a statistically

Table 3. Phylogenetic controlled regression models ($\log_{10} \text{OLD} = \log_{10} \text{intercept} + \text{slope} * \log_{10} \text{BM}$) of osteocyte lacunar density (OLD) on body mass (BM) for different groups.

group	lambda	N	intercept	95% CI	SE	p-value	slope	95% CI	SE	p-value	AIC
All	0.987	42	4.530	[4.342, 4.719]	0.096	<0.001	-0.096	[-0.146, -0.047]	0.025	<0.001	-15.377
Mammals	0.552	13	4.584	[4.491, 4.676]	0.047	<0.001	-0.108	[-0.154, -0.063]	0.023	<0.001	-7.270
Reptiles	1.175	7	4.694	[4.329, 5.060]	0.186	<0.001	-0.159	[-0.338, 0.019]	0.091	0.141	9.565
Reptiles without <i>Alligator</i>	-0.592	6	4.677	[4.644, 4.710]	0.017	<0.001	-0.131	[-0.203, -0.058]	0.037	0.024	6.547
Sauropodomorphs	1.015	12	4.863	[4.627, 5.098]	0.120	<0.001	-0.130	[-0.234, -0.025]	0.053	0.036	-0.460

All = overall regression analyses with all available data. lambda = Page's lambda. N = sample size. 95% CI = 95% confidence interval of the respective regression coefficient. SE = standard error. AIC = Akaike information criterion. For details on calculating the regression models see text.

doi:10.1371/journal.pone.0077109.t003

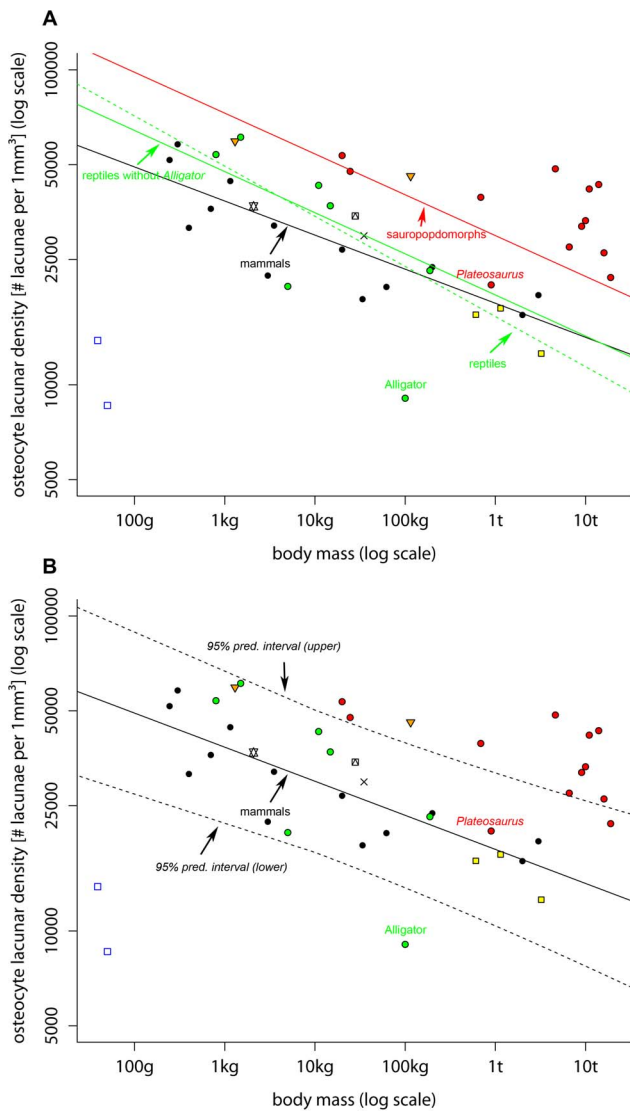


Figure 2. Visualisation of osteocyte lacuna densities in different tetrapods. A. Plot of osteocyte lacunar density on body mass of different taxa on a double logarithmic scale. Lines are the phylogenetic controlled regression lines of the respective taxonomic group. Solid lines represent significant regression models. The scattered line represents a regression model where the slope is not significant different from zero using a significant level of 0.05. For details of the regression models see Table 3. black circles = mammals, red circles = sauropodomorphs, blue open squares = amphibians, yellow squares = theropods, orange triangles = birds, green circles = reptiles, cross = diadectomorphs, star/pentagram = pterosaurs, square with triangle = "pelycosaurs". B. Studied species in comparison to the mammal regression model (solid line). Scattered lines are 95% prediction intervals of the mammal regression model. Symbols as in A. doi:10.1371/journal.pone.0077109.g002

significant relation between body mass and OLD ($p = 0.039$) (see Nexus S1).

Discussion

Our results suggest the relation between OLD and body mass is complex in nature. Carter et al. [90] found highly variable OLD within one single femur section of a young male human. Differences in osteocyte density up to 30%, combined with

differences in general osteocyte morphology, between anterior, posterior, lateral and medial sides were strongly attributed to differences in mechanical loading regimes. Sanchez et al. [2], in their figure 4C, provide a visual representation of such variation in a virtual thin section of the humerus of the salamander *Desmognathus*. We also found strong lacunar density variation in a smaller specimen (femur TMM31025-885) of *Trilophosaurus sp.* (42601 lacunae/mm³ on the anterior side and 33632 lacunae/mm³ on the posterior side). Being aware of these variations, we tried to use standardized locations for measurements, with a sampling location midshaft on the anterior side of the femur. This requirement could not always be met. For example, Bromage et al. [12] did not specify precise locations of measurements, but also when dealing with fossil specimens a femur may not always be available, or preservational reasons prohibit sampling of the desired location. Moreover, a systematic approach with standardized sampling locations would ultimately also account for widely varying locomotion styles and resulting principal loading regimes in the sampled element. Nonetheless, in a general trend among mammals, dinosaurs and reptiles, OLD decreases with increasing body mass. Mullender et al. [18] found a similar relationship for the osteocyte lacunar densities within the cancellous bone tissues of the proximal femur in five mammals. Skedros et al. [91] also observed decreasing OLD with body mass in the turkey ulna. Moreover, they found high lacunar densities in the turkey compared to mammals of a similar size. High lacunar densities in the turkey ulna is consistent with works by Marotti et al. [92] and Remaggi et al. [93] who found high lacunar densities in the domestic chicken. Unfortunately, these authors used surface area measurements, making a direct comparison of the actual values with those presented here difficult. Nevertheless, the two bird species in our study (*Buteo buteo*, *Struthio camelus*) had high lacunar densities in comparison to mammals, too. Skedros et al. [91] speculated that substantially greater lacunar densities in avian species compared to mammals may be a function of their relatively higher specific metabolic rate (metabolic rate per kilogram of body mass), but did not provide further details.

Sauropods have unexpectedly high OLD-values, more than twice as high as expected for scaled up mammals. Also remarkable are the high OLD of the *Tupinambis* and monitor lizards. Even though the large alligator has much lower OLD compared to similar-sized mammals, the squamate high OLD are in contrast with the notion that OLD is directly related to basal metabolic rates. Concomitantly, the much higher lacunar density of the extinct insular bovid *Myotragus* compared to a similar-sized alligator would certainly question its presumed crocodylian metabolic physiology [59].

In an attempt to further test the relation between osteocyte lacunar density and growth rate, we plotted OLD's per kg body mass versus relative growth rates (RGR) for the taxa for which data were available (Figure 3). RGR's are from Werner and Griebeler (this collection) and were calculated from fitted growth models as described in Fitzhugh [94] that is maximal growth rate (of the respective growth model) divided by the body mass at which this rate occurs. OLD's were divided by body mass of the studied taxa to get mass-specific values, too. This approach should also account for body size scaling effects. Interestingly, OLD per kg body mass is significantly correlated with relative growth rate in dinosaurs (including birds) as well as in mammals. On a log-log plot, linear regression analyses show that the regression model for all dinosaurs (including birds) is significantly different from that for mammals (Figure 3). This means for a given lacunar density, dinosaurs (including birds) have a higher relative growth rate than mammals and probably also reptiles (Figure 3). The alligator was

Table 4. Pairwise comparisons of the slopes and intercepts of the different regression models (sauropodomorphs, mammals, reptiles, reptiles without *Alligator*). t = t-value of t-test, df = degree of freedom, p = p-value.

	Mammals		Reptiles		Reptiles without <i>Alligator</i>	
	intercepts	slopes	intercepts	slopes	intercepts	slopes
Sauropodomorphs	¹ t = 7.519	¹ t = 1.283	t = 2.405	t = 0.901	¹ t = 5.242	t = 0.038
	df = 11	df = 11	df = 17	df = 17	df = 5	df = 16
	p < 0.001	p = 0.226	p = 0.028	p = 0.380	p = 0.003	p = 0.960
Mammals			¹ t = 1.546	¹ t = 1.457	¹ t = 6.317	t = 1.619
			df = 6	df = 6	df = 5	df = 17
			p = 0.173	p = 0.195	p = 0.002	p = 0.124

¹t-test for unequal variances.

doi:10.1371/journal.pone.0077109.t004

here taken together with reptiles because of similar physiologies, however, because the sample plots in between regression lines for mammals+reptiles and dinosaurs, it can arguably be taken together with dinosaurs, extending the dinosaur regression to crown-group archosaurs. This may be tested in future projects

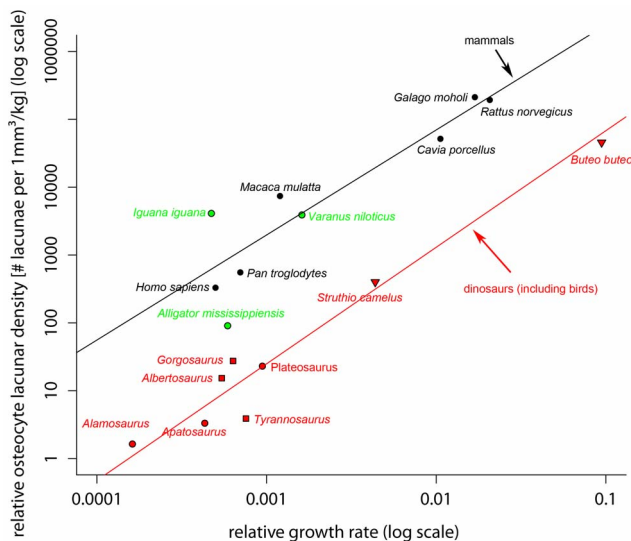


Figure 3. Plot of relative osteocyte lacunar density (ROLD, osteocyte lacunar density per 1 mm³/kg body mass) on relative growth rate (RGR, relative growth per day) on a double logarithmic scale. Red = dinosaurs including birds, black = mammals; green = reptiles. Solid lines are phylogenetic controlled regression models of the respective groups (dinosaurs including birds, mammals). Phylogenetic controlled regression models: log₁₀ ROLD = 6.550 [5.897, 7.203] + 1.718 [1.477, 1.958] * log₁₀ RGR, AIC = 13.456, p < 0.001, lambda = -0.420 (dinosaurs including birds); log₁₀ ROLD = 7.939 [7.325, 8.553] + 1.548 [1.548, 1.548] * log₁₀ RGR, AIC = 10.359, p < 0.001, lambda = 1.111 (mammals). 95% confidence intervals of regression coefficients in square brackets. Residuals of both regressions were normally distributed (Shapiro-Wilk normality test; dinosaurs including birds: W = 0.955, p-value = 0.760; mammals: W = 0.900, p-value = 0.374). Regression lines were significantly different from each other (t-test; slopes: t value = 3.917 df = 5, p = 0.011 intercepts: t value = 7.917, df = 12, p < 0.001). Note: For the species *Rattus norvegicus* and the *Galago moholi* no RGR were available, therefore we used the RGR's of phylogenetic closely related species (same genus) with similar body masses (*Rattus rattus*, *Galago senegalensis*).

doi:10.1371/journal.pone.0077109.g003

with other crurotarsal archosaurs with known relative growth rates.

Cao et al. [11] found much more developed lacunocanicular networks in terrestrial tetrapods versus teleost fish. They suggested these differences may not be related to the aquatic habitat, however, the amphibians in our analysis, as well as the amphibious alligator have the lowest OLD values. The non-amniote *Diadectes* has relatively high OLD, but this animal probably was a relatively terrestrial animal [95]. Similarly, the actively hunting and foraging squamate reptiles also have high lacunar densities compared to the amphibious poikilotherm alligator. Locomotion and biomechanics thus most likely have a significant influence on the density of the lacunocanicular network. Moreover, it is interesting to note that the bipedal *Plateosaurus* in our analysis have lacunar density values closer to those of theropods than to sauropods but not *Thecodontosaurus* and *Saturnalia*.

Other aspects of the lacunocanicular network in tetrapod bones may reflect functional signals too. Rensberger and Watabe [96] observed differences between lacunocanicular features in secondary osteons of theropod and birds and those of ornithomorphs and mammals. These features most likely do not represent true differences in lacunocanicular morphology, but rather differences in the orientation of the osteocytes [28]. Nevertheless, the suggestion that birds and theropods have osteocytes oriented mostly parallel with the long bone axis, whereas ornithomorphs and mammals have osteocytes generally oriented more perpendicular to the long bone axis, may reflect differences in biomechanics and/or locomotion style. This hypothesis receives strong support from modern *in vivo* studies on bioapatite c-axis orientation [97,98]. The hypotheses presented here can be tested by sampling large and small ornithomorph dinosaurs, as well as a wider variety of theropods and birds, but also amphibians and squamate reptiles. To test the individual contributing effects of growth rates, principal mechanical loading and bone apposition rates on the density of the lacunocanicular network, more detailed measurements of these features *in vivo* and analysis with variation partitioning methods are required. These are, however, beyond the scope of the current paper.

Conclusions

The precise cause and origin of high lacunar densities in Sauropodomorpha relative to other tetrapods remains unclear to this point. Further testing on extant amniotes with known behavioural ecology, growth rate and metabolic rate may provide a better resolution on the factors determining osteocyte lacunar

density. When accounting for body mass effects and phylogeny, growth rates are a main factor determining the density of the lacunocanicular network. However, functional aspects most likely play an equally important determining role as well.

Supporting Information

Nexus S1 Nexus file containing calibrated tree and analysis of osteocyte lacuna density with pairwise comparison. (NEX)

Acknowledgments

The authors thank P.M. Sander, M. Clauss, S. Werning and one anonymous reviewer for reading earlier drafts of this manuscript and C.

References

- Cubo J, Le Roy N, Martinez-Maza C, Montes L (2012) Paleohistological estimation of bone growth rate in extinct archosaurs. *Paleobiology* 38: 335–349.
- Sanchez S, Dupret V, Tafforeau P, Trinajstić K, Ryll B, et al. (2013) 3D microstructural architecture of muscle attachments in extant and fossil vertebrates revealed by synchrotron microtomography. *PLoS One* 8: e56992.
- Lindgren J, Uvdal P, Engdahl A, Lee AH, Alwmark C, et al. (2011) Microspectroscopic evidence of Cretaceous bone proteins. *PLoS One* 6: e19445.
- Schweitzer MH, Zheng W, Cleland TP, Bern M (2013) Molecular analyses of dinosaur osteocytes supports the presence of endogenous molecules. *Bone* 52: 414–423.
- Franz-Odenaal TA, Hall BK, Eckhard Witten P (2006) Buried alive: how osteoblasts become osteocytes. *Developmental Dynamics* 235: 176–190.
- Francillon-Vieillot H, Buffrénil Vd, Castanet J, Géraudie J, Meunier FJ, et al. (1990) Microstructure and mineralization of vertebrate skeletal tissues. In: CARTER JG, editor. *Skeletal biomineralization: Patterns, processes and evolutionary trends Vol 1*. New York: Van Nostrand Reinhold. pp. 471–530.
- Marotti G (2000) The osteocyte as a wiring transmission system. *Journal of Musculoskeletal and Neuronal Interaction* 1: 133–136.
- Noble BS (2008) The osteocyte lineage. *Bone* 473: 106–111.
- Klein-Nulend J, Bakker AD, Bacabac RG, Vatsa A, Weinbaum S (2013) Mechanosensation and transduction in osteocytes. *Bone* 54: 182–190.
- Tei A, Zallone A (2009) Do osteocytes contribute to bone mineral homeostasis? Osteocytic osteolysis revisited. *Bone* 44: 11–16.
- Cao L, Moriishi T, Miyazaki T, Iimura T, Hamagaki M, et al. (2011) Comparative morphology of the osteocyte lacunocanicular system in various vertebrates. *Journal of Bone and Mineral Metabolism* 29: 662–670.
- Bromage T, Lacruz RS, Hogg R, Goldman HM, McFarlin SC, et al. (2009) Lamellar bone is an incremental tissue reconciling enamel rhythms, body size, and organismal life history. *Calcified Tissue International* 84: 388–404.
- Mullender MG, Van Der Meer DD, Huiskes R, Lips P (1996) Osteocyte density changes in aging and osteoporosis. *Bone* 18: 109–113.
- Vashishth D, Verborgt O, Divine G, Schaffler MB, Fyhrie DP (2000) Decline in osteocyte lacunar density in human cortical bone is associated with accumulation of microcracks with age. *Bone* 26: 375–380.
- Parfitt AM (2002) Life history of osteocytes: relationship to bone age, bone remodeling, and bone fragility. *Journal of Musculoskeletal Neuronal Interaction* 2: 499–500.
- Qiu S, Rao DS, Palnitkar S, Parfitt AM (2002) Relationships between osteocyte density and bone formation rate in human cancellous bone. *Bone* 31: 709–711.
- Canè V, Marotti G, Volpi G, Zaffè D, Palazzini S, et al. (1982) Size and density of osteocyte lacunae in different regions of long bones. *Calcif Tissue Int* 34: 558–563.
- Mullender MG, Huiskes R, Versleyen H, Buma P (1996) Osteocyte density and histomorphometric parameters in cancellous bone of the proximal femur in five mammalian species. *Journal of Orthopaedic Research* 14: 972–979.
- Hernandez JC, Majeska RJ, Schaffler MB (2004) Osteocyte density in woven bone. *Bone* 35: 1095–1099.
- Skedros JG, Grunander TR, Hamrick MW (2005) Spatial distribution of osteocyte lacunae in equine radii and third metacarpals: considerations for cellular communication, microdamage detection and metabolism. *Cells, Tissues, Organs* 180: 215–236.
- Ma Y-L, Dai R-C, Sheng Z-F, Jin Y, Zhang Y-H, et al. (2008) Quantitative associations between osteocyte density and biomechanics, microcrack and microstructure in OVX rats vertebral trabeculae. *Journal of Biomechanics* 41: 1324–1332.
- Curry KA (1999) Ontogenetic histology of *Apatosaurus* (Dinosauria: Sauropoda): New insights on growth rates and longevity. *Journal of Vertebrate Paleontology* 19: 654–665.
- Erickson GM, Rogers KC, Yerby SA (2001) Dinosaurian growth patterns and rapid avian growth rates. *Nature* 412: 429–433.
- Lehman T, Woodward H (2008) Modeling growth rates for sauropod dinosaurs. *Paleobiology* 34: 264–281.
- Organ, E. Prondvai, R. Benson and M Laurin for insightful discussions on statistical analysis and tree calibration. C. Organ and one anonymous reviewer provided constructive criticism on the submitted manuscript. U. Joger, M.C. Langer, W. Langston Jr., O. Rauhut, J. Reumer, T. Rowe, C. Schultz, K. Siber and V. Suthethorn are greatly acknowledged for allowing sampling of specimens in their care. V. de Buffrénil, G. Erickson, C. Shelton, P. Skutchas, and S. Werning are thanked for providing access to thin sections of selected taxa. This is contribution 152 of the DFG Research Unit FOR533 ‘Biology of the Sauropod Dinosaurs’.
- Sander PM (2000) Long bone histology of the Tendaguru sauropods: Implications for growth and biology. *Paleobiology* 26: 466–488.
- Sander PM, Christian A, Clauss M, Fechner R, Gee CT, et al. (2010) Biology of the sauropod dinosaurs: the evolution of gigantism. *Biological Reviews* 86: 117–155.
- Sander PM, Klein N, Stein K, Wings O (2011) Sauropod Bone Histology and Its Implications for Sauropod Biology. In: Klein N, Remes K, Sander PM, editors. *Biology of the Sauropod Dinosaurs*: Indiana University Press.
- Stein K, Prondvai E (2013) Rethinking the nature of fibrolamellar bone: An integrative biological revision of sauropod pelfiform bone formation. *Biological Reviews* doi: 10.1111/brv.12041.
- Ricqlès AJ, Padian K, Horner JR (2003) On the bone histology of some Triassic pseudosuchian archosaurs and related taxa. *Annales de Paléontologie* 89: 67–101.
- Ricqlès Ad, Padian K, Knoll F, Horner JR (2008) On the origin of high growth rates in archosaurs and their ancient relatives: Complementary histological studies on Triassic archosauriforms and the problem of a “phylogenetic signal” in bone histology. *Annales de Paléontologie* 94: 57–76.
- Werning S, Irmis RB, Smith N, Turner AH, Padian K (2011) Archosauriform bone histology reveals early evolution of elevated growth and metabolic rates. *Journal of Vertebrate Paleontology* 31: 213A.
- Chinsamy-Turan A, editor (2012) *Forerunners of mammals: radiation, histology, biology*. Bloomington, Indiana: Indiana University Press.
- Ray S, Botha J, Chinsamy A (2004) Bone histology and growth patterns of some non-mammalian therapsids. *Journal of Vertebrate Paleontology* 24: 634–648.
- Chinsamy A (1993) Bone histology and growth trajectory of the prosauropod dinosaur *Massospondylus carinatus* (Owen). *Modern Geology* 18: 319–329.
- Chinsamy A, Elzanowski A (2001) Bone histology. Evolution of growth pattern in birds. *Nature* 412: 402–403.
- Erickson G, Mackovicky PJ, Currie PJ, Norell MA, Yerby SA, et al. (2004) Gigantism and comparative life-history parameters of tyrannosaurid dinosaurs. *Nature* 430: 772–775.
- Woodward H, Horner JR, Farlow JO (2011) Osteological evidence for determinate growth in the American alligator. *Journal of Herpetology* 45: 339–342.
- Woodward H, Rich TH, Chinsamy A, Vickers-Rich P (2011) Growth dynamics of Australia’s polar dinosaurs. *PLoS One* 6: e23339.
- Prondvai E, Stein K, Ósi A, Sander MP (2012) Life history of *Rhamphorhynchus* inferred from bone histology and the diversity of pterosaur growth strategies. *PLoS One* 7: e31392.
- Werning S (2012) The ontogenetic osteohistology of *Tenontosaurus tilletti*. *PLoS One* 7: e33539.
- Woodward H, Padian K, Lee AH (2013) Skeletochronology. In: Padian K, Lamm E-T, editors. *Bone histology of fossil tetrapods: advancing methods, analysis, and interpretation*. Berkeley: University of California Press. pp. 187–207.
- Padian K, Stein K (2013) Evolution of growth rates and their implications for paleobiology. In: Padian K, Lamm E-T, editors. *Bone histology of fossil tetrapods: advancing methods, analysis, and interpretation*. Berkeley: University of California Press.
- Castanet J, Smirina E (1990) Introduction to the skeletochronological method in amphibians and reptiles. *Ann Sci Nat Zool Paris, 13 Série* 11: 191–196.
- Buffrénil Vd, Castanet J (2000) Age estimation by skeletochronology in the Nile monitor lizard (*Varanus niloticus*), a highly exploited species. *Journal of Herpetology* 34: 414–424.
- Castanet J, Croci S, Aujard F, Perret M, Cubo J, et al. (2004) Lines of arrested growth in bone and age estimation in a small primate: *Microcebus murinus*. *Journal of Zoology*, London 263: 31–39.
- Köhler M, Marin-Moratalla N, Jordana X, Aanes R (2012) Seasonal bone growth and physiology in endotherms shed light on dinosaur physiology. *Nature* 487: 358–361.

47. Klein N, Scheyer T, Tütken T (2009) Skeletochronology and isotopic analysis of a captive individual of *Alligator mississippiensis* Daudin, 1802. *Fossil Record* 12: 121–131.
48. Sander PM, Mateus O, Laven T, Knöschke N (2006) Bone histology indicates insular dwarfism in a new Late Jurassic sauropod dinosaur. *Nature* 441: 739–741.
49. Horner JR, Padian K, Ricqlès Ad (1999) Variation in dinosaur skeletochronology indicators: implications for age assessment. *Paleobiology* 25: 49–78.
50. Case TJ (1978) On the evolution and adaptive significance of post-natal growth rates in the terrestrial vertebrates. *Quarterly Reviews in Biology* 53: 243–282.
51. Chinsamy-Turan A (2005) The microstructure of dinosaur bone. Baltimore: Johns Hopkins University Press. 195 p.
52. Klein N, Sander PM (2007) Bone histology and growth of the prosauropod *Plateosaurus engelhardti* MEYER, 1837 from the Norian bonebeds of Trossingen (Germany) and Frick (Switzerland). *Special Papers in Palaeontology* 77: 169–206.
53. Stein K, Sander M (2009) Histological core drilling: a less destructive method for studying bone histology. In: Brown MA, Kane JF, Parker WG, editors. *Methods In Fossil Preparation: Proceedings of the first Annual Fossil Preparation and Collections Symposium*. pp. 69–80.
54. Shelton CD, Sander PM, Stein K, Winkelhorst H (In Press) Long bone histology indicates sympatric species of *Dimetrodon* (Lower Permian, Sphenacodontidae). *Transactions of the Royal Society of Edinburgh*.
55. Petermann H, Sander M (2013) Histological evidence for muscle insertion in extant amniote femora: implications for muscle reconstruction in fossils. *Journal of Anatomy* 222: 419–436.
56. Erickson G (2005) Assessing dinosaur growth patterns: a microscopic revolution. *Trends in Ecology and Evolution* 20: 677–684.
57. Erickson G, Currie PJ, Inouye BD, Winn AA (2006) Tyrannosaur life tables: an example of nonavian dinosaur population biology. *Science* 313: 213–217.
58. Skutchav P, Martin T (2011) Cranial anatomy of the stem salamander *Kokartus honorarius* (Amphibia: Caudata) from the Middle Jurassic of Kyrgyzstan. *Zoological Journal of the Linnean Society* 161: 816–838.
59. Köhler M, Moya-Sola S (2009) Physiological and life history strategies of a fossil large mammal in a resource-limited environment. *Proceedings of the National Academy of Sciences, USA* 106: 20354–20358.
60. Klein N, Sander M (2008) Ontogenetic stages in the long bone histology of sauropod dinosaurs. *Paleobiology* 34: 248–264.
61. Stein K, Csiki Z, Curry Rogers K, Weishampel DB, Redelstorff R, et al. (2010) Small body size and extreme cortical bone remodeling indicate phyletic dwarfism in *Magyarosaurus dacus* (Sauropoda: Titanosauria). *Proceedings of the National Academy of Sciences, USA* 107 9258–9263.
62. Stoinski S, Suthau T, Gunga H-C (2011) Reconstructing body volume and surface area of dinosaurs using laser scanning and photogrammetry. In: Klein N, Remes K, Gee CT, Sander M, editors. *Biology of the sauropod dinosaurs: understanding the life of giants*. Bloomington: Indiana University Press. pp. 94–104.
63. Ganse B, Stahn A, Stoinski S, Suthau T, Gunga H-C (2011) Body mass estimation, thermoregulation, and cardiovascular physiology of large sauropods. In: Klein N, Remes K, Gee CT, Sander M, editors. *Biology of the sauropod dinosaurs: understanding the life of giants*. Bloomington: Indiana University Press. pp. 105–115.
64. Pagel M (1997) Inferring evolutionary processes from phylogenies. *Zoologica Scripta 25th Anniversary Special Issue on Phylogenetics and Systematics* 26: 331–348.
65. Pagel M (1999) Inferring the historical patterns of biological evolution. *Nature* 401: 877–884.
66. Freckleton R, Harvey PH, Pagel M (2002) Phylogenetic analysis and ecological data: a review of the evidence. *American Naturalist* 160: 712–726.
67. R Development Core Team (2012) R: A language and environment for statistical computing. Vienna, Austria: R Foundation for Statistical Computing. URL <http://www.R-project.org>.
68. Vidal N, Hedges SB (2005) The phylogeny of squamate reptiles (lizards, snakes, and amphisbaenians) inferred from nine nuclear protein-coding genes. *Comptes Rendus Biologies* 328: 1000–1008.
69. Mulcahy DG, Noonan BP, Moss T, Townsend TM, Reeder TW, et al. (2010) Estimating divergence dates and evaluating dating methods using phylogenomic and mitochondrial data in squamate reptiles. *Molecular Phylogenetics and Evolution* 65: 974–991.
70. Amer SAM, Kumazawa Y (2008) Timing of a mtDNA gene rearrangement and intercontinental dispersal of varanid lizards. *Genes and Genetic Systems* 83: 275–280.
71. Hackett SJ, Kimball RT, Reddy S, Bowie RCK, Braun EL, et al. (2008) A phylogenomic study of birds reveals their evolutionary history. *Science* 320: 1763–1768.
72. Marjanovic D, Laurin M (2013) The origin(s) of extant amphibians: a review with emphasis on the “lepospondyl hypothesis”. *Geodiversitas* 35: 207–272.
73. Clack (2012) Gaining ground: the origin and evolution of tetrapods. Bloomington: Indiana University Press.
74. Bennet SC (2012) The phylogenetic position of the Pterosauria within the Archosauromorpha re-examined. *Historical Biology* Doi:10.1080/08912963.2012.725727.
75. Nesbitt S (2011) The early evolution of archosaurs: relationships and the origin of major clades. *Bulletin of the American Museum of Natural History* 352: 1–292.
76. Pisani D, Yates AM, Langer MC, Benton MJ (2002) A genus-level supertree of the Dinosauria. *Proceedings of the Royal Society B* 269: 915–921.
77. Brusatte S, Norell MA, Carr TD, Erickson GM, Hutchinson JR, et al. (2010) Tyrannosaur paleobiology: new research on ancient exemplar organisms. *Science* 329: 1481–1485.
78. Yates AM (2007) The first complete skull of the Triassic dinosaur *Melanorosaurus* Houghton (Sauropodomorpha: Anchisauria). *Special Papers in Palaeontology* 77: 9–55.
79. Yates AM (2007) Solving a dinosaurian puzzle: the identity of *Alivalia rex* Galton. *Historical Biology* 19: 93–123.
80. Sereno PC (2007) Basal Sauropodomorpha: historical and recent phylogenetic hypotheses, with comments on *Ammosaurus major* (Marsh, 1989). *Special Papers in Palaeontology* 77: 261–289.
81. Allain R, Aquesbi N (2008) Anatomy and phylogenetic relationships of *Tazoudasaurus naimi* (Dinosauria, Sauropoda) from the Early Jurassic of Morocco. *Geodiversitas* 30: 345–424.
82. Remes K, Ortega F, Fierro I, Joger U, Kosma R, et al. (2009) A new basal sauropod dinosaur from the Middle Jurassic of Niger and the early evolution of Sauropoda. *PLoS One* 4: e6924, 6921–6913.
83. Beck RMD, Bininda-Emonds ORP, Cardillo M, Liu F-GR, Purvis A (2006) A higher-level MRP supertree of placental mammals. *BMC Evol Biol* 6: 93.
84. Perelman P, Johnson WE, Roos C, Seuánez HN, Horvath JE, et al. (2011) A molecular phylogeny of living primates. *PLoS Genetics* 7: e1001342.
85. Benton MJ, Donoghue PCJ, Asher RJ (2009) Calibrating and constraining molecular clocks. In: Hedges SB, Kumar S, editors. *The timetree of life*. Oxford: Oxford University Press. pp. 35–86.
86. Müller J, Reisz RR (2005) Four well-constrained calibration points from the vertebrate fossil record for molecular clock estimates. *Bioessays* 27: 1069–1075.
87. Van der Geer A, Lyras G, de Vos J, Dermitzakis M (2010) Evolution of Island Mammals: Adaptation and Extinction of Placental Mammals on Islands.
88. Maddison WP (2006) Pairwise comparisons package for Mesquite, version 1.1. <http://mesquiteproject.org>.
89. Maddison WP, Maddison DR (2011) Mesquite: a modular system for evolutionary analysis. Version 2.75 cd: <http://mesquiteproject.org>.
90. Carter Y, Thomas CDL, Clement JG, Peele AG, Hannah K, et al. (2013) Variation in osteocyte lacunar morphology and density in the human femur - a synchrotron radiation micro-CT study. *Bone* 52: 126–132.
91. Skedros JG, Hunt KJ, Hughes PE, Winet H (2003) Ontogenetic and regional morphologic variations in the turkey ulna diaphysis: implications for functional adaptation of cortical bone. *Anatomical Record Part A* 273A: 609–629.
92. Marotti G, Canè V, Palazzini S, Palumbo C (1990) Structure-function relationships in the osteocyte. *Ital J Miner Electrolyte Metab* 4: 93–106.
93. Remaggi F, Canè V, Palumbo C, Ferretti M (1998) Histomorphometric study on the osteocyte lacuno-canalicular network in animals of different species. I. Woven-fibred and parallel-fibred bones. *Ital J Anat Embryol* 103: 145–155.
94. Fitzhugh HA (1976) Analysis of growth curves and strategies for altering their shape. *Journal of Animal Science* 42: 1036–1051.
95. Berman DS, Henrici AC (2003) Homology of the astragalus and structure and function of the tarsus of diacetyidae. *Journal of Paleontology* 77: 172–188.
96. Rensberger JM, Watabe M (2000) Fine structure of bone in dinosaurs, birds and mammals. *Nature* 406: 619–622.
97. Matsugaki A, Aramoto G, Nakano T (2012) The alignment of MC3T3-E1 osteoblasts on steps of slip traces introduced by dislocation motion. *Biomaterials* 33: 7327–7335.
98. Ishimoto T, Nakano T, Umakoshi Y, Yamamoto M, Tabata Y (2013) Degree of Biological Apatite c-Axis Orientation Rather Than Bone Mineral Density Controls Mechanical Function in Bone Regenerated Using Recombinant Bone Morphogenetic Protein-2. *Journal of Bone and Mineral Research* 28: 1170–1179.
99. Campione NE, Evans DC (2012) A universal scaling relationship between body mass and proximal limb bone dimensions in quadrupedal terrestrial tetrapods. *BMC Biology* 10: 60.
100. Niven J (2007) Brains, islands and evolution: breaking all the rules. *Trends in Ecology and Evolution* 22: 57–59.

Sauropod Necks: Are They Really for Heat Loss?

Donald M. Henderson*

Royal Tyrrell Museum of Palaeontology, Drumheller, Alberta, Canada

Abstract

Three-dimensional digital models of 16 different sauropods were used to examine the scaling relationship between metabolism and surface areas of the whole body, the neck, and the tail in an attempt to see if the necks could have functioned as radiators for the elimination of excess body heat. The sauropod taxa sample ranged in body mass from a 639 kg juvenile *Camarasaurus* to a 25 t adult *Brachiosaurus*. Metabolism was assumed to be directly proportional to body mass raised to the $\frac{3}{4}$ power, and estimates of body mass accounted for the presence of lungs and systems of air sacs in the trunk and neck. Surface areas were determined by decomposing the model surfaces into triangles and their areas being computed by vector methods. It was found that total body surface area was almost isometric with body mass, and that it showed negative allometry when plotted against metabolic rate. In contrast, neck area showed positive allometry when plotted against metabolic rate. Tail area show negative allometry with respect to metabolic rate. The many uncertainties about the biology of sauropods, and the variety of environmental conditions that different species experienced during the groups 150 million years of existence, make it difficult to be absolutely certain about the function of the neck as a radiator. However, the functional combination of the allometric increase of neck area, the systems of air sacs in the neck and trunk, the active control of blood flow between the core and surface of the body, changing skin color, and strategic orientation of the neck with respect to wind, make it plausible that the neck could have functioned as a radiator to avoid over-heating.

Citation: Henderson DM (2013) Sauropod Necks: Are They Really for Heat Loss? PLoS ONE 8(10): e77108. doi:10.1371/journal.pone.0077108

Editor: David C. Evans, Royal Ontario Museum, Canada

Received: March 27, 2013; **Accepted:** September 3, 2013; **Published:** October 30, 2013

Copyright: © 2013 Henderson. This is an open-access article distributed under the terms of the Creative Commons Attribution License, which permits unrestricted use, distribution, and reproduction in any medium, provided the original author and source are credited.

Funding: The author has no support or funding to report.

Competing Interests: The author has declared that no competing interests exist.

* E-mail: don.henderson@gov.ab.ca

Introduction

Metabolic activity results in the production of body heat, and for large animals elimination of excess body heat is an important factor [1]. As the largest land animals known to have existed, sauropods are expected to have been more susceptible to overheating than even the largest extant tropical forms such as elephants [2]. It has been suggested that the exceptionally long necks of sauropods, in addition to being food-gathering adaptations [3,4], may have also functioned as a way of cooling the body by using the external surface area of the neck as a radiator [3,5,6,7]. An alternative suggestion involving the long necks of sauropods for cooling was that the jugular veins and carotid arteries could mutually exchange heat during the transit of blood from body to head, and thus avoid suffusing the brain with excessively warm blood [8]. The hypothesis that sexual selection was the primary driver of the evolution of long necks in sauropods [16] has been challenged by [4], and it will not be dealt with further in this paper.

Sauropods are not alone amongst extinct animals in being suggested to have had a specialized anatomy to deal with excess body heat. The dorsal 'sails' of late Palaeozoic synapsids such as those of *Dimetrodon* and *Edaphosaurus* have been argued to have functioned as radiators [9–12]. Stegosaurian dinosaurs, with their prominent, plate-like osteoderms mounted high on their backs, have also inspired speculations about their ability to lose heat via the extensive vascularization of the plates [13,14]. However, in the case of the synapsids, it has been shown that the sails were more likely to have been for sexual display based on scaling arguments,

and that dorsal sails in small species of *Dimetrodon* would have been ineffective as radiators [15].

There is good evidence that extant animals use the skin as a way to eliminate excess body heat. A well-documented case is the use of the surface of the ears and other body regions in African elephants as radiators [40]. This study found that these regions were highly vascularized, and when examined with infrared thermography, these patches showed elevated temperatures that would encourage heat flow away from the body. They also found that the frequency of use of these high-heat patches increased with increasing environmental temperature and with the size of the animals being observed. An earlier study [41] defined an index for the ability of mammals to use the skin as a radiator. This study found that the ability to eliminate heat via the skin scaled positively with body mass. Both of these studies are relevant to the study of heat loss in sauropods.

With the availability of three-dimensional digital models of various sauropods [17], it is possible to test the idea that the geometry of the necks of these animals may have something to do with the elimination of excess body heat. The hypothesis is that the surface area of the necks, if they really are acting as radiators, should show a correlation with a predicted metabolic rate. When plotted on a log-log plot of the type typically used for analyses of scaling relationships [18], the scaling coefficient (the slope of the regression line) for neck area as a function of metabolism should show a slope of at least 1.0. A slope less than unity would imply that the neck area was not keeping pace with increasing metabolic heat production as body size increased during the evolution of increasingly larger and larger sauropods, and unlikely to be correlated with heat loss.

Materials and Methods

Materials

Three-dimensional digital models of sixteen sauropods were generated using published life restorations that showed the animals in lateral and dorsal views. The taxa modeled and their component masses, body lengths and image sources are listed in Table 1. The shapes of the models were obtained using the three-dimensional slicing method outlined in [19]. As the extent of the neck was the body region of primary interest, it was consistently delineated in all the models. The posterior end of the neck was set at a slice crossing the axial body tangent to the anterior-most point of the illustrated pectoral girdle. The anterior neck limit was set at a slice tangent to the posterior-most point of either the cranium or the mandible, whichever was the most posterior. The extent of the neck on all the models is shown with the dark shading in the cervical region in figures 1, 2 and 3. As a comparative check on the area of the neck relative to the total body surface area, the surface area of the tail was also computed. The posterior limit for a tail was its distal-most tip, while the anterior limit was the slice that was tangent to the most posterior component of the pelvis, either the ischium or the ilium, depending on the species. The extent of the tail is also highlighted in the model figures with a dark shading.

Methods

Body Mass Estimations. Determination of the body masses of the sauropod models requires estimating the volumes of the various body parts and assigning those parts specific density values. Volumes of the axial body and the limbs of the sauropod models were calculated using the three-dimensional mathematical slicing method of [19]. The volumes were then multiplied by particular density values to compute their masses. The selection of density values to use were based on observations of living animals with the limbs and tails being assigned a basic density equal to that of water – 1,000 gm/l. The combination of the evidence for extensive pneumatization of the precaudal sauropod axial skeleton [7,20],

the suggestion that sauropods would have required a respiratory system similar to that of birds [21], and the observation that the air sacs of modern birds occupy about 15% of the trunk volume [22], led to the pelvic and trunk regions having their basic density of 1000 gm/l reduced by 15% to 850 gm/l. The pneumatized neck of a goose was observed to have a density of 300 gm/l [23], and this value was used for the necks and heads of all the models. An additional form of mass reduction was done with the inclusion of a lung cavity within the chest region. Lacking any other objective way of estimating a lung volume for sauropods, the scaling relationship between body mass and lung volume determined for birds [18] was used. See [17,25] for more details on assigning densities to pneumatized bodies.

Metabolic Rate. The main purpose of accurately determining the body masses of the various sauropods was to provide a base for estimating metabolic rate. Following the general rule that basal metabolic rates scales to body mass raised to the $\frac{3}{4}$ power [18], a provisional metabolic rate, assuming a unitary coefficient, was computed for all the models. The coefficient of 1.0 was chosen in light of the controversy about the metabolic rates of dinosaurs in general, and sauropods in particular [6], and the probability that it decreased during ontogeny [26,27]. For the purposes of the present study it is not the actual metabolic rate that is of interest, but how the metabolic exponent, 0.75, compares with the exponent associated with body surface magnitude.

It must be noted that there is mounting evidence that the $\frac{3}{4}$ scaling factor cannot be arbitrarily applied to all animals. Not only might it differ from $\frac{3}{4}$, but that it depends on whether the animal is an ectotherm or an endotherm [42]. For the present study it will be assumed that the sauropods were functional endotherms due to their large body size, and based on the analysis in [42], their metabolic scaling factor would not have exceeded 0.75. See Discussion for the implications of different metabolic scaling factors for the present study.

Surface Area Calculations. The forms of the digital sauropod models make it relatively easy to compute their surface

Table 1. Length, masses and sources for sauropod body models.

	Body Length (m)	Total Body Mass (t)	Axial Mass (t)	Single Leg Mass (kg)	Single Arm Mass (kg)	Image Source	Figure Abbreviation
<i>Apatosaurus louisae</i>	21.8	16.4	13.2	1.27×10^3	302	[30]	A.l
<i>Barosaurus lentus</i>	25.0	15.8	13.7	817	233	[30]	B.l
<i>Brachiosaurus branchai</i> *	25.8	26.3	21.1	1.63×10^3	945	[29]	B.b
<i>Camarasaurus lentus</i> (adult)	15.5	12.3	10.3	724	257	[30]	C.l(a)
<i>Camarasaurus lentus</i> (juvenile)	5.73	0.639	0.560	28.6	11.1	[30]	C.l(j)
<i>Dicraeosaurus hansemani</i>	12.1	4.35	3.73	258	48.0	[30]	D.h
<i>Diplodocus carnegii</i>	24.9	11.9	9.97	829	159	[30]	D.c
<i>Haplocanthosaurus priscus</i>	15.0	13.5	11.4	905	166	[30]	H.p
<i>Jobaria tiguidensis</i>	18.2	22.4	18.7	1.40×10^3	449	[24]	J.t
<i>Mamenchisaurus hochuanensis</i>	20.6	12.8	11.4	453	228	[30]	M.h
<i>Mamenchisaurus youngi</i>	16.1	5.36	4.36	335	169	[30]	M.y
<i>Nigersaurus taqueti</i>	14.1	3.64	3.09	326	105	[39]	N.t
<i>Omeisaurus junghsiensis</i>	18.3	6.73	5.73	364	138	[30]	O.j
<i>Patagosaurus fariasi</i>	16.5	7.88	6.89	344	150	[30]	P.f
<i>Saltasaurus loricatus</i>	12.8	6.87	5.63	438	182	[30]	S.l
<i>Shunosaurus lii</i>	9.02	2.16	1.68	173	67.0	[30]	S.li

*Tail extended relative to published illustration based on other sauropod tail and body proportions [17].

doi:10.1371/journal.pone.0077108.t001

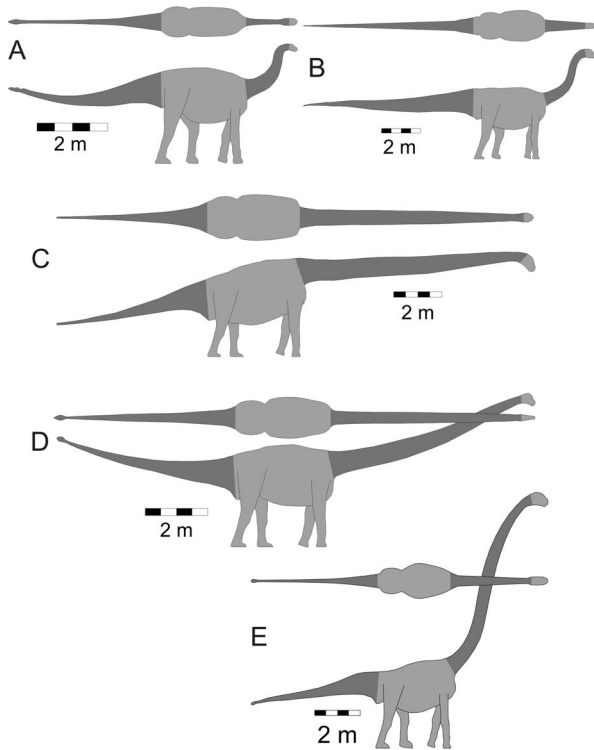


Figure 1. Basal sauropodomorphs. Isometric dorsal and lateral views of the taxa used in the present study. The extent of the neck analyzed for surface area is highlighted with the dark grey colour on each model view. (A) *Shunosaurus lii*. (B) *Patagosaurus fariasi*. (C) *Mamenchisaurus hochuanensis*. (D) *Mamenchisaurus youngi*. (E) *Omeisaurus junghsiensis*. See Table 1 for sources used to generate the models.

doi:10.1371/journal.pone.0077108.g001

areas. The three-dimensional mathematical slicing method used to define a body shape uses ellipses to represent the slices which are transverse sections of the limbs and axial body. These ellipses are further decomposed into discrete sets of points with the same number of points used for all the slices used to define a particular body region. The homologous points on adjacent slices can be linked together and this results in the surface of the body region being decomposed into a set of quadrilateral facets. The full quadrilaterally tessellated surface of the model of *Brachiosaurus* is shown in figure 4A.

The total external area of a limb or axial body is determined by summing the areas of all the component polygons. To compute the area of a polygon each one is divided diagonally into two triangles, and the two sides of each triangle are represented by vectors. (figure 4B). For the n^{th} polygon the vector pair \vec{v}_0^n and \vec{v}_1^n define two sides of the first triangle, while \vec{v}_2^n and \vec{v}_3^n define two sides of the second triangle, and the expression to compute the total surface area of a model component, A_{compo} , is:

$$A_{\text{compo}} = \frac{1}{2} \sum_{n=0}^{P-1} \left\{ \left\| \vec{v}_0^n \times \vec{v}_1^n \right\| + \left\| \vec{v}_2^n \times \vec{v}_3^n \right\| \right\} \quad (1)$$

where \vec{v}_0^n , \vec{v}_1^n , \vec{v}_2^n and \vec{v}_3^n are the vectors defined between, respectively, the first and second, first and fourth, third and fourth, and third and second perimeter points on the n^{th} polygon, and P is the number of polygons comprising the model component. This

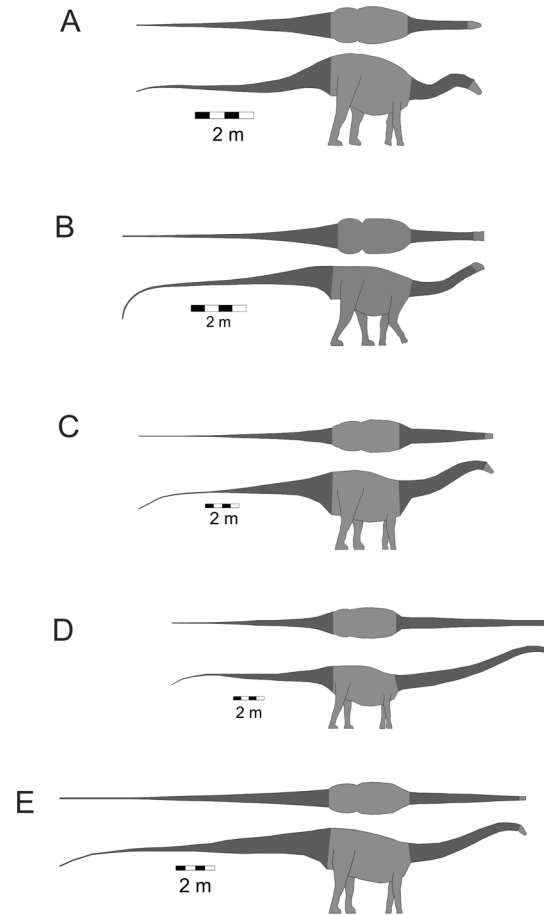


Figure 2. Diplodocoid sauropodomorphs. Isometric dorsal and lateral views of the taxa used in the present study. (A) *Dicraeosaurus hansemani*. (B) *Nigersaurus taqueti*. (C) *Apatosaurus louisae*. (D) *Barosaurus lentus*. (E) *Diplodocus carnegii*. Details as per Figure 1.

doi:10.1371/journal.pone.0077108.g002

expression computes the vector cross-products of the respective vector pairs defining the two triangles to get the areas of the parallelograms spanned by the vector pairs, determines and sums the magnitudes of the two areas, and then divides this result by two as we only need the area of the triangles, not the full parallelograms. Using the two planar triangles to approximate the surface area of the curved quadrilateral surface results in an average underestimate of approximately 0.6%.

Results

The computed total and regional surface areas for all the models are summarized in Table 2. Figure 5 shows total surface area plotted against body mass with a slope of 0.6769 and a very strong correlation coefficient of 0.9944. Surprisingly, the slope of the regression is very close to that expected if the animals increased their size isometrically where the expected slope would be 2/3 (0.66666...) [18]. The fact that the slope is greater than 2/3 indicates that surface area does increase slightly faster than body mass.

Figure 6 shows total surface area plotted against the assumed metabolic rate. The slope can now be seen to be greater than that predicted from isometry, but is still less than 1.0, implying that body heat production might exceed the ability of the body to eliminate it, leading to overheating. However, this ignores internal

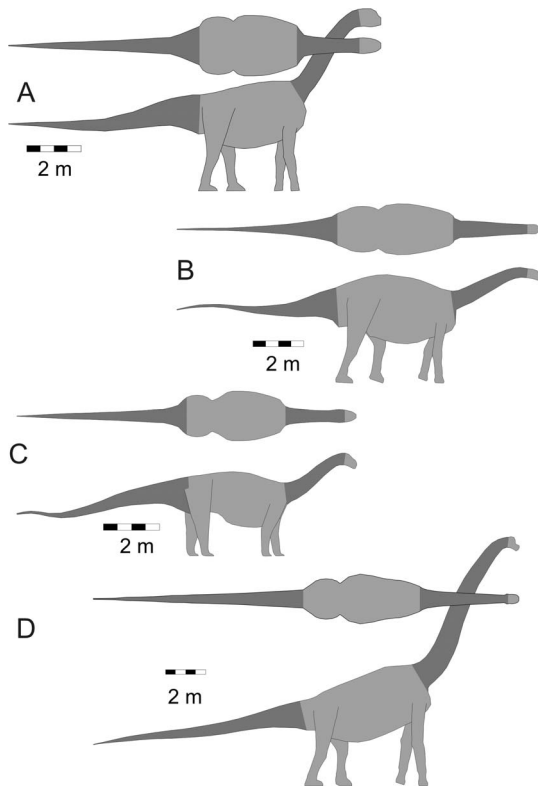


Figure 3. Macronarian sauropodomorphs. Isometric dorsal and lateral views of the taxa used in the present study. *Jobaria tiguidensis* is not shown for space reasons. (A) *Camarasaurus lentus*. (B) *Haplocanthosaurus priscus*. (C) *Saltasaurus loricatus*. (D) *Brachiosaurus brancai*. Details as per Figure 1. doi:10.1371/journal.pone.0077108.g003

blood circulation and the ability of animals to control the flow of heat from the body core to the surface [6].

Figure 7 shows neck surface area plotted against metabolic rate. The computed slope, 1.1664, is now greater than 1.0. It is clear that while the increase in overall body surface area lags behind that of metabolic rate, the neck area shows a positively allometric size increase. This suggests that the neck may have a special role in the elimination of body heat. Those sauropods with noticeable short necks relative to body size – *Shunosaurus*, *Nigersaurus*, *Dicraeosaurus*, *Saltasaurus*, *Patagosaurus*, and *Haplocanthosaurus* do lie below the computed regression line, but closely parallel it. This indicates that a similar scaling factor applies to these taxa, but with a smaller Y-intercept.

The other elongate structure projecting from the body of a sauropod is the tail, and it was felt that a comparison of tail surface area scaling with that of the neck might be informative. Figure 8 shows the surface area of the tail plotted against metabolic rate. The slope of the regression, 0.8198, is less than that for both the neck and the body as a whole. This would seem to indicate that the tail is either not specially adapted for eliminating excess body heat, or that its role in heat loss was a passive one.

Discussion

The present study lumps together 14 genera of which only six were sympatric, the others existed at different times and on different continents. This lumping combines animals that would have experienced different climates with different diurnal and

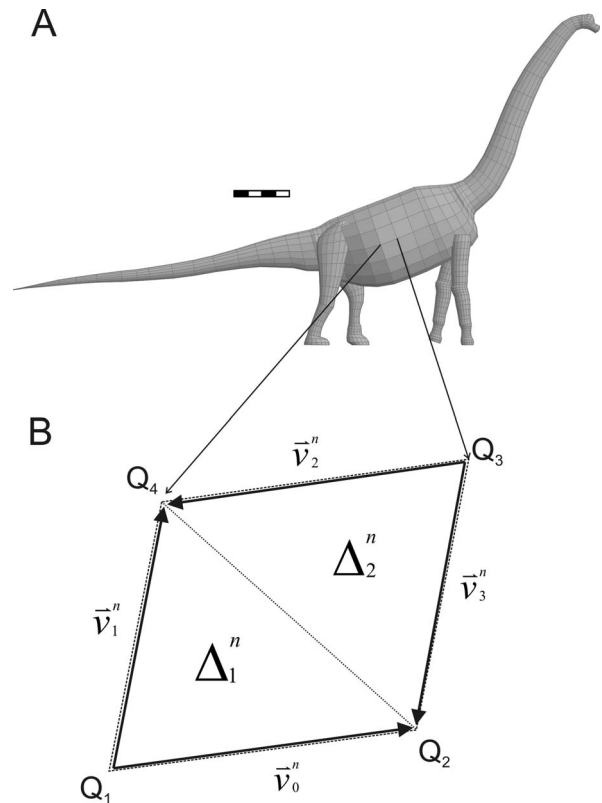


Figure 4. Determining external surface area. (A) *Brachiosaurus* model showing the quadrilateral tessellation used to compute the surface area of the model. The scale bar is 2 m. (B) Decomposition of the n^{th} body surface quadrilateral into two sub-triangles Δ_1^n and Δ_2^n . Q_1 , Q_2 , Q_3 and Q_4 are the four points defining the vertices of the quadrilateral. The edges of the triangles are represented by vectors between the vertices. One half of the magnitude of the vector cross-product of a pair of co-terminal vectors, eg. \vec{v}_0^n and \vec{v}_1^n , gives the area of the triangle Δ_1^n . See Methods: Surface Area Calculations for more detail. doi:10.1371/journal.pone.0077108.g004

seasonal temperature changes, possibly obscuring any anatomically significant patterns related to the dissipation of excess body heat. The sympatric six are those specimens from the Late Jurassic Morrison Formation. *Apatosaurus*, *Camarasaurus* and *Diplodocus* are commonly found in close temporal association [28]. Less frequently, these three genera are variably associated with *Barosaurus*, *Brachiosaurus* and *Haplocanthosaurus* at different levels in the Morrison Formation [28]. However, in an attempt to explain the peculiar anatomy of sauropods as it relates to their control of body temperature, it was felt that it was best to combine all the taxa to have as large a sample size as possible. The results and inferences derived from this study must be taken as preliminary as new discoveries will add to our knowledge of the group.

The evidence that there is no one single metabolic scaling factor of 0.75 for all animals, and that it was most likely less than 0.75 for endotherms [42], increases the contrast between it and the neck area scaling factor of 1.17 identified for sauropods. This probable increased contrast implies an even greater ability in these animals to eliminate excess body heat via the neck. The findings that metabolic scaling varies between different groups of terrestrial vertebrates [43], suggests that different types of sauropods, living at different times and places all over the world, may have had different metabolic scaling factors. This sort of unknown, but likely

Table 2. Sauropod model surface areas. All areas measured in square metres.

	Total	Axial Body	Single Leg	Single Arm	Neck	Tail
<i>Apatosaurus louisae</i>	78.2	53.8	9.04	3.15	16.5	4.75
<i>Barosaurus lentus</i>	75.2	56.4	6.57	2.83	19.5	3.94
<i>Brachiosaurus branchai</i>	114	79.2	10.7	7.12	21.5	16.5
<i>Camarasaurus lentus</i> (adult)	60.8	42.2	6.36	2.97	9.49	11.8
<i>Camarasaurus lentus</i> (juvenile)	8.15	5.65	0.860	0.389	1.03	1.56
<i>Dicraeosaurus hansemanni</i>	29.8	20.9	3.39	1.03	3.33	6.92
<i>Diplodocus carnegii</i>	67.8	50.6	6.55	2.06	9.96	19.3
<i>Haplocanthosaurus priscus</i>	60.3	40.5	7.51	2.39	7.28	8.68
<i>Jobaria tiguidensis</i>	89.7	60.5	9.99	4.57	14.5	14.2
<i>Mamenchisaurus hochuanensis</i>	66.2	51.2	4.63	2.88	18.9	10.0
<i>Mamenchisaurus youngi</i>	40.7	28.4	3.79	2.36	8.94	6.88
<i>Nigersaurus taqueti</i>	30.6	19.9	3.66	1.69	3.23	6.51
<i>Omeisaurus junghsiensis</i>	46.9	33.9	4.34	2.19	12.3	6.69
<i>Patagosaurus fariasi</i>	47.9	34.8	4.36	2.22	5.28	12.6
<i>Saltasaurus loricatus</i>	41.0	27.7	4.32	2.37	4.45	8.23
<i>Shunosaurus lii</i>	20.8	13.1	2.62	1.23	1.67	4.17

doi:10.1371/journal.pone.0077108.t002

variability, means that the findings of this study must be seen as preliminary. However, the existence of variable metabolic scaling does not invalidate the basic finding of the present study.

It has been suggested that the overall attenuated body shape of sauropods with a long thin tail and neck was a sign that they were trying to maximize surface area to avoid overheating. From the present analysis it would seem to not be the case. The finding that surface area scales almost isometrically with body mass in the present sample of sauropods (Fig. 5) may be a true biological signal, or it may be an artifact of the restorations. Most of the illustrations used to generate the models were done by [29,30]

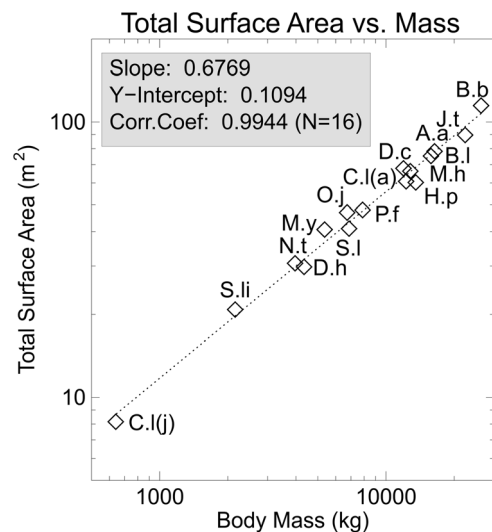


Figure 5. Surface area versus body mass. Log-log plot of total external body surface area plotted against total body mass for all the sauropod models. Note that the slope of the fitted regression line is close to that predicted for isometric size increase – 0.67. See Table 1 for taxa abbreviations.

doi:10.1371/journal.pone.0077108.g005

(Table 1). Given that most sauropods are known from incomplete material [31], there may be a stylistic influence that results in isometric restorations. However, the morphological conservatism of the basic sauropod body plan [31], could be used as an argument that the near-isometric scaling observed is genuine. It has been observed that the expression for surface area (SA) as a function of body mass (M) in vertebrates, $SA = kM^{0.67}$, the value of 'k' typically ranges between 9 and 11 [32], with 10 being an acceptable compromise when mass is measured in kilograms and area measured in decimeters [18]. Converting the square meters

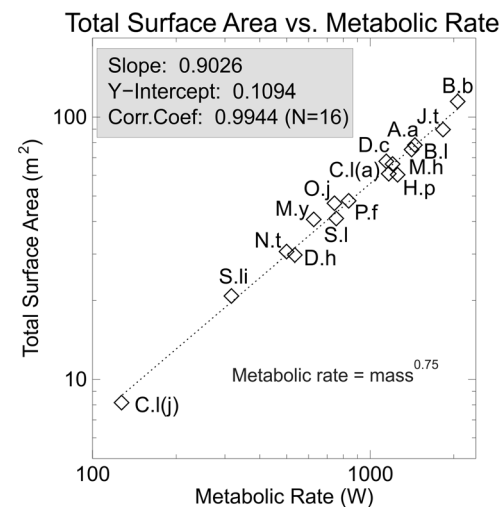


Figure 6. Surface area versus metabolic rate. Log-log plot of total external body surface area plotted against a dimensionless metabolic rate proportional to body mass raised to the $\frac{3}{4}$ power. Note that the fitted regression line is less than 1.0 implying that surface area will lag behind metabolic heat production with phylogenetic size increase. This could lead to overheating due to reduced relative surface area available to radiate excess heat.

doi:10.1371/journal.pone.0077108.g006

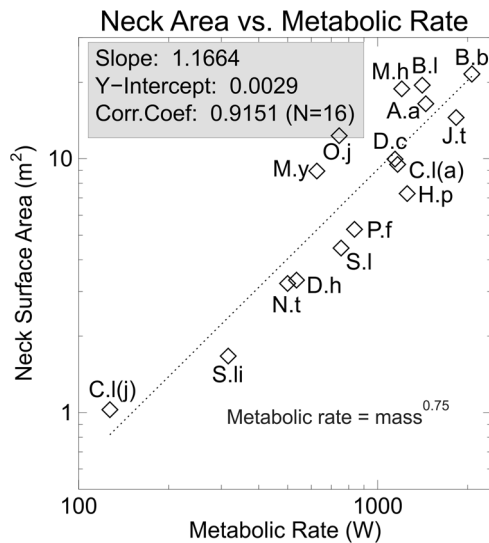


Figure 7. Neck area versus metabolic rate. Log-log plot of neck surface area versus a dimensionless metabolic rate. The scaling exponent is greater than 1.0 implying that neck area increases faster than expected if the animals increased neck size isometrically. The increased neck area could function as a radiator to eliminate excess body heat. doi:10.1371/journal.pone.0077108.g007

used in the present study to decimeters means changing the ‘k’ value (“Y-Intercept” of Fig. 5) from 0.1094 to 10.94, a value similar to that seen in much smaller extant vertebrates.

With the discovery of dermal spines running along the dorsal midline of the body of *Diplodocus* [44], there is the possibility that the dermal spines themselves could have contributed to increasing the surface area of the animal and further enhancing heat loss. As a test of this idea, a diplodocid model with a full set of dermal spines was generated using the configuration shown in [44]. The tallest of these spines was set to 40 cm, and the heights of the

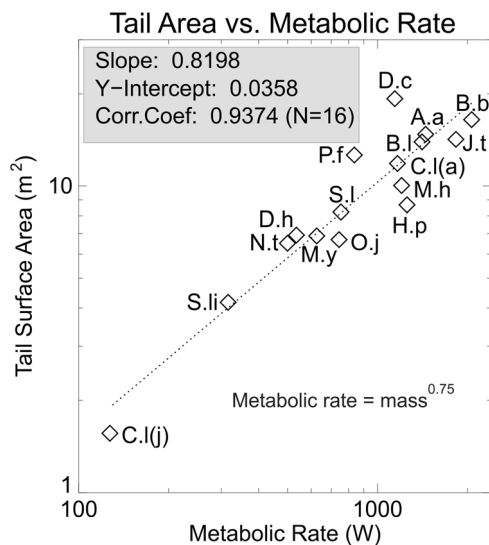


Figure 8. Tail area versus metabolic rate. Log-log plot of tail surface area versus a dimensionless metabolic rate. The scaling exponent is less than 1.0 implying that the tail alone would not be effective in dumping excess body heat. doi:10.1371/journal.pone.0077108.g008

others were set as a sine function of the position of the dermal spine along one of the three body segments – tail, trunk, neck – with the tallest always being in the middle of the body segment. (Fig. 9A). Representing this 40 cm tall spine as a three-dimensional mesh with a narrow elliptical cross-section (Fig. 9B), its total lateral surface area is 855 cm². For the sets of dermal spines along the tail, trunk and neck body segments their combined areas are 4.55 m², 1.38 m² and 2.20 m², respectively, and the total spine area is 7.94 m². The total surface area of the axial body and limbs of the *Diplodocus* model is 67.8 m², so the full dermal spine area represents 11.7% of the body area. If these spines were vascularized then they would have a significant potential to act as radiators. However, there is a great deal of uncertainty about the size, internal structure, and distribution of these spines on the body. Until better fossil material becomes available, the importance of any dermal spines for heat loss in sauropods will have to remain speculative.

It appears to be generally accepted that the long necks of sauropods were food gathering organs that allowed the animal to stand in one place, thus minimizing the energetic cost of movement, while exploiting the large volume of foliage that would be within reach [4,33]. A larger animal needs more food, so it might be expected that a larger animal would have a longer neck. Figure 10 plots neck length against body mass. As can be seen, there is a weak trend for neck length to decrease relative to body mass. However, there is a great deal of scatter in the data as indicated by the low correlation coefficient. Absolute neck length does not follow the same trend as neck area. This scattered plot appears to be a result of lumping diverse group of animals together.

Although morphologically conservative, sauropods were a diverse group of dinosaurs with approximately 200 named species whose remains are found on all continents, and inhabited a variety of environments [34]. As well as having a wide geographic extent, the group also existed for a long time, from the Late Triassic to the end of the Cretaceous, a period of approximately 150 million years. The combination of long duration and wide dispersal means

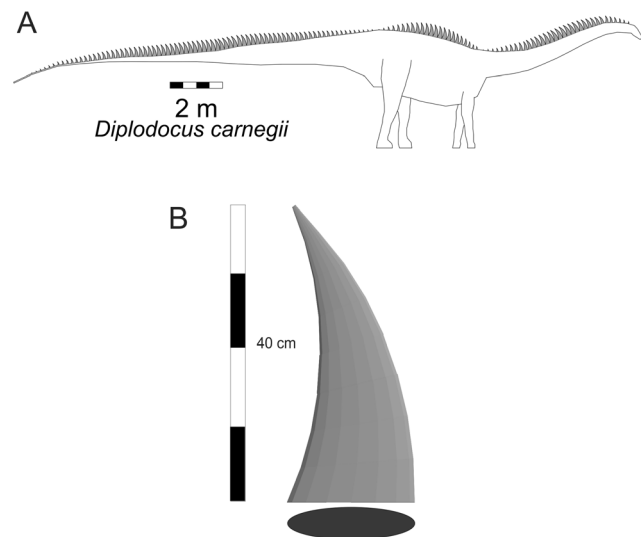


Figure 9. Neck length versus body mass. Log-log plot of absolute neck length plotted against body mass. The great deal of scatter, as indicated by the low correlation coefficient, highlights the variety of neck lengths exhibited by sauropods, and makes it difficult to make broad generalizations about neck function in these animals. doi:10.1371/journal.pone.0077108.g009

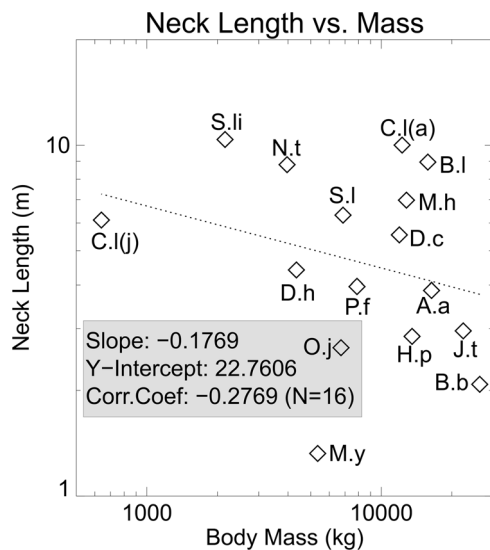


Figure 10. *Diplodocus* with dermal spines. Alternate model with sets of dermal spines running along the dorsal midline of the body. The tallest spine in each of the tail, trunk and neck is 40 cm tall. Size and arrangement of the spines is based on [44]. doi:10.1371/journal.pone.0077108.g010

that these animals must have experienced a diversity of vegetation types that could be exploited as a food source [35]. As can be seen from the few complete skulls known for these animals, they had diverse skull shapes and dentitions [36], with the inference that there was diversity not only in body size, but also in feeding styles and foods eaten. The poor correlation of neck length with body mass might be a reflection of the diversity of feeding strategies used by sauropods. Neck length is intimately associated with the total area of the neck. This diversity of neck lengths makes it difficult to summarize the contribution of the neck to possible cooling strategies used by sauropods.

The thermal environment of any animal is complex with various sources and sinks of heat [6,37], and these will affect how an animal is able to control its body temperature. For elimination of body heat there is evaporative, convective, conductive, and radiative cooling. For sauropods living in semi-arid landscapes such as that recorded by the Morrison Formation [28], water conservation may have been a key concern, thus limiting the potential for evaporative cooling. At large body size the ability of animals to use convective means to eliminate excess heat is reduced due to the thickening of the thermal boundary layer around the body with increasing size [6]. The limited degree of contact with the ground through their feet would have made conductive cooling unlikely in sauropods. However, the capacity for radiative heat loss does not diminish with large body size [6], and the relative increase in neck area with increasing size suggests that sauropods could have been using this method to avoid overheating. Additionally, it has been shown that heat exchangers such as the long limbs of sauropods, or the frills of ceratopsians, are much more effective at large body size [6]. These authors also suggested that the necks of sauropods could be effective radiators. The effectiveness of necks as a radiator will depend on the external temperature and infrared thermal radiation from the environment in which their sauropod owners inhabit [6]. These aspects of the physical environment for extinct sauropods are almost impossible to quantify, and they would not be the same for all sauropods as they lived in different climates at different times in Earth history.

Again, this uncertainty makes it difficult to claim with absolute confidence that the necks functioned as cooling structures, but does not render the idea implausible.

The above discussion has tacitly assumed that heat loss would be passive, with conduction from the core of the body to the external surface being the only mechanism. However, it is well known that animals such as crocodylians are able to increase and decrease the flow of blood between the core and surface of the body to affect heating and cooling rates [14], and birds are able to increase breathing rates to effect elimination of excess body heat (“panting”) [38]. There is also the ability of lizards to change their skin color from light to dark to improve their ability to absorb the warmth of the sun, with the converse being that a lighter colored skin will absorb less infrared radiation and slow the rate of heating. The cervical vertebrae of most sauropods show deep pleurocoels on the sides of their centra, and well-developed systems of airways within the centra (pneumatization), and it is hypothesized that sauropods could have used physiological mechanisms similar to those of birds to facilitate cooling of the body [7]. The scaling exponent for the relationship between whole body surface area and metabolic rate for the sauropod sample is less than 1.0. However, neck area alone has a scaling exponent greater than 1.0. This could be interpreted as showing that the neck is a specialized organ for the elimination of body heat in sauropods. The combined effects of increased neck surface area for radiative heat loss; the elaborate system of air sacs intimately associated with the core of the body; a second system of air sacs in the neck in close association with the blood vascular system of the neck, and close to the external neck surface; and the possibility of changes in neck skin color could all contribute to making the neck a highly effective structure for the elimination of excess body heat. Lastly, modeling studies [6] have shown that increased wind speeds would have a significant cooling effect on large dinosaurs. Properly orienting the sauropod neck with respect to the wind would maximize the ability of the moving air to reduce the thermal boundary layer and further improve heat loss.

Conclusions

The suggestion that the necks of sauropods functioned as cooling structures has not been rejected by the present study. A positive allometric trend with a scaling exponent of 1.1664 for neck surface area to increase with increasing metabolic rate is considered to be an important indicator that the neck was capable of being a radiator. In combination with a system of thoracic and cervical air sacs, and active control of blood flow from the internal regions of the body to the surface, the neck would have made an effective heat loss structure. The effectiveness of a cooling mechanisms such as convection would be reduced for sauropods on account of their immense size. Similarly, evaporative cooling would seem unlikely given their apparent preference for dry habitats. Their unique anatomy, extreme body size, and lack of living descendants make sauropods difficult to interpret as living organisms. However, observations of analogous structures and cooling functions in living relatives such as birds and crocodiles enables plausible interpretations of aspects of sauropod thermal biology.

Author Contributions

Conceived and designed the experiments: DMH. Performed the experiments: DMH. Analyzed the data: DMH. Contributed reagents/materials/analysis tools: DMH. Wrote the paper: DMH.

References

- Alexander RM (1998) All-time giants: the largest animals and their problems. *Palaentology* 41: 1231–1245.
- Wright PG (1984) Why do elephants flap their ears? *South African Journal of Zoology* 19: 266–269.
- Sander PM, Christian A, Clauss M, Fechner R, Gee CT, et al. (2010) Biology of the sauropod dinosaurs: the evolution of gigantism. *Biological Reviews* 86: 117–155.
- Taylor MP, Hone DWE, Wedel MJ, Naish D (2011) The long necks of sauropods did not evolve primarily through sexual selection. *Journal of Zoological Society London* 285: 150–161.
- Bakker RT (1971) Dinosaur physiology and the origin of mammals. *Evolution* 25: 636–658.
- O'Connor MP, Dodson P (1999) Biophysical constraints on the thermal ecology of dinosaurs. *Paleobiology* 25:341–368.
- Wedel MJ (2003) Vertebral pneumaticity, air sacs, and the physiology of sauropod dinosaurs. *Paleobiology* 29: 243–255.
- Wheeler PE (1978) Elaborate CNS cooling structures in large dinosaurs. *Nature* 275: 441–443.
- Bramwell CD, Fellgett PB (1973) Thermal regulation in sail lizards. *Nature* 242: 203–205.
- Bennett SC (1996) Aerodynamics and thermoregulatory function of the dorsal sail of the *Edaphosaurus*. *Paleobiology* 22: 496–506.
- Haack SC (1986) A thermal model of the sailback pelycosaur. *Paleobiology* 21: 450–458.
- Romer AS, Price LI (1940) Review of the Pelycosauria. *Geological Society of America Special Paper* 28: 1–538.
- Farlow JO, Thompson CV, Rosner DE (1976) Plates of the dinosaur *Stegosaurus*: forced convection heat loss fins? *Science* 192: 1123–1125.
- Farlow JO, Hayashi S, Tattersall GJ (2010) Internal vascularity of the dermal plates of *Stegosaurus* (Ornithischia, Thyreophora). *Swiss Journal of Geosciences* 103: 173–185.
- Tomkins JL, LeBas NR, Witton MP, Martill DM, Humphries S (2010) Positive allometry and the prehistory of sexual selection. *The American Naturalist* 176: 1–9.
- Senter P (2006) Necks for sex: sexual selection as an explanation for sauropod dinosaur neck elongation. *Journal of Zoological Society London* 271: 45–53.
- Henderson DM (2006) Burlly gaits: centers of mass, stability, and the trackways of sauropod dinosaurs. *Journal of Vertebrate Paleontology* 26: 907–921.
- Schmidt-Nielsen K (1984) *Scaling: why is animal size so important*. Cambridge University Press, Cambridge, 241p.
- Henderson DM (1999) Estimating the mass and centers of mass of extinct animals by 3D mathematical slicing. *Paleobiology* 25: 88–106.
- Wedel MJ (2007) What pneumaticity tells us about 'prosauropods', and vice versa. *Special Papers in Paleontology* 77: 207–222.
- Daniels CB, Pratt J (1992) Breathing in long necked dinosaurs; did the sauropods have bird lungs? *Comp Biochem Physiol* 101A: 43–46.
- Proctor NS, Lynch PJ (1993) *Manual of ornithology*. Yale University Press, New Haven.
- Bramwell CB, Whitfield GR (1974) *Biomechanics of Pteranodon*. Philosophical Transactions of the Royal Society, Series B 267: 503–581
- Sereno PC, Beck AL, Dutheil DB, Larsson HCE, Lyon GH et al. (1999) Cretaceous sauropods from the Sahara, and the uneven rate of skeletal evolution among dinosaurs. *Science* 286: 1342–1347.
- Henderson DM (2010) Pterosaur body mass estimates from three-dimensional mathematical slicing. *Journal of Vertebrate Paleontology* 30: 768–785.
- Perry S, Christian A, Breuer T, Pajor N, and Codd J (2009) Implications of an avian-style respiratory system for gigantism in sauropod dinosaurs. *Journal of Experimental Zoology, Part A: Ecological Genetics and Physiology* 14: 115–114.
- Farlow JO (1990) Dinosaur energetic and thermal biology. In: Weishampel DB, Dodson P, Osmolska H editors. *The Dinosauria*, pp 43–55. University of California Press, Berkeley.
- Dodson P, Behremsmeyer AK, Bakker RT, McIntosh JS (1980) Taphonomy and paleoecology of the dinosaur beds of the Jurassic Morrison Formation. *Paleobiology* 6: 208–232.
- Paul GS (1987). The science and art of restoring the life appearance of dinosaurs and their relatives: a rigorous how-to guide. In: Czerkas SJ, Olson EC editors. *Dinosaurs Past and Present Volume II*. pp. 5–49, Natural History Museum of Los Angeles County and University of Washington Press, Seattle.
- Paul GS (1997) Dinosaur models: the good, the bad, and using them to estimate the mass of dinosaurs. *Dinofest International Proceedings*: 129–154.
- Upchurch P, Barrett PM, Dodson P (2004) Sauropoda. In: Weishampel DB, Dodson P, Osmolska H editors. *The Dinosauria 2nd edition*, pp 259–322. University of California Press, Berkeley.
- Benedict FG (1934) Die Oberflächenbestimmung verschiedener Tiergattungen. *Ergeb. Physiologie* 36: 300–346.
- Preuschoft H, Hohn B, Stoinski S, Witzel U (2011) Why so huge? Biomechanical reasons for the acquisition of large size in sauropod and theropod dinosaurs. In: Klein N, Remes K, Gee CT, Sander PM editors. *Biology of the Sauropod Dinosaurs*. pp 197–218. Indiana University Press, Bloomington
- Mannion PD, Upchurch P (2010) A quantitative analysis of environmental associations in sauropod dinosaurs. *Paleobiology* 36: 253–282.
- Gee CT (2010) Dietary options for the sauropod dinosaurs from an integrated botanical and paleobotanical perspective. In: Klein N, Remes K, Gee CT, Sander PM editors. *Biology of the Sauropod Dinosaurs*. pp 34–56. Indiana University Press, Bloomington
- Barrett PM, Upchurch P (2005) Sauropod diversity through time: possible macroevolutionary and palaeoecological implications. In: Curry-Rogers KA, Wilson J editors. *The Sauropods: Evolution and Paleobiology*. pp 125–156. University of California Press, Berkeley.
- Pough FH, Janis CM, Heiser JB (1999) *Vertebrate Life 5th edition*. Prentice Hall, Upper Saddle River, New Jersey, 733p.
- Schmidt-Nielsen K, Kanwisher J, Lasiewski RC, Cohn JE, Bretz WL (1969) Temperature regulation and respiration in the ostrich. *Condor* 71: 341–352
- Sereno PC, Wilson JA, Witmer LM, Whitlock JA, Maga A, et al. (2007) Structural extremes in a Cretaceous dinosaur. *PLoS ONE* 2: e1230.
- Weissenböck NM, Weiss CM, Schwammer HM, Kratochvil H (2010) Thermal windows on the body surface of African elephants (*Loxodonta africana*) studied by infrared thermography. *Journal of Thermal Biology* 35: 182–188.
- Phillips PK, Heath JE (1995) Dependency of surface temperature regulation on the body size of terrestrial mammals. *Journal of Thermal Biology* 20: 281–289.
- White CR, Cassey P, Blackburn TM (2007) Allometric exponents do not support a universal metabolic allometry. *Ecology* 88: 315–323.
- Nagy KA (2005) Field metabolic rate and body size. *Journal of Experimental Biology* 208: 1621–1625.
- Czerkas SA (1992) Discovery of dermal spines reveals a new look for sauropod dinosaurs. *Geology* 20: 1068–1070.

Body Temperatures in Dinosaurs: What Can Growth Curves Tell Us?

Eva Maria Griebeler*

Department of Ecology, Zoological Institute, University of Mainz, Mainz, Germany

Abstract

To estimate the body temperature (BT) of seven dinosaurs Gillooly et al. (2006) used an equation that predicts BT from the body mass and maximum growth rate (MGR) with the latter preserved in ontogenetic growth trajectories (BT-equation). The results of these authors evidence inertial homeothermy in Dinosauria and suggest that, due to overheating, the maximum body size in Dinosauria was ultimately limited by BT. In this paper, I revisit this hypothesis of Gillooly et al. (2006). I first studied whether BTs derived from the BT-equation of today's crocodiles, birds and mammals are consistent with core temperatures of animals. Second, I applied the BT-equation to a larger number of dinosaurs than Gillooly et al. (2006) did. In particular, I estimated BT of *Archaeopteryx* (from two MGRs), ornithischians (two), theropods (three), prosauropods (three), and sauropods (nine). For extant species, the BT value estimated from the BT-equation was a poor estimate of an animal's core temperature. For birds, BT was always strongly overestimated and for crocodiles underestimated; for mammals the accuracy of BT was moderate. I argue that taxon-specific differences in the scaling of MGR (intercept and exponent of the regression line, log-log-transformed) and in the parameterization of the Arrhenius model both used in the BT-equation as well as ecological and evolutionary adaptations of species cause these inaccuracies. Irrespective of the found inaccuracy of BTs estimated from the BT-equation and contrary to the results of Gillooly et al. (2006) I found no increase in BT with increasing body mass across all dinosaurs (Sauropodomorpha, Sauropoda) studied. This observation questions that, due to overheating, the maximum size in Dinosauria was ultimately limited by BT. However, the general high inaccuracy of dinosaurian BTs derived from the BT-equation makes a reliable test of whether body size in dinosaurs was ultimately limited by overheating impossible.

Citation: Griebeler EM (2013) Body Temperatures in Dinosaurs: What Can Growth Curves Tell Us? PLoS ONE 8(10): e74317. doi:10.1371/journal.pone.0074317

Editor: Andrew A. Farke, Raymond M. Alf Museum of Paleontology, United States of America

Received: April 26, 2013; **Accepted:** July 23, 2013; **Published:** October 30, 2013

Copyright: © 2013 Eva Maria Griebeler. This is an open-access article distributed under the terms of the Creative Commons Attribution License, which permits unrestricted use, distribution, and reproduction in any medium, provided the original author and source are credited.

Funding: The author's research was generously funded by the Deutsche Forschungsgemeinschaft (GR2625/2-1, GR2625/2-2). The funders had no role in study design, data collection and analysis, decision to publish, or preparation of the manuscript.

Competing Interests: The author has declared that no competing interests exist.

* E-mail: em.griebeler@uni-mainz.de

Introduction

The thermal physiology of dinosaurs has long been a topic of interest and is still intensively discussed [1–7]. The debate mainly focuses on the question whether dinosaurs were endotherms or ectotherms [3]. As in extant species, the process of thermoregulation is very complex; this endotherm/ectotherm dichotomy seems to be too simplistic [3,8].

Endotherms, such as today's mammals and birds make use of an internal heat source. They show high body temperatures that are relatively constant. The rather constant core temperature of endothermic animals comes at a metabolic cost [9–11], which is particularly significant in very small individuals [12] and in those living in environments with temperatures strongly deviating from their preferred body temperature [13]. When ambient temperatures are much higher (e.g. in deserts) or lower (e.g. at higher latitudes or altitudes) than the preferred core temperature, an endothermic animal has a higher field energy expenditure per mass unit than under ambient temperatures close to its core temperature. Diurnal or seasonal torpor, hibernation (throughout winter), and estivation (throughout summer) are states where individuals become relatively inactive and cease feeding to spare their food reserves [12]. Alternatively, migration to more thermally favourable habitats is a good option (e.g. birds in temperate and higher latitudes migrate to subtropical and tropical

regions in the winter) when metabolic costs of endothermy become too high [13].

In extant ectotherms, the main source of internal heat in animals comes from the environment. Animals can thermoregulate behaviourally by exploiting different thermal microhabitats [12,13]. Basking in the sun or cooling in water is the most typical thermal behaviour seen in reptiles [14]. Winter torpor of reptiles is described as hibernation and is found in seasonal climates at moderate and high latitudes. In addition, many reptiles can, to some extent, adapt physiologically to changing temperatures [15]. Phenotypic changes in response to variation in environmental conditions (acclimatisation) can be facilitated by the number of mitochondria in cells [16], different metabolic isozymes [17–19], and regulation of transcription and expression of enzymes [20–22]. Migration to more favourable habitats is also an option for ectothermic animals to escape seasonal adverse environmental conditions [13].

Since the surface-to-volume ratio decreases with increasing body mass, the “inertial homeothermy hypothesis” under an ectothermic thermoregulation model has been suggested for large dinosaurs [1,2]. Large dinosaurs maintained higher, more constant body temperatures than smaller-sized reptiles, because large ectothermic animals heat up and cool down slower than smaller ectothermic animals (= gigantothermy). In other words,

the body temperature of a dinosaur increases and body temperature fluctuations decrease with increasing body mass because of a decreasing surface-to-volume ratio with increasing body mass [3].

To test the inertial homeothermy hypothesis, Seebacher [3] developed a biophysical model that was calibrated with field data from eleven free-ranging crocodiles (*Crocodylus porosus*, [23]) and successfully validated on two other free-ranging crocodiles [24]. The body temperature of the crocodiles was measured with calibrated temperature-sensitive radio transmitters that animals of different masses swallowed and retained as pseudogastroliths in their stomachs. Body temperatures of the crocodiles were sampled during the whole day as well as during one summer and winter month to capture diurnal and seasonal variability. The biophysical model derived by Seebacher [3] predicted for crocodiles an increase in body temperature and decreasing fluctuations in body temperature with increasing body mass as expected under the inertial homeothermy hypothesis.

McNab [5] proposed a hypothesis on the limitation of dinosaurian metabolism and thus indirectly on the body temperature of dinosaurs, especially in large Theropoda and Sauropoda. The maximum size of vertebrates is determined by resource abundance and how it is used by a species. Assuming that the food intake of the largest herbivorous mammals defines the maximal rate at which terrestrial plant resources can be consumed, he demonstrated that the large size of sauropods is consistent with a field energy expenditure extrapolated from extant varanid lizards (corroborating Seebacher [3]). Analogously, assuming that the maximal size of carnivorous theropods is limited by the maximal capacity to consume vertebrates, as seen in extant terrestrial mammals, the size of the largest theropods agrees with a field energy expenditure extrapolated from varanid lizards (contrary to Seebacher [3]). From his calculations McNab [5] concluded that large herbivorous and carnivorous dinosaurs were homeothermic as a result of their very large body masses [25]. The dinosaurs in his model were not characterised by rates of metabolism seen in modern mammals and flighted birds, and had intermediate body temperatures. McNab [5] also noted a potential conflict with his model. Maximum growth rate estimates of large theropod and sauropod dinosaurs are large and close to those of modern mammals and precocial birds (scaled-up). The high growth rates could indicate a higher level of metabolism and thus higher body temperatures than observed in scaled-up varanid lizards. In amniotes (based on a dataset that includes *Varanus exanthematicus* and *Varanus niloticus* [26,27]; for ruminants [6]) a strong relationship between resting metabolic rate and growth rate has been shown.

Gillooly et al. [4] established a link between body temperature and maximum growth rate. In particular, they used an equation ([28], hereafter MGR- T_b -equation) to assess the average body temperature of animals $T_{b,MGR}$ (°C), that is basically derived from the maximum growth rate, MGR (kg day⁻¹) and the mass at maximum growth, M (kg) of the animal. This MGR- T_b -equation relies on a 3/4 power scaling of MGR with body mass. It additionally uses an Arrhenius approach to model body temperature effects on the biochemical reactions controlling individual growth and individual metabolic rate [29,30].

$$MGR = g_0 \cdot M^{0.75} \cdot e^{(-E/k \cdot T)} \quad (1)$$

Rearranging the terms in equation (1) and setting Boltzmann's factor $e^{-E/k \cdot T}$ (E: average activation energy, k: Boltzmann's

constant, T: body temperature in Kelvin) to $e^{0.1T_b}$ (T in °C) reveals the estimator $T_{b,MGR}$ for body temperature (in °C) given in Gillooly et al. [4].

$$T_{b,MGR} = 10 \cdot \ln(MGR \cdot M^{-0.75} / g_0). \quad (2)$$

Gillooly et al. [4] then estimated parameter g_0 in equation (1) and the MGR- T_b -equation (2) from data on scaling of maximum growth rates with body mass in reptiles [31] and in mammals [32]. Body temperature T_b was set to 30°C for reptiles [33] and 37°C for mammals [12]. This approach estimated parameter g_0 as $1.7 \cdot 10^{-4}$ (kg^{1/4} day⁻¹) in reptiles and as $2.3 \cdot 10^{-4}$ (kg^{1/4} day⁻¹) in mammals. The estimation of g_0 was based on the geometric mean of 12 estimates of $MGR \cdot M^{-0.75} e^{0.1T_b}$ for reptiles [31] and on the mean of 163 estimates for mammals [32], respectively. Because g_0 values of reptiles and mammals differed only slightly, Gillooly et al. [4] finally averaged the reptilian and mammalian g_0 value ($2 \cdot 10^{-4}$ kg^{1/4} day⁻¹) when applying their MGR- T_b -equation to dinosaurs. Parameter values of MGR and of the asymptotic mass (M_A) for dinosaurs were estimated from ontogenetic growth trajectories obtained from fossil long bones. Gillooly et al. [4] used trajectories of seven dinosaurs from a larger database of different dinosaurian lineages and geological periods to assess the body temperature of dinosaurs. The size of selected fully-grown dinosaurs ranged from 12 to 12,979 kg. Body temperature estimates of dinosaurs indicated a curvilinear increase in body temperature with the logarithm of body mass. While body temperatures of smaller dinosaurs were consistent with those seen in extant crocodiles (from the study of Seebacher et al. [23] and Seebacher [3]) and close to the average environmental temperature in their habitats (25°C), the larger *Tyrannosaurus rex* and *Apatosaurus excelsus* had with approximately 33°C and 41°C, respectively clearly higher body temperatures than paleotemperature estimates (20–30°C, [3]) suggest. Gillooly et al. [4] concluded that dinosaurs were reptiles that exhibited inertial homeothermy. Since the observed relationship between body mass and body temperature was curvilinear and it predicted a body temperature for the largest dinosaurs (55,000 kg, 48°C) beyond the upper limit tolerated by most of today's animals (45°C), Gillooly et al. [4] hypothesized that maximum body size in Dinosauria was ultimately limited by body temperature.

However, several more recent studies have questioned the results of Gillooly et al. [4]. First, the conclusion of Gillooly et al. [4] on the limitation of maximum size mathematically relies on the maximum growth rate estimate of the *Apatosaurus* specimen. This growth rate represents a clear overestimate [34–36]. Secondly, body temperatures calculated by Gillooly et al. [4] for dinosaurs contradict the ranges found in isotope thermometric studies [37,38].

In this paper, I analyse the accuracy of body temperature estimated from the MGR- T_b -equation and revisit the hypothesis of Gillooly et al. [4] that the maximum body size in Dinosauria was ultimately limited by body temperature. First, I study whether body temperatures measured in today's reptiles, birds and mammals are consistent with those predicted by the MGR- T_b -equation. I will therefore use datasets on core temperature of crocodiles [19,23], birds [39] and mammals [40] and compare these to respective body temperatures predicted from maximum growth rates. Second, I will apply the MGR- T_b -equation to a larger data set of dinosaurs than those studied by Gillooly et al. [4] to study the relationship between body mass and body temperature in dinosaurs. This tests whether the results of Gillooly et al.

[4] on inertial homeothermy and the limitation of maximal body size still hold for a larger number of dinosaurs. Finally, I will compare estimated body temperatures of dinosaurs to two models that have been suggested by other authors: a crocodile model [3] and a varanid lizard model [5].

Materials and Methods

Body Temperatures in Extant Species and the MGR- T_b -equation

The comparison of core temperatures (T_b) measured in extant species and those calculated from the MGR- T_b -equation ($T_{b,MGR}$) was carried out for extant species from non-avian reptiles (Table S1), from precocial, and altricial birds (Table S2), as well as from marsupials and eutherian mammals (Table S3). For T_b of non-avian reptiles, I chose the field data on *Crocodylus porosus* from Seebacher et al. ([23], $N = 10$) and Seebacher [3] as well as from *Alligator mississippiensis* in Seebacher et al. ([19], $N = 7$). All reptilian T_b s are annual averages obtained from calibrated temperature sensitive radio transmitters swallowed by the animals. T_b s of mammals were extracted from the dataset of McNab ([40], $N = 447$) on basal metabolic rate and body temperature; for birds the dataset on T_b from McNab ([39], $N = 88$) was used. Since Case [32] has shown that scaling of MGR with body mass differs strongly between altricial and precocial bird species, I analysed the scaling of body temperature with mass in altricial and precocial birds separately. Bird species were assigned to a precocial or an altricial developmental mode following Dial [41]. Dial [41] distinguishes seven developmental stages of birds and assigns those to different bird orders. The precocial birds considered in my study ($N = 41$), included all birds from McNab [39], belong to Dial's [41] super-precocial, precocial or sub-precocial orders; the altricial birds ($N = 39$) included those from Dial's [41] semi-altricial, altricial and super-altricial orders. As the scaling of MGR with body mass differs between eutherian mammals and marsupials [32,42], the scaling of body temperature in these two mammalian lineages was also analysed separately (eutherian mammals: $N = 384$; marsupials: $N = 63$).

For the estimation of MGR from body mass, I used three different regressions for each taxon: one from Case ([32]; hereafter Case-regression) and two from Werner and Griebeler [42]. The regressions from Werner and Griebeler [42] assume either that the slopes and intercepts are taxon-specific (hereafter MGR-regression) or that the slopes are fixed (0.75) and the intercepts are taxon-specific (as assumed in equation (1) and the MGR- T_b -equation; hereafter fixed-slope-MGR-regression). The MGR-regression and the fixed-slope-MGR-regression linking log MGR to log body mass are based on much larger datasets on extant taxa than the respective regressions from Case [32]. Specifically for non-avian reptiles' MGRs, three chelonians [43], five crocodiles (this study) and ten varanid lizards (this study) are added to the original dataset of Case [32] ($N = 66$, Table S4). The fixed-slope-MGR-regression assumes an equal scaling of body temperature and MGR with body mass, resulting in an independence of $T_{b,MGR}$ from body mass (equations 1 and 2). Thus, $T_{b,MGR}$ values calculated from fixed-slope-MGR-regressions for a taxon can be interpreted as the average body temperatures in this taxon. If MGR scales with body mass at an exponent larger (smaller) than 0.75, body temperature estimated from the MGR- T_b -equation increases (decreases) with increasing mass.

Since $T_{b,MGR}$ is not only calculated from MGR but also from the mass at which MGR is observed, and there is a high natural variability in the body masses at maximum growth of species, I considered three different standard sigmoidal growth models to

estimate the mass at maximum growth. These standard models had been successfully applied to ontogenetic growth series of non-avian reptiles, birds and mammals. Under the von Bertalanffy growth model ([44,45], vBGM) MGR is found at about 30% ($= 100 \cdot 8/27$, [46]) of asymptotic mass (M_A). In contrast, under the Gompertz growth model (GGM), MGR is about 37% ($= 100/e$, [46]), and under the logistic growth model (LGM) at 50% [46]. All three growth models have been successfully used to describe growth in extant non-avian reptilian taxa. The vBGM was used for extant snakes, lizards [47], turtles [48], crocodiles [49,50], and even extinct sauropod dinosaurs [34]. LGMs were applied to smaller extant reptiles [49] including tortoises [43] and to extinct dinosaurs from different lineages [36,51–54]. GGMs worked well for extant chelonians [31,55]. The increase in body mass of birds was successfully described by vBGMs [56], GGMs [57] and LGMs [58]. LGMs were applicable to extant eutherian mammals [59], but GGMs have also been used for mammals [59,60]. Based on these empirical observations, I considered for both non-avian reptiles and birds 30% of M_A (vBGM) as lower limit and 50% of M_A (LGM) as an upper limit of the body mass at maximum growth, and for mammals 37% of M_A (GGM) and 50% of M_A (LGM). My approach revealed an interval with $T_{b,MGR}$ that is realistic for a species of a given body mass.

Body Temperatures in Dinosaurs

Dinosaur specimen studied. Gillooly et al. [4] assessed body temperatures in dinosaurs based on the ontogenetic growth series of seven dinosaurs *Psittacosaurus mongoliensis* (12 kg), *Albertosaurus sarcophagus* (614 kg), *Gorgosaurus libratus* (622 kg), *Daspletosaurus torosus* (869 kg), *Tyrannosaurus rex* (2,780 kg), *Massospondylus carinatus* (140 kg), and *Apatosaurus excelsus* (12,979 kg) published in Erickson et al. [51,52]. Gillooly et al. [4] excluded based on the following arguments three specimens from these two papers: the feathered dinosaur bird *Shuuuua deserti* (1.9 kg) with a presumed different thermoregulation than the other dinosaurs, *Syntarsus rhodesiensis* (18.8 kg) because the MGR of this species is an outlier, and *Maiasaurus peeblesorum* (1,660 kg) because of its bad growth curve (only three mass estimates). Hatchling weights predicted by the fitted growth curves of these three specimens are unrealistic (*Shuuuua deserti*: 0.45 kg compared to an asymptotic mass of 1.9 kg, *Syntarsus rhodesiensis*: 4.1 kg vs. 18.8 kg, *Maiasaurus peeblesorum*: 160 kg vs. 1,660 kg), providing further support for the exclusion of the three specimens from the study of Gillooly et al. [4]. I additionally excluded the growth curve of *D. torosus* from my analysis because it is only based on three mass estimates during ontogeny. I also excluded the curve of *A. excelsus* because the MGR of this specimen is clearly an overestimate [34–36]. In my analysis, I additionally considered more recently published growth curves of *Archaeopteryx* (0.9 kg) from Erickson et al. [53], of *Psittacosaurus lujiatunensis* (37.4 kg) from Erickson et al. [54], of *Alamosaurus* (32,000 kg) from Lehman and Woodward [34], of six sauropod dinosaur specimens (one mamenchisaurid sauropod (25,075 kg), two *Apatosaurus* sp. (18,178 kg, 20,206 kg), two indeterminate diplodocids (4,144 kg, 11,632 kg), and one *Camarasaurus* sp. (14,247 kg) from Griebeler et al. [36] and of one basal sauropodomorph dinosaur individual (*Plateosaurus engelhardti*, 1,587 kg) from Griebeler et al. [36]. In total, for 15 dinosaurs belonging to five clades among Dinosauria (one *Archaeopteryx* individual, two Ceratosauroidea, four Tyrannosauroidea, two Prosauropoda and seven Sauropoda) I estimated body temperature from MGRs applying the MGR- T_b -equation. For *Archaeopteryx* and *Plateosaurus engelhardti* the authors provided two and for *Alamosaurus* three growth models yielding different MGR estimates for each of these specimens, whereas for the other twelve dinosaurs

only one growth curve is available. Overall, from 19 dinosaurian growth trajectories/MGR estimates I estimated body temperatures (Table S5). Except for *Alamosaurus* (vBGM), LGMs had been successfully fitted by the authors to dinosaurs. To estimate $T_{b,MGR}$ from the MGR- T_b -equation, I therefore assumed for all dinosaurs that the mass at maximum growth is reached at half of the asymptotic mass, except for *Alamosaurus* (at 30%).

To test whether body temperature in dinosaurs (Sauropodomorpha, Sauropoda) increases with increasing body mass I established regressions linking estimated $T_{b,MGR}$ from MGR and the mass at maximum growth to the logarithm of body mass of dinosaurs (Sauropodomorpha, Sauropoda) (M_A). These regressions were calculated based on all dinosaurian MGRs (19), but also on all sauropodomorph MGRs (twelve) and sauropod MGRs (nine). From the results of Gillooly et al. [4] I expected the body temperature in dinosaurs (Sauropodomorpha, Sauropoda) to increase with increasing body mass.

I further studied $T_{b,MGR}$ estimates of crocodiles and varanid lizards, because both taxa have been suggested as models for dinosaurs.

Crocodile model. Gillooly et al. [4] estimated body temperatures of crocodiles from the biophysical model developed by Seebacher [3] and considered a mean annual ambient temperature of 25°C. Seebacher's [3] biophysical model was calibrated with field data from eleven free-ranging crocodiles (*Crocodylus porosus*). However, the body temperatures from this field study are measurements of core temperatures of animals of different body mass. For dinosaurs, body temperature was estimated from the MGR- T_b -equation and is thus based on growth in body mass under ambient temperature conditions. For this reason, I also calculated $T_{b,MGR}$ from MGRs for crocodiles of different mass. To assess potential differences between T_b and $T_{b,MGR}$, I additionally compiled literature for MGRs and adult body mass (M_A) of crocodiles. The dataset of Case [32] comprises of only one data point for crocodiles (*Alligator mississippiensis*). For details on species, sources, methods, body masses of species, MGR estimates and calculated $T_{b,MGR}$ please refer to (Table S6). When estimating $T_{b,MGR}$ from the MGR- T_b -equation for crocodiles, I assumed the mass at maximum growth as 30% of the body mass of the individual. Empirical studies have shown that growth in crocodiles follows a vBGM [49,50]. Finally, I established a regression line using all crocodylian data points (hereafter crocodile model) to test whether T_b [3], but also $T_{b,MGR}$, increases with the logarithm of body mass. This would also test whether body temperatures estimated for dinosaurs fit to the crocodile model.

Varanid lizard model. McNab [5] had pointed out in his paper that the varanid lizards have 3.6 times higher rates of field energy expenditure than other lizards of equal size. As field energy expenditure is linked to metabolism [8], this could indicate higher body temperatures in varanid lizards than in other lizards and crocodiles of equal size. To the best of my knowledge, only one study on *Varanus varius* has measured core temperatures in varanid lizards [61] like Seebacher and colleagues [19,23] did for crocodiles. In this study, however, the varanid lizards were only monitored for 4 up to 13 days during summer, whereas Seebacher and colleagues monitored crocodiles over approximately one winter and summer month. Since intra-annual variability in environmental temperature was not captured in the study of *Varanus varius* a reliable comparison of T_b and $T_{b,MGR}$ estimates was impossible for varanid lizards. Nevertheless, I was able to test whether body temperatures estimated for dinosaurs ($T_{b,MGR}$) fit to this varanid lizard model. I therefore gathered information on MGRs and adult body mass (M_A) of varanid lizards in literature. Note that no varanid lizard is included in the dataset of Case [32].

For details on species, sources, methods, body masses of species, MGR estimates and calculated $T_{b,MGR}$ please refer to (Table S7). Since varanid lizards grow according to the vBGM [62,63], to estimate $T_{b,MGR}$ from the MGR- T_b -equation I assumed that the mass at maximum growth is 30% of the body mass of the individual. Based on the values of $T_{b,MGR}$ and body mass of varanid lizards, I finally established a regression line (hereafter varanid lizard model) linking $T_{b,MGR}$ to the logarithm in body mass in varanid lizards.

Statistical Analyses

In all extant taxa I analysed the relationships between body mass and T_b ($T_{b,MGR}$) using ordinary linear least squares regression analysis. In dinosaurs the relationship between body mass and $T_{b,MGR}$ was also analysed by ordinary least squares regression analysis, but I assumed both linear and non-linear models. In particular, I considered a non-linear model to test for a curvilinear increase in $T_{b,MGR}$ with increasing body mass across all dinosaurs (Sauropodomorpha, Sauropoda) that was expected from the results of Gillooly et al. [4]. In all regression analysis body mass was log-transformed, while T_b and $T_{b,MGR}$ were not. The significance of differences in slopes and intercepts between two regression lines was tested by comparing the respective 95% confidence intervals of estimates. Overlapping confidence intervals of estimated slopes and intercepts indicate no statistical support ($p > 0.05$) of differences between regression lines. All statistical analyses were conducted in STATISTICA 7.1 (StatSoft, Inc. 1984–2005).

The estimation of $T_{b,MGR}$ from individual MGR estimates and the MGR- T_b -equation carried out for extant reptilian taxa and extinct dinosaurs was done in Excel 2003 (Microsoft Corporation).

Results

Body Temperatures in Extant Species and the MGR- T_b -equation

Body temperatures predicted from the MGR- T_b -equation ($T_{b,MGR}$) did not fit very well to the T_b values for any of the three studied extant vertebrate lineages (Figure 1, Table 1 and 2). This observation was independent of the three different regression functions used for estimating $T_{b,MGR}$. Fixed-slope-MGR-regressions revealed, as expected, a constant body temperature for all studied vertebrate lineages that was independent of body mass, but differed strongly between lineages (Figure 1). T_b values predicted under the vBGM were always the highest. Those obtained from the GGM were intermediate, and those from the LGM revealed the lowest values for a given body mass (Figure 1).

Non-avian reptiles. As expected [3], T_b in crocodiles significantly increased with increasing body mass (Table 2). In contrast, when applying the Case-regression or the MGR-regression to extant non-avian reptiles, $T_{b,MGR}$ decreased with increasing body mass. $T_{b,MGR}$ values derived from the fixed-slope-MGR-regression on non-avian-reptiles (vBGM: 18.838°C; LGM: 15.007°C) were on average considerably lower than the T_b values of crocodiles (mean $26.635 \pm$ standard deviation s.d. 2.175°C).

Different scaling regression lines linking MGR to log body mass were derived for Lacertilia, Serpentes, Chelonia, Crocodylia and Varanidae (Table 1, Figure 2), but none of the slopes and intercepts differed significantly between these taxa.

Precocial, and altricial birds. T_b in precocial and altricial birds significantly decreased with increasing body mass (Table 2). On average, T_b in precocial birds (mean $40.520 \pm$ s.d. 1.328°C) was slightly lower than in altricial birds (mean $40.969 \pm$ s.d. 1.654°C), but this difference was not significant. $T_{b,MGR}$ in

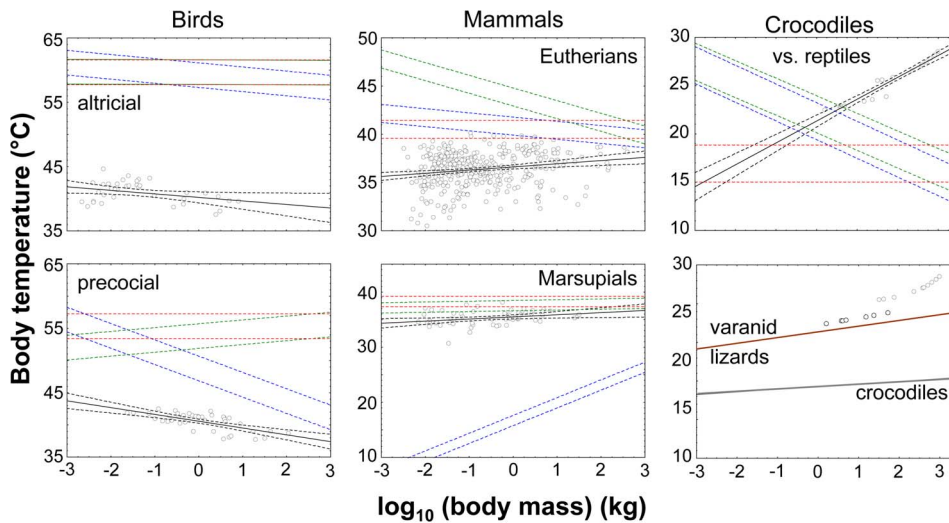


Figure 1. T_b and $T_{b,MGR}$ against the logarithm of body mass in extant taxa. T_b in birds from McNab [39], in mammals from McNab [40] and in crocodiles from Seebacher [3], Seebacher et al. [19], and Seebacher et al. [23]. Bird species were assigned to a precocial or an altricial developmental mode following Dial [41]. For regressions linking T_b and $T_{b,MGR}$, respectively to log body mass and statistics of regressions, please refer to Table 2. Black: regression line and 95% confidence interval of scaling of T_b in the taxon; blue: $T_{b,MGR}$ derived from the Case-regression [32]; green: $T_{b,MGR}$ derived from the MGR-regression [42]; red: $T_{b,MGR}$ derived from the fixed-MGR-regression [42]; upper and lower limits of $T_{b,MGR}$ were calculated based on different growth models that had been successfully applied to the taxon. Brown: my varanid lizard model (Table 2), grey: my crocodile model (Table 2).
doi:10.1371/journal.pone.0074317.g001

precocial and altricial birds based on the Case-regression and the MGR-regression also decreased with increasing body mass. $T_{b,MGR}$ values estimated from the respective Case-regression

and MGR-regression for precocial and altricial birds were unrealistically higher than the respective T_b values (Figure 1). $T_{b,MGR}$ values derived from the respective Case-regression and

Table 1. Logarithm of absolute maximum growth rate (g/day) against logarithm of body mass (kg) in extant taxa.

Taxon	Model	N	Slope	95% CI	Intercept	95% CI	R ²	Source
Non-avian reptiles	Case-regression	42	0.666		-0.334			[32]
	MGR-regression	49	0.671		-0.288			[42]
	Fixed-MGR-regression	49	(0.75)		-0.273			[42]
Lacertilia	MGR-regression	18	0.634***	[0.329, 0.948]	-0.323 ^{n.s.}	[-0.905, 0.258]	0.545	
Serpentes	MGR-regression	15	0.701***	[0.457, 0.945]	-0.371*	[-0.689, -0.052]	0.748	
Chelonia	MGR-regression	10	0.603***	[0.337, 0.868]	-0.205 ^{n.s.}	[-0.698, 0.287]	0.694	
Crocodylia	MGR-regression	6	0.765 ^{n.s.}	[-0.101, 1.630]	-0.471 ^{n.s.}	[-2.046, 1.103]	0.601	
Varanidae	MGR-regression	13	0.782***	[0.657, 0.908]	-0.162*	[-0.312, -0.012]	0.945	
Altricial birds	Case-regression	56	0.722		1.480			[32]
	MGR-regression	387	0.749		1.581			[42]
	Fixed-MGR-regression	387	(0.75)		1.583			[42]
Precocial birds	Case-regression	14	0.640		0.780			[32]
	MGR-regression	194	0.776		1.407			[42]
	Fixed-MGR-regression	194	(0.75)		1.396			[42]
Eutherian mammals	Case-regression	163	0.731		0.750			[32]
	MGR-regression	322	0.693		0.769			[42]
	Fixed-MGR-regression	322	(0.75)		0.794			[42]
Marsupials	Case-regression	4	0.820		-0.030			[32]
Marsupials	MGR-regression	21	0.756		-0.683			[42]
Marsupials	Fixed-MGR-regression	21	(0.75)		-0.697			[42]

Model: allometric regression used (for details refer to the text); slope, intercept: slope and intercept of the allometric regression; significance levels: n.s. $p > 0.05$, * $p \leq 0.05$, ** $p < 0.01$, *** $p < 0.001$; 95% CI: 95% confidence interval; R²: variance explained by the linear regression.
doi:10.1371/journal.pone.0074317.t001

Table 2. Body temperature (°C) against the logarithm of body mass (kg) in extant taxa.

Taxon	Body temperature	Scaling model	M _{inflection point}	Slope	Intercept
Non-avian reptiles	T _{b,MGR}	Case	vBGM	1.934	23.236
	T _{b,MGR}	MGR	vBGM	1.819	23.950
	T _{b,MGR}	Fixed-MGR	vBGM	(0.75)	18.838
Non-avian reptiles	T _{b,MGR}	Case	LGM	1.934	19.405
	T _{b,MGR}	MGR	LGM	1.819	20.119
	T _{b,MGR}	Fixed-MGR	LGM	(0.75)	15.007
Crocodylia	T _{b,MGR}		vBGM	0.341	14.270
Crocodylia	T _b			2.263***	21.331***
Varanidae	T _{b,MGR}		vBGM	0.744	21.396
Altricial birds	T _{b,MGR}	Case	vBGM	0.645	61.137
	T _{b,MGR}	MGR	vBGM	0.023	61.600
	T _{b,MGR}	Fixed-MGR	vBGM	(0.75)	61.574
Altricial birds	T _{b,MGR}	Case	LGM	0.645	57.305
	T _{b,MGR}	MGR	LGM	0.023	57.766
	T _{b,MGR}	Fixed-MGR	LGM	(0.75)	57.743
Altricial birds	T _b			-0.548*	40.217***
Precocial birds	T _{b,MGR}	Case	vBGM	-2.533	50.683
	T _{b,MGR}	MGR	vBGM	0.599	55.726
	T _{b,MGR}	Fixed-MGR	vBGM	(0.75)	57.268
Precocial birds	T _{b,MGR}	Case	LGM	-2.533	46.852
	T _{b,MGR}	MGR	LGM	0.599	51.894
	T _{b,MGR}	Fixed-MGR	LGM	(0.75)	53.437
Precocial birds	T _b			-1.058*	40.574***
Eutherian mammals	T _{b,MGR}	Case	GGM	0.437	41.784
	T _{b,MGR}	MGR	GGM	1.312	44.801
	T _{b,MGR}	Fixed-MGR	GGM	(0.75)	41.439
Eutherian mammals	T _{b,MGR}	Case	LGM	0.437	39.921
	T _{b,MGR}	MGR	LGM	1.312	42.937
	T _{b,MGR}	Fixed-MGR	LGM	(0.75)	39.576
Eutherian mammals	T _b			0.329***	36.622***
Marsupials	T _{b,MGR}	Case	GGM	3.224	17.630
	T _{b,MGR}	MGR	GGM	0.138	36.605
	T _{b,MGR}	Fixed-MGR	GGM	(0.75)	39.205
Marsupials	T _{b,MGR}	Case	LGM	3.224	15.767
	T _{b,MGR}	MGR	LGM	0.138	36.605
	T _{b,MGR}	Fixed-MGR	LGM	(0.75)	37.342
Marsupials	T _b			0.385*	35.492***

Comparison of T_{b,MGR} and T_b. T_{b,MGR} was estimated from different allometric regressions linking the log of maximum growth rate (MGR) to the log of body mass (Case-regression, MGR-regression, and fixed-MGR-regression; for details refer to the text and Table 1). M_{inflection point}: mass at the maximum growth rate of the individual used in the MGR-T_b-equation, vBGM (30% of asymptotic mass of the individual), GGM (37%) and LGM (50%). T_b: body temperatures of vertebrate taxa from different datasets [3,19,23,39,40]. Slope, intercept: slope and intercept of the linear regression linking body temperature to log body mass. Significance levels: n.s. p>0.05,

*p ≤ 0.05,

**p<0.01,

***p<0.001.

doi:10.1371/journal.pone.0074317.t002

MGR-regression for altricial birds exceeded those of precocial birds. T_{b,MGR} estimated from the fixed-slope-MGR-regression of precocial birds was 53.427°C under the vBGM and 57.268°C under the LGM and for altricial birds 57.743°C and 61.674°C, respectively. Thus all T_{b,MGR} of birds were clearly physiologically unrealistic.

Marsupials and eutherian mammals. T_b in marsupials and eutherian mammals significantly increased with increasing log body mass (Table 2). Marsupials had on average (mean 35.275± s.d. 1.296°C) a lower T_b than eutherian mammals (mean 36.365± s.d. 1.752°C). T_{b,MGR} values estimated from the Case-regression and MGR-regression for marsupials increased again with increasing body mass, whereas T_{b,MGR} of eutherian mammals decreased

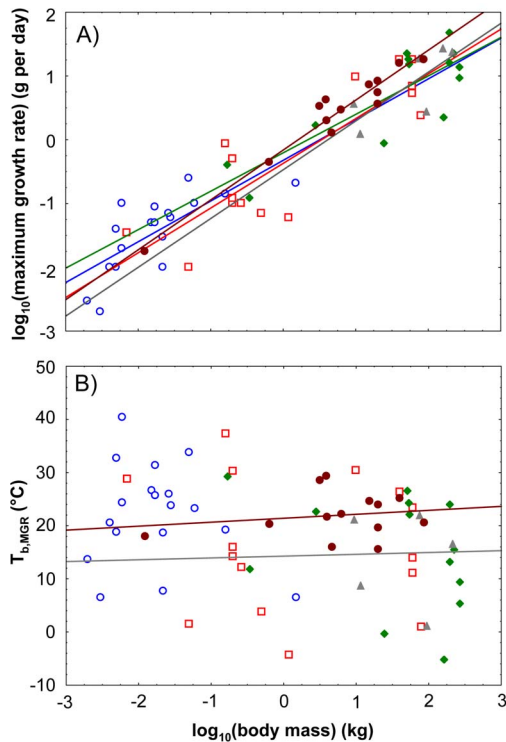


Figure 2. MGR and $T_{b,MGR}$ against the logarithm of body mass in extant non-avian reptiles. Log MGR is shown in panel (A) and $T_{b,MGR}$ in (B). For regressions on log MGR and $T_{b,MGR}$, respectively against log body mass, please refer to Tables 1 and 2. Lacertilia (open blue dots, blue line), Serpentes (open red squares, red line), Chelononia (filled green diamonds, green line), Crocodylia (grey filled triangles, grey line) and Varanidae (filled brown dots, brown line). doi:10.1371/journal.pone.0074317.g002

for both regressions. $T_{b,MGR}$ estimated from the fixed-slope-MGR-regression of marsupials was 39.205°C under the GGM, and 37.342°C under the LGM; for eutherian mammals 41.439°C, and 39.576°C, respectively. Thus, $T_{b,MGR}$ values of marsupials and eutherian mammals showed the lowest deviation from the respective T_b within the three studied extant vertebrate lineages.

Body Temperatures in Dinosaurs

$T_{b,MGR}$ was independent of body mass (linear scaling, slope: $p > 0.05$, Table 3, Figure 3) across all dinosaurs (28.033°C), all Sauropodomorpha (28.712°C) and all Sauropoda (28.712°C). In Sauropodomorpha (Table 3, Figure 3), however, a curvilinear (quadratic polynomial) relationship between body temperature and body mass was significant after excluding the indeterminate diplodocid (MfN.R.2625) from the dataset. The MGR estimate of this specimen is the poorest of the seven Sauropodomorpha studied in Griebeler et al. [36]. In comparison to the other Sauropodomorpha studied in this paper the MfN.R.2625 specimen has the lowest number of growth cycles preserved (9 vs. 9–22) and its growth record does only document the linear phase of growth, which hampers a good fit of a sigmoidal growth model [36]. Three other Sauropodomorpha specimens having also nine growth cycles preserved were not excluded (*Camarasaurus* sp. from Griebeler et al. [36], *Alamosaurus sanjuanensis* from Lehman and Woodward [34], *Massospondylus carinatus* from Erickson et al. [52]) because their growth records clearly document a sigmoidal growth trajectory.

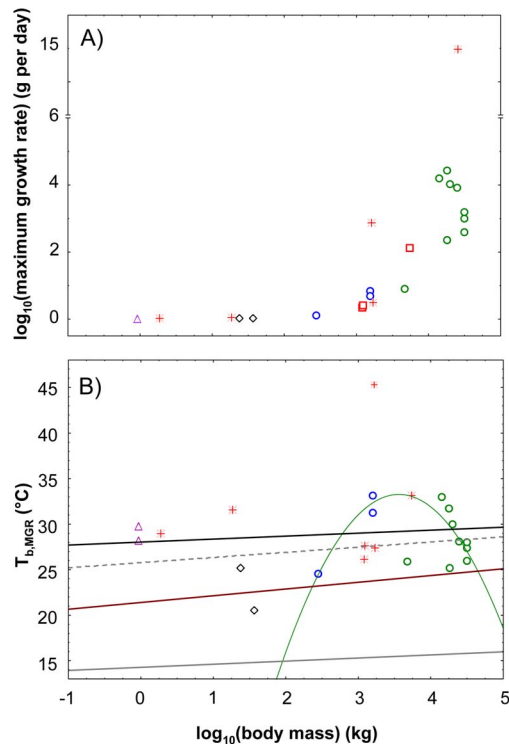


Figure 3. MGR and $T_{b,MGR}$ against the logarithm of body mass in dinosaurs. Log MGR is shown in panel (A) and $T_{b,MGR}$ in (B). Open symbols (included in this study [34,36,51–54]): sauropods (green dots), prosauropods (blue dots), theropods (red squares), ornithischians *Psittacosaurus* (black diamond), *Archaeopteryx* (purple triangle); red crosses (excluded from the study Erickson et al. [51,52]): *Shuvuuia deserti*, *Syntarsus rhodesiensis*, *Maiasaurus peeblesorum*, *Daspletosaurus torosus*, *Apatosaurus excelsus*; black line: overall scaling of $T_{b,MGR}$ in dinosaurs, green line: curvature of $T_{b,MGR}$ in Sauropodomorpha (MfN.R.2625 from Griebeler et al. [36] excluded, Table 3); grey solid line: my crocodile model, grey dashed line: crocodile model from Gillooly et al. [4]; brown line: my varanid lizard model. For statistics of regressions please refer to Tables 2 and 3. doi:10.1371/journal.pone.0074317.g003

Except for *Psittacosaurus lujiatunensis*, $T_{b,MGR}$ of all dinosaurs studied were higher than predicted by the varanid lizard model. As the varanid lizard model revealed higher $T_{b,MGR}$ values for dinosaurs than the crocodile model, $T_{b,MGR}$ were also higher than under the crocodile model (Figure 3).

Discussion

Body Temperatures in Extant Species and the MGR- T_b -equation

The overall dependency (increase, decrease, independence) between T_b and log body mass was correctly reproduced by the regressions linking $T_{b,MGR}$ to log body mass in crocodiles, birds and marsupials, but not in eutherian mammals. In crocodiles, both $T_{b,MGR}$ (derived from the MGR-regression) and T_b increased with increasing body mass. This positive scaling of body temperature is consistent with the results of Seebacher [3] and corroborates the inertial homeothermy for crocodiles not only for T_b , but also for $T_{b,MGR}$.

In precocial birds, altricial birds and marsupials, both $T_{b,MGR}$ (derived from the Case-regression and the MGR-regression) and T_b significantly decreased with increasing body mass. In contrast, in eutherian mammals T_b significantly increased and $T_{b,MGR}$

Table 3. Scaling of $T_{b,MGR}$ ($^{\circ}C$) with the logarithm of body mass (kg) in dinosaurs.

Taxon	Model	N	β_0	95% CI	β_1	95% CI	β_2	95% CI	R ²
all dinosaurs	linear	19	26.460***	[22.481, 30.439]	0.520 ^{n.s.}	[-0.624, 1.664]			0.051
Sauropodomorpha	linear	12	40.261***	[24.247, 56.275]	-2.750 ^{n.s.}	[-6.640, 1.140]			0.221
Sauropodomorpha	quadratic	12	-27.061 ^{n.s.}	[-92.306, 38.183]	32.406 ^{n.s.}	[-5.037, 69.850]	-4.514n.s.	[-9.712, 0.684]	0.221
Sauropodomorpha without MFN.R.2625	quadratic	11	-56.863*	[-110.116, -3.610]	50.617**	[19.686, 81.548]	-7.106**	[-11.422, -2.790]	0.364
Sauropoda	linear	9	27.890 ^{n.s.}	[-11.793, 67.577]	0.099 ^{n.s.}	[-9.145, 9.342]			0.001
Sauropoda without MFN.R.2625	linear	8	21.634 ^{n.s.}	[-12.506, 55.772]	1.418 ^{n.s.}	[-6.502, 9.338]			0.031
Prosauropoda	linear	3	-0.226 ^{n.s.}	[-80.712, 80.260]	10.124 ^{n.s.}	[-16.989, 37.219]			0.958
Theropoda	linear	3	-2.928 ^{n.s.}	[-87.315, 81.560]	9.628 ^{n.s.}	[-15.760, 35.015]			0.959

Model: linear $T_{b,MGR} = \beta_0 + \beta_1 M$, quadratic $T_{b,MGR} = \beta_0 + \beta_1 M + \beta_2 M^2$; significance levels: n.s. $p > 0.05$,

* $p \leq 0.05$,

** $p < 0.01$,

*** $p < 0.001$; 95% CI: 95% confidence interval; R²: variance explained by the regression model.

doi:10.1371/journal.pone.0074317.t003

values (derived from the Case-regression and the MGR-regression) decreased with increasing body mass.

Most of my results on the dependencies between T_b and log body mass in extant species are corroborated by other studies. Based on an analysis of a very small data set on birds and mammals, Rodbard [64] argued that T_b inversely scales with body mass in both lineages. McNab [39] was able to corroborate his finding using a larger dataset for birds, but demonstrated different scaling in T_b for different taxonomic groups within mammals. White and Seymour [65] compiled an extensive dataset on mammals and found an overall increase in T_b with increasing body mass, which is contrary to Rodbard [64]. The most recent extensive study on scaling of T_b in mammals and birds is the one of Clarke and Rothery [66]. Contrary to all other studies before, these authors examined the variation in T_b associated without and with phylogeny. When ignoring phylogenetic effects (as I did) their analysis supported the results of McNab [39], a positive scaling of T_b in mammals and an inverse scaling in birds. When allowing for phylogenetic effects in their analysis, the inverse scaling in birds was corroborated but no relationship between body mass and T_b in mammals was identified. Within taxonomic groups of birds and mammals, a positive scaling, a negative scaling and no relationship between T_b and body mass was observed by Clarke and Rothery [66]. Contrary to the negative scaling found in my study for altricial and precocial birds, Clarke and Rothery [66] showed a weakly positive scaling of T_b in the altricial Passeriformes [41]. In the altricial Piciformes and precocial Anseriformes [41], T_b was independent of body mass. Differences in scaling relationships between taxonomic groups were even more pronounced in mammals than in birds and differed between orders [66]. Contrary to my results, the scaling of T_b was positive in marsupials, but this overall relationship was not statistically supported for any marsupialian order [66]. The results of Clarke and Rothery [66] recommend that any overall relationship between T_b and body mass in a taxon should be interpreted cautiously because the overall pattern of scaling is strongly influenced by the mixture of different scaling relationships existing at lower phylogenetic levels and their proportion of species in the sample. Nevertheless, for both birds and eutherian mammals Clarke and Rothery [66] observed that in taxonomic groups containing species of a large body size, scaling of T_b is negative. In non-passerine birds, artiodactyles and carnivores big species have

a lower T_b than smaller species. This negative scaling of T_b in larger birds and eutherian mammals is corroborated by $T_{b,MGR}$, and suggest that the MGR- T_b -equation is useful to assess in larger species of mammals and birds whether body temperature is independent of log body mass or scales positive or negative.

However, for a given body mass/species the accuracy of $T_{b,MGR}$ in comparison to T_b was low and strongly differed between the vertebrate lineages studied. For endothermic birds and mammals, body temperatures predicted by the MGR- T_b -equation ($T_{b,MGR}$) for a species of a given body mass were always higher than T_b ; for ectothermic crocodiles, T_b was much higher than $T_{b,MGR}$. Nevertheless, the ranking seen in T_b values of extant taxa was well reflected in $T_{b,MGR}$. Altricial birds have the highest T_b and $T_{b,MGR}$ values, and both are lower than in precocial birds. T_b and $T_{b,MGR}$ values in eutherians are lower than in birds, and crocodiles have the lowest T_b and $T_{b,MGR}$.

Several hypotheses could explain the quantitative differences between T_b and $T_{b,MGR}$, which are considerably larger in birds and crocodiles than in mammals. First, the MGR- T_b -equation ($T_{b,MGR}$) was calibrated by Gillooly et al. [4] to reveal $T_{b,MGR}$ values of $30^{\circ}C$ for reptiles and $37^{\circ}C$ for mammals. These values were identified with $g_0 = 2 \cdot 10^{-4} \text{ kg}^{1/4} \text{ day}^{-1}$ thereby assuming a $3/4$ scaling of MGR (equation 1) and an average activation energy of 0.65 eV (term $e^{0.1T_b}$, equation 1) for the biochemical reactions underlying the metabolism of an individual. However, the specific g_0 estimated by Gillooly et al. [4] for reptiles was $1.7 \cdot 10^{-4} \text{ kg}^{1/4} \text{ day}^{-1}$ and for mammals $2.3 \cdot 10^{-4} \text{ kg}^{1/4} \text{ day}^{-1}$. The value of g_0 of reptiles was based only on twelve species, whereas g_0 of mammals was based on 163 species. The $3/4$ scaling of MGR underlying the MGR- T_b -equation is not observed in all vertebrate taxa, although for none of the taxa studied herein a deviation from a $3/4$ scaling is statistically significant ([42], Table 1). Downs et al. [67] have shown that also the activation energy differs between taxonomic groups. While in birds ($1.005 \pm 0.212 \text{ eV}$) and in mammals ($0.856 \pm 0.068 \text{ eV}$) the activation energy is on average much higher than assumed by the MGR- T_b -equation (0.65 eV), in reptiles the activation energy ($0.757 \pm 0.043 \text{ eV}$) is closer to this value. Nevertheless, according to a translation of activation energy in Q_{10} values, the taxon-specific activation energies of birds, mammals and reptiles still correspond to the typical range of Q_{10} for whole body metabolism (i.e. Q_{10} c. 2–3 over the range of 0 – $40^{\circ}C$, [67]). Figure 4 displays the results of my small sensitivity

analyses. The analysis was carried out to gain insights into the influence of the values assumed for g_0 , for the scaling exponent of MGR and for the activation energy on estimated $T_{b,MGR}$ for species of different body masses. Errors in $T_{b,MGR}$ introduced by averaging g_0 of non-avian reptiles and mammals are very small. Setting g_0 for reptiles to $1.7 \cdot 10^{-4} \text{ kg}^{1/4} \text{ day}^{-1}$ and for mammals to $2.3 \cdot 10^{-4} \text{ kg}^{1/4} \text{ day}^{-1}$ (instead of $2 \cdot 10^{-4} \text{ kg}^{1/4} \text{ day}^{-1}$ as assumed by the MGR- T_b -equation) increased $T_{b,MGR}$ by about 2°C in reptiles and decreased $T_{b,MGR}$ by about 2°C in mammals. Errors introduced by a deviation from a $3/4$ scaling of MGR increase with increasing body mass. Smaller exponents than 0.75 (0.65, reptiles, Table 1) lead to higher $T_{b,MGR}$ and higher exponents (0.85, marsupials, Table 1) to lower $T_{b,MGR}$ for reptiles and mammals for the body masses studied in my sensitivity analysis. Whereas for a 1 kg reptile or mammal the error introduced by a deviation of the exponent from 0.75 is low (about 2°C), for a reptile or mammal with a body mass of 1,000 kg it is already about 6°C (0.65 scaling exponent, Table 1). Small errors in the activation energy resulted in even stronger changes in $T_{b,MGR}$ as predicted by the MGR- T_b -equation. Specifically, for reptiles, mammals and birds, all having on average larger activation energies than 0.65 eV [67], $T_{b,MGR}$ considerably decreased when the correct activation energy was used in the MGR- T_b -equation. For example, an activation energy of 0.89 eV (mammals) decreases $T_{b,MGR}$ of a mammal between 7 and 8°C . For crocodiles, an average (non-avian) reptilian activation energy (0.757 eV , [67]) results in an even stronger underestimation of T_b [19,23] by $T_{b,MGR}$. In total, my small sensitivity analyses suggests that values assumed in the MGR- T_b -equation for g_0 , the scaling exponent of MGR and the average activation energy can introduce very large inaccuracies in estimated body temperatures of species (Figure 4).

For reptiles I found a strong underestimation of T_b by $T_{b,MGR}$. A known caveat of the MGR- T_b -equation [68] linking individual growth to body mass (M_A) is the disregard for reproduction in West et al. [28] and Gillooly et al. [4]. For the so-called determinate growers (most mammals and birds) modelled by the MGR- T_b -equation, all growth occurs before reproduction begins. In so-called indeterminate growers (many fish and non-avian reptiles), individuals continue to grow after first reproduction. Thus, in indeterminate growers growth is substantially slowed down before reaching M_A because materials and energy are not only allocated to individual growth and maintenance but also to reproduction. A lower MGR results in lower body temperatures predicted by the MGR- T_b -equation. This inherent underestimation of T_b in indeterminate growers by the MGR- T_b -equation is important in extant non-avian reptiles, but could also be significant in several dinosaurs presumed to reproduce well before reaching full size M_A [35,36,69]. In non-avian reptiles, growth can also be highly variable, reflecting environmental inconsistencies within and between years in general [70] and in ambient temperatures in particular [70,71]. For example, the most northerly distributed extant crocodylian species, the American Alligator, stops eating when ambient temperature drops below 16°C . It is only during the warmer months of the year during active feeding that growth occurs [71]. During winter torpor (hibernation), growth in non-avian reptiles stops completely [70]. Since MGR of larger reptiles and dinosaurs (annual growth marks are preserved in long bones; for a review on the establishment of growth trajectories, see [35,36]) is calculated at a yearly basis, phases of growth and not growth within the year are averaged. Annual MGRs (although transformed to a daily basis) therefore underestimate the real maximum daily growth rate of the specimen. For example, if an American alligator with a body mass of 160 kg and a MGR of 27.0 g per day estimated at a yearly

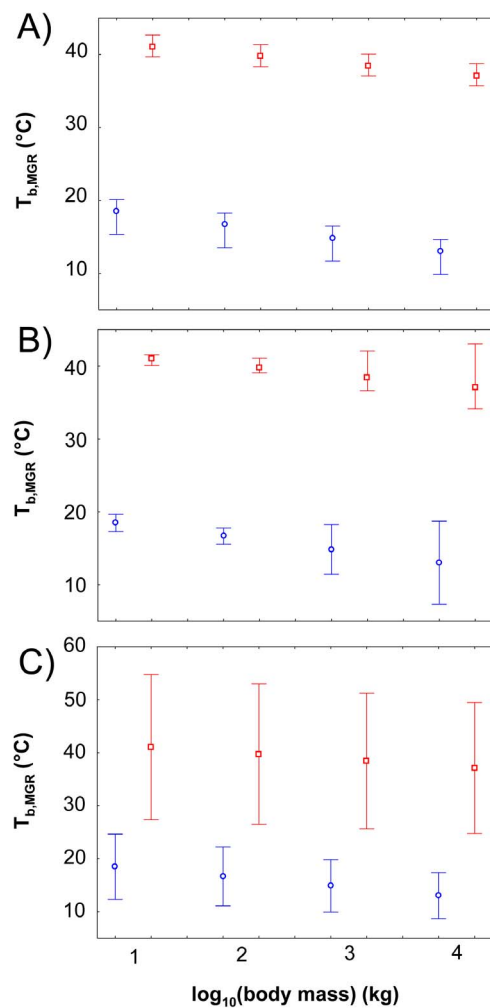


Figure 4. Results of the sensitivity analysis on the influence of values assumed for g_0 , the scaling exponent of MGR, and the activation energy term $e^{0.1T_b}$ on estimated $T_{b,MGR}$ of extant (non-avian) reptilian and mammalian species. For different body masses (1, 10, 100, 1000 kg), $T_{b,MGR}$ was calculated from the MGR- T_b -equation in Gillooly et al. [4] applying the MGR-regression for reptiles and mammals, respectively to estimate MGR from body mass (Table 1). Tested parameter values: (A) in the MGR- T_b -equation g_0 was set to 0.00017 (reptiles, [4]), 0.0002 (average of reptiles and mammals, [4]) and 0.00023 (mammals, [4]); (B) scaling exponent used in the MGR- T_b -equation was 0.65, 0.75 (default) and 0.85; (C) 0.075, 0.1 and 0.15 was used as an exponent in the activation energy term $e^{0.1T_b}$, or an activation energy of 0.447, 0.65 and 0.894 eV, respectively. The average values used by Gillooly et al. [4] result in average $T_{b,MGR}$ for reptiles (open dots) and mammals (open squares). The reptilian g_0 (upper whisker mark) reveals higher $T_{b,MGR}$ than the mammalian value (lower whisker mark). Scaling exponents smaller than 0.75 (upper whisker mark) result in higher $T_{b,MGR}$ and higher exponents (lower whisker mark) in lower $T_{b,MGR}$ than observed under a $3/4$ scaling of MGR. Note: MGR scales in non-avian reptiles with about 0.65, in mammals and birds with about 0.75 (Table 1). An exponent of 0.075 in the activation energy term (upper whisker mark) reveals the highest $T_{b,MGR}$ and an exponent of 0.15 the lowest $T_{b,MGR}$ (lower whisker mark). Note: Average activation energies of non-avian reptiles (0.757 eV), mammals (0.856 eV) and birds (1.005 eV) are all higher than the 0.65 eV used in the MGR- T_b -equation [67]. A usage of the specific activation energies for these three vertebrate lineages results in lower $T_{b,MGR}$ values than predicted by the MGR- T_b -equation. The average activation energy of ectothermic fish is 0.433 eV (Downs et al. 2008 [67], upper whiskers). doi:10.1371/journal.pone.0074317.g004

base [32] does not grow between October and March (=6 months, [71]), the respective (daily) MGR is doubled when only referring to the growth phase (54 g per day) and $T_{b,MGR}$ rises from 20.02 to 26.95°C. This revised $T_{b,MGR}$ is very close to a T_b of 26.24°C (=25+1.24°C, with 25°C average annual temperature, [4]) estimated from the biophysical model of Seebacher [3] and to the average T_b of about 24°C measured by Seebacher et al. [19] in a field study on the American alligator (Figure 1). In conclusion, the MGR- T_b -equation underestimates T_b for non-avian reptiles when a species shows considerable, long phases of no growth within the year. This underestimation could explain the higher ranges of body temperatures found in isotope thermometric studies for dinosaurs [37,38] than by Gillooly et al. [4].

The accuracy of estimated $T_{b,MGR}$ was best in mammals which is expected because Gillooly et al. [4] calibrated the MGR- T_b -equation based on this vertebrates. For eutherian mammals $T_{b,MGR}$ values derived from the fixed-slope-MGR-regression and the Case-regression were closer to T_b than the $T_{b,MGR}$ values derived from MGR-regression. In particular, the MGR-regression revealed unrealistically high T_b values for animals smaller than 1 kg (Figure 1). However, differences in the slope of the MGR-regression and the Case-regression are not significant and they include the 0.75 of the fixed-slope-MGR-regression [42]. Thus, the higher $T_{b,MGR}$ derived from the MGR-regression compared to the other two regressions (0.731 for Case-regression and 0.75 for fixed-slope regression, Table 1) are not statistically supported. The generally higher $T_{b,MGR}$ values derived from the fixed-slope-MGR-regression and the Case-regression are consistent with a higher activation energy observed in mammals (0.856 ± 0.068 eV, [67]) than assumed by the MGR- T_b -equation (0.65 eV) (Figure 4).

For marsupials $T_{b,MGR}$ values derived from the MGR-regression and the fixed-slope regression were close to T_b values. Contrarily, the Case-regression revealed unrealistically low $T_{b,MGR}$ values for marsupials, but this regression is only based on four species (Table 1). In marsupials a $\frac{3}{4}$ scaling of MGR assumed in the MGR- T_b -equation is indeed observed ([42], Table 1). Thus a lower g_0 and/or higher activation energy than assumed by the MGR- T_b -equation could have caused the small overestimation of $T_{b,MGR}$ by the MGR-regression and the fixed-slope-MGR-regression in marsupials.

However, for birds, I found the strongest overestimation of T_b by the MGR- T_b -equation. This is contrary to the other determinate growers, mammals. While body temperatures of adult birds and mammals are very similar, differences in metabolic rates exist between these two taxa attributed to the expensive and expansive form of avian flight. White et al. [72] found that smaller (<1 kg) birds have a higher standard metabolic rate (normalized to 38°C) than mammals (about 1.2 times at a mass of 10 g), whereas in larger birds the opposite is true. Based on a very extensive analysis, McNab [40,73] suggested that birds have on average basal metabolic rates 30–40% greater than mammals. Since both studies demonstrated only small differences in the metabolism of adult bird and mammal individuals, these results are unable to fully explain the large differences seen between T_b and $T_{b,MGR}$ in birds over a body mass range of five orders of magnitude. However, the observation that birds generally have higher T_b and $T_{b,MGR}$ than mammals is consistent with the results of Western and Ssemakula [74]. Western and Ssemakula [74] found that most of the variation in MGR observed between birds and mammals can be attributed to body temperature, metabolic rate and brain weight (e.g. primates have very large brains compared to other species of equal size and grow slower).

Altricial birds and precocial birds have MGRs about five times and three times higher than eutherian mammals (fixed-MGR-

regression, Table 1), but these values are reached in this determinate growers during the juvenile phase. In altricial nestlings, the thermoregulation and muscle coordination develops slowly during the growth phase and parents heat the young by sitting on the nest. In contrast, the young of precocial birds are endothermic and quite mobile after hatching [75]. The resulting energy saved in altricial young compared to precocial young during the juvenile phase could at least partially explain the higher MGRs in altricial than in precocial birds. Case [32] formulated a preliminary idea explaining the large difference in MGR of precocial and altricial birds. Birds which grow quickly are fed frequently by both parents, while slow growers are either self-feeding or are fed large food parcels at infrequent intervals by their parents. In many altricial birds, e.g. passerines, growth rates are very high; the lowest avian growth rates have been measured in the young of precocial and self-feeding birds. Ricklefs [58] confirmed in a model his alternative hypothesis, that interspecific variation in growth rates of altricial birds is the result of adaptations to levels of predation and the requirement for, and availability of, energy to the nestling. This model questions the reasoning of Case [32]. Independent of factors driving the differences in MGR between altricial and precocial young, altricial chicks save energy during the juvenile phase compared to precocial chicks. This energy could be allocated to their growth.

In conclusion, my results on the comparison of T_b and $T_{b,MGR}$ in different extant vertebrate lineages suggest that the dependency (increase, decrease, independence) between body mass and body temperature can be assessed from the MGR- T_b -equation for crocodiles, birds, and larger mammals. However, the accuracy of $T_{b,MGR}$ derived from this equation was poor in all vertebrate lineages studied. Taxon-specific differences in the scaling of MGR (g_0 , scaling exponent) and in the activation energy of biochemical reactions assumed in Arrhenius model as well as ecological and evolutionary adaptations of species cause the observed differences in T_b and $T_{b,MGR}$. This suggests that we can not expect that the MGR- T_b -equation will reveal accurate body temperatures for dinosaurs. This in turn strongly questions the applicability of the MGR- T_b -equation to study a potential limitation of body mass in Dinosauria due to overheating.

Body Temperatures in Dinosaurs

Irrespective of the inaccuracy of $T_{b,MGR}$ values observed in extant species I expected a curvilinear increase of $T_{b,MGR}$ with increasing log body mass in dinosaurs from the results of Gillooly et al. [4]. But contrary to my expectation, across all dinosaurs, Sauropodomorpha and Sauropoda, $T_{b,MGR}$ was independent of body mass (linear scaling of $T_{b,MGR}$ with increasing log body mass, Table 3). All $T_{b,MGR}$ values derived for dinosaurs were largely consistent with paleotemperature estimates (20–30°C, [3]). These two results strongly contradict Gillooly et al. [4] and also question the conclusion of these authors on the limitation of body mass in Dinosauria. Only *Plateosaurus*, *Apatosaurus* (BYU601-17328) and *Tyrannosaurus rex* had slightly higher $T_{b,MGR}$ than 30°C [3]. The overall range of $T_{b,MGR}$ of dinosaurs (24.55–31.12°C; *Massospondylus carinatus*, *T. rex*) was smaller than the range of $T_{b,MGR}$ seen in extant non-avian reptiles (–5.29–40.47°C; *Caretta caretta*, *Chemidophorus sexlineatus*), extant crocodiles (1.04–21.89°C; *Crocodylus porosus*, female American alligator) and extant varanid lizards (15.57–29.33°C; *Varanus salvator*, *Varanus niloticus*). The lower variability of $T_{b,MGR}$ found at a given body size in the larger Dinosauria compared with the smaller variability seen in extant non-avian reptiles conforms with inertial homeothermy in Dinosauria. According to the biophysical model of Seebacher [3], larger ectothermic animals have more stable body tempera-

tures than smaller. However, reasons for the natural variability seen in growth rates of extant similar-sized individuals are not only ambient temperature and thermoregulation but also food availability, quality and intake, and water availability [70]. Moreover, the sample size of studied extant non-avian reptiles is much larger than that of Dinosauria. We can expect that the natural variability covered by a smaller sample is lower than by a larger sample, even if two (statistical) populations have equal ranges.

While in the two prosauropods $T_{b,MGR}$ increases with increasing body mass, in sauropods $T_{b,MGR}$ decreases with increasing body mass. However, neither the trend in $T_{b,MGR}$ of prosauropods nor the trend in $T_{b,MGR}$ of sauropods is statistically significant. Nevertheless, a curvilinear relationship between $T_{b,MGR}$ and body mass was significant when excluding the MfN.R.2625 specimen from the dataset (Figure 3, Table 3). The decrease in body temperature with increasing body mass in sauropods, which is statistically supported by the fitted parabola (Figure 3), again strongly contradicts the hypothesis that the body mass of the largest dinosaurs was ultimately limited by body temperature. This is not to say that sauropods did not exhibit inertial homeothermy [3,5], but that they were able to efficiently cool themselves down [76].

For all dinosaurs studied, $T_{b,MGR}$ values predicted by my crocodile model were lower than the $T_{b,MGR}$ values derived from the varanid lizard model. The higher $T_{b,MGR}$ of varanid lizards compared to crocodiles supports McNab [5]. The aggressively predatory varanid lizards have considerably higher field energy expenditures and metabolic rates than most other lizards [5].

Except for *Psittacosaurus*, in all dinosaurs studied $T_{b,MGR}$ values were even higher than assumed under my varanid lizard model. This model was inspired by the energetics model developed by McNab [5] that illustrates the link between food intake and metabolic rate. When assuming that the food intake of the largest herbivorous (carnivorous) mammals defines the maximal rate at which a terrestrial environments' plant resources (vertebrate species) can be consumed, McNab [5] showed that the large size of sauropods (carnivorous theropods) is consistent with a field energy expenditure extrapolated from extant ectothermic varanid lizards. This shows a significantly lower metabolic rate in sauropods and theropods than in extant endothermic mammals and birds. Since body temperature is linked to metabolic rate, the high $T_{b,MGR}$ (compared to extant varanid lizards) of all dinosaurs studied is not in accordance with food intake under an ectothermic metabolism of extant varanid lizard. This could indicate a higher rate of metabolism in dinosaurs than in varanid lizards (as already pointed out in McNab [5]). The observation that $T_{b,MGR}$ is more or less consistent with paleotemperature estimates (20–30°C, [3]) in all dinosaurs studied could eventually question endothermy in these dinosaurs. The latter argument against endothermy in

dinosaurs, however, is based on precise estimates of T_b in dinosaurs, which are unfortunately not derivable from the MGR- T_b -equation.

In total, the high inaccuracy of dinosaurian $T_{b,MGR}$ as evidenced by the application of the MGR- T_b -equation to different extant vertebrate lineages makes a reliable test of the limitation of maximal body size in Dinosauria impossible. Irrespective of this inaccuracy of body temperatures a larger dataset of dinosaurian MGRs than studied by Gillooly et al. [4] provided no support for this hypothesis.

Supporting Information

Table S1 Body mass and body temperature of crocodiles studied.

(XLS)

Table S2 Body mass and body temperature in birds.

(XLS)

Table S3 Body mass and body temperature in mammals.

(XLS)

Table S4 Body mass, maximum growth rate and source of data of reptiles studied.

(XLS)

Table S5 Body mass, maximum growth rate and source of data of dinosaurs studied.

(XLS)

Table S6 Sex, adult mass, estimated maximum daily growth rates and sources of data for several species of Crocodylians.

(DOC)

Table S7 Neonate mass, sex, adult mass, estimated maximum daily growth rates and sources of data for several species of the genus *Varanus*.

(DOC)

Acknowledgments

I'm grateful to two anonymous reviewers for many helpful and insightful comments and to Rebecca Nagel for her linguistic improvement of this manuscript. This is contribution number 154 of the DFG Research Unit 533, "Biology of the Sauropod Dinosaurs".

Author Contributions

Conceived and designed the experiments: EMG. Performed the experiments: EMG. Analyzed the data: EMG. Contributed reagents/materials/analysis tools: EMG. Wrote the paper: EMG.

References

- Colbert EH, Cowles RB, Bogert CM (1947) Rates of temperature increase in dinosaurs. *Copeia* 1947: 141–142.
- Spotila JR, Lommen PW, Bakken GS, Gates DM (1973) A mathematical model for body temperature in large reptiles: Implications for dinosaur ecology. *Am Nat* 107: 391–404.
- Seebacher F (2003) Dinosaur body temperatures: occurrence of endothermy and ectothermy. *Paleobiology* 29: 105–122.
- Gillooly JF, Alleen AP, Charnov EL (2006) Dinosaur fossils predict body temperatures. *PLoS Biology* 4: 1467–1469.
- McNab BK (2009a) Resources and energetics determined dinosaur maximal size. *Proc Natl Acad Sci U S A* 106: 12184–12188.
- Köhler M, Marín-Moratalla N, Jordana X, Aanes R (2012) Seasonal bone growth and physiology in endotherms shed light on dinosaur physiology. *Nature* 487: 358–361.
- Wilkinson DM, Ruxton GD (2003) High C/N ratio (not low-energy content) of vegetation may have driven gigantism in sauropod dinosaurs and perhaps omnivory and/or endothermy in their juveniles. *Func Ecol* 27: 131–135.
- Clarke A, Pörtner H-O (2010) Temperature, metabolic power and the evolution of endothermy. *Biol Rev* 85: 703–727.
- Guderley HE, St Pierre J (1996) Phenotypic plasticity and evolutionary adaptations of mitochondria to temperature. In: Johnston IA, Bennet AF, eds. *Animals and temperature: phenotypic and evolutionary adaptation*, Vol. 59. Cambridge: Cambridge University Press. 127–152.
- Rolfe DFS, Brown GC (1997) Cellular energy metabolism and molecular origin of standard metabolic rate in mammals. *Physiological Reviews* 77: 731–758.
- Lowell BB, Spiegelman BM (2000) Towards a molecular understanding of adaptive thermogenesis. *Nature* 353: 748–750.
- Schmidt-Nielson K (1997) *Animal physiology*. New York: Cambridge University Press. 607p.

13. Willmer P, Stone G, Johnston I (2005) Environmental physiology of animals. Oxford: Blackwell Publishing Ltd. 754p.
14. Pough FH, Andrews RM, Cadle JE, Crump ML, Savitzky AH, et al. (2003) Herpetology. San Francisco: Benjamin Cummings. 736p.
15. Seebacher F, Franklin CE (2005) Physiological mechanisms of thermoregulation in reptiles: a review. *J Comp Physiol B* 175: 533–541.
16. St Pierre J, Charest P-M, Guderley H (1998) Relative contribution of quantitative and qualitative changes in mitochondria to metabolic compensation during seasonal acclimatization of rainbow trout *Oncorhynchus mykiss*. *J Exp Biol* 201: 2961–2970.
17. Lin J-J, Somero GN (1995) Thermal adaptation of cytoplasmic malate dehydrogenase of eastern pacific barracuda (*Sphyræna* spp): the role of differential gene expression. *J Exp Biol* 198: 551–560.
18. Fields PA, Somero GN (1997) Amino acid sequence differences cannot fully explain interspecific variation in thermal sensitivities of gobiid fish A₁-lactate dehydrogenases (A₁-LDHS). *J Exp Biol* 200: 1839–1850.
19. Seebacher F, Guderley H, Eisey RM, Trosclair PL III (2003) Seasonal acclimatization of muscle enzymes in a reptile (*Alligator mississippiensis*). *J Exp Biol* 206: 1193–1200.
20. Crawford DL, Powers DA (1989) Molecular basis of evolutionary adaptation at the lactate dehydrogenase-B locus in the fish *Fundulus heteroclitus*. *Proc Natl Acad Sci U S A* 86: 9365–9369.
21. Crawford DL, Powers DA (1992) Evolutionary adaptation to different thermal environments via transcriptional regulation. *Mol Biol Evol* 9: 806–813.
22. Seebacher F, Sparrow J, Thompson MB (2004) Turtles (*Chelonia longicollis*) regulate muscle metabolic enzyme activity in response to seasonal variation in body temperature. *J Comp Physiol B* 174: 205–210.
23. Seebacher F, Grigg GC, Beard LA (1999) Crocodiles as dinosaurs: Behavioural thermoregulation in very large ectotherms leads to high and stable body temperatures. *J Exp Biol* 202: 77–86.
24. Seebacher F, Grigg GC (1997) Patterns in body temperature in wild freshwater crocodiles, *Crocodylus johnstoni*: Thermoregulation versus thermoconformity, seasonal acclimatization, and the effect of social interactions. *Copeia* 3: 549–557.
25. O'Connor MP, Dodson P (1999) Biophysical constraints on the thermal ecology of dinosaurs. *Paleobiology* 25: 341–368.
26. Montes L, Le Roy N, Perret M, de Buffrenil V, Castanet J, et al. (2007) Relationships between bone growth rate, body mass and resting metabolic rate in growing amniotes: a phylogenetic approach. *Biol J Linn Soc* 92: 63–76.
27. Cubo J, Legendre P, de Ricqlès A, Montes L, de Margerie E, et al. (2008) Phylogenetic, functional, and structural components of variation in bone growth rate of amniotes. *Evolution & Development* 10: 217–227.
28. West GB, Brown JH, Enquist BJ (2001) A general model for ontogenetic growth. *Nature* 413: 628–631.
29. Gillooly JF, Brown JF, West GB, Savage VM, Charnov EL (2001) Effects of size and temperature on metabolic rate. *Science* 293: 2248–2251.
30. Gillooly JF, Charnov EL, West GB, Savage VM, Brown JH (2002) Effects of size and temperature on developmental time. *Nature* 417: 70–73.
31. Andrews RM (1982) Patterns of growth in reptiles. In: Gans C, Pough FH, eds. *Biology of the Reptilia* Vol. 13, Physiology D. New York: Academic Press. 273–320.
32. Case TJ (1978) On the evolution and adaptive significance of postnatal growth rates in the terrestrial vertebrates. *Q Rev Biol* 53: 242–282.
33. Brattstrom BH (1965) Body temperatures in reptiles. *Am Midl Nat* 73: 376–422.
34. Lehman TM, Woodward HN (2008) Modelling growth rates for sauropod dinosaurs. *Paleobiology* 34: 264–281.
35. Sander PM, Klein N, Stein K, Wings O (2011a) Sauropod bone histology and its implications for sauropod biology. In: Klein N, Remes K, Gee CT, Sander PM, eds. *Biology of the Sauropod Dinosaurs: Understanding the Life of Giants*. Bloomington: Indiana University Press. 276–302.
36. Griebeler EM, Klein N, Sander PM (2013) Aging, maturation and growth of sauropodomorph dinosaurs as deduced from growth curves using long bone histological data: an assessment of methodological constraints and solutions. *PLoS ONE* 8(6): e67012. doi:10.1371/journal.pone.0067012.
37. Amiot R, Lécuyer C, Buffetaut E, Escarguel G, Fluteau F, et al. (2006) Oxygen isotopes from biogenic apatites suggest widespread endothermy in Cretaceous dinosaurs. *Earth Planet Sci Lett* 246: 41–54.
38. Eagle RA, Tütken T, Martin TS, Tripathi AK, Fricke HC, et al. (2011) Dinosaur body temperature determined from isotopic (¹³C-¹⁸O) ordering in fossil biominerals. *Science* 333: 443–445.
39. McNab BK (1966) An analysis of the body temperatures of birds. *Condor* 68: 47–55.
40. McNab BK (2008) An analysis of the factors that influence the level and scaling of mammalian BMR. *Comp Biochem Physiol A* 151: 5–28.
41. Dial KP (2003) Evolution of avian locomotion: Correlates of flight style, locomotor modules, nesting biology, body size, development, and the origin of flapping flight. *The Auk* 120: 941–952.
42. Werner J, Griebeler EM (submitted for this collection) Case curves on growth rate and body mass revised: dinosaurs had rather growth rates like ectotherms than endotherms. *PLoS ONE*.
43. Ritz J, Griebeler EM, Huber R, Clauss M (2010) Body size development of captive and free-ranging African spurred tortoises (*Geochelone sulcata*): high plasticity in reptilian growth rates. *Herpetological Journal* 20: 213–216.
44. von Bertalanffy L (1938) A quantitative theory of organic growth. *Human Biology* 10: 181–213.
45. von Bertalanffy L (1957) Quantitative laws in metabolism and growth. *Q Rev Biol* 32: 217–231.
46. Fitzhugh HA (1976) Analysis of growth curves and strategies for altering their shape. *J Anim Sci* 42: 1036–1051.
47. Shine R, Charnov EL (1992) Patterns of survival, growth and maturation in snakes and lizards. *Am Nat* 139: 1257–1269.
48. Frazer NB, Ehrhart LM (1985) Preliminary growth models for Green, *Chelonia mydas*, and Loggerhead, *Caretta caretta*, turtles in the wild. *Copeia* 1: 73–79.
49. Magnusson WE, Sanaïotti TM (1995) Growth of Caiman crocodilus in Central Amazonia, Brazil. *Copeia* 2: 498–501.
50. Eaton MJ, Link WA (2011) Estimating age from recapture data: integrating incremental growth measures with ancillary data to infer age-at-length. *Ecol Appl* 21: 2487–2497.
51. Erickson GM, Curry Rogers K, Yerby SA (2001) Dinosaurian growth patterns and rapid avian growth rates. *Nature* 412: 429–433.
52. Erickson GM, Currie PJ, Inouye BD, Winn AS (2004) Gigantism and comparative life-history parameters of tyrannosaurid dinosaurs. *Nature* 430: 772–775.
53. Erickson GM, Rauhut OWM, Zhou Z, Turner AH, Inouye BD, et al. (2009a) Was dinosaurian physiology inherited by birds? Reconciling slow growth in *Archaeopteryx*. *PLoS ONE* 4(10): doi:10.1371/journal.pone.0007390.
54. Erickson GM, Makovicky PJ, Inouye BD, Chang-Fu Z, Gao K-Q (2009b) A life table for *Psittacosaurus lujiatunensis*: initial insights into ornithischian population biology. *Anat Rec* 292: 1514–1521.
55. Hailey A, Coulson IM (1999) The growth pattern of the African tortoise *Geochelone pardalis* and other chelonians. *Can J Zool* 77: 181–193.
56. Ricklefs RE (1968) Patterns of growth in birds. *Ibis* 110: 419–451.
57. Cooper RG, Mahroze KM (2004) Anatomy and physiology of the gastrointestinal tract and growth curves of the ostrich (*Struthio camelus*). *Anim Sci J* 75: 491–498.
58. Ricklefs RE (1984) The optimization of growth rate in altricial birds. *Ecology* 65: 1602–1616.
59. Gaillard J-M, Pontier D, Allaine D, Loison A, Herve J-C, et al. (1997) Variation in growth form and precocity at birth in eutherian mammals. *Proc R Soc Lond B* 264: 859–868.
60. Zullinger EM, Ricklefs RE, Redford KH, Mace GM (1984) Fitting sigmoidal equations to mammalian growth curves. *J Mammal* 65: 607–636.
61. Seebacher F, Grigg GC (2001) Changes in heart rate are important for thermoregulation in the varanid lizard *Varanus varius*. *J Comp Physiol B* 171: 395–400.
62. James CD (1996) Ecology of the pygmy goanna (*Varanus brevicauda*) in spinifex grasslands of central Australia. *Aust J Zool* 44: 177–192.
63. De Buffrenil V, Hémery G (2002) Variation in longevity, growth, and morphology in exploited Nile Monitors (*Varanus niloticus*) from Sahelian Africa. *J Herpetol* 36: 419–426.
64. Rodbard S (1950) Weight and body temperature. *Science* 111: 465–466.
65. White CR, Seymour RS (2003) Mammalian basal metabolic rate is proportional to body mass 2/3. *Proc Natl Acad Sci U S A* 100: 4046–4049.
66. Clarke A, Rothery P (2008) Scaling of body temperature in mammals and birds. *Funct Ecol* 22: 58–67.
67. Downs CJ, Hayes JP, Tracy CR (2008) Scaling metabolic rate with body mass and inverse body temperature: a test of the Arrhenius fractal supply model. *Funct Ecol* 22: 239–244.
68. Kerkhoff AJ (2012) Modelling metazoan growth and ontogeny. In: Sibly RM, Brown JH, Kodric-Brown A, eds. *Metabolic Ecology. A scaling approach*. Chichester: Wiley-Blackwell. 48–56.
69. Lee AH, Werning S (2008) Sexual maturity in growing dinosaurs does not fit reptilian growth models. *Proc Natl Acad Sci U S A* 105: 582–587.
70. Avery RA (1994) Growth in reptiles. *Gerontology* 40: 193–199.
71. Lance VA (2003) Alligator physiology and life history: the importance of temperature. *Experimental Gerontology* 38: 801–805.
72. White CR, Phillips NF, Seymour RS (2006) The scaling and temperature dependence of vertebrate metabolism. *Biol Letters* 2: 125–127.
73. McNab BK (2009b) Ecological factors affect the level and scaling of avian BMR. *Comp Biochem Physiol A* 152: 22–45.
74. Western D, Ssemakula J (1982) Life history patterns in birds and mammals and their evolutionary interpretation. *Oecologia* 54: 281–290.
75. Ricklefs RE (1979) Adaptation, constraint, and compromise in avian postnatal development. *Biol Rev* 54: 269–290.
76. Sander PM, Christian A, Clauss M, Fechner R, Gee CT, et al. (2011b) Biology of the sauropod dinosaurs: the evolution of gigantism. *Biol Rev Camb Philos Soc* 86: 117–155.

Caudal Pneumaticity and Pneumatic Hiatuses in the Sauropod Dinosaurs *Giraffatitan* and *Apatosaurus*

Mathew J. Wedel^{1*}, Michael P. Taylor^{2*}

1 College of Osteopathic Medicine of the Pacific and College of Podiatric Medicine, Western University of Health Sciences, Pomona, California, United States of America, **2** Department of Earth Sciences, University of Bristol, United Kingdom

Abstract

Skeletal pneumaticity is found in the presacral vertebrae of most sauropod dinosaurs, but pneumaticity is much less common in the vertebrae of the tail. We describe previously unrecognized pneumatic fossae in the mid-caudal vertebrae of specimens of *Giraffatitan* and *Apatosaurus*. In both taxa, the most distal pneumatic vertebrae are separated from other pneumatic vertebrae by sequences of three to seven apneumatic vertebrae. Caudal pneumaticity is not prominent in most individuals of either of these taxa, and its unpredictable development means that it may be more widespread than previously recognised within Sauropoda and elsewhere in Saurischia. The erratic patterns of caudal pneumatization in *Giraffatitan* and *Apatosaurus*, including the pneumatic hiatuses, show that pneumatic diverticula were more broadly distributed in the bodies of the living animals than are their traces in the skeleton. Together with recently published evidence of cryptic diverticula—those that leave few or no skeletal traces—in basal sauropodomorphs and in pterosaurs, this is further evidence that pneumatic diverticula were widespread in ornithomirans, both across phylogeny and throughout anatomy.

Citation: Wedel MJ, Taylor MP (2013) Caudal Pneumaticity and Pneumatic Hiatuses in the Sauropod Dinosaurs *Giraffatitan* and *Apatosaurus*. PLoS ONE 8(10): e78213. doi:10.1371/journal.pone.0078213

Editor: Peter Dodson, University of Pennsylvania, United States of America

Received: April 16, 2013; **Accepted:** September 12, 2013; **Published:** October 30, 2013

Copyright: © 2013 Wedel and Taylor. This is an open-access article distributed under the terms of the Creative Commons Attribution License, which permits unrestricted use, distribution, and reproduction in any medium, provided the original author and source are credited.

Funding: Research for this study was conducted on a field trip sponsored by DFG Research Unit 533: Biology of the Sauropod Dinosaurs; DFG 533 also supported our travel to Germany. The authors thank Martin Sander (University of Bonn) and the organisers and participants of the field trip. The Field Museum of Natural History supported our travel to Chicago. Research at the Carnegie Museum was supported by a grant from the Jurassic Foundation. The funders had no role in study design, data collection and analysis, decision to publish, or preparation of the manuscript.

Competing Interests: The authors have declared that no competing interests exist.

* E-mail: mathew.wedel@gmail.com (MJW); dino@miketaylor.org.uk (MPT)

Introduction

Postcranial skeletal pneumaticity (PSP) is the modification of the postcranial skeleton by pneumatic diverticula of the respiratory system. It is widespread in saurischian dinosaurs including birds, other theropods, and sauropods, and it is also present in pterosaurs. PSP in archosaurs is of interest as a morphogenetic system and source of phylogenetic information [1–3], for its effect in lightening the skeleton [4–8], as the skeletal footprint of the lungs and air sacs [9–17], and as the osteological correlate of a system of pneumatic diverticula, which developed from the lungs and air sacs and may have had important non-respiratory functions [18,19]. The extent of PSP varied greatly among sauropod taxa, among individuals and among regions of the skeleton. Cervical vertebrae are pneumatic in basal eusauropods; cervical, dorsal and sacral vertebrae are pneumatic in mamenchisaurids and most neosauropods; and all of these plus caudal vertebrae are extensively pneumatic in diplodocines and in some titanosaurs [1,4,12,20]. Cervical and dorsal ribs are pneumatic in many, maybe most, titanosauriforms (e.g., [21]: p. 239; [22]: p. 52) and some diplodocids (e.g., [23]: figs. 9–10; 24: p. 212; [25]: p. 534). Pectoral girdle elements are pneumatic in some derived titanosaurs [20], and pneumatization of pelvic girdle elements apparently evolved independently in rebbachisaurid diplodocids [26–27] and somphospondylan macronarians ([20], [28]: p. 233). Most of the elements listed above are also pneumatized in at least some pterosaurs [7], non-avian theropods [13,15], and birds

[6,13,14,29], although caudal pneumaticity has not yet been demonstrated in pterosaurs, and ischial pneumaticity is not yet known in non-avian theropods [27]. The acquisition of PSP in parallel in so many ornithomiran lineages suggests that a diverticular lung and air sac system may be primitive for Ornithomira as a whole [12,15–17].

To date, caudal pneumaticity has received less attention than pneumaticity in other parts of the skeleton (but see [30]), but it is of particular interest because of its possible independent origins and parallel evolution in diplodocids and macronarians. Here we describe complex patterns of caudal pneumaticity in *Giraffatitan brancai* (formerly assigned to the genus *Brachiosaurus*; see [31]) and *Apatosaurus*, and discuss the functional and phylogenetic implications.

Institutional Abbreviations

AMNH, American Museum of Natural History, New York City, New York, USA; **CM**, Carnegie Museum of Natural History, Pittsburgh, Pennsylvania, USA; **DMNH**, Denver Museum of Natural History, Denver, Colorado, USA; **FMNH**, Field Museum of Natural History, Chicago, Illinois, USA; **HMN**, Humboldt Museum für Naturkunde, Berlin, Germany; **KLR**, Henan Geological Museum, Zhengzhou, China; **LACM**, Natural History Museum of Los Angeles County, Los Angeles, California, USA; **MAL**, Malawi Department of Antiquities Collection, Lilongwe and Nguludi, Malawi; **MB.R.**, Museum für Naturkunde Berlin, Berlin, Germany; **MCS**, Museo de Cinco Saltos, Río

Negro Province, Argentina; **MCT**, Collection of the Earth Science Museum of the National Department of Mineral Production, Río de Janeiro; **MIWG**, Museum of Isle of Wight Geology, Sandown, Isle of Wight, United Kingdom; **ML**, Museu da Lourinhã, Portugal; **MN**, Museu Nacional, Rio de Janeiro, Brazil; **MPCA-Pv**, Colección de Paleovertebrados de la Museum Provincial de Cipolletti “Carlos Ameghino”, Cipolletti, Río Negro Province, Argentina; **MPS**, Museo de Dinosaurios e Paleontología, Salas de los Infantes, Burgos, Spain; **MUCPv**, Museo de Geología y Paleontología de la Universidad Nacional del Comahue, Neuquén, Argentina; **NHM**, Natural History Museum, London, United Kingdom; **NMST**, National Science Museum, Tokyo, Japan; **OMNH**, Oklahoma Museum of Natural History, Norman, Oklahoma, USA; **ONM**, Office National Des Mines, Service Patrimoine Géologique, Tunis, Tunisia; **PVL**, Colección de Paleontología de Vertebrados de la Fundación Instituto Miguel Lillo, Tucumán, Argentina; **UNPSJB**, Universidad Nacional de la Patagonia San Juan Bosco, Comodoro Rivadavia, Argentina; **USNM**, National Museum of Natural History, Smithsonian Institution, Washington, D.C., USA; **WDC**, Wyoming Dinosaur Center, Thermopolis, Wyoming, USA; **YPM**, Yale Peabody Museum, New Haven, Connecticut, USA.

Results and Discussion

Overview of pneumatic features

The interaction of pneumatic epithelium and bone tissue produces a spectrum of osteological features, including pneumatic tracks, fossae, foramina, and internal chambers of various shapes and sizes [1,4,9,10,14,32] (**Figure 1**). Not all of these features are diagnostic for pneumaticity in isolation. Pneumatic fossae are particularly problematic: fossae on the surface of vertebrae can be associated with numerous soft tissues, including cartilage, adipose tissue, muscles, and pneumatic diverticula [14]. Although distinctly emarginated and sharply lipped fossae are usually inferred to represent pneumatic invasion [9], apneumatic fossae sometimes have distinct margins and pneumatic fossae sometimes do not [16,17,32]. It is worth noting that vertebral fossae are present in numerous basal and pseudosuchian archosaurus [16,17,33] and in some synapsids (see discussion in [15]: p. 172), and although it is possible that some of these were pneumatic, it is unlikely that all of them were.

In equivocal cases, the diagnosis of a fossa as pneumatic may be strengthened by the presence of other pneumatic features on the same bone [4]. Unequivocally pneumatic fossae (e.g. those containing pneumatic foramina) often have multiple subfossae [17,34], which may represent the resorption of adjacent cortical bone by a complex diverticulum that consists of multiple tubes or sacs, such as the complex diverticula of some birds ([11]: fig. 2). Apneumatic fossae usually have no margins or only weakly developed margins; the only strongly emarginated apneumatic fossae are muscle attachments that are easily identified by their location and texture, such as the temporal fossae of the human skull and the muscle attachment fossae on the ilia of birds. PSP in saurischians is typically variable: the presence and form of pneumatic features varies among individuals, serially along the vertebral column, and even on the left and right sides of a single vertebra (e.g., [35]: p. 1552).

Although fossae are less diagnostic for PSP than more invasive foramina and internal chambers, the differences between pneumatic and apneumatic fossae listed above can be used to develop a profile for distinguishing the two ([9,17]; see also [14]: fig. 12). In descending order of usefulness, pneumatic fossae are expected to (1) occur together with other correlates of PSP, (2) have a scalloped

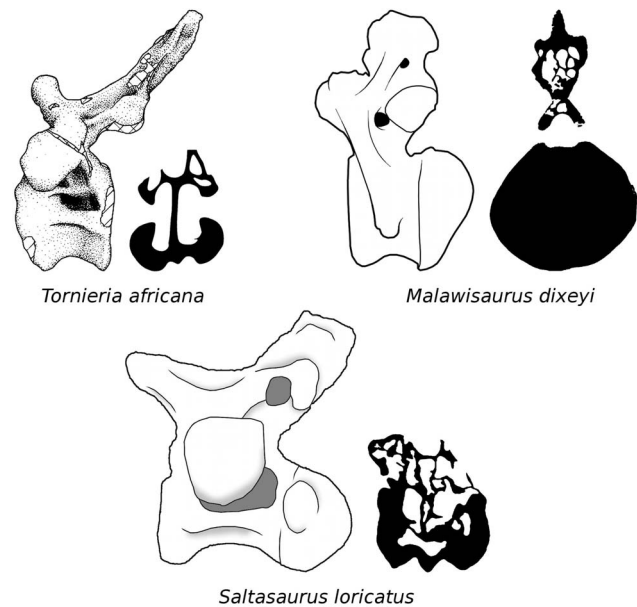


Figure 1. Caudal pneumaticity varies among sauropods. In the diplodocid *Tornieria*, the first 15–20 caudal vertebrae have neural arch laminae and fossae, and lateral pneumatic foramina opening into large internal chambers. Images traced from Remes ([51]: fig. 31 [lateral view]) and Janensch ([72]: fig. 7 [cross-section]); the two views are from different vertebrae. In the basal titanosaurian *Malawisaurus*, caudal pneumaticity is restricted to a handful of proximal caudal vertebrae, in which the neural arches are honeycombed with pneumatic chambers but the vertebral centra are solid. Images traced from Wedel ([12]: fig. 2A [lateral view] and 2C [cross-section]). In the derived titanosaurian *Saltasaurus*, the first 20–25 caudal vertebrae have large external fossae but small external foramina, and both the neural arches and centra are honeycombed with chambers. Images traced from Powell ([59]: plate 53 [lateral view]) and Cerda *et al* [20]: fig. 4F [cross-section]); the two views are from different vertebrae.
doi:10.1371/journal.pone.0078213.g001

texture or subfossae, (3) occur on bone surfaces not occupied by muscle attachments, or in the same locations as pneumatic foramina in related taxa, and (4) vary in expression among individuals, serially along the axial skeleton, and from left to right in single vertebra. There is no reason to assume that putatively pneumatic fossae were originally occupied by some other soft tissue (e.g., muscle, cartilage, or adipose tissue) which was then replaced by pneumatic diverticula that produced more diagnostic bony traces [17], especially given the mounting evidence that a diverticular lung was present in the ancestral saurischian and possibly in the ancestral ornithodiran [12,15–17]. Nevertheless, it is often difficult to tell which fossae may have been pneumatic, especially in basal taxa or those in which the presence of PSP is unexpected or not well established [16].

Caudal pneumaticity in Ornithodira

The phylogenetic distribution of caudal pneumaticity in sauropods and in ornithodirans more generally is complex (**Figure 2**). To date, there are no reports of caudal pneumaticity in pterosaurs. There are several possible explanations for this. Although the presence of PSP in pterosaurs has been widely acknowledged since the mid-1800s (e.g., [36]), and although it has received more attention in recent years (e.g., [7,37]), there has still been less work on pneumaticity in pterosaurs than in sauropods or theropods. So possibly caudal pneumaticity is present in pterosaurs but hasn't been recognized yet. Caudal vertebrae in pterosaurs are

small and at small scale it can be difficult to distinguish pneumatic and vascular foramina, and to tell pneumatic chambers from marrow-filled trabecular bone ([16]: p. 18). It does not help that the pterosaurs with long tails were mostly small-bodied, whereas the large-bodied pterodactyloids had tiny tails. The absolutely small tails of pterosaurs may have created little demand or opportunity for pneumatization, and if any pneumatic traces are present in pterosaur tails they would be difficult to diagnose.

Caudal pneumaticity is uncommon in non-avian theropods. The most comprehensive survey to date is that of Benson *et al* [15], who found caudal pneumaticity in only 12 of the 159 taxa they surveyed. Note, however, that 67 taxa could not be scored, so caudal pneumaticity could be positively ruled out in only half of the sampled taxa (80 out of 159). Only the proximal caudals, if any, are pneumatic in megalosaurids (*Torvosaurus*) and therizinosauroids (*Nothronychus*, *Neimongosaurus*); proximal and middle caudals are pneumatic in some allosauroids (*Aerosteon*, *Megaraptor*, *Carcharodontosaurus*); and proximal, middle, and distal caudals are pneumatic in some—but not all—oviraptorosaurs (*Chiroteles*, *Citipati*, *Khaan*; see fig. 4, table 4, and appendix S1 in [15]). In contrast, caudal pneumaticity is fairly common in extant birds, at least in medium-to-large-bodied taxa: O'Connor [6]: table 2 found caudal pneumaticity in at least some members of 6 out of 10 higher-level clades (mostly corresponding to traditional Linnean orders). In addition to the volant taxa surveyed by O'Connor [6], the large ratites (ostriches, emus, cassowaries, and rheas) all have pneumatic caudals (pers. obs., **Figure 3**).

In general, caudal pneumaticity is common in neosauropods and rare or absent in non-neosauropod sauropodomorphs (**Table 1**). A proximal caudal of '*Bothriospondylus madagascarensis*', NHM 2599, has fossae on the lateral sides of the centrum, but lacks large pneumatic foramina or internal pneumatic chambers [38]. The phylogenetic position of the '*B. madagascarensis*' material is uncertain and it may not all pertain to the same taxon [38]. Mannion [38] suggested that it might best be regarded as a non-neosauropod eusauropod, at least until more complete and diagnostic material comes to light. If NHM 2599 does belong to a eusauropod, it is probably the best documented case of caudal pneumaticity in a non-neosauropod sauropodomorph. Caudal pneumaticity has not been reported in the Mamenchisauridae, a clade which otherwise shows some derived pneumatic features, including complex pneumatic chambers in the cervical vertebrae [39].

The first caudal vertebra of *Haplocanthosaurus* CM 879, has pneumatic fossae on both the centrum and the neural arch ([40]: plate 2; [12]: figs. 7 and 9). The phylogenetic position of *Haplocanthosaurus* is uncertain; it has been recovered as a basal diplodocoid [41], a basal macronarian [22,42], and a non-neosauropod close to the origin of Neosauropoda [43] in different analyses, although recent analyses tend to support a position within Diplodocoidea [25,44]. Here we regard it as a neosauropod of uncertain affinities (**Figure 2**); moving it into either Diplodocoidea or Macronaria would have no great effect on the phylogenetic distribution of caudal pneumaticity in sauropods. In more derived diplodocoids, caudal pneumaticity is present in rebbachisaurids and diplodocids but apparently absent in dicraeosaurids (see [45]). In rebbachisaurids the neural arches and transverse processes of the proximal caudals often have pronounced laminae and deep, irregular fossae characteristic of pneumaticity ([46]: figs. 1-3; [47]), and pneumatic foramina leading to large internal chambers are present in at least the proximal caudals of the rebbachisaurid *Tataouinea* (the middle and distal caudals are as yet unknown) [27]. The same is true in diplodocids, and in diplodocines such as *Diplodocus*, *Barosaurus*, and

Torniera, these pneumatic foramina persist down to caudal 15 or 20 (48: fig. 13; [49]: p. 35 and plate 9; [50]: p. 54 and fig. 2.6; [51]: fig. 3). Although some authors have reported pneumatic features in the most proximal caudal vertebrae of *Apatosaurus* (e.g., [52,53]), pneumatic features have not previously been observed further back than the fifth caudal vertebra; below we report isolated pneumatic fossae more distally in the tail.

Pneumaticity is absent in the caudal vertebrae of *Camarasaurus* (see [54]: plates 74–77) but caudal pneumaticity is otherwise prevalent in Macronaria. Pneumatic fossae have been reported in the caudals of the brachiosaurids *Cedarosaurus* [55] and *Venosaurus* [56], and Janensch [57] briefly mentioned fossae in proximal caudal vertebrae in three specimens of *Giraffatitan* (discussed in more detail below). Below, we describe additional pneumatic fossae distributed unevenly through the tail in another specimen of *Giraffatitan*. Caudal pneumaticity is also widespread in Titanosauria ([30]; **Table 1**), with *Opisthocoelicaudia* being one of the few titanosaurs that appears to lack caudal pneumaticity (see [58]: plates 4–5). Caudal pneumaticity reached its apex among sauropods in the saltasaurines *Rocasaurus*, *Neuquensaurus*, and *Saltasaurus*, as did appendicular pneumaticity [20]. Known saltasaurines are uniformly small, with femur lengths well under one meter [59–61]—compare to femur lengths of 1–1.2 meters in dicraeosaurids and 1.5–2.0 meters in most other neosauropods ([62]: table 1). It is not yet clear why PSP, which is suspected to have been a key innovation in facilitating the evolution of large body size in sauropods [63], achieved its maximum expression in these small-bodied taxa.

Caudal pneumaticity in *Giraffatitan*

Caudal vertebrae of *Giraffatitan* personally examined by us in this study are listed in **Table 2**, and described below.

MB.R.5000 ('Fund no', Figures 4 and 5). The mounted skeleton of *Giraffatitan brancai* at the Humboldt Museum für Naturkunde Berlin consists primarily of elements of the paratype, MB.R.2181 (formerly cataloged as HMN SII), but missing parts of the skeleton were provided from the remains of other similarly sized individuals [64]. The tail of the mounted skeleton, MB.R.5000 (formerly HMN 'Fund no'), consists of the second to fifty-first caudal vertebrae, "not articulated, with the exception of a few at the end, but altogether relatively in sequence" ([57]: p. 64, plate IV; **Figure 6**). The first caudal vertebra was not recovered, and it is modeled in plaster in the mounted skeleton. The preserved caudals are discussed in groups of serially adjacent vertebrae based on pneumatic characters.

MB.R.5000 ('Fund no'): Caudal vertebrae 2–7. All of these vertebrae have fossae on the right side of the centrum, and all but Ca4 and Ca7 also on the left. The fossae of these vertebrae are all located ventral to the transverse processes on the dorsolateral faces of the centra. Some of the fossae are multipartite; that is, divided into subfossae by bony septa. Fossae are absent from the neural arches and spines. Caudals 4 and 7 have fossae only on the right side of the centrum: similar asymmetry in the expression of pneumatic fossae is present in the sacrum of the CM 879 specimen of *Haplocanthosaurus* [12].

MB.R.5000 ('Fund no'): Caudal vertebrae 8–10. Although these vertebrae present a series of intermediate forms relative to the vertebrae anterior and posterior to them, and all are deeply waisted, they have no apparent pneumatic features on their centra, neural arches, or neural spines. As there are obvious traces of pneumaticity in caudal vertebrae 11–15 (see below), pneumatic diverticula must have passed by these vertebrae and may even have been in contact with the bone, but they left no macroscopic traces. It is possible that correlates of PSP might be found in the

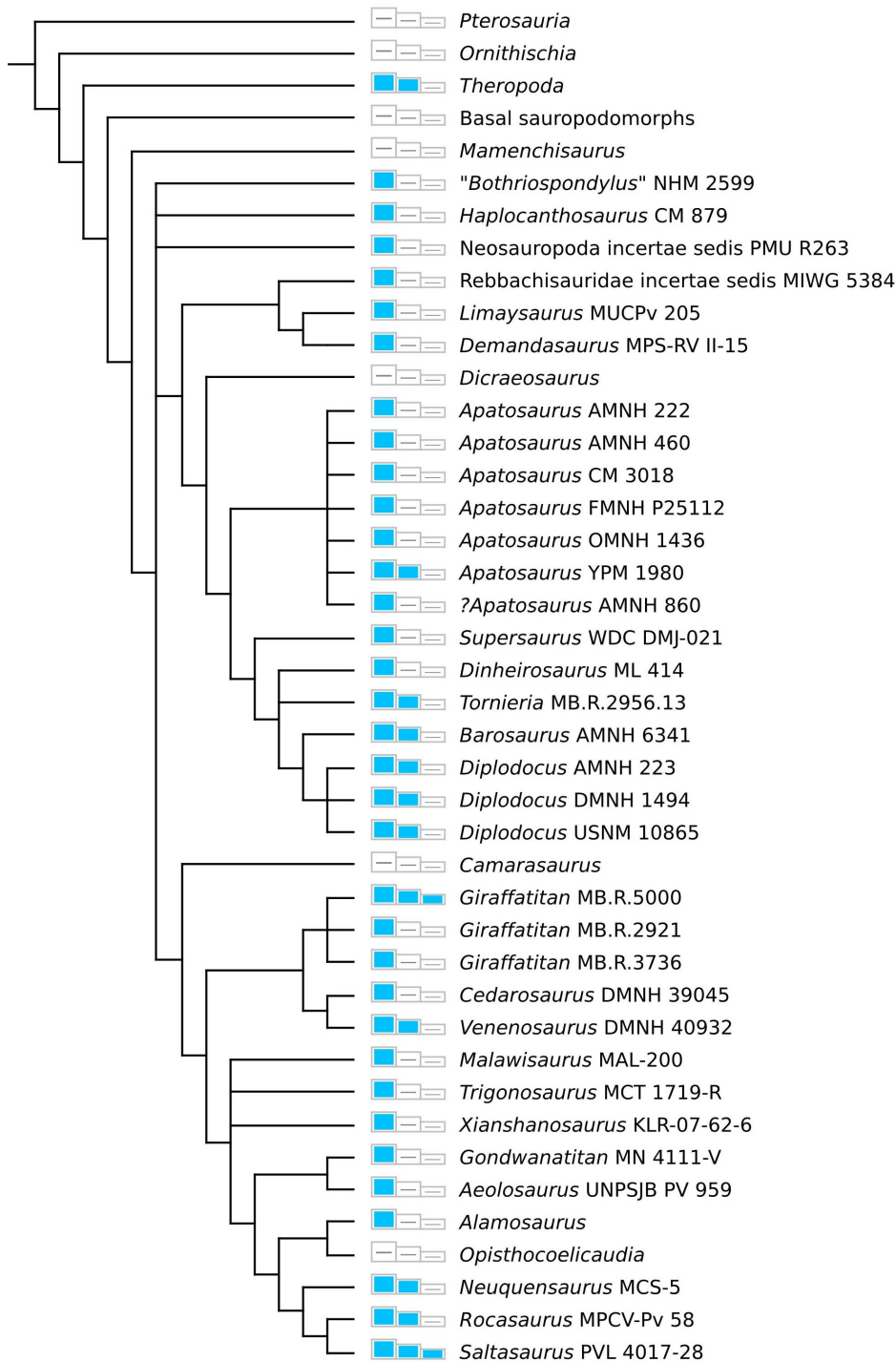


Figure 2. The phylogenetic distribution of caudal pneumaticity in sauropods and other dinosaurs is complex. Boxes represent proximal, middle, and distal caudal vertebrae, arbitrarily defined for sauropods as caudals 1–10, 11–20, and 21 on, respectively; blue boxes indicate that pneumaticity is present in that part of the tail. Pneumaticity data for theropods come from Benson *et al* [15]—note that although Theropoda is collapsed to a single node in this figure, caudal pneumaticity is not primitive for the clade, but evolved independently several times in both non-avian theropods and birds [6,15,29]. Data from sauropods come from the sources listed in Table 1. The figure also shows the phylogenetic framework we use in this paper. The phylogenetic framework is drawn from Whitlock [44] for diplodocoids, Mannion *et al* [30] for basal macronarians and *Xianshanosaurus*, Calvo *et al* [96] for most titanosaurs, and Campos *et al* [93] for *Trigonosaurus*. Basal sauropodomorphs are a grade, not a clade, but they are listed together here for convenience since they all lack caudal pneumaticity. doi:10.1371/journal.pone.0078213.g002

bone microtexture or histology of these vertebrae, but such correlates have not been identified to date in any vertebrae so resolution of this question must wait. This block of three vertebrae

is bounded anteriorly and posteriorly by pneumatic vertebrae and thus constitutes a pneumatic hiatus [11,12]; the implications of this hiatus are explored below.



Figure 3. The caudal vertebrae of ostriches are highly pneumatic. This mid-caudal vertebra of an ostrich (*Struthio camelus*), LACM Bj342, is shown in dorsal view (top), anterior, left lateral, and posterior views (middle, left to right), and ventral view (bottom). The vertebra is approximately 5cm wide across the transverse processes. Note the pneumatic foramina on the dorsal, ventral, and lateral sides of the vertebra.
doi:10.1371/journal.pone.0078213.g003

MB.R.5000 ('Fund no'): Caudal vertebrae 11–15. All of these vertebrae have pneumatic fossae, and the distribution and morphology of these fossae is considerably more complex than in caudals 2–7. The most obvious difference between these ranges is that those in the posterior range have pneumatic fossae on both the centrum and neural arch, whereas more anteriorly fossae are present only on the centrum. Caudal vertebra 11 has fossae on both sides of the neural arch, and these fossae are weakly subdivided by bony septa. No fossae are apparent on either side of the centrum. Caudal vertebra 12 has the most complex pneumatic features of any vertebra in the entire tail, with multipartite fossae on both sides of the centrum and both sides of the neural arch. Caudal vertebra 13 has a very large fossa on the right side of the centrum, which in its size and form approximates the large pneumatic fossae or “pleurocoels” in the dorsal vertebrae of more basal taxa like *Haplocanthosaurus*. A small subdivided fossa is also present on the right side of the neural spine. Pneumatic features are absent from both the centrum and neural arch on the left side. Caudal 13 is therefore similar to caudals 4 and 7 in having pneumatic features present only on the right side. Caudal 14 has large pneumatic fossae on both sides of the centrum, and a smaller multipartite fossa on the right side of the neural arch. Caudal 15 has a pair of pneumatic fossae on the left side of the centrum, but no fossae on the neural arch or anywhere on the right side of the vertebra. This is the first vertebra in the series in which PSP is present only on the left side; all of the previous vertebrae that are unilaterally apneumatic (caudals 4, 7 and 13) have their fossae on the right side.

MB.R.5000 ('Fund no'): Caudal vertebrae 16–18. These three vertebrae, like caudals 8–10, are deeply waisted but lack distinct fossae. They constitute a second bilateral pneumatic hiatus.

MB.R.5000 ('Fund no'): Caudal vertebrae 19–24. These six vertebrae again present a complex suite of pneumatic features. Caudals 19, 21, and 23 have pneumatic fossae only on the left side, like caudal 15, whereas caudals 20, 22, and 24 have pneumatic fossae on both sides of the centrum. Caudal 22 has a multipartite

fossa on the right side, on the border between the centrum and neural arch; fossae are otherwise absent from the neural arches and spines of all six vertebrae. In contrast, pneumatic fossae on the centra of these six vertebrae are better defined than in almost all of the preceding vertebrae, with the fossae of caudals 20, 22, and 24 being particularly large, deep, and well subdivided.

MB.R.5000 ('Fund no'): Caudal vertebrae 25–51. No obvious pneumatic features are present on any of these vertebrae. The vertebrae that make up the last 26 cm of the tail (i.e. from caudal 52 on) were not recovered and are reconstructed in plaster in the mounted skeleton ([64]: p. 98). We assume that the missing vertebrae were also apneumatic, based on the absence of pneumaticity in the preceding 27 vertebrae and in the distal tails of all other known non-avian saurischians.

MB.R.2921 ('Fund Aa', Figure 7). MB.R.2921 ('Fund Aa') consists of the first 18 caudal vertebrae and their chevrons, found in an articulated sequence behind the last sacral vertebra ([57]: p. 60). Regarding possible pneumatic features, Janensch ([57]: p. 61) wrote, “Pleurocentral excavations are absent; only under the root of the transverse process of the second is an elongated, about four centimeter long depression clearly developed, particularly on the right.” We have confirmed that small fossae are present on both sides of the centrum in the second caudal, and that they are absent from the first caudal. These fossae are similar to those found in the first pneumatic block (caudals 2–7) of MB.R.5000 ('Fund no'; see above). Fossae are absent on the neural arch of the second caudal, and in all the other caudal vertebrae that make up the specimen. The first caudal vertebra of MB.R.2921 ('Fund Aa') therefore constitutes another (short) pneumatic hiatus.

MB.R.3736 ('Fund D'). MB.R.3736 ('Fund D') includes 31 caudal vertebrae, of which caudals 1–23 were found in articulation, with the rest associated. According to Janensch ([57] p. 63), “As in Aa [MB.R.2921], a short and narrow cavity is present below the transverse process of only the second vertebra.” We confirmed that fossae are present on both sides of the centrum in caudal 2 but absent in caudals 1 and 3. This specimen therefore also contains a pneumatic hiatus.

Caudal vertebrae from the G1 quarry. Janensch ([57]: p. 66) reported: “The site G1 in the Middle Saurian Marl has yielded weathered remains of *Brachiosaurus* [= *Giraffatitan*], portions of extremity bones, and centra from various regions of the tail. Among 15 complete and 6 half centra, one (G1 4), with ample 25-cm-high posterior end surfaces, distinguishes itself as the second caudal vertebra by its extraordinarily wide ventral surface. It possesses, in accordance with tails Aa and D [MB.R.2921 and 3736], a small lateral depression that is, however, much more clearly formed.” We were unable to locate this vertebra but the distribution of pneumaticity described by Janensch is consistent with MB.R.2921 ('Fund Aa') and MB.R.3736 ('Fund D').

Summary of caudal pneumaticity in *Giraffatitan*

Patterns of PSP along the tail. The pattern of pneumatization along the MB.R.5000 ('Fund no') tail is more complex than in any other known dinosaur (Figure 8). PSP varies serially along the tail, from the left to the right side in many of the vertebrae, between the centra and neural arches, and in complex combinations of all three parameters. Proceeding serially from the first preserved vertebrae (caudal 2), there is a block of six pneumatic vertebrae, followed by a bilateral pneumatic hiatus of three vertebrae, then a block of five pneumatic vertebrae, then a second bilateral pneumatic hiatus of three vertebrae, a final block of six pneumatic vertebrae, and finally the apneumatic remainder of the tail. Caudals 2–24 may be considered the total pneumatic domain of the tail, in which skeletal pneumaticity is often but not always

Table 1. Most posterior pneumatic caudal vertebra in several sauropods.

Clade	Genus	Specimen	Caudal # ^a	Reference
Eusauropoda	<i>'Bothriospondylus'</i>	NHM 2599	proximal	[38]
Neosauropoda	<i>Haplocanthosaurus</i>	CM 879	1	[12]
	Neosauropoda incertae sedis	PMU R263	proximal	[87]
Rebbachisauridae ^b	<i>Demandsaurus</i>	MPS-RV II-15	proximal	[47]
	<i>Limaysaurus</i>	MUCPv 205	proximal	[46]: fig. 3
	<i>Tataouinea</i>	ONM DT 1-36	proximal	[27]
	Rebbachisauridae incertae sedis	MIWG 5384	proximal	[46]: figs. 1-2
	Rebbachisauridae incertae sedis	NHM R36636	proximal	[88]
Diplodocidae	<i>Apatosaurus</i>	AMNH 222	proximal	[74]
		AMNH 460	5	[53]: 188
		CM 3018	3	pers. obs.
		FMNH P25112	5	[53]: 189
		OMNH 1436	proximal	pers. obs.
		YPM 1980	13	pers. obs.
	? <i>Apatosaurus</i>	AMNH 860	proximal	pers. obs.
	<i>Dinheirosaurus</i>	ML 414	proximal	[89]
	<i>Supersaurus</i>	WDC DMJ-021	proximal	[25]
	<i>Barosaurus</i>	AMNH 6341	14	pers. obs.
		YPM 429	17 or 19	[50,90]
	<i>Diplodocus</i>	AMNH 223	18	[48]
		DMNH 1494	16	pers. obs.
		USNM 10865	19	[65]
	<i>Tornieria</i>	MB.R.2956.13	middle	[51]
Brachiosauridae	<i>Giraffatitan</i>	MB.R.2181	24	pers. obs.
		MB.R.2921	2	pers. obs.
		MB.R.3736	2	pers. obs.
		'Fund G1'	2	[57]
	<i>Cedarosaurus</i>	DMNH 39045	proximal	[55]
	<i>Venenosaurus</i>	DMNH 40932	middle	[56]
Titanosauria	<i>Malawisaurus</i>	MAL-200	proximal	[12]
	<i>Gondwanatitan</i>	MN 4111-V	?3	[91]
	<i>Aelosaurus</i>	UNPSJB PV 959	proximal	[92]
	<i>Trigonosaurus</i>	MCT 1719-R	?2	[93]
	<i>Xianshanosaurus</i>	KLR-07-62-06	proximal	[94]
	<i>Alamosaurus</i>	(unspecified)	proximal	[95]
	<i>Rocasaurus</i>	MPCV-Pv 58	middle	[20]
	<i>Neuquensaurus</i>	MCS-5	middle	[20]
	<i>Saltasaurus</i>	PVL 4017-28	distal	[20]

^aIn several specimens the precise serial position is unknown; in these cases the approximate location in the tail is given as proximal (caudals 1–10), middle (caudals 11–20), or distal (caudals 21 and higher).

^bFor more discussion on caudal pneumaticity in rebbachisaurids, see [46] and [88].

doi:10.1371/journal.pone.0078213.t001

present. Asymmetrically pneumatic vertebrae in the anterior half of the domain are apneumatic on the left but never on the right, whereas in the posterior half they are apneumatic on the right but never on the left. The last vertebra that is pneumatic only on the right is caudal 13, and the first vertebra that is pneumatic only on the left is caudal 15, so the switch between these two regions of asymmetric pneumatization occurs in the middle of the second block of pneumatic vertebrae rather than at one of the pneumatic hiatuses.

The *a priori* expectation based on caudal pneumatization in diplodocids [48–50,65] is that PSP would be best developed in the anterior caudals and pneumatic features would diminish monotonically in successively posterior vertebrae. However, this is not the case in MB.R.5000 ('Fund no'). Except for a fossa in caudal 22 that encroaches on the right side of the neural arch, pneumaticity of the neural elements is found only in four adjacent vertebrae (caudals 11–14) in the second pneumatic block. Furthermore,

Table 2. Caudal vertebrae of *Giraffatitan* in the Museum für Naturkunde Berlin personally examined by us in this study.

Specimen	Field #	Caudal #	Pneumatic?	Fossae and Foramina
MB.R.5000 ^a	no	2–51	Yes	scattered fossae to Ca24
MB.R.2921	Aa	1–18	Yes	fossae only on Ca2
MB.R.3736	D	1–31	Yes	fossae only on Ca2
MB.R.3748	dd	middle caudal	No	
MB.R.3786	St 10	middle caudal	No	
MB.R.3787	St 274	middle caudal	No	
MB.R.4029 ^b	P	proximal centrum	No	
uncatalogued	G1	proximal series	Yes	fossae reported in Ca2 by [57] ^c
MB.R.3450 ^d	?	proximal centrum	No	
MB.R.4030	?	middle caudal	No	
MB.R.4038	?	proximal centrum	No	
MB.R.4041	?	proximal centrum	No	neurovascular foramina only

^aMB.R.5000 ('Fund no') is incorporated into the famous mounted skeleton with MB.R.2181.

^bMB.R.4029 may pertain to *Janenschia* rather than *Giraffatitan*, but as it shows no evidence of pneumaticity it does affect our findings.

^cWe were unable to locate the pneumatic vertebra from site G1 reported by [57], although we did examine several apneumatic vertebrae from the site. We were also unable to locate the vertebrae from site Y.

^dMB.R.3450 might be part of the caudal series from site G1.

doi:10.1371/journal.pone.0078213.t002

fossae on the lateral sides of the centra are best developed in the most posterior pneumatic block, caudals 19–24.

The combination of an apneumatic first caudal and pneumatic second caudal is found in at least two specimens, MB.R.2921 ('Fund Aa') and MB.R.3736 ('Fund D'). Janensch described a similar pattern in the vertebrae from the G1 quarry [57], although we were unable to relocate the presumed second caudal with the pneumatic fossae. Although the first caudal of MB.R.5000 ('Fund no') is missing, the preserved material is consistent with the same

pattern. It will be interesting to see if this pattern holds as the skeletons of more brachiosaurs are discovered in the future.

The differing extent of caudal pneumatization between MB.R.5000 ('Fund no') on one hand and MB.R.2921 ('Fund Aa') and MB.R.3736 ('Fund D') on the other is striking. With so few samples, the cause of the difference is unclear; it could represent ontogenetic or phylogenetic changes or intraspecific variation. MB.R.5000 ('Fund no') represents a slightly larger individual than either of the other specimens, and it might have been more mature. However, it would be unusual to have such a large change in the pneumatic domain so late in ontogeny. Taylor [31,66] has argued on the basis of Migeod's specimen [67] that

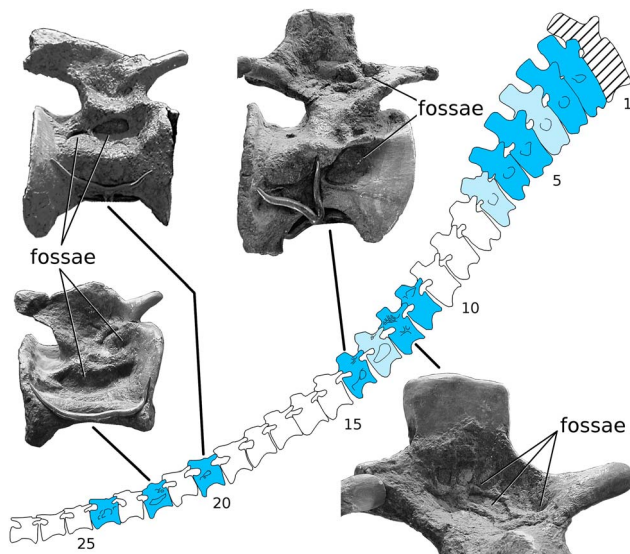


Figure 4. *Giraffatitan brancai* tail MB.R.5000 ('Fund no') in right lateral view. Dark blue vertebrae have pneumatic fossae on both sides, light blue vertebrae have pneumatic fossae only on the right side, and white vertebrae have no pneumatic fossae on either side. The first caudal vertebra (hatched) was not recovered and is reconstructed in plaster.

doi:10.1371/journal.pone.0078213.g004

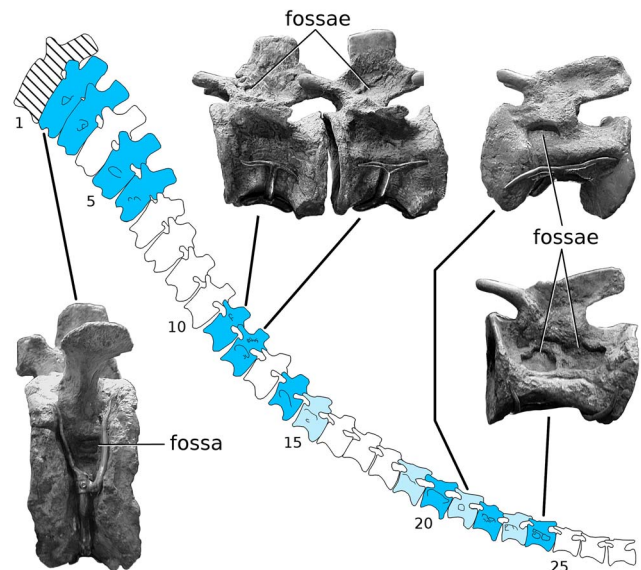


Figure 5. *Giraffatitan brancai* tail MB.R.5000 ('Fund no') in left lateral view. Shading conventions follow Figure 4, with light blue vertebrae having pneumatic fossae only the left side.

doi:10.1371/journal.pone.0078213.g005



Figure 6. The ‘Fund no’ quarry at Tendaguru preserved a tail of *Giraffatitan* with the vertebrae roughly in order. The series of caudal vertebrae catalogued as MB.R.5000 and incorporated in the famous mounted skeleton of *Giraffatitan* are visible near the bottom of the photo. The photo appears courtesy of the Museum für Naturkunde Berlin.

doi:10.1371/journal.pone.0078213.g006

there is more than one brachiosaurid taxon present in the Tendaguru Formation. It is possible that the variation in caudal pneumaticity between MB.R.5000 (‘Fund no’) and the other Tendaguru brachiosaur specimens carries a phylogenetic signal. For now, though, we assume that all the Tendaguru brachiosaur tails belong to *Giraffatitan*. Pneumatic diverticula show high levels of intraspecific variation in many clades and in different parts of

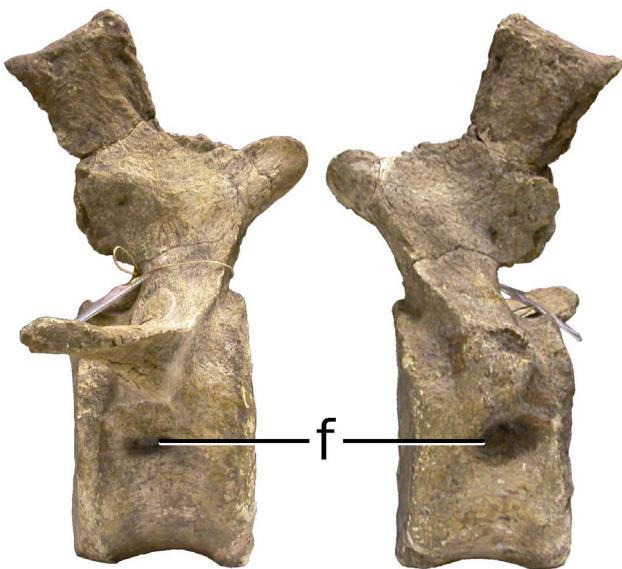


Figure 7. Pneumatic fossae are present only in the second caudal vertebra in several specimens of *Giraffatitan*. Caudal vertebra 2 from the MB.R.2921 (‘Fund Aa’) is shown here in right lateral (left) and left lateral (right) views. Small pneumatic fossae (f) are present on both sides of the centrum, but absent in the rest of the tail. The same pattern of pneumaticity is present in MB.R.3736 (‘Fund D’) and, according to Janensch [57], in the caudal series from the ‘Fund G1’ quarry.

doi:10.1371/journal.pone.0078213.g007

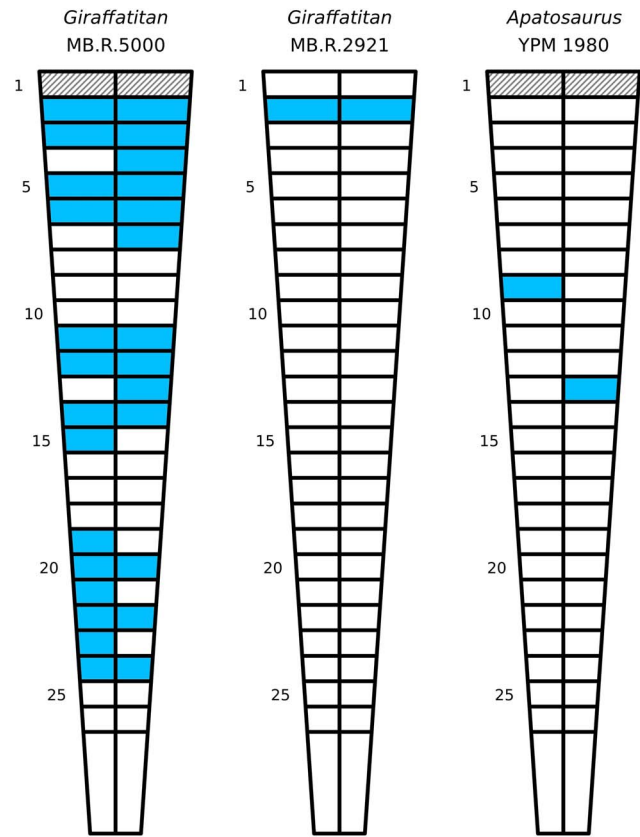


Figure 8. Patterns of caudal pneumaticity in *Giraffatitan* and *Apatosaurus* are complex and frequently include pneumatic hiatuses. Shading conventions follow Figure 4. The intermittent unilateral and bilateral pneumatic hiatuses (i.e., gaps in pneumatization) in *Giraffatitan* MB.R.5000 (‘Fund no’) contrast sharply with the very restricted pneumaticity in MB.R.2921 (‘Fund Aa’) and the isolated pneumatic features in *Apatosaurus* YPM 1980. YPM 1980 has the longest pneumatic hiatuses, unilaterally and bilaterally, that we have found to date in any dinosaur.

doi:10.1371/journal.pone.0078213.g008

the body (e.g., [68–70]), and the seemingly erratic patterns of PSP discussed here could simply represent variation within a population. At least, intraspecific variation is the closest to a null hypothesis among these alternatives.

Comparisons to other sauropods. *Giraffatitan* MB.R.5000 (‘Fund no’) is remarkable in having PSP farther posteriorly in its vertebral column than almost any other known sauropod, out to caudal 24. The only other taxa with PSP so far down the tail are saltosaurine titanosaurs: Cerda *et al* ([20]: fig. 4) illustrate pneumaticity down to caudal 25 in *Saltasaurus*. Furthermore, *Giraffatitan* MB.R.5000 (‘Fund no’) has a much larger proportion of its tail pneumatized than the diplodocines. Janensch ([64]) reconstructed *Giraffatitan* with only 55 caudal vertebrae, whereas diplodocines have long caudal series of up to 80 vertebrae ([24]: p. 204). Diplodocines therefore pneumatized only the anterior one quarter of the caudal vertebrae, whereas in *Giraffatitan* PSP is found almost halfway down the caudal series. The situation in saltosaurines is unclear; although rod-like distal caudals were present in some saltosaurines [71], none have been found associated with the same skeletons that preserve extensive caudal pneumaticity. Cerda *et al* ([20]: fig. 4) illustrate between 40 and 50 caudal vertebrae in *Saltasaurus*, in which case PSP was present in 50–60% of the caudal vertebrae.

That Janensch did not mention the numerous pneumatic features in MB.R.5000 ('Fund no') is puzzling, given his extensive discussions of PSP elsewhere [57,72]. From his writing he seems to have considered the anterior and middle caudal vertebrae to be best represented by MB.R.2921 ('Fund Aa') and MB.R.3736 ('Fund D'), respectively, and he valued MB.R.5000 ('Fund no') mainly as a source of information about the morphology of distal caudal vertebrae, which were not preserved in the other specimens and which lack pneumatic fossae.

Caudal pneumaticity in *Apatosaurus*

Although the caudal vertebrae of *Apatosaurus* have been scored as lacking pneumatic fossae or foramina in phylogenetic analyses (e.g., [41]: character 119; [42]: character 181; [73]: character 170), caudal pneumatic features have been documented in the literature for several specimens.

In his description of the "*Brontosaurus*" (now *Apatosaurus*) *excelsus* holotype YPM 1980, the earliest adequate description of any *Apatosaurus* material, Marsh ([52]: p. 417) wrote that "the first three caudals are lightened by excavations in their sides", and expanded on this saying that "the three vertebrae next behind the sacrum [meaning caudals 1–3] have moderate sized cavities between the base of the neural arch and the transverse processes. These shallow pockets extend into the base of the processes" ([52]: p. 420).

Riggs ([53]: p. 188) observed of AMNH 460 that "the number of anterior [caudal] vertebrae having lateral cavities in the centra is five in the Museum specimen" and noted that in the first caudal of his own specimen FMNH P25112 "the interior of the centrum contains numerous small cavities, the pedicles are hollow [...] the prezygapophyses [...] are excavated at their bases by deep lateral fossae". He further observed that in the first caudal, "two sets of cavities occur in the centra of the anterior caudal vertebrae, the first above and the second below [...] the root of the caudal rib. [...] The lateral cavities in the centra persist as far back as caudal V in this specimen" ([53]: p. 189). We have confirmed these observations (**Figure 9**). Riggs ([53]: p. 189) was also first to note the unpredictable distribution of pneumatic features in the tail: "these cavities cannot be regarded as constant characteristics, as they are sometimes present on one side and absent on the other."



Figure 9. Pneumatic fossae are present in the proximal caudal vertebrae in many specimens of *Apatosaurus*. Here the first part of the tail of FMNH P25112, the mounted *Apatosaurus* skeleton in Chicago, is shown in left lateral view.
doi:10.1371/journal.pone.0078213.g009

AMNH 222 includes some dorsal, sacral, and caudal vertebrae, originally considered to belong to *Camarasaurus* [74] but since 1900 universally regarded as pertaining to *Apatosaurus*, and in fact incorporated into the mounted skeleton of *Apatosaurus* at the AMNH ([75]: 70; [76]: 375). The proximal caudal vertebrae have complex pneumatic fossae on the neural spines ([74]: fig. 5) and transverse processes ([74]: figs. 3 and 4), and the third caudal vertebra has a prominent pneumatic fossa on the left side of the centrum ([74]: fig. 5).

Gilmore ([24]: p. 203–209), in his detailed discussion of the caudal vertebrae of the *Apatosaurus louisae* holotype CM 3018, surprisingly did not describe any pneumatic features. However, our personal observations show that pneumatic fossae are present on the first three caudals.

Upchurch *et al* [77] reported no caudal pneumaticity in *Apatosaurus ajax* NMST-PV 20375, and wrote, "All caudal centra are solid with no lateral depressions or pleurocoels" ([77]: p. 42). Shallow lateral depressions are illustrated in the anterior caudals ([77]: pl. 5), but these may represent waisting of the vertebrae rather than pneumatic invasion of the bone (see [32]: pp. 212–213 for further discussion of waisting versus pneumatization).

YPM 1980. In our own examination of the mounted *Apatosaurus excelsus* skeleton YPM 1980, we have been unable to locate the lateral excavations described by Marsh. This is surprising because, although many elements of this skeleton were over-enthusiastically "restored" with plaster, obscuring genuine osteological features, the caudal centra after the first are an exception to this, and the bone of the vertebrae, particularly on the right side, is in good condition. The centra of the first dozen or so caudals do feature irregularly positioned lateral foramina (pers. obs., [76]: plates 33–35), but these are very small – less than 1 cm in diameter – and are almost certainly neurovascular rather than pneumatic. It seems unlikely that Marsh was referring to these, especially as they persist long after the first three caudals, but no other features of the bone can be interpreted as matching his description. Much more convincing, however, are two isolated lateral fossae: one on the left side of caudal 9, the other on the right side of caudal 13 (**Figure 10**). Both of these are much larger than the aforementioned foramina – about 6 cm across – and have distinct lips. There is absolutely no trace of similar fossae in any of the other caudals, so these fossae represent a bilateral pneumatic hiatus of at least seven vertebrae (since caudal 1 is extensively reconstructed and may have had pneumatic fossae that cannot be observed) and a unilateral hiatus (on the right side) of at least eleven vertebrae.

Implications for the development of PSP and its recognition in fossil taxa

Two characteristics of the caudal pneumaticity in *Giraffatitan* and *Apatosaurus* deserve special comment. The first is that the development of pneumatic fossae varies strongly among individuals. MB.R.5000 ('Fund no') has numerous distinct, multipartite fossae scattered on the anterior and middle caudal vertebrae, whereas in MB.R.2921 ('Fund Aa'), MB.R.3736 ('Fund D'), and the vertebrae from the G1 quarry, caudal pneumaticity is limited to small fossae on the lateral faces of the second caudal centrum. Similarly, YPM 1980 has pneumatic fossae much farther down the tail than in any other known specimen of *Apatosaurus*. The variability of pneumatic traces within the single individuals *Giraffatitan* MB.R.5000 ('Fund no') and *Apatosaurus* YPM 1980 is also surprising. PSP is not expressed consistently down the tail, and vertebrae with pneumatic fossae are separated by blocks of vertebrae with no traces of pneumaticity. This inter- and intra-individual variation has several important implications:



Figure 10. An isolated pneumatic fossa is present on the right side of caudal vertebra 13 in *Apatosaurus excelsus* holotype YPM 1980. The front of the vertebra and the fossa are reconstructed, but enough of the original fossil is visible to show that the feature is genuine.
doi:10.1371/journal.pone.0078213.g010

Pneumatic diverticula were more widespread than their skeletal traces directly indicate. This is not a new insight: in extant birds pneumatic diverticula pass under the skin, in between the muscles, and among the viscera, and only a few of these diverticula leave traces on the skeleton [78]. But it presents a particular problem for paleobiologists because in most cases skeletal evidence is all that we have to work with. Pneumatic hiatuses are present in several articulated caudal series of *Giraffatitan*. The apneumatic first caudal vertebrae of MB.R.2921 ('Fund Aa') and MB.R.3736 ('Fund D') represent pneumatic hiatuses of one vertebra each, similar to the pneumatic hiatus in the fifth sacral of *Haplocanthosaurus* CM 879 [12]. In MB.R.5000 ('Fund no') the pneumatic caudal vertebrae are interrupted by two bilateral pneumatic hiatuses each of three vertebrae. The tail of *Apatosaurus* YPM 1980 has the longest pneumatic hiatus we have found to date—at least seven vertebrae bilaterally, and at least eleven vertebrae unilaterally. Presumably the tails of these sauropods were pneumatized by diverticula of abdominal air sacs which spread distally along the tail during development. Caudal pneumatic hiatuses show that pneumatic diverticula are capable of "leapfrogging" over single vertebrae and even sequences of multiple vertebrae without leaving any diagnostic skeletal traces.

As mentioned above, pneumatic diverticula that leave no traces on the skeleton are common in birds. Within non-avian ornithomirans, pneumatization of distal forelimb elements in pterosaurs suggests the presence of a system of subcutaneous diverticula [7]. We refer to diverticula that do not leave diagnostic skeletal traces as 'cryptic' diverticula. The presence of long pneumatic hiatuses in *Giraffatitan* and *Apatosaurus*, the evidence for subcutaneous diverticula in pterosaurs, and the numerous non-skeletal diverticula of birds suggest that cryptic diverticula are a general feature of ornithomiran respiratory systems. Therefore skeletal traces of pneumaticity provide only a lower bound on the

extent of the diverticular system, which is often much more extensive and complex in extant birds, and may have been equally extensive and complex in extinct ornithomirans.

Asymmetry of inference. Pneumatization of a single element is enough to establish the presence of pneumatic diverticula in a particular region of the body, but even a long string of apneumatic elements does not necessarily indicate that diverticula are absent – as seen with the seven-vertebra bilateral hiatus in the tail of *Apatosaurus* YPM 1980. This asymmetry of evidence and inference is particularly troubling in the case of caudal pneumaticity. As the number of specimens of a taxon without caudal pneumaticity mounts, the likelihood that caudal pneumaticity is absent in the taxon increases, but it can never be truly ruled out because only a single counterexample is needed to demonstrate its presence. The absence of caudal pneumaticity in the many well-described specimens of *Camarasaurus* probably represents a genuine absence (see, e.g., [54]). The same cannot be said for *Brachiosaurus altithorax*, for which the only known caudal vertebrae are the two most anterior caudals of the holotype individual. As *Giraffatitan* demonstrates, *Brachiosaurus* could have invasive caudal pneumaticity that was expressed farther down the tail or in another individual. This seems particularly possible given that Riggs ([21]: p. 235) described a pneumatic hiatus in the sacrum of the *Brachiosaurus* holotype FMNH P25107, in which pneumatic cavities are apparently absent from the second sacral vertebra but present in the first, third and fourth (we have been unable to confirm the presence of this hiatus because the size and fragility of the specimen prevent close examination of the sacral centra).

Pneumatic hiatuses do not always indicate separate sources of pneumatization. Pneumatic hiatuses (*sensu* [11]) are less informative than previously supposed. In birds, the only sources of vertebral diverticula posterior to the middle of the dorsal series are the abdominal air sacs, and this was probably true for non-avian saurischians as well ([13,14], contra [79,80]). The caudal vertebral diverticula of *Giraffatitan* are therefore inferred to have originated from abdominal air sacs. However, the tail of MB.R.5000 ('Fund no') shows that the caudal vertebral diverticula were able to leapfrog over sequences of several vertebrae without leaving any distinct or diagnostic traces, so pneumatic hiatuses do not always indicate that the vertebrae before and behind them were pneumatized by different sources of diverticula. This possibility was recognised by Wedel ([12]: p. 619), but its likelihood was underestimated. The utility of pneumatic hiatuses in determining which air-sacs were the sources of pneumatising diverticula is further undermined by the observation that in juvenile chickens, the middle cervical vertebrae are the first to be completely pneumatised ([12]: fig. 3; [81]). This pneumatization is by diverticula of the cervical air-sacs, and those diverticula leave no osteological traces on the more posterior cervicals that they are also adjacent to: in effect the posterior part of the neck is a cervicodorsal pneumatic hiatus (*sensu* [12]). The same was presumably true in *Pantyraco*, which probably also had pneumatic middle cervicals [32,82].

This does not mean that pneumatic hiatuses are never produced by multiple sources of diverticula: some of the pneumatic hiatuses of chickens certainly are. (Compare patterns of vertebral pneumatisation in [68]: fig. 1 with mapping of pneumatisation domains to air sacs reported by [13,14]; also see pp. 8-9 and figure 4 in [12].) However, there is currently no way to distinguish hiatuses produced by multiple sources of diverticula from those produced by leapfrogging diverticula, as in *Giraffatitan* and *Apatosaurus*.

Pneumatization through ontogeny. It may not be safe to assume that pneumatization of the postcranial skeleton in sauropods is completed in early ontogeny, as it is in the few extant birds in which it has been studied [81,83]. The restriction of PSP to the second caudal vertebra in all *Giraffatitan* specimens other than MB.R.5000 (“Fund no”) – assuming they really are all *Giraffatitan*, and not another, as-yet unrecognised taxon – implies that pneumatization of the rest of the tail may have progressed piecemeal throughout ontogeny, and there is no reason to assume that the mounted tail represents the culmination of caudal pneumatization. It is likely that this animal was about the same size as the one represented by MB.R.2181 (HMN SII), from which most of the rest of the mounted skeleton is drawn ([64]: p. 98). However, MB.R.2181 (HMN SII) was probably not fully mature when it died: the suture between the scapula and coracoid is still open, and the individual represented by the fibula MB.R.2688 (HMN XV2) is about 13% larger in linear dimensions. It is possible that fully mature individuals of *Giraffatitan* might have caudal pneumaticity as continuous and invasive as that of diplodocines but extending further down the tail.

Morphogenetic rules of postcranial pneumatization. Benson *et al* ([15]: p. 180) identified two morphogenetic rules that appear to govern posterior dorsal and sacral pneumaticity in non-avian theropods. The first is the “neural arch first” rule for posterior expansions of pneumaticity beyond the anterior dorsals. In posterior dorsal and sacral vertebrae of non-avian theropods, if pneumaticity is present, it is always present in the neural arches. The centra may also be pneumatic, but only alongside the arches; one never finds a pneumatic centrum and an apneumatic arch. This is contrast to the “centrum-first” pattern of pneumatic invasion in the cervical vertebrae.

It is not clear if the “neural arch first rule” applies to caudal vertebrae in theropods; Benson *et al* [15] only discussed this rule in the context of dorsal and sacral vertebrae. Using character optimization, Fanti *et al* [27] found that the “neural arch first” rule held for caudal pneumatization in rebbachisaurid sauropods. They interpreted the rule as also applying to theropod caudal vertebrae, and on that basis they proposed that the “neural arch first” pneumatization pattern was synapomorphic for Saurischia ([27]: p. 6).

The second morphogenetic pattern identified by Benson *et al* [15] is the “no gaps” rule, which simply means that there are no gaps in the pneumatization of the vertebral column. The most anterior and posterior pneumatic vertebrae in the entire vertebral column are connected by an unbroken chain of pneumatic vertebrae.

As we discuss above, caudal pneumaticity in *Giraffatitan* and *Apatosaurus* breaks both the “neural arch first” and “no gaps” rules. Regarding the “neural arch first” rule, fossae are occasionally present on the centra but absent on the neural arches in *Giraffatitan* (e.g., the second caudal vertebrae of MB.R.2921 and MB.R.3736, and proximal caudals of MB.R.5000) and *Apatosaurus* (e.g., caudals 9 and 13 of YPM 1980). The same is true of the most distal pneumatic vertebrae in *Diplodocus* (e.g., caudal 18 in AMNH 223, [48]: fig. 13, and caudals 15–19 in USNM 10865, [65]: fig. 3). The situation in some of the mid-caudals in *Giraffatitan* MB.R.5000 is less clear, since the fossae straddle the base of the neural arch and the dorsal part of the lateral centrum. As it stands, “neural arch first” pneumatization of caudal appears to hold in rebbachisaurids [27] but not diplodocines or brachiosaurids, and its status in theropods is unclear. Fanti *et al* [27] proposed “neural arch first” caudal pneumatization as a synapomorphy of Saurischia but that is not supported by this work. Even determining which pattern

(“arch first” or “centrum first”) dominates in Sauropoda will require more work.

The “no gaps” rule proposed for non-avian theropods by Benson *et al* [15] does not hold for sauropods. The pneumatic hiatuses described above in both *Giraffatitan* and *Apatosaurus* break this rule, as do those previously described in *Haplocanthosaurus* [12] and *Brachiosaurus* ([21]: p. 235). A pneumatic hiatus may also be present in the basal sauropod *Tazoudasaurus* and in several other basal sauropodomorphs and basal sauropods ([17]: p. 95 and fig. 12). What is most interesting about this apparent pattern is that the very thorough survey of Benson *et al* [15] found no exceptions to the “no gaps” rule among non-avian theropods, but pneumatic hiatuses are present in sauropods and birds [12], which bracket non-avian theropods both phylogenetically and in terms of body size. Clearly more comparative work is needed to elucidate the evolutionary, ecological, and developmental drivers of skeletal pneumatization across Archosauria—the analyses of O’Connor [6,29], Benson *et al* [15], and Smith [3] are welcome advances, but there are plenty of mysteries left to solve.

Functional Implications

In the specimens of *Giraffatitan* and *Apatosaurus* discussed herein, PSP does not invade the caudal vertebrae to a significant extent. Reduction of the mass of the vertebrae by pneumatization would have been negligible, a characteristic shared with PSP in early saurischians like *Coelophysis* and *Pantyraco* [32]. This is in sharp contrast to the presacral and sacral vertebrae in *Giraffatitan* and *Apatosaurus*, which were more than 60% air by volume and as lightly built, on average, as the pneumatic long bones of birds [4,8].

The first postcranial bones to be pneumatised, both ontogenetically in birds and evolutionarily in saurischians, are vertebrae that are not adjacent to the lungs or air sacs, implying that diverticula evolved, and develop, before they interact with the skeleton ([12]: fig. 3; [32]: text-fig. 2). Furthermore, many of the diverticula of extant birds do not pneumatize the skeleton at any point in ontogeny (i.e., all visceral and most intermuscular and subcutaneous diverticula; [78]). These observations suggest that pneumatic diverticula did not evolve to pneumatize the skeleton. (Numerous other possible functions for diverticula are reviewed by Witmer [84].) The very limited resorption of bone during pneumatization in basal saurischians further implies that neither did PSP initially evolve to lighten the skeleton, but it was later exapted for that purpose in lineages where weight loss was important due to great size (sauropods) or flight (birds). Now we find that even in *Giraffatitan* and *Apatosaurus*, both large neosauropods with extensive pneumatization of the presacral and sacral vertebrae, caudal pneumaticity contributed very little to lightening the skeleton. The model of diverticula as “opportunistic pneumatizing machines” ([84]: p. 64) is consistent with many aspects of the development and evolution of skeletal pneumaticity in amniotes. However, it does not explain why presacral and sacral pneumatization in *Giraffatitan* and *Apatosaurus* is so aggressive, whereas caudal pneumatization in the same taxa and the same individuals is so minimal and erratic. This is particularly surprising in light of the fact that, while the torso’s mass is suspended between the fore- and hind-limb girdles, the tail is cantilevered, and so its mass induces a large bending moment. It is unlikely that mechanical demands would permit extensive pneumatization of the long, cantilevered neck but prevent pneumatization of the similarly cantilevered tail, which in *Giraffatitan* accounted for only about a third as much volume as the neck ([31]: table 4). The tail of *Apatosaurus* was proportionally much larger, but extensive pneumatization of the tail in the closely related diplodocines

(*Diplodocus*, *Barosaurus*, and *Tomieria*), which also had proportionally large tails, suggests that mechanical factors alone are insufficient to explain the very limited caudal pneumatization in *Apatosaurus*.

We hypothesize that in its earliest evolutionary stages, in any part of the body and in any taxon, skeletal pneumaticity has no selective value. In those early stages it confers no disadvantages but does not affect the skeleton enough, through lightening or remodeling individual bones, to offer a selective advantage. It may therefore be invisible to natural selection and free to evolve neutrally (*sensu* [85]). Skeletal pneumaticity can only be favored in those cases where, by chance, it lightens the skeleton enough to become visible to selection. The very limited mass reduction from caudal pneumatization in *Giraffatitan* and *Apatosaurus* suggests that this process of neutral evolution eventually leading, in some cases, to extensive and exaptive skeletal remodeling took place repeatedly in different parts of the body in sauropods. An alternative possibility is that caudal pneumatization was limited by some as-yet-unknown aspect of the developmental program. Cranial skeletal pneumaticity is widespread in extant mammals and archosaurs, and PSP in birds, but the levels of control of the pneumatization process are poorly known. Therefore, neither of these hypotheses can be falsified on the basis of current knowledge, but both could conceivably be tested in extant animals.

Conclusions

Although it has not been previously recognised, caudal pneumaticity was present in *Apatosaurus* and *Giraffatitan*. Pneumatic fossae in the mid-caudal vertebrae of these animals were not detected for decades following their initial descriptions, despite the fact that two of the most important specimens were on display for most of the twentieth century. Furthermore, the pattern of caudal pneumatization in both taxa appears to have been erratic, although this may be at least partly caused by incomplete ontogenetic sampling. Taken together, these facts suggest that caudal pneumaticity, or at least the capacity to develop it, may be more widely distributed in sauropods (and possibly theropods) than is currently appreciated. We predict that more examples of caudal pneumaticity in otherwise well-known taxa will be discovered in the future.

The discovery of long pneumatic hiatuses in the tails of *Giraffatitan* and *Apatosaurus* complicates our understanding of the development and evolution of PSP in extinct archosaurs, and undermines the utility of hiatuses for identifying the air-sac systems responsible for pneumatization. On one hand, the presence of multiple pneumatic hiatuses within the inferred domain of a single pair of air sacs shows that such hiatuses can be produced by leapfrogging diverticula and do not always indicate pneumatization from multiple sources as originally proposed by Wedel [11]. The pneumatic hiatus reported in *Haplocanthosaurus* [12] seems likely to have been produced by diverticula that simply affected adjacent vertebrae inconsistently. If more pneumatic hiatuses are discovered in extinct ornithomirans, criteria will be needed to distinguish those caused by multiple sources of diverticula from those caused by “leapfrogging” diverticula. Until such criteria are established, the inference that pneumatic hiatuses always indicate multiple air sacs is falsified. However, the case for an essentially avian air sac system in pterosaurs and saurischians is also based on several other lines of evidence [7,12], and remains robust.

The other major implication of the pneumatic hiatuses in *Giraffatitan* and *Apatosaurus* is that pneumatic diverticula were even more widespread in sauropods than previously thought. This

should not be surprising, given the many visceral, intermuscular, and subcutaneous diverticula of extant birds that leave no skeletal traces. The anatomical breadth of diverticular systems in saurischians and pterosaurs is also underscored by distal forelimb pneumaticity in pterosaurs [7].

A common discovery pattern for PSP in pterosaurs and saurischians has been emerging over the past few years: the more we look, the more we find. Compelling evidence of PSP is now known in early representatives of both clades, and patterns of pneumatization in derived pterosaurs, sauropods, and non-avian theropods are diagnostic for the air sacs required for flow-through lung ventilation [7,12–15]. The discovery of more pneumaticity in pterosaurs, sauropodomorphs, and non-avian theropods emphasises how strange is the absence of reported pneumaticity in ornithischians ([16]: p. 19; the putative pneumatic foramen in a dorsal rib of the iguanodont *Delapparentia* [86] is not convincing). If, as seems increasingly likely, an air sac system is primitive for Ornithodira, why did ornithischians never discover PSP (in a developmental sense)? And if an air sac system is not primitive for Ornithodira, why did the three other major lineages evolve PSP so soon after their divergence from one another and from Ornithischia?

It is possible that ornithischians did have pneumatic diverticula, but that—following the hypothesis of initially neutral evolution described above—these diverticula did not impact the skeleton enough to become visible to selection. This is a complex scenario that will be difficult to test, since we currently have no way of identifying pneumatic diverticula in fossil taxa other than by their skeletal traces. In basal sauropodomorphs, potentially pneumatic fossae can be difficult to assess because the recesses ventral to the diapophyses are often obscured by sediment, even in apparently well-prepared specimens ([16]: p. 16; [17]: 95). Largely because of this difficulty, PSP went unrecognized in basal sauropodomorphs until very recently. By analogy, we think it is at least possible that pneumatic fossae in ornithischians, if present, may have escaped detection. We therefore encourage paleobiologists to keep an eye out for even rudimentary indications of PSP in ornithischians.

Acknowledgments

For curatorial assistance we thank Mark Norell and Carl Mehling (American Museum of Natural History), Matt Lamanna, David Berman, and Amy Henrici (Carnegie Museum), Pete Makovicky, Nate Smith, and William Simpson (Field Museum of Natural History), Kenneth Campbell and Kimball Garrett (Natural History Museum of Los Angeles County), Richard Cifelli, Nicholas Czaplewski, Kyle Davies, and Jennifer Larson (Oklahoma Museum of Natural History), Daniel Brinkman and Marilyn Fox (Yale Peabody Museum), and especially Daniela Schwarz-Wings, Oliver Wings, and Heinrich Mallison (Museum für Naturkunde Berlin). All our quotations of Janensch [57,64] were made by Gerhard Maier, and are available at the Polyglot Paleontologist website (<http://www.paleoglot.org/>); we thank Gerhard for his effort. The photograph of the ‘Fund no’ quarry used in Figure 6 appears courtesy of Daniela Schwarz-Wings at the Museum für Naturkunde Berlin. Pat O’Connor and John Whitlock reviewed an earlier version of this manuscript and made many helpful comments, for which we are grateful. We also thank Daniela Schwarz-Wings and Roger Benson for thoughtful review comments.

Author Contributions

Conceived and designed the experiments: MJW MPT. Performed the experiments: MJW MPT. Analyzed the data: MJW MPT. Contributed reagents/materials/analysis tools: MJW MPT. Wrote the paper: MJW MPT.

References

- Wedel MJ (2003b) The evolution of vertebral pneumaticity in sauropod dinosaurs. *Journal of Vertebrate Paleontology* 23: 344–357.
- Wilson JA, Mohabey DM. (2006) A titanosauriform (Dinosauria: Sauropoda) axis from the Lameta Formation (Upper Cretaceous: Maastrichtian) of Nand, central India. *Journal of Vertebrate Paleontology* 26: 471–479.
- Smith ND (2012) Body mass and foraging ecology predict evolutionary patterns of skeletal pneumaticity in the diverse “waterbird” clade. *Evolution* 66(4): 1059–1078.
- Wedel MJ (2005) Postcranial skeletal pneumaticity in sauropods and its implications for mass estimates. In Wilson JA, Curry-Rogers K, The sauropods: evolution and paleobiology. Berkeley: University of California Press. pp.201–228.
- Schwarz D, Fritsch G (2006) Pneumatic structures in the cervical vertebrae of the Late Jurassic Tendaguru sauropods *Brachiosaurus brancai* and *Dicraeosaurus*. *Eclogae Geologicae Helvetiae* 99: 65–78.
- O'Connor PM (2009) Evolution of archosaurian body plans: skeletal adaptations of an air-sac-based breathing apparatus in birds and other archosaurs. *Journal of Experimental Zoology Part A: Ecological Genetics and Physiology* 311(8): 629–646.
- Claessens LPAM, O'Connor PM, Unwin DM (2009) Respiratory evolution facilitated the origin of pterosaur flight and aerial gigantism. *PLoS ONE* 4(2): e4497. doi:10.1371/journal.pone.0004497.
- Taylor MP, Wedel MJ (2013) Why sauropods had long necks; and why giraffes have short necks. *PeerJ* 1: e36.
- Britt BB (1993) Pneumatic postcranial bones in dinosaurs and other archosaurs. Calgary: University of Calgary. 383pp.
- Britt BB (1997) Postcranial pneumaticity. In Currie PJ, Padian K, editors. *The Encyclopedia of Dinosaurs*. San Diego: Academic Press. pp.590–593.
- Wedel MJ (2003a) Vertebral pneumaticity, air sacs, and the physiology of sauropod dinosaurs. *Paleobiology* 29: 243–255.
- Wedel MJ (2009) Evidence for bird-like air sacs in saurischian dinosaurs. *Journal of Experimental Zoology* 311A. DOI: 10.1002/jez.513.
- O'Connor P, Claessens LPAM (2005) Basic avian pulmonary design and flow-through ventilation in non-avian theropod dinosaurs. *Nature* 436: 253–256.
- O'Connor PM (2006) Postcranial pneumaticity: an evaluation of soft-tissue influences on the postcranial skeleton and the reconstruction of pulmonary anatomy in archosaurs. *Journal of Morphology* 267: 1199–1226.
- Benson RB, Butler RJ, Carrano MT, O'Connor PM (2012) Air-filled postcranial bones in theropod dinosaurs: physiological implications and the ‘reptile’–bird transition. *Biological Reviews* 87(1): 168–193.
- Butler RJ, Barrett PM, Gower DJ (2012) Reassessment of the evidence for postcranial skeletal pneumaticity in Triassic archosaurs, and the early evolution of the avian respiratory system. *PLOS One* 7(3): e34094.
- Yates AM, Wedel MJ, Bonnan MF (2012) The early evolution of postcranial skeletal pneumaticity in sauropodomorph dinosaurs. *Acta Palaeontologica Polonica* 57(1): 85–100.
- Schwarz D, Frey E, Meyer CA (2007) Pneumaticity and soft-tissue reconstructions in the neck of diplodocid and dicraeosaurid sauropods. *Acta Palaeontologica Polonica* 52: 167–188.
- Schwarz-Wings D, Frey E (2008) Is there an option for a pneumatic stabilization of sauropod necks? – an experimental and anatomical approach. *Palaeontologia Electronica* 11(3): 17A. Available: http://palaeo-electronica.org/2008_3/155/index.html. Accessed 2013 Sep 24.
- Cerda IA, Salgado L, Powell JE (2012) Extreme postcranial pneumaticity in sauropod dinosaurs from South America. *Paläontologische Zeitschrift*, 86(4): 441–449.
- Riggs ES (1904) Structure and relationships of the opisthocoelian dinosaurs, part II: the Brachiosauridae. *Field Columbian Museum Publications in Geology* 2: 229–247.
- Wilson JA, Sereno PC (1998) Early evolution and higher-level phylogeny of sauropod dinosaurs. *Society of Vertebrate Paleontology Memoir* 5: 1–68.
- Marsh OC (1896) The dinosaurs of North America. US Geological Survey, Sixteenth Annual Report, 1894–95: 133–414.
- Gilmore CW (1936) Osteology of *Apatosaurus* with special reference to specimens in the Carnegie Museum. *Memoirs of the Carnegie Museum* 11: 175–300.
- Lovelace DM, Hartman SA, Wahl WR (2008) Morphology of a specimen of *Supersaurus* (Dinosauria, Sauropoda) from the Morrison Formation of Wyoming, and a re-evaluation of diplodocid phylogeny. *Arquivos do Museu Nacional, Rio de Janeiro* 65: 527–544.
- Carvalho IS, Avilla LS, Salgado L (2003) *Amazonsaurus maranhensis* gen. et sp.nov. (Sauropoda, Diplodocoidea) from the Lower Cretaceous (Aptian-Albian) of Brazil. *Cretaceous Research* 24:697–713.
- Fanti F, Cau A, Hassine M, Contessi M (2013). A new sauropod dinosaur from the Early Cretaceous of Tunisia with extreme avian-like pneumatization. *Nature Communications* 4: 2080. doi:10.1038/ncomms3080
- Wilson JA, Upchurch P (2009) Redescription and reassessment of the phylogenetic affinities of *Euhelopus zdanskyi* (Dinosauria: Sauropoda) from the Early Cretaceous of China. *Journal of Systematic Palaeontology* 7 (2): 199–239.
- O'Connor PM (2004) Pulmonary pneumaticity in the postcranial skeleton of extant Aves: a case study examining Anseriformes. *Journal of Morphology* 261: 141–161.
- Mannion PD, Upchurch P, Barnes RN, Mateus O (2013) Osteology of the Late Jurassic Portuguese sauropod dinosaur *Lusotitan atalaiensis* (Macronaria) and the evolutionary history of basal titanosauriforms. *Zoological Journal of the Linnean Society*. doi: 10.1111/zoj.12029.
- Taylor MP (2009) A re-evaluation of *Brachiosaurus altithorax* Riggs 1903 (Dinosauria, Sauropoda) and its generic separation from *Giraffatitan brancai* (Janensch 1914). *Journal of Vertebrate Paleontology* 29: 787–806.
- Wedel MJ (2007) What pneumaticity tells us about ‘prosauropods’, and vice versa. *Special Papers in Palaeontology* 77: 207–222.
- Gower DJ (2001) Possible postcranial pneumaticity in the last common ancestor of birds and crocodylians: evidence from *Erythrosuchus* and other Mesozoic archosaurs. *Naturwissenschaften* 88: 119–122.
- Wilson JA (1999) A nomenclature for vertebral laminae in sauropods and other saurischian dinosaurs. *Journal of Vertebrate Paleontology* 19: 639–653.
- Taylor MP, Naish D (2007) An unusual new neosauropod dinosaur from the Lower Cretaceous Hastings Beds Group of East Sussex, England. *Palaeontology* 50: 1547–1564.
- Owen R (1859) Monograph on the fossil Reptilia of the Cretaceous Formations. Supplement No. 1. Pterosauria (*Pterodactylus*). *Palaeontographical Society*. pp.1–19.
- Bonde N, Christiansen P (2003) The detailed anatomy of *Rhamphorhynchus*: axial pneumaticity and its implications. In: Buffetaut E, Mazin J-M, editors. *Evolution and paleobiology of pterosaurs*. London: Geological Society. pp.217–232.
- Mannion PD (2010) A revision of the sauropod dinosaur genus ‘*Bothriospondylus*’ with a redescription of the type material of the Middle Jurassic form ‘*B. madagascarensis*’. *Palaeontology* 53: 277–296.
- Russell DA, Zheng Z. (1993). A large mamenchisaurid from the Junggar Basin, Xinjiang, People’s Republic of China. *Canadian Journal of Earth Sciences* 30(10): 2082–2095.
- Hatcher JB (1903) Osteology of *Haplocanthosaurus*, with a description of a new species, and remarks on the probable habits of the Sauropoda, and the age and origin of *Atlantosaurus* beds. *Memoirs of the Carnegie Museum* 2: 1–72.
- Wilson JA (2002) Sauropod dinosaur phylogeny: critique and cladistic analysis. *Zoological Journal of the Linnean Society* 136: 217–276.
- Upchurch P, Barrett PM, Dodson P (2004) Sauropoda. In: Weishampel DB, Dodson P, Osmolska H, editors. *The Dinosauria*, second edition. Berkeley: University of California Press. pp.259–322.
- Upchurch P (1998) The phylogenetic relationships of sauropod dinosaurs. *Zoological Journal of the Linnean Society* 124(1): 43–103.
- Whitlock JA (2011) A phylogenetic analysis of Diplodocoidea (Saurischia: Sauropoda). *Zoological Journal of the Linnean Society* 161(4): 872–915.
- Janensch W (1929) Die Wirbelsäule der Gattung *Dicraeosaurus*. *Palaeontographica*, Supplement 7, 2: 35–133.
- Mannion PD, Upchurch P, Hutt S (2011) New rebbachisaurid (Dinosauria: Sauropoda) material from the Wessex Formation (Barremian, Early Cretaceous), Isle of Wight, United Kingdom. *Cretaceous Research* 32(6): 774–780.
- Torcida Fernández-Baldor F, Canudo JI, Huerta P, Montero D, Suberbiola XP, et al (2011) *Demandsaurus darwini*, a new rebbachisaurid sauropod from the Early Cretaceous of the Iberian Peninsula. *Acta Palaeontologica Polonica* 56(3): 535–552.
- Osborn HF (1899) A skeleton of *Diplodocus*. *Memoirs of the American Museum of Natural History* 1: 191–214.
- Hatcher JB (1901) *Diplodocus* (Marsh): its osteology, taxonomy, and probable habits, with a restoration of the skeleton. *Memoirs of the Carnegie Museum* 1: 1–63.
- McIntosh JS (2005) The genus *Barosaurus* Marsh (Sauropoda, Diplodocidae). In: Tidwell V, Carpenter K, editors. *Thunder lizards: the sauropodomorph dinosaurs*. Bloomington: Indiana University Press. pp.38–77.
- Remes K (2006) Revision of the Tendaguru sauropod dinosaur *Tomieria africana* (Fraas) and its relevance for sauropod paleobiogeography. *Journal of Vertebrate Paleontology* 26(3): 651–669.
- Marsh OC (1881) Principal characters of American Jurassic dinosaurs, Part V., *American Journal of Science*, Series 3 21: 417–423.
- Riggs ES (1903) Structure and relationships of the opisthocoelian dinosaurs, part I: *Apatosaurus* Marsh. *Field Columbian Museum Publications in Geology* 2: 165–196.
- Osborn HF, Mook CC (1921) *Camarasaurus*, *Amphicoelias* and other sauropods of Cope. *Memoirs of the American Museum of Natural History*, New Series, 3: 247–387.
- Tidwell V, Carpenter K, Brooks W (1999) New sauropod from the Lower Cretaceous of Utah, USA. *Oryctos* 2: 21–37.
- Tidwell V, Carpenter K, Meyer S (2001) New titanosauriform (Sauropoda) from the Poison Strip Member of the Cedar Mountain Formation (Lower Cretaceous), Utah. In: Tanke DH, Carpenter K, editors. *Mesozoic vertebrate life*. Bloomington: Indiana University Press. pp.139–165.
- Janensch W (1950a) Die Wirbelsäule von *Brachiosaurus brancai*. *Palaeontographica*, Supplement 7, 3(2): 27–93.
- Borsuk-Bialynicka M (1977) A new camarasaurid sauropod *Opisthocoelecaudia skarzynskii* gen. n., sp. n. from the Upper Cretaceous of Mongolia. *Palaeontologia Polonica* 37(5): 5–64.

59. Powell JE (2003) Revision of South American titanosaurid dinosaurs: palaeobiological, palaeobiogeographical and phylogenetic aspects. *Records of the Queen Victoria Museum* 111: 1–173.
60. Martinelli A, Forasiepi AM (2004) Late Cretaceous vertebrates from Bajo de Santa Rosa (Allen Formation), Rio Negro province, Argentina, with the description of a new sauropod dinosaur (Titanosauridae). *Revista del Museo Argentino de Ciencias Naturales* 6(2): 257–305.
61. Otero A (2010) The appendicular skeleton of *Neuquensaurus*, a Late Cretaceous saltasaurine sauropod from Patagonia, Argentina. *Acta Palaeontologica Polonica* 55 (3): 399–426.
62. Mazzetta GV, Christiansen P, Farina RA (2004) Giants and bizarres: body size of some southern South American Cretaceous dinosaurs. *Historical Biology* 2004: 1–13.
63. Sander PM, Christian A, Clauss M, Fechner R, Gee TC, et al (2010) Biology of the sauropod dinosaurs: the evolution of gigantism. *Biological Reviews* 86: 117–155. DOI: 10.1111/j.1469-185X.2010.00137.x.
64. Janensch W (1950b) Die Skelettrekonstruktion von *Brachiosaurus brancai*. *Palaeontographica*, Supplement 7, 3(2): 95–102.
65. Gilmore CW (1932) On a newly mounted skeleton of *Diplodocus* in the United States National Museum. *Proceedings of the United States National Museum* 81(18): 1–21.
66. Taylor MP (2005) Sweet seventy-five and never been kissed: the Natural History Museum's Tendaguru brachiosaur. In: Barrett PM, editors. 53rd Symposium of Vertebrate Palaeontology and Comparative Anatomy, Abstracts. London: The Natural History Museum. p.25.
67. Migeod FWH (1931) British Museum East Africa Expedition: Account of the work done in 1930. *Natural History Magazine* 3: 87–103.
68. King AS (1957) The aerated bones of *Gallus domesticus*. *Cells Tissues Organs* 31(2): 220–230.
69. Cranford TW, Amundin M, Norris KS (1996) Functional morphology and homology in the odontocete nasal complex: implications for sound generation. *Journal of Morphology* 228(3): 223–285.
70. Weiglein AH (1999). Development of the paranasal sinuses in humans. In: Koppe T, Nagai H, Alt KW, editors. The paranasal sinuses of higher primates. Chicago: Quintessence. pp.35–50.
71. Wilson JA, Martínez RN, Alcober O (1999). Distal tail segment of a titanosaur (Dinosauria: Sauropoda) from the Upper Cretaceous of Mendoza, Argentina. *Journal of Vertebrate Paleontology* 19(3): 591–594.
72. Janensch W (1947) Pneumatizität bei Wirbeln von Sauropoden und anderen Saurischien. *Palaeontographica*, Supplement 7, 3(1): 1–25.
73. Harris JD (2006) The significance of *Suuwassea emiliae* (Dinosauria: Sauropoda) for flagella-caudata intrarelationships and evolution. *Journal of Systematic Palaeontology* 4: 185–198.
74. Osborn HF (1898) Additional characters of the great herbivorous dinosaur *Camarasaurus*. *Bulletin of the American Museum of Natural History* 10: 219–233.
75. Matthew WD (1905) The mounted skeleton of *Brontosaurus*. *American Museum Journal* 5: 62–70.
76. Ostrom JH, McIntosh JS (1966) Marsh's dinosaurs: the collections from Como Bluff. New Haven: Yale University Press. 388p.
77. Upchurch P, Tomida Y, Barrett PM (2004b) A new specimen of *Apatosaurus ajax* (Sauropoda: Diplodocidae) from the Morrison Formation (Upper Jurassic) of Wyoming, USA. *National Science Museum Monographs (Tokyo)* 26: 1–107.
78. Duncker HR. (1971) The lung air sac system of birds. *Advances in Anatomy, Embryology, and Cell Biology* 45: 1–171.
79. Ruben JA, Jones TD, Geist NR, Hillenius WJ (1997) Lung structure and ventilation in theropod dinosaurs and early birds. *Science* 278: 1267–1270.
80. Sereno PC, Martínez RN, Wilson JA, Varricchio DJ, Alcober OA, et al (2008) Evidence for avian intrathoracic air sacs in a new predatory dinosaur from Argentina. *PLoS ONE* 3(9): e3303. doi:10.1371/journal.pone.0003303
81. Hogg DA (1984) The development of pneumatization in the skeleton of the adult domestic fowl. *Journal of Anatomy* 139: 105–113.
82. Yates AM (2003) A new species of the primitive dinosaur *Thecodontosaurus* (Saurischia: Sauropodomorpha) and its implications for the systematics of early dinosaurs. *Journal of Systematic Palaeontology* 1: 1–42.
83. Cover MS (1953) Gross and microscopic anatomy of the respiratory system of the turkey. III. The air sacs. *American Journal of Veterinary Research* 14: 239–245.
84. Witmer LM (1997) The evolution of the antorbital cavity of archosaurs: a study in soft-tissue reconstruction in the fossil record with an analysis of the function of pneumaticity. *Society of Vertebrate Paleontology Memoir* 3: 1–73.
85. Kimura M (1968) Evolutionary rate at the molecular level. *Nature* 217: 624–626.
86. Ruiz-Omeñaca JI (2011) *Delapparentia turoloensis* nov. gen et sp., un nuevo dinosaurio iguanodontoideo (Ornithischia: Ornithomimidae) en el Cretácico Inferior de Galve. *Estudios Geológicos* 67 (1): 83–110. doi:10.3989/egol.40276.124
87. Upchurch P, Mannion PD (2009) The first diplodocid from Asia and its implications for the evolutionary history of sauropod dinosaurs. *Palaeontology* 52(6): 1195–1207.
88. Mannion PD, Barrett P (2013) Additions to the sauropod dinosaur fauna of the Cenomanian (early Late Cretaceous) Kem Kem beds of Morocco: Palaeobiogeographical implications of the mid-Cretaceous African sauropod fossil record. *Cretaceous Research* 45: 49–59.
89. Mannion PD, Upchurch P, Mateus O, Barnes RN, Jones MEH (2011) New information on the anatomy and systematic position of *Dinheirosaurus lourinhanensis* (Sauropoda: Diplodocoidea) from the Late Jurassic of Portugal, with a review of European diplodocoids. *Journal of Systematic Palaeontology* 10(3): 521–551.
90. Lull RS (1919) The sauropod dinosaur *Barosaurus* Marsh. *Memoirs of the Connecticut Academy of Arts and Sciences* 6: 1–42.
91. Kellner AWA, Azevedo SD (1999) A new sauropod dinosaur (Titanosauria) from the Late Cretaceous of Brazil. *National Science Museum Monographs*, 15: 111–142.
92. Casal G, Martínez R, Luna M, Sciotto JC, Lamanna M (2007) *Aeolosaurus colhuehuapensis* sp. nov. (Sauropoda, Titanosauria) de la Formación Bajo Barreal, Cretácico Superior de Argentina. *Revista Brasileira de Paleontología*, 10(1): 53–62.
93. Campos DD, Kellner AWA, Bertini RJ, Santucci RM (2005) On a titanosaurid (Dinosauria, Sauropoda) vertebral column from the Bauru group, Late Cretaceous of Brazil. *Arquivos do Museu Nacional, Rio de Janeiro* 63(3): 565–593.
94. Lü J, Xu L, Jiang X, Jia S, Li M, et al (2009) A preliminary report on the new dinosaurian fauna from the Cretaceous of the Ruyang Basin, Henan Province of central China. *Journal of the Paleontological Society of Korea* 25: 43–56.
95. Fronimos J (2011) Patterns of postcranial pneumaticity in the Late Cretaceous titanosaur *Alamosaurus sanjuanensis*. *Journal of Vertebrate Paleontology (Supplement 2)* 31: 112–113A.
96. Calvo JO, Porfiri JD, González-Riga BJ, Kellner AWA (2007) A new Cretaceous terrestrial ecosystem from Gondwana with the description of a new sauropod dinosaur. *Anais da Academia Brasileira de Ciências* 79(3): 529–541.

Ecological Interactions in Dinosaur Communities: Influences of Small Offspring and Complex Ontogenetic Life Histories

Daryl Codron^{1,2,3,4*}, Chris Carbone⁵, Marcus Clauss¹

1 Clinic for Zoo Animals, Exotic Pets and Wildlife, Vetsuisse Faculty, University of Zürich, Zürich, Switzerland, **2** Florisbad Quaternary Research, National Museum, Bloemfontein, South Africa, **3** School of Biological and Conservation Sciences, University of KwaZulu-Natal, Pietermaritzburg, South Africa, **4** Department of Anthropology, University of Colorado at Boulder, Boulder, Colorado, United States of America, **5** Institute of Zoology, Zoological Society of London, London, United Kingdom

Abstract

Because egg-laying meant that even the largest dinosaurs gave birth to very small offspring, they had to pass through multiple ontogenetic life stages to adulthood. Dinosaurs' successors as the dominant terrestrial vertebrate life form, the mammals, give birth to live young, and have much larger offspring and less complex ontogenetic histories. The larger number of juveniles in dinosaur as compared to mammal ecosystems represents both a greater diversity of food available to predators, and competitors for similar-sized individuals of sympatric species. Models of population abundances across different-sized species of dinosaurs and mammals, based on simulated ecological life tables, are employed to investigate how differences in predation and competition pressure influenced dinosaur communities. Higher small- to medium-sized prey availability leads to a normal body mass-species richness (*M-S*) distribution of carnivorous dinosaurs (as found in the theropod fossil record), in contrast to the right-skewed *M-S* distribution of carnivorous mammals (as found living members of the order Carnivora). Higher levels of interspecific competition leads to a left-skewed *M-S* distribution in herbivorous dinosaurs (as found in sauropods and ornithomimids), in contrast to the normal *M-S* distribution of large herbivorous mammals. Thus, our models suggest that differences in reproductive strategy, and consequently ontogeny, explain observed differences in community structure between dinosaur and mammal faunas. Models also show that the largest dinosaurian predators could have subsisted on similar-sized prey by including younger life stages of the largest herbivore species, but that large predators likely avoided prey much smaller than themselves because, despite predicted higher abundances of smaller than larger-bodied prey, contributions of small prey to biomass intake would be insufficient to satisfy meat requirements. A lack of large carnivores feeding on small prey exists in mammals larger than 21.5 kg, and it seems a similar minimum prey-size threshold could have affected dinosaurs as well.

Citation: Codron D, Carbone C, Clauss M (2013) Ecological Interactions in Dinosaur Communities: Influences of Small Offspring and Complex Ontogenetic Life Histories. PLoS ONE 8(10): e77110. doi:10.1371/journal.pone.0077110

Editor: Andrew A. Farke, Raymond M. Alf Museum of Paleontology, United States of America

Received: May 5, 2013; **Accepted:** September 4, 2013; **Published:** October 30, 2013

Copyright: © 2013 Codron et al. This is an open-access article distributed under the terms of the Creative Commons Attribution License, which permits unrestricted use, distribution, and reproduction in any medium, provided the original author and source are credited.

Funding: This is contribution no. 155 of the Deutsche Forschungsgemeinschaft, DFG Research Unit 533 "The Biology of Sauropod Dinosaurs". The funders had no role in study design, data collection and analysis, decision to publish, or preparation of the manuscript.

Competing Interests: The authors have declared that no competing interests exist.

* E-mail: d.codron@nasmus.co.za

Introduction

Modern terrestrial vertebrate systems are dominated by mammals, whereas birds and herpetiles are smaller-bodied and less conspicuous components of our landscapes. This presents a limitation to our understanding of dinosaurian ecology: no contemporary analogue exists from which conclusions can be securely made. One way to overcome this hurdle is to draw from known major differences between mammals and dinosaurs, and to use this information to make inferences about dinosaur ecology and the functioning of Mesozoic land systems. Dinosaurs and mammals differ in multiple aspects of biology, life history, and ecology [1,2], but it is the difference in reproductive strategies that is likely to have most relevance to arising ecological trends [3–6].

Dinosaurs, like their living descendents (birds), and extant herpetiles, were oviparous - numerous eggs and nesting sites have been described from the fossil record, and in some cases these have even been associated with particular taxa [5–9]. Mammals, by contrast, are viviparous, and their ancestors were likely giving

birth to live young from as early as the Mesozoic [10]. This contrast means that dinosaurs had the higher reproductive output, since oviparous animals can generally produce more offspring (eggs) than the number of live offspring produced by mammals [3,11]. In terms of life history strategies, species that produce more offspring tend to experience lower survival rates during younger life stages than do species with a lower reproductive output [12]. When survival rates are plotted against age, the patterns that emerge are known as either a type 3 or type B1 survivorship [12–14]. In the former, mortality rates level off amongst older individuals such that a negatively concave curve is produced, and in the latter mortality rates become relatively low during the species' middle years of life, with survivorship decreasing only later in life - the resultant curve is sigmoid in shape. Life tables reconstructed for specific dinosaur taxa directly from the fossil record indicate that they followed type B1 survivorship schedules [13,14]. Survivorship curves for species with lower reproductive rates (like many mammals) tend to be convex, exhibiting low mortality rates amongst juveniles [15]. Species can achieve this

type 1 survivorship by, for example, providing a level of parental care sufficient to ensure that the majority of juveniles escape death by predation, starvation, or disease. Since a species' survivorship schedule is strongly linked to the growth rate of populations [16], dinosaur populations surely experienced growth and dynamics that were different than those of mammals.

Another outcome of the disparity in reproductive strategies, of equal or potentially even greater significance, is that dinosaurs gave birth to much smaller offspring than do similar-sized mammals [7,11]. This occurred because, whereas mammals of larger size give birth to offspring of ever-increasing size, dinosaur egg size could not have increased indefinitely. Larger eggs need to be protected by thicker eggshells, but the eggshell cannot be so thick as to prevent sufficient oxygen from diffusing and reaching the growing embryo [9,17,18]. Thus, limits to eggshell thickness place limits on maximum egg size, and indeed eggs recovered from the dinosaur fossil record are relatively small compared to the extreme size of the adults, probably not weighing much more than 10 kg (and usually much less than this) in life [7,9,11]. As a comparison, offspring of the largest land mammals - the African elephant *Loxodonta africana* and Indian elephant *Elephas maximus* - weigh on average ~100 kg at birth, respectively [19]. At smaller body sizes, differences in relative offspring size of dinosaurs and mammals were small, but amongst larger size classes the effect is much more notable, with dinosaurs having massive adult-offspring size differences. These dinosaurs would have experienced more complex ontogenetic histories than mammals, with numerous morphological shifts through life [11,20,21]. These would have been accompanied by multiple shifts in ecological niches [11], as individuals/species with different morphologies and body masses are often assumed to occupy different niches. Ontogenetic niche shifts would have been even more pronounced in dinosaurs due to limited parental care [22] (young of mammals, which suckle from their mothers, probably have fewer niche shifts through life). Consequently, dinosaur communities must have included a greater diversity of individuals exploiting ecological niches associated with specific body sizes than do mammals, which would have meant a) greater availability of food for predators of the affected size classes, and b) a greater number of individuals competing for shared resources [4,23]. In the case of the former, younger individuals of the largest dinosaurs would have been available as prey, contrasting with the trophic energy sinks [23] represented by the megaherbivores of modern mammalian ecosystems (whose populations are hardly affected by pressure from predators).

Complex morphological ontogenetic series, and a link between ontogeny and demographic structure, have been described for dinosaur communities [5,20,21], but the influence of this structure on the ecology of Mesozoic fauna have hardly been considered in detail. On the other hand, attempts to reconstruct the age/size structure of dinosaur communities directly from the fossil record [13,14] are questionable because of small sample sizes [24]. Here, we explore size-structured ecological models that reflect the different intensities of key ecological interactions (predation and competition) between dinosaur and mammal communities, to assess how these differences influenced their respective body mass-species richness (M - S) distributions, and extinction patterns. We simulate communities comprising size-structured populations across the full range of body size classes expected for both vertebrate groups, and hypothetical life tables for each population based on predicted survivorship schedules (type B1 for dinosaurs, type 1 for mammals). Results are compared with M - S distributions from the fossil record (and of extant mammals and birds), to test the hypotheses that 1) middle- and large-sized carnivorous dinosaurs were relatively more diverse than carnivorous mammals

[25–27] because the former had access to a wider diversity and abundance of prey in this size range [23]; and 2) dinosaurs were poorly represented amongst small-to-middle size class species due to high competition intensity with juveniles from larger species in this range [4]. We also discuss trends in prey size selection that emerge in terms of resource partitioning that occurs amongst different-sized carnivorous dinosaurs in our models.

Methods

Vertebrate Body Masses

Body mass data for Mesozoic non-avian dinosaurs, mammals, and birds are from datasets presented in Codron et al. [4] (see references therein for primary literature sources). These include over 120 non-avian dinosaur, 31 bird, and 80 mammal taxa (see Table S1). All data were \log_2 -transformed for evaluating M - S distributions of each group, as well as for the three major non-avian dinosaur clades separately: Ornithischia, Sauropodomorpha, and Theropoda. The shape of the distributions for each group were evaluated by their skewness, and assessed for normality using the Shapiro Wilks' test [28]. M - S distributions for extant mammals and birds are also presented for comparison. The mammal dataset was extracted from [29], pruned to exclude duplicated species (taking mean body masses for species across continents), the marine Orders Cetacea and Sirenia, and the egg-laying Monotremata. Of the remaining 3501 entries, 214 represent taxa that went extinct by the end of the Pleistocene, and a further 658 are airborne bats (Order Chiroptera) and colugos (Order Dermoptera, $n=2$), thus the analyses of M - S distributions in modern mammals were repeated with both these groups excluded. Further, for comparison with clade-specific trends in dinosaurs, we evaluated M - S distributions amongst extant mammalian herbivores and carnivores separately. For the latter, however, we included only mammal groups comprising relatively large taxa, as these were expected to be most comparable with dinosaur communities. Thus, mammalian herbivores are represented by the four living terrestrial ungulate orders (Artiodactyla, Perissodactyla, Proboscidea, and Hyracoidea), and mammalian carnivores by the Order Carnivora. The dataset for bird body masses was taken from [30], including recent updates to that database [31]. We took averages (means) across sexes of the same taxon (including separate means for subspecies), in cases where data for both sexes were provided. The updated data adds numerous new taxa (species and subspecies) to the database, and mass estimates deemed as "better" by the author of the update replaced the earlier estimates. Finally, for taxa where no mean body mass was given, but minimum and maximum masses were, we took the average of the latter. Data for modern mammals and birds are included in Table S1.

Simulation of Size-Structured Communities

To simulate structure and abundances of dinosaurian and mammalian communities, we specified species (populations) over a variety of size (body mass, M , in kg \log_2 -transformed) classes, representing the full body mass range described for both groups. For dinosaurs, this range (i) extended in $\log_2 M$ increments from -9 to 17 , and for mammals from -9 to 14 , i.e. species ranged in M from ~ 2 g to 131 and 16 tons, respectively (see Sander et al. [32] for size limits of dinosaur and mammal species). Life tables for each population were constructed, sub-divided by mass classes (x) ranging from offspring to adult M , again in $\log_2 M$ increments. Offspring body masses were estimated by allometric relationships with adult body mass, using a smaller scaling exponent for dinosaurs (0.6) than for mammals (0.9) to incorporate differences

in ontogenetic history due to relatively smaller offspring in dinosaurs [3]. These scaling exponents are consistent with available data for extant herpetiles and birds, and for mammals, respectively [3,18,33–35].

In order to reconstruct survivorship schedules for simulated life tables, we first simulated age-specific survivorships (g_x) using the arbitrary equation

$$g_x = a + \frac{b}{x^\rho} \quad (1)$$

where a and b are constants greater than and less than zero, respectively, and x is the age (body mass) class. Equation 1 produces a negatively concave relationship between g_x and x for negative ρ , mirroring the hypothetical g_x schedule of populations exhibiting a Type 1 survivorship. For positive values of ρ , equation 1 yields a positively concave slope as expected for species that exhibit Type 3 survivorship. Because equation 1 produces the desired shape but arbitrary values, g_x schedules had to be standardized across all species in the model. Based on real life tables for 18 mammal and 11 herpetile taxa [36–50], which show maximum and minimum g_x values of 0.07 and 0.91, respectively, we standardized our schedules from 0.1 to 0.9. These schedules were then used to estimate mortality rates (q_x , i.e. $1 - g_x$), and more importantly for life table analyses the standardized survivorships (l_x , i.e. $l_{x-1}g_{x-1}$, where $l_0 = 1$) for each population [12,16]. Standardized survivorship schedules thus produced convex l_x curves (plotted over x) for type 1 survivorships, and concave curves for type 3 survivorships. For dinosaurs, we used a type 1 survivorship, but with g_0 set to the minimum value (i.e. 0.1) to reflect the high mortality rates of the youngest individuals, resulting in the sigmoid curve assumed for type B1 survivorships [13]. Despite concerns about the validity of this type of schedule for dinosaurs [24], we opted to retain the B1 curve since results of an earlier, similar model showed no qualitative differences in final outcomes from a Type 3 survivorship [4] - note that both strategies imply high reproductive output coupled with high infant mortality, reflecting the r -strategy predicted for dinosaurs [6]. For mammals, we assumed a Type 1 survivorship, typical for species which practice parental care to a greater degree than most herpetiles, and indeed than what is believed to have occurred in dinosaurs [22].

Fecundity schedules (m_x) of extant mammals and herpetiles are notably asymptotic in shape (when plotted against age); for examples, see [15,39,41,43,45,49]. To incorporate this pattern into our simulated life tables, we modeled m_x of each age/size class (x) according to the following (arbitrarily-selected) asymptotic equation:

$$m_x = a - b\rho^x; \text{ where } 0 < \rho < 1 \quad (2)$$

The minimum breeding stage was set amongst individuals with body masses 10% that of adults for their specific population, although shifting this figure as high as 90% had negligible influences on the end results. Fecundity schedules were then standardized for each population, where maximum m_x scaled negatively (with exponents 0.1) with M_{adult} [35].

Finally, we simulated abundances of each age class (n_x), both in terms of numbers available for predation (mortalities in the life tables) and numbers remaining after predation had occurred. Initial abundances for each population were established for the largest size class (k) based on negative allometric scaling (exponents -0.75) of body mass with abundance recorded for extant mammals and birds [51–53]. Initial abundances for younger age

classes were subsequently calculated by multiplying n of the largest age class by l_x and dividing by the lowest l_x in the series (i.e.). Abundances of the smallest group (n_0) were added to the number of births, the sum of the fertility schedule (F_x) for each population, where (i.e. the number of individuals in each size class multiplied by their estimated birth rate and survival probability, multiplied by 0.5 assuming only half the population is female). From the series of initial abundances, the numbers eaten by predators were calculated as $n_x q_x$ (assuming all mortalities are due to predation) and numbers of survivors were calculated as $n_x(1 - q_x)$.

Models of Ecological Interactions

The combined $n_x q_x$ schedules (assuming these to represent herbivores only, i.e. predation by carnivores on carnivores is omitted here for simplicity) for all populations yielded prey available for carnivores. Our model of predator-prey interactions is based on random encounters between predator and prey individuals of randomly-drawn body masses, similar to an approach used by Carbone et al. [54]. For these simulations, we used the entire mass range as prey, but carnivores ranged in $\log_2 M$ from only -9 to 13 (~ 8 000 kg) for dinosaurs, and from -9 to 10 (~ 1 000 kg) in mammals, since the largest carnivores species that ever existed were somewhat smaller than the largest herbivores. To avoid artificially setting minimum prey sizes taken by a predator, we retained the smallest individuals ($\log_2 M = -9$) for both prey and predators. Two versions of the model were run, incorporating two scenarios. In the first, prey partitioning was assumed *a priori*, so that during any random encounter a successful attack occurred if the predator and prey were of equal body mass. In the second, we assumed niche overlap, with predators consuming any prey individual they encountered that was equal to or smaller than their own mass. Simulations were repeated until the entire prey base was diminished, or results no longer changed with additional simulations - requiring more than 3×10^8 iterations for each scenario for dinosaurs and mammals, respectively. Ultimately, a matrix of predator-prey mass relationships was produced, from where prey partitioning amongst differently-sized predators could be evaluated, and the M - S distributions of predators could be inferred. For the latter, we estimated the number of predator individuals that could be supported by the available prey base from the total mass consumed (kg) by each size class, i.e. the product of numbers of prey eaten and their respective masses. This figure was then divided by the meat requirements for a predator of a particular body mass, which in modern vertebrates typically scales as mass to the exponent 0.75, consistent with allometries of both basal metabolic and field metabolic rates [55,56]. Meat requirements of herpetiles and mammals likely scale similarly, although the absolute intake (given by the intercept of log-log allometries) may have differed by an order of magnitude depending on whether dinosaurs were ecto- or endothermic [57,58]. Nonetheless, since ultimately intakes are calculated in relative terms here (i.e. proportions of diet), such physiologically-based differences need not be considered at this stage. In all, our models of predator-prey interactions represent outcomes when only body mass and availability (encounter rates) are considered, but for simplicity we do not include factors such as hunting velocity, energy expenditure, prey defense and predator attack mechanisms, or search areas.

Incorporating Size-Specific Competition

To incorporate density-dependent competition effects across species, we followed procedures used in a previous version of our models [4]. In brief, only similar-sized individuals (from life tables produced above) “compete”, resulting in mortalities in each size

class. The number of deaths were calculated as the total number of individuals of a particular size class, minus the number of individuals in that size class of the population of interest (i.e. competition effects are strictly interspecific), weighted by an arbitrary competition co-efficient (α). In these models, we also evaluate results that incorporate interactions between dinosaurs and mammals as well as those restricted within their respective groups. Finally, following Codron et al. [4], we simulated outcomes of size-specific competition in systems post-dating the non-avian dinosaur extinctions that occurred at the Cretaceous-Tertiary (K-T) boundary. Since these extinctions affected only larger individuals [59,60], we simply set initial abundances for individuals >25 kg to zero to mimic post K-T conditions.

Results

Body Mass-Species Richness Distributions of Dinosaurs, Mammals and Birds

The M - S distribution of non-avian dinosaurs in our dataset parallels results from analysis of a much larger dataset [61], and of a spatially-restricted dataset specific to the Dinosaur Park Formation, Alberta [62]. In all three datasets, dinosaurs exhibit a distinct bias against smaller taxa, resulting in left-skewed M - S distribution (Fig. 1a). This pattern, however, pertains only to the Ornithischia (Fig. 1b) and Sauropodomorpha (Fig. 1c), whereas the Theropoda - which were evidently better represented amongst smaller and medium-sized classes - display a normal M - S distribution, despite peaks at roughly 80 and 1000 kg, respectively (Fig. 1d; $SW-W=0.952$, $SW-p=0.127$; see Table 1 for a descriptive comparison of distributions and skewness in these groups). Analysis of a dataset comprising nearly 400 non-avian dinosaur taxa revealed a similar difference in M - S distributions of ornithischian and sauropodomorph dinosaurs on the one hand, and theropods on the other [61].

Mammals and birds, by contrast, exhibit more right-skewed M - S distributions (normal in the case of Mesozoic birds, but data for this group are limited), both amongst Mesozoic and extant faunas (Figs. 1e-h; Table 1). Similar left-skewed M - S distributions have previously been reported for extant mammal and bird assemblages [63–65]. An interesting pattern also emerges if data for all oviparous Mesozoic vertebrates are assessed together - because of the small maximum size of Mesozoic birds, the overall Mesozoic terrestrial vertebrate M - S distribution is bimodal, and a size gap appears in the size range of several to roughly a thousand kg (Figs. 1a and g; see also Codron et al. [4]). Mammals, which have dominated terrestrial life since the extinction of non-avian dinosaurs 65.6 million years ago, have always had continuous M - S distributions [4].

The difference in M - S distributions between ornithischian and sauropod compared with theropod dinosaurs is likely related to differences in trophic positions, since the former comprise largely herbivorous taxa, whereas the latter were primarily carnivores [2,66]. If this is the case, a further disparity with living mammals can be demonstrated: the large herbivorous land mammals of today (the ungulates) exhibit normal M - S distributions across taxa (Fig. 2a; Table 1), whereas the large-bodied carnivores (Order: Carnivora) exhibit strongly right-skewed M - S distributions (Fig. 2b). Both groups differ markedly from their Mesozoic dinosaurian counterparts, which had either left-skewed (herbivores) or normal (carnivores) M - S distributions, respectively.

Predator M - S Distributions and Prey Partitioning

The M - S distribution of dinosaur predators resulting from our model of predator-prey interactions reflects expectations based on

prey availability of different sizes, and the intake (biomass) required to support predators of different sizes. The high numbers of intermediate-sized dinosaur prey (i.e. including medium-sized taxa and the younger life stages of larger taxa) presents a richly available food resource for carnivorous dinosaurs. Consequently, the model results in a normal M - S distribution of carnivorous dinosaurs, regardless of whether or not prey partitioning is assumed, i.e. whether predators are assumed to consume prey of their size only, or prey of their size and smaller (Figs. 3a and b). This result mirrors the M - S distribution of theropod dinosaurs (Fig. 1d), which is normal and contrasts with the strongly left-skewed M - S distribution of the primarily herbivorous ornithischian and sauropodomorph groups (Figs. 1b and c). For mammals, a normal M - S distribution is also predicted when prey partitioning is assumed (Fig. 3c), but the pattern is distinctly right-skewed when partitioning is not assumed (Fig. 3d). The latter finding is not unlike the M - S distribution observed in living members of the Order Carnivora (Fig. 2b).

Models in which we assumed no prey partitioning *a priori* yielded results that are informative about the ways in which prey might have been partitioned across carnivorous dinosaurs of different size classes, and in fact how carnivores in general might partition the prey base. In this version of our models, predators were allowed to consume prey up to and including their own mass. The results reflect differences in prey availability across mass classes, such that the smallest predators consume only the smallest prey while larger predators consume an ever-increasing number of prey types (Fig. 4a). Because prey availability (i.e. herbivore density) is negatively correlated with body mass [67], large prey items make up a smaller number of the victims of larger carnivores. However, when relative contributions to a predator's diet (based on body mass of each item consumed rather than on numbers eaten) are considered, larger prey make up the biggest proportion of the diets of larger predators (Fig. 4b). Actually, above a certain predator mass, proportions of smaller prey items in the total biomass intake of a predator are so small they can be considered negligible. As a result, calculated niche breadths [68] (which are based on relative proportions of different prey items consumed) only increase with predator body mass until about 16 to 32 kg, after which increasing the number of prey items in the diet does not increase dietary diversity (Fig. 4c). The implication is that whereas larger predators can take prey of ever-increasing size, smaller prey items only make substantial contributions to the diets of predators below the 16–32 kg range in our model.

Size-specific Competition

Effects of size-specific competition on Mesozoic vertebrate communities have been reported previously, based on an earlier version of the models used here [4]. In that study, we predicted that the high degree of size (niche) overlap amongst individuals of small-to-medium size regardless of species resulted in limited niche opportunity for small-to-medium dinosaur species. The net effect is that dinosaur M - S distributions would have been bimodal, with a gap in the intermediate size range. Competition from small-bodied mammals would have further reduced niche opportunity for the smallest dinosaur taxa. Thus, if competition between small dinosaurs and mammals was an issue, this would have further reduced the body mass range of the former, leading to their exclusion and/or necessitating adoption of a alternative (i.e. airborne) niches. By contrast, mammal M - S distributions would have been continuous except at unrealistically high competition intensities (high α values in the model), but would have been limited to smaller mass classes due to competition pressure from dinosaurs. We predicted that the low species diversity of non-avian

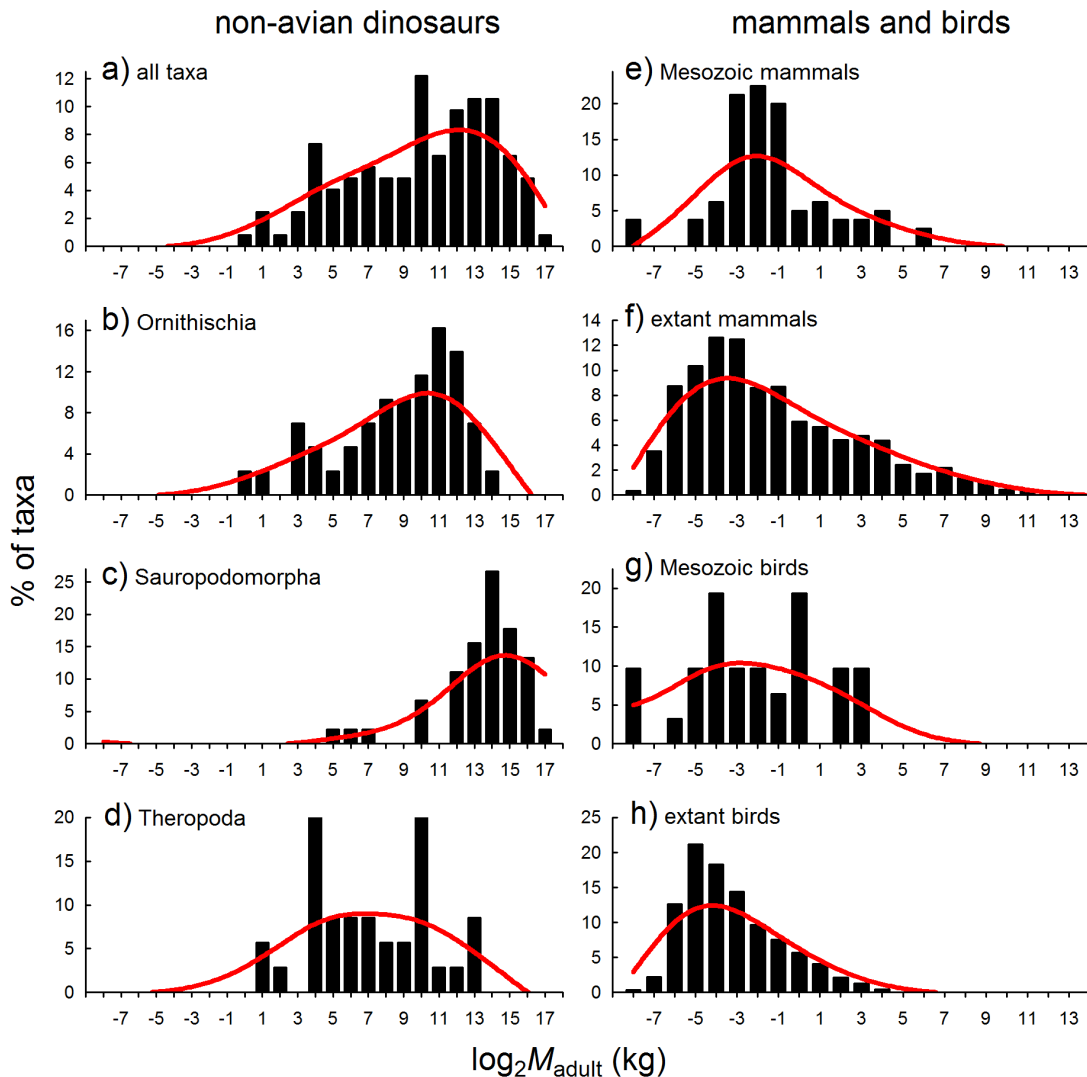


Figure 1. Body mass-species richness (M - S) distributions, represented on a \log_2 -scale, of extinct (non-avian) dinosaurs, in comparison with distributions of mammals and birds from the Mesozoic and present-day distributions. Data for Mesozoic vertebrates compiled in [4], see references therein for primary sources, and data for extant mammals and birds are from [29–31]. Red curves are fitted visually to aid interpretation.

doi:10.1371/journal.pone.0077110.g001

dinosaurs amongst the smaller mass range would have prevented the recovery of populations after the K-T extinction events, whereas mammals were able to recover (not having experienced the size gap) and even proliferate into larger mass classes.

Having considered effects of predation on size-structured dinosaur communities in the model versions presented above, it is worth revisiting whether our earlier results of size-specific competitive interactions [4] persist (and also since those effects cannot now be excluded from a detailed analysis of how size structure influenced the ecology of dinosaur communities). In [4], we assumed dinosaurs to have displayed type 3 rather than type B1 survivorships as used here, but we showed in sensitivity analyses that this difference did not influence model outcomes qualitatively. Thus we are only concerned here with the difference in species abundances simulated by the two modelling approaches (here mortalities are also influenced by predation, rather than on mass-abundance scaling alone), and also with the more complex fertility schedules used here (in earlier versions, only the largest individuals within populations produced offspring).

As expected, incorporating size-specific interspecies competition in the present models yielded results that are qualitatively similar to those discussed previously [4], indicating that the high degree of size overlap is a quintessential ecological parameter for dinosaur communities. In the absence of competition, the simulated dinosaur community exhibits a continuous M - S distribution (Fig. 5a), but competition-induced mortalities lead to population extinctions in the middle size class range (between several and one thousand kg) resulting in a bimodal M - S distribution (Fig. 5b). The lower end of the M - S distribution is consistent with minimum and maximum size of Mesozoic birds, whereas few non-avian dinosaur taxa existed in this range (see Figs. 1a and g). In addition, the upper size classes of the small end of the dinosaur M - S distribution is further reduced when pressure from competition with other dinosaurs is coupled with competition with similar-sized mammals (Fig. 5c). Finally, results of our simulation of post K-T scenarios (initially excluding all individuals >25 kg) indicate that the body size gap - the explicit outcome of size-specific competition amongst

Table 1. Descriptive statistics for $\log_2 M_{\text{adult}}$ (kg) of Mesozoic dinosaur, mammal, and bird taxa, and for living mammals and birds.

Group	<i>n</i>	Median	Min	Max	Q25	Q75	Skewness	SW- <i>W</i>	SW- <i>p</i>
Non-avian dinosaurs									
All taxa	123	10.5	0	17.2	7	13.3	-0.491	0.959	<0.001
Ornithischia	43	9.8	0	14.5	6.7	11.4	-0.826	0.93	0.012
Sauropodomorpha	45	13.7	4.6	17.2	12.7	14.8	-1.599	0.862	<0.001
Theropoda	35	7.3	1.1	12.7	4.3	10	-0.008	0.952	0.127
Mammals									
Mesozoic	80	-3.6	-7.2	4.1	-5	-2.4	1.043	0.921	<0.001
Modern									
Extant	3277	-3.3	-9.2	11.9	-5.3	0.1	0.8	0.939	<0.0001
Incl. recent extinctions	3501	-2.9	-9.2	13.3	-5.2	1.2	0.9	0.928	<0.0001
Excl. airborne groups	2619	-2.3	-9.2	11.9	-4.5	1.3	0.7	0.953	<0.0001
Extant herbivores	223	5.8	1.3	11.9	4.3	7.4	0.2	0.990	0.110
Extant carnivores	258	1.8	-3.3	10.6	0.5	3.8	0.6	0.959	<0.0001
Birds									
Mesozoic	31	-4	-9	1.3	-6.2	-1.6	0.169	0.951	0.168
Extant	9991	-4.8	-9.0	6.8	-6.1	-2.9	0.827	0.999	<0.0001

n = number of taxa; SW = Shapiro Wilks' test for normal distribution.

Modern mammal subgroups: Incl. recent extinctions = data includes species that went extinct in the Late Pleistocene; Excl. airborne groups = data excludes the airborne mammalian orders Chiroptera (bats) and Dermoptera (colugos); carnivores = members of the Order Carnivora; Herbivores = members of the Orders Artiodactyla, Perissodactyla, Proboscidea, and Hyracoidea.

doi:10.1371/journal.pone.0077110.t001

dinosaurs - prevented recovery of populations of larger (non-avian) dinosaur faunas (Fig. 5d).

Effects of size-specific competition are weaker in mammals, due to their less complex ontogenetic histories and lower degrees of size and niche overlaps across species. Our model yields a continuous *M-S* distribution for mammals with and without competition (Figs. 5e and f); size gaps do emerge for mammals, but only at much higher competition intensities than for dinosaurs (e.g. four- or fivefold increases in α). Interestingly, competition with similar-sized dinosaur individuals, including younger life stages of larger dinosaur species, is sufficient enough to result in population extinctions of mammal species above 8 kg (Fig. 5g). Low diversity of mammal species above this size is not unlike what is known about Mesozoic mammals based on the fossil record (see Fig. 1e) - indeed, the largest Mesozoic mammal was only around 30 kg, and this is considered exceptionally large for mammal faunas of the times [69]. In the absence of competition from dinosaurs, post K-T mammals did not suffer this constraint in our model, and populations are able to recover and invade even larger size classes despite initial conditions excluding all individuals above 25 kg (Fig. 5h). Hence, size-specific competition effects, incorporating differences in ontogenetic niche complexities between dinosaurs and mammals, are consistent both with trends observed in the Mesozoic fossil record, and with changes in terrestrial vertebrate diversity after the K-T events.

Discussion

Dinosaurs differed in numerous ways from mammals, in terms of life history and biology [1,2]. The respective reproductive strategies of these two groups is a major life history difference, that would have influenced the ecology of both types of communities differently. Notably, no oviparous species since the Mesozoic have reached the massive sizes achieved by dinosaurs, nor even rivalled those of the largest mammals. Yet, even today oviparous and

viviparous taxa have disparate life histories, as evident from data collected to construct ecological life tables for mammals and herpetiles [15,39,41,43,45,49]. In the case of dinosaurs, an oviparous reproductive strategy coupled with extremely large body size resulted in adult:offspring mass ratios that were substantially higher than those of similar-sized mammals [7]. We hypothesized that this led to a more pronounced and complex ontogenetic series experienced by dinosaurs than mammals, which resulted in a higher frequency of density-dependent ecological interactions in dinosaur- than in mammal-dominated systems.

How ontogenetic niche shifts and resultant changes in the frequency of ecological interactions affect communities is not well understood even in extant systems, but it is likely that population numbers and dynamics would be influenced [70,71]. Our study focused on resultant changes to community structure, in particular the contrast between extant mammal-dominated and Mesozoic dinosaur-dominated systems. One potential influence at the community level is that more small- to medium-sized prey must have been available to dinosaurian than mammal carnivores. Also, dinosaurs would have experienced more ecological niche shifts through life, as occurs during ontogeny in many species both oviparous and viviparous [70-74]. Since similar-sized individuals of a given trophic level often share a similar niche space, the relatively high niche diversity within dinosaur species surely meant more overlaps - and hence more frequent competitive interactions - across species.

Model Limitations

The size-structured models we used make a number of assumptions about dinosaur life history and ecology which would have influenced our results to some degree. The choice to simulate Type B1 survivorships for dinosaurs (as opposed to Type 1 schedules for mammals) was based on evidence for dinosaur life histories in the fossil record [13,14]. However, small sample sizes

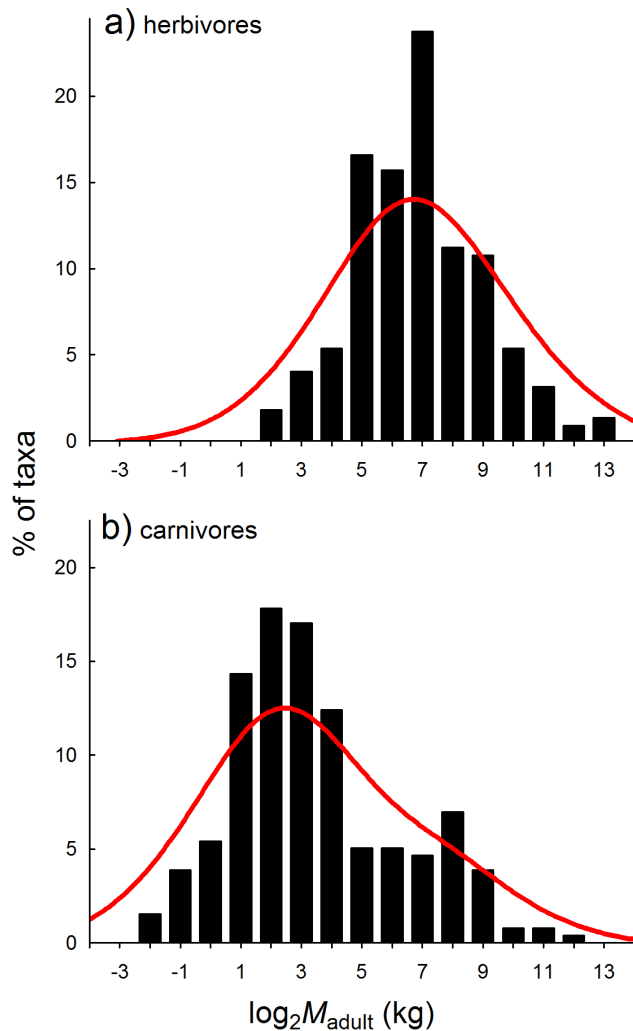


Figure 2. *M-S* distributions of extant mammal herbivores and carnivores. For comparison with *M-S* dinosaur distributions, only larger-bodied groups of mammals were included here, i.e. we omitted data for rodents, insectivores, and other smaller-bodied mammal groups. Thus, herbivores are represented only by the four living ungulate Orders (Artiodactyla, Perissodactyla, Proboscidea, and Hyracoidea), and carnivores by the Order Carnivora. Red curves are fitted visually to aid interpretation.
doi:10.1371/journal.pone.0077110.g002

used to construct those life tables may have misleadingly led to inference of concave curves, and only minor adjustments to the data are necessary for convex (Type 3) curves to emerge [24]. Moreover, many if not most modern herpetiles display Type 3 survivorships [39,41–50], and, given the *r*-life history strategy (i.e. high reproductive output) [1,6] and low levels of parental care typically expected for non-avian dinosaurs [22], this life history schedule may be more appropriate. Nonetheless, in earlier versions of the model (which focused only on size-specific competition), model outcomes did not differ qualitatively across any type of survivorship schedule, described in Table S1 to [4]. Clearly, the impacts of a more complex size-structure in dinosaur populations than in mammals more significantly influenced community properties than did the shape of species' survivorship curves. It remains, though, that our models lack variability in life histories across species, and further work is needed to determine

what effects - if any - differences in life history of small versus large dinosaurs might have had.

A key assumption of our model is that similar-sized individuals occupy overlapping niche space, and that predators and competitors are strongly influenced by this. While links between body size and niche occupancy should be expected, morphological, physiological, and behavioural constraints could easily dictate an individual's realized niches and - in theory - lead to niche separation between individuals/species of similar size (recall that these models also do not take differences in carnivore behaviour into account). Our assumption therefore is very general, and makes a broad statement that niche overlaps within body size classes are more frequent than those across body size classes. Thus, our models should not be treated as attempts to quantitatively reconstruct dinosaur communities, but rather to make inferences about broad-scale trends within them.

The assertion that size-specific competition was a major limiting factor in dinosaur-dominated systems is upheld not only by being a logical conclusion deduced from a well-known pattern (the relatively small offspring of dinosaurs), but also because results presented here are consistent with those presented in an earlier study [4]. The models used in that study lacked effects of predation, and the complexity of breeding schedules used here. Further modification of these approaches will help us to work towards building ever more realistic simulations of past communities and community interactions.

Comparison to the Fossil Record

The fossil record reveals vastly disparate structures of dinosaur-versus mammal-dominated systems: in the former, *M-S* distributions are bimodal, with a gap in the middle size range between several to around 1 000 kg, whereas *M-S* distributions of the latter are continuous, and have been so throughout the Cenozoic [4]. The size gap in dinosaur-dominated vertebrate systems occurs because of a strong bias towards larger species amongst non-avian dinosaurs [4,61], and bias towards smaller body size in Mesozoic birds and mammals. Bias towards larger species amongst non-avian dinosaurs means their *M-S* distributions were left-skewed along the mass gradient (whereas mammalian systems are typically right-skewed), although this trend was only consistent amongst herbivorous groups (ornithischians and sauropodomorphs); theropods, having been largely carnivorous, show a more normal pattern. Conversely, the pattern for modern mammalian carnivores is right-skewed, whilst large mammalian herbivores (ungulates) are normally distributed across their body mass range.

The influence of taphonomic effects which could bias *M-S* distributions recovered from the fossil record is debatable. While several studies have found no evidence for taphonomic size biases in dinosaur assemblages [8,61,75], a recent analysis of a well-constrained assemblage (Dinosaur Park Formation, DPF) suggests that taphonomic effects and researcher bias have resulted in underrepresentation of small-bodied dinosaurs in at least some datasets [62]. However, further analyses of the species accumulation curves (an important source of information for inferring how closely current sampling approximates true diversity) presented in that study reveals that only theropods, not ornithischian dinosaurs, may have been undersampled at DPF (i.e. the curve for ornithischian species richness does reach an asymptote; see also [76]). Hence, even in this spatially-restricted case, the left-skewed *M-S* distribution of the herbivorous group is a consistent trend. Further, the DPF assemblage lacks sauropods, so may in fact underrepresent large-bodied taxa. Whether theropod *M-S* distributions other than normal will emerge from future discoveries is at this stage unclear. Other factors arguing against a major

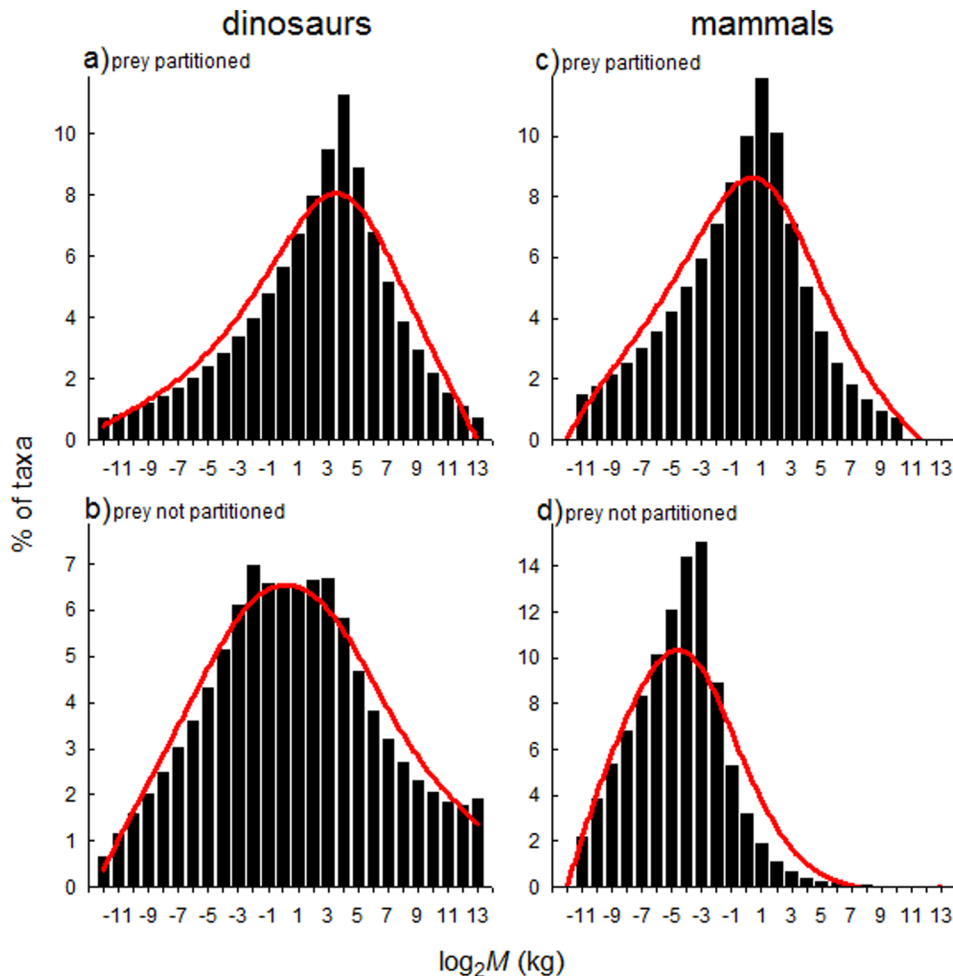


Figure 3. Predicted M - S distributions of carnivorous dinosaur and mammal assemblages, based on a model incorporating differences in availability of prey of different body sizes, and the resultant biomass intake (and requirements) by predators. Prey partitioning was assumed by setting prey:predator mass ratios at 1:1, i.e. each predator is assumed to eat prey of its size only. When prey partitioning was not assumed, predators were allowed to feed on any prey they encountered of their size or smaller. Red curves are fitted visually to aid interpretation.

doi:10.1371/journal.pone.0077110.g003

taphonomic effect is that numerous small-bodied mammals and birds have been recovered from a variety of Mesozoic deposits from where small-bodied non-avian dinosaurs are few in number or absent [10]. A recent analysis of a globally-representative dataset found no evidence for taphonomic bias, and in fact reported similar M - S distributions as described here [61]. Whatever future discoveries may reveal about Mesozoic dinosaurian and other vertebrate faunas, it seems unlikely that the M - S distributions presented here will ever change substantially: for skewness to differ entirely from current predictions, over 95% of non-avian dinosaur taxa still await discovery, all of which would have to be very small [4,61].

Results of models presented here actually mirror the M - S distribution patterns of the dinosaur and mammal fossil records. These results show that left-skewed M - S distributions of herbivorous non-avian dinosaurs, and relative scarcity of medium- to small-sized species of this group, could easily have arisen because of size-specific competition for niche space in this mass range. Similarly, the increased availability of medium-sized prey in dinosaur-dominated ecosystems could account for the normal M - S distribution so far recorded for theropods, as well as a higher

carnivore:herbivore species ratio in dinosaur versus mammal communities [25–27]. Thus, our approach offers an ecological explanation for patterns observed in the fossil record, such that we might even expect these patterns rather than predicting that taphonomic effects have taken place.

Complex Size Structure and the Ecology of Non-Avian Dinosaur Communities

The complex size structure of non-avian dinosaur populations likely influenced carnivores and herbivores in different ways. Whereas here and previously we have predicted a left-skewed M - S distribution for non-avian dinosaurs in general [4], data presented here and elsewhere [61] reveal a normal M - S distribution amongst the (largely carnivorous) theropods. Our models depict that a high abundance and diversity of prey in the small-medium mass range was available to theropod dinosaurs, because of the numerous younger life stages of very large herbivores that would have been present. This complexity of age/size diversity has also been reported from analyses of dinosaur trackways [5]. Given that carnivores tend to feed on prey at or below their body mass [77,78], this hypothesized prey diversity could easily explain the

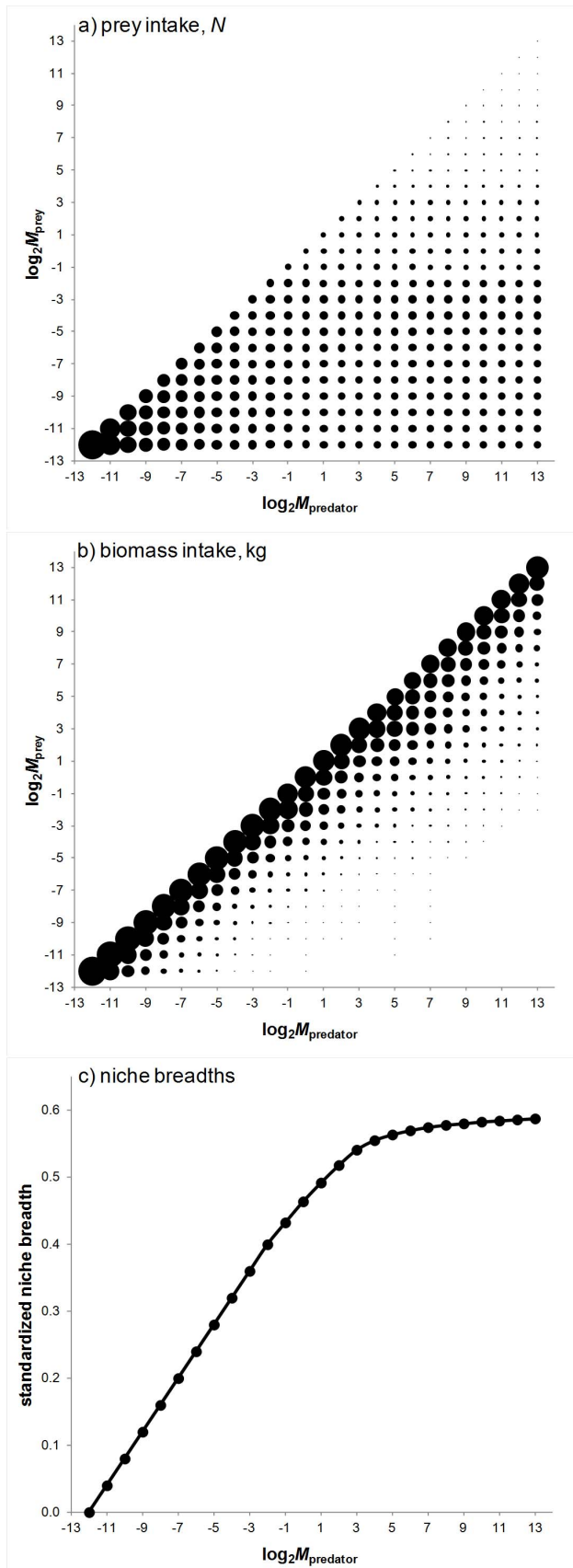


Figure 4. Prey partitioning amongst different-sized predators that arises in models where no prey partitioning was assumed

a priori. In a) and b) bubbles represent relative contributions of different-sized prey to predator diets, based on numbers or total biomass (kg) consumed, respectively; for c) niche breadths were calculated based relative numbers of prey consumed per size class. doi:10.1371/journal.pone.0077110.g004

higher prevalence of small- and medium-sized carnivorous dinosaurs than observed in the largely herbivorous sauropod and ornithischian clades. A difference from mammal-dominated systems is that megaherbivores did not represent trophic energy sinks [23], as they do in today's mammalian-dominated systems in which predator pressure on the largest herbivores is small or negligible [79]. Similarly, greater diversity and abundance of small- and medium-sized prey in the Mesozoic could have equated to a greater relative (and perhaps absolute) diversity of predators in this size range, explaining the high carnivore:herbivore ratios in these compared with extant mammalian systems (see above). Models converged on this outcome for carnivorous dinosaur assemblages even when prey partitioning was not assumed. Thus, even if the fundamental diet niches of dinosaurian carnivores had overlapped entirely - at least in as much as all had equal access to prey items below their own body size - they still would have been affected differently by prey availability than mammalian carnivores.

When competing for prey in this way, carnivores are likely to partition the prey base due to the interaction between prey availability (which is negatively related to prey size) and energy gain (the mass of the prey). In our models, predators did not consume nearly as many large compared with smaller prey individuals, due to the lower abundances of the former, yet net energy gain (total biomass consumed) made smaller prey items somewhat unprofitable for larger carnivores. Thus, despite the high availability of small prey (in numbers), they contributed little to the overall biomass intake of larger predators. In modern mammals, a switchpoint has been described, around which carnivores smaller than 21.5 kg are represented by taxa that feed primarily at their own body mass and taxa feeding on much smaller prey (including insectivorous species), whereas carnivores larger than 21.5 kg feed only on prey of their own mass [80]. Explanations for this pattern have focused on energetics, a claim supported by models that balance daily net energy expenditure and gain [80,81]. Our models reveal a similar switchpoint (between ~16 and 32 kg), which suggests the interaction between prey availability and mass of each meal gained at least partly explains the pattern observed in mammals.

The implication of a prey-size switchpoint is that in dinosaurian carnivore systems - and perhaps amongst vertebrate carnivores in general - there is a high cost associated with feeding on small prey that is related to availability, i.e. above a certain body mass, encounter rates with small prey are insufficient relative to the low energy gain for large predators to forage efficiently. This would force carnivores to focus on larger prey sizes as they themselves increase in size. Nevertheless, given the high productivity of herbivorous dinosaurs in the medium body mass range, most carnivorous dinosaurs would have occupied this feeding niche rather than the high energy requirements needed to catch and subdue very large prey. In other words, by focusing on younger life stages as prey, dinosaurian predators would have been able to ensure that trophic energy was not lost even from populations of the largest herbivore species [23].

Aside from carnivory, our study - consistent with results from an earlier version of these models [4], indicates that size-specific competition was a likely factor driving the bimodal M - S distribution of Mesozoic communities, both in terms of limiting niche opportunity for populations of small- and medium-sized non-avian dinosaur populations to flourish, and restricting

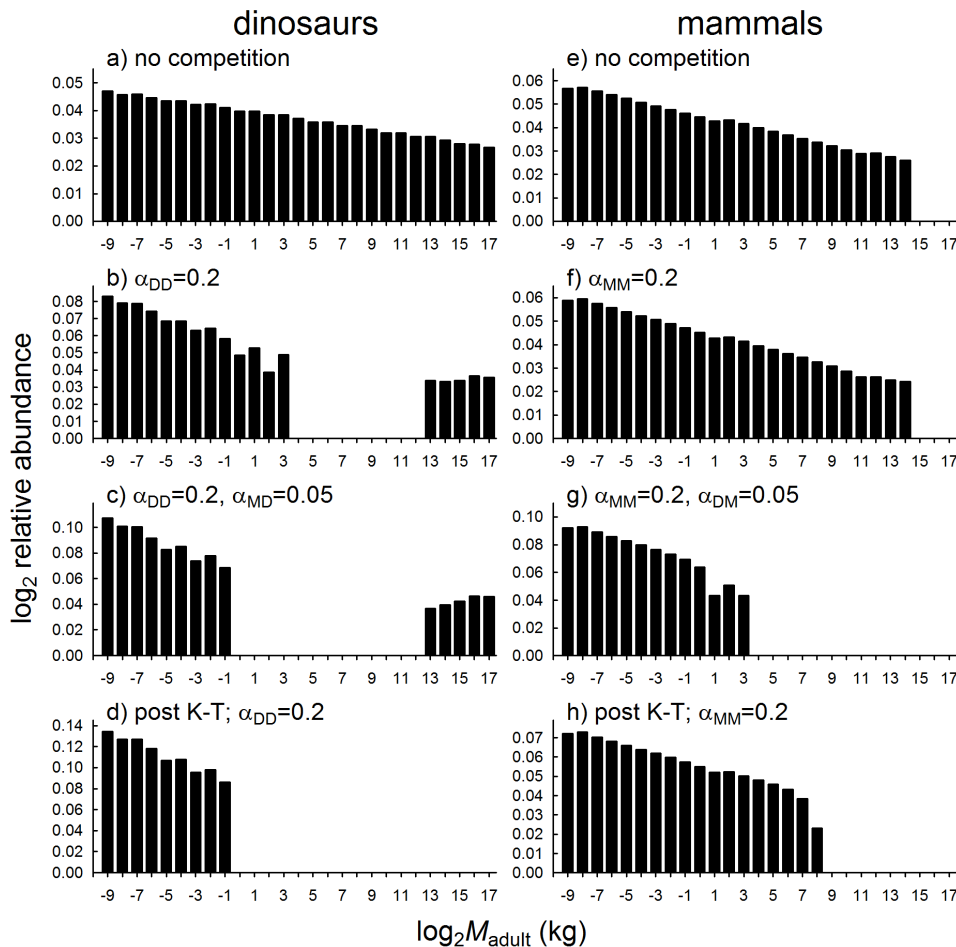


Figure 5. Outcomes of the size-specific competition model, comparing outcomes for M - S distributions of dinosaur (with a higher number of size-specific niche overlaps due to their more complex ontogenetic histories) and mammal communities. Competition coefficients (α) represent the proportion of density-dependent mortalities that occur, due to competition between dinosaurs (subscript DD), between mammals (MM), from mammals on dinosaurs (MD), and from dinosaurs on mammals (DM). Post K-T extinction scenarios were simulated by setting initial conditions to exclude all individuals above 25 kg. doi:10.1371/journal.pone.0077110.g005

Mesozoic mammals to small size classes. The combined pressure of competition from mammals and other dinosaurs, if these groups were also competing, could have further restricted niche space available to the smallest dinosaurs. One possible outcome is that very small dinosaurs adopted alternate niches altogether, and the proposed mechanism could thus provide an explanation for the emergence of flight earlier in the Mesozoic. In the absence of large, oviparous taxa having to pass through so many ontogenetic niche stages during growth, size-specific competition has not been as big of an issue for Cenozoic communities.

Oviparity is associated with a higher net reproductive output than viviparity, implying that during the Mesozoic dinosaurs had an advantage over mammals over the various environmental and extinction episodes that occurred [3,11,82]. Moreover, their complex ontogenetic histories, including a diversity of niches utilized throughout life, possibly ensured that at least some life stages of dinosaurian populations would have survived through loss of particular habitats during short periods of environmental disturbance. By contrast, loss of only a few habitats during such times would have had far more drastic impacts on mammal populations. However, the K-T events were unique, with events selectively killing individuals above a certain size, probably

between 20–25 kg [59,60]. Our model shows how the lack of species diversity in non-avian dinosaurs at small sizes prevented post K-T recovery of this group. Mammals, and even birds if they were affected, were able to recover because sufficient small-bodied species were present before and after the events. Subsequently, mammals and birds were able to evolve into larger body size classes as well, consistent with the rapid increase of maximum mammal body mass, and increases in avian diversity, from relatively early in the Cenozoic [83,84].

Dinosaurs are renowned for their large body sizes, and for having had growth rates which were nearly as high as those of endothermic, viviparous mammals [1,85,86]. Whether the combined pressure from predation and competition on medium-sized prey populations, and the relative immunity of large adults to these factors, could have been responsible for the evolution of large size and relatively fast growth (for notions linking biology to body size in dinosaurs, see [3,87]) is an important question for future research, and may shed light on other key aspects of dinosaur evolutionary biology, including the origins of endothermy in them and their living descendents, the birds.

Supporting Information

Table S1 Body mass estimates for Mesozoic vertebrates, modern mammals, and modern birds.
(XLSX)

Acknowledgements

We thank Christopher Noto and an anonymous reviewer for comments that improved the quality of this manuscript.

References

- Sander PM, Christian A, Clauss M, Fechner R, Gee CT, et al. (2011) Biology of the sauropod dinosaurs: the evolution of gigantism. *Biol Rev (Camb)* 86: 117–155.
- Weishampel DB, Dodson P, Osmólska H (2004) *The Dinosauria*. Berkeley/Los Angeles, CA: University of California Press.
- Werner J, Griebeler EM (2011) Reproductive biology and its impact on body size: comparative analysis of mammalian, avian and dinosaurian reproduction. *PLoS ONE* 6: e28442.
- Codron D, Carbone C, Müller DWH, Clauss M (2012) Ontogenetic niche shifts in dinosaurs influenced size, diversity and extinction in terrestrial vertebrates. *Biol Lett* 8: 620–623.
- Lockley MG (1994) Dinosaur ontogeny and population structure: interpretations and speculations based on fossil footprints. In: Carpenter K, Hirsch KF, Horner JR, editors. *Dinosaur eggs and babies*. Cambridge: Cambridge University Press. 347–354.
- Paul GS (1999) Dinosaur reproduction in the fast lane: implications for size, success, and extinction. In: Carpenter K, Hirsch KF, Horner JR, editors. *Dinosaur eggs and babies*. Cambridge: Cambridge University Press. 244–255.
- Sander PM, Peitz C (2008) Upper Cretaceous titanosaur nesting sites and their implications for sauropod dinosaur reproductive biology. *Palaeontogr Abt A Palaeozool-Stratigr* 284: 69–107.
- Carrano MT (2006) Body-size evolution in the Dinosauria. In: Carrano MT, Blob RW, Gaudin T, Wible JR, editors. *Amniote paleobiology: perspectives on the evolution of mammals, birds, and reptiles*. Chicago: University of Chicago Press. 225–268.
- Seymour RS (1979) Dinosaur eggs: gas conductance through the shell, water loss during incubation and clutch size. *Paleobiol* 5: 1–11.
- Benton MJ (2006) *Vertebrate palaeontology*, third edition. Massachusetts: Blackwell Publishing.
- Janis CM, Carrano M (1992) Scaling of reproductive turnover in archosaurs and mammals: why are large terrestrial mammals so rare? *Ann Zool Fenn* 28: 201–216.
- Begon M, Townsend CR, Harper JL (2006) *Ecology, from individuals to ecosystems*, fourth edition. Oxford: Blackwell Publishing.
- Erickson GM, Currie PJ, Inouye BD, Winn AA (2006) Tyrannosaur life tables: An example of nonavian dinosaur population biology. *Science* 313: 213–217.
- Erickson GM, Makovicky PJ, Inouye BD, Zhou C-F, Gao K-Q (2009) A life table for *Psittacosaurus lujiatunensis*: initial insights into ornithischian dinosaur population biology. *Anatomical Record: Advances in Integrative Anatomy and Evolutionary Biology* 292: 1514–1521.
- Heppell SS, Caswell H, Crowder LB (2000) Life histories and elasticity patterns: perturbation analysis for species with minimal demographic data. *Ecology* 81: 654–665.
- Akçakaya HRM, Burgman MA, Ginzburg LR (1999) *Applied population ecology*, second edition. Sunderland Massachusetts: Sinauer Associates. 285 p.
- Ar A, Rahn H, Paganelli CV (1979) The avian egg: mass and strength. *Condor* 81: 331–337.
- Rahn H, Paganelli CV, Ar A (1975) Relation of avian egg weight to body weight. *Auk* 92: 750–765.
- Jones KE, Bielby J, Cardillo M, Fritz SA, O'Dell J, et al. (2009) PanTHERIA: a species-level database of life history, ecology, and geography of extant and recently extinct mammals. *Ecology* 90: 2648 (Ecological Archives E2090–2184).
- Klein N, Sander M (2008) Ontogenetic stages in the long bone histology of sauropod dinosaurs. *Paleobiol* 34: 247–263.
- Chiappe LM (2001) Embryonic skulls of titanosaur sauropod dinosaurs. *Science* 293: 2444–2446.
- Birchard GF, Ruta M, Deeming DC (2013) Evolution of parental incubation behaviour in dinosaurs cannot be inferred from clutch mass in birds. *Biol Lett* 9. doi:10.1098/rsbl.2013.0036.
- Hummel J, Clauss M (2008) Megaherbivores as pacemakers of carnivore diversity and biomass: distributing or sinking trophic energy? *Evol Ecol Res* 10: 925–930.
- Steinsaltz D, Orzack SH (2011) Statistical methods for paleodemography on fossil assemblages having small numbers of specimens: an investigation of dinosaur survival rates. *Paleobiol* 37: 113–125.
- Läng E, Boudad L, Maio L, Samankassou E, Tabouelle J, et al. (2013) Unbalanced food web in a Late Cretaceous dinosaur assemblage. *Palaeogeogr Palaeoclimatol Palaeoecol* 381–382: 26–32.
- Farlow JO, Holtz TRJ (2002) The fossil record of predation in dinosaurs. In: Kowalewski M, Kelley PH, editors. *The fossil record of predation: Paleontological Society Papers*. 251–265.
- Horner JR, Goodwin MB, Myhrvold N (2011) Dinosaur census reveals abundant *Tyrannosaurus* and rare ontogenetic stages in the Upper Cretaceous Hell Creek Formation (Maastrichtian), Montana, USA. *PLoS ONE* 6: e16574.
- Statsoft_Inc (2007) STATISTICA. Version 8.0 [computer program]. Statsoft Inc. Tulsa, Oklahoma.
- Smith FA, Lyons K, Morgan Ernest SK, Jones KE, Kaufman DM, et al. (2003) Body mass of Late Quaternary mammals. *Ecology* 84: 3403 (Ecological Archives: E3084–3094).
- Dunning JB (2007) *CRC handbook of avian body masses*, second edition: CRC Press.
- Dunning JB (2013) Updates to the second edition of the CRC handbook of avian body masses: <https://ag.purdue.edu/fnr/Documents/BodyMassesBirds.pdf>.
- Sander PM, Clauss M (2008) Sauropod gigantism. *Science* 322: 200–201.
- Blueweiss L, Fox H, Kudzma V, Nakashima D, Peters R, et al. (1978) Relationships between body size and some life history parameters. *Oecologia* 37: 257–272.
- Cabana G, Frewin A, Peters RH, Randall L (1982) The effect of sexual size dimorphism on variations in reproductive effort of birds and mammals. *Am Nat* 120: 17–25.
- Hendriks AJ, Mulder C (2008) Scaling of offspring number and mass to plant and animal size: model and meta-analysis. *Oecologia* 155: 705–716.
- Armitage KB, Downhower JF (1974) Demography of yellow-bellied marmot populations. *Ecology* 55: 1233–1245.
- Barkalow FS, Jr., Hamilton RB, Soots RF, Jr. (1970) The vital statistics of an unexploited gray squirrel population. *J Wildl Manag* 34: 489–500.
- Barlow J, Boveng P (1991) Modeling age-specific mortality for marine mammal populations. *Mar Mamm Sci* 7: 50–65.
- Berglund S-A (2000) Demography and management of relict sand lizard *Lacerta agilis* populations on the edge of extinction. *Ecol Bull* 48: 123–142.
- Ericsson G, Wallin K, Ball JP, Broberg M (2001) Age-related reproductive effort and senescence in free-ranging moose, *Alces alces*. *Ecology* 82: 1613–1620.
- Ortega-Rubio A, Halffter G, Barbault R (2000) Bunch grass lizard, *Sceloporus scalaris*, population dynamics at La Michilia Biosphere Reserve, Mexico. *Herpetol J* 10: 33–39.
- Parker WS (1974) Demography of the fence lizard, *Sceloporus undulatus*, in Northern Mississippi. *Copeia* 1994: 136–152.
- Galán P (1999) Demography and population dynamics of the lacertid lizard *Podarcis bocagei* in north-west Spain. *J Zool* 249.
- Abts ML (1985) The life history strategy of the Saxicolous desert lizard, *Sauromalus obesus*. Portland State University.
- Gadgon JD, Dunham AE, van Loben Sels RC (1994) Demographics of common snapping turtles (*Chelydra serpentina*): implications for conservation and management of long-lived organisms. *Am Zool* 34: 397–408.
- Punzo F (2007) Life history, demography, diet and habitat associations in the southwestern earless lizard, *Cophosaurus texanus scitulus* from northern and southern limits of its geographical range. *Amphibia-Reptilia* 28: 65–76.
- Vinegar MB (1975) Demography of the striped plateau lizard, *Sceloporus virgatus*. *Ecology* 56: 172–182.
- Tinkle DW, Dunham AE (1983) Demography of the tree lizard, *Urosaurus ornatus*, in central Arizona. *Copeia* 1983: 585–598.
- Van Devender RW (1982) Comparative demography of the lizard *Basiliscus basiliscus*. *Herpetologica* 38: 189–208.
- Gadsden H, Estrada-Rodríguez JL (2008) Demography of the Yarrow's spiny lizard, *Sceloporus jarrovi*, from the central Chihuahuan desert. *West N Am Nat* 68: 46–57.
- Damuth J (1981) Home range, home range overlap, and species energy use among herbivorous mammals. *Biol J Linn Soc* 15: 185–193.
- Damuth J (2007) A macroevolutionary explanation for energy equivalence in the scaling of body size and population density. *Am Nat* 169: 621–631.
- Blackburn TM, Gates S, Lawton JH, Greenwood JJD (1994) Relations between body size, abundance and taxonomy of birds wintering in Britain and Ireland. *Philos Trans R Soc Lond B* 343: 135–144.
- Carbone C, Turvey SJ, Bielby J (2011) Intra-guild competition and its implications for one of the biggest terrestrial predators, *Tyrannosaurus rex*. *Proc R Soc Lond B Biol Sci* 278: 2682–2690.

Author Contributions

Conceived and designed the experiments: DC CC MC. Performed the experiments: DC CC. Analyzed the data: DC CC. Contributed reagents/materials/analysis tools: DC CC. Wrote the paper: DC MC.

55. McNab BK (2008) An analysis of the factors that influence the level and scaling of mammalian BMR. *Comp Biochem Physiol A* 151: 5–28.
56. Nagy KA, Girard IA, Brown TK (1999) Energetics of free-ranging mammals, reptiles, and birds. *Annu Rev Nutr* 19: 247–277.
57. Brett-Surman MK, Farlow JO (1997) Some irrelevant thoughts about dinosaur metabolic physiology: jurispthagous food consumption rates of *Tyrannosaurus rex*. In: Farlow JO, Brett-Surman MK, editors. *The complete dinosaur*. Bloomington: Indiana University Press. 350–351.
58. Clauss M, Steuer P, Müller DWH, Codron D, Hummel J (2013) Herbivory and body size: allometries of diet quality and gastrointestinal physiology, and implications for herbivore ecology and dinosaur gigantism. *PLoS ONE* (this issue).
59. Robertson DS, McKenna MC, Toon OB, Hope S, Lillegraven JA (2004) Survival in the first hours of the Cenozoic. *GSA Bulletin* 116: 760–768.
60. Archibald JD (1996) *Dinosaur extinction and the end of an era*. New York: Columbia University Press.
61. O’Gorman EJ, Hone DWE (2013) Body size distribution of the dinosaurs. *PLoS ONE* 7: e51925.
62. Brown CM, Evans DC, Campione NE, O’Brien LJ, Eberth DA (2012) Evidence for taphonomic size bias in the Dinosaur Park Formation (Campanian, Alberta), a model Mesozoic terrestrial alluvial-paralic system. *Palaeogeogr Palaeoclimatol Palaeoecol* 372: 108–122.
63. Smith FA, Brown JH, Haskell JP, Lyons SK, Alroy J, et al. (2004) Similarity of mammalian body size across the taxonomic hierarchy and across space and time. *Am Nat* 163: 672–691.
64. Brown JH, Maurer BA (1989) Macroecology - the division of food and space among species on the continents. *Science* 243: 1145–1150.
65. Blackburn TM, Gaston KJ (1994) The distribution of body sizes of the world’s bird species. *Oikos* 70: 127–130.
66. Zanno LE, Makovicky PJ (2011) Herbivorous ecomorphology and specialization patterns in theropod dinosaur evolution. *Proc Natl Acad Sci USA* 108: 232–237.
67. Damuth J (1981) Population density and body size in mammals. *Nature* 290: 699–700.
68. Levins R (1968) *Evolution in changing environments*. Princeton, NJ: Princeton University Press.
69. Hu Y, Meng J, Wang Y, Li C (2005) Large Mesozoic mammals fed on young dinosaurs. *Nature* 433: 149–152.
70. Wissinger SA (1992) Niche overlap and the potential for competition and intraguild predation between size-structured populations. *Ecology* 73: 1431–1444.
71. Werner EE, Gilliam JF (1984) The ontogenetic niche and species interactions in size-structured populations. *Annu Rev Ecol Syst* 15: 393–425.
72. Radloff FGT, Hobson KA, Leslie AJ (2012) Characterising ontogenetic niche shifts in Nile crocodile using stable isotope ($\delta^{13}\text{C}$, $\delta^{15}\text{N}$) analyses of scute keratin. *Isotopes Environ Health Stud* 48: 439–456.
73. Woolley L-A, Page B, Slotow R (2011) Foraging strategy within African elephant family units: Why body size matters. *Biotropica* 43: 489–495.
74. Codron J, Kirkman K, Duffy KJ, Sponheimer M, Lee-Thorp JA, et al. (2013) Stable isotope turnover and variability in tail hairs of captive and free-ranging African elephants (*Loxodonta africana*) reveal dietary niche differences within populations. *Can J Zool* 91: 124–134.
75. Foster JR (2007) *Jurassic West. The dinosaurs of the Morrison Formation and their World*. Bloomington: Indiana University Press.
76. Codron D, Carbone C, Müller DWH, Clauss M (2012) Ecological modelling, size distributions and taphonomic size bias in dinosaur faunas: reply to Brown *et al.* *Biol Lett* doi: 10.1098/rsbl.2012.0922.
77. Brose U, Jonsson T, Berlow EL, Warren P, Banasek-Richter C, et al. (2006) Consumer-resource body-size relationships in natural food webs. *Ecology* 87: 2411–2417.
78. Troost TA, Kooi BW, Dieckmann U (2008) Joint evolution of predator body size and prey-size preference. *Evol Ecol* 22: 771–799.
79. Sinclair ARE, Mduma S, Brashares JS (2003) Patterns of predation in a diverse predator–prey system. *Nature* 425: 288–290.
80. Carbone C, Mace GM, Roberts SC, Macdonald DW (1999) Energetic constraints on the diet of terrestrial carnivores. *Nature* 402: 286–288.
81. Carbone C, Teacher A, Rowcliffe JM (2007) The costs of carnivory. *PLoS Biology* 5: e22.
82. Werner J (2010) Die Reproduktion von Dinosauriern, speziell der Sauropoden und deren Bedeutung für ihren Gigantismus: Johannes Gutenberg-Universität Mainz.
83. Smith FA, Boyer AG, Brown JH, Costa DP, Dayan T, et al. (2010) The evolution of maximum body size of terrestrial mammals. *Science* 330: 1216–1219.
84. Feduccia A (2003) ‘Big bang’ for tertiary birds? *Trends Ecol Evol* 18: 172–176.
85. Clarke A (2013) Dinosaur energetics: setting the bounds on feasible physiologies and ecologies. *Am Nat* 182: 283–297.
86. Werner J, Griebeler E (2013) Case curves on growth rate and body mass revised: dinosaurs had rather growth rates like ectotherms than endotherms. *PLoS ONE* (this issue).
87. Sookias RB, Benson RBJ, Butler RJ (2012) Biology, not environment, drives major patterns in maximum tetrapod body size through time. *Biol Lett* 8: 674–677.

New Insights into Non-Avian Dinosaur Reproduction and Their Evolutionary and Ecological Implications: Linking Fossil Evidence to Allometries of Extant Close Relatives

Jan Werner*, Eva Maria Griebeler

Department of Ecology, Zoological Institute, University of Mainz, Mainz, Germany

Abstract

It has been hypothesized that a high reproductive output contributes to the unique gigantism in large dinosaur taxa. In order to infer more information on dinosaur reproduction, we established allometries between body mass and different reproductive traits (egg mass, clutch mass, annual clutch mass) for extant phylogenetic brackets (birds, crocodiles and tortoises) of extinct non-avian dinosaurs. Allometries were applied to nine non-avian dinosaur taxa (theropods, hadrosaurs, and sauropodomorphs) for which fossil estimates on relevant traits are currently available. We found that the reproductive traits of most dinosaurs conformed to similar-sized or scaled-up extant reptiles or birds. The reproductive traits of theropods, which are considered more bird-like, were indeed consistent with birds, while the traits of sauropodomorphs conformed better to reptiles. Reproductive traits of hadrosaurs corresponded to both reptiles and birds. Excluding *Massospondylus carinatus*, all dinosaurs studied had an intermediary egg to body mass relationship to reptiles and birds. In contrast, dinosaur clutch masses fitted with either the masses predicted from allometries of birds (theropods) or to the masses of reptiles (all other taxa). Theropods studied had probably one clutch per year. For sauropodomorphs and hadrosaurs, more than one clutch per year was predicted. Contrary to current hypotheses, large dinosaurs did not have exceptionally high annual egg numbers (AEN). Independent of the extant model, the estimated dinosaur AEN did not exceed 850 eggs (75,000 kg sauropod) for any of the taxa studied. This estimated maximum is probably an overestimation due to unrealistic assumptions. According to most AEN estimations, the dinosaurs studied laid less than 200 eggs per year. Only some AEN estimates obtained for medium to large sized sauropods were higher (200–400 eggs). Our results provide new (testable) hypotheses, especially for reproductive traits that are insufficiently documented or lacking from the fossil record. This contributes to the understanding of their evolution.

Citation: Werner J, Griebeler EM (2013) New Insights into Non-Avian Dinosaur Reproduction and Their Evolutionary and Ecological Implications: Linking Fossil Evidence to Allometries of Extant Close Relatives. PLoS ONE 8(8): e72862. doi:10.1371/journal.pone.0072862

Editor: Ulrich Joger, State Natural History Museum, Germany

Received: February 26, 2013; **Accepted:** July 15, 2013; **Published:** August 21, 2013

Copyright: © 2013 Werner et al. This is an open-access article distributed under the terms of the Creative Commons Attribution License, which permits unrestricted use, distribution, and reproduction in any medium, provided the original author and source are credited.

Funding: The project was financed by the German Research Foundation (grant GR 2625/2-1). The funders had no role in study design, data collection and analysis, decision to publish, or preparation of the manuscript.

Competing interests: The authors have declared that no competing interests exist.

* E-mail: wernerja@uni-mainz.de

Introduction

The discovery of the gigantic sauropods and other large dinosaurs has stimulated scientists to understand the biology of dinosaurs. Several researchers [1–3] recently argued that the reproductive strategy of producing many small offspring contributed to the exceptional gigantism seen in the sauropods, a hypothesis introduced by Janis and Carrano [4] and recently corroborated by Werner and Griebeler [5].

In contrast to any living species, our information on dinosaurs and their reproduction is limited to fossils. Unfortunately, fossils do not allow for the complete reconstruction of an organisms' traits (e.g. of the life history). Traits are often inaccurately preserved or simply absent from the fossil record (e.g. clutches can be incomplete and breeding

frequency is simply not documented in the fossil record). This hampers our understanding of the reproductive strategies employed by dinosaurs.

Equations linking body mass to other traits derived from extant taxa are commonly used to estimate these traits for extinct species, including those dealing with reproduction (e.g. [6–8]). While the correlations between clutch/litter size or annual offspring number and body mass differ between different extant amniotic taxa [4,5,9,10], mass specific reproductive traits such as egg mass, clutch mass and annual reproductive mass (clutch mass × number of clutches per year) do significantly, positively correlate with body mass [9,11–17]. The relationships between traits (Y) and body mass (BM) follow a power function $Y = c \times BM^b$, where c is a normalization constant and b is an exponent. These so-called allometric

(allometric because b usually differs from one) functions are usually log-log plotted, whereby the normalization constant c is the intercept and the exponent b is the slope of a straight line. The exponent b differs between different amniotic groups when egg mass is plotted against body mass [9,10]. Conversely, b is often very similar between different amniotic groups when clutch mass or annual reproductive mass is plotted against body mass [9,10,16]. While the slopes b are often statistically indistinguishable for annual clutch/litter mass, the normalization constants vary significantly among taxa [16,18]. These normalization constants are frequently similar among species/taxa with similar lifestyles [18]. We assume from these observations that analogous allometries on body mass and reproductive traits exist within close extant phylogenetic relatives of non-avian dinosaurs. We expect that these allometries are applicable to extinct non-avian dinosaurs as well.

To derive information on dinosaur reproduction, the procedure presented by Bryant and Russell [19] and Witmer [20] was employed, specifically a combination of phylogenetic inference and extrapolatory analysis. As an extant phylogenetic bracket (EPB, [20]) for non-avian dinosaurs, we chose phylogenetically close relatives with reproductive characteristics similar to those assumed for non-avian dinosaurs. Reproductive traits included, among others, ground breeding, and calcified, rigid-shelled eggs (for the distribution of egg types over the phylogeny of early amniotes, see Sander [21]). For the extant bird and reptile species which meet these specifications, we established allometries between body mass and different reproductive traits (egg mass, clutch mass, annual clutch mass). Allometries were then applied to nine non-avian dinosaur taxa for which information on body mass, egg mass and clutch mass is currently available from the fossil record. We expected, (i) reproductive trait estimates of non-avian dinosaurs, which are considered to be more “bird-like” in their reproductive mode (e.g. theropods [22–24]), to conform to those seen in extant birds. Similarly, those dinosaurs expressing traits probably more “reptile-like” in their reproductive mode (e.g. sauropods [24]) were expected to fit to those of extant reptiles.

Our established allometries between body mass and clutch mass might also provide further support for the hypothesis of Seymour [25], who argued that the buried clutch mass of large sauropods is limited due to physiological constraints imposed on the clutch. Assuming a sea turtle model, Seymour [26] showed that unfavorable respiratory gas pressures can occur inside large buried clutches. If clutches are too large, buried eggs do not receive enough oxygen through the soil [25]. Because of this physiological limitation of clutch mass, Seymour [25] suggested that fully buried sauropod eggs were distributed over several small clutches, each clutch containing not more than 13 eggs. Sander et al. [27] also hypothesized that the clutch mass of buried sauropod clutches is smaller than expected given their body mass, suggesting that these sauropods produced several clutches per year. According to these hypotheses, we expected (ii) the clutch masses of buried clutches of large dinosaurs, e.g. of the sauropods producing *Megaloolithus mammilare* eggs [27], to be smaller than those

predicted from any extant species studied. Assuming that the annual clutch mass allometries derived from extant taxa are also valid for dinosaurs, (iii) we estimated annual breeding frequencies of dinosaurs from their fossil clutch mass. Finally, (iv) we estimated the total number of eggs laid per year for each dinosaur taxon, calculated from the annual clutch mass allometries of extant taxa using the respective fossil egg masses.

Material and Methods

Phylogenetic framework and EPB

For our analyses, we selected three extant taxa (birds $N=217$, crocodiles $N=22$ and tortoises $N=20$; Table S2), each of which is phylogenetically close to non-avian dinosaurs and/or has reproductive characteristics similar to non-avian dinosaurs. We chose the extant phylogenetic bracket of non-avian dinosaurs, i.e. birds and crocodiles, as the closest phylogenetic relatives of ancient dinosaurs [28–30]. Given that dinosaurs were most probably terrestrial and ground breeding [27,31,32], we also aimed to restrict our dataset to ground breeding and terrestrial bird species. We initially focused on avian orders presumed to have less derived reproductive characteristics (e.g. ground breeding and precocial). According to traditional taxonomy, these include Paleognathae with the orders Struthioniformes and Tinamiformes. Since the sample sizes obtained for Paleognathae were too small, we also included the orders Galliformes and Anseriformes in our analysis; both are phylogenetically closely related to Paleognathae and are ground breeding and precocial. For Struthioniformes, data from only seven species (two kiwi species and five other ratites) were available, with the two kiwi species (~ 1-3 kg, cave breeding) strongly differing from the other ratites (~ 20-90 kg, open breeding) in terms of body masses and reproductive strategies [33,34]. For Tinamiformes, we found no single species for which information on body mass and all studied reproductive traits was available. Our allometries were finally based on 60 galliforme, 150 anseriforme and 7 ratite species. The allometries obtained from these avian species are hereafter referred to as bird model.

For the crocodile model, we chose all extant crocodylian species ($N = 22$). Since crocodiles are non-terrestrial, we also included tortoises ($N = 20$) in our allometric analyses. Molecular data suggest that turtles are more closely related to archosaurs than to lepidosaurs [35–37] and, similar to crocodiles and birds, and tortoises have calcified, rigid-shelled eggs. For both the crocodile and tortoises model, all extant species for which information on reproductive traits and body mass was available were included in the model. For each of the three extant taxa, we established allometries linking reproductive traits of species to their body mass.

Dinosaurs

We applied established allometries to all dinosaur taxa for which body mass estimates and assignments of fossil eggs or clutches to taxa are currently available (Table S1). These assignments only exist for four theropods (*Troodon formosus*, *Oviraptor philoceratops*, *Citipati osmolskae*, and

Lourinhanosaurus antunesi), two hadrosaurs (*Maiasaura peeblesorum*, lambeosaurine dinosaur), two sauropod oospecies (*Megaloolithus patagonicus*, *Megaloolithus mammillare*) and one prosauropod (*Massospondylus carinatus*). It should be noted that *Megaloolithus siruguei* is considered a junior synonym of *Megaloolithus mammillare*.

Life-history traits

For all extant species, we gathered data on adult body mass (BM), egg mass (EM), clutch size (CS) and number of clutches per year (CY). When more than one trait value was found in the literature for the same species, the mean value was calculated (Table S2). For body mass estimates, data on females was preferentially used because mass is more strongly linked to reproductive traits in females than in males. In some cases, however, it was not possible to distinguish between male and female body masses because only the averages of both sexes were available or the sex was not denoted in the source or was unknown (especially for all dinosaurs). To maximize our sample size while minimizing any bias introduced by male body masses, we used female body masses wherever possible and otherwise averaged body masses.

For dinosaurs (for details, see Table S1, supporting information), we used the average species body masses for our estimations when eggs were assigned to a specific dinosaur species (*Troodon formosus*, *Oviraptor philoceratops*, *Citipati osmolskae*, *Lourinhanosaurus antunesi*, *Maiasaura peeblesorum*, *Massospondylus carinatus*). When eggs were assigned instead to a taxonomic group, we used averages of the specific taxonomic group (*Megaloolithus patagonicus*, *Megaloolithus mammillare*, lambeosaurine dinosaur). Dinosaur egg masses were calculated from an egg's volume, assuming an egg density of 1.13 g/cm³ (birds [38]; mean egg density of the six bird orders from Table 3 in this reference; crocodiles [39]; Table 3 in this reference). Egg volume was calculated from fossil egg dimensions (mean) using either the equation $V = 0.51L * D^2$ (asymmetrical, bird-like, theropods) or $V = 0.524L * D^2$ (ellipse/globular, crocodile-like, sauropodomorphs and hadrosaurs), where V is the egg volume, L the egg length and D the egg diameter [39,40].

Given that all studied extant birds and reptiles lay at least one clutch per year, an initial conservative estimate of the unknown annual breeding frequency was assumed to be one clutch per year for all non-avian dinosaurs. Clutch mass is egg mass multiplied by clutch size. Annual clutch mass is clutch mass multiplied by the number of clutches per year.

Statistical analyses

Establishment of allometries for birds, crocodiles and tortoises. We began by separately analysing the relationship between body mass and reproductive traits for extant birds, crocodiles and tortoises. For each taxa and each of the three reproductive traits, we calculated regression slopes and normalization constants using ordinary least square regressions (OLS) on log-log-transformed data (Table S3).

In these regression analyses, we did not control for phylogenetic effects on reproductive traits. In general, phylogenetic comparative methods perform best when the

Table 3. Reproductive characteristics of hadrosaurs as documented in the fossil record and estimated by the reptile (crocodiles, tortoises) and the bird model.

Taxon	Fossil		Reptile model				Bird model			
	BM (kg)	EM (kg)	CS	CS ^T	CS ^C	AEN	CY	CS ^B	AEN	CY
lambeosaurine	2390	4.737	22	3.5	9.9	10.3	0.5	23.2	25.7	1.2
lambeosaurine	3344	4.737	22	4.4	12.6	13.1	0.6	29.5	32.7	1.5
lambeosaurine	5057	4.737	22	6.0	16.9	17.7	0.8	39.7	44.1	2.0
<i>Maiasaura peeblesorum</i>	1500	1.023	16	11.6	32.9	34.0	2.1	77.1	84.8	5.3
<i>Maiasaura peeblesorum</i>	2556	1.023	16	16.9	48.2	50.1	3.1	112.8	124.7	7.8
<i>Maiasaura peeblesorum</i>	4079	1.023	16	23.7	67.3	70.2	4.4	157.6	174.9	10.9

BM: minimum, mean and maximum fossil body mass of a taxon taken from literature in kilograms; CS: mean clutch size observed in fossil record, with minimum and maximum fossil values given in square brackets or CS calculated from an allometric clutch mass (CM) model (CS^T = tortoise model, CS^C = crocodile model, CS^B = bird model) using the fossil egg mass (EM, for calculating of fossil egg mass see Material and Method), CS = CM divided by EM. AEN (annual egg number): total number of eggs laid per year, calculated from an allometric ACM (annual clutch mass) model using the fossil egg mass, AEN = ACM divided by EM. CY: number of clutches per year, calculated from an allometric ACM model using the fossil CS and estimated AEN, CY = AEN divided by CS. Minima and maxima are given in brackets. References for fossil data are given in Table S3 (supplementary). Equations for the reptile and the bird model are given in Table S6. Note: For the lambeosaurine and *Maiasaura peeblesorum* only one CS estimate was available.

phylogeny itself and branch lengths are correct [41–43]. However, to the best of our knowledge, no phylogenetic trees resolving to the species level are currently available for birds, crocodiles and tortoises. More notably, a phylogenetic tree containing all studied species with reliable branch lengths is not available. Furthermore, the purpose of taking phylogeny into account is to reduce the variance in the estimated regression or correlation coefficients. However, the estimates of regression coefficients are unbiased and independent of phylogeny; estimates of correlation coefficients are only slightly biased [44]. Because we were mainly interested in the mean coefficient values, and we obtained highly significant coefficients, controlling for phylogeny would not have improved our analyses.

Next, we tested the homogeneity of the regression lines obtained for the three taxonomic groups within each reproductive trait (Table S4, S5). Therein, the calculated regression slopes and the normalization constants of all taxonomic groups of one reproductive trait were compared (analyses of covariance ANCOVA, groups as categorical variable). When these overall analyses indicated that normalization constants and/or slopes of more than one taxonomic group differed for a reproductive trait, we used ANCOVA for an additional pairwise comparison. This aimed to identify potential differences or similarities in normalization constants and/or slopes within groups.

The previous analyses could either reveal no statistical differences in regression slopes between at least two taxonomic groups or a significant difference between groups for a reproductive trait. If slopes were statistically homogeneous but intercepts differed between taxonomic groups, we calculated a new OLS regression function with a common regression slope for each group. We used this common regression slope (average value of taxa) as a fixed parameter in these regression models and only estimated the normalization constant for each group. If both slopes and intercepts of taxonomic groups were statistically homogeneous, we determined a common regression function (with the average slope and average intercept of taxa) for these taxa. If a slope of a single taxonomic group statistically differed from all other groups, the initially found OLS regression function was used as allometry for the respective taxon and reproductive trait (Table S6). This statistical procedure led to the development of three allometries/models for egg mass and clutch mass (birds, crocodiles, tortoises, Figures 1 and 2, Table S6) and two allometries for annual clutch mass (birds, reptiles = crocodiles + tortoises, see results, Figure 3, Table S6).

Finally, as a measure of variability in residuals and the deviation of single species from the expected average, we calculated 95% prediction intervals for each regression line (Figures 1-3).

Application of allometries to non-avian dinosaurs. Each of the trait pairs (body mass and reproductive trait) of non-avian dinosaurs were compared to the regression lines and to the respective 95% prediction intervals for the bird, the crocodile, and the tortoise model (Figures 1-3). Due to uncertainties in dinosaur body masses and clutch masses, we considered not only the mean fossil values but also their known variability (determined by reported minimum and maximum values taken from literature). For egg masses however, only the mean values were used. We assume that errors in egg mass are negligible in comparison to errors in the estimates of body mass and clutch size and mass.

Estimation of clutch sizes, annual egg numbers and clutches per year. Clutch size for non-avian dinosaurs was calculated from fossil egg mass and the clutch mass estimates from the regression lines derived for birds, crocodiles and tortoises. Analogously, the total number of eggs per year (AEN) for dinosaurs was calculated from annual clutch mass (ACM). Since the regression lines for crocodiles and tortoises did not differ statistically (see results), the ACM was estimated from the regression lines of birds and the common regression line for reptiles, and from the fossil egg mass. The number of clutches per year (CY) under the bird and reptile model was calculated from the respective annual egg numbers and from fossil clutch sizes.

Software used. The calculations of clutch sizes, number of eggs per year and clutches per year, estimated from the regression models, were done with Excel 2010. All other analyses were carried out in R (Version 2.14.1 [45]). For calculations of OLS regressions, common regression slopes and normalization constants, we used the “lm” function (basic) and the “gnls” function (“nlme” package) implemented in R. ANCOVAs were also conducted in R (“lm” function).

Results

Regression functions and estimation of dinosaur reproductive traits

Reproductive investment in terms of EM, CM, and ACM highly correlated with BM in birds, crocodiles and tortoises (Table S3). We found three different allometric models predicting EM from BM, with the models for crocodiles and tortoises only differing in their normalization constants (Tables S3-S6). For CM versus BM we also derived three different models; each model had different normalization constants (Tables S3-S6). For ACM versus BM we obtained only two different models (bird and reptile model, slopes and intercepts of the regression models of crocodiles and tortoises did not statistically differ) with different normalization constants (Tables S3-S6). All established models (Table S6) were used to compare the reproductive traits of dinosaurs documented in the fossil record with the respective reproductive traits seen in similar-sized or scaled-up extant species. The two models on ACM versus BM were applied to estimate AEN and CY for dinosaurs.

Application of allometries to dinosaurs

Egg mass. Except for the prosauropod *M. carinatus* and the sauropod *M. patagonicus*, all dinosaur EMs fell outside the 95% prediction interval of all extant models (Figure 1, B–D). *Massospondylus carinatus* fitted very well to the crocodile and the tortoise model (Figure 1, C and D). The EM of *M. patagonicus* fitted the tortoise model, but only when we assume that its BM is equal to or higher than the mean BM of 22,399 kg, as given in literature (Figure 1D). None of the other dinosaur EMs fitted to the EM estimates of similar-sized or scaled-up birds or reptiles. Instead, they were intermediately located between these two models (Figure 1). In particular, the theropods (*T. formosus*, *O. philoceratops*, *C. osmolskae*, and *L. antunesi*) had EMs somewhat closer to those of birds than to reptiles, whereas the EMs of the hadrosaur *M. peeblesorum* and of the sauropod *M. patagonicus* were closer to those of reptiles (Figure 1). EMs of the lambeosaurine dinosaur (hadrosaur) and of the sauropod *M. mammilare* ranged between the predicted EM in the bird and the two reptile models (Figure 1).

Clutch mass. All fossil dinosaur CMs fell within the 95% prediction interval of at least one of the extant models (Figure 2, B–D). All non-theropod CMs matched at least one of the two reptile models (crocodiles, tortoises, Figure 2, C and D), while all theropod CMs matched the bird model (Figure 2B). However, the extant model best suited for the CM of a specific dinosaur differed between dinosaur taxa. Theropod CMs and the CM of the lambeosaurine dinosaur clearly conformed best to the bird model (Figure 2B), but the lambeosaurine dinosaur was in the 95% prediction interval of the crocodile model, too (Figure 2C). Sauropod CMs and the CM of the hadrosaur *M. peeblesorum* matched the tortoise model best, but were still realistic under the crocodile model (Figure 2, C and D). The CM of the prosauropod *M. carinatus* corresponded well to both the crocodile and the tortoise model (Figure 2, C and D). The CM of the sauropod *M. mammilare* fell within the 95%

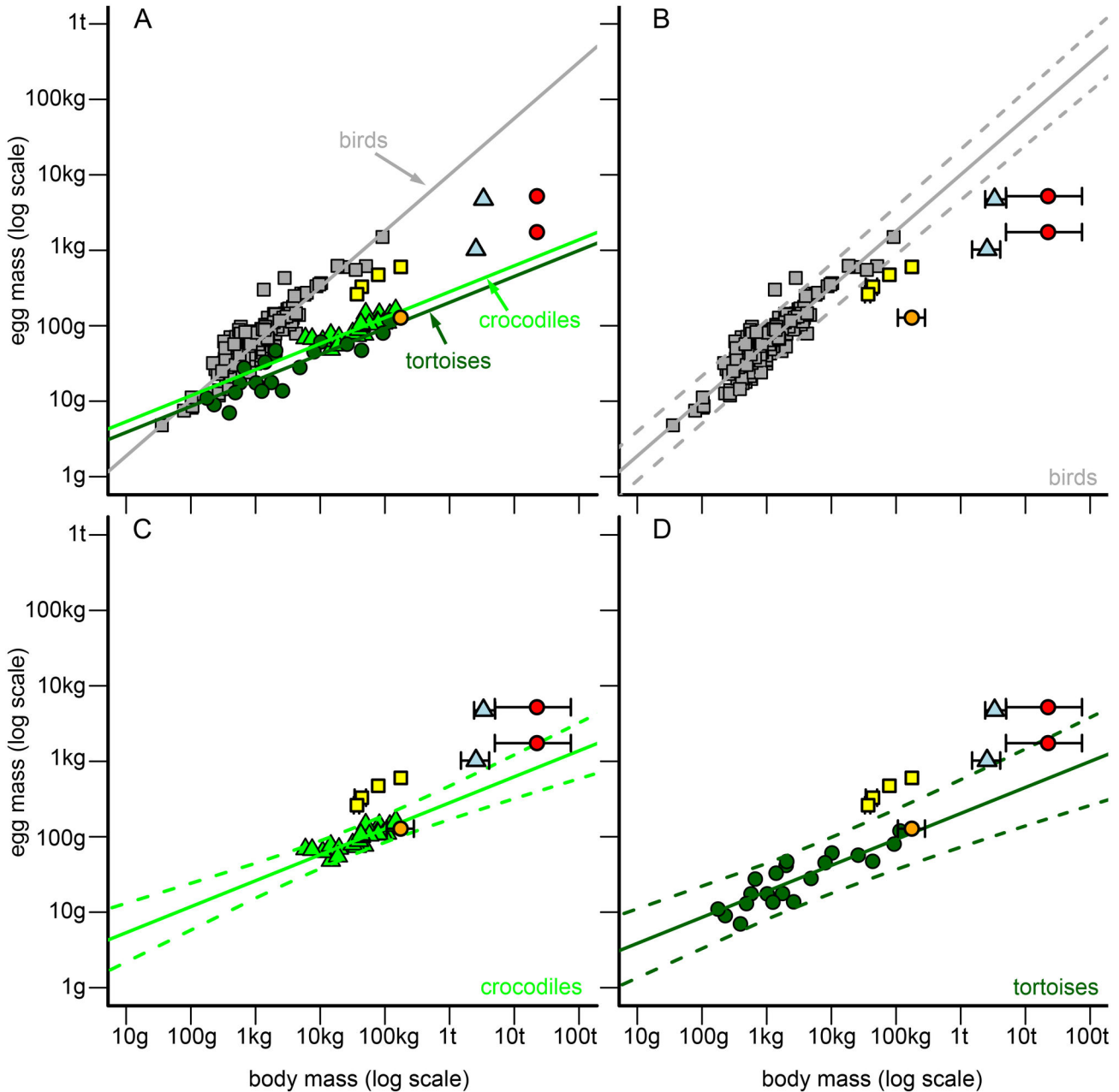


Figure 1. Allometries between body mass (BM) and egg mass (EM) of birds, crocodiles, and tortoises and their comparison to non-avian dinosaurs. (A) General comparison of dinosaur EMs to the EM allometry of birds (grey squares/line), crocodiles (green triangles/line) and tortoises (dark green circles/line). (B) Detailed comparison of dinosaur EMs to the EM allometry of birds. Grey continuous line = regression line of birds. Grey scattered lines = 95% prediction interval of the bird regression. Dinosaurs in the graphs = theropods (yellow squares, from left to right): *Troodon formosus*, *Oviraptor philoceratops*, *Citipati osmolskae*, *Lourinhanosaurus antunesi*; hadrosaurs (light blue triangles, from bottom to top): *Maiasaura peeblesorum*, lambeosaurine dinosaur; sauropod oospecies (red circles, from bottom to top): *Megaloolithus patagonicus*, *Megaloolithus mammilare*; prosauropod (orange circle): *Massospondylus carinatus*. Black error bars = possible value ranges for a non-avian dinosaur taxon (left/lower bar = minimum value derived from the fossil record, right/upper bar = maximum value). (C) Analogous to (B), but for crocodiles (green triangles/lines) and dinosaurs. (D) Analogous to (B), but for tortoises (dark green circles/lines) and dinosaurs.

doi: 10.1371/journal.pone.0072862.g001

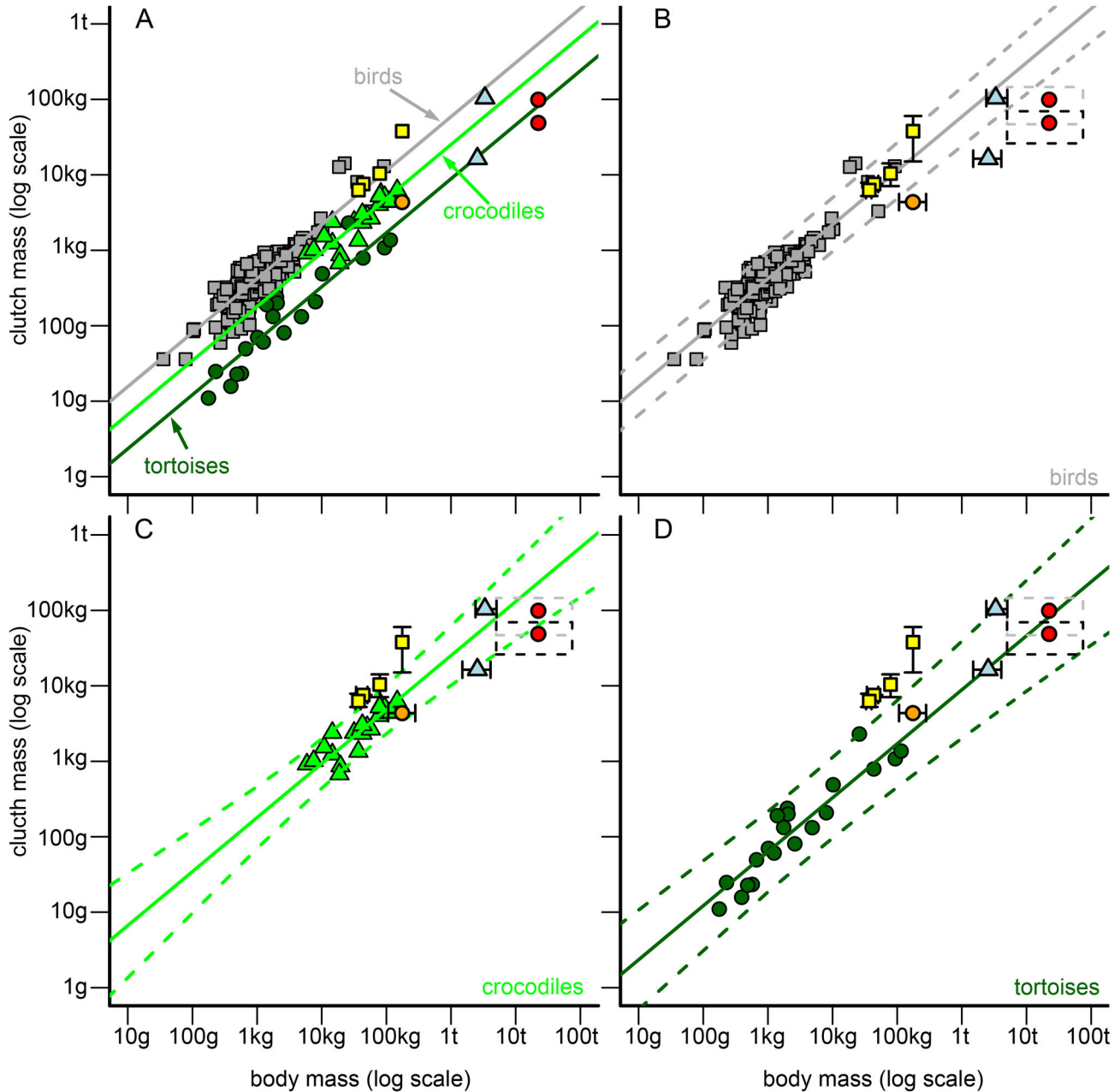


Figure 2. Allometries between body mass (BM) and clutch mass (CM) of birds, crocodiles, and tortoises and their comparison to non-avian dinosaurs. (A) General comparison of dinosaur CMs to the CM allometry of birds (grey squares/line), crocodiles (green triangles/line) and tortoises (dark green circles/line). (B) Detailed comparison of dinosaur CMs to the CM allometry of birds. Grey continuous line = regression line of birds. Grey scattered lines = 95% prediction interval of the bird regression. Dinosaurs in the graph = theropods (yellow squares, from left to right): *Troodon formosus*, *Oviraptor philoceratops*, *Citipati osmolskae*, *Lourinhanosaurus antunesi*; hadrosaurs (light blue triangles, from bottom to top): *Maiasaura peeblesorum*, lambeosaurine dinosaur; sauropod oospecies (red circles, from bottom to top): *Megaloolithus patagonicus*, *Megaloolithus mammillare*; prosauropod (orange circle): *Massospondylus carinatus*. Black error bars/scattered rectangles = possible value ranges for a non-avian dinosaur taxon (left/lower bar/edge = minimum value derived from the fossil record, right/upper bar/edge = maximum value). (C) Analogous to (B), but for crocodiles (green triangles/lines) and dinosaurs. (D) Analogous to (B), but for tortoises (dark green circles/lines) and dinosaurs.

doi: 10.1371/journal.pone.0072862.g002

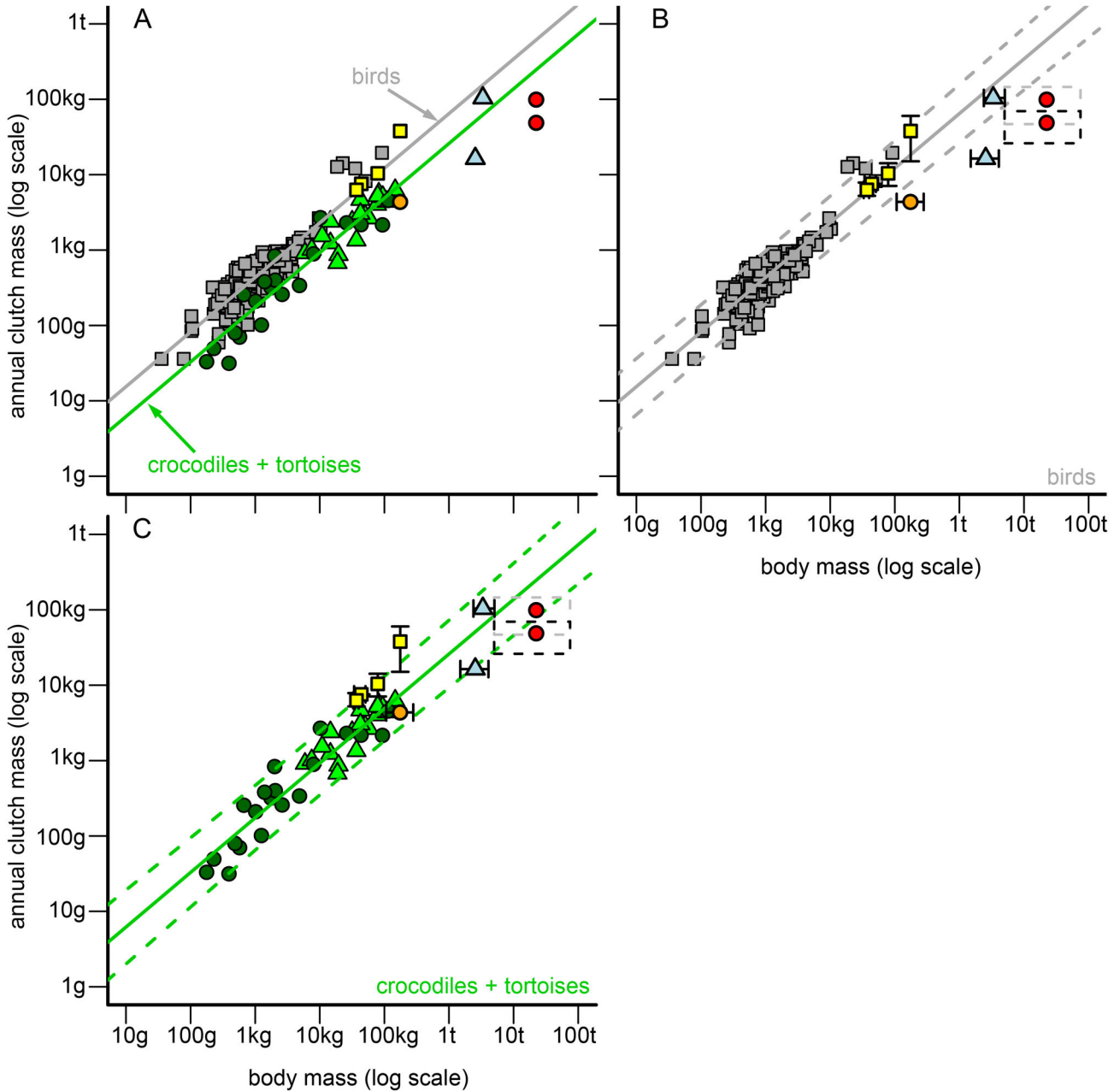


Figure 3. Allometries between body mass (BM) and clutch mass (ACM) of birds, crocodiles, and tortoises and their comparison to non-avian dinosaurs. (A) General comparison of dinosaur ACMs to the ACM allometry of birds (grey squares/line), crocodiles (green triangles/line) and tortoises (dark green circles/line). (B) Detailed comparison of dinosaur ACMs to the ACM allometry of birds. Grey continuous line = regression line of birds. Grey scattered lines = 95% prediction interval of the bird regression. Dinosaurs in the graph = theropods (yellow squares, from left to right): *Troodon formosus*, *Oviraptor philoceratops*, *Citipati osmolskae*, *Lourinhanosaurus antunesi*; hadrosaurs (light blue triangles, from bottom to top): *Maiasaura peeblesorum*, lambeosaurine dinosaur; sauropod oospecies (red circles, from bottom to top): *Megaloolithus patagonicus*, *Megaloolithus mammilare*; prosauropod (orange circle): *Massospondylus carinatus*. Black error bars/scattered rectangles = possible value ranges for a non-avian dinosaur taxon (left/lower bar/edge = minimum value derived from the fossil record, right/upper bar/edge = maximum value). (C) Analogous to (B), but for reptiles (crocodiles + tortoises, green triangles/lines) and dinosaurs.

doi: 10.1371/journal.pone.0072862.g003

Table 1. Reproductive characteristics of sauropodomorphs as documented in the fossil record and estimated by the reptile (crocodiles, tortoises) and the bird model.

Taxon	Fossil			Reptile model				Bird model		
	BM (kg)	EM (kg)	CS	CS ^T	CS ^C	AEN	CY	CS ^B	AEN	CY
<i>Massospondylus carinatus</i>	107	0.128	34	14.0	39.7	40.2	1.2	93.1	100.0	2.9
<i>Massospondylus carinatus</i>	175	0.128	34	19.9	56.5	57.3	1.7	132.4	142.9	4.2
<i>Massospondylus carinatus</i>	280	0.128	34	27.8	79.1	80.6	2.4	185.3	200.8	5.9
<i>Megaloolithus mammilare</i>	5000	5.211	19 [9, 28]	5.4	15.3	16.0	0.8 [0.6, 1.8]	35.8	39.8	2.1 [1.4, 4.4]
<i>Megaloolithus mammilare</i>	22399	5.211	19 [9, 28]	15.7	44.7	47.3	2.5 [1.7, 5.3]	104.7	118.0	6.2 [4.2, 13.1]
<i>Megaloolithus mammilare</i>	75000	5.211	19 [9, 28]	37.3	106.1	113.6	6.0 [4.1, 12.6]	248.6	283.1	14.9 [10.1, 31.5]
<i>Megaloolithus patagonicus</i>	5000	1.741	28 [15, 40]	16.1	45.7	47.8	1.7 [1.2, 3.2]	107.2	119.1	4.3 [3.0, 7.9]
<i>Megaloolithus patagonicus</i>	22399	1.741	28 [15, 40]	47.1	133.8	141.7	5.1 [3.5, 9.4]	313.4	353.0	12.6 [8.8, 23.5]
<i>Megaloolithus patagonicus</i>	75000	1.741	28 [15, 40]	111.8	317.6	340.1	12.1 [8.5, 22.7]	744.0	847.3	30.3 [21.2, 56.5]

BM: minimum, mean and maximum fossil body mass of a taxon taken from literature in kilograms; CS: mean clutch size observed in fossil record, with minimum and maximum fossil values given in square brackets or CS calculated from an allometric clutch mass (CM) model (CS^T = tortoise model, CS^C = crocodile model, CS^B = bird model) using the fossil egg mass (EM, for calculating of fossil egg mass see Material and Method), CS = CM divided by EM. AEN (annual egg number): total number of eggs laid per year, calculated from an allometric ACM (annual clutch mass) model using the fossil egg mass, AEN = ACM divided by EM. CY: number of clutches per year, calculated from an allometric ACM model using the fossil CS and estimated AEN, CY = AEN divided by CS. Minima and maxima are given in brackets. References for fossil data are given in Table S3. Equations for the reptile and the bird model are given in Table S6. Note: For *Massospondylus carinatus* only one CS estimate was available.

prediction interval of the crocodile model (Figure 2C). The CM of the sauropod *M. patagonicus* and of the hadrosaur *M. peeblesorum* also conform to the crocodile model (Figure 2C) when assuming a lower BM for both taxa (*M. patagonicus*: 5,000-10,000 kg, *M. peeblesorum*: minimum reported BM of 1,500 kg), or in the case of *M. patagonicus* when the maximum CS reported in literature was used for predicting CM (40 eggs).

Annual clutch mass. When assuming one clutch per year, all estimated ACMs of non-avian dinosaurs fell within the 95% prediction interval of at least one of the extant models, with the exception of the sauropod *M. patagonicus* and the hadrosaur *M. peeblesorum* (Figure 3). All ACMs of theropods conformed well to the bird model (Figure 3B). In contrast, with the exception of the lambeosaurine dinosaur, none of the non-theropod dinosaur ACMs coincided with the bird model when assuming one clutch per year (Figure 3B). The ACM of the lambeosaurine dinosaur was intermediary when referring to the mass expected under the bird model and the reptile model (Figure 3). For the sauropod *M. patagonicus* and the hadrosaur *M. peeblesorum*, the ACMs derived from the assumption of one clutch per year coincided with the reptile model only when assuming body masses lower than the mean body masses derived from literature (Figure 3C). Combining *M. patagonicus* EMs and sauropod BMs with the maximum CS of 40 eggs reported in literature also leads to an ACM that conforms to the reptile model. ACMs of very large sauropods (75,000 kg and more) conformed neither to the bird nor to the reptile model when assuming the CS and EM reported in literature (for *M. patagonicus* or *M. mammilare*) and only one clutch per year (Figure 3).

Estimates of annual egg numbers and clutches per year from allometries

Independent of the extant model used, the estimated dinosaur AEN did not exceed 850 eggs (75,000 kg sauropod)

for any of the taxa studied. According to most estimations, dinosaurs lay less than 200 eggs per year and only some estimates obtained for medium to large sized sauropods were higher (Table 1). Assuming the bird model, for example, the AENs of theropods were comparable to fossil clutch sizes. This suggests that theropods had one clutch per year (Table 2). By contrast, hadrosaurs and sauropodomorphs probably had more than one clutch per year. This is supported by AEN estimates of nearly all BM and CM combinations (minimum, maximum and average values for BM and CM are considered). For all hadrosaurs and sauropodomorphs, these AEN estimates exceeded the egg number of fossil clutches, independent of the extant model assumed. The AENs of the lambeosaurine dinosaur calculated under the reptile and bird model indicated that this taxon probably had one or a maximum of two clutches per year. The *M. peeblesorum* had at least two clutches per year under the reptile model, and up to 11 clutches under the bird model (Table 3). Depending on the extant models applied for *M. carinatus* this taxon might have had one up to two (reptile model) or three up to six (bird model) clutches per year (Table 1). Small / young sauropods (BM ~ 5,000 kg), likely producers of oospecies *M. mammilare* or *M. patagonicus* eggs, might have had one (reptile model) up to two (bird model) or two (reptile model) up to four (bird model) clutches per year (Table 1). Medium sized sauropods (BM ~ 22,399 kg) might have laid two or three (*M. mammilare*, reptile model), but up to six (*M. mammilare*, bird model) clutches per year, depending on the model employed. For *M. patagonicus*, the number of clutches per year ranged from five (reptile model) to a maximum of 13 (*M. patagonicus*, bird model). The AEN estimate for very large sauropods (BM ~ 75,000 kg) was also variable depending on the species and model used. Estimates range from six (*M. mammilare*, reptile model) up to 15 (*M. mammilare*, bird model) or even 13 (*M. patagonicus*, reptile model) up to 30 (*M. patagonicus*, bird model) clutches per year (Table 1).

Table 2. Reproductive characteristics of theropods as documented in the fossil record and estimated by the reptile (crocodiles, tortoises) and the bird model.

Taxon	Fossil			Reptile model				Bird model		
	BM (kg)	EM (kg)	CS	CS ^T	CS ^C	AEN	CY	CS ^B	AEN	CY
<i>Troodon formosus</i>	34	0.329	23 [22, 24]	2.4	6.8	6.8	0.3 [0.3, 0.3]	15.9	17.0	0.7 [0.7, 0.8]
<i>Troodon formosus</i>	44	0.329	23 [22, 24]	2.9	8.2	8.2	0.4 [0.3, 0.4]	19.2	20.4	0.9 [0.9, 0.9]
<i>Troodon formosus</i>	51	0.329	23 [22, 24]	3.2	9.1	9.1	0.4 [0.4, 0.4]	21.3	22.8	1.0 [0.9, 1.0]
<i>Oviraptor philoceratops</i>	33	0.262	24 [20, 30]	2.9	8.4	8.4	0.3 [0.3, 0.4]	19.6	20.8	0.9 [0.7, 1.0]
<i>Oviraptor philoceratops</i>	37	0.262	24 [20, 30]	3.2	9.1	9.1	0.4 [0.3, 0.5]	21.3	22.6	0.9 [0.8, 1.1]
<i>Oviraptor philoceratops</i>	40	0.262	24 [20, 30]	3.4	9.6	9.6	0.4 [0.3, 0.5]	22.5	24.0	1.0 [0.8, 1.2]
<i>Citipati osmolskae</i>	79	0.473	22 [15, 30]	3.0	8.7	8.7	0.4 [0.3, 0.6]	20.3	21.7	1.0 [0.7, 1.4]
<i>Lourinhanosaurus atunesis</i>	176	0.602	63 [25, 100]	4.2	12.1	12.2	0.2 [0.1, 0.5]	28.3	30.5	0.5 [0.3, 1.2]

BM: minimum, mean and maximum fossil body mass of a taxon taken from literature in kilograms; CS: mean clutch size observed in fossil record, with minimum and maximum fossil values given in square brackets or CS calculated from an allometric clutch mass (CM) model (CS^T = tortoise model, CS^C = crocodile model, CS^B = bird model) using the fossil egg mass (EM, for calculating of fossil egg mass see Material and Method), CS = CM divided by EM. AEN (annual egg number): total number of eggs laid per year, calculated from an allometric ACM (annual clutch mass) model using the fossil egg mass, AEN = ACM divided by EM. CY: number of clutches per year, calculated from an allometric ACM model using the fossil CS and estimated AEN, CY = AEN divided by CS. Minima and maxima are given in brackets. References for fossil data are given in Table S3 (supplementary). Equations for the reptile and the bird model are given in Table S6. Note: For *Citipati osmolskae* and *Lourinhanosaurus antunesi* only one BM estimate was available.

Discussion

The allometries of body mass and reproductive investment in extant amniotes

Our results corroborate that body mass and reproductive investment (in terms of egg mass, clutch mass or annual clutch mass) are highly correlated in extant reptiles and birds [9,11–17]. In amniotes, the relative reproductive investment generally declines with body mass, whereas the absolute reproductive investment increases ([16,46], Figures 1–3, Table S3). Our analysis provides additional evidence [9,15] that the egg mass of large birds is higher compared to similar-sized reptiles (Figure 1). In contrast, large reptiles have a larger number of eggs per clutch and/or per year than similar-sized birds [9,15]. This results in less distinction between clutch masses/annual clutch masses of large birds and reptiles than in egg masses (Figures 1, 2 and 3).

Reproductive investment in dinosaurs

In summary, our results revealed four important insights into dinosaur reproductive biology. First, corroborating our hypothesis (i), the reproductive traits of dinosaurs that are considered to be more bird-like (theropods) did indeed coincide with reproductive traits of birds. Similarly, those traits of dinosaurs that were probably more reptile-like (prosauropods, sauropods) coincided with those of reptiles. Second, although the size difference between a dinosaur egg and the egg-laying female is very impressive, for all dinosaurs studied the egg to body mass relationship was similar to similar-sized or scaled-up extant reptiles (in *M. carinatus*) or even higher (in all other dinosaurs). However, it was lower than in similar-sized or scaled-up birds. Third, contrary to our hypothesis (ii) clutch masses of all dinosaurs and even of sauropods matched at least one of the extant models. We thus did not find any evidence that sauropods clutch sizes are small in comparison

to their body mass. This in turn questions the idea that a physiological limitation imposed on the clutch [25] leads to the “small” clutch size of fully buried sauropod clutches. Under such a limitation, the predicted CM to BM relationship would be too high in large dinosaurs, regardless of the extant model used. Fourth, annual clutch mass estimates (iii) suggest that theropods had only one clutch per year, whereas all other studied dinosaurs had probably several clutches per year (except for the lambeosaurine hadrosaur, for which one clutch per year is also realistic). This is especially true for the large sauropods. However, contrary to our expectation (iv), most of the dinosaurs studied probably laid no more than 200 eggs per year (Tables 1, 2 and 3). Even large sauropods (75,000 kg) probably had less than 400 eggs per year (Table 1), which is a smaller annual egg number than extant sea turtles (up to 513 eggs [47]).

Egg mass. Our results suggest that the egg masses of most dinosaurs match neither the egg masses of similar-sized or scaled-up birds nor those of reptiles, but were in fact in-between (Figure 1). This could reflect the reproductive strategy differences of most dinosaurs compared to the reproductive strategy seen in extant birds or reptiles [1] and suggests that their reproductive strategy was intermediary [24]. The great variability in egg mass to body mass relations found in dinosaurs (Figure 1) could indicate that different reproductive strategies existed in dinosaurs. The suggested variability in reproduction strategies is corroborated by the variability seen in dinosaur egg shapes and eggshell structures [31,32,48,49]. As observed in extant reptiles and birds, dinosaur egg mass (EM) increased significantly with body mass (BM; $EM = 0.090 \cdot BM^{0.311}$ $p = 0.031$; $r = 0.680$ (Pearson's correlation coefficient); $N = 9$, all dinosaur taxa studied). According to the assumption that the reptile reproductive model is plesiomorphic and the bird model is phylogenetically derived, none of the studied dinosaurs with egg masses close to the reptile model belong to the theropods (Figure 1). Furthermore, the egg mass of the

most basal sauropodomorph (*M. carinatus*) matched both the crocodile and tortoise model well. Thus our results corroborate our hypothesis (i).

Clutch mass/size. In contrast to the egg masses, all dinosaur (mean) clutch masses matched the masses of similar-sized or scaled-up birds or reptiles.

Theropods. As expected under our initial hypothesis, the bird model was the best model for theropods. Fossils indicate that at least some avian reproductive characteristics, such as adult brooding [22,50–52], asymmetrical eggs [22,50,53,54], unornamented eggshell surface and complex eggshell ultrastructure, existed in non-avian theropods [55]. Thus, our results provide further evidence of a bird-like reproduction mode in theropods. Furthermore, our results on theropods suggest accurate body mass and egg mass estimates and the completeness of fossil clutches. The stronger deviation of *L. antunesi* from the bird model could possibly be explained by a higher inaccuracy in the estimates of its body mass (a not fully grown sub-adult individual is the holotype of this taxon, Mateus et al. [56]) and fossil clutch size (eggs of the clutch could come from different females [57]) than in the other theropods.

Varricchio et al. [23] assumed that some theropods received/provided paternal care, because clutch-associated adults lack the maternal and reproductively associated histological feature common to extant archosaurs, including the medullary bone. Furthermore, theropods have relatively large clutch volumes. However, our analyses revealed no large clutch masses relative to body masses for theropods when compared to the studied extant birds showing bipaternal or maternal care. Thus, our data provide no evidence for the postulation presented in Varricchio et al. [23], that the theropods “sitting” on eggs were really males. The discrepancy in the results could have been caused by different sample compositions. We focused only on precocial birds in our analyses and used female body masses, as far as possible. We did not take into consideration the different parental care strategies of species. In contrast, Varricchio et al. [23] mixed different development modes of birds and used body mass averages without accounting for differences between sexes, but did allow for different parental care strategies. However, a recent study [58] corroborates our conclusion, showing that the development mode is a better predictor of the parental care strategy than clutch mass.

Sauropodomorpha. Contrary to our initial hypothesis (ii) clutch masses of sauropods were consistent with an extant species model, the tortoise model (Figure 2D). Several authors have argued that the clutch sizes of buried clutches in sauropods are bounded by physiological constraints [25,27,59], resulting in lower clutch mass to body mass relations compared to smaller taxa. Our analysis showed that the mean clutch masses for all studied dinosaurs matched the 95% prediction interval of at least one of the extant species models (birds, crocodiles or tortoises). Hence, they could be still consistent with the extant variability. For the two analyzed sauropods, the largest dinosaurs in our dataset, body mass and clutch size (particularly for *M. mammilare*) [27,49, but see 60] is uncertain. However, even when assuming large errors in the body mass and clutch mass/size estimates for these two sauropods (Figure 2, scattered rectangles), the clutch mass to body mass

relations did not conflict with those seen in scaled-up recent taxa (Figure 2D, the rectangles are completely located within the 95% prediction interval of the tortoise model). Additionally, the clutch mass of the prosauropod *M. carinatus* is also well described by the tortoise model (Figure 2D). All these observations suggest that the tortoise model might be appropriate for sauropodomorphs in general. Thus, our results provided no evidence that the “small” clutch sizes of *M. mammilare* are caused by physiological limits imposed on the clutch [25,27,59]. We think that the use of a sea turtle model, as Seymour [25] did, to determine physiological limits on a large buried sauropod clutch is problematic. Sea turtles bury their clutches much deeper than most other reptiles [61]. In crocodylian clutches, for example, the respiratory gas pressure is closer to the atmospheric level than in sea turtle clutches [61]. In a buried clutch of the turtle species *Chelodina expansa* the respiratory gas pressure is also similar to the atmospheric pressure [62]. Thus, oxygen availability plays a stronger role in sea turtle clutch size than in other egg-burying reptiles, and is presumably not such a limiting factor in sauropods.

Hadrosaurs. The applicability of allometric models for clutch mass differed between the two hadrosaurs. For the lambeosaurine hadrosaur, the bird model was best, but the crocodile model was also applicable. For *M. peeblesorum*, the tortoise model was best; the crocodile model was also applicable, but only when assuming the lowest body mass estimates for that species. This discrepancy could indicate that reproduction strategies differed in hadrosaurs, as already suggested by Horner [63]. However, our results could be biased by an incomplete *M. peeblesorum* fossil clutch count. This would lead to a low assumed clutch mass. Horner [63] noted that counting individual eggs in a *M. peeblesorum* clutch was very difficult and for this reason assumed that one clutch consisted of at least 16 eggs.

Annual clutch mass/clutch per year/annual egg number. A reliable estimate of the number of clutches per year and the annual egg number for dinosaurs is uncertain because of the high variability observed in traits of extant species. Furthermore, there is a high inaccuracy in body mass and clutch mass estimates of dinosaurs, making it difficult to completely rule out any of the extant models for dinosaur taxa. Irrespective of all these limitations, we are able to provide qualitative estimates for the number of clutches per year and the annual egg number laid by dinosaurs. By using further information from the fossil record, we were able to identify the most likely extant model for a taxon.

Theropods. Fossil egg masses and clutch masses of theropods are consistent with the bird model, which suggests a general applicability of allometries on reproductive traits of birds to theropods. Assuming one clutch per year for theropods, the theropod ACMs match the bird model (Figure 3B). Furthermore, the low annual breeding frequency of theropods might provide further evidence for parental care in this taxon [23].

Sauropodomorpha. ACMs of sauropodomorphs were lower than all “average” extant species studied when assuming the studied sauropodomorphs (Figure 3) to have one clutch per year and mean values for BM and CM/CS. However, with the

exception of *M. patagonicus*, ACMs still fall within the 95% prediction interval of the reptile model (Figure 3C). Due to this observation and the finding that sauropods/sauropodomorphs were more “reptile-like” in their reproductive mode [24], we think that the reptile model is more appropriate for Sauropodomorpha than the bird model. The bird model provided high numbers of clutches per year, which could be flawed. These high estimates could be the result of incomplete fossil clutches (estimated clutch size is too small) or an assumed body mass too large for the producer. It is also possible that the bird model is not applicable for sauropods in general because of the more “reptile-like” reproduction strategy in sauropods.

Under the reptile model, an “average” *M. carinatus* could have had one or a maximum of two clutches, and laid between 40 and 81 eggs per year. Our estimates of the number of clutches per year for sauropods are more imprecise than those for the theropods and prosauropod. The two studied oospecies were assigned to the taxon *Titanosauria*, which covers a wide range of body masses for the potential egg producer. However, even if the body mass of a fully grown adult would be known, a wide range of body masses for the egg producer is still possible because sauropods probably became sexually mature well before they were fully-grown [64,65]. Irrespective of all these uncertainties, the reptile model revealed reliable estimates of the number of eggs and clutches per year for Sauropodomorpha. A sauropod weighing 75,000 kg could have laid the eggs of the *M. patagonicus* oospecies and is predicted to have had twelve clutches per year. This would result in an annual egg number of 340. However, the small eggs of the *M. patagonicus* oospecies imply that they were likely produced by a small to medium sized sauropod. Based on the smaller clutch size found in *M. mammilare* compared to *M. patagonicus*, Sander et al. [27] argued that *M. mammilare* had several clutches per year, whereas *M. patagonicus* had only one clutch per year. Contrary to these authors, our results indicate that both sauropods had multiple clutches per year, assuming that the egg laying individuals were not very small sauropods (BM < 5,000 kg, Table 1). Based on the reptile model, we suggest that *M. patagonicus* had between two and five clutches per year resulting in an annual egg production between 48 and 142, whereas *M. mammilare* could have laid one up to six clutches per year resulting in around 16 but up to 114 eggs per year.

Altogether, our results imply that sauropods probably had several clutches per year, resulting in more than one hundred eggs per year. However, sauropod clutch and egg numbers probably did not exceed the numbers found in some recent reptile species (e.g. sea turtles [66]). Nevertheless, the high annual egg numbers estimated for Sauropodomorpha in comparison to other non-avian dinosaurs, recent birds or mammals could indicate a high predation rate of hatchlings and little parental care in this dinosaurian lineage.

Hadrosaurs. We could not clearly identify the most likely extant model for the ACM of hadrosaurs. The ACM to BM relation of the lambeosaurine hadrosaur was intermediary to both the bird and reptile model; for *M. peeblesorum* its relation was lower than observed in any extant model. Nevertheless, our results suggest that hadrosaurs probably had several

clutches per year. For the lambeosaurine hadrosaur, one (reptile model) but up to two clutches (bird model) per year is estimated (Table 3). *Maiasaura peeblesorum* probably had more clutches per year than the lambeosaurine hadrosaur. The reptile model estimates two, up to four clutches per year and the bird model five up to eleven (Table 3). However, as discussed before, the assumed clutch size and mass of *M. peeblesorum* could be too low. The resulting number of clutches per year estimated could therefore be much closer to those of the lambeosaurine hadrosaur. In any case, the annual egg numbers of hadrosaurs studied were less than 200 (Table 3).

Ecological implications

Why should some dinosaurs have several clutches per year and others not? As seen in extant species, they could have lived in different environments, each favoring different reproductive strategies. Producing several small clutches within a breeding season could reflect a bet-hedging strategy [67–69]. If few of many clutches are lost to predation or other unfavorable environmental conditions cause considerable egg mortality, the eggs/hatchlings from other clutches may survive by chance. Such a strategy is favorable in environments with a long breeding season and when the time intervals between clutches are relatively long. This is also true in environments with a short breeding season, when clutches are laid more or less simultaneously. Dinosaurs which had one clutch per year could have lived in environments with a short breeding season. Under such environmental conditions putting all eggs into a single clutch/reproductive event (producing all eggs in a specific time period) is the only option, even at high rates of egg mortality, because the length of the breeding season limits reproduction [70]. Irrespective of the length of the breeding season, one clutch per year can be sufficient if offspring mortality due to environmental conditions is low.

Evolutionary implications

Since birds are dinosaurs, there must have been an evolutionary shift in the reproductive mode from the basal reptilian/non-avian dinosaur mode to that currently observed in birds. This shift might be observable in the studied dinosaurs. As expected, all studied reproductive traits of Sauropodomorpha were more reptile-like, whereas traits of studied theropods conform well to those of recent birds. Furthermore, it is likely that within the dinosaur lineage (including birds), an increase in egg size was linked to a decrease in egg numbers per clutch/year and vice versa. The prosauropod had many small eggs for its body mass. The two sauropods had in fact larger eggs than the prosauropod, but they still had many eggs in comparison to other dinosaurs because of their large size (Figure 1, Tables 1, 2 and 3). The four theropods had larger but fewer eggs than the sauropodomorphs (Figure 1, Tables 1 and 2), whereas recent birds have the largest eggs in comparison to their body mass (Figure 1) and also the fewest egg numbers (2.2–4.5 eggs per clutch, geometric mean of 5290 bird species [33]). This evolutionary change in egg size and number observed in the dinosaurian clade probably coincides with other changes in life

history traits. High mortality during the egg and juvenile phase could have led to the evolution of and selection for parental care; in birds, this would have sustained viable populations over evolutionary time. A similar shift in life history traits might have also occurred in the hadrosaurian lineage (Ornithischia). Interestingly, other researchers have also assumed extended parental care for species of this lineage based on fossil clutches with “altricial hatchlings” (e.g. *Maiasaura peeblesorum* [71,72], but see 48,73). However, our results imply that extended parental care was more likely in the studied lambeosaurine hadrosaur than in *M. peeblesorum*. This is due to the increased size observed in eggs and estimated fewer egg/clutch numbers in the former taxon.

Conclusion

From our study we conclude i) that allometric regression functions are a suitable approach to describe the relation between body mass and the studied reproductive traits in birds or reptiles. It is ii) appropriate to transfer these established allometries to specific taxa of extinct non-avian dinosaurs. Although we found a high variability in reproductive traits around the (average) allometric regression lines in extant species, we think that the results provide new testable hypotheses about dinosaur reproduction, its evolution and their ecological implications, especially for reproductive traits that are insufficiently documented or lacking in the fossil record.

Supporting Information

Table S1. Average body mass and reproductive characteristics of dinosaurs as documented in the fossil record. The *Megaloolithus patagonicus* oospecies is assigned to a titanosaurian sauropod based on embryonic remains in the eggs, and the *Megaloolithus sirugueilmammillare* egg type (with a highly porous shell) is commonly assigned to titanosaurian sauropod dinosaurs, because titanosaur bones had been found in the same horizon or formation as the eggs. It should be noted that *Megaloolithus siruguei* is considered as a junior synonym of *Megaloolithus mammillare*. *Megaloolithus* eggs have also been assigned to titanosaurs because of the find of a hatchling in a nest of *Megaloolithus* eggs from India. Although taxonomic identification of the eggs and their producers is problematic in sauropods, species with a mass of at least 5000 kg were assigned to both *Megaloolithus* oospecies. BM = body mass. ES = egg size, expressed in length (L) and diameter (D). EM = egg mass. CS = clutch size, number of eggs per clutch. CM/ACM = clutch mass (CM; CM = EM x CS) respectively annual clutch mass (ACM). ACM equals CM because as a first approximation we assumed one clutch per year for all dinosaurs studied. Values in brackets are minimum and maximum values, where no maxima are given only one value was available. Note: the mean BMs for both titanosaur taxa were established from body masses of sauropods larger than 5000 kg (because sauropod species with a BM of at least 5000 kg were assigned to both *Megaloolithus* oospecies) and for which the body mass estimation method was given in the source. The exact body mass range is 6853 kg to 72936 kg,

however we assumed, as a somewhat more conservative measure, minimum and maximum body masses of 5000 kg and of 75000 kg. (DOCX)

Table S2. Data used in the allometric analyses of extant species. G = Galliformes, A = Anseriformes, S = Struthioniformes, C = Crocodylia, T = Testudinidae, BM = body mass, EM = egg mass, CM = clutch mass, ACM = annual clutch mass. (DOCX)

Table S3. Results of the OLS regression analyses carried out for body mass against several reproductive traits for tortoises, crocodiles and birds. Allometric functions follow $c \times BM^b$ ($c + b \times BM$, log-log-plot), where BM is the body mass in kilograms, c is the intercept and b the slope of the line in a log-log-plot. N = sample size. 95% CI = 95% confidence interval of c or b . EM = egg mass. CM = clutch mass. ACM = annual clutch mass. (DOCX)

Table S4. Summary of results obtained in ANCOVAs. With these analyses we tested for differences in regression slopes ((a); for EM, CM, ACM) and intercepts ((b); CM, ACM) obtained for birds, crocodiles and tortoises under ordinary least squares regression analysis. EM = egg mass, CM = clutch mass, ACM = annual clutch mass, group = categorical variable, coding whether the species is a bird, crocodile or tortoises, log = logarithm to the base 10. n.a. = not applicable. For sample sizes refer to Table S3. (DOCX)

Table S5. Summary of results obtained in ANCOVAs. With these analyses we tested for differences in regression slopes ((a); for EM, CM, ACM) and intercepts ((b); CM, ACM) obtained for crocodiles and tortoises under ordinary least squares regression analysis. EM = egg mass, CM = clutch mass, ACM = annual clutch mass, group = categorical variable, coding whether the species is a crocodile or tortoises, log = logarithm to the base 10. n.a. = not applicable. For sample sizes refer to Table S3. (DOCX)

Table S6. Allometric models used to estimate reproductive traits of non-avian dinosaurs. EM = egg mass, CM = clutch mass, ACM = annual clutch mass; c = intercept and b = slope of the respective allometry. (DOCX)

Acknowledgements

We thank two reviewers for their valuable comments and all members of the DFG Research Unit 533 and the participants of the 2nd workshop on sauropod gigantism for valuable discussions, especially Martin Sander who introduced us to dinosaur reproductive biology. We are grateful to Rebecca Nagel for some linguistic improvements. This paper is part of

the PhD thesis of JW. this is contribution number 145 of the DFG Research Unit 533 "Biology of the Sauropod Dinosaurs: The Evolution of Gigantism".

Contributed reagents/materials/analysis tools: JW EMG. Wrote the manuscript: JW EMG.

Author Contributions

Conceived and designed the experiments: JW EMG.

Performed the experiments: JW. Analyzed the data: JW.

References

- Sander PM, Clauss M (2008) Sauropod gigantism. *Science* 322: 200-201. doi:10.1126/science.1160904. PubMed: 18845734.
- Griebeler EM, Werner J (2011) The life-cycle of sauropods. In: N KleinC RemesCT GeePM Sander. *Biology of the sauropod dinosaurs: understanding the life of giants*. Bloomington: Indian University Press. pp. 263-275.
- Sander PM, Christian A, Clauss M, Fechner R, Gee CT et al. (2011) Biology of the sauropod dinosaurs: the evolution of gigantism. *Biol Rev* 86: 117-155. doi:10.1111/j.1469-185X.2010.00137.x. PubMed: 21251189.
- Janis CM, Carrano M (1992) Scaling of reproductive turnover in archosaurs and mammals: why are large terrestrial mammals so rare? *Ann Zool Fenn* 28: 201-216.
- Werner J, Griebeler EM (2011) Reproductive biology and its impact on body size: comparative analysis of mammalian, avian and dinosaurian reproduction. *PLOS ONE* 6: e28442. doi:10.1371/journal.pone.0028442. PubMed: 22194835.
- Schmidt-Nielsen K (1984) *Scaling, why is animal size so important?* Cambridge: Cambridge University Press.
- Werner J, Griebeler E (2012) Reproductive investment in moa: a K-selected life-history strategy? *Evol Ecol* 26: 1391-1419. doi:10.1007/s10682-011-9552-0.
- Peters RH (1983) *The ecological implications of body size*. Cambridge: Cambridge University Press. 344pp.
- Blueweiss L, Fox H, Kudzma V, Nakashima D, Peters R et al. (1978) Relationships between body size and some life history parameters. *Oecologia* 37: 257-272. doi:10.1007/BF00344996.
- Hendriks AJ, Mulder C (2008) Scaling of offspring number and mass to plant and animal size: model and meta-analysis. *Oecologia* 155: 705-716. doi:10.1007/s00442-007-0952-3. PubMed: 18196279.
- Rahn H, Paganelli CV, Ar A (1975) Relation of avian egg weight to body weight. *Auk* 92: 750-765. doi:10.2307/4084786.
- Rohwer FC (1988) Inter- and intraspecific relationships between egg size and clutch size in waterfowl. *Auk* 105: 161-176.
- Iverson JB (1992) Correlates of reproductive output in turtles (Order Testudines). *Herpetol Monogr* 6: 25-42. doi:10.2307/1466960.
- Thorbjarnarson JB (1996) Reproductive characteristics of the order Crocodylia. *Herpetologica* 52: 8-24.
- Dol'nik VR (2000) Allometry of reproduction in poikilotherm and homoiotherm vertebrates. *Biol Bull* 27: 702-712.
- Ernest SKM, Enquist BJ, Brown JH, Charnov EL, Gillooly JF et al. (2003) Thermodynamic and metabolic effects on the scaling of production and population energy use. *Ecol Lett* 6: 990-995. doi: 10.1046/j.1461-0248.2003.00526.x.
- Figuerola J, Green A (2006) A comparative study of egg mass and clutch size in the Anseriformes. *J Ornithol* 147: 57-68. doi:10.1007/s10336-005-0017-5.
- Sibly RM, Brown JH (2007) Effects of body size and lifestyle on evolution of mammal life histories. *Proc Natl Acad Sci U S A* 104: 17707-17712. doi:10.1073/pnas.0707725104. PubMed: 17940028.
- Bryant HN, Russell AP (1992) The role of phylogenetic analysis in the inference of unpreserved attributes of extinct taxa. *Philos Trans R Soc Lond B Biol Sci* 337: 405-418. doi:10.1098/rstb.1992.0117.
- Witmer LM (1995) The extant phylogenetic bracket and the importance of reconstructing soft tissues in fossils. In: J Thomason. *Functional Morphology in Vertebrate Paleontology*. Cambridge: Cambridge University Press. pp. 19-33.
- Sander PM (2012) Reproduction in early amniotes. *Science* 337: 806-808. doi:10.1126/science.1224301. PubMed: 22904001.
- Varricchio DJ, Jackson F, Borkowski JJ, Horner JR (1997) Nest and egg clutches of the dinosaur *Troodon formosus* and the evolution of avian reproductive traits. *Nature* 385: 247-250. doi:10.1038/385247a0.
- Varricchio DJ, Moore JR, Erickson GM, Norell MA, Jackson FD et al. (2008) Avian paternal care had dinosaur origin. *Science* 322: 1826-1828. doi:10.1126/science.1163245. PubMed: 19095938.
- Grellet-Tinner G, Chiappe L, Norell M, Bottjer D (2006) Dinosaur eggs and nesting behaviors: a paleobiological investigation. *Palaeogeogr Palaeoclimatol Palaeoecol* 232: 294-321. doi:10.1016/j.palaeo.2005.10.029.
- Seymour RS (1979) Dinosaur eggs: gas conductance through the shell, water loss during incubation and clutch size. *Paleobiology* 5: 1-11.
- Ackerman RA (1977) Respiratory gas exchange of sea turtle nests. *Respir Physiol* 31: 19-38. doi:10.1016/0034-5687(77)90062-7. PubMed: 918411.
- Sander PM, Peitz C, Jackson FD, Chiappe LM (2008) Upper Cretaceous titanosaur nesting sites and their implications for sauropod dinosaur reproductive biology. *Palaeontogr Abt A* 284: 69-107.
- Padian K, de Ricqlès AJ, Horner JR (2001) Dinosaurian growth rates and bird origins. *Nature* 412: 405-408. doi:10.1038/35086500. PubMed: 11473307.
- Weishampel DB, Dodson P, Osmólska H, editors (2004) *The Dinosauria*: University of California Press.
- Turner AH, Pol D, Clarke JA, Erickson GM, Norell MA (2007) A basal dromaeosaurid and size evolution preceding avian flight. *Science* 317: 1378-1381. doi:10.1126/science.1144066. PubMed: 17823350.
- Paul GS (1994) Dinosaur reproduction in the fast lane: implications for size, success, and extinction. In: K CarpenterKF HirschJR Horner. *Dinosaur eggs and babies*. New York: Cambridge University Press. pp. 244-255.
- Horner JR (2000) Dinosaur reproduction and parenting. *Annu Rev Earth Pl Sc* 28: 19-45.
- Jetz W, Sekercioglu CH, Böhning-Gaese K (2008) The worldwide variation in avian clutch size across species and space. *PLOS Biol* 6: 2650-2657. PubMed: 19071959.
- Martin TE, Li P (1992) Life history traits of open- vs. cavity-nesting birds. *Ecology* 73: 579-592. doi:10.2307/1940764.
- Zardoya R, Meyer A (2001) The evolutionary position of turtles revised. *Naturwissenschaften* 88: 193-200. doi:10.1007/s001140100228. PubMed: 11482432.
- Iwabe N, Hara Y, Kumazawa Y, Shibamoto K, Saito Y et al. (2005) Sister group relationship of turtles to the bird-crocodylian clade revealed by nuclear DNA-coded proteins. *Mol Biol Evol* 22: 810-813. doi: 10.1093/molbev/msi075. PubMed: 15625185.
- Chiari Y, Cahais V, Galtier N, Delsuc F (2012) Phylogenomic analyses support the position of turtles as the sister group of birds and crocodiles (Archosauria). *BMC Biol* 10: 65. doi:10.1186/1741-7007-10-65. PubMed: 22839781.
- Rahn H, Paganelli CV (1989) The initial density of avian eggs derived from the tables of Schönwetter. *J Ornithol* 130: 207-215. doi:10.1007/BF01649755.
- Ferguson MWJ (1985) Reproductive biology and embryology of the crocodylians. In: C GansF BilletPFA Maderson. *Biology of the reptilia*. New York: John Wiley and Sons. pp. 451-460.
- Hoyt DF (1979) Practical methods of estimating volume and fresh weight of bird eggs. *Auk* 96: 73-77.
- Felsenstein J (1985) Phylogenies and the comparative method. *Am Nat* 125: 1-15. doi:10.1086/284325.
- Felsenstein J (1988) Phylogenies and quantitative characters. *Annu Rev Ecol Syst* 19: 445-471. doi:10.1146/annurev.es.19.110188.002305.
- Martins EP, Diniz-Filho JAF, Housworth EA (2002) Adaptive constraints and the phylogenetic comparative method: a computer simulation test. *Evolution* 56: 1-13. doi:10.1111/j.0014-3820.2002.tb00844.x. PubMed: 11913655.
- Rohlf FJ (2006) A comment on phylogenetic correction. *Evolution* 60: 1509-1515. doi:10.1554/05-550.1. PubMed: 16929667.
- Core R Team (2012) R: a language and environment for statistical computing. Vienna, Austria: R Foundation for Statistical Computing. ISBN 3-900051-07-0 Available: <http://www.R-project.org/>. Accessed 2012 January

46. Reiss MJ (1985) The allometry of reproduction - why larger species invest relatively less in their offspring. *J Theor Biol* 113: 529-544. doi: 10.1016/S0022-5193(85)80037-0.
47. Hirth HF (1980) Some aspects of the nesting behavior and reproductive biology of sea turtles. *Am Zool* 20: 507-523.
48. Carpenter K (1999) Eggs, nests, and baby dinosaurs: a look at dinosaur reproduction. Bloomington: Indiana University Press.
49. Jackson FD, Varricchio DJ, Jackson RA, Vila B, Chiappe LM (2008) Comparison of water vapor conductance in a titanosaur egg from the Upper Cretaceous of Argentina and a *Megaloolithus siruguei* egg from Spain. *Paleobiology* 34: 229-246. doi: 10.1666/0094-8373(2008)034[0229:COWVCI]2.0.CO;2.
50. Norell MA, Clark JM, Chiappe LM, Dashzeveg D (1995) A nesting dinosaur. *Nature* 378: 774-776. doi:10.1038/378774a0.
51. Dong ZM, Currie PJ (1996) On the discovery of an oviraptorid skeleton on a nest of eggs at Bayan Mandahu, Inner Mongolia, People's Republic of China. *Can J Earth Sci* 33: 631-636. doi:10.1139/e96-046.
52. Varricchio DJ, Jackson F, Trueman CN (1999) A nesting trace with eggs for the Cretaceous theropod dinosaur *Troodon formosus*. *J Vertebr Paleontol* 19: 91-100. doi:10.1080/02724634.1999.10011125.
53. Horner JR, Weishampel DB (1988) A comparative embryological study of two ornithischian dinosaurs. *Nature* 332: 256-257. doi: 10.1038/332256a0.
54. Horner JR, Weishampel DB (1996) A comparative embryological study of two ornithischian dinosaurs (vol 332, pg 256, 1988). *Nature* 383: 103-103. doi:10.1038/383103a0. PubMed: 8779724.
55. Zelenitsky DK, Therrien F (2008a) Phylogenetic analysis of reproductive traits of maniraptoran theropods and its implications for egg parataxonomy. *Palaeontology* 51: 807-816. doi:10.1111/j.1475-4983.2008.00770.x.
56. Mateus O, Walen A, Antunes MT (2006) The large theropod fauna of the Lourinhã Formation (Portugal) and its similarity to that of the Morrison Formation, with a description of a new species of *Allosaurus*. In: JR FosterSG Lucas. *Paleontology and geology of the Upper Jurassic Morrison Formation*. New Mexico: Museum of Natural History & Science Bulletin 36. pp. 123-130
57. Mateus I, Mateus H, Antunes MT, Mateus O, Taquet P et al. (1998) Upper Jurassic theropod dinosaur embryos from Lourinhã (Portugal) 37. *Mem Acad Ci Lisboa*. pp. 101-109.
58. Birchard GF, Ruta M, Deeming DC (2013) Evolution of parental incubation behaviour in dinosaurs cannot be inferred from clutch mass in birds. *Biol Lett* 9: 20130036. PubMed: 23676654.
59. Seymour RS, Ackerman RA (1980) Adaptations to underground nesting in birds and reptiles. *Am Zool* 20: 437-447.
60. Vila B, Jackson FD, Fortuny J, Sellés AG, Galobart À (2010) 3-D modelling of megaloolithid clutches: insights about nest construction and dinosaur behaviour. *PLOS ONE* 5: e10362. doi:10.1371/journal.pone.0010362. PubMed: 20463953.
61. Booth DT, Thompson MB (1991) A comparison of reptilian eggs with those of megapode birds. In: DC DeemingMWJ Ferguson. *Egg incubation: its effects on embryonic development in birds and reptiles*. Cambridge, UK: Cambridge University Press. pp. 117-146.
62. Booth DT (1998) Nest temperature and respiratory gases during natural incubation in the broad-shelled river turtle, *Chelodina expansa* (Testudinata : Chelidae). *Aust J Zool* 46: 183-191. doi:10.1071/ZO98003.
63. Horner JR (1999) Egg clutches and embryos of two hadrosaurian dinosaurs. *J Vertebr Paleontol* 19: 607-611. doi: 10.1080/02724634.1999.10011174.
64. Sander PM (2000) Long bone histology of the Tendaguru sauropods: implications for growth and biology. *Paleobiology* 26: 466-488. doi: 10.1666/0094-8373(2000)026.
65. Griebeler EM, Klein N, Sander PM (2013) Aging, maturation and growth of sauropodomorph dinosaurs as deduced from growth curves using long bone histological data: an assessment of methodological constraints and solutions. *PLOS ONE* 8: e67012. doi:10.1371/journal.pone.0067012. PubMed: 23840575.
66. SWOT (2012) The state of the world's sea turtles. Available: <http://seaturtlestatus.org/learn/meet-the-turtles>. Accessed 2012 November 13.
67. Slatkin M (1974) Hedging one's evolutionary bets. *Nature* 250: 704-705. doi:10.1038/250704b0.
68. Olofsson H, Ripa J, Jonzén N (2009) Bet-hedging as an evolutionary game: the trade-off between egg size and number. *Proc R Soc Lond B Biol Sci* 276: 2963-2969. doi:10.1098/rspb.2009.0500. PubMed: 19474039.
69. Beaumont HJE, Gallie J, Kost C, Ferguson GC, Rainey PB (2009) Experimental evolution of bet hedging. *Nature* 462: 90-93. doi:10.1038/nature08504. PubMed: 19890329.
70. Griebeler EM, Caprano T, Böhning-Gaese K (2010) Evolution of avian clutch size along latitudinal gradients: do seasonality, nest predation or breeding season length matter? *J Evol Biol* 23: 888-901. doi:10.1111/j.1420-9101.2010.01958.x. PubMed: 20210827.
71. Horner JR, Makela R (1979) Nest of juveniles provides evidence of family-structure among dinosaurs. *Nature* 282: 296-298. doi: 10.1038/282296a0.
72. Horner JR (1982) Evidence of colonial nesting and site fidelity among ornithischian dinosaurs. *Nature* 297: 675-676. doi:10.1038/297675a0.
73. Geist NR, Jones TD (1996) Juvenile skeletal structure and the reproductive habits of dinosaurs. *Science* 272: 712-714. doi:10.1126/science.272.5262.712. PubMed: 8662567.



PLOS is a nonprofit organization that accelerates progress in science and medicine by leading a transformation in research communication

U.S. HEADQUARTERS
1160 Battery Street
Koshland Building East, Ste. 100
San Francisco, CA 94111 US
+ 1 415.624.1200 PHONE
+ 1 415.546.4090 FAX

EUROPEAN EDITORIAL OFFICE
Carlyle House
Carlyle Road
Cambridge CB4 3DN UK
+ 44 0.1223.442.810 PHONE
+ 44 0.1223.442.833 FAX

©2013 Public Library of Science
info@plos.org
plos.org